Investigating the Importance of Hydrophobicity and Hydration of Carbohydrates and Antifreeze Glycoprotein Analogues to Ice Recrystallization Inhibition Activity and Cryopreservation

Elisabeth von Moos

Thesis submitted to the Faculty of Graduate & Postdoctoral Studies

University of Ottawa

In partial fulfillment of the requirements for the Ph.D. degree in the Ottawa-Carleton Chemistry Institute

Candidate	Supervisor
_____	_____
Elisabeth von Moos	Robert N. Ben

Abstract

Cryopreservation is a vitally important field of study, and although significant advances have been made in the last 60 years, many challenges still exist. The exact mechanisms by which injury occurs are still debated, and therefore the design of cryoprotectants is uniquely challenging. A key event during cryopreservation is the recrystallization of ice, which results in damage to cells. Antifreeze glycoproteins (AFGPs) are a subclass of biological antifreezes found in many species of Arctic and Antarctic teleost fish, and these possess potent recrystallization inhibition (RI) activity. Consequently, our lab has explored the rational design of chemically and biologically stable AFGP analogues for use in cryopreservation. In this study, we have prepared *C*-linked AFGP analogues and their derivatives to probe the mechanism of RI, and explored the relationship between RI activity and cryopreservation.

Recently, our lab prepared a series of *C*-linked AFGP analogues substituted with different monosaccharides in order to explore the connection between the stereochemistry of the carbohydrate moiety and recrystallization activity. A subsequent study of a series of commercially available *O*-linked mono- and disaccharides confirmed that the hydration of the carbohydrate, which is determined by its stereochemistry, is correlated to its RI activity. The hydration of a compound is further related to its hydrophobicity. Consequently, we designed a series of analogues to investigate the importance of hydrophobicity and hydration of *C*-linked AFGP analogues and their components to RI activity. AFGP analogues substituted with a carbohydrate moiety containing a double bond, AFGP analogue building blocks substituted with both saturated and unsaturated carbohydrate moieties, and a series of *C*-linked carbohydrate derivatives bearing a variety of hydrophobic groups were prepared and tested for RI activity. The data obtained reinforced the importance of stereochemistry for RI activity. The double bond would have disturbed the stereochemistry of the hydroxyl groups compared to the saturated carbohydrate, and this resulted in a decrease in RI activity. Further, it was found that increasing the hydrophobicity of *C*-linked carbohydrate derivatives does not necessarily improve RI activity. Lastly, the AFGP analogues had much greater RI

activity than their individual components, and the components cannot be used to predict the RI activity of the polymer.

Our cryopreservation studies were carried out using two cell types, a hepatocyte-like cell line (WRL 68), and hematopoietic stem cells (HSCs) from umbilical cord blood (UCB). Hematopoietic stem cells (HSCs) are immature hematopoietic precursor cells also found in bone marrow and peripheral blood. Transplantation of both HSCs and hepatocytes is indicated for myriad conditions, and a reliable supply of cells is paramount. There is a need for improved cryopreservation conditions for both cell types to achieve this goal.

Based on the extensive work done by our lab on the effect of hydration of carbohydrates on RI, we investigated the cryopreservation potential of several carbohydrates, representing a spectrum of RI activity. It was found that that low concentrations of carbohydrates can be used for successful cryopreservation of WRL 68 cells, and further, the addition of low concentration of carbohydrates can allow the concentration of DMSO in the cryopreservation medium to be reduced without adversely affecting the cryopreservation outcome. For UCB cells, 5% DMSO can be completely replaced with galactose, without a decrease in cell viability. For both cell types, in the presence of DMSO, the type of carbohydrate was more important than its concentration for a successful cryopreservation outcome. Further, carbohydrates are most effective when employed as extracellular cryoprotectants. Significantly, when used as the sole cryoprotectant, we determined that carbohydrate cryopreservation activity correlated with RI activity. Carbohydrates with good RI activity may therefore be able to effectively manage the ice formed during cryopreservation.

Acknowledgements

I would first like to thank my supervisor, Dr. Robert Ben, for providing a stimulating and challenging environment that caused me to grow as a person and as a scientist. He was available for helpful discussions and suggestions for my research, and he also made it possible for me to attend several scientific conferences during my studies. Dr. Ben was also helpful in proof-reading the various drafts of this thesis. I would also like to thank all of the past and present members of the Ben group for their assistance and friendship including: Dr. Vincent Bouvet, Dr. Suhuai Liu, Dr. Pawel Czechura, Jessica Jackman, Dr. Roger Tam, Dr. Jennifer Chaytor, John F. Trant, Ruoying Gong, Sandra Ferreira, Wendy Campbell, Taline Boghossian, and Jacqueline Tokarew. Special thanks also to Dr. Mathieu Leclere and Dr. Michael Souweha, members of the Fallis group.

Thank you to the members of my Research Proposal Committee and members of my Thesis Committee for valuable discussions and suggestions to improve these documents.

I was privileged to supervise two undergraduate students, John F. Trant, and Louise Guolla. I would like to thank John for his help with chemistry, preparing starting materials for this project, and Louise for her help with cell biology, particularly with the cytotoxicity assays.

I would also like to thank Luke Wu for his help with the cryopreservation experiments, and Dr. David Allen for helpful discussions and valuable insight regarding the umbilical cord blood studies. Thanks also to Dr. Scott Findlay for his help with statistical analysis, and Dr. Glenn Facey for NMR assistance.

I would like to thank the National Research Council for allowing us access to their confocal microscope, and particularly to Dr. Robert Monette for his invaluable assistance.

I would like to acknowledge the National Sciences and Engineering Research Council and the University of Ottawa for their generous scholarships that assisted me financially during the course of this research.

Thank you to my friends and family, for their love, support, and constant encouragement during the course of my studies, and especially, thank you to Martin, who always believed in me, and without whom I could not have completed this work.

Table of Contents

CHAPTER 1: INTRODUCTION TO CRYOPRESERVATION 1
1.1 Cryobiology 2
1.1.1 Fast-Freezing Injury 3
1.1.2 Slow-Freezing Injury 4
1.1.3 Effects of Slow and Fast Warming and Thawing Rates 6
1.2 Effects of Cryopreservation on Cells 7
1.2.1 Ice Recrystallization 7
1.2.2 Innocuous Intracellular Ice 8
1.2.3 Biochemical Mechanisms of Cell Death 9
1.2.3.1 Necrosis 9
1.2.3.2 Apoptosis 10
1.2.4 Effects of Cryopreservation on Cells: Summary 12
1.3 Cryopreservation Agents 13
1.3.1 Colligative Mechanism of Action of Cryoprotective Agents 13
1.3.2 DMSO and DMSO Toxicity 15
1.4 Biological Antifreezes 16
1.4.1 Antifreeze Proteins (AFPs) 16
1.4.2 Antifreeze Glycoproteins (AFGPs) 17
1.5 Antifreeze Activity 19
1.5.1 Thermal Hysteresis (TH) of Biological Antifreezes 19
1.5.2 Recrystallization Inhibition (RI) of Biological Antifreezes 21
1.5.3 AF(G)Ps and Ice-Binding 22
1.5.4 Membrane Protection 23
1.6 AF(G)Ps and Cryopreservation 24
1.7 Sugars, Antifreeze Activity, and Cryopreservation 25
1.8 Umbilical Cord Blood and Hematopoietic Stem Cells 28
1.9 Hepatocytes: Orthotopic Liver Transplantation vs. Hepatocyte Transplantation 30
1.10 Summary 31

CHAPTER 2: OBJECTIVES 42
2.1 Structure-Function Studies of AFGP and *O*-Linked AFGP Analogues 42
2.2 Synthesis and Structure-Function Studies of *C*-Linked AFGP Analogues 46
2.3 Hydration of the Carbohydrate Moiety of AFGP Analogues 50
2.4 Recrystallization Inhibition (RI) Activity of Carbohydrates 53
2.5 *In vitro* Effects and Cellular Interactions of a *C*-linked AFGP 8 Analogue and native AFGP 8 55

2.6 Project Goals 59
Goal 1: Design of New *C*-Linked AFGP 8 Analogues 59
Objective 1.1: Investigating the Importance of Hydrophobicity of C-Linked AFGP 8 Analogues to Recrystallization Inhibition (RI) Activity (Series I Analogues) 59
Objective 1.2: Investigating the Importance of Hydration of the AFGP 8 Analogues to Recrystallization Inhibition (RI) Activity (Series II Analogues) 60
Goal 2: Investigating the Cryopreservation Potential of the Ornithine Analogue and Several Carbohydrates *in Vitro* 62
Objective 2.1: Assessing the Cryopreservation Activity of Carbohydrates 62
Objective 2.2: Assessing the Cryopreservation Activity of the Ornithine Analogue 62

CHAPTER 3: DESIGN OF NEW *C*-LINKED AFGP 8 ANALOGUES 66
Part 1: Preparation of *C*-Linked Analogues 66
3.1. Retrosynthetic Analysis 66
3.1.1. Investigating the Importance of Hydrophobicity of the AFGP 8 Analogues to Recrystallization Inhibition (RI) Activity (Series I Analogues) 66
3.1.2 Investigating the Importance of Hydration of the AFGP 8 Analogues to Recrystallization Inhibition (RI) Activity (Series II Analogues) 69
3.2 Synthesis 72
3.2.1 Investigating the Importance of Hydrophobicity of the AFGP 8 Analogues to Recrystallization Inhibition (RI) Activity (Series I Analogues) 72
3.2.2 Investigating the Importance of Hydration of the AFGP 8 Analogues to Recrystallization Inhibition (RI) Activity (Series II Analogues) 79
3.2.3 Assessing the Cryopreservation Activity of the Ornithine Analogue: Synthesis of the Ornithine Analogue 105
Part II: Assessing Antifreeze Activity 107
3.3 Thermal Hysteresis (TH) Activity 107
3.4 Recrystallization Inhibition (RI) Activity 110
3.5 Antifreeze Activity Testing: Summary 120

CHAPTER 4: CRYOPRESERVATION STUDIES 123
4.1 State of the Art: Cryopreservation Conditions for Umbilical Cord Blood (UCB) Hematopoietic Stem Cells (HSCs) and Hepatocytes 123
4.2 Cryopreservation Protocol Developed for the Current Study 127
4.3 Cryopreservation Using Carbohydrates: Precedent 127
4.3.1 Umbilical Cord Blood (UCB) Hematopoietic Stem Cells (HSCs) 127
4.3.2 Hepatocytes 129
4.3.3 Carbohydrates and Carbohydrate Concentrations for Cryopreservation 131

4.4 Analysis of Cryopreservation Outcomes 131
4.4.1 Cytotoxicity of Cryopreservation Agents 131
4.4.2 Cell Viability Post-Cryopreservation 133
4.5 Cytotoxicity Studies with WRL 68 Cells: 136
4.5.1 Cytotoxicity of carbohydrates to WRL 68 cells 136
4.5.1.1 Interactions of Carbohydrates and Cells 138
4.5.2 Cytotoxicity of Dimethyl Sulfoxide (DMSO) to WRL 68 Cells 141
4.6 Permeable versus Impermeable Cryoprotectants 141
4.7 Cryopreservation Studies with WRL 68 Cells 143
4.7.1 Cryopreservation of WRL 68 Cells with Dimethyl Sulfoxide (DMSO) 143
4.7.2 Cryopreservation of WRL 68 Cells with Carbohydrates 145
4.7.3 Cryopreservation of WRL 68 Cells with Carbohydrates and 5% Dimethyl Sulfoxide (DMSO) 148
4.7.4 Cryopreservation of WRL 68 Cells with Combinations of Carbohydrates and Dimethyl Sulfoxide (DMSO) 150
4.7.4.1 Cryopreservation of WRL 68 Cells with Carbohydrates and Dimethyl Sulfoxide (DMSO) 153
4.7.5 Cryopreservation of WRL 68 Cells with Carbohydrates: Significant Successes using Carbohydrates 158
4.7.6 Cryopreservation of WRL 68 Cells: Mechanism of Action of Carbohydrates 159
4.7.6.1 Cryopreservation of WRL 68 Cells Versus Recrystallization Inhibition (RI) Activity 160
4.7.7 Assessing the Cryopreservation Activity of the Ornithine Analogue 163
4.7.8 Cryopreservation Studies with WRL 68 Cells: Summary 167
4.8 Cryopreservation of Umbilical Cord Blood (UCB): 168
4.8.1 Cryopreservation of Umbilical Cord Blood (UCB) with Dimethyl Sulfoxide (DMSO) 169
4.8.2 Cryopreservation of Umbilical Cord Blood (UCB): Pre-Cryopreservation Data 171
4.8.3 Cryopreservation of Umbilical Cord Blood (UCB) with Carbohydrates and Dimethyl Sulfoxide (DMSO) 173
4.8.3.1 Cryopreservation of Umbilical Cord Blood (UCB) with Galactose 174
4.8.3.2 Cryopreservation of UCB with Combinations of Carbohydrates and Dimethyl Sulfoxide (DMSO): Correlations Between Cell Populations 176
4.8.3.3 Cryopreservation of Umbilical Cord Blood (UCB) with Glucose and 3-O-Methylglucose 180
4.8.3.4 Cryopreservation of Umbilical Cord Blood (UCB): Melibiose 181
4.8.3.5 Cryopreservation of Umbilical Cord Blood (UCB) with Trehalose 183
4.8.3.6 Cryopreservation of Umbilical Cord Blood (UCB) with Sucrose 184
4.8.4 Cryopreservation of Umbilical Cord Blood (UCB): Significant Successes Using Carbohydrates 186

4.8.5 Cryopreservation of Umbilical Cord Blood (UCB) Versus Recrystallization Inhibition (RI) Activity 188
4.8.6 Cryopreservation of Umbilical Cord Blood (UCB): Summary 192

CHAPTER 5: CONCLUSIONS 201
5.1 Goal 1: Design of New C-Linked AFGP 8 Analogues 201
Objective 1.1: Investigating the Importance of Hydrophobicity of C-Linked AFGP 8 Analogues to Recrystallization Inhibition (RI) Activity (Series I Analogues) 201
Objective 1.2: Investigating the Importance of Hydrophobicity of C-Linked AFGP 8 Analogues to Recrystallization Inhibition (RI) Activity (Series II Analogues) 202
5.1.1 Antifreeze Activity Testing: Thermal Hysteresis (TH) and Recrystallization Inhibition (RI) 203
5.2 Goal 2: Investigating the Cryopreservation Potential of the Ornithine Analogue and Several Carbohydrates in Vitro 204
Objective 2.1 Assessing the Cryopreservation Activity of Carbohydrates 204
Objective 2.2: Assessing the Cryopreservation Activity of the Ornithine Analogue 208
5.3 Future Directions 208
5.3.1 Analogue Synthesis and Recrystallization Inhibition (RI) 209
5.3.2 Cryopreservation Studies with WRL 68 cells and Umbilical Cord Blood (UCB) 209

CHAPTER 6: EXPERIMENTAL 211
6.1 General Experimental 215
6.2 Compound Preparation Procedures and Experimental Data 216
6.3 Procedures for Assessing Antifreeze Activity 280
6.3.1: Assessing Thermal Hysteresis (TH) and Dynamic Ice-Shaping (DIS) Activities 280
6.3.2: Assessing Recrystallization Inhibition (RI) Activity 281
6.4 Methods for Assessing Cytotoxicity and Cryopreservation Activity 281
6.4.1 Cell Culture 281
6.4.1 MTT Cytotoxicity Assay 282
6.4.3 Cryopreservation 282
6.4.4 Flow Cytometry 283
6.5 Statistical Analysis 284

APPENDIX 1 COMPOUND CHARACTERIZATION 288
APPENDIX 2 CRYOPRESERVATION DATA 366

List of Figures

Figure 1.1 "Inverted U" Cooling Curves: comparative effects of cooling velocity on the survival of various cells cooled to -196 °C and thawed rapidly; the yeast and human red cells (RBC) were frozen in distilled water and blood, respectively. The marrow stem cells and hamster cells were suspended in balanced salt solutions containing 1.25 M glycerol.[10] 3

Figure 1.2 Necrosis vs. Apoptosis[59] 10

Figure 1.3 Cryopreservation-Induced Apoptosis: A) membrane-mediated apoptosis: schematic diagram of the Fas and TNF surface receptor-mediated apoptotic pathways; open arrows (⟹) indicated stages in the apoptotic cascade that have been implicated in cell death following cryopreservation; B) Mitochondrial-induced apoptosis: schematic diagram of apoptotic progression following induction through mitochondrial alterations; open arrows (⟹) indicate stages in the apoptotic cascade that have been implicated in cell death following cryopreservation[50] 11

Figure 1.4 General structures of antifreeze glycoproteins and abbreviations: (A) AFGP the most common structural motif with n = 4-50; (B) AFGP-Pro in which Pro replaces Ala; (C) AFGP-Arg in which Arg replaces Thr, with the loss of a disaccharide group, frequently at the C-terminus of the sequences; AFGP-Pro and AFGP-Arg constitue < 5% of the naturally occurring glycoproteins[94] 18

Figure 1.5 Interaction between antifreeze proteins and ice: A) in a dilute solution of AFPs (nM), the AFPs absorb onto the prism faces of the ice crystal and limit growth along the a_1-, a_2-, and a_3-axes, forming a crystal that is hexagonal in shape; B) in solutions containing higher concentrations of AFPs (μM), the preferred direction of ice crystal growth is along the c-axis, so that the crystal forms a hexagonal bipyramid[114] 20

Figure 1.6 Proposed mechanisms of growth inhibition based on the Kelvin effect: (A) step pinning model; (B) mattress model[124] 22

Figure 1.7 Proposed mechanism of action of type I AFP: schematic of proposed mechanism for inhibition of leakage from membrane by type I AFP (TTTT) by insertion of the N-terminal region of the AFGP into the membrane[139] 24

Figure 2.1 Helical wheel representation of type 1 proteins: the hydrophobic face is indicated by bold residues; in the case of threonine this is achieved with γ-methyl group oriented on the surface[7] 43

Figure 2.2 Structure-activity relationship: AFGP analogues synthesized by Nishimura and co-workers; all compounds were used for the activity evaluation studies in polymeric form[16] 45

Figure 2.3 Structure-activity relationship: example of AFGP analogues synthesized by Heggemann and co-workers[17] 46

Figure 2.4 Model for AFGP structure-activity relationship studies[25] 47

Figure 2.5 AFGP 8 and novel C-linked AFGP analogues; the red colour indicates differences between the analogue and AFGP 8. 48

Figure 2.6 RI activity: mean largest grain size of AFGP-8, C-linked analogues (**14-16**), and controls at -6.4 °C after 30 min anneal time; error bars indicate SEM 49

Figure 2.7 Structure of C-linked AFGP 8 analogues 50

Figure 2.8 RI activity: mean largest grain size of AFGP 8, C-linked analogues (**14**, **18-20**), and PBS standard at -6.4 °C after 30 min anneal time; error bars indicate SEM 51

Figure 2.9 Partial molar compressibilities of monosaccharides in aqueous solution at 298 K (K_2° (s) x 10^4, cm^3 mol^{-1} bar^{-1}); values are given for the dominant conformer in solution... 52

Figure 2.10 Monosaccharides and disaccharides assessed for recrystallization-inhibition activity by Tam and co-workers[35] 53

Figure 2.11 RI activities of carbohydrates (**21-29**) plotted against their respective hydration index (hydration number/partial molar volume) (mol^1cm^{-3}) 54

Figure 2.12 RI activity of various concentrations of DMSO and 0.022 M solutions of D-galactose in PBS solution 55

Figure 2.13 Internalization study of fluorescently labeled AFGP 8 (F-AFGP 8) and fluorescently labeled serine analogue 16 (F-**16**) in human embryonic liver cells (WRL 68 cell line); WRL 68 cells were incubated with 10 μM RH-237 membrane probe solution in Eagle's minimum essential medium (EMEM) and 1.5 mg/mL F-AFGP 8 or F-**16**, solution in EMEM. F-AFGP 8 and F-**16** appear green, and RH-237 appears red; (A) WRL 68 cells were incubated with F-AFGP 8 at 37 °C for 10 min; (B) WRL 68 cells were incubated with F-**16**,

at 37 °C for 10 min; (C) WRL 68 cells were incubated with F-AFGP 8 at 0 °C for 50 min; the scale bar = 25 μm 56

Figure 2.14 Vybrant apoptosis assay of WRL 68 cells incubated with AFGP 8; WRL 68 cells were incubated with 8.1 μM Hoechst 33342, 1.5 μM propidium iodide and 0.1 μM YO-PRO-1 solutions in Eagle's minimum essential medium (EMEM) at 0 °C for 30 min.; Hoechst 33342 stains the nuclei of all cells blue; propidium iodide stains dead cells and late apoptotic cells red; YO-PRO-1 stains early apoptotic cells green; (A) negative control: WRL 68 cells were pre-incubated with EMEM; (B) WRL 68 cells were pre-incubated with 5 mg/mL AFGP 8 solution in EMEM at 37 °C for 4 h; (C) WRL 68 cells were pre-incubated with 20 μM staurosporine solution in EMEM at 37 °C for 4 h; the scale bar = 50 μm 57

Figure 2.15 The evolution of the AFGP 8 analogues that led to the synthesis of the hydrophobic analogues 30 (series 1 analogues)..... 60
Figure 2.16 Series two analogues……..…..……...61

Figure 3.1 Summary of all compounds synthesized for antifreeze testing 104

Figure 3.2 Structure of the carbohydrates and C-linked carbohydrates tested for recrystallization inhibition (RI) activity (data in Figure 3.3)..... 110

Figure 3.3 Recrystallization inhibition (RI) activity of several carbohydrates in PBS; RI activity is reported as a ratio of the mean grain size (MGS) of the carbohydrate solution to the MGS of the PBS solution. 111

Figure 3.4 Structure of the polymers and building blocks tested for recrystallization inhibition (RI) activity (data in Figure 3.5) 113

Figure 3.5 Recrystallization inhibition (RI) activity of several building blocks in PBS; RI activity is reported as a ratio of the mean grain size (MGS) of the building block solution to the MGS of the PBS solution. 114

Figure 3.6 Structure of the C-linked carbohydrates, building blocks, and polymers tested for recrystallization inhibition (RI) activity (data in Figure 3.7)..... 115

Figure 3.7 Recrystallization inhibition (RI) activity of several polymers and their corresponding building blocks and carbohydrate derivatives in PBS; RI activity is reported as a ratio of the mean grain size (MGS) of the test solution to the MGS of the PBS solution. 116

Figure 3.8 Structure of the ornithine analogue (**14**) and corresponding building block (**137**) and carbohydrate derivative (**135**) tested for recrystallization inhibition (RI) activity (data in Figure 3.9)..... 117

Figure 3.9 Recrystallization inhibition (RI) activity of the ornithine analogue and the corresponding building block and carbohydrate derivative in PBS; RI activity is reported as a ratio of the mean grain size (MGS) of the test solution to the MGS of the PBS solution. ... 118

Figure 3.10 Structure of the polymers tested for recrystallization inhibition (RI) activity (data in Figure 3.11)..... 119

Figure 3.11 Recrystallization inhibition (RI) activity of several polymers in PBS; RI activity is reported as a ratio of the mean grain size (MGS) of the test solution to the MGS of the PBS solution..... 119

Figure 4.1 Schematic of a typical cryopreservation protocol. 124

Figure 4.2 Living cells reduce the yellow MTT tetrazole (3-(4,5-dimethylthiazol-2-yl)-2,5-diphenyltetrazolium bromide) to insoluble purple formazan crystals. 132

Figure 4.3 MTT cell viability assay of WRL 68 cells in carbohydrate solutions; WRL 68 cells were incubated at 37 °C for 24 h with different concentrations of monosaccharides and disaccharides in EMEM. Optical density (OD) was measured at 570 nm. Cells treated only with EMEM were used as the positive control and were considered to be 100% viable. The error bars indicate SEM. 137

Figure 4.4 MTT cell viability assay of WRL 68 cells in DMSO solutions; WRL 68 cells were incubated at 37 °C for 24 h with different concentrations of DMSO in EMEM. Optical density (OD) was measured at 570 nm. Cells treated only with EMEM were used as the positive control and were considered to be 100% viable. The error bars indicate SEM. 141

Figure 4.5 Annexin V/7AAD flow cytometry assay of WRL 68 cells after cryopreservation; WRL 68 cells were treated with different concentrations of DMSO in HTK, and then treated according to the standard protocol given in the Chapter 6. The total cell count was taken as 100% of cells. The error bars indicate SEM. 144

Figure 4.6 Annexin V/7AAD flow cytometry assay of WRL 68 cells after cryopreservation; WRL 68 cells were treated with different concentrations of different carbohydrates in HTK, and then treated according to the standard protocol given in Chapter 6. The total cell count was taken as 100% of cells. The error bars indicate SEM. 146

Figure 4.7 Annexin V/7AAD flow cytometry assay of WRL 68 cells after cryopreservation; WRL 68 cells were treated with different concentrations of different carbohydrates with 5% DMSO in HTK, and then treated according to the standard protocol given in Chapter 6. The total cell count was taken as 100% of cells. The error bars indicate SEM. 149

Figure 4.8 Annexin V/7AAD flow cytometry assay of WRL 68 cells after cryopreservation; WRL 68 cells were treated with different concentrations of galactose and DMSO in HTK, and then treated according to the standard protocol given in Chapter 6. The total cell count was taken as 100% of cells. The error bars indicate SEM. 150

Figure 4.9 Percentage of viable cells versus percentage of late apoptotic/necrotic cells as determined by Annexin V/7AAD flow cytometry assay of WRL 68 cells after cryopreservation; WRL 68 cells were treated with different concentrations of carbohydrates and DMSO in HTK, and then treated according to the standard protocol given in Chapter 6. The total cell count was taken as 100% of cells. 151

Figure 4.10 Percentage of viable cells versus percentage of early apoptotic cells as determined by Annexin V/7AAD flow cytometry assay of WRL 68 cells after cryopreservation; WRL 68 cells were treated with different concentrations of carbohydrates and DMSO in HTK, and then treated according to the standard protocol given in Chapter 6. The total cell count was taken as 100% of cells. 152

Figure 4.11 Annexin V/7AAD flow cytometry assay of WRL 68 cells after cryopreservation; WRL 68 cells were treated with different concentrations of carbohydrates and DMSO in HTK, and then treated according to the standard protocol given in Chapter 6. The total cell count was taken as 100% of cells. The error bars indicate SEM. 153

Figure 4.12 Annexin V/7AAD flow cytometry assay of WRL 68 cells after cryopreservation; WRL 68 cells were treated with different concentrations of carbohydrates and 2.5% DMSO in HTK, and then treated according to the standard protocol given in Chapter 6. The total cell count was taken as 100% of cells. The error bars indicate SEM. . 155

Figure 4.13 Annexin V/7AAD flow cytometry assay of WRL 68 cells after cryopreservation; WRL 68 cells were treated with different concentrations of carbohydrates with 5% DMSO in HTK, and then treated according to the standard protocol given in Chapter 6. The total cell count was taken as 100% of cells. The error bars indicate SEM. . 156

Figure 4.14 Annexin V/7AAD flow cytometry assay of WRL 68 cells after cryopreservation; WRL 68 cells were treated with different concentrations of carbohydrates and DMSO in HTK, and then treated according to the standard protocol given in Chapter 6. The total cell count was taken as 100% of cells. The error bars indicate SEM. 158

Figure 4.15 Percentage of viable cells versus the RI ratio (sample/PBS) for the same treatment; percentage of viable cells was obtained by Annexin V/7AAD flow cytometry assay of WRL 68 cells after cryopreservation, where the total cell count was taken as 100% of cells. RI ratio of carbohydrates at 220 mM was compared to cryopreservation data of 200 mM carbohydrates. Cryopreservation and RI data were obtained according to the protocols given in Chapter 6. The error bars indicate SEM. 161

Figure 4.16 Annexin V/7AAD flow cytometry assay of WRL 68 cells after cryopreservation; WRL 68 cells were treated with different concentrations of AFGP 8 and DMSO in HTK, and then treated according to the standard protocol given in Chapter 6. The total cell count was taken as 100% of cells. The error bars indicate SEM. 164

Figure 4.17 Annexin V/7AAD flow cytometry assay of WRL 68 cells after cryopreservation; WRL 68 cells were treated with different concentrations of ornithine analogue **14** and DMSO in HTK, and then treated according to the standard protocol given in Chapter 6. The total cell count was taken as 100% of cells. The error bars indicate SEM. . 166

Figure 4.18 Annexin V/7AAD flow cytometry assay of UCB MNCs after cryopreservation; UCB cells were treated with different concentrations of DMSO in RPMI, and then treated according to the standard protocol given in Chapter 6. The total MNC count was taken as 100% of cells. The error bars indicate SEM. 169

Figure 4.19 Annexin V/7AAD flow cytometry assay of UCB $CD34^+$ cells after cryopreservation; UCB cells were treated with different concentrations of DMSO in RPMI, and then treated according to the standard protocol given in Chapter 6. The total $CD34^+$ cell count was taken as 100% of cells. The error bars indicate SEM. 170

Figure 4.20 Annexin V/7AAD flow cytometry assay of UCB MNCs prior to cryopreservation; the total $CD34^+$ cell count was taken as 100% of cells. The error bars indicate SEM. 172

Figure 4.21 Annexin V/7AAD flow cytometry assay of UCB $CD34^+$ cells prior to cryopreservation; the total $CD34^+$ cell count was taken as 100% of cells. The error bars indicate SEM. 173

Figure 4.22 Annexin V/7AAD flow cytometry assay of UCB MNCs after cryopreservation; UCB cells were treated with different concentrations of galactose and DMSO in RPMI, and then treated according to the standard protocol given in Chapter 6. The total MNC count was taken as 100% of cells. The error bars indicate SEM. 175

Figure 4.23 Annexin V/7AAD flow cytometry assay of UCB $CD34^+$ cells after cryopreservation; UCB cells were treated with different concentrations of galactose and DMSO in RPMI, and then treated according to the standard protocol given in Chapter 6. The total $CD34^+$ cell count was taken as 100% of cells. The error bars indicate SEM. 175

Figure 4.24 Percentage of viable cells versus percentage of late apoptotic/necrotic cells as determined by Annexin V/7AAD flow cytometry assay of MNCs after cryopreservation; UCB cells were treated with different concentrations of carbohydrates and DMSO in RPMI, and then treated according to the standard protocol given in Chapter 6. The total cell count was taken as 100% of cells. 177

Figure 4.25 Percentage of viable cells versus percentage of early apoptotic cells as determined by Annexin V/7AAD flow cytometry assay of MNCs after cryopreservation; UCB cells were treated with different concentrations of carbohydrates and DMSO in RPMI, and then treated according to the standard protocol given in Chapter 6. The total cell count was taken as 100% of cells. 178

Figure 4.26 Percentage of viable cells versus percentage of late apoptotic/necrotic cells as determined by Annexin V/7AAD flow cytometry assay of $CD34^+$ cells after cryopreservation; UCB cells were treated with different concentrations of carbohydrates and DMSO in RPMI, and then treated according to the standard protocol given in Chapter 6. The total cell count was taken as 100% of cells..... 179

Figure 4.27 Percentage of viable cells versus percentage of early apoptotic cells as determined by Annexin V/7AAD flow cytometry assay of $CD34^+$ cells after cryopreservation; UCB cells were treated with different concentrations of carbohydrates and DMSO in RPMI, and then treated according to the standard protocol given in Chapter 6. The total cell count was taken as 100% of cells..... 179

Figure 4.28 Annexin V/7AAD flow cytometry assay of UCB MNCs after cryopreservation; UCB cells were treated with different concentrations of glucose, 3-O-methylglucose and DMSO in RPMI, and then treated according to the standard protocol given in Chapter 6. The total MNC count was taken as 100% of cells. The error bars indicate SEM. 180

Figure 4.29 Annexin V/7AAD flow cytometry assay of UCB $CD34^+$ cells after cryopreservation; UCB cells were treated with different concentrations of glucose, 3-O-methylglucose and DMSO in RPMI, and then treated according to the standard protocol given in Chapter 6. The total $CD34^+$ cell count was taken as 100% of cells. The error bars indicate SEM. 181

Figure 4.30 Annexin V/7AAD flow cytometry assay of UCB MNCs after cryopreservation; UCB cells were treated with different concentrations of melibiose and DMSO in RPMI, and then treated according to the standard protocol given in Chapter 6. The total MNC count was taken as 100% of cells. The error bars indicate SEM. 182

Figure 4.31 Annexin V/7AAD flow cytometry assay of UCB $CD34^+$ cells after cryopreservation; UCB cells were treated with different concentrations of melibiose and DMSO in RPMI, and then treated according to the standard protocol given in the Chapter 6. The total $CD34^+$ cell count was taken as 100% of cells. The error bars indicate SEM. 182

Figure 4.32 Annexin V/7AAD flow cytometry assay of UCB MNCs after cryopreservation; UCB cells were treated with different concentrations of trehalose and DMSO in RPMI, and then treated according to the standard protocol given in Chapter 6. The total MNC count was taken as 100% of cells. The error bars indicate SEM. 183

Figure 4.33 Annexin V/7AAD flow cytometry assay of UCB $CD34^+$ cells after cryopreservation; UCB cells were treated with different concentrations of trehalose and DMSO in RPMI, and then treated according to the standard protocol given in Chapter 6. The total $CD34^+$ cell count was taken as 100% of cells. The error bars indicate SEM. 184

Figure 4.34 Annexin V/7AAD flow cytometry assay of UCB MNCs after cryopreservation; UCB cells were treated with different concentrations of sucrose and DMSO in RPMI, and then treated according to the standard protocol given in Chapter 6. The total MNC count was taken as 100% of cells. The error bars indicate SEM. 185

Figure 4.35 Annexin V/7AAD flow cytometry assay of UCB $CD34^+$ cells after cryopreservation; UCB cells were treated with different concentrations of DMSO in RPMI, and then treated according to the standard protocol given in Chapter 6. The total $CD34^+$ cell count was taken as 100% of cells. The error bars indicate SEM. 185

Figure 4.36 Annexin V/7AAD flow cytometry assay of UCB MNCs after cryopreservation; UCB cells were treated with different concentrations of carbohydrates and DMSO in RPMI, and then treated according to the standard protocol given in Chapter 6. The total MNC count was taken as 100% of cells. The error bars indicate SEM. 186

List of Tables

Table 1.1 Key structural features and natural sources of AFPs and AFGPs[94] 17

Table 3.1 Reactions of thiazolidine thione chiral auxiliry with test electrophiles 77

Table 3.2 Hydrogenolysis conditions 90

Table 3.3 Results of thermal hysteresis (TH) activity testing: carboxylic acid galactal derivatives and building blocks 107

Table 3.4 Results of thermal hysteresis (TH) activity testing: polymers 109

List of Schemes

Scheme 3.1 Retrosynthesis of Series I AFGP 8 analogues; A α-series (R = H is the ornithine analogue); B β-series 67

Scheme 3.2 Lewis acid mediated cross-coupling reaction of glycals to chiral titanium enolates derived from (S)-**42** and (R)-**40**[1, 2] 68

Scheme 3.3 Retrosynthesis of Series II AFGP analogues 70

Scheme 3.4 Series II AFGP analogues 71

Scheme 3.5 Synthesis of the thiazolidine thione chiral auxiliary to introduce methyl groups at the pseudo-anomeric position 72

Scheme 3.6 Synthesis of thiazolidine thione chiral auxiliaries to introduce various R groups 73

Scheme 3.7 Synthesis of various acyl chlorides from the carboxylic acid derivatives 74

Scheme 3.8 Synthesis of the carbohydrate coupling partner 75

Scheme 3.9 Test reaction with the trichloroimidate-substituted carbohydrate 75

Scheme 3.10 First attempted reaction of the carbohydrate derivative with the chiral titanium enolate 76

Scheme 3.11 Synthesis of alternate electrophilic carbohydrate moieties 76

Scheme 3.12 Reaction of thiazolidine thione chiral auxiliaries with various electrophilic carbohydrates 77

Scheme 3.13 Synthesis of acetyl-protected galactal 79

Scheme 3.14 Reaction of the chiral titanium enolate with protected galactal 80

Scheme 3.15 Reactions of the (S)- and (R)-chiral auxiliary with acetylated galactal 80

Scheme 3.16 Reaction of (S)-chiral auxiliaries with acetylated galactal 81

Scheme 3.17 Reaction of (R)-chiral auxiliaries with acetylated galactal 82

Scheme 3.18 Typical conditions for reaction of thiazolidine thione auxiliary with an acetal; B Transition states for anti (**92**) and syn (**93**) products[1] 83

Scheme 3.19 Dihydroxylation test reaction (I) 84

Scheme 3.20 Dihydroxylation of the β-anomer 84

Scheme 3.21 Dihydroxylation test reaction (II) 84

Scheme 3.22 Dihydroxylation test reaction (III) 85

Scheme 3.23 Dihydroxylation of the α- and β-anomers (new conditions) 85

Scheme 3.24 Dihydroxylation of the β-anomer (catalytic OSO_4 and new conditions) 85

Scheme 3.25 Displacement of the chiral auxiliary from the coupled galactal (**88**) using a primary amine 86

Scheme 3.26 Synthesis of the protected amino acid 87

Scheme 3.27 Displacement of the chiral auxiliary from the coupled galactal (**90b**) using protected ornithine (**37**) 87

Scheme 3.28 Displacement of the chiral auxiliary from various coupled galactals using protected ornithine 88

Scheme 3.29 Hydrogenolysis 89

Scheme 3.30 Attempted synthesis of the carboxylic acid galactal derivative 91

Scheme 3.31 Synthesis of galactal derivatives 92

Scheme 3.32 Successful synthesis of the building blocks for Series II analogues 93

Scheme 3.33 Complete synthesis of the building block for the Series II α-linked analogue containing a double bond in the carbohydrate moiety 94

Scheme 3.34 Complete synthesis of the building block for the Series II β-linked analogue containing a double bond in the carbohydrate moiety 94

Scheme 3.35 Solid-phase peptide synthesis of the Series II α-linked analogue containing a double bond in the carbohydrate moiety 95

Scheme 3.36 Solid-phase peptide synthesis of the Series II β-linked analogue containing a double bond in the carbohydrate moiety 96

Scheme 3.37 Synthesis of the building block for the Series II α-linked analogue containing a saturated carbohydrate moiety 97

Scheme 3.38 Synthesis of the building block for the Series II β-linked analogue containing a saturated carbohydrate moiety 98

Scheme 3.39 Complete deprotection of series II building blocks in preparation for antifreeze activity testing 99

Scheme 3.40 Summary: synthesis of both the building blocks for the Series II α-linked analogues (**117a** and **106a**) and the building blocks to be used for antifreeze activity testing (**121** and **123**) 100

Scheme 3.41 Summary: synthesis of both the building blocks for the Series II β-linked analogues (**115a** and **108a**) and the building blocks to be used for antifreeze activity testing (**122** and **124**) 101

Scheme 3.42 Synthesis of various protected C-linked carboxylic acid galactal derivatives 102

Scheme 3.43 Deprotection of various C-linked carboxylic acid galactal derivatives for antifreeze activity testing 103

Scheme 3.44 Synthesis of building block **134** for the ornithine analogue (**14**) 105

Scheme 3.45 Solid phase synthesis of the ornithine analogue (**14**) 106

List of Abbreviations

7AAD	7-actinomycin D
Ac	acetyl
Ac_2O	acetic anhydride
AcOH	acetic acid
AD	asymmetric dihydroxylation
AFGP(s)	antifreeze glycoprotein(s)
AFGP 8	antifreeze glycoprotein fraction 8
AFP(s)	antifreeze protein(s)
Ala	alanine
ANOVA	analysis of variance
Arg	arginine
Asn	asparagine
ATP	adenosine-5'-triphosphate
$BF3•OEt_2$	boron trifluoride diethyl etherate
Bn	benzyl
BnBr	benzyl bromide
BnOH	benzyl alcohol
Boc	*tert*-butyloxycarbonyl
br	broad
Bu	butyl
BuLi	butyl lithium
CCl_3CN	trichloroacetonitrile
$CDCl_3$	deuterated chloroform
CD_3OD	deuterated methanol
CFU	colony-forming assay
CIDOCD	cryopreservation-induced delayed-onset cell death
cm^{-1}	wavenumber
CPA(s)	cryoprotective agent(s)
CS_2	copper disulfide

$CuSO_4$	copper sulfate
d	doublet
DBU	diaza(1,3)bicyclo[5.4.0]undecane
dd	doublet of doublets
DCC	*N,N'-dicyclohexylcarbodiimide*
DCM	dichloromethane
DIBAL-H	diisobutylaluminum hydride
DIPEA	diisopropylethyl amine
DIS	dynamic ice shaping
DMAP	dimethylaminopyridine
DMEM	Dulbecco's Modified Eagle Medium
DMF	dimethyl formamide
DMSO	dimethyl sulfoxide
DNA	deoxyribonucleic acid
D_2O	deuterated water
dt	doublet of triplets
E^+	elecrophile
EDTA	ethylene diamine tetraacetic acid
EMEM	Eagle's minimum essential media
ESI	electrospray ionization
Et	ethyl
Et_3N	triethylamine
Et_2O	diethyl ether
EtOAc	ethyl acetate
EtOH	ethanol
FBS	fetal bovine serum
FCS	fetal calf serum
FITC	fluorochrome fluorescein isothiocyanate
Fmoc	9-fluorenylmethyloxycarbonyl
Gal	galactose
GalNAc	*N*-acetyl-galactosamine

Glc	glucose
GlcNAc	*N*-acetyl glucosamine
Gln	glutamine
Gly	glycine
GvHD	graft versus host disease
h	hour
HBTU	*O*-benzotriazole-*N*,*N*,*N*',*N*'-tetramethyl-uronium-hexafluoro-phosphate
HCl	hydrochloric acid
HCTU	2-(6-chloro-1H-benzotriazole-1-yl)-1,1,3,3-tetramethylaminium hexafluorophosphate
HBSS	Hank's balanced salt solution
HBr	hydrogen bromide
HDM	hormonally defined medium
HOBT	*N*-hydroxyl benzotriazole
HLA	human leukocyte antigen
HPLC	high performance liquid chromatography
HSC(s)	hematopoietic stem cell(s)
HTK	histidine-tryptophan-ketoglutarate
*i*Pr	isopropyl
*i*PrOH	isopropanol
K_2CO_3	potassium carbonate
KH_2PO_4	potassium dihydrogen phosphate
KOH	potassium hydroxide
kDa	kiloDaltons
LDA	lithium diisopropyl amide
$LiAlH_4$	lithium aluminum hydride
LiOH	lithium hydroxide
Leu	leucine
m	multiplet
M	molar

M^+	parent molecular ion
Man	mannose
Me	methyl
MeCN	acetonitrile (CH_3CN)
MeI	iodomethane (methyl iodide)
MeOH	methanol
MGS	mean grain size
MgSO4	magnesium sulfate
MIM	1-methylimidazole
MLGS	mean largest grain size
mM	millimolar
MNC(s)	mononuclear cell(s)
mOsmol	milliOsmolars
MS	mass spectrometry
MTT	3-(4,5-dimethyldiazol-2-yl)-2,5-diphenyl tetrazolium 6 bromide
$NaBH_4$	sodium borohydride
NAc	*N*-acetyl
$NaClO_2$	sodium chlorite
NaH	sodium hydride
$NaHCO_3$	sodium bicarbonate
NaOCl	sodium hypochlorite
NaOH	sodium hydroxide
NaOMe	sodium methoxide
NBS	*N*-bromosuccinamide
NH_4Cl	*tert*-butyl ammonium chloride
NH_4I	*tert*-butyl ammonium iodide
nm	nanometer
NMO	*N*-methylmorpholine
NMR	nuclear magnetic resonance
NSERC	national science and engineering research council
O_3	ozone

O/N	overnight
OMe	*O*-methyl
Orn	ornithine
OLT	orthotopic liver transplantation
OsO_4	osmium tetroxide
P	protecting group
PBS	phosphate-buffered saline
Pd/C	palladium on carbon
PE	phycoerythrin
Ph	phenyl
PhSH	thiophenol
PI	propidium iodidie
PPh_3	triphenylphosphine
*p*PhOMe	para-methoxy phenyl
*p*PhBr	para-bromo phenyl
p$PhNO_2$	para-nitro phenyl
Pro	proline
PS	phosphatidyl serine
psi	pound per square inch
q	quartet
RBC	red blood cells
ROS	reactive oxygen species
RT	room temperature
s	singlet
SEM	standard error of the mean
SM	starting material
S_N2	bimolecular nucleophilic substitution
$SnCl_4$	tin tetrachloride
SPPS	solid-phase peptide synthesis
SUV(s)	small unilamellar vesicle(s)
syAFGP	synthetic antifreeze glycoprotein

t	triplet
Tal	talose
TBAI	*tert*-butylammonium iodide
*t*BuOH	*tert*-butanol
TEMPO	2,2,6,6-tetramethyl-1-piperidinyloxy free radical
TFA	trifluoroacetic acid
TLC	thin layer chromatography
TH	thermal hysteresis
THF	tetrahydrofuran
Thr	threonine
$TiCl_4$	titanium tetrachloride
TPAP	tetrapropylammonium perruthenate
TS	transition state
UCB	umbilical cord blood
µM	micro molar
Val	valine

All sugars referred to in this thesis are D sugars.

Chapter 1: Introduction to Cryopreservation

Scientists have been interested in studying biological effects at low temperature for over a century. "Low temperature" preservation includes hypothermic storage and cryopreservation. Hypothermic preservation is defined as preservation in the absence of ice formation, while cryopreservation involves cryogenic temperatures and comprises freezing preservation and vitrification.[1] Hypothermic storage of cells is often desirable for the short term. Under hypothermic storage conditions, cell aerobic metabolic rates decrease, but do not stop, and the membrane and metabolic functions become decoupled; cells then become sensitive to hypoxic and hypothermic conditions and suffer metabolic damage.[2] Hypothermic storage is therefore not a viable solution for long-term storage. For the purposes of this thesis, freezing preservation is referred to as cryopreservation. Cryopreservation is equally often referred to as cryobiology, a term coined in 1946 by Alan Parkes in the first issue of the journal *Cryobiology*.[3]

Early work in cryobiology focused largely on the cryopreservation of spermatozoa, and the first of many milestones is credited to Polge *et al.* for the serendipitous discovery that fowl spermatozoa could survive freezing to low sub-zero temperatures when frozen in the presence of glycerol.[4] Since then, researchers have sought to understand what occurs during temperature excursions to low sub-zero temperatures and the implications for cell viability and function upon thawing. Work in the field of reproductive technology has expanded beyond spermatozoa, to include animal and human gamete, oocyte, and embryo cryopreservation. Many types of human cells, including stem cells, and tissues, have successfully undergone hypothermic storage or cryopreservation followed by positive clinical outcomes. Despite remarkable clinical success, cryopreservation remains uniquely challenging. The early biophysical studies are still debated today, and much work is carried out based on phenomenological data. A review of the debate is imperative for the understanding of the current state of the art.

The work presented in this thesis is focused on the design and synthesis of hydrophobic antifreeze glycoprotein analogues, and the cryopreservation of two different cell types, human hepatocytes and human hematopoietic stem cells, using mono- and disaccharides as cryoprotectants. This chapter will discuss: the cryopreservation process and the problems associated with it; cell damage during cryopreservation; typical cryopreservation conditions; cryoprotectants, including dimethyl sulfoxide (DMSO), sugars, and biological antifreezes; and finally, the cryopreservation of human hepatocytes and human umbilical cord blood.

1.1 Cryobiology

Cryopreservation involves the freezing of biological material to low sub-zero temperatures. Typical storage temperature is -196 °C and cells can survive storage at this temperature for centuries. In fact, temperatures below -130 °C effectively stop biological time.[5, 6] Rather, it is the transitions to-and-from very low temperatures that are dangerous to life. Both freezing and thawing present challenges to successful cryopreservation. The challenges of the freezing process are addressed first. Cell survival is poor if the cooling rate is too fast or too slow. While the ideal cooling rate differs between different cell types, plots of cell survival vs. cooling rate for different cell types all describe an "inverted U" (Figure 1).[5, 7] The causes of cell death are different at high and low cooling rates and can be categorized as fast-freezing injury and slow-freezing injury. In general, fast-freezing increases the probability of intracellular ice formation, and slow-freezing results in prolonged exposure to extracellular ice, the consequences of which are cell injury and death.[8] The optimal rate is found through experimentation or modeling,[9] and the exact mechanism by which injury occurs is still debated.

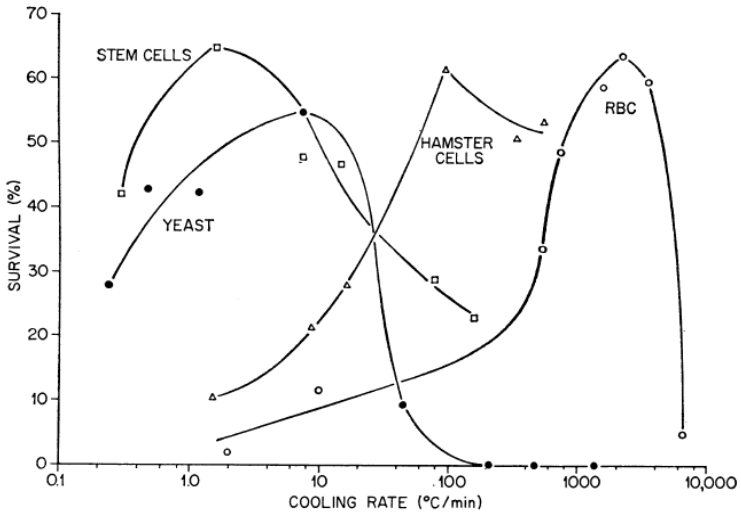

Figure 1.1 "Inverted U" Cooling Curves: comparative effects of cooling velocity on the survival of various cells cooled to -196 °C and thawed rapidly; the yeast and human red cells (RBC) were frozen in distilled water and blood, respectively. The marrow stem cells and hamster cells were suspended in balanced salt solutions containing 1.25 M glycerol.[10]

1.1.1 Fast-Freezing Injury

At supra-optimal cooling rates – fast-freezing – intracellular ice formation occurs. Cooling cells at any rate causes an increase in the concentration of solutes outside the cells, since ice excludes solutes as it forms. The thermodynamic freezing point of most cells is -0.5 °C, however cells remain unfrozen, coexisting with the extracellular ice, until the temperature drops an additional 5 °C to 40 °C. The plasma membrane inhibits ice nucleation, which leads to this supercooling.[5] Supercooling of the water surrounding cells creates a difference in vapour pressure or chemical potential difference across the cell membrane. This difference causes the cell to lose water to the extracellular environment and dehydrate. In order for the cell to stay in equilibrium with the external ice, the cooling rate must not be faster than the cell can lose water.[5] Cooling rates in fast-freezing are such that the cell is no longer in equilibrium, and therefore does not lose water before a temperature is reached that causes intracellular ice formation. However, different cells have different permeability to water, and this accounts for the different ideal cooling rates seen with different cells.[5] Below -30 °C, weak endogenous nucleators can cause ice formation. However, ice nucleation can

occur at temperatures *greater than* -30 °C, particularly in the presence of cryoprotective agents (CPAs). Three theories have been put forward to explain intracellular ice formation above -30 °C. First, the membrane-pore theory postulates that intracellular ice nucleation could result from external ice growth through angstrom-sized pores in the plasma membrane.[5, 11, 12] Even if external ice cannot initially grow through the channel, water leaving the cell as a result of the chemical potential across the membrane, would meet it in the channel and thus facilitate the growth of ice into the cell. Ice growth in the channel and ice recrystallization could cause the pore to enlarge, permitting the growth of ice into the cell interior.[11]The topic of ice recrystallization will be more fully explored in a later section. Secondly, the heterogeneous intracellular ice-nucleation model proposes that the cell membrane can act as an ice nucleator.[5, 13, 14] Extracellular ice can cause structural changes in the plasma membrane or in the water just inside the membrane and therefore indirectly lead to plasma membrane-catalyzed nucleation of the supercooled interior of the cell.[15, 16] Finally, the osmotic rupture hypothesis postulates that thermal fluctuations during cooling ruptures the plasma membrane, which can then cause loss of osmotic responsiveness, expansion-induced lysis, or allow the formation of intracellular ice.[17] Muldrew and McGann provided new evidence for the osmotic rupture hypothesis, and proposed a mechanism of membrane injury, based on the recrystallization of ice.[18, 19] The nature and exact mechanism of cell damage due to fast-freezing therefore remains unsolved.

1.1.2 Slow-Freezing Injury

On the other side of the "inverted U" of cooling rates lies slow-freezing. Although slow-freezing precludes the formation of intracellular ice,[20] sub-optimal cooling rates can cause as much damage as supra-optimal rates, and in fact, the fall-off from optimal is more dramatic. In 1953, Lovelock and co-workers proposed that slow-freezing injury could be due to an increase in electrolyte concentration inside or outside the cell. The term "solute effects" (also called solute toxicity) was coined by Mazur and, according to Pegg et al., "is understood to mean any deleterious effect brought about by changes in the concentration or composition of the solution in which the cells are suspended as freezing progresses."[21, 22]

When cooling is sub-optimal, the cell is unable to stay in equilibrium with the surrounding water and ice; under these conditions, the cells will dehydrate, which results in an increase in intracellular solutes.[23] As extracellular ice continues to form, it will remove water from the solution, causing solutes in the extracellular space to become concentrated. The uptake of solutes during freezing likely injures the cell due to osmotic stress experienced during thawing.[24] The solute effects hypothesis was strongly supported by results obtained by Santarius and Giersh,[25] Pegg and Diaper[26], and Mazur and Cole.[27] Detractors of Lovelock's "solute toxicity" theory, including Fahy and Karow,[24] point out that there is limited direct evidence to support his specific conclusions. They suggest that in their current studies, cryoprotectant toxicity (they used DMSO) may have played a greater role than solute concentration. Nevertheless, Lovelock's basic hypothesis still has widespread acceptance.

Another set of hypotheses put forward contend that cell death is caused by destabilization of the plasma membrane due to cell dehydration. This position is strongly supported by Steponkus and Lynch.[28] The authors argue that cell cooling and dehydration - an attempt to regulate the osmotic balance across the membrane - eventually causes an influx of solutes into the cell. Upon thawing, as the cell tries to attain equilibrium with the surrounding solution, the high intracellular concentration of solutes results in cell swelling. Cell swelling could cause the cell to lyse. Meryman presented a variation on this hypothesis, proposing that such extreme dehydration places mechanical stress on the cell that it cannot withstand.[29] However, much of the work supporting the membrane destabilization hypothesis was conducted with plant cells. Muldrew and co-workers suggested that, rather than membrane destabilization alone resulting in increased intracellular salt concentration, the increasing solute concentration due to dehydration could result in the solubilization of protein salt-bridges, which would increase the levels of intracellular sodium. The increased intracellular level of sodium could cause the cell to burst due to the influx of water during thawing.[30]

The previous hypotheses all agree that, "injury is assumed to be a consequence of the lowered chemical potential of water brought about by the increased solute concentration."[5] However, Mazur and co-workers postulate that solute toxicity is dependent on the size of the unfrozen fraction of water. The unfrozen fraction of water does not remain in the liquid state,

but usually vitrifies to some extent, becoming a glass-phase solid, or a partially crystallized glassy matrix, surrounding the cells.[7, 31] When the fraction of unfrozen water was between 25% and 10% of the initial water content of the cell, Mazur's results corroborated Lovelock's solute toxicity hypothesis (that blood cell survival depends strongly on electrolyte concentration). When the fraction of unfrozen water was greater than 25%, even high salt concentrations did not hinder cell survival. However, as the fraction of unfrozen water decreased below 10%, cell survival dropped dramatically.[5, 27, 32] Mazur theorized that the compression of cells into the small channels between ice crystals caused deformation of the cell membrane and injury to the cells from adverse cell-ice and cell-cell interactions. Pegg *et al*. supported this hypothesis with their studies on the dense packing of cells during freezing,[22] although they later provided alternate explanations for all points in Mazur's hypothesis. [33, 34] Despite the vast volume of research on slow-freezing injury, none of the hypotheses proposed to date are supported by conclusive evidence that delineates one mechanism of action from another.

1.1.3 Effects of Slow and Fast Warming and Thawing Rates

The difficulty with cryopreservation is not with the ability of cells to survive at very low temperatures, but rather, it is the intermediate sub-zero temperatures that are lethal.[5] Cells pass through high sub-zero temperatures during both freezing and cooling. As discussed, during fast-freezing (the right side of the "inverted U") intracellular ice is formed as the cells pass through this potentially lethal zone, while slow-freezing (the left side of the "inverted U") leads to extreme dehydration without intracellular ice formation. However, Rall and co-workers proposed that even with freezing protocols that prevent intracellular ice formation, warming may still cause freezing inside the cell.[35] There is substantial evidence that shows that cells frozen using fast-freezing protocols benefit from rapid warming as compared to slow warming.[36] Muldrew and McGann report that, "[this] effect is usually ascribed to the lack of time for recrystallization of intracellular ice."[19] The situation is more confused for cells cooled with slow-freezing protocols: "the warming rate can have no effect on cell viability, slow warming can be more damaging to cells than rapid warming or, rapid warming can be more damaging than slow warming".[36] Most commonly however, slow

warming is more damaging to cells than rapid warming. There are myriad explanations for the deleterious effects of slow warming, and Mazur suggests that they are likely similar to the damage inflicted by slow cooling.[5] The explanations put forward for the damage inflicted by rapid warming also include the occurrence of osmotic shock due to the membrane becoming temporarily leaky during thawing, allowing normally impermeable solutes to enter.[33] Impermeable solute uptake then results in osmotic swelling, due to a concomitant increase in the uptake of water and permeable solutes. Cells may be injured as a result of devitrification of any glassy-state solid that was formed during cooling.[37, 38]

1.2 Effects of Cryopreservation on Cells

1.2.1 Ice Recrystallization

A key event that almost certainly occurs during warming is the recrystallization of intra- or extracellular ice formed during cooling (or from devitrification). Recrystallization is the process by which larger ice crystals increase in size at the expense of smaller ice crystals. Smaller ice crystals have negative surface curvature while larger ice crystals have a positive curvature; larger ice crystals therefore have lower energy. If subjected to the right temperature and given enough time, grain boundaries migrate from larger ice crystals to swallow up the smaller ice crystals. This process is driven by the reduction in overall grain boundary, the accompanying reduction in the free energy of the system, and a reduction in the internal energy of the ice crystal.[39-41] Recrystallization has been visually observed during the thawing of fast-frozen cells and experimentally correlated to cell death.[5, 42] In fact, slow warming is thought to be harmful because it allows recrystallization to occur.[5, 43] Recrystallization is thought to be damaging to cells since large ice crystals are thought to be more harmful to the cell than small ones. This could be due to their larger size or from the forces generated from their growth process.[5, 36] Recrystallization can cause different amounts of harm depending on where it occurs in relation to the cell.

As detailed earlier, Mazur believes that the presence of membrane pores large enough to admit ice will result in lethal intracellular ice formation.[5] As previously discussed, ice growth can continue through the pore as intracellular water is driven out of the cell by the chemical potential across the membrane. As the cell is warmed during thawing, ice in the pore may undergo recrystallizaiton; this process is thought to enlarge the membrane pore, causing damage to the plasma membrane.[11, 19, 44, 45] The mechanism by which recrystallization damages cells remains unclear. Indirect evidence in support of the theory that recrystallization plays a major role in cellular injury can be found in nature: there are many naturally freeze-tolerant organisms that generate recrystallization inhibitors in response to freezing stress.[31] These "biological antifreezes" - the antifreeze proteins and the antifreeze glycoproteins – are integral to this work and will be revisited and discussed in detail.

1.2.2 Innocuous Intracellular Ice

The critical point regarding the formation of intracellular ice and its recrystallization, is that although intracellular ice formation is generally thought to be lethal to cells, it may in fact be innocuous. Intracellular ice forms during fast freezing of cells, but it can also form as the result of the devitrification of a glassy state formed during slow cooling. Although the precise mechanism by which cells are damaged is not yet known, both mechanical and non-mechanical causes of cell death have been proposed. Mechanical forces due to intracellular ice could damage the plasma membrane or intracellular components. Non-mechanical causes of cell damage include solution effects and thermal shock, osmotic injury, protein denaturation, and gas bubble formation.[46] There is a general consensus however, that *if* the damage that leads to cell death occurs during warming, then the mechanism is mechanical, and is a result of the increase in size of intracellular ice crystals due to recrystallization. However, Fowler and Toner proposed that even substantial amounts of intracellular ice may be innocuous *if* crystal growth and recrystallization can be avoided during warming.[47] Muldrew *et al*. point to the studies that show that the amount of ice formed, the size of the ice crystals, the location of the ice formed, or the mechanism of formation can also be implicated in cell damage.[36] Fowler and Toner wonder in their review of cryopreservation

whether, "a possible future for cryopreservation research may lie in the development of cryopreservation protocols that manage intracellular ice so that it is non-lethal, rather than attempt its prevention".[31] Effective ice recrystallization may therefore be a key step towards successful cryopreservation. This idea forms one part of our cryopreservation strategy. The second part of our strategy is the inhibition of apoptosis.

1.2.3 Biochemical Mechanisms of Cell Death

Many forms of cell death have been identified, and these fall generally into two categories: non-programmed (accidental) cell death called necrosis, and programmed cell death. Programmed cell death comprises at least apoptosis, autophagy, oncosis, and pyroptosis pathways.[48,49] Cell death associated with the cryopreservation process has been attributed to physical rupture of the plasma membrane and intracellular components caused by intracellular ice formation, alterations in cellular ion homeostasis, the occurrence of a mitochondrial permeability transition, as well as necrosis and apoptosis.[50-52] There is emerging consensus that that the stress of cryopreservation induces cell death by apoptosis.[53-57]

1.2.3.1 Necrosis

Necrosis is the passive result of cell injury; it can be caused by severe cellular stresses. Necrosis is generally thought to be an energy-independent (ATP-independent) event and characterized by cellular swelling, compromise of membrane integrity, mitochondrial dysfunction, random DNA fragmentation by cellular endonucleases, and massive oxidative stress. Necrosis causes cell lysis and activates an immune response.[49, 50, 58] Figure 2 shows the morphological changes associated with necrosis and apoptosis.

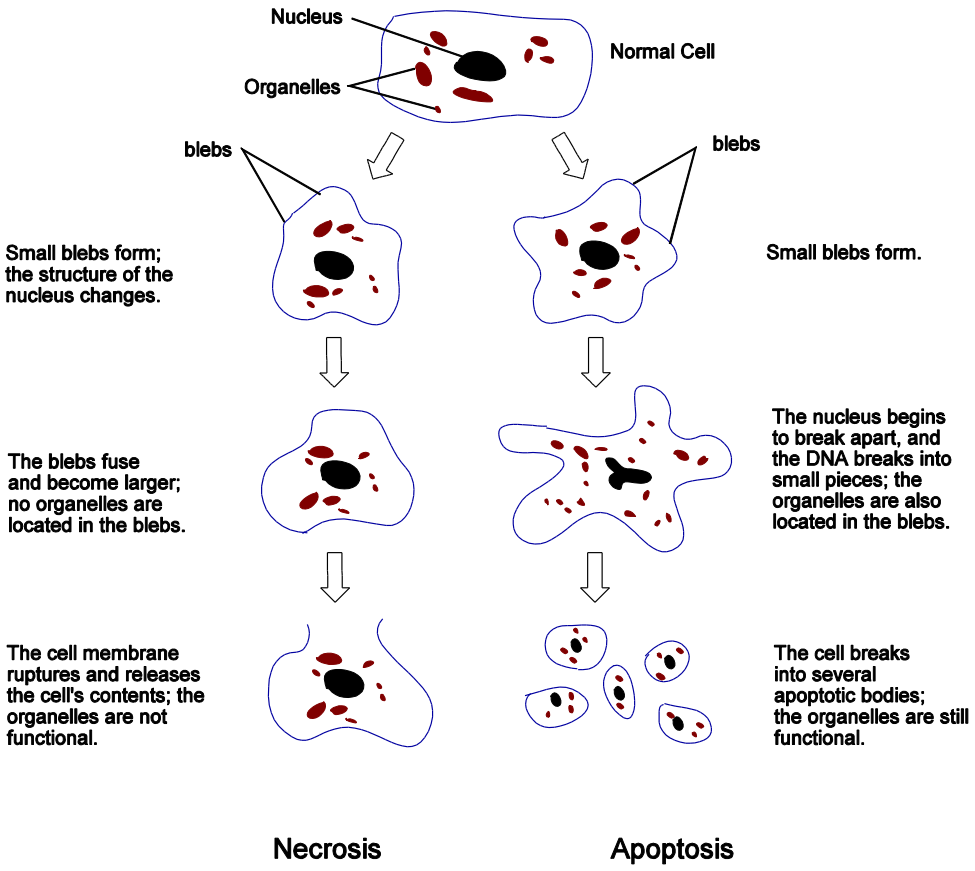

Figure 1.2 Necrosis vs. Apoptosis[59]

1.2.3.2 Apoptosis

Apoptosis is a programmed form of cell death, conserved and uniform in nature. It is an energy-dependant and carefully controlled process, and constitutes an important part of physiological homeostasis. Apoptosis is biochemically, morphologically, and molecularly distinct from necrosis. Morphological changes unique to apoptosis include cell shrinkage, chromatin condensation and fragmentation, compartmentalization of intracellular components, maintenance of an intact cell membrane, cytoplasmic blebbing, and cellular fragmentation into apoptotic bodies; it does not illicit an immune response.[49, 50, 58] Apoptosis can be initiated by both exogenous and endogenous factors, including ultraviolet radiation, toxic stress, growth factor deprivation, nutrient stress, temperature extremes, ischemia, and changes in apoptotic-related gene production. Apoptosis is frequently defined as a pathway

that involves the sequential activation of caspases.[49] Caspases are members of a cysteine protease family; they are thought to be the key players in the disassembly of the cell – the morphological process of apoptosis.[58] Caspaces normally exist as proenzymes (procaspaces) that are converted to their fully active forms by proteolysis. They are ordered into a cascade, in which activated caspases can activate other enzymes, including other procaspases. They are generally grouped into the initiator caspases (caspases 2, 8, 9, 10), and the effector caspases (caspases 3, 6, 7). The former act upstream of the so-called point-of-no-return, while the latter are activated once the cell is committed to the apoptotic pathway.

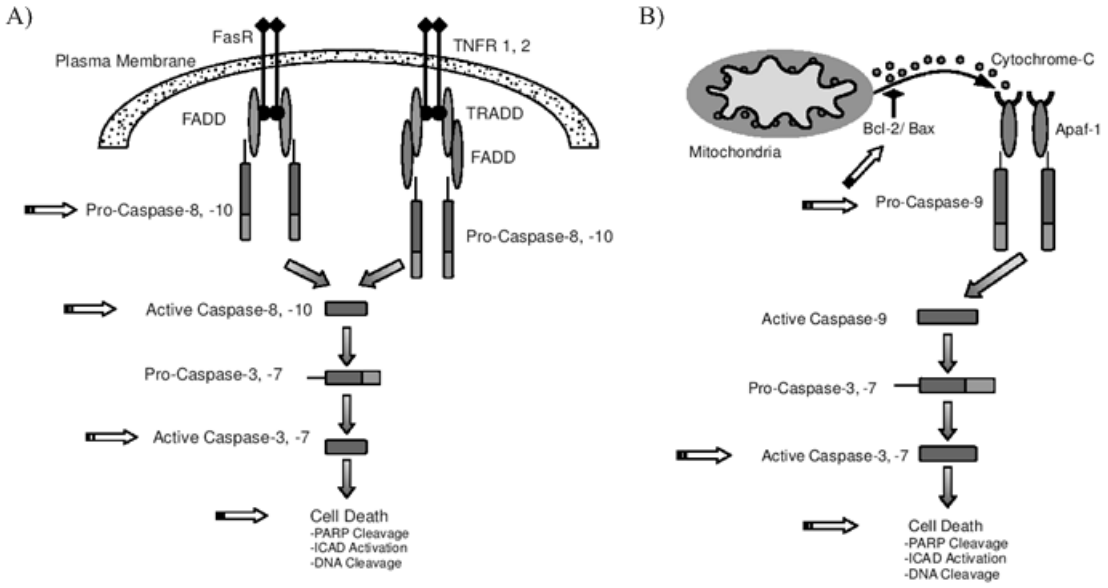

Figure 1.3 Cryopreservation-Induced Apoptosis: A) membrane-mediated apoptosis: schematic diagram of the Fas and TNF surface receptor-mediated apoptotic pathways; open arrows (⇨) indicated stages in the apoptotic cascade that have been implicated in cell death following cryopreservation; B) Mitochondrial-induced apoptosis: schematic diagram of apoptotic progression following induction through mitochondrial alterations; open arrows (⇨) indicate stages in the apoptotic cascade that have been implicated in cell death following cryopreservation[50]

Apoptosis can be initiated by both exogenous and endogenous events, each triggering apoptosis via an apoptosis pathway (Figure 1.3). Three "families" of pathways have been described: receptor-mediated (membrane-mediated), mitochondrial mediated, and nuclear mediated.[49, 50] In his review, Baust presents the sequential caspase activation resulting from

membrane-mediated versus mitochondrial-mediated apoptosis, and indicates the stages in the cascade that have been implicated in cryopreservation-induced cell death.[50]

Caspase inhibitors has been shown to improve cryopreservation outcome.[57, 60, 61] Despite this experimental evidence, the role of caspases in apoptosis and cell death associated with cryopreservation - and therefore the role of caspase inhibitors - is unclear. Recently, it has been shown that upon caspase inhibition, alternative programs of cell death are executed and these may have features characteristic of necrosis.[62, 63]

1.2.4 Effects of Cryopreservation on Cells: Summary

Mazur's two-factor hypothesis for optimal cooling rate was developed in 1965, yet is still the principle behind successful cryopreservation. Optimal freezing protocols must cool the cells quickly enough so that some water is retained inside the cell in order to avoid slow-freezing damage. Yet, cooling must be slow enough so that cells can dehydrate in order to stay in osmotic equilibrium with the extracellular solution. In a sufficiently dehydrated cell the remaining water will vitrify before the cell reaches its homogeneous nucleation temperature.[31, 41] While the mechanisms of cell injury and death are still debated, cryopreservation protocols can be developed through phenomenological work. In attempts to speed up the slow process of experimental work, some groups have developed 'optimal' freezing programs using theoretical models.[64, 65] The optimal cryopreservation condition for a given cell type requires a protocol that, at a minimum, uses the appropriate cooling rate but also the optimal type and concentration of cryoprotectants.[1] Cryoprotective agents, including DMSO, biological antifreezes, and sugars, will be discussed in detail.

1.3 Cryopreservation Agents

Cryoprotective agents (CPAs) have played a key role in cryopreservation since the accidental 1949 discovery by Polge *et al*[4] and the 1953 discovery by Lovelock[66, 67] of the cryoprotective effects of glycerol and DMSO respectively. CPAs can be divided into two broad categories: permeating and non-permeating cryoprotectants. Permeating (or penetrating) cryoprotectants can enter the cell passively through the plasma membrane. They are small, non-ionic molecules that have a high solubility in water at low temperatures. They ideally have a low cellular toxicity. Non-permeating (or non-penetrating) cryoprotectants cannot penetrate the plasma membrane and therefore remain outside of the cell unless they are artificially introduced. Non-permeating cryoprotectants are generally long-chain water-soluble polymers with large osmotic coefficients.[36] The protective capacity of CPAs during slow-freezing is ascribed to two main mechanisms: they may have a colligative mechanism of action, or they may interact specifically with the plasma membrane.

1.3.1 Colligative Mechanism of Action of Cryoprotective Agents

The addition of cryoprotectants to a solution will lower the freezing temperature of the extracellular water. More importantly, both permeating and non-permeating cryoprotectants have a significant effect on the cell nucleation temperature - the temperature at which intracellular ice nucleation occurs - in the presence of extracellular ice. Nucleation temperatures are usually between -10 °C and -15 °C but can range from -5 °C to below -30°C.[5] While this range can be attributed to the difference in cell type,[5] cryoprotectants generally lower the ice nucleation temperature and increase the vitrification temperature.[41] As a result, the cytoplasm doesn't supercool to the same extent so the chances of forming intracellular ice are decreased. Further, permeating cryoprotectants act colligatively to minimize solution effects injury by decreasing the concentration of salts normally found in physiological solutions at a given sub-zero temperature in the presence of ice. They do this by lowering the amount of ice present at a given temperature and by acting as a secondary solvent for salt.[68, 69] Non-permeating cryoprotectants cannot protect against solution effects

since they cannot penetrate to the cell interior. This colligative action of CPAs would increase cell survival after cryopreservation according to both Lovelock's solute effects hypothesis (if permeating cryoprotectants are used), as well as Mazur's unfrozen fraction hypothesis (since lowering the amount of ice present means an increase in the unfrozen fraction). Finally, permeating CPAs increase the volume of the cell (compared to cells without CPAs) when the cell has dehydrated due to freezing. In other words, permeating CPAs can, "reduce excessive cellular shrinking",[31] a phenomenon that has been linked to cell death during slow-freezing.[29, 30] Permeating cryoprotectants have been used extensively for the protection of cells during slow-freezing. However, they have not proven to be effective protectors during fast-freezing (although they are extensively used in vitrification). Finally, non-permeating cryoprotectants are thought to act by dehydrating the cell before freezing. Therefore, once freezing begins they decrease the amount of water that the cell needs to lose to maintain osmotic equilibrium during freezing. Non-permeating cryoprotectants, however, are largely ineffective during slow-freezing and their primary use is with fast-freezing protocols, although they have been used to enhance the effect of permeating cryopreservatives[70, 71]

The second mode of action, the interaction of the cryoprotectant with the plasma membrane, will be discussed in the context of biological antifreezes. Other concerns regarding cryoprotectants are that the addition and removal of cryoprotectants can cause damage to cells due to excessive osmotic forces.[46] Various strategies including step-wise dilution and sucrose dilution have been developed to help overcome this challenge. However, the benefits of slow addition and removal must be balanced with the direct toxic effects that can result from exposure of cells to CPAs under non-frozen conditions.[72] The amount of DMSO or other permeating cryoprotectant required to prevent solute toxicity during slow cooling is in itself damaging or lethal to cells.[31] DMSO has been extensively studied in this regard.

1.3.2 DMSO and DMSO Toxicity

According to Meryman, there are two criteria for permeating reagents. They must easily and rapidly cross the cell membrane, and even at high concentrations they must not be toxic to the cells.[73] Despite the many advances in cryopreservation, no CPAs have been found that fit these ideal criteria. The most commonly used cryoprotectants are glycerol and DMSO; DMSO is the most commonly used cryopreservation agent for hepatocytes, and hematopoietic stem cells (these cells are of primary interest to the research presented here).[73-75] Glycerol is non-toxic, but many cells are impermeable to it or allow it to permeate only slowly. This can create major osmotic problems. The major benefit of glycerol is that it can stabilize macromolecules within the cell.[29, 73, 76] DMSO, on the other hand, permeates cells relatively quickly. However, especially at reduced temperature, it does not do so instantly. Further, DMSO destabilizes macromolecules, and is toxic to cells. However, the relative toxicity of DMSO in the clinical setting has been difficult to ascertain. In the case of hepatocyte transplantation, the cells are washed in order to remove all traces of DMSO.[77] This is not necessarily the case for umbilical cord blood. In the transplantation of hematopoietic stem cells from umbilical cord blood, DMSO has been implicated in a number of dose-dependent adverse effects including gastro-intestinal, cardiovascular, and neurotoxicity effects.[78-82] DMSO toxicity has been called "idiosyncratic", and it "may thus be unpredictable and unavoidable",[81, 83] and despite the findings of some researchers that DMSO is relatively safe and well-tolerated, the same researchers suggest that decreasing the amount of DMSO infused along with umbilical cord blood merits further investigation.[79, 82, 84, 85]

Given the preceding discussion of cryoprotectants, it seems clear that efforts to improve the current cryoprotective strategies are warranted. While DMSO is a commonly used CPA, its disadvantages have also been outlined. A different type of CPA, the biological antifreezes, may present a unique solution in the search for the ideal cryoprotectant. Biological antifreezes will be discussed in detail.

1.4 Biological Antifreezes

The biological 'antifreezes' are a structurally diverse class of proteins that have the ability to interact with ice crystals in supercooled water and prevent their growth.[86, 87] The first biological antifreezes were isolated from Antarctic fish, and described by DeVries and Wohlshlag,[88, 89] DeVries *et al.,*[89] Komatsu *et al.*[90] , and DeVries *et al*.[91] These antifreeze glycoproteins (AFGPs) allow fish to survive in the cold waters at the poles where the water temperature can be as low as -1.9 °C, far below the freezing temperature of the blood serum of most fish. It was found that the presence of colligatively acting salts could only account for about 70% of the freezing point depression seen in the blood serum of arctic and Antarctic fish, and the remaining 30% was attributed to the unusual presence of AFGPs. The AFGPs were found to depress the freezing point of the blood serum to a greater extent than would be expected if they were acting colligatively. Since the discovery of AFGPs, four classes of non-glycosylated antifreeze proteins (AFPs) have been described. AFGP's are synthesized in the pancreas, and are circulated via the bloodstream.[92] Some fish additionally express AFPs in the gill and skin epithelia where they protect cells and tissues that come into direct contact with external ice.[93] Much work has been done on the structure and function of the AF(G)Ps and all five classes of have been reviewed extensively.[39, 87, 93-96]

1.4.1 Antifreeze Proteins (AFPs)

Four distinct classes of AFPs from the blood serum of arctic and Antarctic fish have been isolated and described, and the basic characteristics are outlined in Table 1. While AFGPs are only found in fish, AFPs have been isolated from different species of bacteria, plants, insects, and vertebrates, including frogs. [93] Unlike the AFGPs, the four classes of AFPs have little in common structurally. Type 1 AFPs are comprised of a family of seven independently active compounds. They are alanine rich (~65 mol%), and range in molecular weight from 3.3 kDa to 4.5 kDa. They take on an amphiphilic α-helical structure.[39, 97] Type II AFPs generally have a mass of 14-16 kDa. These AFPs are cysteine rich (8-9 mol%), and consequently form disulfide bridges. Other major components include alanine (Ala) (up to

14.4 mol%), asparagines (Asn), glycine (Gly), and threonine (Thr). [39, 98] Type II AFPs tend to form β-sheets.[99] Type III AFPs differ from the previous two classes in that they do not have a dominant amino acid. They range in molecular weigth from 5 kDa to 6.7 kDa. [99, 100] Type IV is found along with AFP Type I in the longhorn sculpin, although the two AFPs are unrelated. [101] While Type IV also has a high level of α-helical content, at 12.3 kDa, it has a much greater molecular mass. Like AFP Type III, it does not contain any cysteine residues. Unique among the AFPs, it may contain an N-terminal pyroglutamyl group.

Table 1.1 Key structural features and natural sources of AFPs and AFGPs[94]

Characteristic	AFGP	Type I AFP	Type II AFP	Type III AFP	Type IV AFP
Mass (Da)	2600 – 33000	3300 – 4500	11000 – 24000	6500	12000
Key Properties	AAT repeat; disaccharide	Alanine-rich α-helix	Disulfide bonded	β-sandwich	Alanine rich; helical bundle
Representative Structure	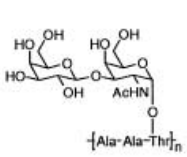				
Natural Source	Antarctic notothenioids; northern cods	Right-eyed flounders; sculpins	Sea raven; smelt; herring	Ocean pout; wolfish; eel pout	Longhorn sculpin

1.4.2 Antifreeze Glycoproteins (AFGPs)

Structurally, AFPs and AFGPs are very different. The AFGPs, isolated from fish blood plasma (in which they are the major protein fraction[94]), are polymers of the repeating tripeptide unit Ala-Ala-Thr, with only minor sequence variation. The disaccharide moiety galactosyl-*N*-acetylgalactosamine (β-D-galatcosyl(1-3)-α-*N*- acetyl-D-galactosamine) is glycosidically linked to the hydroxyl of each Thr residue.

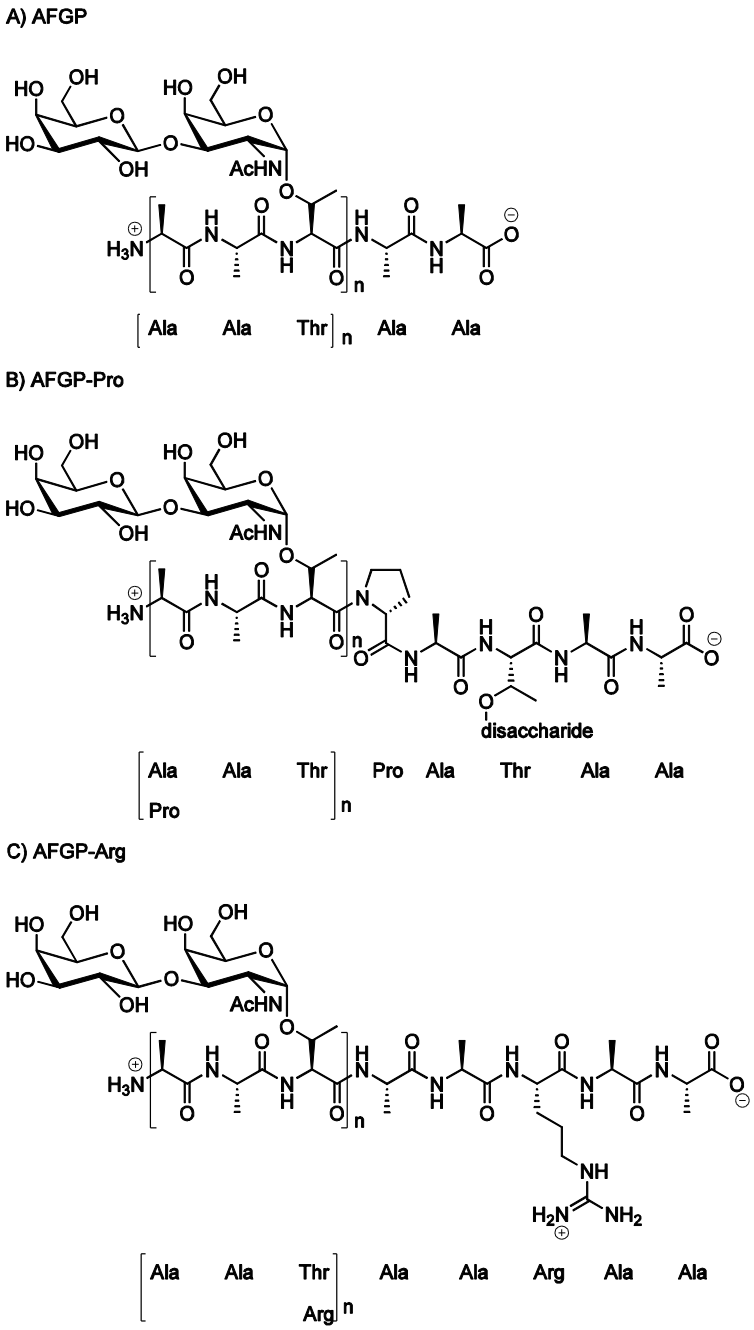

Figure 1.4 General structures of antifreeze glycoproteins and abbreviations: (A) AFGP the most common structural motif with n = 4-50; (B) AFGP-Pro in which Pro replaces Ala; (C) AFGP-Arg in which Arg replaces Thr, with the loss of a disaccharide group, frequently at the *C*-terminus of the sequences; AFGP-Pro and AFGP-Arg constitue < 5% of the naturally occurring glycoproteins[94]

The AFGPs can be divided into 8 categories (AFGP 1-8) based on their relative rates of electrophoresis migration. They range in molecular weight from 2.6 kDa to 33.7 kDa.[102, 103] The abbreviation AFGP x (x = 1-8) refers to a mixture of glycopeptides in an approximate mass range.[94] In AFGP 7 and 8, proline (Pro) occasionally replaces some of the Ala residues in the sequence,[104] and arginine (Arg) occasionally replaces Thr.[105, 106] A novel AFGP comprised of the carbohydrate residue N-acetylglucosamine and the amino acids Asn, glutamine (Gln), Gly, Ala, and traces of Arg, valine (Val), leucine (Leu) and Thr has also been reported.[107]

1.5 Antifreeze Activity

There are two main properties that are used to define AF(G)Ps: thermal hysteresis (TH) and recrystallization inhibition (RI). These will be explored as they relate to the AF(G)Ps, and cryopreservation.

1.5.1 Thermal Hysteresis (TH) of Biological Antifreezes

When AF(G)Ps are present in a solution, the freezing temperature is lowered, while the melting point is unaffected. This non-colligative phenomenon is known as TH,[39] and the difference between the melting and freezing points is termed the thermal hysteresis gap.[102] The observed freezing point lowering is greater than would be expected from that of a molar equivalent of colligatively-acting salts.[39] Ice neither freezes nor melts perceptibly so long as the temperature remains in the TH gap.[102] Using single ice crystals suspended in solutions of AFGPs at temperatures in the TH gap, Raymond *et al.* observed that the most active fraction of AFGPs (AFGP 1-5), prevented all growth on the prism faces, and allowed only limited growth on the basal plane (along the c-axis of the ice crystal) (refer to Figure 1.5). The appearance of hexagonal pits on the basal plane accompanied this slow growth. Crystal growth halted when the basal plane was completely covered in these pits. The smaller AFGP

fractions (AFGP 7-8) allowed greater growth of the ice crystal along the c-axis, as well as some growth of the prism faces.[108] It has been repeatedly confirmed that AFGP 1-5 show greater TH activity than the smaller AFGPs (AFGP 6-8).[103, 109] Raymond *et al.* also observed that the ice crystals in the presence of any AFGP fraction formed a hexagonal bipyramidal structure. This feature of AF(G)Ps is known as dynamic ice shaping (DIS) and always precedes TH.[110] Subsequently, using a variety of techniques, other researchers determined that different AF(G)Ps bind to different planes on the ice crystal.[103, 109, 111-113]

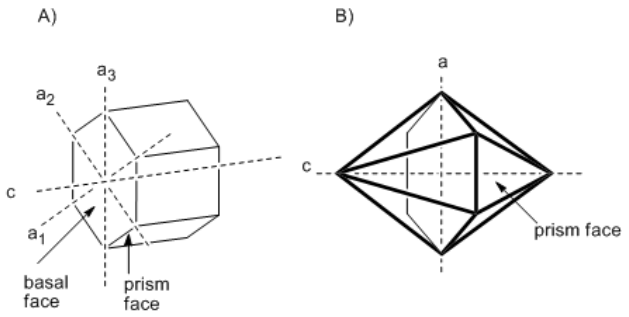

Figure 1.5 Interaction between antifreeze proteins and ice: A) in a dilute solution of AFPs (nM), the AFPs absorb onto the prism faces of the ice crystal and limit growth along the a_1-, a_2-, and a_3-axes, forming a crystal that is hexagonal in shape; B) in solutions containing higher concentrations of AFPs (μM), the preferred direction of ice crystal growth is along the *c*-axis, so that the crystal forms a hexagonal bipyramid[114]

However, once the temperature of the solution falls below the TH gap, the crystal growth habits change dramatically, growing along the c-axis in long spicules. This is unlike crystal growth in pure water, which forms dendrites within the basal plane, and growth is preferentially along the a-axis. In the presence of AFGP, as the degree of supercooling increases, normal dendritic growth resumes.[115] Since fish live in temperatures that stay within the TH gap, AF(G)Ps effectively protect them.[86] From the point of view of the field of cryopreservation however, the DIS in and below the TH gap is an undesirable aspect of AF(G)Ps. Ishigurao and Rubinsky[116] and Carpenter and Hansen[43] observed that increased hemolysis was seen when cells were frozen in the presence of antifreeze proteins (AFPs), and attributed it to the needle-like ice spicules formed from the interaction of AFPs with ice.

They therefore suggest that the shape of the extracellular ice crystals have a strong influence on the survival of cells subjected to slow-freezing.

1.5.2 Recrystallization Inhibition (RI) of Biological Antifreezes

As described earlier in the description of cryopreservation and the problems associated with it, ice recrystallization presents a major problem for the successful cryopreservation of cells. Native AF(G)Ps possess a RI capacity that functions as a compliment to TH. Recrystallization is the spontaneous tendency of all crystalline solids to increase in grain size, while decreasing the number of grains[117] This means that large ice crystals will grow larger at the expense of smaller ones, causing damage to the cell. In 1986 Knight and co-workers reported that concentrations of AFGPs as low as 10^{-12} can prevent ice recrystallization that occurs at temperatures near the melting point.[102] Knight and Duman found that AFPs in insects also showed RI, and speculated that RI may be their major protective role in these organisms.[118] While TH and RI were previously supposed to be correlated, in their work with an antifreeze protein from the ryegrass *Lolium perenne*, Knight *et al.* discovered that there was no correlation between the TH and RI activity.[119] Based on work on synthetic AFGPs in our lab, it is clear that the two activities can indeed be uncoupled.[120] There is much talk in the literature of the potential of recrystallization inhibitors as key compounds for cryopreservation.[119] For example, Acker and McGann[121] speculate that, "improved long-term storage of cells and tissues will result by incorporating innocuous intracellular ice formation into current strategies for cryopreservation." The discovery that TH, and its damaging consequences at temperatures below the TH gap, can be uncoupled from RI should prove to be an important step towards the use of synthetic AFGPs in cryopreservation applications.

1.5.3 AF(G)Ps and Ice-Binding

AF(G)Ps are the only compounds known to bind to ice. Normally, solutes are excluded from the growing ice front and are not incorporated into the ice lattice. The mechanism by which AF(G)Ps are able to inhibit ice growth are still under debate. It is generally described as an adsorption-inhibition process.[122] A number of models have emerged in the literature; predominant among them are the step-pinning model proposed by Raymond *et al*.,[122] and the mattress model, proposed by Knight and Devries[123] (Figure 6). Hall and Lips proposed a third model that will not be discussed.[124] The models are based on irreversible binding of the AF(G)P to the ice surface. Fletcher *et al.* argue that ice-AF(G)P interactions probably have an extensive contact site involving multiple interactions. These would have to be broken simultaneously for the connection to break. They argue that the probability of this happening is zero, and the binding is, for all purposes, irreversible.[93] It is generally accepted that ice growth inhibition involves a Kelvin effect.[124, 125] The two models of growth inhibition are very similar except for their geometrical assumptions. Both models require curvature of the ice-water interface, lowering the local freezing temperature. In the step-growth model, AF(G)P molecules adsorb to the growing crystal in such a way as to inhibit growth across the ice surface. In the mattress pinning model, the AF(G)Ps inhibit growth normal to the surface.[111, 122, 124, 126] A reversible binding model and a compromise between the irreversible and reversible binding models have also been proposed.[39]

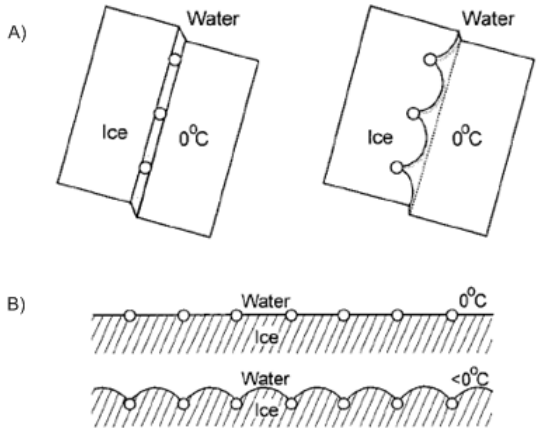

Figure 1.6 Proposed mechanisms of growth inhibition based on the Kelvin effect: (A) step pinning model; (B) mattress model[124]

1.5.4 Membrane Protection

As discussed in the context of the general modes of action, cryopreservatives may stabilize the cell membrane. Cryopreservatives, including the biological antifreezes, may play a role in stabilization of the plasma membrane through solute-specific interaction with phospholipid bilayers.[36] Crowe and co-workers proposed that the permeating cryoprotectant dimethyl sulfoxide (DMSO) helps to stabilize the phospholipid membrane through an electrostatic interaction of the sulfoxide group with the polar head groups of the phospholipids.[127] More recently, molecular dynamics simulations have revealed that DMSO may induce water pores in lipid bilayers, and cause the membrane to become "floppier". This would cause membranes to become more permeable to both water and other cryopreservation agents, facilitate membrane fusion, and enable the cell membrane to better accommodate osmotic and mechanical stresses during cryopreservation.[128, 129] Wu *et al.* agree that AFGPs likely inhibit membrane leakage as the cell passes through the phase transition temperature.[130] The cryoprotection afforded by the disaccharides trehalose, and sucrose, has also been attributed to their ability to stabilize the cell membrane.[131] As will be discussed, biological antifreezes have also been shown to stabilize cell membranes.

While AFGPs are thought to act by inhibiting recrystallization, it has been proposed that RI is not the protective mechanism, but rather, that stabilization of the cell membrane results in increased viability after cryopreservation.[132] In one study, less than 1 mg/mL AFGP fractions 2-6+ and 10 mg/mL AFGP fraction 8 prevented 100% of the leakage from liposomes (phospholipid vesicles served as the model membrane) that normally occurs when going through the phase transition.[133] AFGPs were equally effective during chilling and warming. However, since AFPs did not prevent leakage at any concentration, the authors suggested that these experiments provided no evidence to support the hypothesis that a direct interaction with the bilayer is responsible for the properties of AFGPs. Still, it has also been demonstrated that the efficacy with which AFGP can protect liposome membranes from cold depends on the composition of the cell membrane.[134] Support for the interaction of AFP Type I and AFGPs with membranes emerged from work on spinach thylakoid membranes and liposomes. However, the association of AFP Type I induced concentration-dependant leakage from the liposomes, and caused membrane fusion. This was not the case for AFGP

8, which, at concentrations of up to 10 mg/mL was able to protect membranes to some extent.[135]

It has been proposed that AFP I can block ion channels. [136] A more general interaction between AF(G)Ps and cell membranes has also been proposed based on the protection afforded to pig oocytes in hypothermic storage, and cryopreservation by a physiological combination of AFGPs. [137] [138] Interestingly, this effect was not seen when AFGPs were used separately. [137] This type of interaction with the phospholipid membrane is different than that proposed for DMSO, where the sulfoxide moiety interacts with the polar head groups of the phospholipids (as discussed previously).

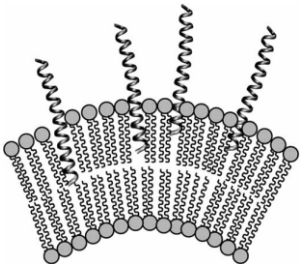

Figure 1.7 Proposed mechanism of action of type I AFP: schematic of proposed mechanism for inhibition of leakage from membrane by type I AFP (TTTT) by insertion of the *N*-terminal region of the AFGP into the membrane[139]

1.6 AF(G)Ps and Cryopreservation

AF(G)Ps have been studied as adjuvants for hypothermic storage as well as for cryopreservation. The results of these studies are complex; in some cases AF(G)Ps were able to enhance the survival of cells stored at sub-zero temperatures, while in others their addition was detrimental. The following studies all involve cryopreservation, rather than hypothermic storage. A hybrid protein containing AFP Type I showed RI activity, and increased the survival of cryopreserved yeast by two-fold compared to cells without the chimeric protein. The protocol included fast freezing, and a moderate rate of warming. The authors cite their result as evidence that ice recrystallization is one mechanism of cell damage during

cryopreservation.[140] The viability of red blood cells was increased compared to controls, using relatively low concentrations (5-160 μg/mL) of Type I AFP in the cryopreservation solution. In these studies, warming was carried out at a suboptimal rate in order to exacerbate the effects of ice recrystallization. However, a 1.54 mg/mL solution of Type I AFP led to preferential growth of ice around the cells during warming, resulting in additional damage. The authors suggested that recrystallization inhibition and preferential ice growth around the cells are in delicate balance.[43] At a concentration of 10 μg/mL, both AFGP and AFP Type I, increased the motility of ram spermatozoa after cryopreservation, compared to the motility seen at 0.1 μg/mL.[141] For those trials, a fast freezing rate, and a moderately fast warming rate were used. At 1 μg/mL, Type I AFP showed no increase compared to the motility seen at 0.1 μg/mL, while AFGP produced only a moderate increase. Cryopreservation of bull sperm was similarly carried out with various AFP II, AFP III, and AFGP proteins. It was found that AFP I, at concentrations of 0.1 μg/mL, 1 μg/mL, and 10 μg/mL (but not 100 μg/mL) increased the osmotic resistance of the cells – a quality correlated with fertility. Only AFP type I and III were observed to bind to the cells, and only the three lower concentrations of AFP I assayed created ice crystals that were visibly different from the control. A study with mouse spermatozoa, on the other hand, concluded that neither AFP I nor AFP III, at concentrations of 1-100 μg/mL, could protect frozen-thawed cells.[142] In fact, the addition of AFPs led to a decrease in survival compared to the controls. For these trials, cooling was carried out at an optimal rate while warming was carried out at a suboptimal rate. The authors speculate that the changes in the ice crystals brought on by the interactions of ice with the AFPs had deleterious consequences to these sensitive cells. Two reviews further summarize studies of hypothermic storage and cryopreservation using AFPs and AFGPs.[139, 143]

1.7 Sugars, Antifreeze Activity, and Cryopreservation

AFGPs appear to have evolved independently in Arctic and Antarctic fish in a rare example of convergent evolution, that is, "…the development of a similar protein from different parent [genes] under similar environmental pressures."[94] A similar convergence is

seen in the AFPs. Sonnichsen *et al.* muse that the fact that AFPs from phylogenetically distinct species can be classified into an established AFP class is an indication that a limited number of structures out of the existing panoply of proteins can serve as antifreezes.[144] Perhaps this holds true for the AFGPs as well. In all fractions of native AFGP, the carbohydrate moiety is a Gal-GalNAc disaccharide.[94] While it has been determined that the Gal-GalNAc disaccharide can be replaced by a GalNAc monosaccharide without loss of antifreeze activity (defined as TH), until recently, the nature of the carbohydrate had only received brief mention.[95] Further, carbohydrates have also been used on their own as cryoprotective agents (examples are presented in Chapter 4).

It has been suggested that the stereochemistry of the carbohydrate determines its compatibility with the three-dimensional hydrogen-bonded network of water,[145, 146] and while the reasons are not yet clear, it is known that carbohydrate hydration is closely correlated to stereochemistry. Galema *et al.* determined the partial molar volumes, isentropic partial molar compressibilities, and hydration numbers of many commercially available hexoses and correlated these to carbohydrate stereochemistry. [147-150] It has been proposed that antifreeze activity is a function of hydration.[151, 152] However, this work defined antifreeze activity as thermal hysteresis, and not recrystallization inhibition. With the work by Galema *et al.* on carbohydrate hydration in mind, our lab synthesized a series of *C*-linked AFGP analogues substituted with different carbohydrate moieties and showed that carbohydrate stereochemistry also modulated recrystallization inhibition (RI). [153] They suggested that analogues containing carbohydrates with low isentropic molar compressibilities (such as galactose) fit poorly into the three-dimensional hydrogen bonded network of bulk water, and may therefore disturb the highly ordered structure of supercooled water. They proposed that this would increase the energy associated with transferring a water molecule to the ice lattice, inhibiting the growth of ice, resulting in increased RI activity. Following, our lab investigated the relationship between the hydration *index* of a carbohydrate, and its RI activity.[110] The hydration *number* reflects the number of tightly bound water molecules to the carbohydrate and is a function of carbohydrate stereochemistry.[147, 150] Dividing the hydration number by the molar volume of the carbohydrate gave the hydration *index*, a description of the number of tightly bound water

molecules per molar volume of carbohydrate.[110] They found that the hydration index of both mono- and disaccharides correlated well with experimentally measured RI activity.

Many organisms use sugars as part of their survival strategy for hypothermic conditions.[154, 155] Of the animals that use a freeze-tolerance strategy (as opposed to freeze-avoidance), many produce low-molecular weight cryoprotectants, which elevate cellular osmolality. Wood frogs and spring peepers produce glucose, while freeze-tolerant insects produce polyhydric alcohols, including glycerol. Other insect cryoprotectants include sorbitol, mannitol, myoinositol, ribitol, erythritol, threitol, ethylene glycol, and, in some cases, sugars such as trehalose. Cell-volume regulation is also important for freeze-tolerance. Important factors for cell-volume regulation include membrane stabilization, and minimizing cell volume decrease. Membrane stabilization can be accomplished using specific low-molecular weight cryoprotectants, such as trehalose and proline. The colligative actions of specifically synthesized cryoprotectants such as sugars and polyols, further aide volume regulation by minimizing cell-volume decrease during freezing.[155] Similarly, during cryopreservation, sugars within cells do not only work colligatively to help maintain cell volume, they have also been shown to interact with and stabilize the cell membrane.[155] Trehalose, sucrose, and glucose have been shown to stabilize small unilamellar vesicles (SUVs) during cryopreservation, maintaining their structural integrity and permeability.[156] Trehalose and sucrose can reduce membrane fusion of SUVs during cryopreservation,[157, 158] and in some cases can be more effective than the standard cryoprotectants, glycerol and DMSO.[159] Saccharides may interact with the acyl chains of the bilayer,[157] and likely form hydrogen bonds to the phospholipid polar head-group,[156, 160] or they may affect the water structure.[158] More recently, the interaction of saccharides, including glucose, trehalose, and maltose, with the lipid bilayer has been demonstrated using molecular dynamics simulations.[161-163] Similarly to DMSO, the saccharides displace water surrounding the polar head group, forming hydrogen bonds with the lipids and water molecules and increasing the stability of the membrane. It is thought that increasing the space between the head groups, lowers the transition temperature of the phospholipids.[164] Unlike DMSO, however, disaccharides are also thought to protect proteins during cooling.[165]

Sugars have been shown to enhance the activity of cryopreservation and vitrification agents. For example, trehalose and other polyhydroxy compounds were found to enhance the antifreeze activity (TH activity) of a beetle antifreeze protein.[166] Sugars, including glucose, fructose, sorbitol, sucrose, trehalose and raffinose were found to influence the vitrification properties of ethylene glycol-based solutions.[167] Since disaccharides are normally found only in the extra-cellular medium, they act to increase the osmolarity of the medium, keeping water molecules from the cell membrane. Freezing of water molecules at the cell surface can cause intra-cellular ice crystals to form; as outlined in earlier sections, intracellular freezing is thought to be detrimental to cells.

A major benefit of sugars in cryopreservation, is that they are non-toxic to many systems.[167] In fact, sugars have been extensively investigated as cryoprotective agents. Examples from studies with hepatocytes and hematopoietic stem cells are given in Chapter 4. Different cell types must not only be cryopreserved using different cryopreservation protocols (different rates of freezing, etc.),[10] but the optimal type and concentration of cryoprotectant also appears to be cell specific. The effect of sugars in cryopreservation of a particular cell type varies depending on the type of sugar used.[168] Mono-, di-, and tri-saccharides, and polyols, have been used alone or in combination with more common cryoprotectants such as DMSO.[169]

1.8 Umbilical Cord Blood and Hematopoietic Stem Cells

Hematopoietic stem cells (HSCs) are immature hematopoietic precursor cells. They are multipotent cells, capable of developing into about 10 hematopoietic lineages, and these form the whole hematopoietic system over a lifetime. In adults, HSC are found primarily in the bone marrow, although they are also present to some extent in the peripheral blood. Since HSC are abundant in the bone marrow, blood, and liver of the developing fetus, they are also found in umbilical cord blood (UCB).[170]

Transplantation of HSCs is currently indicated for as many as 70 hematological and non-hematological disorders; among them are: acute and chronic myeloid and lymphocytic

leukaemias, myelodysplastic syndrome, myeloma, Hodgkin's and non-Hodgkin's lymphoma, solid tumours, bone marrow failure syndromes, hamoglobinopathies, severe combined immunodeficiencies, inborn error of metabolism, and autoimmune diseases. Annually, an estimated 45,000-50,000 UCB transplants are performed worldwide.[171]

HSCs for transplantation can be derived from bone marrow, peripheral blood, and UCB.[170] UCB transplants are a relatively newer field; the first successful UCB transplant was performed in 1988.[172] HSCs from bone marrow or peripheral blood must present a 6/6 or 5/6 match for human leukocyte antigen (HLA) loci between recipient and donor.[173] However, a higher locus-disparity – up to three mismatches (HLA-mismatch) - can be tolerated for UCB.[170, 173-175] HLA-mismatched UCB transplants provide the same success rate as HLA-matched bone marrow transplants.[176] One consequence of this is that they may be the only source of HSC available for patients with rare HLA types (often ethnic minorities).[170] Other advantages of HSCs from UCB over bone marrow or peripheral blood include that it is easily collected, without harm to mother or child, and can then be tested, HLA-typed, and banked (cryopreserved).[171] Cryopreserved UCB is ready for immediate use as needed, and the time to transplant is much lower than that for a bone marrow transplant.[170] Further, UCB transplants present fewer risks of viral infection, and a lower incidence of severe graft vs. host disease (GvHD) both in the case of related donors as well as unrelated donors.[175, 177, 178] The main disadvantages of UCB compared to bone marrow are that it has fewer HSCs per unit, and repeat donations are not possible. As a result, UCB transplants are more successful in children than in adults. On the other hand, in the pediatric setting, UCB transplants may be the preferred alternative over bone marrow or peripheral blood transplants.[171] Delayed hematological and immune reconstitution have also been reported. Several strategies to overcome these shortfalls are currently under study. These include *ex vivo* expansion of UCB stem cells, the use of double unit transplantation,[179] and direct intrabone transplants.[180] However, UCB use and cryopreservation are relatively new areas, and use and cryopreservation protocols have yet to be optimized.[170, 171, 173, 181]

Cryopreservation is critically important for umbilical cord blood since it is collected during childbirth and is used at a later time.[71] UCB transplantation was developed subsequent to bone marrow transplantation, and as a result, the UCB cryopreservation protocols are based on those for bone marrow.[182] Since UCB contains fewer HSCs than bone

marrow, UCB cryopreservation protocols must consequently be more effective than those for bone marrow, in order to limit cell loss.[183] There is no universal cryopreservation method in use for UCB. The general method involves the use of 5-10% DMSO as the cryoprotectant, and a slow cooling and fast warming protocol.[71, 171, 184]

UCB may prove valuable not only as an important source of HSC. More recently, it was found that UCB contains non-hematopoietic stem cells, including mesenchymal stem cells, and vascular endothelial cell precursors. These cells may have potential in tissue revascularization, repair of bone and joint diseases, wound healing, cardiac repair, and others.[170] In a 2007 review, Woods and co-workers point out that there is less expertise with the use of UCB for HSC transplants compared to bone marrow transplants. There is both much promise in UCB for future therapy, and a need for the pre-transplantation and cryopreservation of UCB cells to be optimized.[171]

1.9 Hepatocytes: Orthotopic Liver Transplantation vs. Hepatocyte Transplantation

Human hepatocytes are vitally important for transplantation as well as for research. Hepatocytes have been used in the construction of bioartificial livers for patients with liver damage as a result of acute or chronic liver failure, allowing the patient's liver to recover, or to sustain the patient awaiting transplantation. Hepatocyte transplantation has been used to treat inherited metabolic disorders, and is rapidly emerging as an alternative to orthotopic liver transplantation (OLT).[53, 185-187] Hepatocytes also find important application as *in vitro* models in toxicity and drug metabolism testing.[188, 189] Access to good quality cells is very important both for clinical use, and to ensure the availability of hepatocytes for transplantation.[53, 190, 191] Hepatocyte transplantation has the potential to be superior to OLT since: multiple patients could be treated with hepatocytes from a single tissue donour, the same patient can be treated repeatedly with hepatocytes from multiple tissue donours, hepatocyte transplantation is less invasive than OLT (since only a small portion of hepatocytes need to be replaced, and it does not prevent subsequent OLT), and hepatocytes may be genetically modified prior to transplantation as part of gene therapy.[53, 189, 192, 193]

Cryopreservation plays a vital role in ensuring a reliable supply of hepatocytes . Successful and routine cryopreservation would allow the establishment of hepatocyte banks.[53, 189, 191] Hepatocytes are vulnerable to damage and death during both the cell isolation process, as well as the cryopreservation process.[194, 195] Cryopreservation protocols have been developed that result in hepatocyte viability that is often greater than 90% after cryopreservation. However, function recovery is less reliable.[193] There is as yet no optimized protocol for routine hepatocyte cryopreservation.[53, 77]

1.10 Summary

Cryopreservation and cell death are extremely complicated processes that are not yet fully understood. Cryopreservation of different cell types is carried out using either a fast-freezing or slow-freezing protocol. Even with the use of a slow-freezing protocol, the formation of ice either in the intracellular or extracellular space is inevitable, and ice recrystallization can further damage cells. However, *innocuous* intracellular ice formation may be beneficial for cell survival. Cryoprotective agents are employed to mitigate the damages of the cryopreservation process, including those caused by the formation of ice. The most commonly used cryoprotectant is DMSO; however, as was discussed earlier, DMSO may be toxic, and its infusion into transplant recipients can cause negative side effects. It is of great interest to develop a cryopreservation protocol that will eliminate or reduce the amount of DMSO required for successful cell preservation. The biological antifreezes have been explored as cryoprotective agents, and their ability to prevent ice recrystallization is of particular interest. The synthesis of antifreeze glycoprotein analogues that are effective ice recrystallization inhibitors, without exhibiting thermal hysteresis, is an ongoing challenge. The carbohydrate component of the AFGPs was found to be integral to its ice recrystallization ability, and it is therefore of interest to explore the cyropreservation potential of carbohydrates on their own. This thesis will focus on the cryopreservation of two cell types: hepatocytes, and hematopoietic stem cells from umbilical cord blood.

1. Rubinsky, B., Principles of low temperature cell preservation. *Heart Failure Reviews* **2003,** 8, 277-284.
2. Hochachka, P. W., Defense strategies against hypoxia and hypothermia. *Science* **1986,** 231, 234-241.
3. Parkes, A. S., Cryobiology. *Cryobiology* **1964,** 1, (1), 3.
4. Polge, C.; Smith, A. U.; Parkes, A. S., Revival of spermatozoa after vitrification and dehydration at low temperature. *Nature* **1949,** 164, 666.
5. Mazur, P., Freezing of living cells: mechanisms and implications. *American Journal of Physiology: Cell Physiology* **1984,** 247, C125-C142.
6. Bagchi, A.; Woods, E. J.; Critser, J. K., Cryopreservation and vitrification: recent advances in fertility preservation technologies. *Expert Review of Medical Devices* **2008,** 5, 359-370.
7. Fowler, A. J.; Toner, M., Cryo-injury and biopreservation. *Annals of the New York Academy of Science* **2006,** 1066, 119-135.
8. Mazur, P.; Leibo, S. P.; Chu, E. H. Y., A two-factor hypothesis of freezing injury. *Experimental Cell Research* **1972,** 71, 345-355.
9. Kleinhans, F. W.; Mazur, P., Determination of the water permeability (Lp) of mouse oocytes at -25 °C and its activation energy at subzero temperatures. *Cryobiology* **2009,** 58, 215-224.
10. Mazur, P., Cryobiology: The freezing of biological systems. *Science* **1970,** 168, 939-949.
11. Mazur, P., The role of cell membranes in the freezing of yeast and other single cells. *Annals of the New York Academy of Science* **1965,** 125, 658-676.
12. Kozono, D.; Yasui, M.; King, L. S.; Agre, P., Aquaporin water channels: atomic structure and molecular dynamics meet clinical medicine. *Journal of Clinical Investigation* **2002,** 109, 1395-1399.
13. Toner, M.; Cravalho, E. G.; Karel, M., Thermodynamics and kinetics of intracellular ice formation during freezing of biological cells. *Journal of Applied Physics* **1990,** 67, 1582-1593.
14. Toner, M.; Cravalho, E. G.; Karel, M., Cellular response of mouse oocytes to freezing stress: prediction of intracellular ice formation. *Journal of Biomechanical Engineering* **1993,** 115, 169-174.
15. Callow, R. A.; McGrath, J. J., Thermodynamic modeling and cryomicroscopy of cell-size unilamellar, and paucilamellar liposomes. *Cryobiology* **1985,** 22, 251-267.
16. Pitt, R. E.; Steponkus, P. L., Quantitative analysis of the probability of intracellular ice formation during freezing of isolated protoplasts. *Cryobiology* **1989,** 26, 44-63.
17. Steponkus, P. L.; Dowgert, M. F.; Gordon-Kamm, W. J., Destabilization of the plasma membrane of isolated plant protoplasts during a freeze-thaw cycle: the influence of cold acclimation. *Cryobiology* **1983,** 20, 448-465.
18. Muldrew, K.; McGann, L. E., Mechanism of intracellular ice formation. *Biophysical Journal* **1990,** 57, 525-532.
19. Muldrew, K.; McGann, L. E., The osmotic ruprure hypothesis of intracellular freezing injury. *Biophysical Journal* **1994,** 66, 532-541.
20. Diller, K. R.; Cravalho, E. G.; Huggins, C. E., Intracellular freezing in biomaterials. *Cryobiology* **1972,** 9, 429-440.
21. Miller, R. H.; Mazur, P., Survival of frozen-thawed human red cells as a function of cooling and warming velocities. *Cryobiology* **1976,** 13, 404-414.
22. Pegg, D. E.; Diaper, M. P.; Skaer, H. L.; Hunt, C. J., The effect of cooling rate and warming rate on the packing effect in human erythrocytes frozen and thawed in the presence of 2 M glycerol. *Cryobiology* **1984,** 21, 491-502.
23. Mazur, P., Kinetics of water loss from cells at subzero temperatures and the likelihood of intracellular freezing. *Journal of General Physiology* **1963,** 47, 347-369.
24. Fahy, G. M.; A. M. Karow, J., Ultrastructure-function correlative studies for cardiac cryopreservation. V. Absence of a correlation between electrolyte toxicity and cryoinjury in the slowly frozen, cryoprotected rat heart. *Cryobiology* **1977,** 14, 418-427.

25. Santarius, K. A.; Giersch, C., Cryopreservation of spinach chloroplast membranes by low-molecular-weight carbohydrates. II. Discrimination between colligative and noncolligative protection. *Cryobiology*
1983, 20, 90-99.
26. Pegg, D. E.; Diaper, M. P., The effect of initial tonicity on freeze/thaw injury to human red cells suspended in solutions of sodium chloride. *Cryobiology* **1991,** 28, 18-35.
27. Mazur, P.; Cole, K. W., Roles of unfrozen fraction, salt concentration, and changes in cell volume in the survival of frozen human erythrocytes. *Cryobiology* **1989,** 26, 1-29.
28. Steponkus, P. L.; Lynch, D. V., Freeze/thaw-induced destabilization of the plasma membrane and the effects of cold acclimation. *Journal of Bioenergetics and Biomembranes* **1989,** 21, (1), 21-41.
29. Meryman, H. T., Freezing injury and its prevention in living cells. *Annual Review of Biophysics* **1974,** 3, 341-363.
30. Muldrew, K., The salting-in hypothesis of post-hypertonic lysis. *Cryobiology* **2008,** 57, 251-256.
31. Fowler, A. J.; Toner, M., Cryo-injury and biopreservation. *Annals of the New York Academy of Science* **2005,** 1066, 119-135.
32. Mazur, P.; Rall, W. F.; Rigopoulos, N., Relative contributions of the fraction of unfrozen water and of salt concentration to the survival of slowly frozen human erythrocytes. *Biophysical Journal* **1981,** 36, 653-675.
33. Pegg, D. E.; Diaper, M. P., On the mechanism of injury to slowly frozen erythrocytes. *Biophysical Journal* **1988,** 54, 471-488.
34. Pegg, D. E.; Diaper, M. P., The "unfrozen fraction" hypothesis of freezing injury to human erythrocytes: a critical examination of the evidence. *Cryobiology* **1989,** 26, 30-43.
35. Rall, W. F.; Reid, D. S.; Farrant, J., Innocuous biological freezing during warming. *Nature* **1980,** 286, 511-514.
36. Buller, B. J.; Lane, N.; Benson, E. E., *Life in the Frozen State*. CRC Press: New York, 2004.
37. Koshimoto, C.; Mazur, P., Effects of cooling and warming rate to and from -70 °C, and effect of further cooling from -70 to -196 °C on the motility of mouse spermatozoa. *Biology of Reproduction* **2002,** 66, 1477-1484.
38. Karlsson, J. O. M., A theoretical model of intracellular devitrification. *Cryobiology* **2001,** 42, 154-169.
39. Yeh, Y.; Feeney, R. E., Antifreeze proteins: structure and mechanisms of Function. *Chemical Reviews* **1996,** 96, 601-618.
40. Knight, C. A.; Duman, J. G., Inhibition of recrystallization of ice by insect thermal hysteresis proteins: A possible cryoprotective role. *Cryobiology* **1986,** 23, 256-262.
41. Meryman, H. T., Cryopreservation of living cells: principles and practice. *Transfusion* **2007,** 47, 935-945.
42. Yang, G.; Zhang, A.; Xu, L. X., Experimental study of intracellular ice growth in human umbilical vein endothelial cells. *Cryobiology* **2009,** 58, 96-102.
43. Carpenter, J. F.; Hansen, T. N., Antifreeze protein modulates cell survival during cyopreservation: mediation through influence on ice crystal growth. *Proceedings of the National Academy of Science* **1992,** 89, 8953-8957.
44. Acker, J. P.; Elliott, J. A. W.; McGann, L. E., Intercellular ice propagation: experimental evidence for ice growth through membrane pores. *Biophysical Journal* **2001,** 81, 1389-1397.
45. Muldrew, K.; Schachar, J.; Cheng, P.; Rempel, C.; Liang, S.; Wan, R., The possible influence of osmotic poration on cell membrane water permeability. *Cryobiology* **2009,** 58, 62-68.
46. Karlsson, J. O. M.; Toner, M., Long-term storage of tissues by cryopreservation: critical issues. *Biomaterials* **1996,** 17, 243-256.
47. Fowler, A. J.; Toner, M., Prevention of Hemolysis in Rapidly Frozen Erythrocytes by Using a Laser Pulse. *Annals of the New York Academy of Science* **1998,** 858, 245-252.
48. Tait, J. F., Imaging of Apoptosis. *The Journal of Nuclear Medicine* **2008,** 49, 1573-1576.

49. Degterev, A.; Yuan, J., Expansion and evolution of cell death programmes. *Nature Reviews Molecular Cell Biology* **2008,** 9, 378-390.
50. Baust, J. M., Molecular mechanisms of cellular demise associated with cryopreservation failure. *Cell Preservation Technology* **2002,** 1, 17-31.
51. Baust, J. M.; Vogel, M. J.; Snyder, K. K.; Buskirk, R. G. v.; Baust, J. G., Activation of mitochondrial-associated apoptosis contributes to cryopreservation failure. *Cell Preservation Technology* **2007,** 5, 155-163.
52. Rauen, U.; Groot, H. d., New insights into the cellular and molecular mechanisms of cold storage injury. *Journal of Investigative Medicine* **2004,** 52, 299-309.
53. Terry, C.; Dhawan, A.; Mitry, R. R.; Hughes, R. D., Cryopreservation of isolated human hepatocytes for transplantation: State of the art. *Cryobiology* **2006,** 53, 149-159.
54. Baust, J. G., The management of mammalian cells at low temperature. *Cell Preservation Technology* **2008,** 6, 111-112.
55. Yagi, T.; Hardin, J. A.; Valenzuela, Y. M.; Miyoshi, H.; Gores, G. J.; Nyberg, S. L., Caspase inhibition reduces apoptotic death of cryopreserved porcine hepatocytes. *Hepatology* **2003,** 33, (6), 1432-1440.
56. Paasch, U.; Sharma, R. K.; Gupta, A. K.; Grunewald, S.; Mascha, E. J.; Anthony J. Thomas, J.; Glander, H.-J.; Agarwal, A., Cryopreservation and thawing is associated with varying extent of activation of apoptotic machinery in subsets of ejaculated human spermatozoa. *Biology of Human Reproduction* **2004,** 71, (6), 1828-1837.
57. Stroh, C.; Cassens, U.; Samraj, A. K.; Sibrowski, W.; Schulze-Osthoff, K.; Loss, M., The role of caspases in cryoinjury: caspase inhibition strongly improves the recovery of cryopreserved hematopoietic and other cells. *The FASEB Journal* **2002,** 16, 1651-1653.
58. Vermes, I.; Haanen, C.; Reutelingsperger, C., Flow cytometry of apoptotic cell death. *Journal of Immunological Methods* **2000,** 243, 167-190.
59. Goodlett, C. R.; Horn, K. H., Mechanisms of alcohol-induced damage to the developing nervous system. *Alcohol, Research and Health* **2001,** 25, (3), 175-184.
60. Yagi, T.; Hardin, J. A.; Valenzuela, Y. M.; Miyoshi, H.; Gores, G. J.; Nyberg, S. L., Caspase inhibition reduces apoptotic death of cryopreserved porcine hepatocytes. *Hepatology* **2001,** 33, 1432-1440.
61. Fujita, R.; Hui, T.; Chelly, M.; Demetriou, A. A., The effect of antioxidants and a caspase inhibitor on cryopreserved rat hepatocytes. *Cell Transplantation* **2005,** 14, 391-396.
62. Henriquez, M.; Armisen, R.; Stutzin, A.; Quest, A. F. G., Cell death by necrosis: a regulated way to go. *Current Molecular Medicine* **2008,** 8, 187-206.
63. Green, D. R.; Reed, J. C., Mitochondria and apoptosis. *Science* **1998,** 281, 1309-1312.
64. Karlsson, J. O. M.; Eroglu, A.; Toth, T. L.; Carvalho, E. G.; Toner, M., Fertilization and development of mouse oocytes cryopreserved using a theoretically optimized protocol. *Human Reproduction* **1996,** 11, 1296-1305.
65. Woelders, H.; Chaveiro, A., Theoretical prediction of 'optimal' freezing programmes. *Cryobiology* **2004,** 49, 258-271.
66. Lovelock, J. E., The haemolysis of human red blood-cells by freezing and thawing. *Biochimica et Biophysica Acta* **1953,** 10, 414-426.
67. Lovelock, J. E., Het mechanism of the protective action of glycerol against haemolysis by freezing and thawing. *Biochimica et Biophysica Acta* **1953,** 11, 28-36.
68. Pegg, D. E., Red cell volume in glycerol/sodium chloride/water mixtures. *Cryobiology* **1984,** 21, 234-239.
69. Skoric, D.; Balint, B.; Petakov, M.; Sindjic, M.; Rodic, P., Collection strategies and cryopreservatino of umbilical cord blood. *Transfusion Medicine* **2007,** 17, 107-113.
70. Kuleshova, L. L.; Gouk, S. S.; Hutmacher, D. W., Vitrification as a prospect for cryopreservation of tissue-engineered constructs. *Biomaterials* **2007,** 28, 1585-1596.

71. Berz, D.; McCormack, E. M.; Winer, E. S.; Colvin, G. A.; Quesenberry, P. J., Cryopreservation of hematopoietic stem cells. *American Journal of Hematology* **2007,** 82, (6), 463-472.
72. Toner, M.; Cravalho, E. G.; Stachecki, J.; Fitzgerald, T.; Tompkins, R. G.; Yarmush, M. L.; Armant, D. R., Nonequilibrium freezing of one-cell mouse embryos: membrane integrity and developmental potential. *Biophysical Journal* **1993,** 64, 1908-1921.
73. Baust, J. G., The field of cellular preservation. *Cell Preservation Technology* **2006,** 4, 147-148.
74. Woods, E. J.; Pollok, K. E.; Byers, M. A.; Perry, B. C.; Purtteman, J.; Heimfeld, S.; Gao, D., Cord blood stem cell cryopreservation. *Transfusion Medicine and Hemotherapy* **2006,** 34, 276-285.
75. Hantson, P.; Bauwens, D.; Laterre, P. F.; Michaux, L.; Tourtchaninoff, M. d.; Hernalsteen, D., Recurrent seizure and sustained encephalopathy associated with DMSO. *Clinical Toxicology* **2005,** 43, (5), 513-514.
76. Yancey, P. H., Organic osmolytes as compatible, metabolic and counteracting cryoprotectants in high osmolarity and other stresses. *The Journal of Experimental Biology* **2005,** 208, 2819-2830.
77. Terry, C.; Dhawan, A.; Mitry, R. R.; Lehec, S. C.; Hughes, R. D., Optimization of the cryopreservation and thawing protocol for human hepatocytes for use in cell transplantation. *Liver Transplantation* **2010,** 16, 229-237.
78. Windrum, P.; Morris, T. C. M.; Drake, M. B.; Niederwieser, D.; Ruutu, T., Variation in dimethyl sulfoxide use in stem cell transplantation: a survey of EBMT centres. *Bone Marrow Transplantation* **2005,** 36, 601-603.
79. Rowley, S. D.; Feng, Z.; Yadock, D.; Holmberg, L.; MacLeod, B.; Heimfeld, S., Post-thaw removal of DMSO does not completely abrogate infusional toxicity of the need for pre-infusion histamine blockade. *Cytotherapy* **1999,** 1, 439-446.
80. Fois, E.; Desmartin, M.; Benhamida, S.; Xavier, F.; Vanneaux, V.; Rea, D.; Fermand, J.-P.; Arnulf, B.; Mounier, N.; Ertault, M.; Lotz, J.-P.; Galicier, L.; Raffoux, E.; Benbunan, M.; Marolleau, J.-P.; Largero, J., Recovery, viability and clinical toxicity of thawed and washed haematopoietic progenitor cells: analysis of 952 autologous peripheral blood stem cell transplantations. *Bone Marrow Transplantation* **2007,** 40, 831-835.
81. Junior, A. M.; Arrais, C. A.; Saboya, R.; Velasques, R. D.; Junqueira, P. L.; Dulley, F. L., Neurotoxicity associated with dimethylsulfoxide-preserved hematopoietic progenitor cell infusion. *Bone Marrow Transplantation* **2008,** 41, 95-96.
82. Konuma, T.; Ooi, J.; Takahashi, S.; Tomonari, A.; Tsukada, N.; Kobayashi, T.; Sato, A.; Kato, S.; Kasahara, S.; Ebihara, Y.; Nagamura-Inoue, T.; Tsuji, K.; Tojo, A.; Asano, S., Cardiovascular toxicity of cryopreserved cord blood cell infusion. *Bone Marrow Transplantation* **2008,** 41, 861-865.
83. Petropoulou, A. D.; Bellochine, R.; Norol, F.; Marie, J.-P.; Rio, B., Coronary artery spasm after infusion of cryopreserved cord blood cells. *Bone Marrow Transplantation* **2007,** 40, 397-398.
84. Akkok, C. A.; Holte, M. R.; Tangen, J. M.; Ostenstad, B.; Bruserud, O., Hematopoietic engraftment of dimethyl sulfoxide-depleted autologous peripheral blood progenitor cells. *Transfusion* **2009,** 49, 354-361.
85. Galmes, A.; Gutierrez, A.; Sampol, A.; Canaro, M.; Morey, M.; Iglesias, J.; Matamoros, N.; Duran, M. A.; Novo, A.; Bea, M. D.; Galan, P.; Balansat, J.; Martinez, J.; Bargay, J.; Besalduch, J., Long-term hematologic reconstitution and clinical evaluation of autologous peripheral blood stem cell transplantation after cryopreservation of cell with 5% and 10% dimethylsulfoxide at -80 ^{o}C in a mechanical freezer. *Haematologica* **2007,** 92, 986-989.
86. Knight, C. A., Adding to the antifreeze agenda. *Nature* **2000,** 406, 249-251.
87. Davies, P. L.; Sykes, B. D., Antifreeze proteins. *Current Opinion in Structural Biology* **1997,** 7, 828-834.

88. DeVries, A. L.; Wohlschlag, D. E., Freezing resistance in some Antarctic fishes. *Science* **1969,** 163, 1073-1075.
89. DeVries, A. L.; Komatsu, S. K.; Feeney, R. E., Chemical and physical properties of freezing point-depressing glycoproteins from antarctic fishes. *The Journal of Biological Chemistry* **1970,** 245, 2901-2908.
90. Komatsu, S. K.; DeVries, A. L.; Feeney, R. E., Studies of the structure of freezing point-depressing glycoproteins from an antarctic fish. *The Journal of Biological Chemistry* **1970,** 245, 2909-2913.
91. DeVries, A. L.; Vandenheede, J.; Feeney, R. E., Primary structure of freezing point-depressing glycoproteins. *The Journal of Biological Chemistry* **1971,** 246, 305-308.
92. Cheng, C.-H.; Cziko, P. A.; Evans, C. W., Nonhepatic origin of notothenioid antifreeze reveals pancreatic synthesis as common mechanism in polar fish freezing avoidance. *Proceedings of the National Academy of Science* **2006,** 103, 10491-10496.
93. Fletcher, G. L.; Hew, C. L.; Davies, P. L., Antifreeze proteins of teleost fishes. *Annual Review of Physiology* **2001,** 63, 359-390.
94. Harding, M. M.; Anderberg, P. I.; Haymet, A. D. J., 'Antifreeze' glycoproteins from polar fish. *European Journal of Biochemistry* **2003,** 270, 1381-1392.
95. Tachibana, Y.; Fletcher, G. L.; Fujitani, N.; Tsuda, S.; Monde, K.; Nishimura, S.-I., Antifreeze glycoproteins: elucidation of the structural motifs that are essential for antifreeze activity. *Angewandte Chemie International Edition* **2004,** 43, 856-862.
96. Ewart, K. V.; Lin, Q.; Hew, C. L., Structure, function and evolution of antifreeze proteins. *Cellular and Molecular Life Sciences* **1999,** 55, 271-283.
97. Duman, J. G.; DeVries, A. L., Isolation, characterization, and physical properties of protein antifreezes from the winter flounder, *Pseudopleuronectes americanus*. *Comparative Biochemistry and Physiology, Part B* **1976,** 54B, 375-380.
98. Ng, N. F. L.; Hew, C. L., Structure of an antifreeze polypeptide from the sea raven: disulfide bonds and similarity to lectin-binding proteins. *The Journal of Biological Chemistry* **1992,** 267, 16069-16075.
99. Davies, P. L.; Hew, C. L., Biochemistry of fish antifreeze proteins. *The FASEB Journal* **1990,** 4, 2460-2468.
100. Li, X.-M.; Trinh, K.-Y.; Hew, C. L., Structure of an antifreeze polypeptide and its precursor from the ocean pout, *Macrozoarces americanus*. *The Journal of Biological Chemistry* **1985,** 260, 12904-12909.
101. Deng, G.; Andrews, D. W.; Laursen, R. A., Amino acid sequence of a new type of antifreeze protein, from the longhorn sulpin *Myoxocephalus octodecimspinosis*. *FEBS Letters* **1997,** 402, 17-20.
102. Knight, C. A.; DeVries, A. L.; Oolman, L. D., Fish antifreeze protein and the freezing and recrystallization of ice. *Nature* **1984,** 308, 295-296.
103. Wilson, P. W.; Beaglehole, D.; DeVries, A. L., Antifreeze glycopeptides adsorption on single crystal ice surfaces using ellipsometry. *Biophysical Journal* **1993,** 64, 1878-1884.
104. Morris, H. R.; Thompson, M. R.; Osuga, D. T.; Ahmed, A. I.; Chan, S. M.; Vandenheede, J. R.; Feeney, R. E., Antifreeze glycoproteins from the blood of an antarctic fish: the structure of the proline-containing glycopeptides. *The Journal of Biological Chemistry* **1978,** 253, 5155-5162.
105. Hew, C. L.; Slaughter, D.; Fletcher, G. L.; Joshi, S. B., Antifreeze glycoproteins in the plasma of Newfoundland Atlantic cod (*Gadus morhua*). *Canadian Journal of Zoology* **1981,** 59, 2186-2192.
106. Raymond, J. A.; Lin, Y.; DeVries, A. L., Glycoprotein and protein antifreezes in two alaskan fishes. *Journal of Experimental Zoology* **1975,** 193, 125-130.
107. Wohrmann, A. P. A., Antifreeze glycopeptides and peptides in Antarctic fish species from teh Weddell Sea and the Lazarev Sea. *Marine Ecology Progress Series* **1996,** 130, 47-59.
108. Raymond, J. A.; Wilson, P.; DeVries, A. L., Inhibition of growth of nonbasal planes in ice by fish antifreezes. *Proceedings of the National Academy of Science* **1989,** 86, 881-885.

109. Harding, M. M.; Ward, L. G.; Haymet, A. D. J., Type I 'antifreeze' proteins: structure-activity studies and mechanisms of ice growth inhibition. *European Journal of Biochemistry* **1999,** 264, 653-665.
110. Tam, R. Y.; Ferreira, S. S.; Czechura, P.; Chaytor, J. L.; Ben, R. N., Hydration index: a better parameter for explaining small molecule hydration in inhibition of ice recrystallization. *Journal of the American Chemical Society* **2008,** 130, 17494-17501.
111. Knight, C. A.; Cheng, C. C.; Davies, A. L., Adsorption of α-helical antifreeze peptides on specific ice crystal surface planes. *Biophysical Journal* **1991,** 59, 409-418.
112. Knight, C. A.; Driggers, E.; DeVries, A. L., Adsorption to ice of fish antifreeze glycopeptides 7 and 8. *Biophysical Journal* **1993,** 64, 252-259.
113. Michael E. Housten, J.; Chao, H.; Hodges, R. S.; Sykes, B. D.; Kay, C. M.; Sonnichsen, F. D.; Loewen, M. C.; Davies, P. L., Binding of an oligopeptide to a specific plane of ice. *The Journal of Biological Chemistry* **1998,** 273, 11714-11718.
114. Griffith, M.; Ewart, K. V., Antifreeze proteins and their potential use in frozen foods. *Biotechnology Advances* **1995,** 13, 375-402.
115. Feeney, R. E.; Fink, W. H.; Hallett, J.; Harrison, K.; Vesenka, J. P.; Yeh, Y., Investigations of the differential affinity of antifreeze glycoprotein for single crystals of ice. *Journal of Crystal Growth* **1991,** 113, 417-429.
116. Ishiguro, H.; Rubinsky, B., Mechanical interactions between ice crystals and red blood cells during directional solidification. *Cryobiology* **1994,** 31, 483-500.
117. Knight, C. A.; Wen, D.; Laursen, R. A., Nonequilibrium antifreeze peptides and the recrystallization of ice. *Cryobiology* **1995,** 32, 23-34.
118. Knight, C. A.; Duman, J. G., Inhibition of recystallization of ice by insect thermal hysteresis proteins: a possible cryoprotective role. *Cryobiology* **1986,** 23, 256-262.
119. Sidebottom, C.; Buckley, S.; Pudney, P.; Twigg, S.; Jarman, C.; Holt, C.; Telford, J.; McArthur, A.; Worrall, D.; Hubbard, R.; Lillford, P., Heat-stable antifreeze protein from grass. *Nature* **2000,** 406, 256.
120. Eniade, A.; Purushotham, M.; Ben, R. N.; Wang, J. B.; Horwath, K., A serendipitous discovery of antifreeze protein-specific activity in C-linked antifreeze glycoprotein analogs. *Cell Biochemistry and Biophysics* **2003,** 38, 115-124.
121. Acker, J. P.; McGann, L. E., Innocuous intracellular ice improves survival of frozen cells. *Cell Transplantation* **2002,** 11, 563-571.
122. Raymond, J. A.; DeVries, A. L., Adsorption inhibition as a mechanism of freezing resistance in polar fishes. *Proceedings of the National Academy of Science* **1977,** 74, 2589-2593.
123. Knight, C. A.; DeVries, A. L., Melting inhibition and superheating of ice by an antifreeze glycopeptide. *Science* **1989,** 245, 505-507.
124. Hall, D. G.; Lips, A., Phenomenology and mechanism of antifreeze peptide activity. *Langmuir* **1999,** 15, 1905-1912.
125. Hew, C. L.; Yang, D. S. C., Protein interaction with ice. *European Journal of Biochemistry* **1992,** 203, 33-42.
126. Knight, C. A.; DeVries, A. L., Effects of a polymeric, nonequilibrium "antifreeze" upon ice growth from water. *Journal of Crystal Growth* **1994,** 143, 301-310.
127. Anchordoguy, T. J.; Cecchini, C. A.; Crowe, J. H.; Crowe, L. M., Insight into the cryoprotective mechanism of dimethyl sulfoxide for phospolipid bilayers. *Cryobiology* **1991,** 28, 467-473.
128. Notman, R.; Noro, M.; O'Malley, B.; Anwar, J., Molecular basis for dimethylsulfoxide (DMSO) action on lipid membranes. *Journal of the American Chemical Society* **2006,** 128, 13982-13983.
129. Gurtovenko, A. A.; Anwar, J., Modulating the structure and properties of cell membranes: the molecular mechanism of action of dimethyl sulfoxide. *Journal of Physical Chemistry B* **2007,** 111, 10453-10460.

130. Wu, Y.; Banoub, J.; Goddard, S. V.; Kao, M. H.; Fletcher, G. L., Antifreeze glycoproteins: relationship between molecular weight, thermal hysteresis and the inhibition of leakage from liposomes during thermotropic phase transition. *Comparative Biochemistry and Physiology Part B* **2001,** 128, 265-273.
131. Anchordoguy, T. J.; Rudolph, A. S.; Carpenter, J. F.; Crowe, J. H., Modes of interaction of cryoprotectants with membrane phospholipids during freezing. *Cryobiology* **1987,** 24, 324-331.
132. Rubinsky, B.; Arav, A.; DeVries, A. L., The cryoprotective effect of antifreeze glycopeptides from antarctic fishes. *Cryobiology* **1992,** 29, 69-79.
133. Hays, L. M.; Feeney, R. E.; Crowe, L. M.; Crowe, J. H.; Oliver, A. E., Antifreeze glycoproteins inhibit leakage from liposomes during thermotropic phase transitions. *Proceedings of the National Academy of Science* **1996,** 93, 6835-6840.
134. Wu, Y.; Fletcher, G. L., Efficacy of antifreeze protein types in protecting liposome membrane integrity depends on phospholipid class. *Biochimica et Biophysica Acta* **2000,** 1524, 11-16.
135. Tomczak, M. M.; Hincha, D. K.; Estrada, S. D.; Feeney, R. E.; Crowe, J. H., Antifreeze proteins differentially affect model membranes during freezing. *Biochimica et Biophysica Acta* **2001,** 1511, 255-263.
136. Rubinsky, B.; Mattioli, M.; Arav, A.; Barboni, B.; Fletcher, G. L., Inhibition of Ca^{2+} and K^{+} currents by "antifreeze" proteins. *American Journal of Physiology: Regulatory, Integrative and Comparative Physiology* **1992,** 262, 542-545.
137. Rubinsky, B.; Arav, A.; Mattioli, M.; DeVries, A. L., The effect of antifreeze glycopeptides of membrane potential changes at hypothermic temperatures. *Biochemical and Biophysical Research Communications* **1990,** 173, 1369-1374.
138. Arav, A.; Rubinsky, B.; Fletcher, G.; Seren, E., Cryogenic protection of oocytes with antifreeze proteins. *Molecular Reproduction and Development* **1993,** 36, 488-493.
139. Inglis, S. R.; Turner, J. J.; Harding, M. M., Applications of type I antifreeze proteins: studies with model membranes and cryoprotectant properties. *Current Protein and Peptide Science* **2006,** 7, (7), 509-522.
140. McKown, R. L.; Warren, G. J., Enhanced survival of yeast expressing an antifreeze gene analogue after freezing. *Cryobiology* **1991,** 28, 474-482.
141. Payne, S. R.; Oliver, J. E.; Upreti, G. C., Effect of antifreeze proteins on the motility of ram spermatozoa. *Cryobiology* **1994,** 31, 180-184.
142. Koshimoto, C.; Mazur, P., Effects of warming rate, temperature, and antifreeze proteins on the survival of mouse spermatozoa frozen at an optimal rate. *Cryobiology* **2002,** 45, 49-59.
143. Wang, J.-H., A comprehensive evaluation of the effects and mechanisms of antifreeze proteins during low-temperature preservation. *Cryobiology* **2000,** 41, 1-9.
144. Sonnichsen, F. D.; DeLuca, C. I.; Davies, P. L.; Sykes, B. D., Refined solution of type III antifreeze proteins: hydrophobic groups may be involved in the energetics of the protein-ice interaction. *Structure* **1996,** 4, 1325-1337.
145. Franks, F., Physical chemistry of small carbohydrates - equilibrium solution properties. *Pure and Applied Chemistry* **1987,** 59, 1189-1202.
146. Franks, F.; Lillford, P. J.; Robinson, G., Isomeric equilibria of monosaccharides in solution. *Journal of the Chemical Society Faraday Transactions 1* **1989,** 85, 2417-2426.
147. Dashnau, J. L.; Sharp, K. A.; Vanderkooi, J. M., Carbohydrate intramolecular hydrogen bonding cooperativity and its effect on water structure. *Journal of Physical Chemistry B* **2005,** 109, 24152-24159.
148. Galema, S. A.; Hoiland, H., Stereochemical aspects of hydration of carbohydrates in aqueous solutions. 3. Density and ultrasound measurements. *Journal of Physical Chemistry* **1991,** 95, 5321-5326.

149. Galema, S. A.; Engberts, J. B. F. N.; Hoiland, H.; Forland, G. M., Informative thermodynamic properties of the effect of stereochemistry on carbohydrate hydration. *Journal of Physical Chemistry* **1993,** 97, 6885-6889.
150. Galema, S. A.; Howard, E.; Engberts, J. B. F. N.; Grigera, J. R., The effect of stereochemistry upon carbohydrate hydration. A molecular dynamics simulation of β-D-galactopyranose and (α, β)-D-talopyranose. *Carbohydrate Research* **1994,** 265, 215-225.
151. Furuki, T., Effect of stereochemistry on the anti-freeze characteristics of carbohydrates. A thermal study of aqueous monosaccharides at subzero temperatures. *Carbohydrate Research* **2000,** 323, 185-191.
152. Furuki, T., Effect of molecular structure on thermodynamic properties of carbohydrates. A calorimetric study of aqueous di- and oligosaccharides at subzero temperatures. *Carbohydrate Research* **2002,** 337, 441-450.
153. Czechura, P.; Tam, R. Y.; Dimitrijevic, E.; Murphy, A. V.; Ben, R. N., The importance of hydration for inhibiting ice recrystallization with C-linked antifreeze glycoproteins. *Journal of the American Chemical Society* **2008,** 130, 2928-2929.
154. Storey, K. B.; Storey, J. M., Freeze-tolerant frogs: cryoprotectants and tissue-metabolism during freeze-thaw cycles. *Canadian Journal of Zoology* **1986,** 63, 49-56.
155. Storey, K. B.; Storey, J. M., Natural freezing survival in animals. *Annual Review of Ecology and Systematics* **1996,** 27, 365-386.
156. Strauss, G.; Schurtenberger, P.; Hauser, H., The interaction of saccharides with lipid bilayer vesicles: stabilization during freeze-thawing and freeze-drying. *Biochimica et Biophysica Acta* **1986,** 858, 169-180.
157. Anchordoguy, T. J.; Rudolphe, A. S.; Carpenter, J. F.; Crowe, J. H., Modes of interaction of cryoprotectants with membrane phospholipids during freezing. *Cryobiology* **1987,** 24, 324-331.
158. Strauss, G.; Hauser, H., Stabilization of lipid bilayer vesicles by sucrose during freezing. *Proceedings of the National Academy of Science* **1986,** 83, 2422-2426.
159. Rudolph, A. S.; Crowe, J. H., Membrane stabilization during freezing: the role of two natural cryoprotectants, trehalose and proline. *Cryobiology* **1985,** 22, 367-377.
160. Crowe, J. H.; Crowe, L. M.; Chapman, D., Preservation of membranes in anhydrobiotic organisms: the role of trehalose. *Science* **1984,** 223, 701-703.
161. Pereira, C. S.; Hunenberger, P. H., Effect of trehalose on a phospholipid membrane under mechanical stress. *Biophysical Journal* **2008,** 95, 3525-3534.
162. Pereira, C. S.; Hunenberger, P. H., Interaction of the sugars trehalose, maltose and glucose with a phospholipid bilayer: a comparative molecular dynamics study. *Journal of Physical Chemistry B* **2006,** 110, 15572-15581.
163. Leekumjorn, S.; Sum, A. K., Molecular dynamics study on the stabilization of dehydrated lipid bilayers with glucose and trehalose. *Journal of Physical Chemistry B* **2008,** 112, 10732-10740.
164. Crowe, J. H.; Crowe, L. M.; Carpenter, J. F.; Wistrom, C. A., Stabilization of dry phospholipid bilayers and proteins by sugars. *Biochemical Journal* **1987,** 242, 1-10.
165. Leslie, S. B.; Israeli, E.; Lighthart, B.; Crowe, J. H.; Crowe, L. M., Trehalose and sucrose protect both membranes and proteins in intact bacteria during drying. *Applied and Environmental Microbiology* **1995,** 61, 3592-3597.
166. Amornwittawat, N.; Wang, S.; Banatlao, J.; Chung, M.; Velasco, E.; Duman, J. G.; Wen, X., Effects of polyhydroxy compounds on beetle antifreeze protein activity. *Biochimica et Biophysica Acta* **2009,** 1794, 341-346.
167. Kuleshova, L. L.; MacFarlane, D. R.; Trounson, A. O.; Shaw, J. M., Sugars exert a major influence on the vitrification properties of ethylene glycol-based solutions and have low toxicity to embryos and oocytes. *Cryobiology* **1999,** 38, 119-130.
168. Yildiz, C.; Kaya, A.; Aksoy, M.; Tekeli, T., Influence of sugar supplementation of the extender on motility, viability and acrosomal integrity of dog spermatozoa during freezing. *Theriogenology* **2000,** 54, 579-585.

169. Yildiz, C.; Ottaviani, P.; Law, N.; Ayearst, R.; Liu, L.; McKerlie, C., Effects of cryopreservation on sperm quality, nuclear DNA integrity, *in vitro* fertilization, and *in vitro* embryo development in the mouse. *Reproduction* **2007,** 133, 585-595.
170. Watt, S. M.; Contreras, M., Stem cell medicine: umbilical cord blood and its stem cell potential. *Seminars in Fetal and Neonatal Medicine* **2005,** 10, 209-220.
171. Woods, E. J.; Pollok, K. E.; Byers, M. A.; Perry, B. C.; Purtteman, J.; Heimfeld, S.; Gao, D., Cord blood stem cell cryopreservation. *Transfusion Medicine and Hemotherapy* **2007,** 34, 276-285.
172. Gluckman, E.; Broxmeyer, H. E.; Auerbach, A. D.; Friedman, H. S.; Douglas, G. W., Hematopoietic reconstitution in a patient with Fanconi's Anemia by means of umbilical-cord blood from an HLA-identical sibling. *The New England Journal of Medicine* **1989,** 321, 1174.
173. Brown, J. A.; Boussiotis, V. A., Umbilical cord blood transplantation: basic biology and clinical challenges to immune reconstitution. *Clinical Immunology* **2008,** 127, 286-297.
174. Wagner, J. E.; Barker, J. N.; DeFor, T. E.; Baker, K. S.; Blazar, B. R.; Eide, C.; Goldman, A.; Kersey, J.; Krivit, W.; MacMillan, M. L.; Orchard, P. J.; Peters, C.; Weisdorf, D. J.; Ramsay, N. K. C.; Davies, S. M., Transplantation of unrelated donor umbilical cord blood in 102 patients with malignant and nonmalignant diseases: influence of CD34 cells dose with HLA disparity on treatment-related mortality and survival. *Blood* **2002,** 100, 1611-1618.
175. Arcese, W.; Picardi, A.; Cerretti, R.; Cudillo, L.; Angelis, G. d.; Franceschini, L.; Felice, L. d.; Postorino, M., The therapeutic use of cord blood. *Cell Preservation Technology* **2006,** 4, 161-168.
176. Gluckman, E.; Rocha, V., Cord blood transplantation: state of the art. *Haematologica* **2009,** 94, 451-454.
177. Gluckman, E.; Rocha, V., History of the clinical use of umbilical cord blood hematopoietic cells. *Cytotherapy* **2005,** 7, 219-227.
178. Laughlin, M. J.; Barker, J.; Bambach, B.; Koc, O. N., Hematopoietic engraftment and survival in adult recipients of umbilical-cord blood from unrelated donors. *The New England Journal of Medicine* **2001,** 344, 1815-1822.
179. Nauta, A. J.; Kruisselbrink, A. B.; Lurvink, E.; Mulder, A.; Claas, F. H.; Noort, W. A.; Willemze, R.; Fibbe, W. E., Enhanced engraftment of umbilical cord blood-derived stem cells in NOD/SCID mice by cotransplantation of a second unrelated cord blood unit. *Experimental Hematology* **2005,** 33, 1249-1256.
180. Frassoni, F.; Gualandi, F.; Podesta, M.; Raiola, A. M.; Ibatici, A.; Piaggio, G.; Sessarego, M.; Sessarego, N.; Gobbi, M.; Sacchi, N.; Labopin, M.; Bacigalupo, A., Direct intrabone transplant of unrelated cord-blood cells in acute leukaemia: a phase I/II study. *The Lancet Oncology* **2008,** 9, 831-839.
181. Hofmeister, C. C.; Zhang, J.; Knight, K. L.; Le, P.; Stiff, P. J., *Ex vivo* expansion of umbilical cord blood stem cells for transplantation: growing knowledge from teh hematopoietic niche. *Bone Marrow Transplantation* **2007,** 39, 11-23.
182. Rubinstein, P.; Dobrila, L.; Rosenfield, R. E.; Adamson, J. W.; Migliaccio, G.; Migliaccio, A. R.; Taylor, P. E.; Stevens, C. E., Processing and cryopreservation of placental/umbilical cord blood for unrelated bone marrow reconstitution. *Proceedings of the National Academy of Science* **1995,** 92, 10119-10122.
183. Hunt, C. J.; Armitage, S. E.; Pegg, D. E., Cryopreservation of umbilical cord blood: 1. Osmotically inactive volume, hydraulic conductivity and permeability of CD34+ cells to dimethyl sulphoxide. *Cryobiology* **2003,** 46, 61-75.
184. Hunt, C. J.; Armitage, S. E.; Pegg, D. E., Cryopreservation of umbilical cord blood: 2. Tolerance of CD34+ cells to multimolar dimethyl sulphoxide and the effect of cooling rate on recovery after freezing and thawing. *Cryobiology* **2003,** 46, 76-87.
185. Strain, A. J.; Neuberger, J. M., A Bioartificial Liver - state of the art. *Science* **2002,** 295, 1005-1009.
186. Dhawan, A.; Mitry, R. R.; Hughes, R. D., Hepatocyte transplantation for liver-based metabolic disorders. *Journal of Inherited Metabolic Disease* **2006,** 29, 431-435.

187. Strom, S. C.; Bruzzone, P.; Cai, H.; Ellis, E.; Lehmann, T.; Mitamura, K.; Miki, T., Hepatocyte transplantation: clinical experience and potential for future use. *Cell Transplantation* **2006,** 15, (Supplement 1), 105-110.
188. Terry, C.; Dhawan, A.; Mitry, R. R.; Lehec, S. C.; Hughes, R. D., Preincubation of rat and human hepatocytes with cytoprotectants prior to cryopreservation can improve viability and function upon thawing. *Liver Transplantation* **2005,** 11, 1533-1540.
189. Li, A. P., Human hepatocytes: isolation, cryopreservation and applications in drug development. *Chemico-Biological Interactions* **2007,** 168, 16-29.
190. Zaman, G. J. R.; Roos, J. A. D. M. d.; Blomenrohr, M.; Koppen, C. J. v.; Oosterom, J., Cryopreserved cells facilitate cell-based drug discovery. *Drug Discovery Today* **2007,** 12, 521-526.
191. Ludlow, J. W.; Bruce, A. T.; Kulik, M. J.; Meheux, S. O.; McCoy, D. W.; Asfeldt, T. M., Allogeneic cell therapy for the treatment of liver disease. *Progress in Transplantation* **2005,** 15, 178-184.
192. Vandenheede, J. R.; Ahmed, A. I.; Feeney, R. E., Structure and role of carbohydrate in freezing point-depressing glycoproteins from an antarctic fish. *The Journal of Biological Chemistry* **1972,** 247, 7885-7889.
193. Fiegel, H. C.; Kaufmann, P. M.; Bruns, H.; Kluth, D.; Horch, R. E.; Vacanti, J. P.; Kneser, U., Hepatic tissue engineering: from transplantation to customized cell-based liver directed therapies from the laboratory. *Journal of Cellular and Molecular Medicine* **2008,** 12, (1), 56-66.
194. Illouz, S.; Nakamura, T.; Webb, M.; Thava, B.; bikchandani, J.; Robertson, G.; Lloyd, D.; Berry, D.; Wada, H.; Dennison, A., Comparison of University of Wisconsin and ET-Kyoto preservation solutions for the cryopreservation of primary human hepatocytes. *Transplantation Proceedings* **2008,** 40, 1706-1709.
195. Fu, T.; Guo, D.; Huang, X.; O'Gorman, M. R. G.; Huang, L.; Crawford, S. E.; Soriano, H. E., Apoptosis Occurs in Isolated and Banked Primary Mouse Hepatocytes. *Cell Transplantation* **2001,** 10, 59-66.

Chapter 2: Objectives

The physical interactions of antifreeze glycoproteins (AFGPs) with ice have been studied in some detail, as was outlined in Chapter 1, but are still under debate. The mechanisms of thermal hysteresis (TH), and recrystallization inhibition (RI), are not yet clear, and further, the potential use of AFGPs as cryopreservation agents have not yet been fully explored. The first goal of this work is to modify the physical properties of selected AFGP analogues in an attempt to tailor antifreeze activity. Specifically, modifications that affect the hydrophobicity and hydration characteristics of these AFGP analogues and the subsequent effect on TH and RI activity will be examined. The second goal is the assessment of the cryopreservation potential of these AFGP analogues, and more generally, carbohydrates *in vitro*. The precedents for these goals, as well as the specific objectives related to each, are discussed.

2.1 Structure-Function Studies of AFGP and *O*-Linked AFGP Analogues

As was discussed in Chapter 1, AF(G)Ps are thought to inhibit ice growth via an "adsorption-inhibition" process that is thought to be irreversible. The adsorption of AF(G)Ps has been postulated to result from either hydrophilic or hydrophobic interactions with the water and ice interface. Most of the ice-binding studies have been carried out with AFGP and AFP Type I. It was first proposed that AF(G)Ps bind to ice via hydrogen bonding of their polar groups - hydroxyl groups of the disaccharide of AFGP or the threonines of AFP I - to the ice surface.[1] Based on a series of amino acid substitution studies on HPLC fraction 6 of AFP Type I, which contains an 11 residue repeat unit commencing with threonine, it was shown that hydrophilic interactions between the protein and ice may not be as important as hydrophobic interactions.[2] It was found that hydrophobic interactions of the γ-methyl groups of the threonine residues were at least as important for ice binding as the hydroxyl groups of threonines.[3-5] Further indications that hydrophobic interactions may be important for

antifreeze activity arise from the presence of a well-defined hydrophobic face in AFP Type I. AFP Type 1 polymers are therefore said to be amphiphilic. As shown in Figure 2.1, in the helix, the majority of the hydrophilic amino acid side chains project along the length of one side of the helix (residues labeled in plain text), while the opposite side is predominantly hydrophobic (residues labeled in bold).[6]

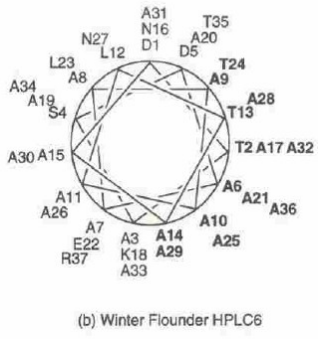

Figure 2.1 Helical wheel representation of type 1 proteins: the hydrophobic face is indicated by bold residues; in the case of threonine this is achieved with γ-methyl group oriented on the surface[7]

Due to the challenges associated with synthesizing AFGPs, early structure-function work was performed using degradation studies.[8] In these early studies, only TH activity was assessed. It was found that while the C-6 hydroxyl groups are required for activity, a negative charge at that position is not tolerated.[9, 10] At least some of the hydroxyl groups on the carbohydrate seem to mandatory.[11-13] The magnitude of freezing point depression may be related to the length of the glycopeptides,[14] and AFGP 8 may be the minimum length for antifreeze activity.[15] AFGP 8 seems to require at least 3 carbohydrate moieties, the terminal galactose of the disaccharide, and free hydroxyl groups on the side chains for activity. These results were summarized in a recent review,[8] although the authors caution that in most cases, the derivatives were not isolated and purified. However, as Nishimura *et al.* point out, AFGPs are structurally complex and exist as numerous isoforms, and they are therefore difficult to isolate in large quantities. As a result, the authors published extensive structure-function work using synthetic AFGP (syAFGP) analogues.[16] The purity of each glycopeptides was demonstrated using analytical reverse-phase HPLC. The authors found

that all of the glycopeptides, including the monomer, displayed concentration-dependant thermal hysteresis, and produced hexagonal bipyramidal ice crystals. While chain length and TH were positively correlated, maximum TH seemed to have been reached by the five-repeat glycopeptides. A collection of syAFGPs that differed in their carbohydrate side-chain were also synthesized and tested for TH activity. The structures are shown in Figure 2.2.

The authors found that the removal of the carbohydrate altogether, as in (**1**), destroyed TH activity, as did the substitution of the α-O-linked glycopeptides of the native system (**2**) for a β-O-linked glycopeptide (**3**). TH activity was similarly destroyed by the inclusion of sialic acid at C3 (**4**), confirming that the oxygen at C3 cannot tolerate a negative charge. In contrast to previous studies[15] however, the terminal galactose residue was not found to be necessary for antifreeze activity, as GalNAc (**5**) showed TH activity. The NAc group seemed to be critical however, as the replacement of GalNAc (**5**) with Galβ1-3Gal (**7**), Gal (**8**), or Lac (**9**) surpressed antifreeze activity. The configuration of the sugar hydroxyls may be important for activity, since the replacement of the GalNAc (**5**) residue with LacNAc (**6**) reduced antifreeze activity. As for the AFPs, the authors concluded that the γ-methyl groups of the Thr residues are required for activity (structure not shown). Conformational studies using NMR and CD indicated that, similar to AFP Type I (Figure 2.1), syAFGP (**2**) is amphipathic in solution: it has a hydrophilic face (due to the disaccharide moieties) and a hydrophobic face (due to the CH_3 groups of the Ala residue and the N-acetyl group).

Very recently (in 2009) a structure-function study of synthetic AFGPs that measured the recrystallization inhibition ability of glycopeptides as a measure of antifreeze activity was published.[17] Recrystallization inhibition was determined according to the technique of Knight *et al*.[18] The authors found that the terminal galactose was not required for RI activity (an example of the analogues synthesized is given in Figure 2.3). The authors further concluded that the RI of AFGPs is highly dependent on the concentration and molar mass, as well as a periodic turn formation (structures not shown).

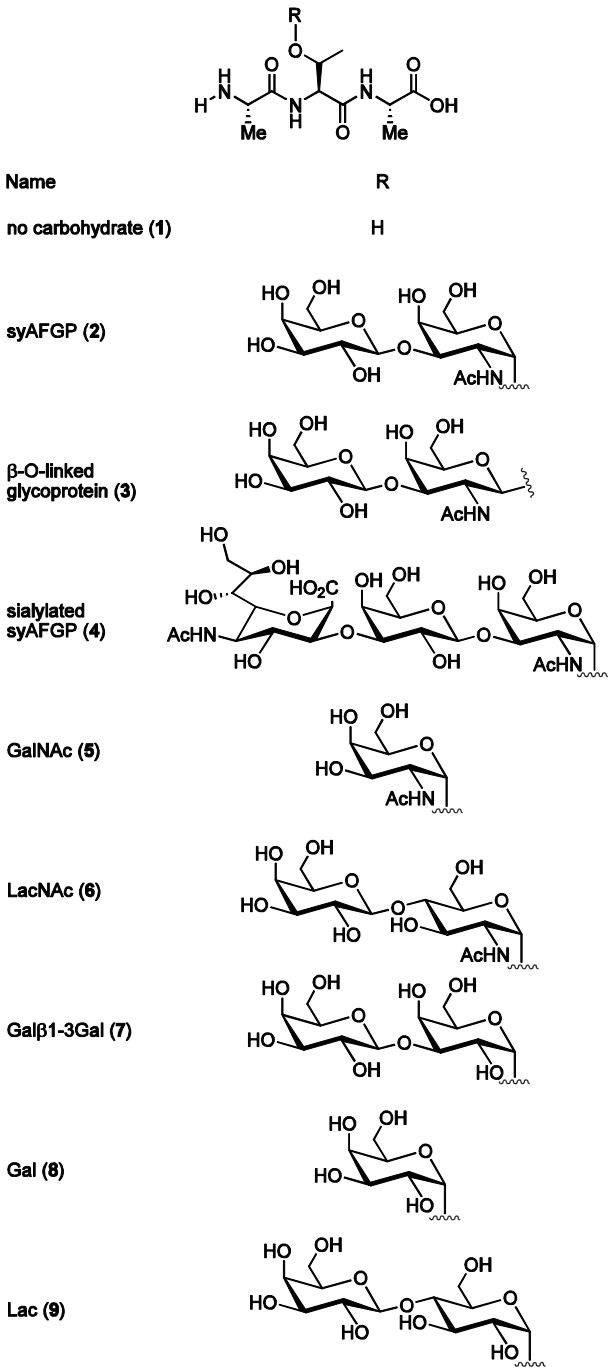

Figure 2.2 Structure-activity relationship: AFGP analogues synthesized by Nishimura and co-workers; all compounds were used for the activity evaluation studies in polymeric form[16]

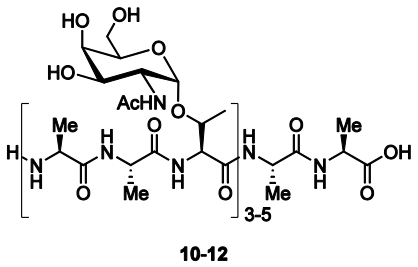

Figure 2.3 Structure-activity relationship: example of AFGP analogues synthesized by Heggemann and co-workers[17]

It seems that, at least for the *O*-linked AFGP analogues, the correct balance and orientation of hydrophobic and hydrophilic residues is critical for TH and RI activity. However, *O*-linked glycosides are unstable to chemical or biological aqueous hydrolytic fragmentation,[19] and are thus difficult to synthesize, and may be unsuitable for biological applications. Consequently, *C*-linked analogues have been investigated.

2.2 Synthesis and Structure-Function Studies of *C*-Linked AFGP Analogues

The first synthesis of a '*C*-disaccharide,' in which a methylene group replaced the inter-unit oxygen atom, was reported by Rouzaud and Sinaÿ.[20] Since then, many strategies have been developed for the synthesis of *C*-linked glycoconjugates, and these have been extensively reviewed.[21, 22] Conformations of *C*-linked glycosides have been shown to be very close to the corresponding *O*-linked glycosides, and further, bind substrates with nearly identical conformations and affinities.[23] *C*-linked glycosides are therefore good analogues for their *O*-linked counterparts. Due to their stability, *C*-linked antifreeze glycoproteins may prove to be superior cryoprotectants compared to the native glycoproteins. The *C*-linkage also provides greater flexibility than the *O*-linkage does,[24] and this may prove to be a benefit for the AFGP analogues.

Our lab has synthesized a number of rationally designed *C*-linked AFGP analogues using a number of different techniques. The general structure of the analogues is given in Figure 2.4.[25] There are three distinct parts to the AFGP analogues: the carbohydrate

component, the side chain, and the peptide backbone. All three regions can be modified to form structurally diverse AFGP analogues. The "building block" refers to the carbohydrate, side chain, and one amino acid (A1).

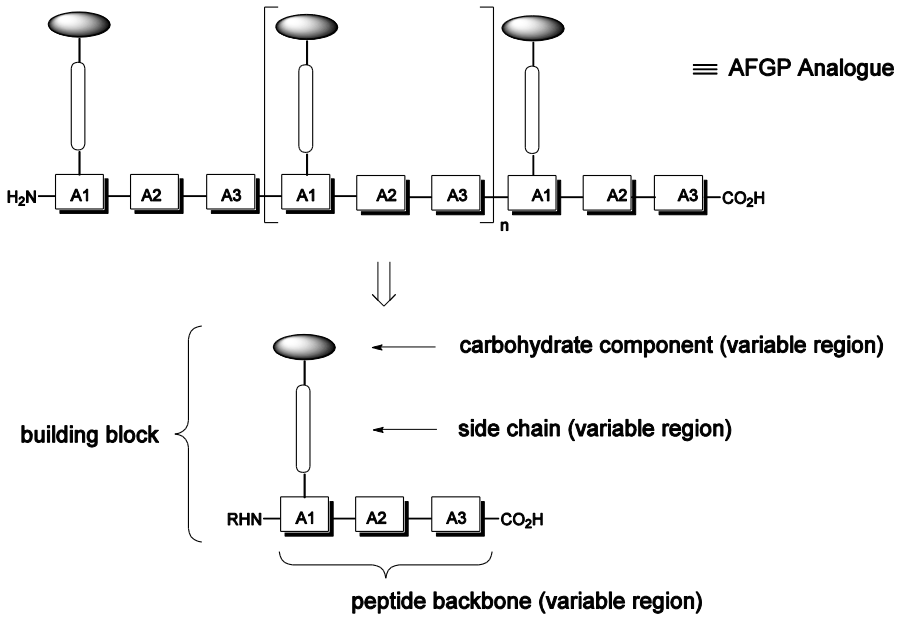

Figure 2.4 Model for AFGP structure-activity relationship studies[25]

Based on the native AFGP structure and this structure-function work, our lab synthesized several series of *C*-linked analogues (Figure 2.5). The first analogues included four tripeptide repeating units in order to resemble the smallest active antifreeze, AFGP 8. Further, the disaccharide was truncated to a monosaccharide, although the α-configuration at the anomeric centre of the native proteins was retained. In order to increase ease of synthesis for this first set of analogues, which were to be a "proof-of-concept", the NAc group was omitted, and the alanine residues in the backbone were replaced with glycine. Interestingly, although Nishimura and co-workers found that removing the NAc group abolished antifreeze activity (as determined by TH measurements), our lab found that their analogues retained good RI activity despite this modification. Lastly, our lab took advantage of the fact that arginine sometimes replaces threonine in native AFGP,[8] and rather than synthesizing *C*-linked threonine, which would entail a lengthy synthesis,[22] a *C*-linked lysine analogue (**15**) that would approximate the structure of arginine, was developed. Replacing lysine with the unnatural amino acid ornithine easily gave the ornithine analogue (**14**) in which the side

chain was shorter by one methylene. The syntheses of both the ornithine (**14**) and lysine (**15**) analogues have been carried out in our lab following a number of different protocols. Subsequently, a serine analogue was developed.[26] The synthesis of this analogue was somewhat more complex, employing catalytic asymmetric hydrogenation.

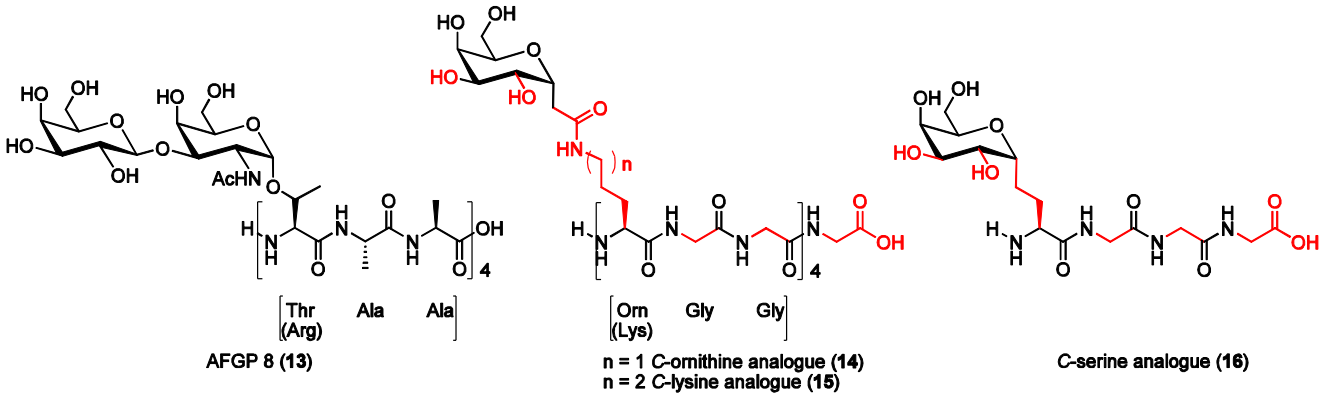

Figure 2.5 AFGP 8 and novel *C*-linked AFGP analogues; the red colour indicates differences between the analogue and AFGP 8.

The antifreeze activity of these novel *C*-linked AFGP analogues was assessed by both TH and RI measurements (the RI data is shown in Figure 2.6)[26-28]. Assessments were carried out according to the protocols given in the experimental section of this document. The *y*-axis depicts the mean largest grain size (MLGS in square millimeters) of ice crystals, measured directly from photographs of the sample. PBS is used as the control since all samples are tested in a PBS solution.

The data indicates that despite the dramatic structural modifications from the native polymer, all analogues showed antifreeze protein-specific activity; however, both TH (data not shown) and RI activity were weaker than the wild-type protein.[27] In fact, the replacement of lysine with ornithine to give analogue **14**, eliminated TH activity (data not shown), and increased RI activity compared to the lysine analogue **15.**

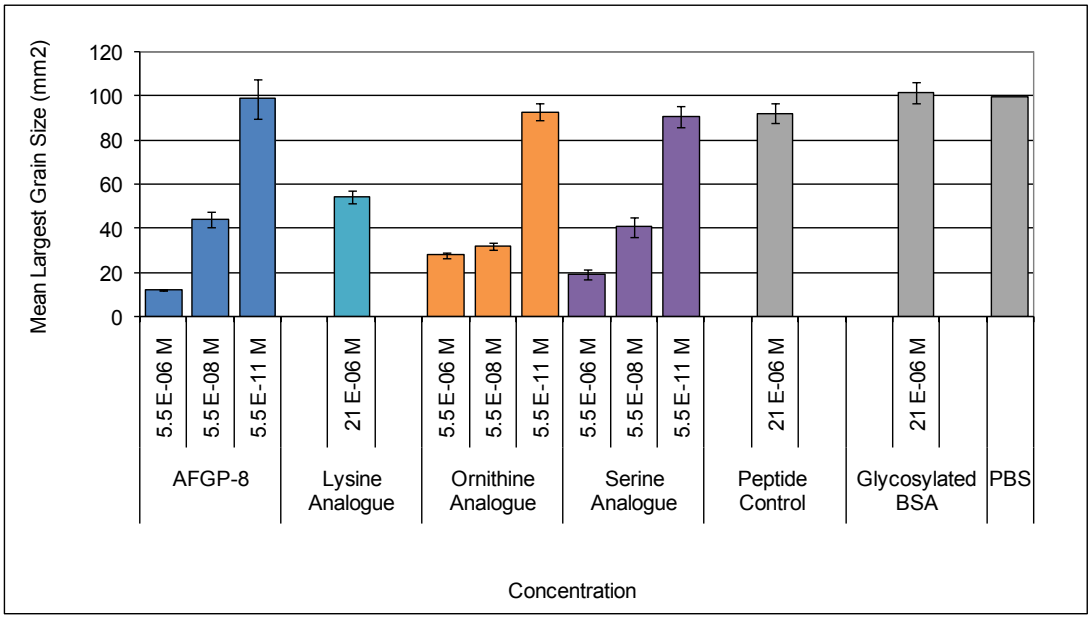

Figure 2.6 RI activity: mean largest grain size of AFGP-8, *C*-linked analogues (**14-16**), and controls at -6.4 °C after 30 min anneal time; error bars indicate SEM

A comparison between the *C*-linked AFGP analogues and AFGP 8 reveals that the lysine analogue (**15**) is only weakly active (i.e. AFGP-8 is approx 90 times more active than the *C*-lysine analogue). The ornithine (**14**) and serine (**16**) analogues showed significantly more activity, although the serine analogue (**16**) showed the best activity. Given the structural modifications of these compounds relative to AFGP-8, the fact that the analogues showed any RI activity was noteworthy. In order to confirm that the activity of the analogues was not the result of a nonspecific RI effect, several controls were examined. The first was a peptide control ((L-lysine-glycine-glycine)$_6$-glycine) composed of 6 tripeptide units analogous to the lysine analogue (**15**), but with no sugars attached to the lysine side chains. The peptide control showed no RI activity compared to the PBS control, highlighting the importance of the carbohydrate residues. This observation is consistent with earlier work demonstrating that the disaccharide residues in native AFGP are crucial to activity.[29] However, commercially available glycosylated BSA (at a concentration of 0.21 mM relative to carbohydrate) similarly showed no RI activity. This suggests that glycosylation is not the only important factor for RI activity. The results of these controls confirm that the antifreeze protein-specific activity observed with each of the *C*-linked analogues is genuine and not the

result of a non-specific RI effect. It seems that, as was the case for the *O*-linked AFGP analogues, there are specific structures that are required for TH and RI activity. It may indeed be that the correct balance and orientation of hydrophobic and hydrophilic residues is critical for TH and RI activity. In order to explore this idea, and given the positive results seen with the early generations of *C*-linked AFGP analogues, new AFGP analogues based on the ornithine analogue (**14**) were explored.

2.3 Hydration of the Carbohydrate Moiety of AFGP Analogues

Based on the encouraging RI data obtained for the ornithine analogue (**14**), coupled with the relative ease of its synthesis compared to that of the serine analogue (**16**), our lab undertook the synthesis of a series of analogues based on the ornithine analogue (**14**) substituted with different monosaccharides, including galactose (**14**), glucose (**18**), mannose (**19**), and talose (**20**) (Figure 2.7).[30] This series of analogues therefore explored the *hydrophilic* component of the AFGPs.

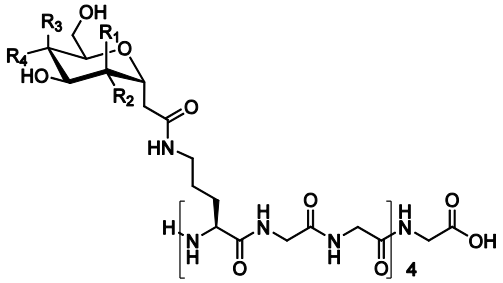

onithine analogue:
14: Gal R_1=H; R_2=OH; R_3=OH; R_4=OH
18: Glc R_1=H; R_2=OH; R_3=H; R_4=OH
19: Man R_1=OH; R_2=H; R_3=H; R_4=OH
20: Tal R_1=OH; R_2=H; R_3=OH; R_4=H

Figure 2.7 Structure of *C*-linked AFGP 8 analogues

Analogues **14**, and **18-20** were tested for recrystallization inhibition (RI) activity, and the data is shown in Figure 2.8. Each sample was tested at three different concentrations to rule out non-specific RI effects. As with the earlier analogues, the results are presented in

comparison to the phosphate buffered saline (PBS) control. Testing for TH was also carried out (data not shown), and it was found that none of the analogues displayed any TH activity.[30]

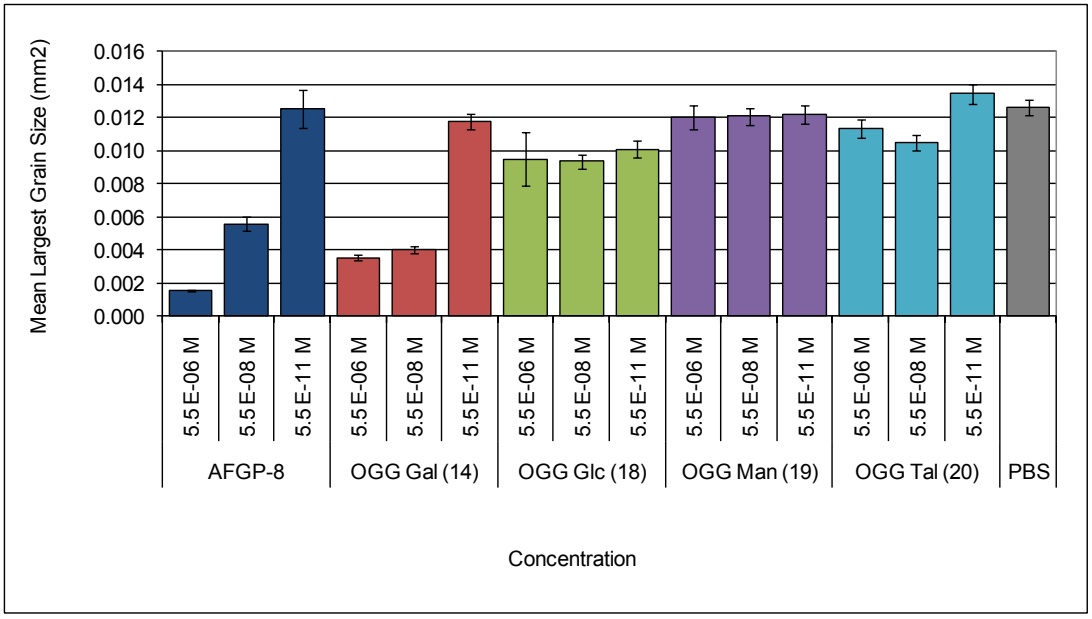

Figure 2.8 RI activity: mean largest grain size of AFGP 8, *C*-linked analogues (**14**, **18**-**20**), and PBS standard at -6.4 °C after 30 min anneal time; error bars indicate SEM

These results provided surprising insight into the role of the hydroxyl groups for RI activity. The mannose and talose analogues (**19** and **20**, respectively) exhibited very weak RI activity with MLGS values similar to PBS. Glucose analogue **18** exhibited moderate RI activity while galactose analogue **14** was the most potent analogue with a MLGS value of 0.00354 mm^2 at 5.54 X 10^{-6} M. We concluded that carbohydrate configuration is very important for RI activity, and that RI activity is maximized when the C4 hydroxyl group is axial and all other hydroxyl groups are in an equatorial position. The trend in RI activity seen with these analogues was found to mirror that found for the *hydration* of their respective carbohydrates.[30]

The hydration numbers of many commercially available hexoses, as well as the partial molar compressibilities, and the partial molar isentropic compressibilities, have been worked out by Galema and co-workers, who correlated them to carbohydrate

stereochemistry.[31-34] Hexoses with the lowest molar compressibility values exhibit the poorest fit in the three-dimensional hydrogen-bonded network of water. The partial molar compressibilities of the monosaccharides galactose (**21**), glucose (**22**), mannose (**23**), and talose (**24**) are given in Figure 2.9. In general, these values relate to the volume of space occupied by a molecule upon hydration by water and quantify the "compatibility" of a carbohydrate with the three-dimensional hydrogen-bonded network of bulk water.

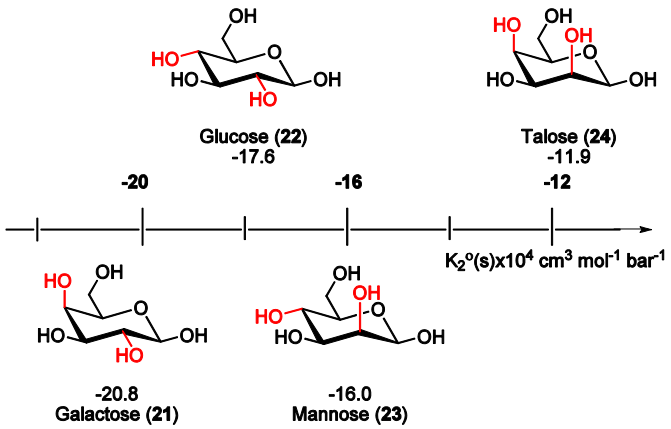

Figure 2.9 Partial molar compressibilities of monosaccharides in aqueous solution at 298 K (K_2° (s) x 10^4, cm^3 mol^{-1} bar^{-1}); values are given for the dominant conformer in solution

Given this data, it appeared that the compatibility of a hexose with the three-dimensional hydrogen-bonded network of water is inversely proportional to its recrystallization-inhibition activity.[30] Indeed, the molar compressibility of these sugars could be correlated to the RI activity of the polymers; that is, the lower the molar compressibility (and hence, the worse the "fit" into the three-dimensional hydrogen-bonded network of water), the better the RI activity. Unfortunately, the hydration of *C*-linked carbohydrate derivatives has not been studied in detail. However, the hydration characteristics between an *O*-linked pyranose and a *C*-linked pyranose are not expected to differ, and in a subsequent paper, our lab showed that *C*-linked derivatives of monosaccharides appear to parallel the RI activity of their *O*-linked native structures.[35]

This correlation between RI activity and the hydration of the carbohydrate led to the speculation that recrystallization-inhibitors (biological antifreezes or our *C*-linked AFGP

analogues) may function by disturbing the highly ordered structure of supercooled water.[30] Therefore, our lab surveyed the RI activity of several simple mono- and disaccharides on their own, in order to further explore the relationship between the hydration of carbohydrates and RI activity.[35]

2.4 Recrystallization Inhibition (RI) Activity of Carbohydrates

Our lab studied four monosaccharides (galactose, glucose, mannose, and talose) and five disaccharides (melibiose, lactose, maltose, trehalose, and sucrose) in terms of their RI activity (Figure 2.10).[35]

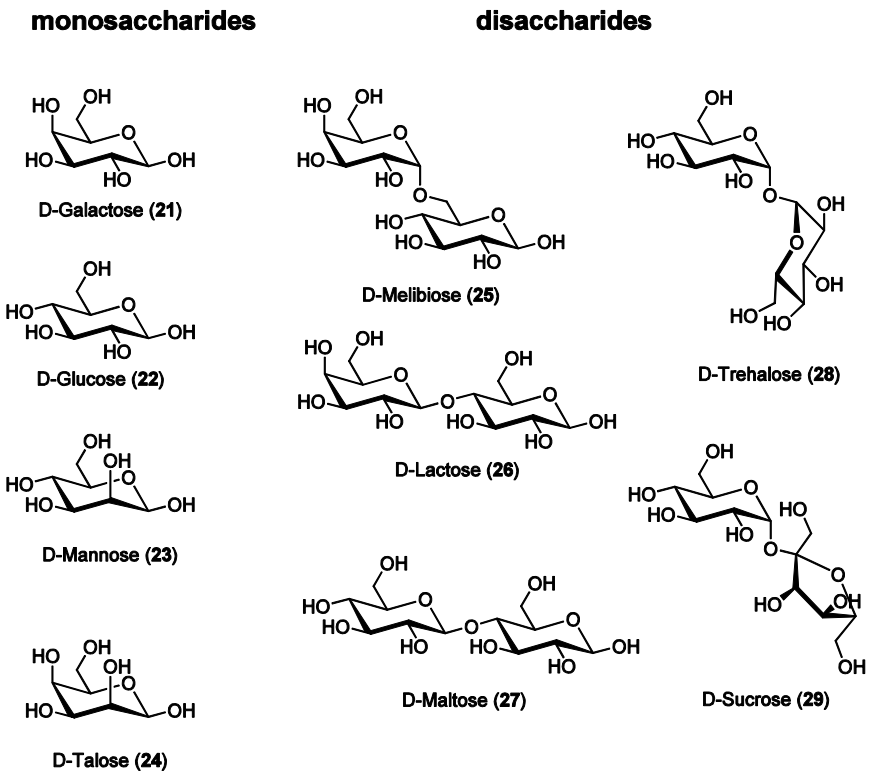

Figure 2.10 Monosaccharides and disaccharides assessed for recrystallization-inhibition activity by Tam and co-workers[35]

The RI activity was tested at several concentrations of galactose (21), and interestingly, it was found that at higher concentrations, the RI activity of galactose seemed

to be non-colligative, as has been observed for biological antifreezes (data not shown). Due to practical consideration, RI activity of the remaining carbohydrates was assessed using carbohydrate concentrations of 0.022 M in PBS.

In order to account for the difference in steric volume between monosaccharides and disaccharides, our lab recorded the RI activity of each sugar in relation to the hydration *index*, rather than in relation to the hydration *number*. They obtained the hydration index by dividing the hydration numbers of each carbohydrate (obtained from the literature) by the partial molar volumes. Therefore, the hydration index is a description of the number of tightly bound water molecules per molar volume of carbohydrate. The graph of RI activity of carbohydrates versus their hydration index is given in Figure 2.11.[35]

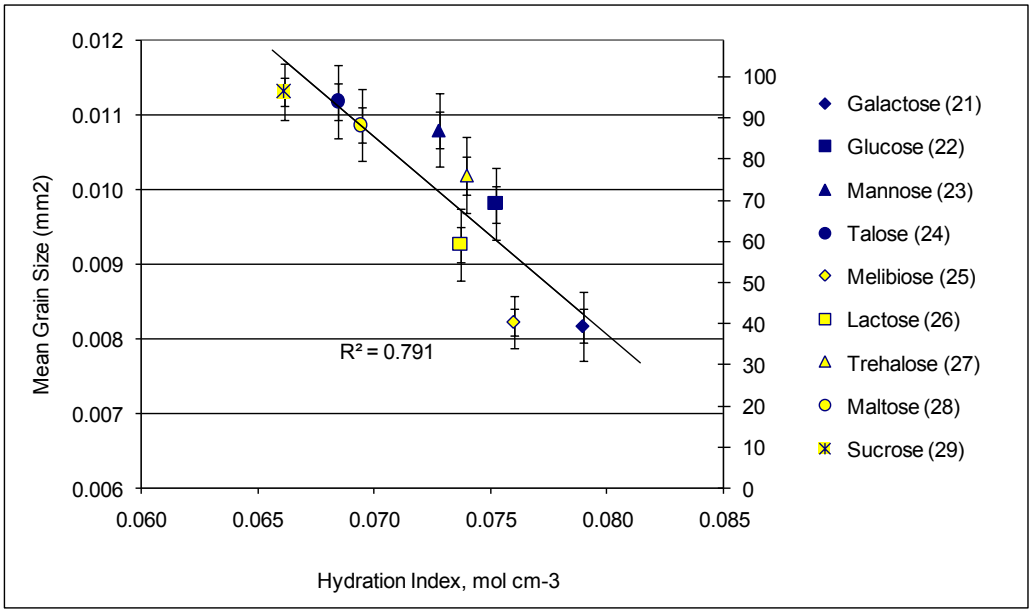

Figure 2.11 RI activities of carbohydrates (**21-29**) plotted against their respective hydration index (hydration number/partial molar volume) ($mol^{1}cm^{-3}$)

Our lab concluded that the hydration of a carbohydrate is correlated to RI activity, and that the hydration index modulates the ability of a sugar to function as a potent recrystallization inhibitor. Further, our lab compared the RI activity of galactose with various concentrations of DMSO, and showed that a 0.022 M solution of galactose is as efficient at

inhibiting recrystallization as a 3% (v/v) DMSO solution (Figure 2.12). We believe that these results suggest that galactose may be a suitable cryoprotectant.[35]

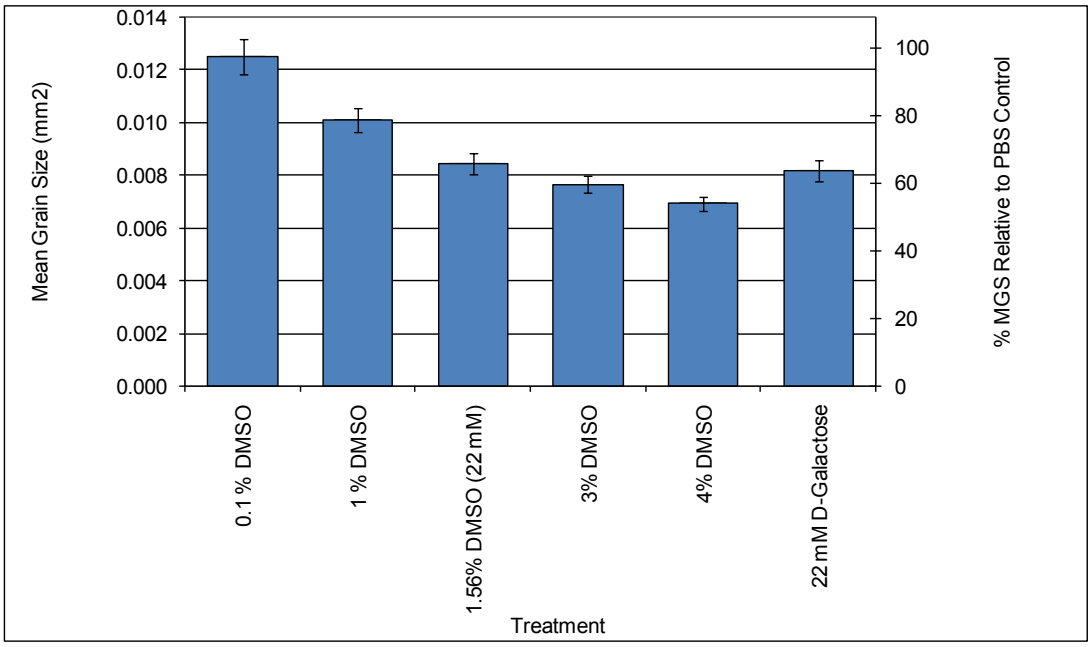

Figure 2.12 RI activity of various concentrations of DMSO and 0.022 M solutions of D-galactose in PBS solution

To compliment the physical structure-function work, our lab began to study the behavior of native AFGP 8 and *C*-linked AFGP 8 analogues in mammalian cells.

2.5 *In vitro* Effects and Cellular Interactions of a *C*-linked AFGP 8 Analogue and native AFGP 8

Since these analogues are intended for use in human applications, the potential for cytotoxicity had to be investigated. Consequently, our lab described the *in vitro* effects and cellular interactions of the serine analogue (**16**), and native AFGP 8 (**13**).[36] Using the MTT cell viability assay,[37] we determined that AFGP 8 is cytotoxic to human embryonic liver cells (WRL 68 cell line)[38] and human embryonic kidney cells (HEK 293 cell line)[36] at concentrations higher than 2 mg/mL and 0.63 mg/mL, respectively. Lower concentrations were not toxic. The broad implications of this observation are that the cytotoxicity of AFGP

8 is not only concentration-dependent but also cell specific. Interestingly, the serine analogue (**16**) did not appear to be cytotoxic to WRL 68 cells even at concentrations as high as 5 mg/mL.

To assess whether the difference in cytotoxicity in human cells was due to selective internalization, our lab studied the internalization of AFGP 8 and the serine analogue (**16**) in WRL 68 cells and a fish cell line (Rtgill-W1)[36] using fluorescently labeled glycoproteins and confocal microscopy. Fluorescently labeled AFGP 8 (F-AFGP 8) and the serine analogue **16** (F-**16**) were prepared by labeling the *N*-terminus of the glycopeptide with Oregon Green 488 (the glycoproteins therefore appear green), and the red membrane stain RH-237 was used as the counter stain. We found that both cell types readily internalized AFGP 8 and the serine analogue (**16**) into the cytoplasmic space after only 10 min of incubation at physiological temperatures (Figures 2.13a and 2.13b). However, there was no evidence of internalization when WRL 68 cells were treated with fluorescently labeled AFGP 8 or the serine analogue at 0 °C (Figure 2.13c).

As was discussed in chapter 1, cell death can be generally classified into two categories: necrosis and apoptosis.[39] During live cell imaging, changes in cell morphology consistent with an apoptotic mechanism of cell death were seen. These changes included nuclear blebbing and the punctate appearance of cell membranes.[40]

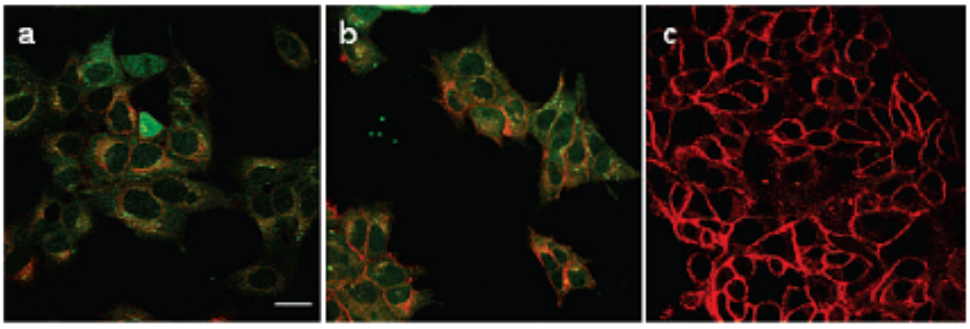

Figure 2.13 Internalization study of fluorescently labeled AFGP 8 (F-AFGP 8) and fluorescently labeled serine analogue 16 (F-**16**) in human embryonic liver cells (WRL 68 cell line); WRL 68 cells were incubated with 10 μM RH-237 membrane probe solution in Eagle's minimum essential medium (EMEM) and 1.5 mg/mL F-AFGP 8 or F-**16**, solution in EMEM. F-AFGP 8 and F-**16** appear green, and RH-237 appears red; (A) WRL 68 cells were incubated with F-AFGP 8 at 37 °C for 10 min; (B) WRL 68 cells were incubated with F-**16**, at 37 °C for 10 min; (C) WRL 68 cells were incubated with F-AFGP 8 at 0 °C for 50 min; the scale bar = 25 μm

To confirm whether cell death was occurring via apoptosis, we performed a caspase-3/7 assay that specifically identifies whether effector caspases 3 and 7 are activated (data not shown). Once these effector caspases are activated, the cell is thought to be committed to the apoptotic pathway. The incubation of WRL 68 cells for 18 h with 5 mg/mL AFGP 8 resulted in significantly increased caspase-3/7 activity relative to the negative control. As expected, this activity increased with time. The results indicate that the treatment of WRL 68 cells with AFGP 8 resulted in the conversion of pro-caspases 3 and 7 into active caspases 3 and 7, suggesting that AFGP 8 is initiating an apoptotic process. This result was independently confirmed using the Vybrant apoptosis assay. For this assay, WRL 68 cells were incubated with three different fluorescent nucleic acid stains: YO-PRO-1, propidium iodide, and Hoechst 33342. YOPRO- 1 stains apoptotic cells green, propidium iodide stains only dead or late apoptotic cells red, and Hoechst 33342 stains both apoptotic cells and live, healthy cells blue, but does not stain necrotic cells. Apoptotic cells are confirmed visually with both green and blue fluorescent stains. Staurosporine, a known inducer of apoptosis, was used as a positive control. After the incubation of human liver cells with 5 mg/mL AFGP 8 for 4 h, most cells were stained green and blue, which indicated that the cells were undergoing apoptosis (Figure 2.14).

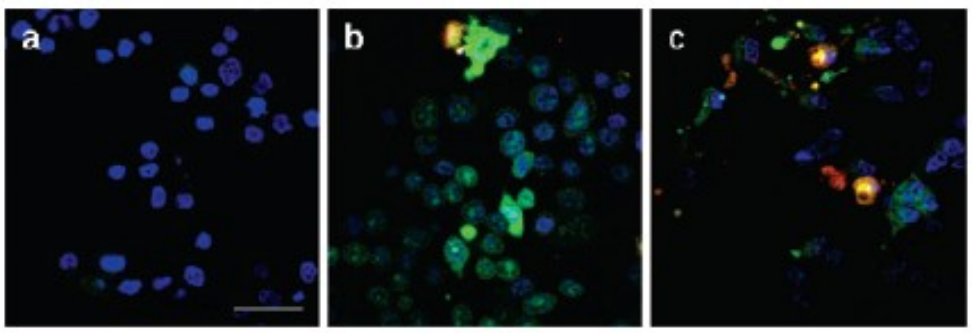

Figure 2.14 Vybrant apoptosis assay of WRL 68 cells incubated with AFGP 8; WRL 68 cells were incubated with 8.1 μM Hoechst 33342, 1.5 μM propidium iodide and 0.1 μM YO-PRO-1 solutions in Eagle's minimum essential medium (EMEM) at 0 °C for 30 min.; Hoechst 33342 stains the nuclei of all cells blue; propidium iodide stains dead cells and late apoptotic cells red; YO-PRO-1 stains early apoptotic cells green; (A) negative control: WRL 68 cells were pre-incubated with EMEM; (B) WRL 68 cells were pre-incubated with 5 mg/mL AFGP 8 solution in EMEM at 37 °C for 4 h; (C) WRL 68 cells were pre-incubated with 20 μM staurosporine solution in EMEM at 37 °C for 4 h; the scale bar = 50 μm

In the negative control, cells were only stained by the blue Hoechst 33342 dye. In the staurosporine-treated control, a large number of cells were stained green and blue as well as red, identifying them as late apoptotic or dead cells. The consequences of the data from the caspase 3/7 assay, and the Vybrant apoptosis assay are that despite the many useful antifreeze properties of AFGP 8, the *in vitro* cytotoxicity will dramatically affect the future use of native AFGP 8 for cryoprotection and hypothermic storage.

Caspase-3/7 levels were also assessed after the treatment of human liver cells with the serine analogue (**16**). After incubation, caspase-3/7 levels in WRL 68 cells did not climb above the negative controls. In fact, caspase-3/7 levels remained significantly lower in cells treated with the serine analogue (**16**) compared to the levels in untreated cells. This was not surprising because this analogue failed to display any *in vitro* cytotoxicity. However, it was surprising that caspase-3/7 activity in human liver cells treated with the serine analogue (**16**) was actually depressed well below that of background activity. Furthermore, this effect occurred in the presence of 2% DMSO (which was used to solubilize staurosporine and was therefore added to all wells). This result suggests that the serine analogue (**16**) possesses caspase-inhibitory activity. The fact that **16** is a potent inhibitor of recrystallization and also appears to suppress caspase activity is extremely encouraging. In fact, recent studies have shown that the addition of caspase inhibitors can prevent cold-induced apoptosis from occurring upon low-temperature preservation of cells.[39, 41] Therefore, AFGP analogue **16** shows tremendous promise as a cryoprotectant since it may also be effective at preventing cold-induced apoptosis. The question remains whether or not the AFGP 8 analogues synthesized in our lab could in fact function as effective cryopreservation agents. As a result of the work by our lab discussed here, we set out the following goals and objectives.

2.6 Project Goals

Goal 1: Design of New *C*-Linked AFGP 8 Analogues

Two series of analogues will be synthesized in order to investigate the importance of the hydrophobicity of *C*-linked AFGP analogues to RI activity.

Objective 1.1: Investigating the Importance of Hydrophobicity of C-Linked AFGP 8 Analogues to Recrystallization Inhibition (RI) Activity (Series I Analogues)

As has been detailed in this chapter, AFP Type I and AFGPs are amphiphilic - the hydrophobic portions of the polymer are found on one side of the helix, and the hydrophilic elements on the other. Further, it has been shown that the γ-methyl groups of the Thr residues of AFGPs are important for antifreeze activity. To date, the analogues synthesized by our lab have not possessed this hydrophobic component. In order to try to gain a better understanding of the involvement of hydrophobic effects for RI, we developed a new series of AFGP analogues that possess a variety of hydrophobic groups in the pseudo-anomeric position. The overall structure of these new analogues is based on ornithine analogue (**14**, Figure 2.15). For analogue **14**, ornithine was chosen as the linker portion of the polymer since it is a structural mimetic of the amino acid arginine that sometimes replaces threonine in the native protein. The placement of the hydrophobic groups in this new series is an attempt to "re-introduce" the γ-methyl group of threonine to the ornithine analogue (**14**). The evolution of the AFGP 8 analogues is shown in Figure 2.15. The new compounds (**30b-j**) will constitute series 1. The change of only one element of the ornithine analogue (**14**) was important in order to limit the factors that could be attributed to any differences in RI activity seen amongst the new analogues, and between the new analogues and the ornithine analogue (**14**).

We hypothesize that the re-introduction of the hydrophobic elements to the ornithine analogue (to give **30b-j**) will lead to an increase in RI activity over that of the ornithine

analogue (**14**/**30a**). We expect that the RI activity will increase with increased hydrophobicity of the R group (**30b-f, j**). The changes in the electronics of the R group (**30g-i**) are unprecedented. We speculate that the partial charges on both the electron-donating and electron-withdrawing elements will have a negative effect on the RI activity, and decrease the RI activity of these compounds compared to their neutral counterpart **30e** (and **30f**).

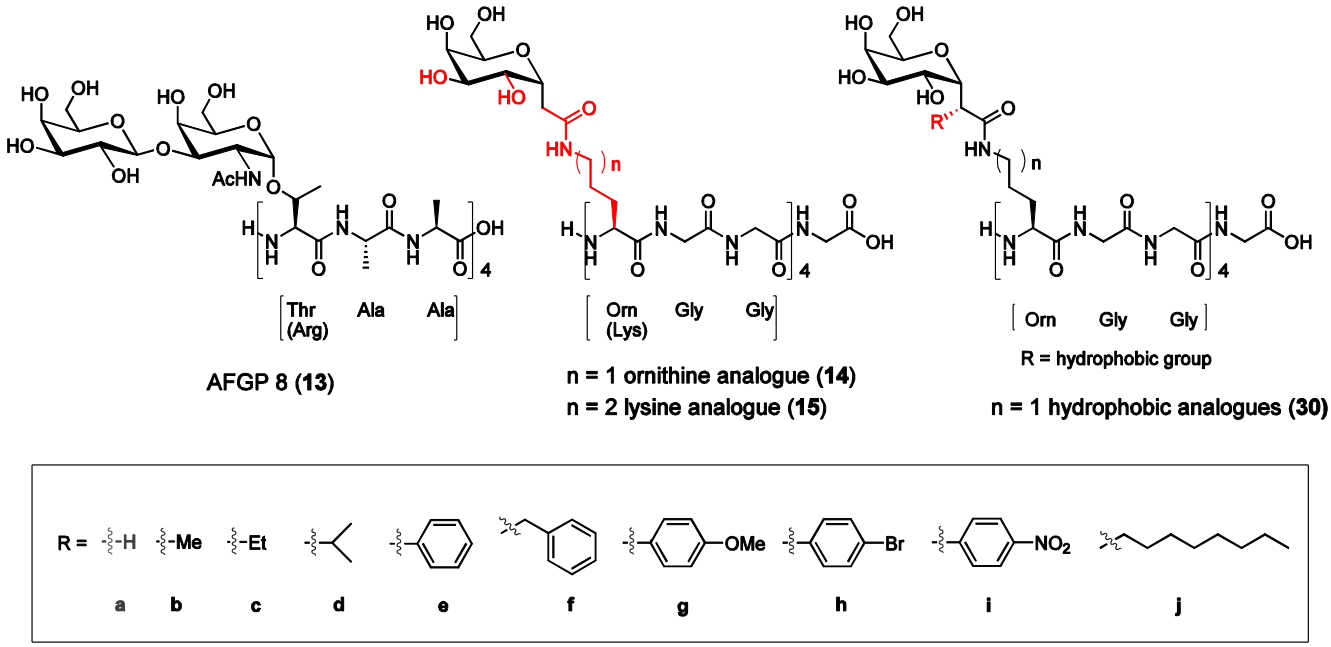

Figure 2.15 The evolution of the AFGP 8 analogues that led to the synthesis of the hydrophobic analogues 30 (series 1 analogues)

Objective 1.2: Investigating the Importance of Hydration of the AFGP 8 Analogues to Recrystallization Inhibition (RI) Activity (Series II Analogues)

It is also of interest to synthesize the closely related AFGP analogues **31-34** shown in Figure 2.16. These will constitute series 2. With series 1, we were primarily interested in investigating what effects various hydrophobic groups would have on the antifreeze activity of the analogue. With this second series, the *hydration* of the polymers was manipulated. As discussed previously in this chapter, the studies published by Tam *et al.*[35] and Czechura *et al.*[30] showed that the orientation of the C2 and C4 hydroxyl groups of *C*-linked carbohydrate derivates and polymers can be directly correlated to their recrystallization ability. We were

therefore interested in manipulating the hydroxyl groups on the carbohydrates of our analogues, and this second series is missing the C2 and C3 hydroxyl groups. The absence of the hydroxyl group at C2 could mean that this series of analogues will have a worse "fit" into the three-dimensional hydrogen-bonded network of water, that is, poorer hydration, than the ornithine analogue, and this modification may therefore increase RI activity. In order to compare this second series of analogues with the ornithine analogue as well as the Series I analogues, we similarly planned to introduce a variety of hydrophobic groups at the pseudo-anomeric position. The dehydroxy analogues **31** and **32**, and the unsaturated dehydroxy analogues **33** and **34** are expected to be accessible from a common intermediate; therefore, the synthesis of the various analogues of this series should be readily accomplished. The double bond in **33** and **34** will change the conformation of the carbohydrate moiety, and it is of interest to see what effect, if any, this difference in conformation will have on antifreeze activity.

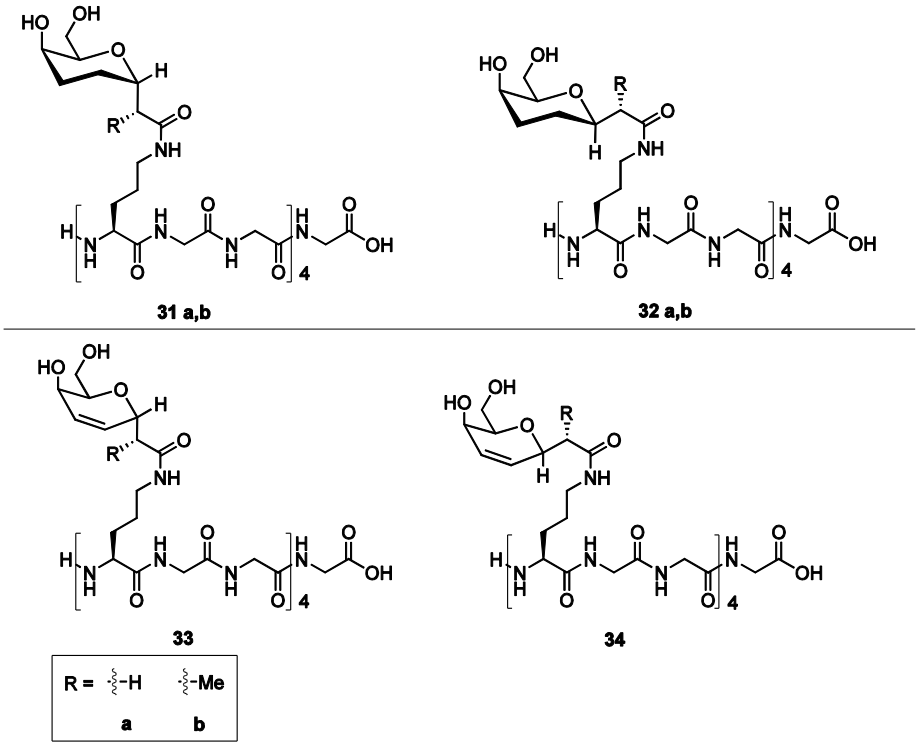

Figure 2.16 Series two analogues

Goal 2: Investigating the Cryopreservation Potential of the Ornithine Analogue and Several Carbohydrates *in Vitro*

Objective 2.1: Assessing the Cryopreservation Activity of Carbohydrates

Based on the extensive work done by our lab on the effect of hydration of carbohydrates on RI, we sought to investigate the cryopreservation potential of several carbohydrates, representing a spectrum of RI activity. We chose to test four monosaccharides (galactose, glucose, 3-*O*-methylglucose, and talose) and four disaccharides (melibiose, lactose, trehalose, and sucrose). Post-thaw analysis using the appropriate assays together with flow cytometry, allows the enumeration of viable, early apoptotic, and late apoptotic/necrotic cells. Since the use of sugars in the cryopreservation medium can enhance the cryopreservation potential and/or allow the amount of DMSO required for successful cryopreservation to be reduced, we will also evaluate the cryopreservation ability of combinations of carbohydrates and DMSO, with the objective of developing a cryopreservation protocol optimized for both type and concentration of carbohydrate, as well as the concentration of DMSO employed. We hypothesize that RI activity will correlate positively with cryopreservation activity: that is, the better the RI activity of a carbohydrate, the greater the number of viable cells after freeze-thaw. For the reasons outlined in chapter 1, the cryopreservation of hepatocytes and hematopoietic stem cells from umbilical cord blood is of particular interest, and we therefore used these cell types for our *in vitro* studies.

Objective 2.2: Assessing the Cryopreservation Activity of the Ornithine Analogue

Since our work is based on the ornithine analogue, we were interested in testing this analogue, as well as the native compound, AFGP 8, for their cryopreservation activity *in vitro*. As for the carbohydrate studies outlined in objective 2.1, we will employ hepatocytes and hematopoietic stem cells from umbilical cord blood for our *in vitro* studies.

1. Chou, K.-C., Energy-optimized structure of antifreeze protein and its binding mechanism. *Journal of Molecular Biology* **1992,** 223, 509-517.
2. Chao, H.; Jr., M. E. H.; Hodges, R. S.; Kay, C. M.; Sykes, B. D.; Loewen, M. C.; Davies, P. L.; Soennichsen, F. D., A diminished role for hydrogen bonds in antifreeze protein binding to ice. *Biochemistry* **1997,** 36, 14652-14660.
3. Haymet, A. D. J.; Ward, L. G.; Harding, M. M.; Knight, C. A., Valine substituted winter flounder 'antifreeze': preservation of ice growth hysteresis. *FEBS Letters* **1998,** 430, 301-306.
4. Zhang, W.; Laursen, R. A., Structure-function relationship in a type I antifreeze polypeptide: the role of threonine methyl and hydroxyl groups in antifreeze activity. *The Journal of Biological Chemistry* **1998,** 273, 34806-34812.
5. Haymet, A. D. J.; Ward, L. G.; Harding, M. M., Winter flounder "antifreeze" proteins: synthesis and ice growth inhibition of analogues that probe the relative importance of hydrophobic and hydrogen-bonding interactions. *Journal of the American Chemical Society* **1999,** 121, 941-948.
6. Rubinsky, B.; Arav, A.; Fletcher, G. L., Hypothermic protection - a fundamental property of "antifreeze" proteins. *Biochemical and Biophysical Research Communications* **1991,** 180, 566-571.
7. Harding, M. M.; Ward, L. G.; Haymet, A. D. J., Type I 'antifreeze' proteins: structure-activity studies and mechanisms of ice growth inhibition. *European Journal of Biochemistry* **1999,** 264, 653-665.
8. Harding, M. M.; Anderberg, P. I.; Haymet, A. D. J., 'Antifreeze' glycoproteins from polar fish. *European Journal of Biochemistry* **2003,** 270, 1381-1392.
9. Vandenheede, J. R.; Ahmed, A. I.; Feeney, R. E., Structure and role of carbohydrate in freezing point-depressing glycoproteins from an antarctic fish. *The Journal of Biological Chemistry* **1972,** 247, 7885-7889.
10. Osuga, D. T.; Feather, M. S.; Shah, M. J.; Feeney, R. E., Modification of galactose and *N*-acetylgalactosamine residues by oxidation of C-6 hydroxyls to the aldehydes followed by reductive amination: model systems and antifreeze glycoproteins. *Journal of Protein Chemistry* **1989,** 8, 519-528.
11. DeVries, A. L., Glycoproteins as biological antifreeze agents in Antarctic fishes. *Science* **1971,** 172, 1152-1155.
12. Ahmed, A. I.; Yeh, Y.; Osuga, D. T.; Feeney, R. E., Antifreeze glycoproteins from antarctic fish: inactivation by borate. *The Journal of Biological Chemistry* **1976,** 251, 3033-3036.
13. Feeney, R. E.; Osuga, D. T.; Yeh, Y., Effect of boronic acids on antifreeze proteins. *Journal of Protein Chemistry* **1991,** 10, 167-170.
14. Schrag, J. D.; O'Grady, S. M.; DeVries, A. L., Relationship of amino acid composition and molecular weight of antifreeze glycopeptides to non-colligative freezing point depression. *Biochimica et Biophysica Acta* **1982,** 717, 322-326.
15. Geoghegan, K. F.; Osuga, D. T.; Ahmed, A. I.; Yeh, Y.; Feeney, R. E., Antifreeze glycoproteins from frozen fish: structural requirements for function of glycopeptide 8. *The Journal of Biological Chemistry* **1980,** 255, 663-667.
16. Tachibana, Y.; Fletcher, G. L.; Fujitani, N.; Tsuda, S.; Monde, K.; Nishimura, S.-I., Antifreeze glycoproteins: elucidation of the structural motifs that are essential for antifreeze activity. *Angewandte Chemie International Edition* **2004,** 43, 856-862.

17. Heggemann, C.; Budke, C.; Schomburg, B.; Majer, Z.; Wissbrock, M.; Koop, T.; Sewald, N., Antifreeze glycopeptide analogues: microwave-enhanced synthesis and functional studies. *Amino Acids* **2009**.
18. Knight, C. A.; Hallett, J.; DeVries, A. L., Solute effects on ice recrystallization: An assessment technique. *Cryobiology* **1988,** 25, 55-60.
19. Wang, J.; Kovac, P.; Sinay, P.; Glaudemans, C. P. J., Synthetic C-oligosaccharides mimic their natural, analogous immunodeterminants in binding to three monoclonal immunoglobulins. *Carbohydrate Research* **1998,** 308, 191-193.
20. Rouzaud, D.; Sinay, P., The fist synthesis of a '*C*-disaccharide'. *Journal of the Chemical Society, Chemical Communications* **1983**, 1353-1354.
21. Dondoni, A.; Marra, A., Methods for anomeric carbon-linked and fused sugar amino acid synthesis: the gateway to artificial glycopeptides. *Chemical Reviews* **2000,** 100, 4395-4421.
22. Moos, E. v.; Ben, R. N., Recent advances in the synthesis of *C*-linked glycoconjugates. *Current Topics in Medicinal Chemistry* **2005,** 5, 1351-1361.
23. Ravishankar, R.; Surolia, A.; Vijayan, M.; Lim, S.; Kishi, Y., Preferred conformation of *C*-lactose at the free and peanut lectin bound states. *Journal of the American Chemical Society* **1998,** 120, 11297-11303.
24. Espinosa, J.-F.; Canada, F. J.; Asensio, J. L.; Martin-Pastor, M.; Dietrich, H.; Martin-Lomas, M.; Schmidt, R. R.; Jimenez-Barbero, J., Experimental evidence of conformational differences between *C*-glycosides and *O*-glycosides in soultion and in the protein-bound state: the *C*-lactose/*O*-lactose case. **1996,** 118, 10862-10871.
25. Ben, R. N.; Eniade, A. A.; Hauer, L., Synthesis of a *C*-linked antifreeze glycoprotein (AFGP) mimic: probes for investigating the mechanism of action. *Organic Letters* **1999,** 1, 1759-1762.
26. Liu, S.; Ben, R. N., *C*-linked galactosyl serine AFGP analogues as potent recrystallization inhibitors. *Organic Letters* **2005,** 7, 2385-2388.
27. Eniade, A.; Purushotham, M.; Ben, R. N.; Wang, J. B.; Horwath, K., A serendipitous discovery of antifreeze protein-specific activity in C-linked antifreeze glycoprotein analogs. *Cell Biochemistry and Biophysics* **2003,** 38, 115-124.
28. Chaytor, J., Unpublished Results. In.
29. Feeney, R. E.; Yeh, Y., Antifreeze Proteins from Fish Bloods. *Advances in Protein Chemistry* **1978,** 32, 191-282.
30. Czechura, P.; Tam, R. Y.; Dimitrijevic, E.; Murphy, A. V.; Ben, R. N., The importance of hydration for inhibiting ice recrystallization with C-linked antifreeze glycoproteins. *Journal of the American Chemical Society* **2008,** 130, 2928-2929.
31. Dashnau, J. L.; Sharp, K. A.; Vanderkooi, J. M., Carbohydrate intramolecular hydrogen bonding cooperativity and its effect on water structure. *Journal of Physical Chemistry B* **2005,** 109, 24152-24159.
32. Galema, S. A.; Hoiland, H., Stereochemical aspects of hydration of carbohydrates in aqueous solutions. 3. Density and ultrasound measurements. *Journal of Physical Chemistry* **1991,** 95, 5321-5326.
33. Galema, S. A.; Engberts, J. B. F. N.; Hoiland, H.; Forland, G. M., Informative thermodynamic properties of the effect of stereochemistry on carbohydrate hydration. *Journal of Physical Chemistry* **1993,** 97, 6885-6889.

34. Galema, S. A.; Howard, E.; Engberts, J. B. F. N.; Grigera, J. R., The effect of stereochemistry upon carbohydrate hydration. A molecular dynamics simulation of β-D-galactopyranose and (α, β)-D-talopyranose. *Carbohydrate Research* **1994,** 265, 215-225.
35. Tam, R. Y.; Ferreira, S. S.; Czechura, P.; Chaytor, J. L.; Ben, R. N., Hydration index: a better parameter for explaining small molecule hydration in inhibition of ice recrystallization. *Journal of the American Chemical Society* **2008,** 130, 17494-17501.
36. Liu, S.; Wang, W.; von Moos, E.; Jackman, J.; Mealing, G.; Monette, R.; Ben, R. N., *In vitro* studies of antifreeze glycoprotein (AFGP) and a *C*-linked AFGP analogue. *Biomacromolecules* **2007,** 8, 1456-1462.
37. The details of the MTT viability assay are given in Chapter 4, and in the Appendix.
38. The details of the WRL 68 cell line are given in Chapter 4.
39. Baust, J. M., Molecular mechanisms of cellular demise associated with cryopreservation failure. *Cell Preservation Technology* **2002,** 1, 17-31.
40. Shi, Y., A structural view of mitochondria-mediated apoptosis. *Nature Structural Biology* **2001,** 8, (5), 394-401.
41. Stroh, C.; Cassens, U.; Samraj, A. K.; Sibrowski, W.; Schulze-Osthoff, K.; Loss, M., The role of caspases in cryoinjury: caspase inhibition strongly improves the recovery of cryopreserved hematopoietic and other cells. *The FASEB Journal* **2002,** 16, 1651-1653.

Chapter 3: Design of New *C*-Linked AFGP 8 Analogues

Part 1: Preparation of *C*-Linked Analogues

The synthetic strategies towards the antifreeze glycoprotein (AFGP) 8 analogues outlined in the objectives of Chapter 2 are given in this chapter. The retrosynthetic strategies for each analogue, as well as the synthesis steps carried out are detailed. Following, the antifreeze activity of the synthesized analogues is presented and analyzed.

3.1. Retrosynthetic Analysis

3.1.1. Investigating the Importance of Hydrophobicity of the AFGP 8 Analogues to Recrystallization Inhibition (RI) Activity (Series I Analogues)

The first objective was to explore what effect manipulating the hydrophobicity of AFGP 8 analogues would have on antifreeze activity, and specifically what effect it would have on recystallization inhibition (RI) activity. As outlined in Chapter 2, in order to pursue this objective we designed AFGP 8 analogues into which we could incorporate various hydrophobic groups. The retrosyntheses for the AFGP 8 analogues of Series I are presented in Scheme 3.1. The general structure of the Series I AFGP 8 analogues is given by compounds **30** and **40**. The desired polymer **30** (or **40**) can be prepared using solid-phase synthesis by the sequential addition of either Fmoc-protected *C*-glycosyl amino acid building block **35** (or **41**), or Fmoc-protected glycine. Building blocks **35** (and **41**) should be available

from the direct displacement of the auxiliary from compounds **36** (or **42**), respectively, using the amine of the protected amino acid **37**.

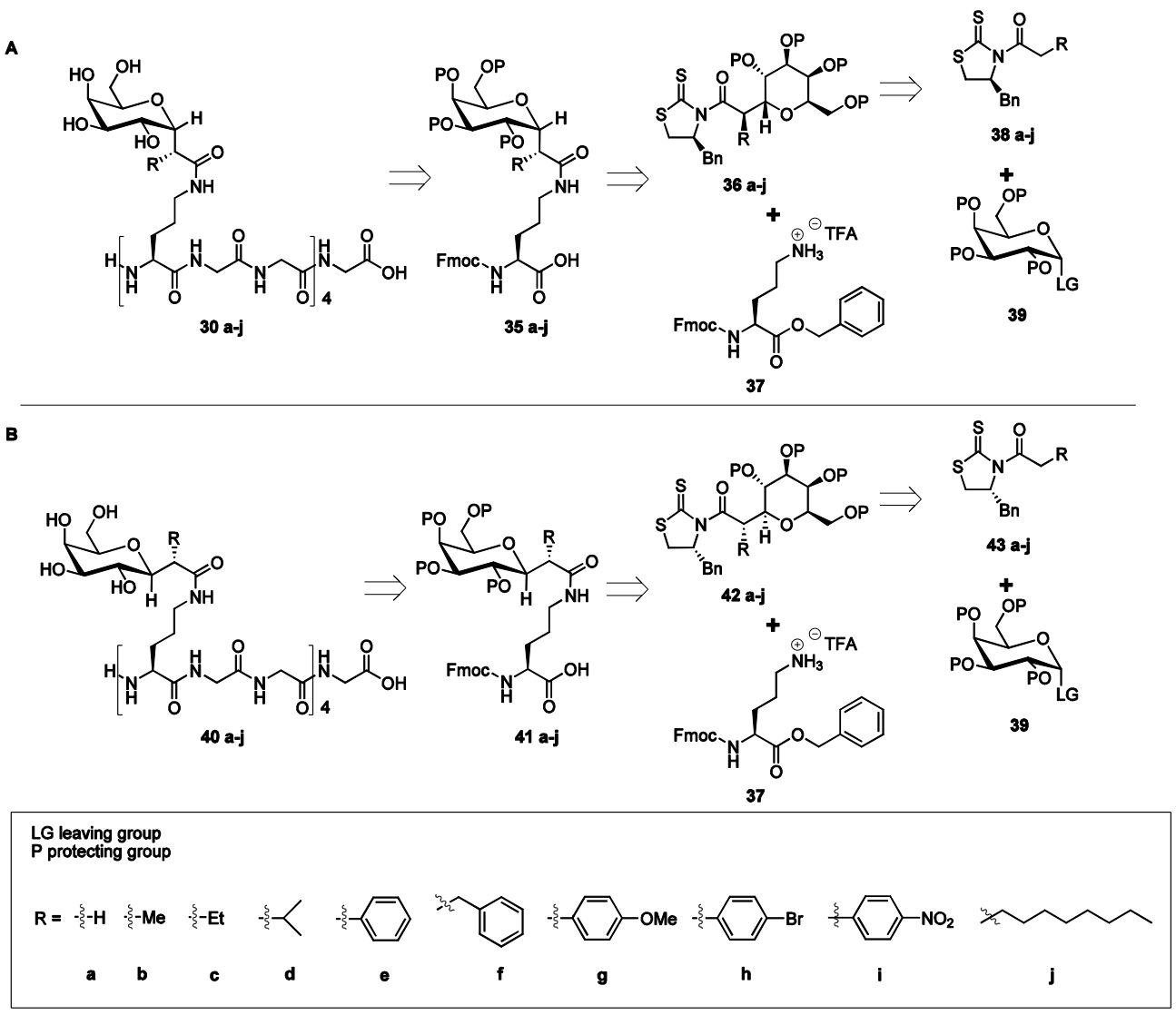

Scheme 3.1 Retrosynthesis of Series I AFGP 8 analogues; A α-series (R = H is the ornithine analogue); B β-series

The protected amino acid (**37**) has been previously synthesized by our lab, and is available by selective protection and deprotection steps from commercially available Fmoc- and Boc-protected ornithine. The hydrophobic groups will be introduced stereoselectively at the 1' position of the carbohydrate (pseudo-anomeric position) with the use of a chiral 1,3-

thiazolidine-2-thione-derived titanium enolate **38** (or **43**). The chiral auxiliary will also allow the stereoselective formation of the desired α-linkage or β-linkage. This approach is based on methodology developed by Urpi and co-workers shown in Scheme 3.2.[1, 2] Urpi and co-workers showed that Lewis-acid mediated addition of chiral titanium enolates to glycals provides either the α- or β-1'-methyl-substituted *C*-glycosides. This methodology proved to be highly stereoselective. As shown in Scheme 3.2, when the (S)-auxiliary (**42**) was used in a reaction with protected glycal (**41**), the α-linked 1'-methyl-substituted *C*-glycoside **43** was obtained in 70% yield with a diastereomeric ratio of 99:1. The same reaction with the (R)-auxiliary (**40**) provided the β-1'-methyl-substituted *C*-glycoside **39** in 71% yield with a diastereomeric ratio of 99:1.[2]

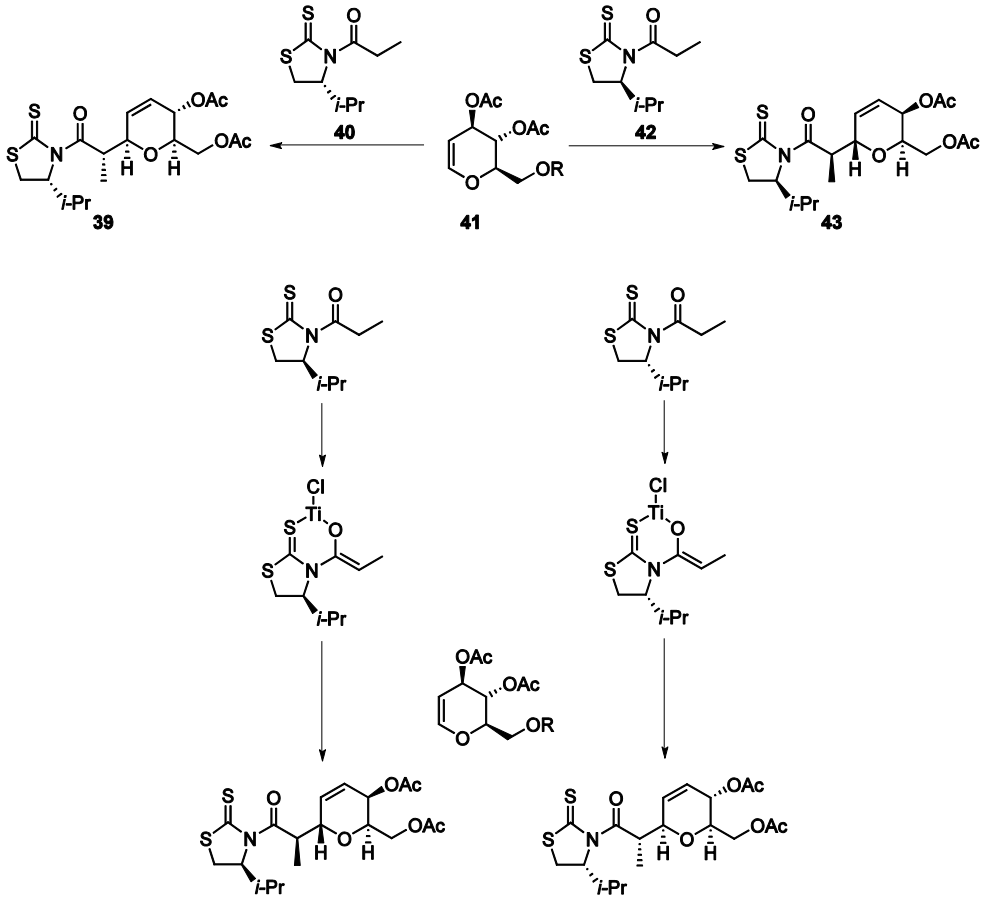

Scheme 3.2 Lewis acid mediated cross-coupling reaction of glycals to chiral titanium enolates derived from (*S*)-**42** and (*R*)-**40**[1, 2]

Based on this precedent our desired compounds **36** (or **42**) should be available from the titanium-mediated coupling of the chiral auxiliary **38** (or **43**) with the carbohydrate moiety **39** (Scheme 3.1). We expect that the reaction will take place either as an S_N2-type displacement on the anomeric centre or, via attack of the enolate of **38** (or **43**) on the oxocarbenium ion. As with the reaction carried out by Urpi and co-workers, the chirality of the auxiliary should determine the final configuration about the anomeric centre. Reacting the carbohydrate moiety **39** with the (S)-chiral auxiliary **38** will install the hydrophobic group, as well as ensure the desired α-configuration at the anomeric centre. The β-analogues **42** should similarly be accessible by using chiral titanium enolate of auxiliary **43**. This is the key step of the synthesis as it serves to install the hydrophobic R group at the pseudo-anomeric position of the carbohydrate moiety. The R groups **a-j** encompass a variety of substituents that differ in their sterics and electronics. Throughout this thesis, the letters **a-j** will refer to the R group of the chiral auxiliary, and at the pseudo-anomeric position of the resulting coupled galactals and glycosylated amino acids. Analogue **30a**, where R = H is the ornithine analogue (**14**), which will serve as a control in the antifreeze activity assessments. Finally, the carbohydrate moiety **39** can be accessed from commercially available galactose.

3.1.2 Investigating the Importance of Hydration of the AFGP 8 Analogues to Recrystallization Inhibition (RI) Activity (Series II Analogues)

The second series of analogues (Series II) is comprised of polymers **31** and **32** (Scheme 3.3), as well as polymers **33** and **34** (Scheme 3.4). Both sets of polymers should be readily accessible since their synthesis is based directly on the synthetic scheme developed by Urpi and co-workers (as was shown in Scheme 3.2), employing a protected galactal (**52**), rather than a protected galactose (**39**). As with the Series I analogues (polymers **30** and **40**, Scheme 3.1), polymers **31** and **32** of Series II can be prepared via solid-phase synthesis using Fmoc-protected glycine and the *C*-glycosyl amino acid building blocks **49** and **53**, respectively.

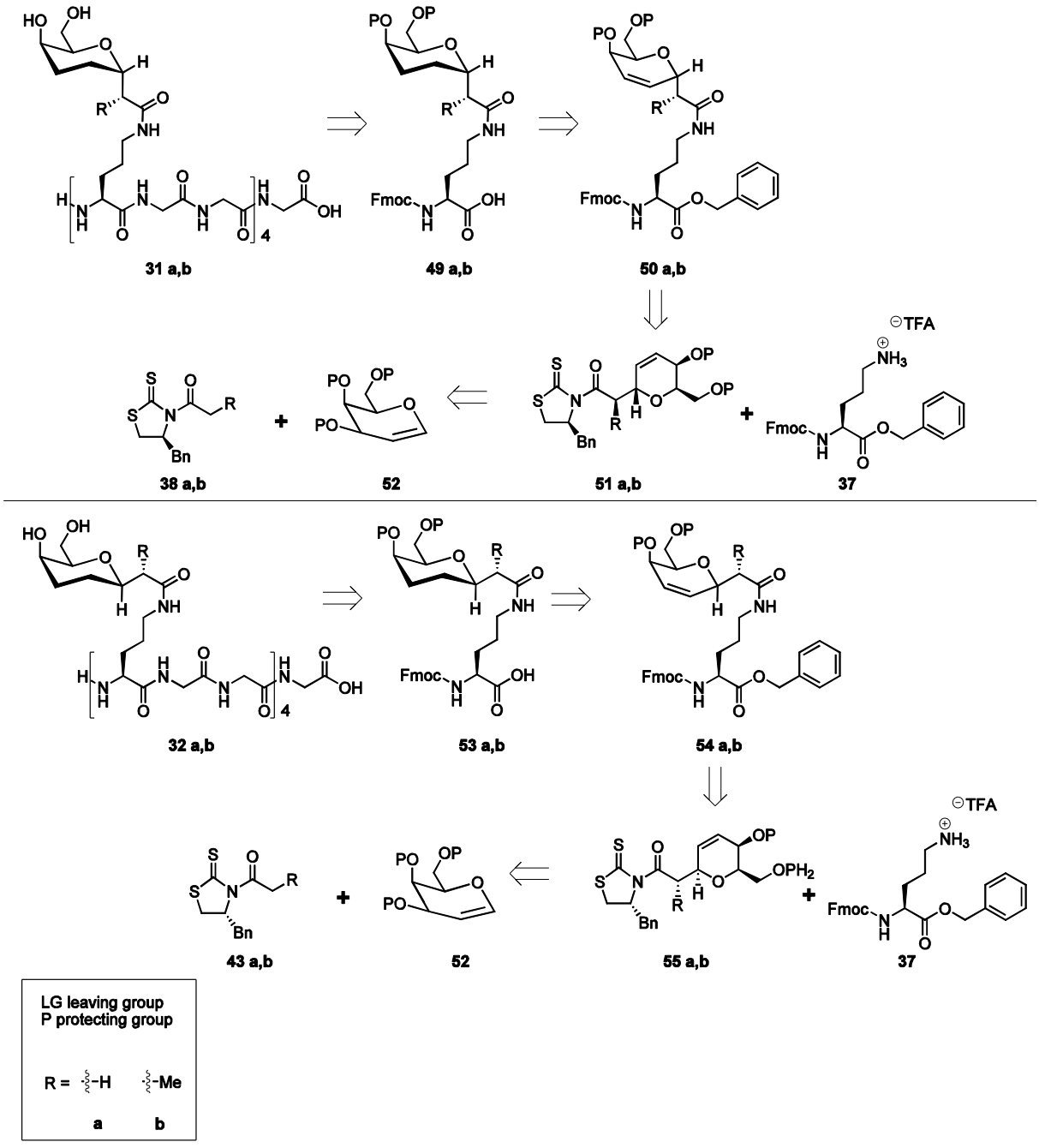

Scheme 3.3 Retrosynthesis of Series II AFGP analogues

The desired building blocks **49** (or **53**) should be available by hydrolysis and deprotection of **50** (or **54**). These protected building blocks can in turn be prepared by displacing the auxiliary from **51** (or **55**) with protected amino acid **37**. Compounds **51** (or **55**) should be available from the titanium-mediated coupling of the chiral auxiliary **38** (or **43**)

with the protected galactal **52**, according to the protocol of Urpi and co-workers.[2] As for the series I analogues, the chirality of the auxiliary will determine the configuration at the anomeric centre. Reacting the carbohydrate moiety **48** with the (S)-chiral titanium enolate of auxiliary **38** should install the R group as well as ensure the desired α-configuration at the anomeric centre. Similarly, the reaction of the carbohydrate moiety **52** with the (R)-chiral titanium enolate of auxiliary **43** should install the R group as well as ensure the desired β-configuration at the anomeric centre. As for Series I, this is the key step of the synthesis as it serves to install the hydrophobic R group at the pseudo-anomeric position on the carbohydrate moiety. Likewise, the protected galactal **52** can be synthesized from commercially available galactose.

Series II analogues that possess a double bond in the carbohydrate moiety will also be synthesized (polymers **33** and **34,** Scheme 3.4). The syntheses of all the Series II analogues are closely related; analogue **33** (or **34**) should be available from a similar sequence to that presented in Scheme 3.3 for analogues **31** (or **32**). The required building blocks for analogue **33** (or **34**) should be available from **50** (or **54**) (Scheme 3.3), as long as the carboxylic acid protecting group is removed without hydrogenation of the double bond of the carboxylic acid moiety. In order to avoid hydrogenation of the double bond, the carboxylic acid protecting group of the amino acid will have to be carefully considered.

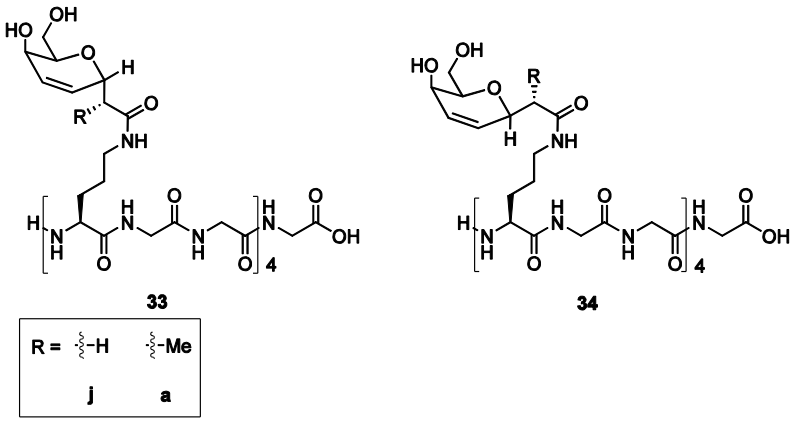

Scheme 3.4 Series II AFGP analogues

3.2 Synthesis

3.2.1 Investigating the Importance of Hydrophobicity of the AFGP 8 Analogues to Recrystallization Inhibition (RI) Activity (Series I Analogues)

The syntheses of both Series I and II AFGP 8 analogues rely on the chiral titanium enolate used by Urpi and co-workers in their synthesis of *C*-linked carbohydrate derivatives.[1, 2] The authors point out that the auxiliary can be easily removed, and the products transformed into a wide range of derivatives in high yields, using mild conditions. This suited our purposes, and for this reason, we adopted the thiazolidine thione chiral auxiliary into our synthesis.

We first carried out the synthesis of the auxiliary that would be used to install a methyl group at the pseudo-anomeric position (Scheme 3.5). Commercially available (L)-phenylalanine (**56**) or (D)-phenylalanine (**61**) was reduced to the corresponding alcohol **57** or **62**, respectively, with lithium aluminum hydride.[3] The amino alcohols were cyclized using CS_2 with excess base according to the protocol of Crimmins *et al.,*[4] to give **58** and **63**. Finally, the cyclized products **58** and **63** were acylated with acyl chloride **59** to provide the (R)- or (S)-chiral auxiliaries **38b** and **43b**, respectively.

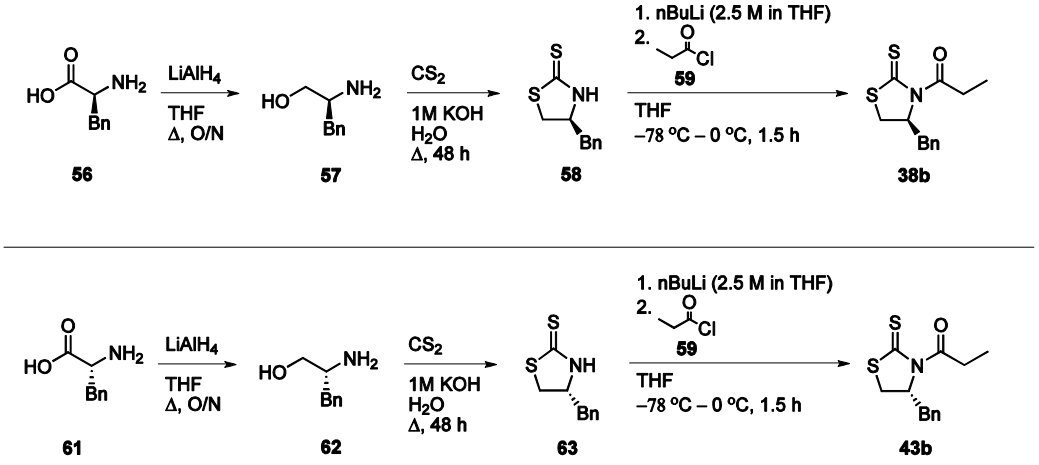

Scheme 3.5 Synthesis of the thiazolidine thione chiral auxiliary to introduce methyl groups at the pseudo-anomeric position

Using this methodology, we were able to synthesize several (R)- and (S)-chiral auxiliaries; these are shown in Scheme 3.6. John F. Trant, an NSERC summer student at the time, synthesized several of the auxiliaries. Most of the acyl chlorides used were commercially available. Those that were not commercially available were synthesized from the corresponding commercially available carboxylic acid derivatives according to the methodology shown in Scheme 3.7 The synthesized acyl chlorides **65**, **67**, and **69** were used in the synthesis of the corresponding chiral auxiliaries (Scheme 3.6).

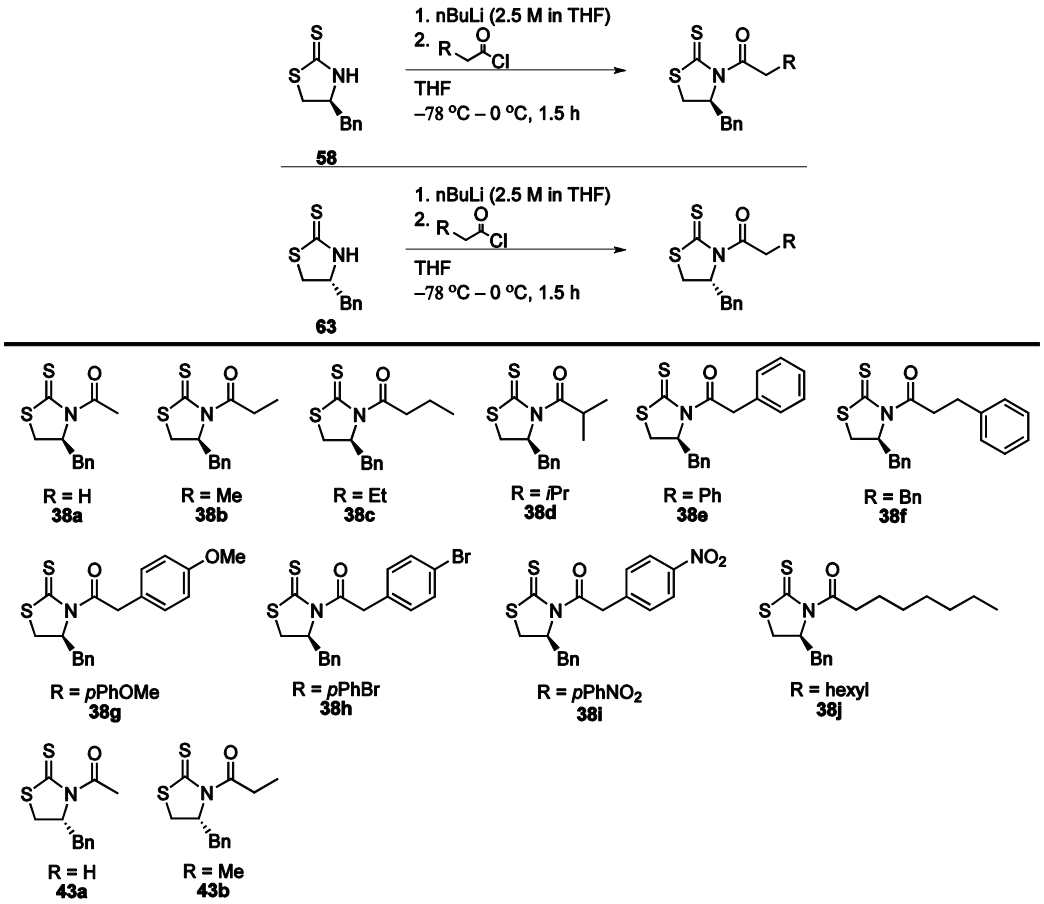

Scheme 3.6 Synthesis of thiazolidine thione chiral auxiliaries to introduce various R groups

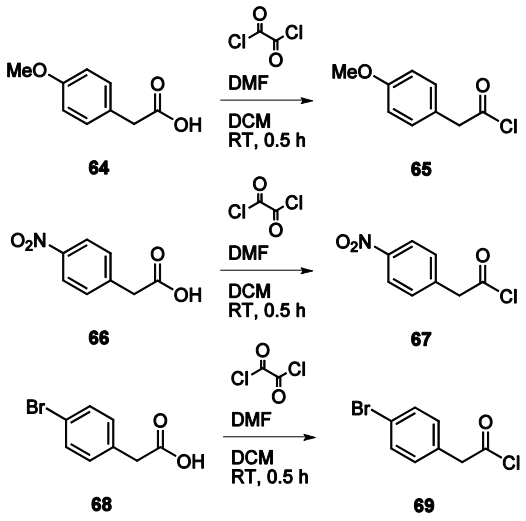

Scheme 3.7 Synthesis of various acyl chlorides from the carboxylic acid derivatives

The carbohydrate moiety to be used in the coupling reaction with the chiral auxiliary (compound **76**) was synthesized starting from commercially available galactose according to a protocol developed in our lab (Scheme 3.8). Acetylation of commercially available galactose (**70**), provided **71**, although commercially available β-galactose pentaacetate was also used. Installation of thiophenol at the anomeric centre of **71** followed to give **72**. As a result of the anchimeric effect, only the β-anomer was formed; however this stereocentre was later destroyed so its stereospecific formation was irrelevant. Near-quantitative deprotection of the hydroxyl groups using sodium methoxide to give compound **73**, was followed by the installation of four benzyl protecting groups to give compound **74**. The anomeric thiophenol was replaced by a hydroxyl group using *N*-bromosuccinamide to give compound **75**, and finally, the trichloroimidate was installed under mildly basic conditions to yield the β-anomer (**76**). The formation of the electrophilic carbohydrate **76** was confirmed using ^{1}H NMR and MS, and despite the presence of some impurities in the crude product, **76** was used without further purification.

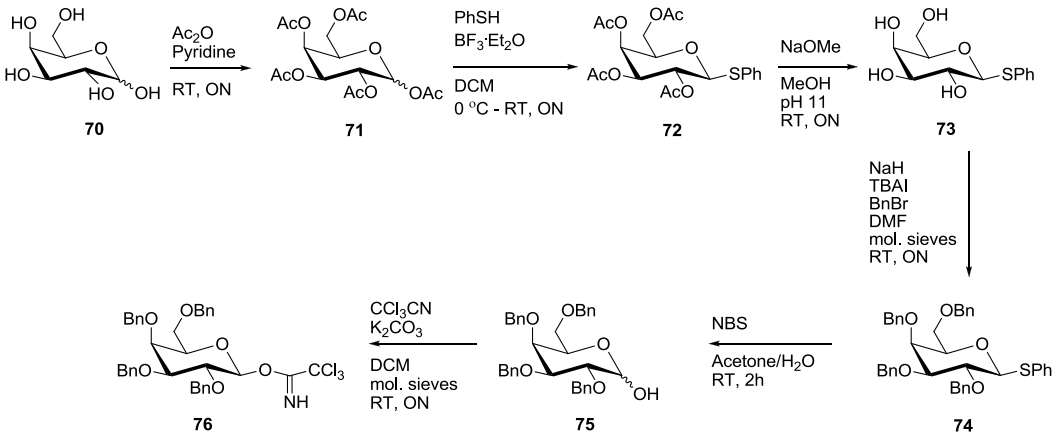

Scheme 3.8 Synthesis of the carbohydrate coupling partner

Before employing the trichloroimidate-substituted carbohydrate **76** in the key step, we ran a test reaction with the simple nucleophile isopropanol in order to confirm that the trichloroimidate had been properly installed. The test reaction is given in Scheme 3.9. Analysis of the crude reaction product (**78**) by ^{1}H NMR and mass spectroscopy indicated that the desired product **79** was formed, and with minimal concurrent side-product formation. The crude product was not purified; nevertheless, we confidently attempted the key step.

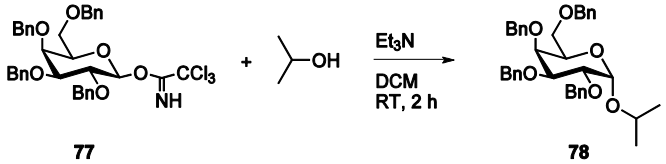

Scheme 3.9 Test reaction with the trichloroimidate-substituted carbohydrate

Unfortunately, the reaction of the carbohydrate moiety with the chiral auxiliary (Scheme 3.10) did not provide any desired product (**79**). The resulting product mixture was difficult to separate, and therefore its composition could not be determined.

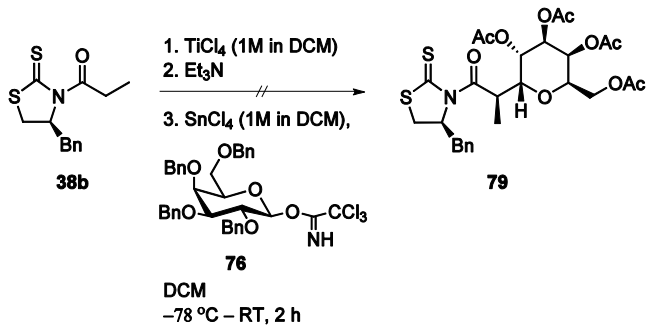

Scheme 3.10 First attempted reaction of the carbohydrate derivative with the chiral titanium enolate

Consequently, we synthesized additional electrophilic carbohydrates in order to test different leaving group and protecting group combinations. Their syntheses are given in Scheme 3.11.

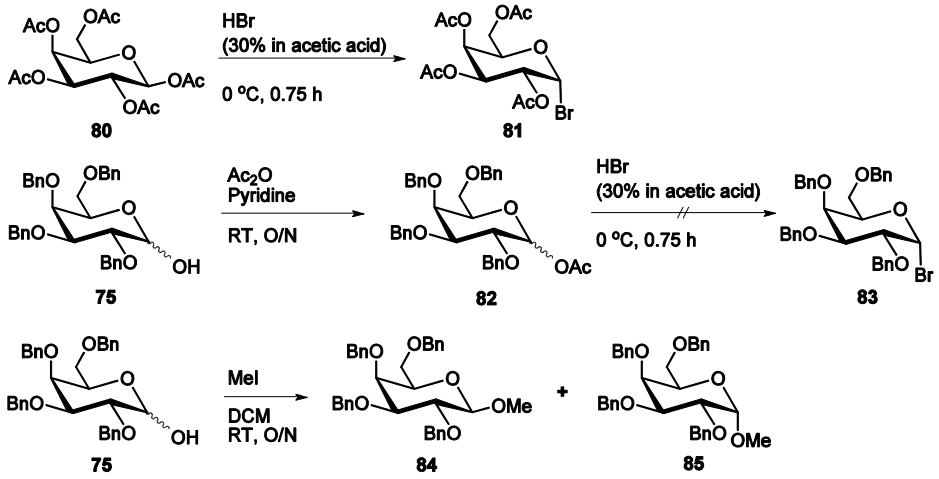

Scheme 3.11 Synthesis of alternate electrophilic carbohydrate moieties

Compound **81** (Scheme 3.11) was obtained in good yield by bromination of commercially available β-galactose pentaacetate using a 30% solution of hydrogen bromide in acetic acid. Compound **82** was accessible by acetylation of **75** using acetic anhydride and pyridine; however, bromination of **82**, carried out as for **81**, did not provide the desired product **83**. Lastly, compounds **84** and **85**, which were separated using silica flash

chromatography, were available from methylation of **75**. However, when the new electrophilic carbohydrates (**81**, **84**, and **85**) were reacted with the chiral auxiliary (**38b**), no desired product was obtained in any of the reactions (Scheme 3.12).

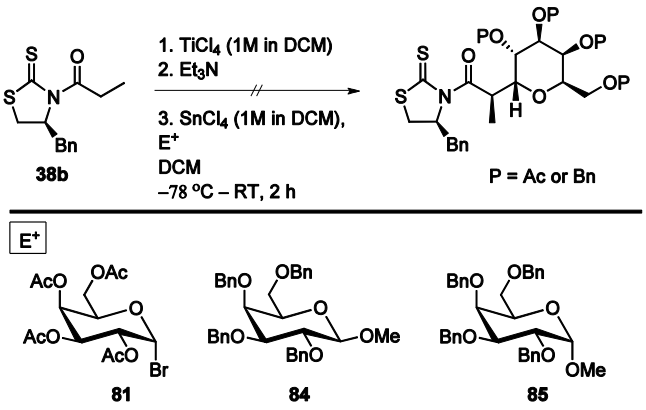

Scheme 3.12 Reaction of thiazolidine thione chiral auxiliaries with various electrophilic carbohydrates

Following, a series of test reactions of the chiral auxiliary **38b** with simpler electrophiles was carried out (Table 3.1). As indicated in Table 3.1, the nature of the base was varied with several of the electrophiles tested.

Table 3.1 Reactions of thiazolidine thione chiral auxiliry with test electrophiles

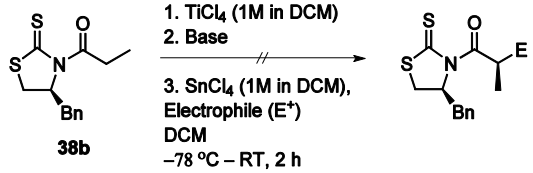

Entry	Electrophile (E^+)	Base	Expected Product	Isolated Product
1	MeI	DIPEA	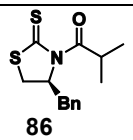 86	SM

Entry	Electrophile (E^+)	Base	Expected Product	Isolated Product
2	MeI	Et_3N	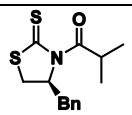 **86**	SM
3	MeI	(-)-sparteine	 **86**	SM
4	MeI	LDA	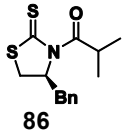 **86**	SM
5	Dihydro-cinnamaldehyde	Et_3N	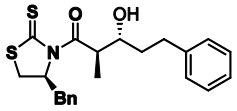 **87**	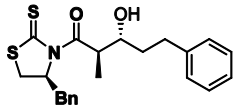 **87**
6	Dihydro-cinnamaldehyde	(-)-sparteine	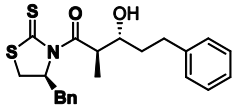 **87**	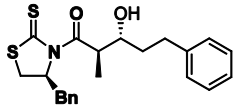 **87**
7	Allylbromide	DIPEA	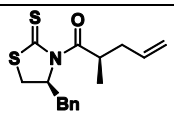 **88**	SM
8	Allylbromide	LDA	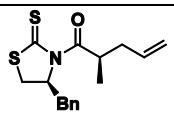 **88**	SM + 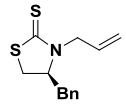 **89**
9	Allylbromide	LDA (no $TiCl_4$)	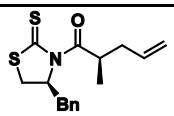 **88**	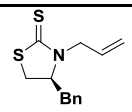 **89**

As indicated in Table 3.1, with the exception of entries 5 and 6, the experimental conditions did not provide the desired products. Most trials (entries 1-4, and 7) returned starting material exclusively. In the presence of lithium diisopropyl amine (LDA), reaction with allylbromide (entries 8 and 9) resulted in unexpected removal of the acyl group from the starting material **38b** by the base, followed by nucleophilic attack by the nitrogen on the electrophile to provide compound **89**. Given the poor results of these trials, the current

approach to the Series I analogues was abandoned, and we focused our attention on the synthesis of the Series II analogues.

3.2.2 Investigating the Importance of Hydration of the AFGP 8 Analogues to Recrystallization Inhibition (RI) Activity (Series II Analogues)

The syntheses of the polymers in Series II were subsequently undertaken. The synthesis of protected galactal **44** was carried out as shown in Scheme 3.13. As was previously shown in Scheme 3.11, the brominated product **81** was obtained from commercially available β-galactose pentaacetate in good yield. Analysis by ^{1}H NMR analysis showed the exlusive formation of the α-anomer. Since the bromination reaction progresses through an oxocarbenium ion, both α- and β-linked bromination products can be formed. However, the reaction is reversible, and since the anomeric effect favours the thermodynamically more stable α-anomeric configuration, only the α-anomer is found in the final product.[5] From brominated carbohydrate **81**, protected galactal **44** was prepared according to the procedure developed by Somsak and Nemeth.[6]

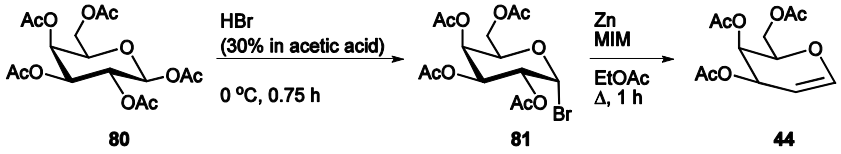

80 81 44

Scheme 3.13 Synthesis of acetyl-protected galactal

As expected based on the precedent by Urpi and co-workers[2], the reaction of (S)-chiral auxiliary **38b** with protected galactal **44** as the electrophilic carbohydrate moiety proceeded smoothly to provide the desired coupled product **90b** in good yield (Scheme 3.14A). Similarly, the reaction of the (R)-chiral auxiliary **43b** with the protected galactal **44** provided the β-anomer **91b** (Scheme 3.14B).

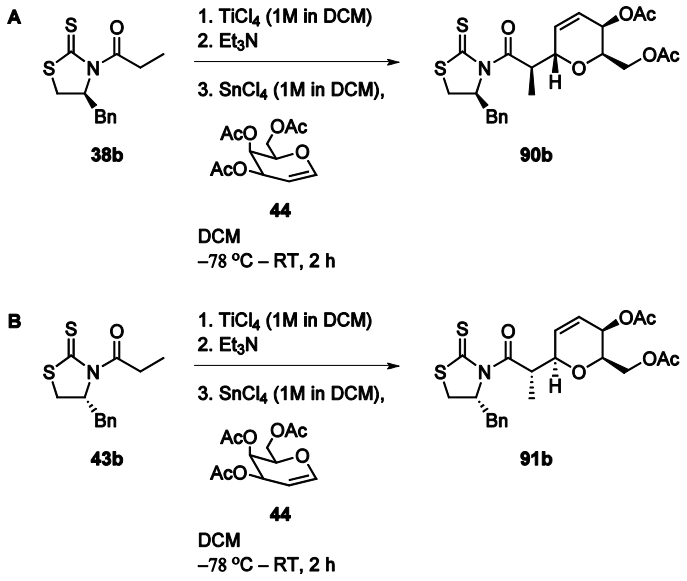

Scheme 3.14 Reaction of the chiral titanium enolate with protected galactal

The reactions of the (R)- and (S)-chiral auxiliaries with the protected galactal are summarized in Scheme 3.15.

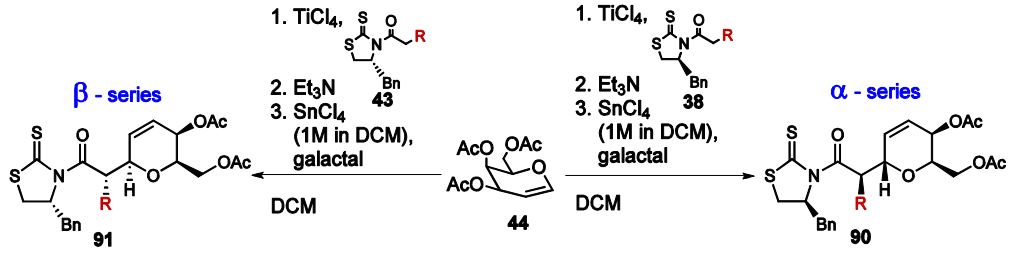

Scheme 3.15 Reactions of the (S)- and (R)-chiral auxiliary with acetylated galactal

All (S)- and (R)-chiral auxiliaries with diverse R groups (Scheme 3.6) reacted readily with protected galactal (**44**) to give the expected products. The results are shown in Schemes 3.16 and 3.17. While most reactions were highly selective for one diastereomer, chiral auxiliaries in which R = H were less stereoselective, and the resulting two diastereomers (the α- and β-linked coupled galactal) were difficult to separate completely.

Consequently, some of the unwanted diastereomer was carried forward to the next reactions in both cases.

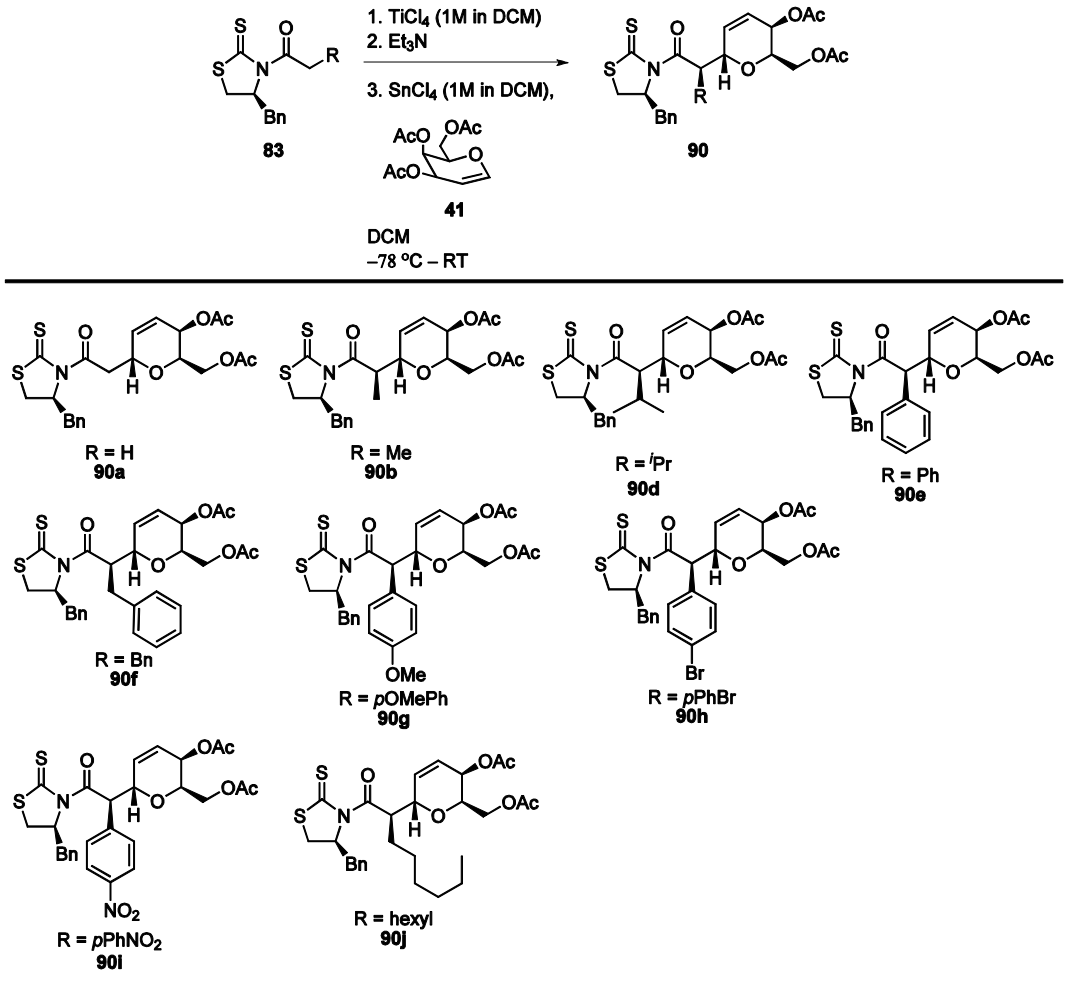

Scheme 3.16 Reaction of (S)-chiral auxiliaries with acetylated galactal

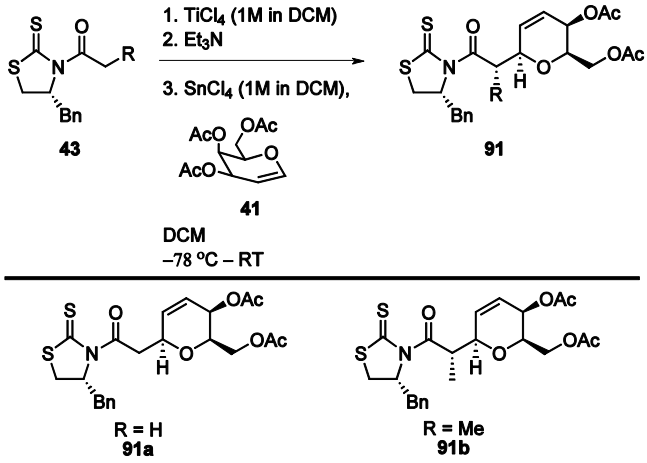

Scheme 3.17 Reaction of (R)-chiral auxiliaries with acetylated galactal

The chiral auxiliary determines the stereochemistry at both the anomeric and pseudo-anomeric positions. Urpi and co-workers first presented the reaction of the chiral titanium enolate with acetals to give *anti* α-methyl-β-alkoxy carbonyl structures (Scheme 3.18A),[1] and subsequently expanded their work to the glycosidation reactions (as discussed previously).[2] Based on their studies, the authors speculated that the reactions proceed via an S_N1-like process. To rationalize the observed stereochemistry of the α-methyl-β-alkoxy carbonyl structures the authors invoke the transition states TS-A and TS-B (Scheme 3.18B).[1] The observed stereochemistry might therefore result from an open transition state in which the intermediate oxocarbenium ion approaches the less hindered face of a putative chelated Z-enolate and determines the R configuration at the α-centre. The stereochemistry of the glycosidation products, however, is notT exclusively governed by the chiral auxiliary. Urpi and co-workers found that when the glycal reacting partner bore acetate protecting groups, "the configuration at [the anomeric centre] C1 arises from a compromise between the induction exerted by the auxiliary and [the induction exerted] by the glycal." Urpi and co-workers provided proof for their stereochemical outcomes by the synthesis of derivatives of their coupled glycals, as well as by crystallographic data of one coupled glycal. The stereochemical proof is detailed in the supporting information for their key glycosidation paper. [2] The spectral data for our newly synthesized coupled galactal products was in agreement with their published spectral data.

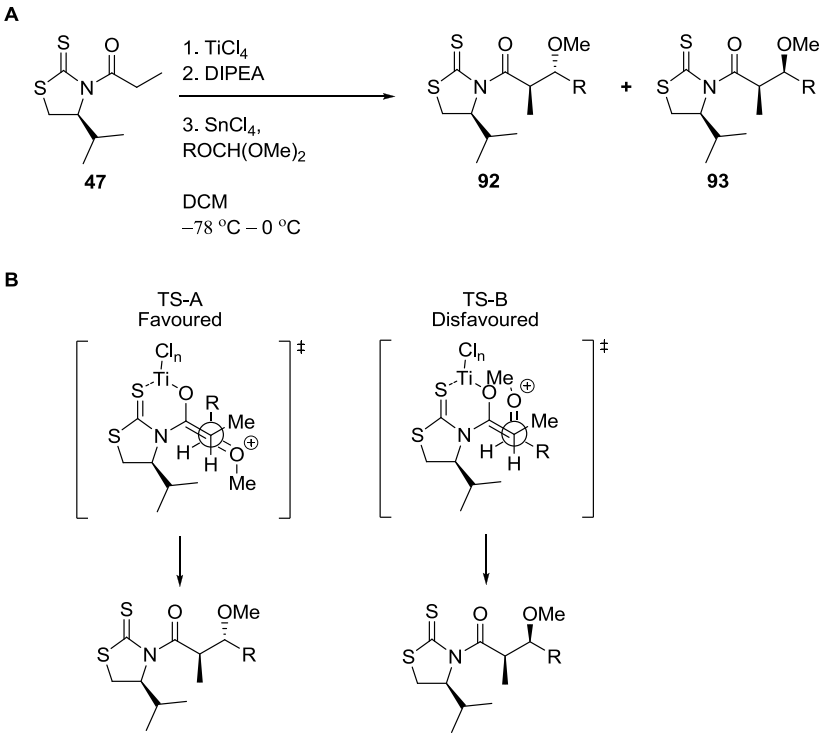

Scheme 3.18 Typical conditions for reaction of thiazolidine thione auxiliary with an acetal; B Transition states for *anti* (**92**) and *syn* (**93**) products[1]

In the meantime, although we were pleased with the successful syntheses of the coupled galactal products, we were still intent on the synthesis of the Series I analogues - the fully hydroxylated analogues (Scheme 3.1). We therefore attempted the dihydroxylation of the double bond of the coupled galactal **90b** according to the protocol of Sharpless *et al*.[7] in order to obtain a fully-hydroxylated carbohydrate. The test reaction, the dihydroxylation of cyclohexene using AD-mixα (Scheme 3.19) was successful, as determined by ^{1}H NMR and MS analysis of the product. However, the same conditions did not result in any reaction when applied to the coupled galactal **91b** (Schemes 3.20). In all attempted dihydroxylation reactions with the coupled galactals only starting material was recovered, despite the long reaction times employed.

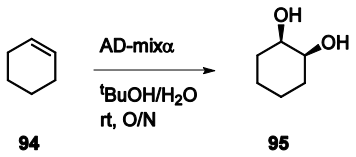

Scheme 3.19 Dihydroxylation test reaction (I)

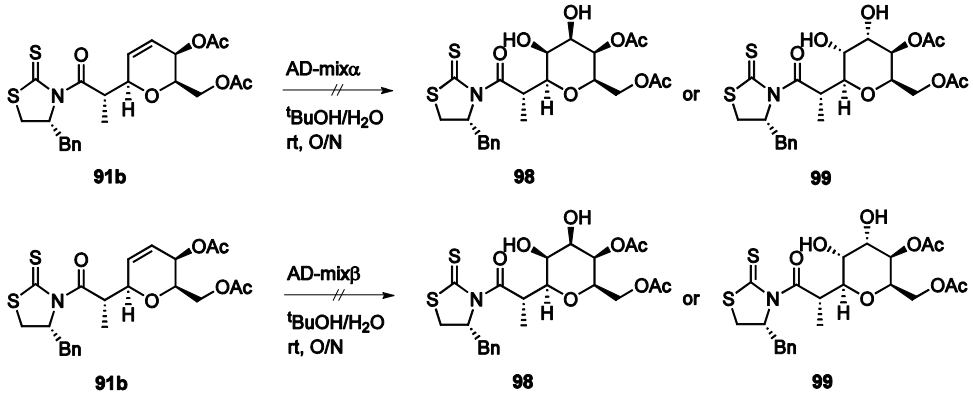

Scheme 3.20 Dihydroxylation of the β-anomer

In order to determine whether or not the chiral auxiliary was preventing dihydroxylation, we applied the same conditions to the protected galactal **44** alone (Scheme 3.21). In both cases (using AD-mixα or AD-mixβ) no dihydroxylation took place and only starting material was recovered.

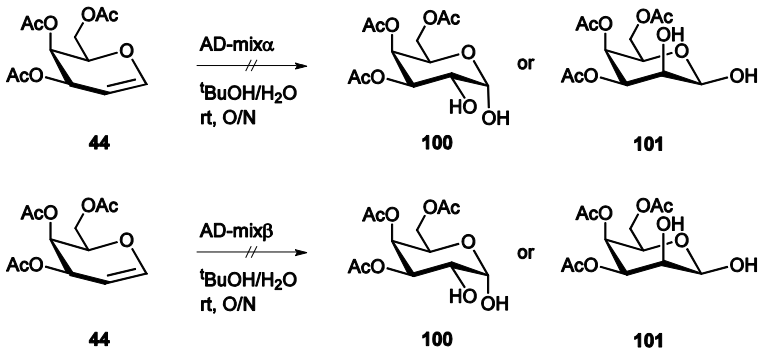

Scheme 3.21 Dihydroxylation test reaction (II)

The dihydroxylation was next attempted using OsO_4 and NMO rather than AD-mix. Under these conditions,[8] the test reaction readily provided dihydroxylated cyclohexane from cyclohexene (Scheme 3.22). However, the same conditions were unable to provide the desired dihydroxylation product when applied to the coupled galactals (**90b** or **91b**) (Scheme 3.23). Using OsO_4 in catalytic amounts, and employing a different reaction medium[9] similarly failed to produce any desired product (Scheme 3.24).

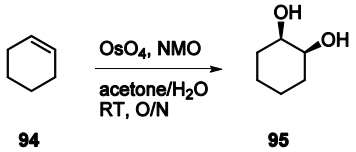

Scheme 3.22 Dihydroxylation test reaction (III)

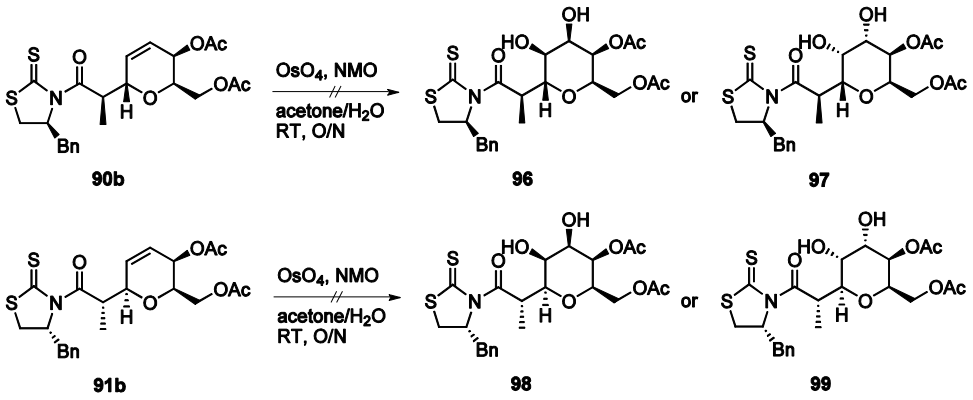

Scheme 3.23 Dihydroxylation of the α- and β-anomers (new conditions)

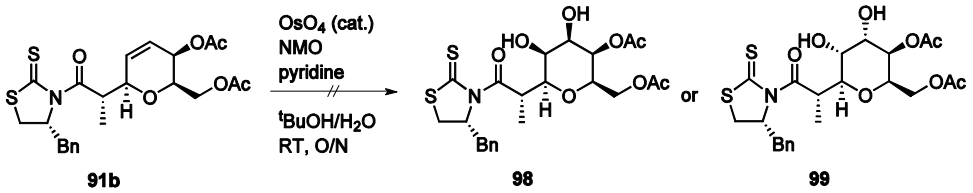

Scheme 3.24 Dihydroxylation of the β-anomer (catalytic OSO_4 and new conditions)

At this point, the dihydroxylation strategy was abandoned, and we returned our attention to the completion of the dehydro-analogues of Series II (**31** and **32**, Scheme 3.3). Consequently, the displacement of the chiral auxiliary from the coupled galactals **90b** and **91b** with the δ-amine of the ornithine (**37**) was investigated (Scheme 3.26). First, a test reaction using a simpler amine, benzylamine, was attempted (Scheme 3.25).

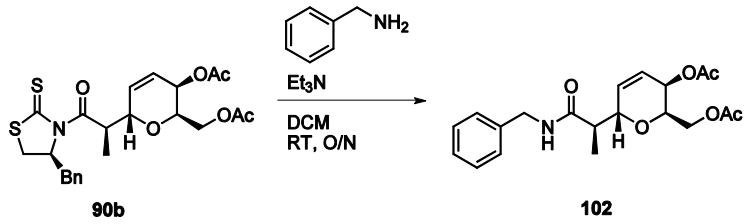

Scheme 3.25 Displacement of the chiral auxiliary from the coupled galactal (**88**) using a primary amine

Gratifyingly, benzylamine easily displaced the chiral auxiliary from coupled galactal **90b** to provide **102** in 89% crude yield after simple purification (Scheme 3.26). The formation of the desired product was verified by ^{1}H NMR and MS, and ^{1}H NMR further verified that the purity of the desired product was high. Therefore, the displacement with ornithine (**37**) was attempted.

As shown in Scheme 3.27, the synthesis of the amino acid coupling partner (**37**) was readily accomplished in two steps. The benzyl protecting group was installed on the commercially available Fmoc- and Boc-protected starting material (**103**) using benzyl alcohol, with *N*,*N*′-dicyclohexylcarbodiimide (DCC) and 4-(dimethylamino)pyridine (DMAP) in dichloromethane (DCM), to provide **104**. The Boc group was subsequently removed in quantitative yield using trifluoroacetic acid (TFA), and the resulting product (**37**) was purified by recrystallization.

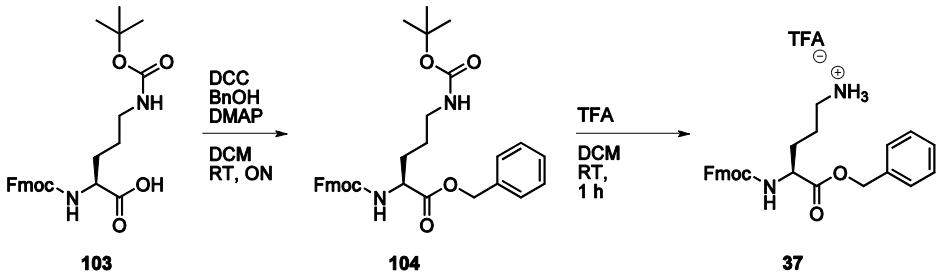

Scheme 3.26 Synthesis of the protected amino acid

The displacement of the auxiliary from the coupled galactal (**90b**) with the amino acid was carried out in the presence of excess triethylamine (Scheme 3.27). While the desired product was obtained, as determined by ^{1}H NMR and MS analysis, the yield was very poor, and multiple side-products were formed. The isolation of the desired product proved to be very difficult, and ultimately, not enough material could be obtained (in sufficient purity) to make the synthesis of the polymer feasible. Similar results were obtained when the β-analogue was reacted (not shown). Despite the low yield obtained in these first reactions, the direct displacement was attempted using several of the coupled galactals (Scheme 3.28).

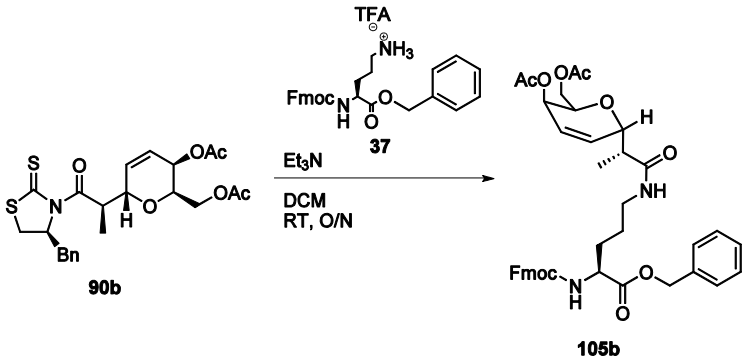

Scheme 3.27 Displacement of the chiral auxiliary from the coupled galactal (**90b**) using protected ornithine (**37**)

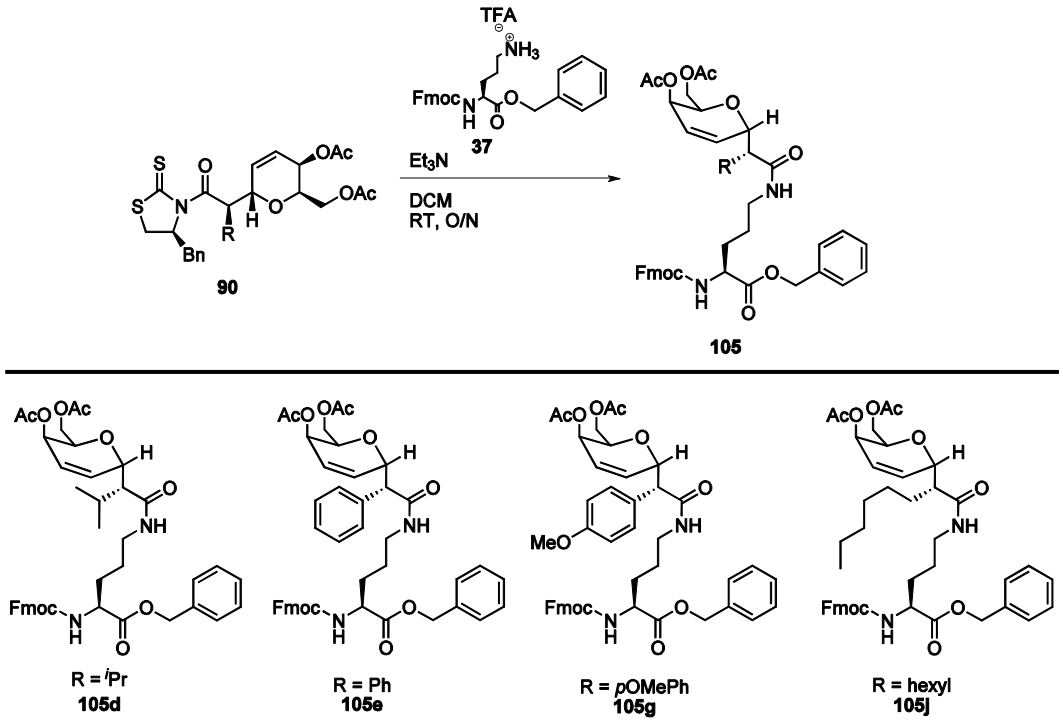

Scheme 3.28 Displacement of the chiral auxiliary from various coupled galactals using protected ornithine

However, the yields for these reactions were poorer still, and the isolation of the desired product proved to be even more difficult. The products with the largest R groups, that is, the most hydrophobic products, were most difficult to isolate. If the yields of these reactions had been greater, the deprotection of either the carboxylic acid terminus of the ornithine, or the hydroxyl groups of the carbohydrate component might have allowed for the purification of these products. Unfortunately, given the low yields of the displacement products (α- and β-ornithine-coupled galactals), we ruled out this approach.

Despite the low yields of the α- and β-ornithine-coupled galactals (**105b** and **107b**) obtained, we proceeded with the hydrogenolysis of the benzyl protecting group with the small amount of reasonably pure material in hand (Scheme 3.29). The removal of the benzyl group (with concomitant hydrolysis of the double bond) of the β-analogue (**107b**) under hydrogenolysis conditions proceeded readily to give **108b**. However, under the same reaction conditions, the α-linked analogue (**105b**) did not react.

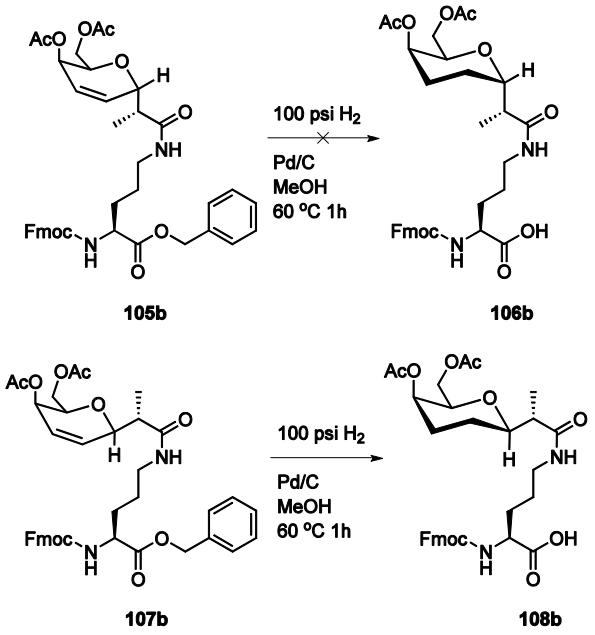

Scheme 3.29 Hydrogenolysis

In order to carry out the hydrogenolysis, a number of different conditions were assayed (Table 3.2). Under all but the reaction conditions given in entries 3 and 7, no reaction occurred, and all of the starting material was recovered. Dissolving metal reduction (entry 3) and high temperature and pressure (entry 7), both gave multiple products, and no desired product was recovered.

Table 3.2 Hydrogenolysis conditions

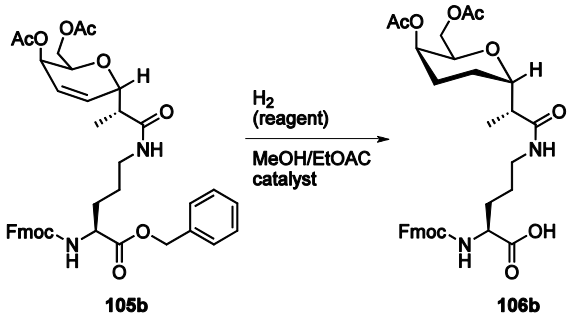

Entry	Reagent	Catalyst	Pressure	Temperature	Time	Yield
1	none	10% Pd/C	ambient	RT	24 h	no reaction
2	none	10% Pd/C	100 psi	RT	18 h	no reaction
3[10]	none	Na/NH_3	ambient	-78 °C	0.5 h	decomposition
4	HCO_2H	10% Pd/C	ambient	RT	18 h	no reaction
5	HCO_2NH_4	10% Pd/C	ambient	RT	18 h	no reaction
6	HCO_2NH_4	10% Pd/C	500 psi	RT	2 h	no reaction
7	HCO_2NH_4	10% Pd/C	600 psi	75 °C	5 h	decomposition

The failure of these reactions seemed highly unusual. It is possible that impurity in the starting material was the cause. Since it was very difficult to purify the starting materials for the hydrogenolysis reactions (**105b** and **107b**), it is possible that a trace of the chiral auxiliary from the previous reaction (the displacement of the chiral auxiliary from the coupled-galactal with ornithine) remained. It is possible that sulfur from the chiral auxiliary poisoned the palladium catalyst in the hydrogenolysis reaction. Since the starting materials

were only available in low yields, and further, had proven to be difficult to purify, we developed a new strategy to access the building blocks: rather than displacing the chiral auxiliary from the coupled galactals with the amino acid, we chose to remove the chiral auxiliary and to install a carboxylic acid moiety in its place. In order to use relatively gentle conditions, we opted for a step-wise approach to access the carboxylic acid galactal derivative (**111**); therefore, the first step was the transformation of the coupled galactal into the alcohol derivative. The conditions employed are given in Scheme 3.31.

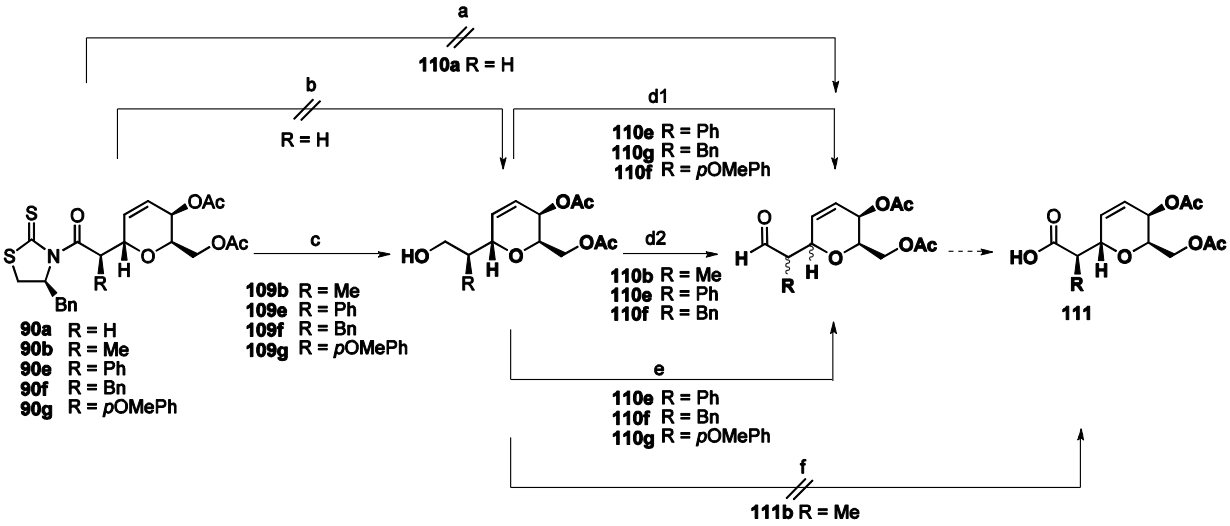

(a) DIBAL-H, THF, -78 °C, 3 h; (b) $NaBH_4$, DCM, 0 °C; (c) $NaBH_4$, THF/H_2O, RT, 0.3 h; (d1) TPAP/NMO, DCM/CH_3CN, RT, 2 h, work-up 1; (d2) TPAP/NMO, DCM/CH_3CN, RT, 2 h work-up 2; (e) $(COCl)_2$, DMSO, Et_3N, DCM, - 60 °C, 0.25 h; (f) TEMPO, MeCN, sodium phospohate buffer pH 7, $NaClO_2$, NaOCl, 35 °C, 24 h;

Scheme 3.30 Attempted synthesis of the carboxylic acid galactal derivative

The alcohol derivatives **109b**, **109e**, **109f**, and **109g** were readily available from the corresponding starting materials **90b**, **90e**, **90f**, and **90g,** respectively, using sodium borohydride in THF/water.[2] However, the oxidation of the alcohols to give the aldehyde derivatives proved to be problematic. Oxidation with TPAP and NMO, using two different protocols for the reaction work-up,[11, 12] did provide the desired aldehyde products **110b**, **110e**, **110f**, and **110g** from their respective starting materials, however, only **110f** and **110g** could be isolated. In every case, an inseperable diastereomer of the desired product was produced. Compound **110f** clearly showed two diastereomers in a ratio of about 2:1, and

analysis of the ^{1}H and ^{13}C NMR data was readily accomplished. Compound **110g**, however, showed two diastereomers in a ratio of 1:1, and ^{1}H NMR analysis could not be carried out. It could not be determined which stereocentre had isomerized. Swern oxidation conditions[13] applied to the alcohol derivatives also resulted in two inseparable diastereomers, and attempted production of the aldehyde derivative **110a** directly from the coupled galactal (**90a**) did not provide any of the desired product. Synthesis of the carboxylic acid derivative **111b** directly from the alcohol derivative **90b** using TEMPO and bleach[14] was also unsuccessful.

Urpi and co-workers have also shown that the chiral auxiliary of coupled galactals such as **90b** could be transformed into the methyl ester or Weinreb's amide derivatives.[2] Consequently, we undertook the synthesis of a number of new derivatives. However, only the Weinreb's amide derivatives could be accessed.

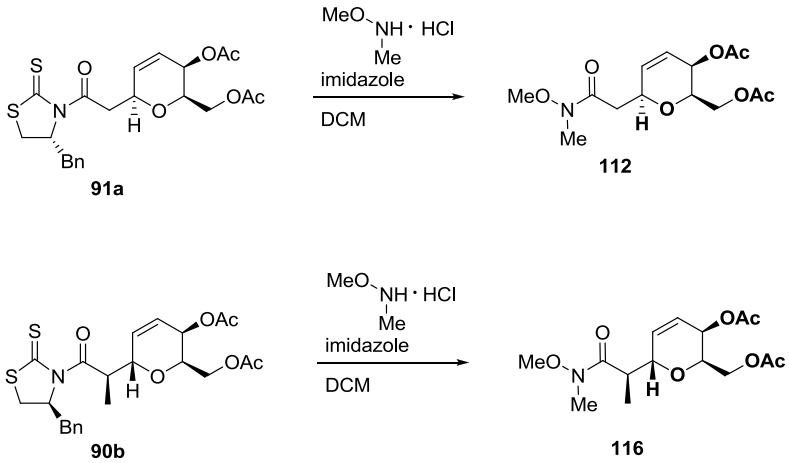

Scheme 3.31 Synthesis of galactal derivatives

For both the β-coupled galactal **91a**, and the α-coupled galactal **90b**, the Weinreb's amide derivatives (**112** and **116,** respectively) were readily available using the reaction conditions given in Scheme 3.31.[15] However, attempted displacements of the amide using amines returned only starting material. Interestingly, the known reduction[16] of the Weinreb's amide derivative **116** to the aldehyde derivative did not give the desired product.

Faced with the failures of these efforts, we re-examined the first attempts at the displacement of the chiral auxiliary from the coupled-galactal with protected ornithine **37** (refer to Scheme 3.27). One reason for the poor yield of the displacement reactions may have been that an intra-molecular attack by the γ-amine on the benzyl ester of the ornithine resulting in the formation of a six-membered ring was taking place. Despite the fact that the leaving group must be an alkoxide or alcohol group, the intramolecular reaction may be faster than the desired intermolecular one. In an attempt to overcome this potential problem, we replaced **37** with an Fmoc-protected ornithine bearing a free carboxylic acid terminus (**114**). The amino acid **114** was obtained by quantitative deprotection of the Boc protecting group of commercially available Fmoc- and Boc-protected ornithine **103.** The subsequent chiral auxiliary displacement reactions using **114** provided the desired products in good yield (Scheme 3.32). After purification, these products will be used as the building blocks in solid-phase peptide synthesis.

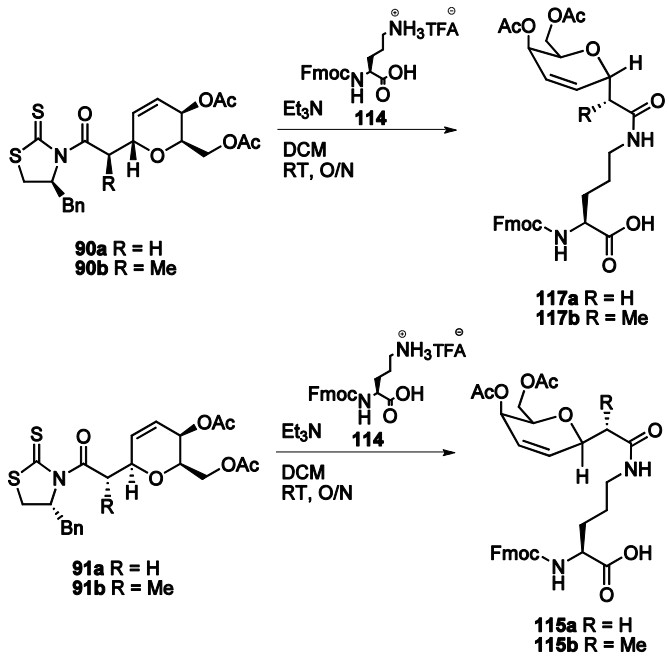

Scheme 3.32 Successful synthesis of the building blocks for Series II analogues

The complete syntheses of building blocks **115** and **117** for the Series II analogues (those peptides containing a double bond in the carbohydrate moiety: peptides **33** and **34**, Scheme 3.4) are summarized in Schemes 3.33 and 3.34, respectively. The syntheses each began with one enantiomer of phenylalanine: D-phenylalanine ultimately provided the α-

analogue and L-phenylalanine ultimately provided the β-analogue. The key step was the reaction of the (R)- or (S)-chiral auxiliary (**38a** and **43a,** respectively) with the protected galactal (**44**) to give the α- or β-coupled galactals **90a**, and **90b**, respectively. Displacement with the protected ornithine (**114**) provided the desired building blocks **117a** and **115a**.

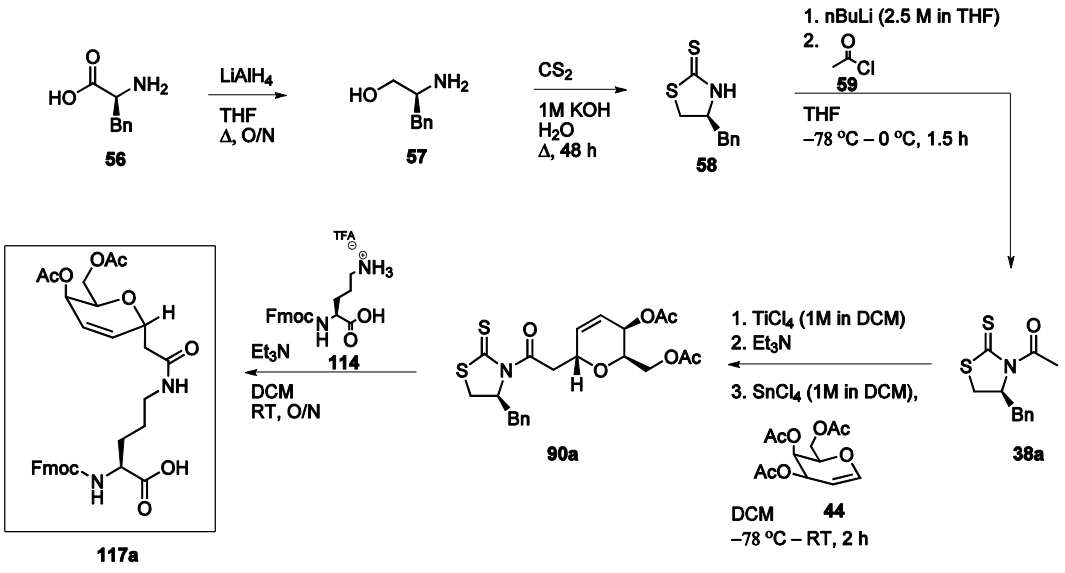

Scheme 3.33 Complete synthesis of the building block for the Series II α-linked analogue containing a double bond in the carbohydrate moiety

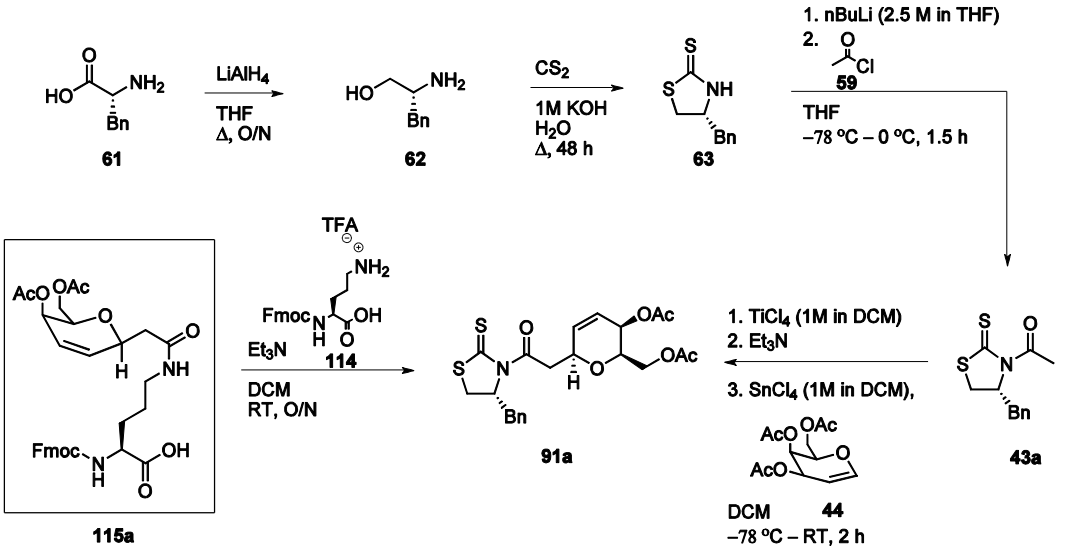

Scheme 3.34 Complete synthesis of the building block for the Series II β-linked analogue containing a double bond in the carbohydrate moiety

Unfortunately, despite the free carboxylic acid, the building blocks in which R = Me (**117b** and **115b**, Scheme 3.32) could not be sufficiently purified to be used for solid-phase synthesis. The unsubstituted building blocks (R = H, **117a** and **115a**, schemes 3.33 and 3.34) were readily purified by reverse-phase high-pressure liquid chromatography (HPLC) and used for solid-phase synthesis of the respective Series II analogues. Solid-phase synthesis was carried out on Wang Resin using an HBTU coupling protocol (Schemes 3.35 and 3.36). The Fmoc-Gly-Gly-OH was synthesized by Mathieu Leclere. The completed polymer was cleaved from the bead using a solution of TFA, and deprotected using sodium methoxide in methanol. The completed polymers **33a** and **34a** were then tested for antifreeze activity (refer to Part II).

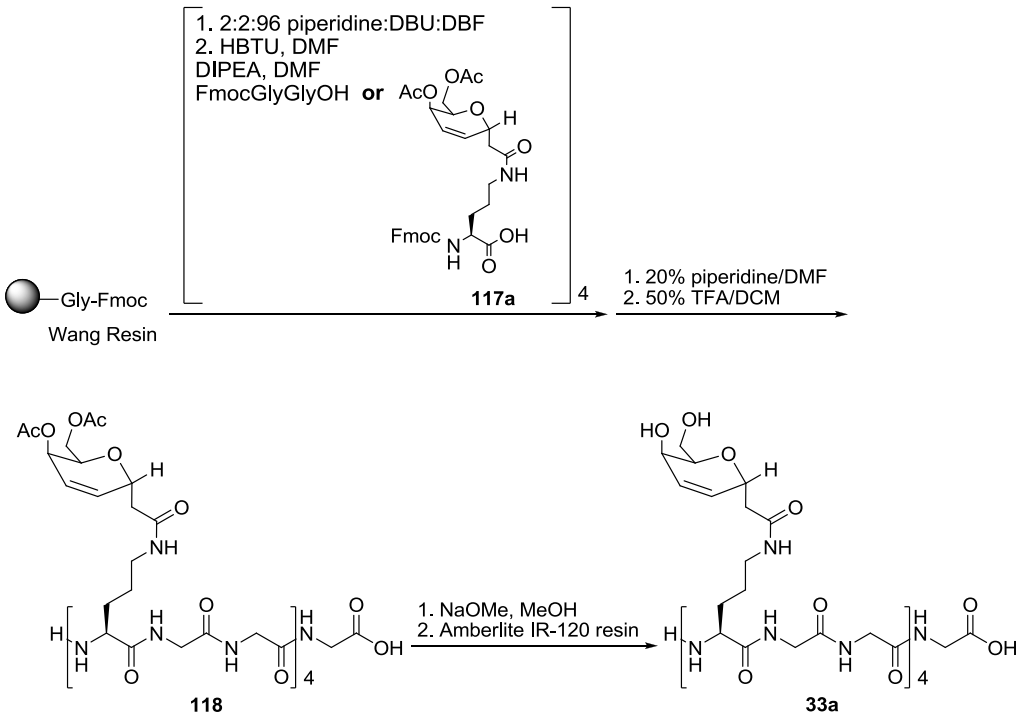

Scheme 3.35 Solid-phase peptide synthesis of the Series II α-linked analogue containing a double bond in the carbohydrate moiety

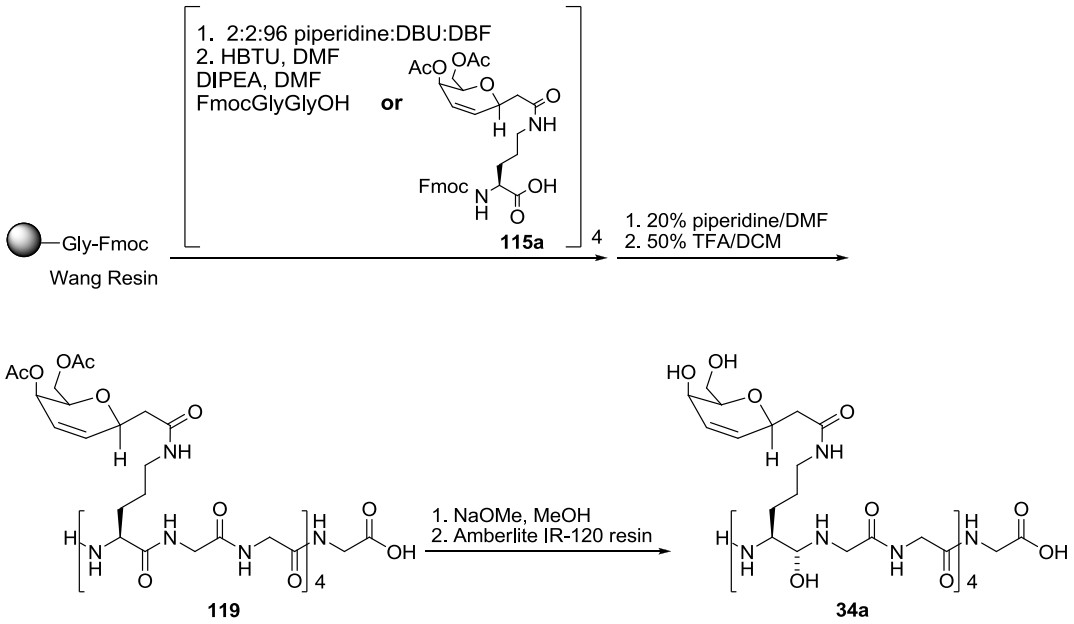

Scheme 3.36 Solid-phase peptide synthesis of the Series II β-linked analogue containing a double bond in the carbohydrate moiety

The building blocks for the above analogues (Series II analogues possessing a double bond in the carbohydrate moiety) were obtained by the displacement of the auxiliary from the coupled galactal using the amino acid, and while the yields of this step were sufficiently high for the syntheses of their respective analogues, they were not ideal and we were interested in improving the synthesis. As a result, to synthesize the fully-hydrogenated Series II analogues (compounds **31** and **32**, Scheme 3.3), we explored a new approach. Since at this point it became of interest to test the antifreeze activity of the carbohydrate moiety at the carboxylic acid derivative stage, the development of a route to the building block that proceeded via the carboxylic acid galactal derivative was of great interest to us. Therefore, rather than attempting the hydrogenation of the previously synthesized building blocks (compounds **117a** and **115a**, Schemes 3.33 and 3.34, respectively) to obtain the desired building blocks with the saturated carbohydrate moiety, we instead attempted the removal of the auxiliary from the coupled-galactal (**90a**) with concomitant carboxylic acid formation. We had not been able to effect this transformation previously; however, in our previous attempts at the formation of the carboxylic acid galactal derivative (**111,** Scheme 3.30) we had not attempted the direct transformation from the coupled-galactals (**90**), and had instead

tried to access it via the alcohol derivatives (**109b**). Fortunately, aqueous lithium hydroxide and hydrogen peroxide in THF[17] provided the carboxylic acid galactal derivatives **111a** and **111b** in good yield from the coupled galactal **90a** and **90b**, respectively (Scheme 3.37). This approach proved to be a very effective route for the synthesis of the building blocks, as the carboxylic acid galactal derivative was readily coupled to the protected ornithine **37** to give compounds **105a** and **105b**. Exposure to palladium on carbon effected the removal of the benzyl protecting group, as well as the hydrogenation of the double bond, to give the Series II unsaturated building blocks **106a** and **106b**. The β-analogue was also accessible using this protocol (Scheme 3.38). The fact that building blocks **106a** and **106b** were readily obtained via the hydrogenation/hydrogenolysis of compounds **105a** and **105b** obtained in this way**,** when the hydrogenation/hydrogenolysis product **106b** from **105b** obtained by the direct displacement of the chiral auxiliary (Scheme 3.28) had been unsuccessful, supports our hypothesis that in that reaction, sulfur from chiral auxiliary impurities poisoned the palladium catalyst, preventing the reaction.

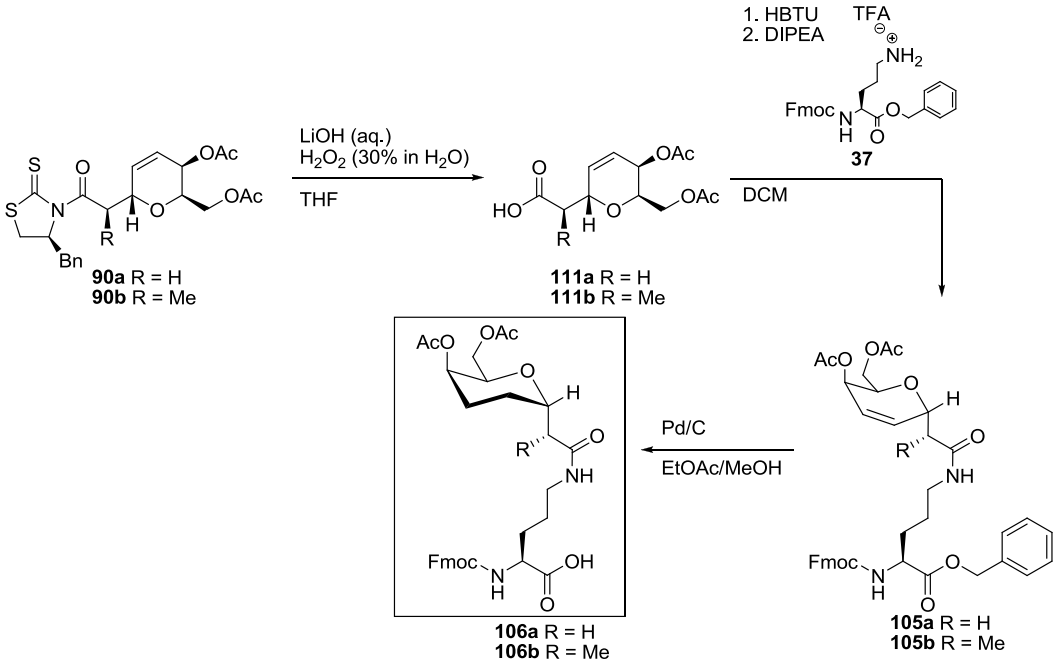

Scheme 3.37 Synthesis of the building block for the Series II α-linked analogue containing a saturated carbohydrate moiety

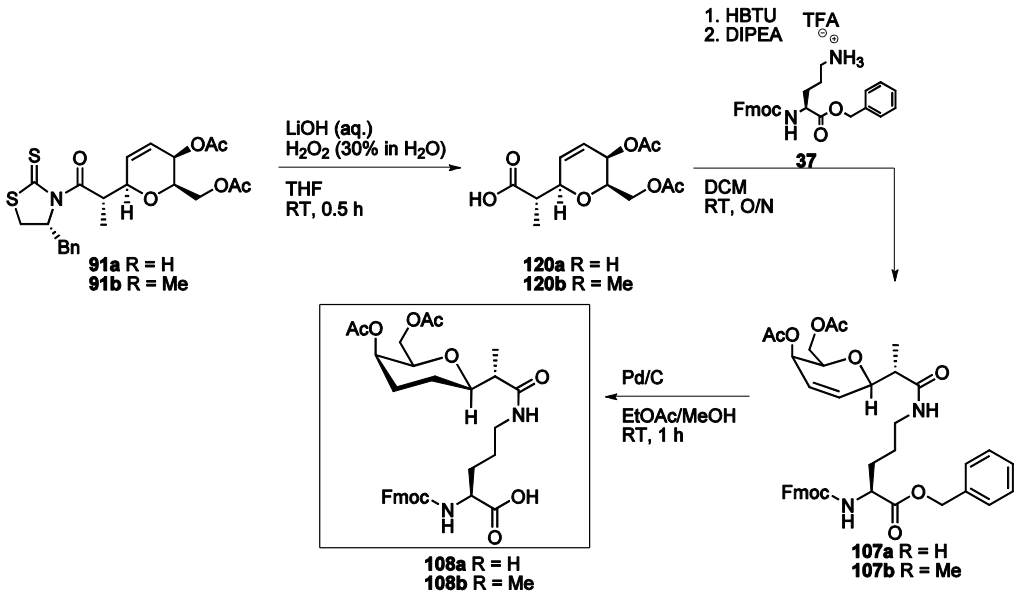

Scheme 3.38 Synthesis of the building block for the Series II β-linked analogue containing a saturated carbohydrate moiety

As shown in Scheme 3.37 and 3.38, this route was also employed for the analogues bearing a methyl group at the pseudo-anomeric position (R = Me). The α- and β-linked carboxylic acid galactal derivatives were readily obtained, and couplings with the ornithine derivative were also successful. However, while the hydrogenolysis reactions provided the wanted products (as determined by ^{1}H NMR and MS), these could not be adequately purified for peptide synthesis.

In the meantime, it had been shown by our lab that relative antifreeze activity could be rapidly gauged by testing just the *C*-linked carbohydrates (the carboxylic acid galactal derivatives), or the building blocks alone. Therefore, all Series II building blocks were fully deprotected using sodium methoxide (Scheme 3.39). Compounds **121**-**124** were then purified by preparative thin-layer chromatography and assessed for antifreeze activity (refer to Part II).

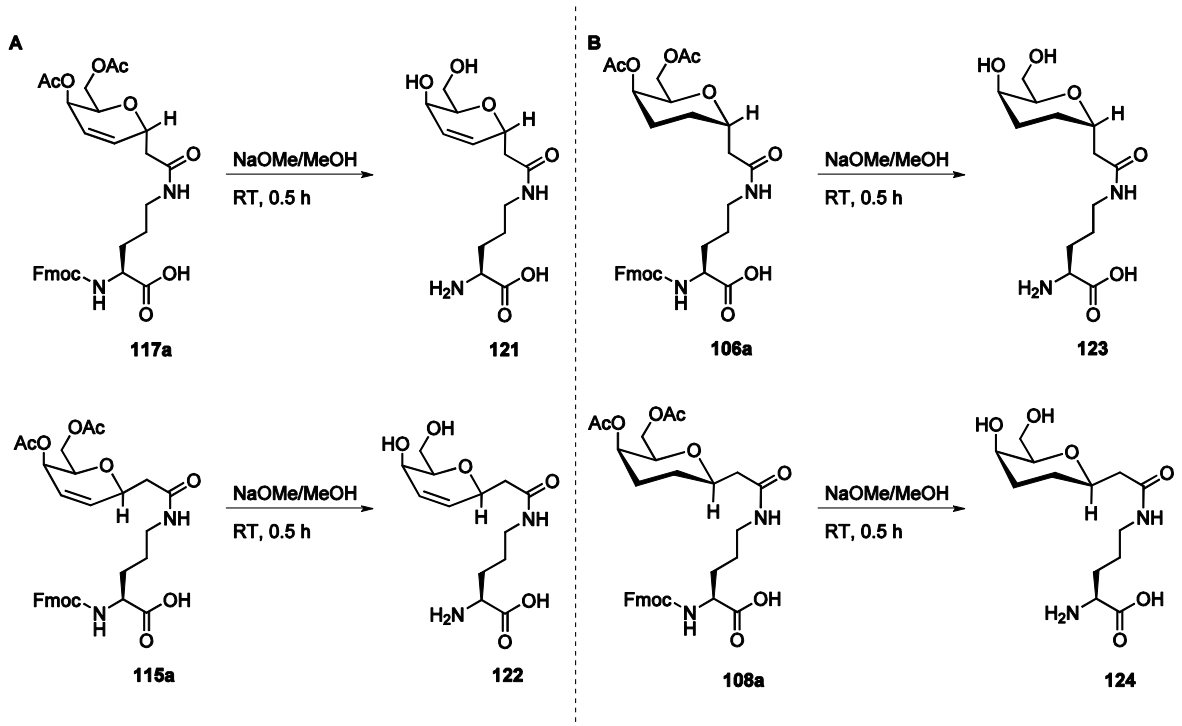

Scheme 3.39 Complete deprotection of series II building blocks in preparation for antifreeze activity testing

An overview of the syntheses of each of the products – building blocks for solid-phase synthesis (**106a**, **108a**, **115a**, and **117a**), and deprotected building blocks ready for antifreeze activity (**121**, **122**, **123** and **124**) - are presented in Schemes 3.40 and 3.41.

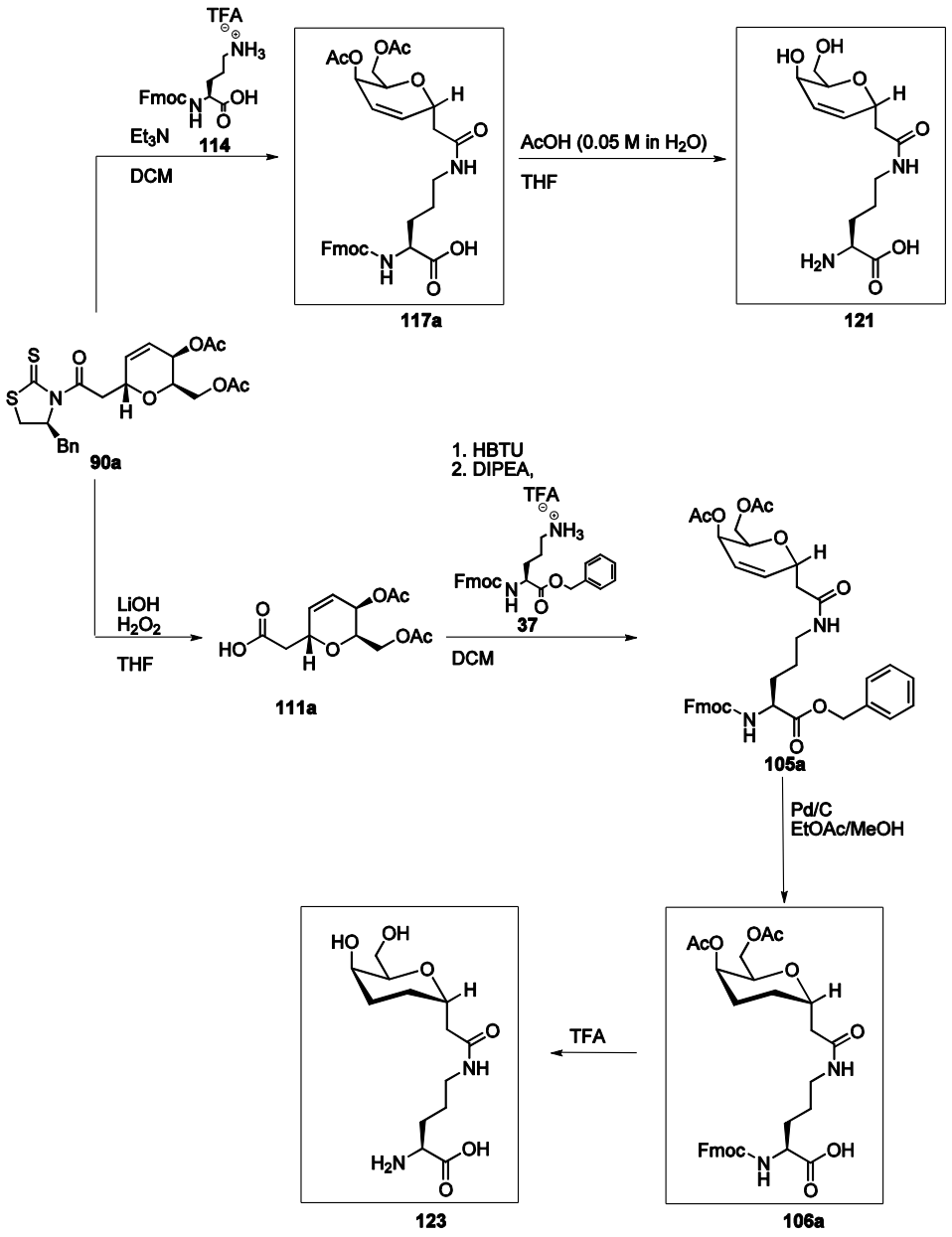

Scheme 3.40 Summary: synthesis of both the building blocks for the Series II α-linked analogues (**117a** and **106a**) and the building blocks to be used for antifreeze activity testing (**121** and **123**)

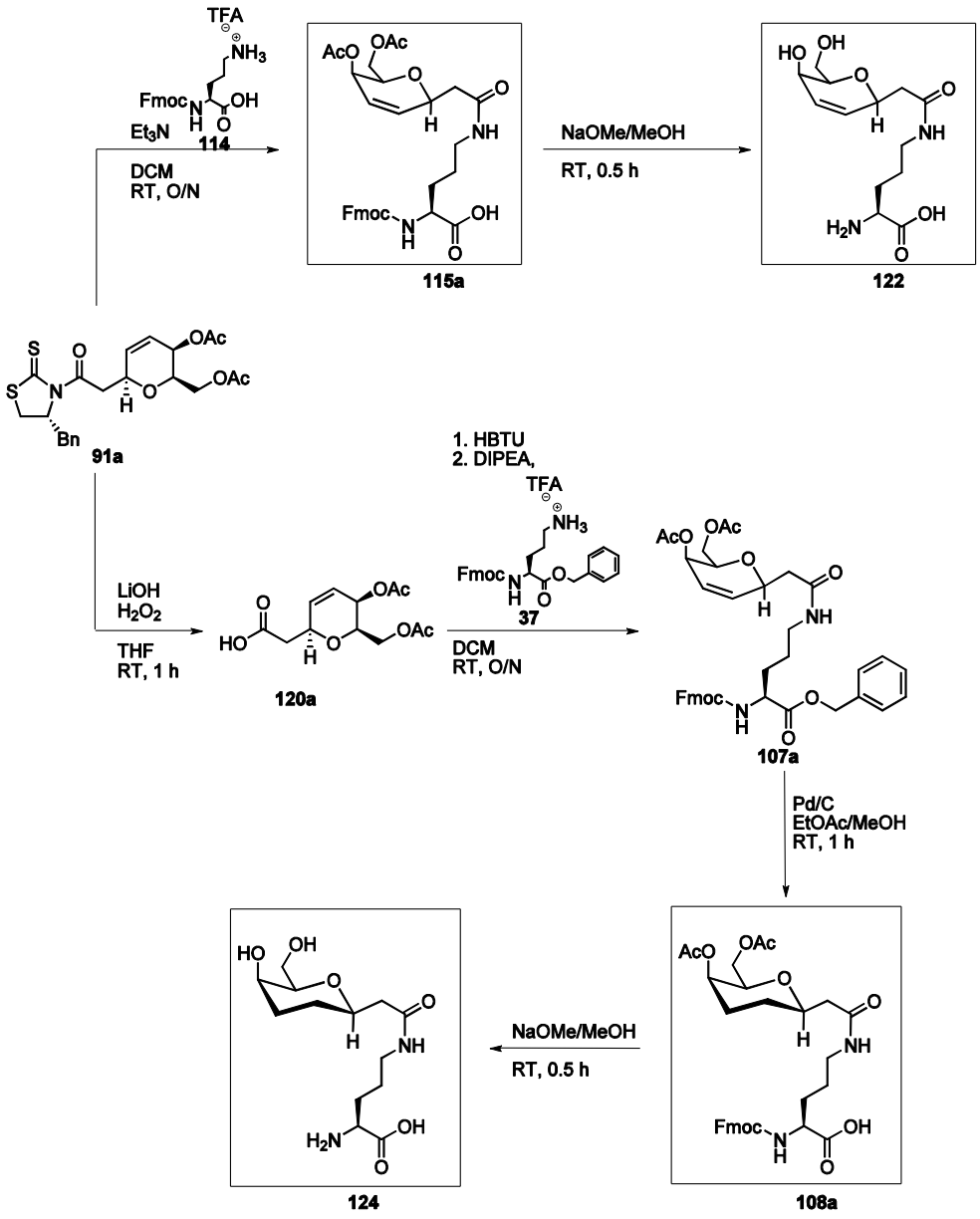

Scheme 3.41 Summary: synthesis of both the building blocks for the Series II β-linked analogues (**115a** and **108a**) and the building blocks to be used for antifreeze activity testing (**122** and **124**)

Several more *C*-linked carboxylic acid galactal derivatives were synthesized using the same protocol previously used for the simple analogues **111a** and **120a** in Schemes 3.40 and 3.41, respectively. The newly synthesized compounds are shown in Scheme 3.42. Since the work-up for these compounds was carried out using an acid-base extraction, in some

cases, the acetate protecting groups were partially or completely hydrolyzed. As a result, the acetylated compounds were difficult to isolate and characterize. The final, de-acetylated compounds were fully characterized, and therefore we were confident in the identity of the acetylated precursors.

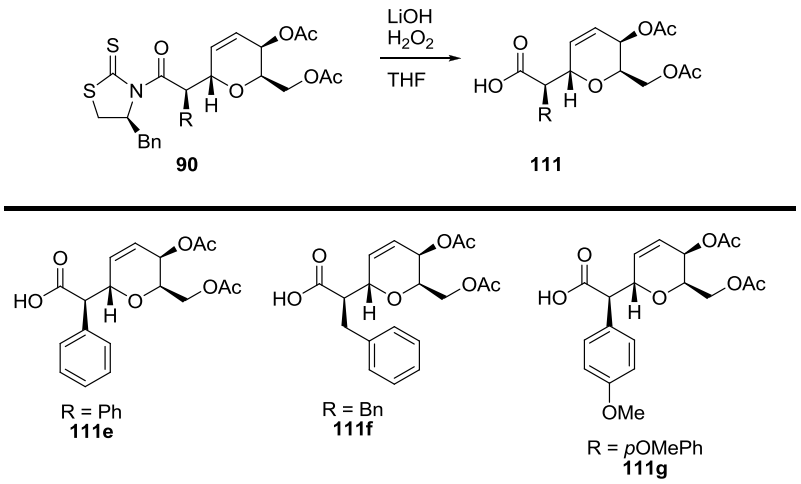

Scheme 3.42 Synthesis of various protected *C*-linked carboxylic acid galactal derivatives

The protected *C*-linked carboxylic acid galactal derivatives were easily deprotected using sodium in methanol. The deprotected *C*-linked carboxylic acid galactal derivatives are shown in Scheme 3.43 (including both the α- and β-anomers). After purification by preparative thin layer chromatography, these analogues were tested for antifreeze activity (refer to Part II).

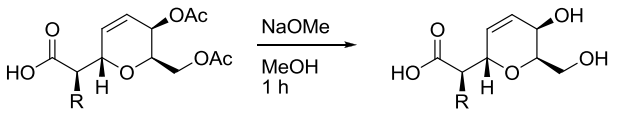

111 **125**

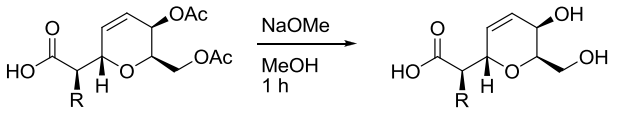

120 **126**

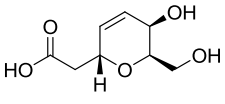

R = H
125a

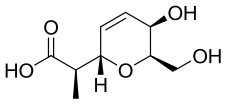

R = Me
125b

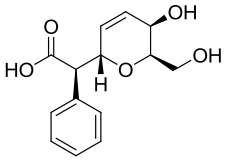

R = Ph
125e

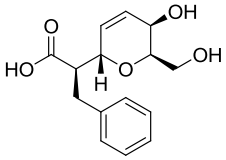

R = Bn
125f

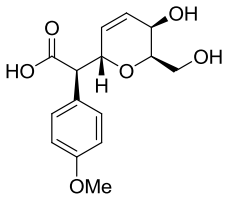

R = *p*OMePh
125g

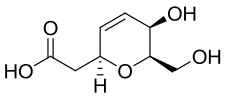

R = H
126a

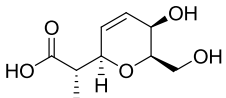

R = Me
126b

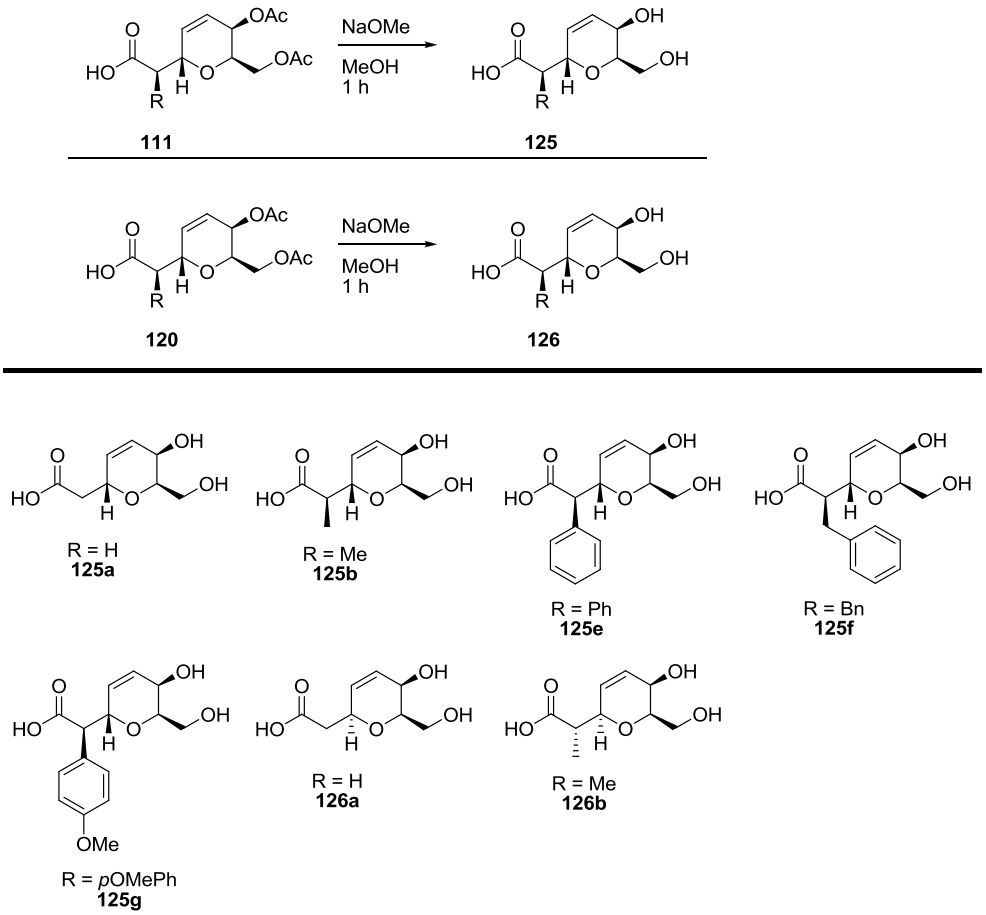

Scheme 3.43 Deprotection of various *C*-linked carboxylic acid galactal derivatives for antifreeze activity testing

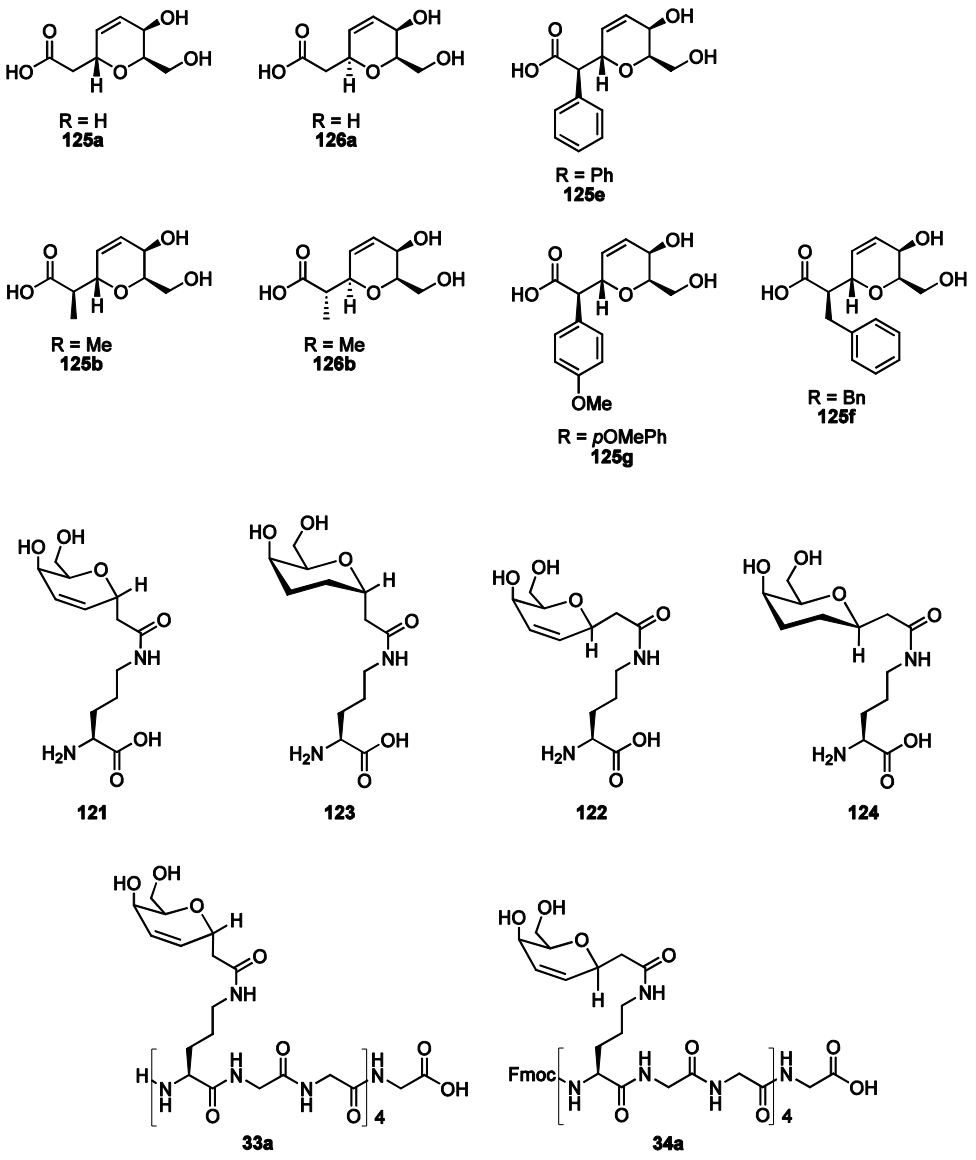

Figure 3.1 Summary of all compounds synthesized for antifreeze testing

Part II of this chapter explores the results of the antifreeze activity testing that was carried out with the polymers, building blocks, and *C*-linked carboxylic acid galactal derivatives just described.

3.2.3 Assessing the Cryopreservation Activity of the Ornithine Analogue: Synthesis of the Ornithine Analogue

Objectives 2.1 and 2.2 deal with the assessment of cryopreservation potential and will be addressed in Chapter 4. However, the synthesis of the ornithine analogue (compound **14**, Scheme 3.44) is detailed here. The ornithine analogue has previously been synthesized in our lab; however, since we intended to carry out cryopreservation studies with this analogue, it was re-synthesized as part of the current study. The protocol for synthesis of the building block is shown in Scheme 3.45.

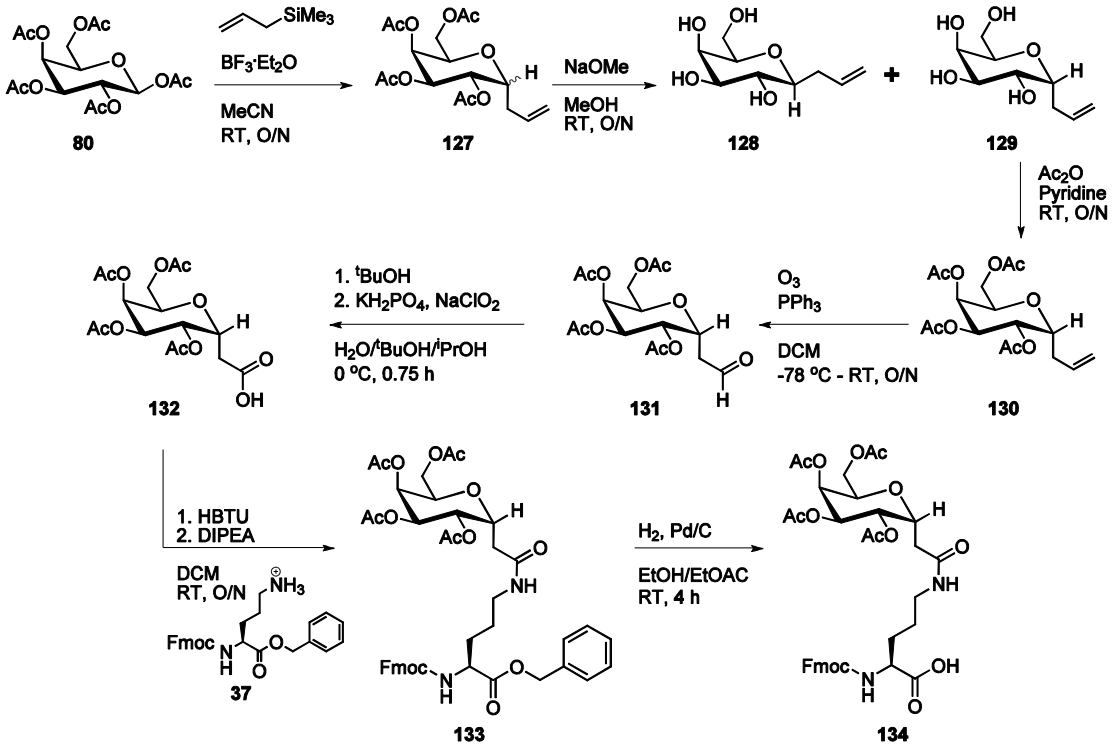

Scheme 3.44 Synthesis of building block **134** for the ornithine analogue (**14**)

The carbon linkage was installed in a Lewis acid-mediated step to give the epimeric *C*-linked product **127**. De-acetylation allows the separation of the two diastereomers by recrystallization to give the desired α-anomer **129**, and re-acetyllation was followed by a

two-step oxidation to provide the carboxylic acid **132**. Coupling **132** with the protected ornithine **37** using HBTU was followed by hydrogenolysis to provide the ornithine building block **134**. At this point, the building block was combined with material synthesized by Mathieu Leclere, who purified all of the material and carried out the solid-phase synthesis to produce the polymer. The solid-phase synthesis was carried out on Wang Resin using an HBTU coupling protocol (Scheme 3.46). The completed polymer was cleaved from the bead using a solution of TFA, and deprotected using sodium methoxide in methanol to provide the final compound.

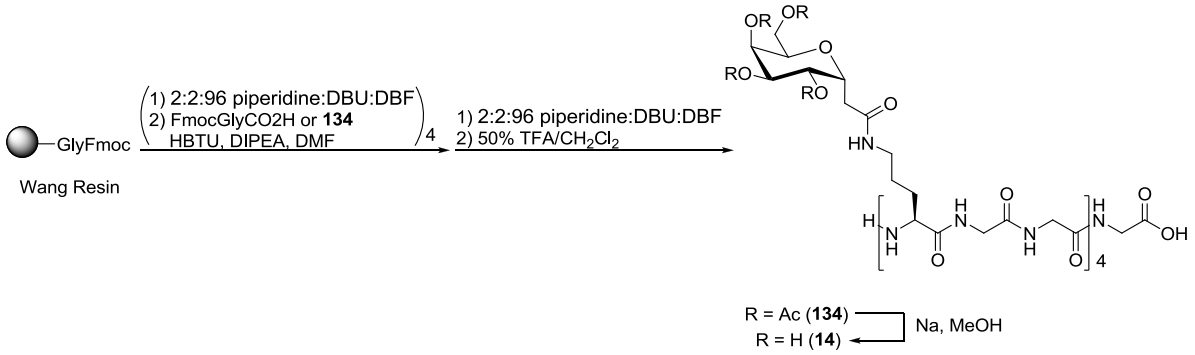

Scheme 3.45 Solid phase synthesis of the ornithine analogue (**14**)

Part II: Assessing Antifreeze Activity

3.3 Thermal Hysteresis (TH) Activity

All of the analogues – polymers and carbohydrates – that were synthesized as detailed in Part I were tested for RI and TH activity. The results of TH testing are shown in Table 3.3. Our lab has shown previously that the ornithine analogue (**14**) does not possess any TH acitivty, although both the ornithine analogue (**14**) and AFGP 8 (**13**) showed dynamic ice shaping (DIS), indicating that they do interact with ice crystals. In the course of the current work, the newly synthesized carbohydrates and AFGP analogues were tested for TH, and similarly showed no activity. DIS was only seen with the polymers (**33a** and **34a**). Photos of ice crystals in the presence of each compound are provided in Tables 3.3 and 3.4. The arrow in each picture indicates the location of the ice crystal in the water drop submerged in the oil.

Table 3.3 Results of thermal hysteresis (TH) activity testing: carboxylic acid galactal derivatives and building blocks

Compound	Melting Point	Photo	TH	Compound	Melting Point	Photo	TH
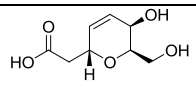 R = H **125a**	-0.09 ºC	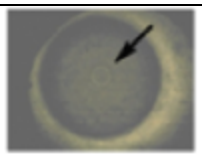	no	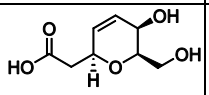 R = H **126a**	-0.15 ºC	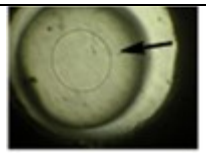	no
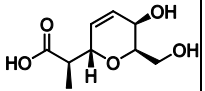 R = Me **125b**	-0.11 ºC	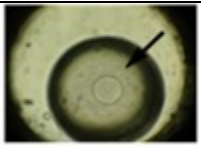	no	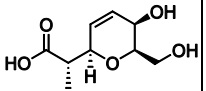 R = Me **126b**	-0.01 ºC	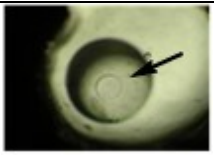	no

Compound	Melting Point	Photo	TH	Compound	Melting Point	Photo	TH
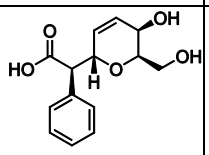 R = Ph **125e**	-0.02 ºC	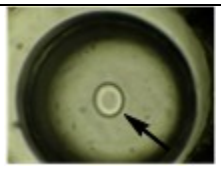	no	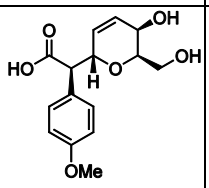 R = *p*OMePh **125g**	-0.02 ºC	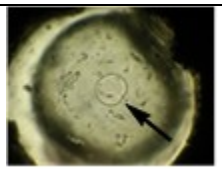 a	no
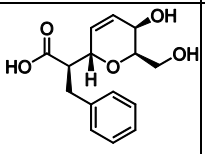 R = Bn **125f**	-0.05 ºC	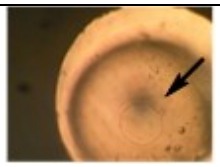	no				
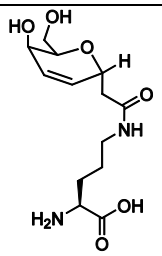 **121**	-1.01 ºC	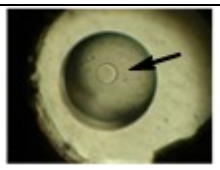	no	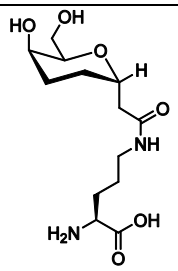 **123**	-0.07 ºC	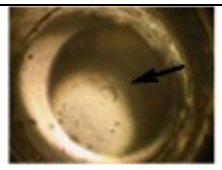	no
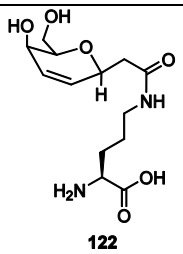 **122**	-0.4 ºC	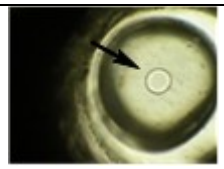	no	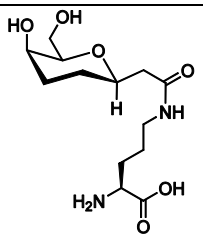 **124**	-0.41 ºC	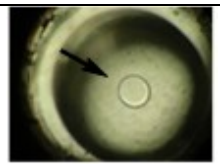	no

[a] arrow indicates two ice crystals fused together

Table 3.4 Results of thermal hysteresis (TH) activity testing: polymers

Compound	Melting Point	Photo	TH
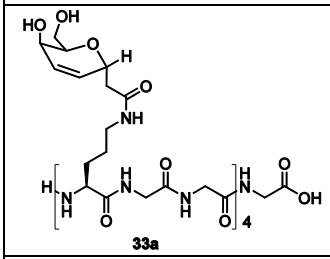 **33a**	-0.18 ºC	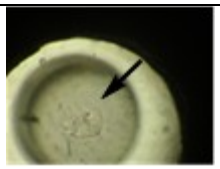	no
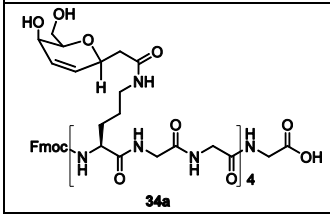 **34a**	-0.04 ºC	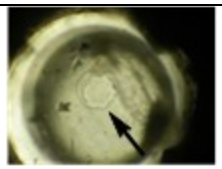	no

The AFGP 8 analogues **33a** and **34a**, building blocks **121-124**, and carboxylic acid galactal derivatives **125a**,**125b**, **125e**, **125f**, **125g**, **126a**, and **126b** as 10 mg/mL solutions in de-ionized water depressed the freezing point of water to between -0.01 ºC and -1.01 ºC. However, the solubility of the compounds varied widely and this likely had a significant effect on the freezing point depression. Of the carboxylic acid galactal derivatives, compounds **125e** and **125f** were slightly insoluble and compound **125g** was very poorly soluble. In fact, the solid particles could be clearly seen in the picture provided for compound **125g**. The remaining carboxylic acid galactal derivatives were readily soluble in water, as were all of the building blocks. Both polymers also displayed poor solubility in water, and as for compound **125g**, the solid particles could be clearly seen under the microsope. Not surprisingly, it appears that, in general, the more-soluble compounds were able to depress the freezing point to a greater extent than those with limited solubility. Consequently, we propose that the difference in freezing point depression among the compounds is relatively narrow.

Dynamic ice shaping (DIS) was not seen with the carboxylic acid galactal derivatives, nor with the building blocks. Interestingly, the two polymers did show DIS. While it was clear that polymer **33a** affected the shape of the ice crystal to some extent, as can be seen from the picture, the shape was not clearly defined. Polymer **34a**, on the other

hand, clearly caused the ice crystal to assume a hexagonal shape. Although it was difficult to draw a conclusion based on this limited sample set, it appeared that, at least in this case, the length of the compound had an influence on DIS activity; that is, the building blocks monomers were insufficient for DIS. In any case, none of the compounds tested showed any TH activity. Since TH activity is not desirable for cryopreservation, the absence of any TH activity was encouraging.

3.4 Recrystallization Inhibition (RI) Activity

Next, each newly synthesized compound was tested for RI activity. Phosphate-buffered saline (PBS) was tested for RI activity on every day that RI testing of compounds was carried out. The data was reported as the ratio of the mean grain size (MGS) of the test compound to the MGS of the PBS sample measured that day. PBS was therefore reported as having a ratio of 1.0 and served as the negative control. Importantly, the smaller the mean grain size (mm^2) found for a given compound, the greater that compound's RI activity. The carbohydrates were tested at a concentration of 22 mM in PBS, and their RI activity is shown in Figure 3.3. Commercially available galactose and 2-deoxygalactose, as well as synthesized α-*C*-acid-galactose were previously tested in our lab by Jennifer L. Chaytor and Jacqeuline Tokarew, and are included in the figure for comparison.

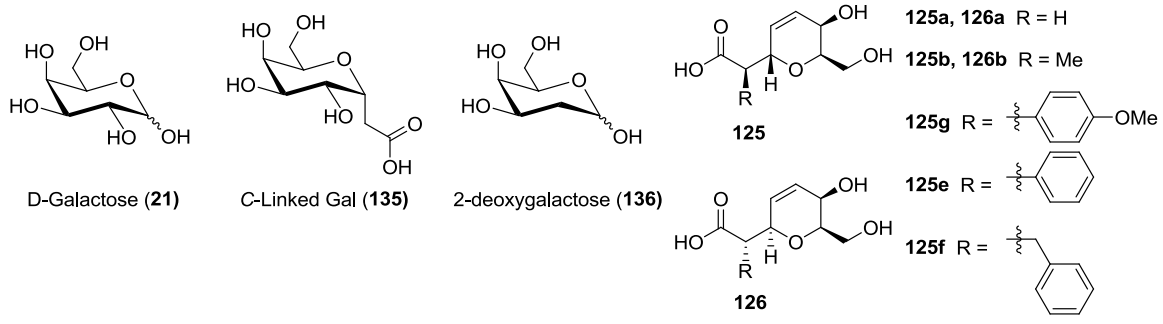

Figure 3.2 Structure of the carbohydrates and *C*-linked carbohydrates tested for recrystallization inhibition (RI) activity (data in Figure 3.3)

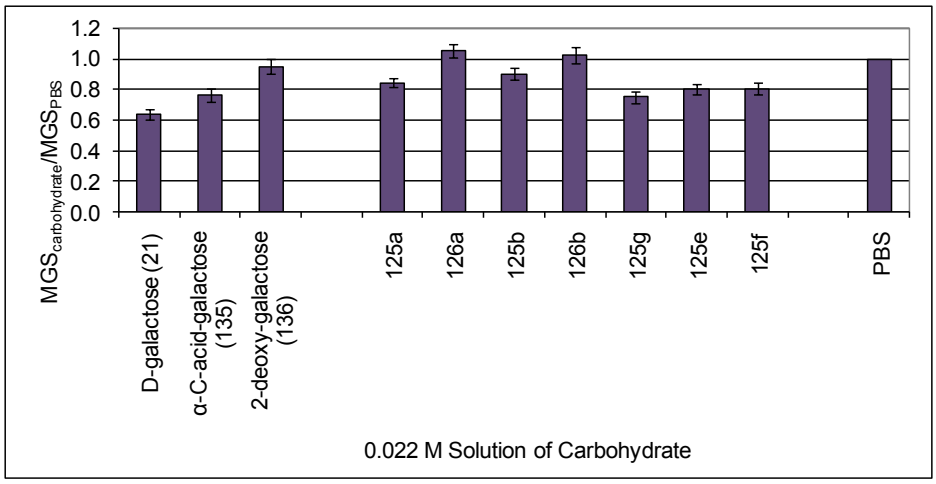

Figure 3.3 Recrystallization inhibition (RI) activity of several carbohydrates in PBS; RI activity is reported as a ratio of the mean grain size (MGS) of the carbohydrate solution to the MGS of the PBS solution.

As was shown in Chapter 2, galactose had the greatest RI activity of the monosaccharides. It therefore served as a benchmark value against which the newly synthesized carbohydrate derivatives could be compared. The α-*C*-acid galactose was included to show that while the derivatization of galactose to produce a *C*-linked carboxylic acid galactose derivative did decrease the RI activity relative to galactose, it did not eradicate activity. The difference in RI activity between the newly synthesized derivatives and galactose was only partly due to the addition of the carboxylic acid moiety, or the addition of a *C*-linkage to the anomeric centre. The removal of the C2 hydroxyl group from galactose to give 2-deoxygalactose, on the other hand, nearly eradicated RI activity. As discussed in Chapter 2, our lab has shown that carbohydrate configuration seems to be very important for RI activity, and RI activity is maximized when the C4 hydroxyl group is axial and all other hydroxyl groups are in an equatorial position.[18] The poor RI activity exhibited by 2-deoxygalactose supports the hypothesis that the C2 hydroxyl group plays an important role in RI activity. Consequently, the newly synthesized analogues were not expected to have very good RI activity. It is interesting, therefore, that some of the newly synthesized analogues did show RI activity comparable to that of α-*C*-acid galactose. In fact, the α-linked derivatives bearing aromatic groups, including **125e**, **125f**, and **125g** all showed RI activity equivalent to

that of α-*C*-acid galactose. However, none of the derivatives showed activity equivalent to that of galactose.

The RI activity of the non-aromatic analogues (**125a**, **125b**, **126a**, and **126b**) was also somewhat surprising. It was hypothesized that, at least for the polymers (AFGP analogues), the addition of the methyl group (R = Me) next to the anomeric centre would increase RI activity compared to that of the unsubstituted (R = H) analogue. Further, it was expected that the same trend would be reflected by the carboxylic acid galactal derivatives; however, Figure 3.3 shows that **126a** (R = H) had a slightly greater RI activity than **126b** (R = Me), although the difference was not statistically significant. While **125a** (R = H) had greater RI activity than 2-deoxygalactose, the difference between **125b** (R = Me) and 2-deoxygalactose was not statistically significant. However, for both R = H, and R = Me, the α-anomer had greater RI activity than the corresponding β-anomer. In fact, the β-anomers **126a** (R = H), and **126b** (R = Me) did not show any RI activity (they showed activity equivalent to that of PBS). Based on previously studied analogues, this was the expected trend for RI activity of the α-anomers and their respective β-anomers.

The fact that the *C*-linked analogues showed RI activity at all, despite the dramatic structural modifications compared to galactose or *C*-linked Gal (**135**), is interesting in itself. These analogues lack both the C2 and C3 hydroxyl groups, and further, the double bond will prevent the cyclohexane ring from adopting the chair conformation of the saturated ring. Therefore, the orientation of the remaining substituents will also differ from the orientation of the hydroxyl groups of 2-deoxygalactose and galactose. It may be that the new analogues are positioned at the ice/water interface in a very different way than either the 2-deoxygalactose or galactose, and therefore have slightly different requirements for activity. The best of these analogues, those bearing the aromatic substituents (compounds **125e**, **125f**, **125g**), had equivalent RI activity to *C*-linked Gal, despite their structural differences; therefore, it is unlikely that these very different compounds would be interacting with ice in the same manner. It is difficult, therefore, to draw clear conclusions from this data. The difference in RI between the different α-anomers (**125**) was not very great, and while all of them show some RI activity, none of the α-anomers have activity comparable to that of galactose. Therefore, while the data obtained for the new *C*-linked carboxylic acid galactal derivatives showed a slight internal trend of increasing RI activity with increasing

hydrophobicity, these analgoues did not surpass the RI activity of galactose, and this data does not appear to support the conclusion that increasing the hydrophobicity of the *C*-linked carbohydrate derivatives necessarily improves RI activity.

Subsequently, the four newly synthesized building blocks (**122**-**124**, Figure 3.4) were also tested for RI activity, and the results are shown in Figure 3.5. The mean grain size ratios were obtained as described above, and PBS remains the negative control. Previously tested commercially available galactose and 2-deoxygalactose (each at a concentration of 22 mM), as well as AFGP 8 (**13**) and the ornithine analogue (**14**) (each at a concentration of 5.5 x 10^{-6} M) were included in the figure for comparison.[18]

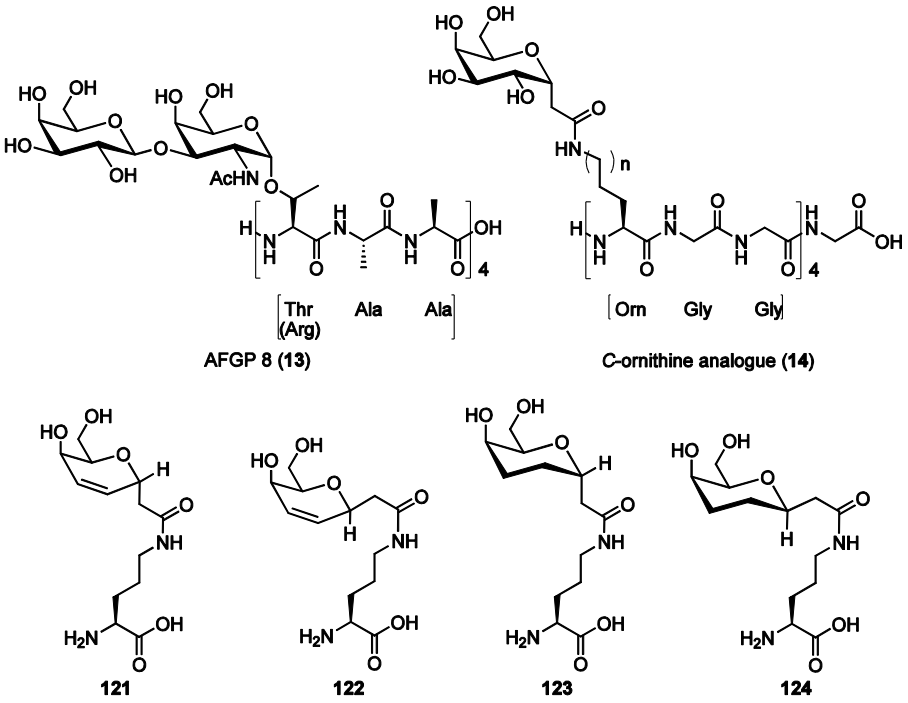

Figure 3.4 Structure of the polymers and building blocks tested for recrystallization inhibition (RI) activity (data in Figure 3.5)

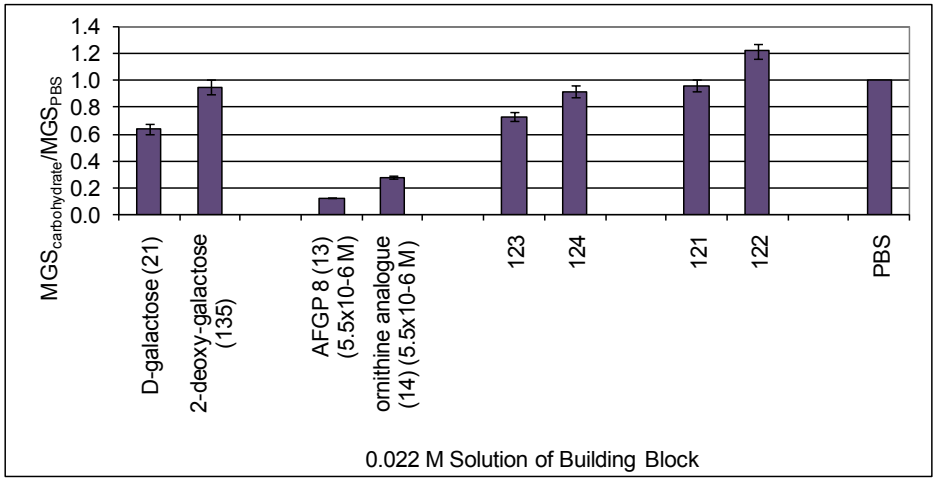

Figure 3.5 Recrystallization inhibition (RI) activity of several building blocks in PBS; RI activity is reported as a ratio of the mean grain size (MGS) of the building block solution to the MGS of the PBS solution.

It can be clearly seen in Figure 3.5, that the polymers AFGP 8 and ornithine analogue **14** have significantly better RI activity than galactose, even though they were tested at a much lower concentration: the polymers were tested at a concentration of only 5.5 x 10^{-6} M in PBS, while carbohydrates were tested at a concentration of 2.2 x 10^{-2} M in PBS. Therefore, the concentration of polymer in PBS required for significant RI activity is much lower than the concentration of carbohydrate in PBS required for RI activity. Unfortunately, the RI activity of the building blocks (**121-124**) was much poorer than that of any of AFGP 8 (**13**), the ornithine analogue (**14**), or galactose (**21**). The RI activity exhibited by the building blocks varied widely. In each case, the RI activity of the α-anomers was significantly greater than that of the β-anomers. The α-anomer **124** had greater activity than the α-anomer **121**, and similarly, the β-anomer **124** had greater activity than the β-anomer **122**. However, the β-anomer **124** showed RI activity comparable to that of the α-anomer **121**, and further, neither compound showed better RI activity than that of 2-deoxygalactose. Oddly, the RI activity of the β-linked building block **122** was seemingly much poorer than PBS, and this suggests that either the accuracy of that measurement was poor, or that **122** actually aided recrystallization. The absence or presence of a double bond in the carbohydrate moiety was the only difference between analogues **123** and **124**, and **121** and **122**, respectively; therefore, the double bond in the carbohydrate moiety of analogues **121** and **122** increased

the RI activity over that of analogues **123** and **124**. As was the case for the carboxylic galactal derivatives **125** and **126** (Figure 3.1), both compounds are without the C2 and C3 hydroxyl groups, and the double bond in analogues **121** and **122** likely changes the orientation of the remaining constituents of the carbohydrate moiety compared to those of compounds **123** and **124**. This seems to confirm that the addition of the double bond and the resulting change in orientation of the hydroxyl groups (or of the side chain at the anomeric position) does in fact reduce RI activity.

Figure 3.7 presents the RI activity of the newly synthesized AFGP 8 analogues **33a** and **43a**, the carbohydrate-bearing building blocks **121** and **122** used in their respective syntheses, as well as the corresponding carboxylic acid galactal derivatives **125a** and **126a**. As before, the polymers were tested at a concentration of only 5.5 x 10^{-6} M in PBS, while carbohydrates were tested at a concentration of 2.2 x 10^{-2} M in PBS. The best RI activity was seen with the α-*C*-linked polymer **33a**; however, the RI activity of the polymer was not as good as that of galactose. As expected (based on results obtained previously by our lab, as well as the data presented in Figure 3.3), the α-anomers had better RI activity than their β-*C*-linked counterparts. The magnitude of the difference in RI between α- and β-anomers was similar for each of the three types of compounds (polymer, building block, or carbohydrate derivative).

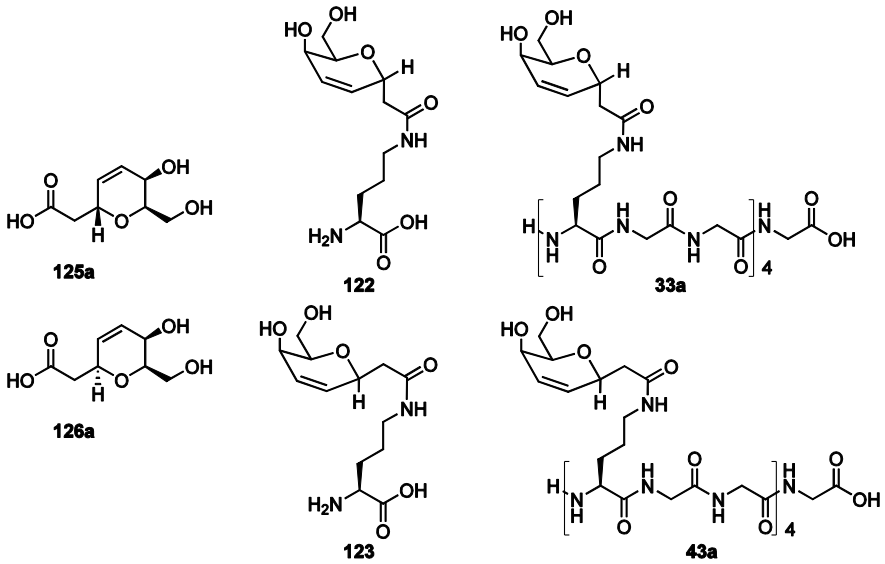

Figure 3.6 Structure of the *C*-linked carbohydrates, building blocks, and polymers tested for recrystallization inhibition (RI) activity (data in Figure 3.7)

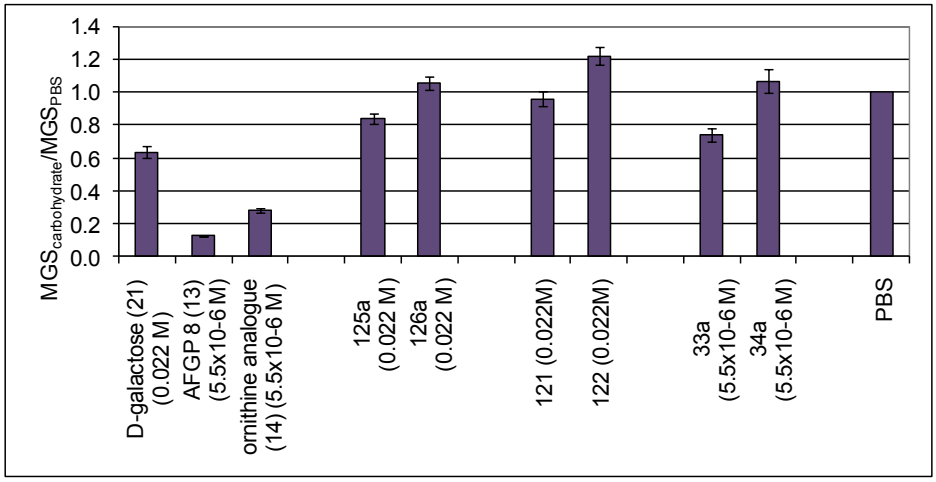

Figure 3.7 Recrystallization inhibition (RI) activity of several polymers and their corresponding building blocks and carbohydrate derivatives in PBS; RI activity is reported as a ratio of the mean grain size (MGS) of the test solution to the MGS of the PBS solution.

Further, none of the β-*C*-linked analogues showed any RI activity. In all cases, in fact, the RI appears to be *worse* than that of PBS. The relationship of the α-*C*-linked compounds, however, is different: the polymer **33a** shows the best RI activity, the building block **121** shows the worst RI activity (it is nearly equal to PBS), while the carbohydrate derivative falls in the middle. All differences are statistically significant. The RI activity of the AFGP 8 analogue **33a** was not quite as good as that of galactose alone, and very much poorer than that of the ornithine analogue (**14**). This data suggests that the addition of a side chain to the *C*-linked carbohydrate derivative (building block **121** compared to *C*-linked carbohydrate derivative **125a**) does not necessarily result in increased RI activity. This was somewhat surprising, since unpublished work by our lab – carried out by Chantelle Capicciotti – suggests that the addition of side chains at some positions to *C*-linked carbohydrates dramatically increases RI activity. However, in this case, the addition of the side chain adds three additional methylene groups compared to the *C*-linked carbohydrate, but it also adds the highly hydrophilic amine and carboxylic acid of the amino acid, and therefore predicting its effect was difficult. The amino and carboxylic acid groups will exist as a zwitterion, and given the building block's small size compared to the polymer, the zwitterions will likely have a significant effect on the mechanism of action/activity of the

building block. Given that the native AFGP is a polymer, it was not surprising that AFGP 8 analogue **33a** showed the greatest RI activity of the group.

The fact that the three components are significantly different suggests that the building block and carbohydrate derivatives cannot be used as reasonable predictors of the RI activity of the polymer. However, it is possible that the differences are relatively constant between any set of polymer, building block, and carbohydrate derivative, and if this is the case, then testing the carbohydrate derivative or building block may serve as a useful tool to predict the RI activity of the corresponding polymer. It would therefore be interesting to see whether or not the same trend in RI activity (polymer > carbohydrate > building block) holds for the remaining carbohydrate derivatives and building blocks tested. Fortunately, John F. Trant from our lab recently synthesized the building block for the ornithine analogue and tested it for RI activity. The RI data for the carbohydrate derivative, building block, and polymer (shown in Figure 3.8) are compared in Figure 3.9.

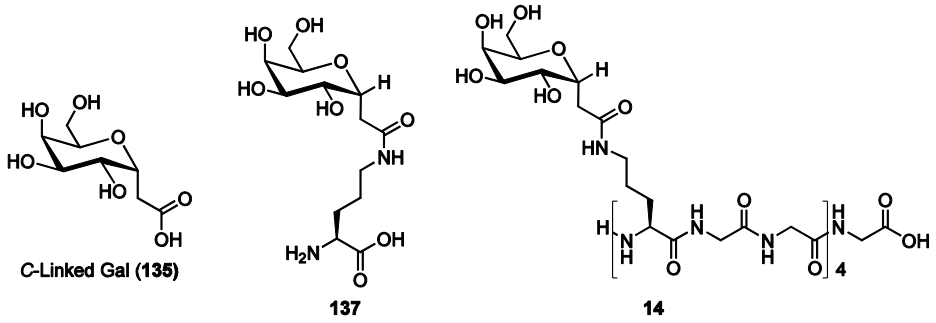

Figure 3.8 Structure of the ornithine analogue (**14**) and corresponding building block (**137**) and carbohydrate derivative (**135**) tested for recrystallization inhibition (RI) activity (data in Figure 3.9)

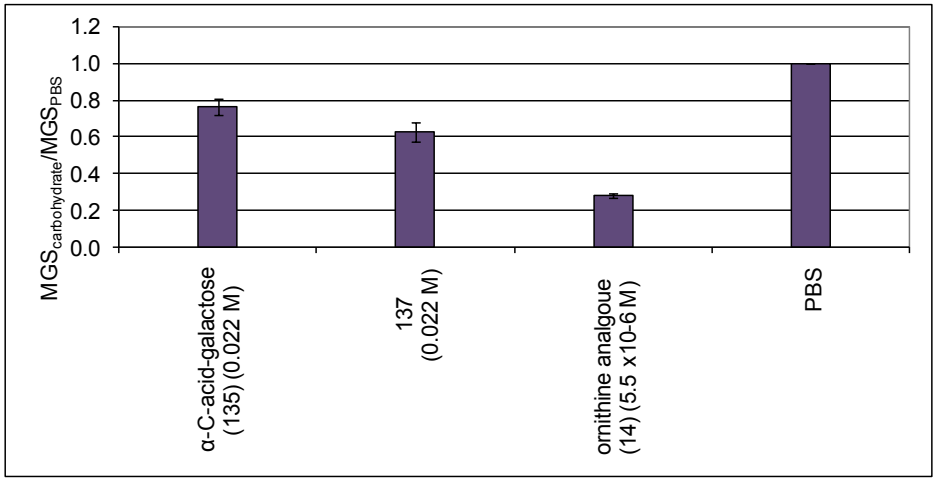

Figure 3.9 Recrystallization inhibition (RI) activity of the ornithine analogue and the corresponding building block and carbohydrate derivative in PBS; RI activity is reported as a ratio of the mean grain size (MGS) of the test solution to the MGS of the PBS solution.

Interestingly, the ornithine analogue (**14**), its building block (**137**) and the carboxylic acid galactose derivative (**135**) did not follow the same trend as that seen in with the deydro analogues in Figure 3.7. For ornithine, the RI activity of the polymer was greater than that of the building block, which in turn had greater RI activity than the carbohydrate component. As was previously stated, for analogues **33a** and **33b**, the carbohydrate showed better activity than the building block. Therefore, based on this small sample set (the ornithine analogue and its components, and analogues **33a** and **34a** and their respective components), it appeared that the trend in RI activity among the three components was not always the same, and could not be predicted, and therefore, in general, the RI of one compound in the "set" likely cannot be used to predict the RI activity of the others.

Finally, Figure 3.11 shows the RI activity of the newly synthesized analogues **33a** and **33b** compared to the series of analogues previously synthesized in our lab that explored the hydrophilic component of the AFGPs[18] and prompted the current study. The analogues are based on the ornithine analogue (**14**) substituted with different monosaccharides, including galactose (**14**), glucose (**18**), mannose (**19**), and talose (**20**).

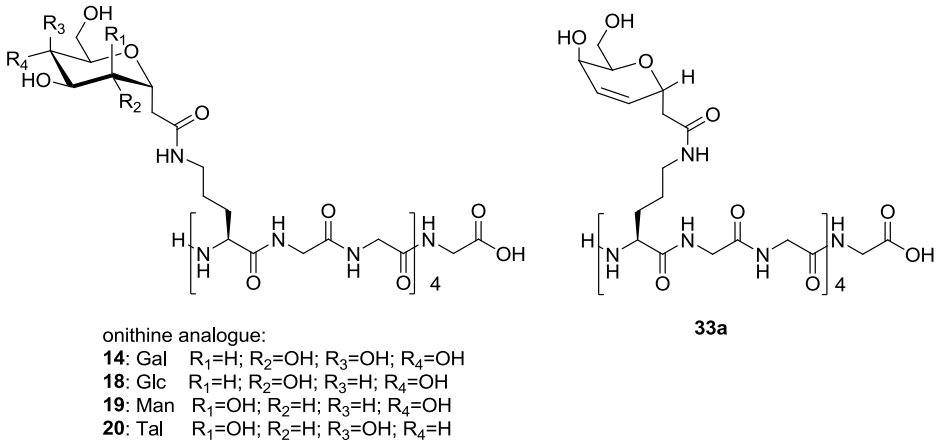

Figure 3.10 Structure of the polymers tested for recrystallization inhibition (RI) activity (data in Figure 3.11)

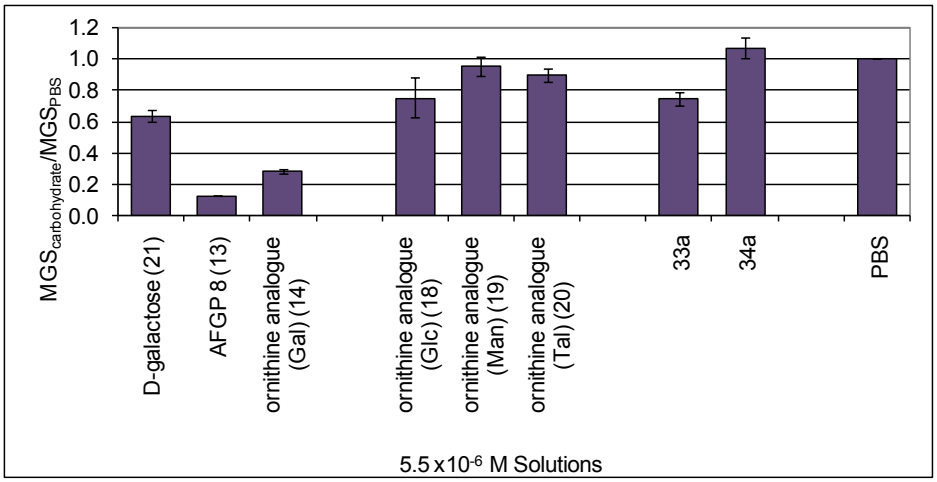

Figure 3.11 Recrystallization inhibition (RI) activity of several polymers in PBS; RI activity is reported as a ratio of the mean grain size (MGS) of the test solution to the MGS of the PBS solution.

The RI activity of analogue **33a** was equivalent to that of the ornithine analogue **18**, in which galactose has been substituted with glucose, and better than that of the mannose- and talose-substituted ornithine analogues **19** and **20**, respectively. Our group previously concluded from the relationship between ornithine analogues **14**, and **18-20**, that carbohydrate configuration was very important for RI activity, and that RI activity was

maximized when the C4 hydroxyl group was axial and all other hydroxyl groups were in an equatorial position.[18] Although glucose has an equatorial hydroxyl group at C4, this was not as detrimental as an axial hydroxyl group at C2, such as that of mannose or talose, since the glucose-substituted analogue **18** shows better RI activity than either the mannose- or talose-substituted analogues (**19** or **20**, respectively). The data shown in Figure 3.11 seemed to indicate that the carbohydrate moiety of analogue **33a** was equivalent to that of glucose (the carbohydrate moiety of **18**). While this finding was somewhat surprising, since the glucose and the carbohydrate moiety of analogue **33a** share neither a common number nor orientation of hydroxyl groups, this result seemed to reinforce that a non-axial hydroxyl group at C2 (no hydroxyl group in the case of the analogue) improved RI activity. However, when the carbohydrate moieties were tested alone (Figure 3.3), 2-deoxygalactose had been found to have poorer RI activity than the newly synthesized analogues, and we had therefore concluded that *C*-linked galactose, 2-deoxygalactose, and newly synthesized carbohydrate moieties may be binding to ice in different ways. The conclusions drawn from Figures 3.3 and 3.11 were therefore difficult to reconcile, although the difference may be related to the general differences between carbohydrate derivatives and polymers. More analogues, including an ornithine analogue substituted with 2-deoxygalactose and 2-deoxyglucose should be tested in order to draw more accurate conclusions. Nevertheless, modifications to analogue **33a** that provide new compounds that incorporate hydrophobic groups on the carbohydrate may result in a potent RI inhibitor.

3.5 Antifreeze Activity Testing: Summary

In conclusion, none of the newly synthesized analogues showed TH activity, and only the polymers showed DIS. Accurate assessment of the melting point in the presence of some of the carboxylic acid galactal derivatives (notably those bearing an aromatic substituent) as well as the polymers was hampered by their limited solubility in the de-ionized water they were tested in. RI activity was observed for all compounds; however, all compounds showed poorer RI activity that either galactose (**21**) or the ornithine analogue (**14**). As expected, the

α-linked compounds showed better RI activity than their corresponding β-linked compounds, and notably, carboxylic acid galactal derivatives **125e,f,g** bearing aromatic substituents at the pseudo-anomeric position showed RI activity that was equal to that of the carboxylic acid galactose derivative **135**. However, we concluded that increasing the hydrophobicity of the carbohydrate analogue does not necessarily increase RI activity. For future studies, it would be interesting to append aromatic groups to the pseudo-anomeric position of *C*-linked carboxylic acid galactose derivatives, rather than to the galactal derivatives, in order to study the influence of the additional groups in isolation. A different synthetic approach than the one employed for the galactal derivatives would be required, however, since we were unable to synthesize the galactose derivatives in this study.

With the newly synthesized analogues, it was found that RI activity decreased on moving from the polymer, to the carbohydrate, and then to the building block. However, for the ornithine analogue (**14**) and its components it was found that while the polymer had the greatest RI activity, the RI activity of the building block was greater than that of the carbohydrate, and therefore, no general conclusions could be derived regarding the trend of the three component types.

Lastly, we found evidence that the carbohydrate-derived moiety of the newly synthesized polymers was equivalent to that of the glucose moiety of the reference polymers in terms of RI activity. However, it was difficult to reconcile this interpretation of the data with the conclusion we drew based only on the carbohydrate data that the unsaturated carbohydrate moiety may bind to the ice-water interface differently than the saturated carbohydrate moieties. More studies will have to be carried out to further investigate these ideas.

1. Cosp, A.; Romea, P.; Talavera, P.; Urpi, F.; Vilarrasa, J.; Font-Bardia, M.; Solans, X., Enantioselective addition of a chiral thiazolidinethione-derived titanium enolate to acetals. *Organic Letters* **2001,** 3, 615-617.
2. Larrosa, I.; Romea, P.; Urpi, F.; Balsells, D.; Vilarrasa, J.; Font-Bardia, M.; Solans, X., Unprecedented highly stereoselective α- and β-C-glycosidation with chiral titanium enolates. *Organic Letters* **2002,** 4, 4651-4654.
3. McKennon, M. J.; Meyers, A. I., A covalent reduction of amino acids and their derivatives. *Journal of Organic Chemistry* **1993,** 58, 3568-3571.
4. Crimmins, M. T.; King, B. W.; Tabet, E. A.; Chaudhary, K., Asymmetric aldol additions: use of titanium tetrachloride and (-)-sparteine for teh soft enolization of *N*-acyl oxazolidinones, oxazoladinethiones, and thiazolidinethiones. *Journal of Organic Chemistry* **2001,** 66, 894-902.
5. Boons, G.-J.; Hale, K. J., *Organic Synthesis with Carbohydrates*. Blackwell Science, Inc.: Malden, 2000; p 348.
6. Somsak, L.; Nemeth, I., A simple method for the synthesis of acylated pyranoid glycals under aprotic conditions. *Journal of Carbohydrate Chemistry* **1993,** 12, (4), 679-684.
7. Sharpless, K. B.; Amberg, W.; Bennani, Y. L.; Crispino, G. A.; Hartung, J.; Jeong, K.-S.; Kwong, H.-L.; Morikawa, K.; Wang, Z.-M.; Xu, D.; Zhang, X.-L., The osmium-catalyzed asymmetric dihydroxylation: a new ligand class and a process improvement. *Journal of Organic Chemistry* 57, 2768-2771.
8. VanRheenen, V.; Cha, D. Y.; Hartley, W. M., Catalytic osmium tetroxide oxidation of olefins: cis-1,2-cyclohexanediol. *Organic Syntheses* **1978,** 58, 43.
9. Ray, R.; Matteson, D. S., Osmium tetroxide catalyzed hydroxylation of hindered olefins. *Tetrahedron Letters* **1980,** 21, 449-450.
10. Roberts, C. W., The synthesis of L-cysteinyl-L-tyrosyl-L-isoleucine. *Journal of the American Chemical Society* **1954,** 76, 6203-6204.
11. Griffith, W. P.; Ley, S. V.; Whitcombe, G. P.; White, A. D., Preparation and use of tetra-n-butylammonium per-ruthenate (TBAP reagent) and tetra-n-propylammonium per-ruthenate (TPAP reagent) as new catalytic oxidants for alcohols. *Journal of the Chemical Society Chemical Communications* **1987**, 1625-1627.
12. Ley, S. V.; Norman, J.; Griffith, W. P.; Marsden, S. P., Tetrapropylammonium perruthenate, $Pr_4N^+RuO_4^-$, TPAP: a catalytic oxidant for organic synthesis. *Synthesis* **1994**, 639-666.
13. Omura, K.; Swern, D., Oxidation of alcohols by "activated dimethyl sulfoxide. A preparative, steric and mechanistic study. *Tetrahedron* **1978,** 34, 1651-1660.
14. Zhao, M. M.; Li, J.; Mano, E.; Song, Z. J.; Tschaen, D. M., Oxidation of primary alcohols to carboxylic acids with sodium chlorite catalyzed by tempo and bleach: 4-methophenylacetic acid. *Organic Syntheses* **2005,** 81, 195-199.
15. Nahm, S.; Weinreb, S. M., N-Methoxy-N-methylamides as effective acylating agents. *Tetrahedron Letters* **1981,** 22, 3815-3818.
16. Zakarian, A.; Batch, A.; Holton, R. A., A convergent total synthesis of hemibrevetoxin B. *Journal of the American Chemical Society* **2003,** 125, 7822-7824.
17. Evans, D. A.; Britton, T. C.; Ellman, j. A., Contrasteric carboximide hydrolysis with lithium hydroperoxide. *Tetrahedron letters* **1987,** 28, 6141-6144.
18. Czechura, P.; Tam, R. Y.; Dimitrijevic, E.; Murphy, A. V.; Ben, R. N., The importance of hydration for inhibiting ice recrystallization with C-linked antifreeze glycoproteins. *Journal of the American Chemical Society* **2008,** 130, 2928-2929.

Chapter 4: Cryopreservation Studies

This chapter will detail the experiments carried out to determine the value of various carbohydrates as cryoprotectants for cells. The goal was to devise a cryopreservation protocol that employs carbohydrates as the cryopreservation agents. The cells of interest are human umbilical cord blood hematopoietic stem cells, and human hepatocytes. The details of these cell types, as well as the particular protocols currently used for their cryopreservation, will be discussed first.

4.1 State of the Art: Cryopreservation Conditions for Umbilical Cord Blood (UCB) Hematopoietic Stem Cells (HSCs) and Hepatocytes

In order to determine the relative efficacy of different cryoprotective agents, we first established a cryopreservation assay appropriate for the cells types we were studying. There is no universally used cryopreservation protocol for either UCB hematopoietic stem cells or hepatocytes; consequently, a literature survey was carried out in order to establish a suitable protocol for this study. The key steps of the cryopreservation sequence that must be taken into consideration are given in Figure 4.1.

The concentration of DMSO generally employed, the cell concentration in the freezing vial, the method used for the addition and removal of the cryoprotectant, the appropriate freezing rate, storage temperature, and thawing rate, were all carefully considered based on literature precedent for both umbilical cord blood and hepatocytes. Since cryopreservation was carried out using the cell line WRL 68 rather than primary hepatocytes - the cell line is more robust than the primary cells - the conditions used for the cryopreservation of the WRL 68 cells could be adapted slightly from the ideal hepatocyte cryopreservation conditions found in the literature. A discussion of each stage of the cryopreservation process follows.

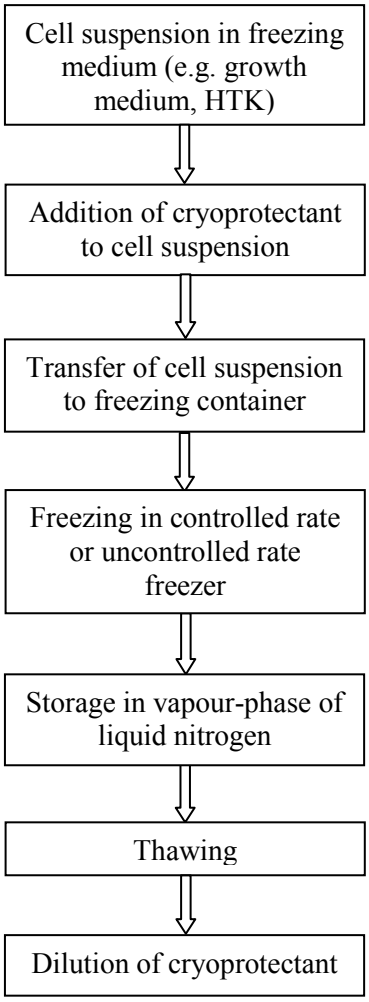

Figure 4.1 Schematic of a typical cryopreservation protocol.

Recently, a number of studies have shown that UCB can be successfully cryopreserved using only 5% DMSO or a combination of 5% DMSO and other additives;[1-3] however, successful cryopreservation may also depend on the concentration of cells.[3] This also appears to be true for other HSC sources.[3-7] It has been shown that UCB cells can tolerate DMSO concentrations up to 10% without incurring damage;[8] however, it is desirable to use a minimum of DMSO in order to decrease the chance of adverse reaction in the recipient.[9] Hepatocytes, on the other hand, are generally cryopreserved using 10% DMSO,[10, 11] although final concentrations of 12% DMSO and 20.5% DMSO have also been reported.[11]

The question of DMSO toxicity was discussed in detail in Chapter 1. The freezing medium may be the same as the cell culture medium, although freezing medium such as University of Wisconsin (UW) solution, and histidine–tryptophan–ketoglutarate (HTK) have been used for hepatocyte and orthotopic liver cryopreservation.[11-15]

Regarding cell concentration, it has been reported that UCB cells easily tolerate high cell concentrations (up to 5.6 x 10^8 cells/mL).[9] A different study assayed cell concentrations of 5 x 10^6 cells/mL, 1.5 x 10^7 cells/mL, and 5 x 10^7 cells/mL.[16] While cell viability after cryopreservation was highest with 5 x 10^7 cells/mL, the study employed a concentration of 1.5 x 10^7 cells/mL for their trials due to the limited availability of UCB. For hepatocyte cryopreservation, cell concentration ranging from 1 x 10^5 cells/mL to 1 x 10^7 cells/mL have been used,[11, 17-19] and unlike UCB cells, hepatocytes may suffer negatively from higher cell densities due to increased membrane-membrane contact;[20] however, there has been little study of the optimum cell density.[11]

The addition and elution of DMSO to and from UCB was modeled by Hunt and co-workers.[8, 21] They determined that both DMSO addition and elution should be step-wise; protocols should therefore allow longer equilibration time to ensure that $CD34^+$ cells do not exceed tolerable limits. Based on experimental evidence, it was determined by Meyer *et al.* that fast addition and removal of DMSO was optimal for $CD34^+$ recovery;[16] however, the authors found that very similar results were obtained with fast addition and slow removal of DMSO. Further, other reports, such as that by Tarasov *et al.* suggested that post-hypertonic and hypotonic stress are the cause of damage to $CD34^+$ cells during cryopreservation.[22] It has also been suggested that the addition of cryoprotectants is less damaging than their removal.[23] DMSO has been assumed to be toxic to $CD34^+$ cells, but newer data has emerged that suggests that DMSO is only minimally toxic to these cells.[24] Washing cells has been reported to result in substantial cell loss;[25, 26] however, it appears that washing cells to remove DMSO is currently still standard.[9, 23] Similarly conflicting reports exist for hepatocyte cryopreservation.[11] Some reports found that different rates of addition of DMSO did not result in differences in viability,[27] while others found that gradual addition was the optimal approach.[28] There seems to be consensus, however, that slow dilution of the cryoprotectant upon thawing is ideal.[11]

Berz *et al.* report a summary of controlled vs. uncontrolled rate freezing in their review of hematopoietic stem cells.[9] Controlled rate freezing is carried out using a programmable freezer, and attempts to compensate for the heat liberated at the eutactic point, which is thought to negatively affect hematopoietic stem cells. The cells are frozen at a rate of 1-2 °C/min until about -40 °C is reached. The freezing rate is then increased to about 3-5 °C/min, until -120 °C is reached. They further report that for umbilical cord stem cells, bone marrow, and peripheral blood stem cells, the controlled rate freezing process is considered standard. The main disadvantages of controlled rate freezing are that it is time-consuming, and requires staff with specific expertise. In uncontrolled rate freezing, cells are cooled to -4 °C, and then placed in a -80 °C freezer or placed directly into liquid nitrogen. Berz *et al.* further report that there is evidence that uncontrolled rate freezing is a viable option for umbilical cord blood stem cells. Uncontrolled rate freezing includes using a freezing container such as the Nalgene® "Mr. Frosty", which aides in maintaining a constant freezing rate of about 1 ºC per minute in a mechanical, low-temperature freezer. The main advantage of uncontrolled rate freezing is its simplicity and low cost. A disadvantage of uncontrolled rate freezing was reported in a similar review by Erik J. Woods *et al.*, who report that uncontrolled rate freezing tends to yield variable results for UCB HSC.[23] Other studies have found that controlled and uncontrolled rate freezing produce similar results.[29] Similarly for hepatocytes, slow freezing at a rate of 1 °C/min is reported to be optimal. While uncontrolled rate freezing provides satisfactory results, the best results are achieved using a controlled rate freezer with more specific protocol.[11]

Regardless of freezing rate, UCB samples are stored at -80 °C (in a mechanical freezer) or at -196 °C (in liquid nitrogen). However, it is recommended that cell samples be stored at -156 °C (in the vapour phase of liquid nitrogen) in order to reduce the potential for contamination.[9, 30] Further, it has been found that the length of storage time does not affect the function of hematopoietic stem cells.[31] Hepatocytes are treated in the same way.[11]

Several UCB cryopreservation reviews and research papers state that there is generally consensus that fast warming in a 37 °C water bath is the optimal procedure.[9, 16, 23] Fast warming should reduce the chance that any innocuous intracellular ice formed will recrystallize and thereby form damaging intracellular ice. The same is true for hepatocytes.[11]

4.2 Cryopreservation Protocol Developed for the Current Study

Based on the above precedent, we developed a protocol that we could apply to the cryopreservation of both the hematopoietic stem cells and the WRL 68 cells. Due to the limited availability of UCB MNC samples, all trials in the present work were carried out using a concentration of 1.5 x 10^7 cells/mL. We similarly used a concentration of 1.5 x 10^7 cells/mL for all WRL 68 trials. UCB cells were suspended in cell culture medium for cryopreservation, while WRL 68 cells were suspended in HTK. Further, we employed fast addition of the cryoprotectants, and a step-wise dilution protocol in an attempt to avoid osmotic shock. Since uncontrolled rate freezing is acceptable for both cell types, and this is the simpler freezing-rate option, uncontrolled rate freezing was used for both cell types. Consequently, the cells were cooled by placing the cryopreservation vials in a "Mr. Frosty" freezing container in a -80 °C mechanical freezer for 24 hours before placement in a liquid nitrogen tank for storage in the vapour phase for 6 days. The "Mr. Frosty" container maintains the freezing rate at about 1 °C/minute. Fast thawing was employed to return the cells to physiological temperature.

4.3 Cryopreservation Using Carbohydrates: Precedent

4.3.1 Umbilical Cord Blood (UCB) Hematopoietic Stem Cells (HSCs)

The use of carbohydrates in the cryopreservation medium can enhance the cryopreservation potential and/or allow the amount of DMSO required for successful cryopreservation to be reduced. Trehalose, which has been applied to the cryopreservation of a number of human cells[32] including hepatoctyes, has been extensively studied in the UCB context. One study found that the addition of 5% trehalose to 5% or 10% DMSO significantly improved the cryopreservation outcome of UCB cells, as determined using a variety of colony-forming unit (CFU) assays. However, 5% trehalose used alone was only about 33% as effective as trehalose combined with either 5% or 10% DMSO.[32] In another

study, the addition of 100 μg/mL of the bio-antioxidant catalase and 25 μg/mL of trehalose to 10% DMSO provided better graft quality, as measured by the protection of growth factor receptors, adhesion molecules, and functionality of hematopoietic cells, than 10% DMSO alone.[33] The same combination was also shown to improve migration and adhesion-related properties of the hematopoietic graft compared to 10% DMSO.[34] The authors had previously shown that the combination of catalase and trehalose was more effective than the use of either alone.[35] The addition of 100 μg catalase and 25 μg trehalose to 10% DMSO also improved the cryopreservation outcome of murine bone marrow compared to 10% DMSO alone, as determined by a variety of assays after engraftment in a murine model. Notably, the addition of trehalose and catalase reduced the level of apoptosis and reactive oxygen species (ROS) generation.[36] In a study of human bone marrow, 0.5 M trehalose had a similar cryopreservation effect to that of 10% DMSO. The efficacy of trehalose varied depending on the exact source of bone marrow. The authors suggest that trehalose "…could possibly replace DMSO at least in part as a cryoprotectant in the setting of hematopoietic cell transplantation".[37] Using a human hematopoietic cell line, another study found that 200 mM trehalose, when present both intra- and extracellularly was only slightly inferior (92% of control) to 10% DMSO (98% of control) in its ability to preserve clonogenic potential during cryopreservation. When trehalose was present on only one side of the membrane, clonogenic capacity was greatly reduced. Trehalose was introduced into cells using a genetically-engineered mutant of the pore-forming protein α-hemolysin from *Staphylococcus auerus.*[38] Similar results were found when trehalose was loaded into cells from a human hematopoietic stem cell line by taking advantage of the transient membrane permeabilization using the adenosidetriphosphate-dependent P2Z receptor channel. Cells cryopreserved with 200 mM trehalose on both sides of the cell membrane showed 90% of the activity of cells cryopreserved with 10% DMSO.[39] More recently, sucrose has also been assayed as a cryoprotectant. One study found that 0.3 M sucrose with 5% DMSO resulted in comparable viability in human fetal liver hematopoietic stem cells compared to 10% DMSO. Further, 0.3 M sucrose in 5% DMSO resulted in increased metabolic activity after cryopreservation as compared to 5% DMSO alone, and was comparable to the viability found after cryopreservation with 5% DMSO with 10% fetal calf serum (FCS). The authors propose that sucrose may therefore be useful as an FCS substitute, since FCS is commonly used in the

hematopoietic stem cell cryopreservation media.[40] In a study using human HSC from UCB, trehalose and sucrose were both assayed in combination with varying concentrations of DMSO. Using flow cytometry and CFU assays to ascertain cell viability and clonogenic potential respectively, the authors found that a solution of 30 mM trehalose with 2.5% DMSO, or 60 mM sucrose with 5% DMSO afforded similar cryoprotection to 10% DMSO. Carbohydrates may therefore allow the percentage of DMSO to be further decreased from 5% to 2.5%.[41]

4.3.2 Hepatocytes

Many naturally occurring mono- and disaccharides have been used for the cryopreservation of rat and human hepatocytes. Glucose, glucose-derived 3-*O*-methyl glucose, and trehalose have shown improvement over cryopreservation medium supplemented only with 10% DMSO.[42] Pre-incubation at 4 °C and 37 °C of human hepatocytes with 100-300 mM glucose or fructose for 2h before cryopreservation with 10% DMSO was found to be beneficial for cell survival - as assessed using the Trypan blue exclusion test - and for proper cell function after cryopreservation. Pre-incubation with glucose resulted in increased viability and increased plating efficiency of frozen-thawed cells as compared to cells not pre-treated before cryopreservation. Pre-incubation with fructose showed increased plating efficiency and increased albumin production over cells that had not been pre-incubated. Also, pre-incubation of human hepatocytes for 30 min at 37 °C in Krebs-Henseleit buffer that comprised only 15 mM glucose before cryopreservation with 13.3% DMSO (cells stored in liquid nitrogen until needed – at least 6 days) returned viable cells after cryopreservation as determined by trypan blue uptake, with increased plating efficiency as compared to cells not pre-treated with buffer.[43] Further, after cryopreservation, pre-incubated rat and human hepatocytes responded to cytochrome P450 inducers in a manner similar to that of cells not cryopreserved. Supplementing a 10% DMSO cryopreservation solution with the glucose dimer trehalose improved the recovery of primary human hepatocytes after cryopreservation.[44] Primary human hepatocytes were cryopreserved using cell culture media containing 10% fetal calf serum (FCS), and supplemented with 10%

DMSO and 100-300 mM trehalose. Cells were stored at -156 °C in an ultra-low temperature freezer. They found that cells frozen with 100-300 mM trehalose had increased viability post-thaw than cells in the control group. The addition of 150-200 mM trehalose increased plating efficiency post-thaw, while 200-300 mM trehalose was slightly beneficial for membrane stability. The cryopreservation of rat hepatocytes preincubated with the non-metabolizable, and minimally-toxic glucose derivative 3-*O*-methylglucose in glucose-free Dulbecco's Modified Eagle Medium (DMEM) resulted in more than 50% greater viability after cryopreservation, compared to glucose-free controls.[45] Viability was determined using the Trypan blue exclusion test. Cells were pre-incubated with 200 mM carbohydrate for 60 min at 37 °C before cryopreservation. The same group found that neither supplementing the cryopreservation medium with 200 mM glucose nor 200 mM sucrose resulted in cell viability over 15%. All carbohydrates used were found to be minimally toxic at 200 mM. Son *et al.* found that rat hepatocytes could not be successfully cryopreserved with 10-40% (w/v) sucrose in hormonally defined medium (HDM) supplemented with fetal bovine serum (FBS).[18] Cells were incubated at room temperature for 10 min before cryopreservation and stored at -70 °C for 24h. The thawed cells were cultured for 24h hours and the cell densities were subsequently measured using the MTT test. The study found that hepatocytes cryporeserved with sucrose for 24 h could not survive after thawing. Miyamoto *et al.* found improved rat hepatocyte viability (determine by Trypan blue exclusion assay) and plating efficiency (1.2-1.8 fold improvement), compared to controls, after freezing in cryopreservation medium supplemented with 10% DMSO and one of the di- tri- and tetra-saccharides glucose, trehalose, or maltose.[46] Use of oligosaccharides with higher molecular weights resulted in the greatest improvement in viability. Compared to controls, human hepatocyte viability was similarly improved after cryopreservation. Lastly, it is important to remember that cells have variable permeability to different cryoprotectants and this will be addressed in a later section.

4.3.3 Carbohydrates and Carbohydrate Concentrations for Cryopreservation

As was discussed in Chapter 2, we tested three monosaccharides (galactose, glucose, and talose) and four disaccharides (melibiose, lactose, trehalose, and sucrose) for cytotoxicity and cryopreservation ability. The concentrations of mono- and disaccharides assayed were chosen based on the RI work previously carried out by our lab, as well as precedent in the UCB HSC and hepatocyte literature just presented. The lowest concentration assayed was 22 mM, since the RI data collected by our lab was obtained at that concentration. The cryopreservation literature just presented shows that, in general, higher concentrations of carbohydrates (100-500 mM) are required for successful cryopreservation when carbohydrates are used as the sole cryopreservatives. Lower concentrations of carbohydrates (15-60 mM) are used when they are used in conjunction with DMSO.

4.4 Analysis of Cryopreservation Outcomes

In order to assess and compare the cryopreservation potential of the carbohydrates in our study, we were interested in their cytotoxicity to the cells at physiological temperature, as well as their ability to protect cells during cryopreservation. Therefore, we used the MTT assay to determine the cytotoxicity of the carbohydrates to cells in physiological conditions. To determine the ability of the carbohydrates to cryopreserve cells, we used flow cytometry to determine the number of cells that were viable, apoptotic, or necrotic after cryopreservation. Both assays are high-throughput *in vitro* assays.

4.4.1 Cytotoxicity of Cryopreservation Agents

The MTT assay is a colorimetric cell proliferation assay, and has been found to be a good, sensitive test for early cytotoxicity.[47] This assay measures the metabolic activity of cells and is often used as an indirect measure of cell viability. This is based upon the premise

that dying cells are less metabolically active. The cells to be tested are plated in a 96-well plate, and growth medium containing the compound to be tested is then added to each well. After an incubation time (24 h in our study), the growth medium is removed and fresh medium containing the MTT reagent is added, and the plate is re-incubated for a short time (3 h in our study). In cells in which the metabolic system is functional, the yellow-coloured MTT (3-(4,5-Dimethylthiazol-2-yl)-2,5-diphenyltetrazolium bromide) is reduced by enzymes (mitochondrial dehydrogenases) to insoluble purple formazan crystals (Figure 4.2). Cells with compromised metabolic function cannot reduce the tetrazole. After incubation of the treated cells with MTT, the addition of an acidic isopropanol solution dissolves any purple formazan crystals formed, producing a purple solution. The absorbance of this colored solution is quantified using a spectrophotometer. At a given wavelength of light, the absorbance reading is positively correlated to the number of viable cells; that is, the greater the absorbance the greater the number of viable cells. In order to determine the toxicity of the agent tested, the amount of formazan produced by the treated cells is compared to the amount of formazan of untreated (control) cells. The assay is relatively simple and rapid, and requires a relatively small number of cells. Further, a single assay plate may be used to test replicate samples, multiple concentrations of the test compound, or multiple compounds. However, a limitation of the assay is that the solubilisation process is error prone. Since the assay requires adherent cells, in our studies, this assay could only be carried out with the WRL-68 cell line.[48-50]

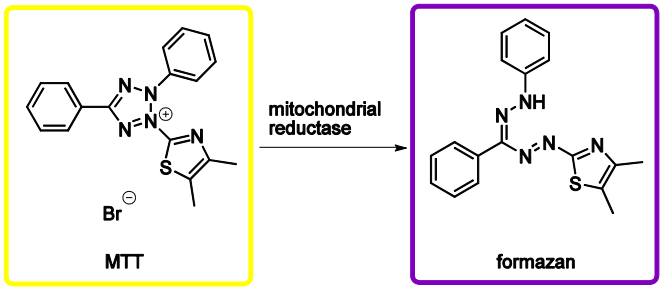

Figure 4.2 Living cells reduce the yellow MTT tetrazole (3-(4,5-dimethylthiazol-2-yl)-2,5-diphenyltetrazolium bromide) to insoluble purple formazan crystals.

4.4.2 Cell Viability Post-Cryopreservation

Determining the degree of success of a cryopreservation protocol requires consideration of the mechanism of cell death associated with cryopreservation. As was alluded to in chapter 1, it has been well-documented that cryopreservation can cause cells to undergo apoptosis, although the exact mechanism of cold-induced apoptosis is not known.[51-54] Baust *et al.* have further identified the phenomenon of cryopreservation-induced delayed-onset cell death (CIDOCD).[55] They define delayed onset-cell death as, "cell death associated with cryopreservation not apparent immediately post-thaw, but extending over the post-thaw recovery period." They found that cell death ("complete cryopreservation failure") was often not seen until 20 hours post-thaw. The implication of CIDOCD is that the number of cells in a sample that are judged to be viable after cryopreservation may not accurately predict the number of cells that will remain viable over time, and therefore, may not accurately predict the number of cells in a sample that are suitable for transplantation. As a result, it is important that the number of completely viable cells be differentiated from apoptotic cells after cryopreservation.

Traditional methods for determining cell viability, including nuclear counts, trypan blue dye exclusion, and membrane integrity staining (eg. 7AAD), can differentiate living cells from necrotic cells, but do not identify the apoptotic cell fraction. A recent study of multiple laboratories found wide inter-laboratory ranges for cell viability reported after cryopreservation, and concluded that all of the viability assays used over-estimated functional progenitor cells.[56] Other studies have found similar conclusions.[57] CFU assays are a reliable way to determine the true engraftment potential of hematopoietic stem cells;[58] however, cells must be grown for 14 days before colonies are counted. Consequently, this strategy is impractical in the clinical setting. The use of assays that employ flow cytometry to measure the cryopreservation outcomes, on the other hand, have proven to be successful as long as samples are assessed rapidly after thawing.[59] A common assay to define apoptotic cells is the annexin V-affinity assay, first described by Koopman and co-workers,[60] and subsequently improved by Reutelingsperger and co-workers.[52, 61-63] Annexin V is commonly labeled with the fluorochrome fluorescein isothiocyanate (FITC). Upon addition to a cell

suspension, and in the presence of Ca^{2+}, Annexin V binds immediately to the exposed phosphatidyl serine (PS) residues of apoptotic cells. PS exposure is thought to be universal to all cell types, and occurs as a result of the initiation of the apoptotic pathway, as the plasma membrane changes in structure and the distribution of phospholipids loses its asymmetry.[62, 63] Since annexin V cannot pass through the cell membrane, and loss of asymmetry does not compromise membrane integrity, annexin V cannot label viable, non-apoptotic cells. In order to further distinguish between early apoptotic and late apoptotic or necrotic cells, a membrane impermeable DNA stain (such as propidium iodidie (PI) or 7AAD[64]) is often used simultaneously with Annexin V.[62, 63] Simultaneous staining therefore allows the differentiation between viable, early apoptotic, and late apoptotic or necrotic cells. The viable cells will not be associated with either PI/7AAD or Annexin V-FITC, apoptotic cells with intact plasma membranes will be bound only by Annexin V, and late apoptotic cells and necrotic cells will be associated with both. This combination of Annexin V and a non-vital dye exclusion test (7AAD is used) is successful since the cell membrane remains intact during early apoptosis, but fails early during necrosis (and necrotic cells will therefore expose PS once their membranes have been compromised). While the Annexin V/7AAD technique is therefore excellent for distinguishing viable and early apoptotic cells, this technique does not allow late apoptotic cells to be distinguished from necrotic ones.[61, 63, 65]

There is some debate as to whether or not cells that bind annexin V are committed to the apoptotic pathway, since there is some debate as to the timing of PS exposure during apoptosis. It is generally believed that the loss of membrane asymmetry is a very early phenomenon during apoptosis.[66] However, although it is seen prior to the detection of DNA strand breaks, it is a downstream event of early caspase activation (the caspase cascade was discussed in Chapter 1).[62, 67] DNA fragmentation may follow as rapidly as within 1 hour of PS translocation, after which the final phase, membrane leakage, will occur.[68] PS exposure may therefore be an early phenomenon of the so-called execution phases of apoptosis,[62] and some studies place PS translocation past the point-of-no-return.[63] However, it has also been found that membrane asymmetry may be reversible,[69] and that detection of PS asymmetry by annexin V does not always condemn the cell to apoptotic cell death.[68] Importantly, however, PS exposure is one of the first apoptotic events that can be experimentally detected,[70] and

should therefore provide an adequate indication of the health of the cell population after cryopreservation for the purposes of the current study.

The annexin V assay is relatively easy to perform, and avoids prolonged incubation periods and washing steps, making it an ideal technique for the rapid analysis of cells.[63] With flow cytometry, cells can be analyzed at rates of 1000 to 10 000 cells/sec. However, analysis is limited to liquid cell cultures and cells derived from the hematopoietic system.[63] Nevertheless, this technique is ideal for the immediate assessment of the viability of frozen-thawed cells. The disadvantages of annexin V are that it requires the presence of Ca^{2+} ions for PS binding, and its binding specificity may be affected by detergents in the medium, or cell-harvesting techniques that employ trypsin.[71] It may also be able to associate with membrane surfaces containing negatively charged bi-products of lipid peroxidation. Consequently, care must be taken to avoid using disadvantageous conditions.

While the annexin V/7AAD system is sufficient for the analysis of our WRL 68 cell line, in the case of UCB, the hematopoietic stem cells ($CD34^+$ cells) must also be differentiated from the remaining cells in the MNC fraction. Many studies do assess the viability profile of the entire MNC fraction, disregarding the contribution of the $CD34^+$ cells; however, it has been reported that the number of viable $CD34^+$ cells in the MNC fraction significantly impacts clinical outcomes (although the optimal dose is dependent on both the type of donor and the stem cell source).[52, 72, 73] Further, it has been found that it is the total $CD34^+$ dose that determines *long-term* hematopoietic reconstitution.[74] For example, Abramsen *et al.* point to a study of DMSO toxicity where the authors noted that washing the PBPC sample to remove DMSO did not eliminate side effects in patients after infusion.[75] Abramsen and co-workers feel that this suggests possible harmful effects of re-infusing poorly cryopreserved non-viable cells. If this proves correct, then accurate post-thaw quality assessment of $CD34^+$ cells specifically becomes even more important.[52, 76, 77] Currently, in hematopoietic stem cell analyses, phycoerythrin (PE)-conjugated anti-$CD34^+$ is used to distinguish hematopoietic cells from other mononuclear cells in the analyzed cell fraction.

In summary, flow cytometry is readily amenable for the evaluation of nucleated cells, and it was therefore appropriate for the cryopreservation studies with both the UCB cells and

the WRL 68 cell line. We chose to assess cryopreservation success using the annexin V/7AAD assay to differentiate between viable, apoptotic, and late apoptotic/necrotic cells in the MNC fraction of UCB, and WRL 68 cells. From the hematopoietic MNC fraction, the hematopoietic stem cells ($CD34^+$ cells) were identified using the PE-conjugated anti-$CD34^+$ marker. The results were displayed graphically, and statistical analysis was carried out using one-way analysis of variance (ANOVA).

4.5 Cytotoxicity Studies with WRL 68 Cells:

The cytotoxicity to WRL 68 cells of DMSO and each of the carbohydrates to be used in the cryopreservation studies was assessed using the MTT assay.

4.5.1 Cytotoxicity of carbohydrates to WRL 68 cells

The cytotoxicity of each of the seven carbohydrates tested was assessed using the MTT assay (Figure 4.4). WRL 68 cells were cultured in 96-well plates and then incubated with various concentrations of carbohydrates in the growth medium, Eagle's Minimum Essential Medium (EMEM), for 24 hours. The EMEM was introduced to the cells using fast addition. Cells incubated with only EMEM served as the control, and were considered to be "100%" viable (this data point is not shown on the graph). The results for the other treatments were calculated in relation to the control. The carbohydrates were tested at concentrations of 22 mM, 200 mM, and 500 mM in EMEM. These concentrations are the main concentrations at which these carbohydrates were tested for cryopreservation activity. Cells were exposed to each of the solutions for 24 hours at physiological temperature (37 °C). All experiments were done in triplicate. Statistical analysis of the data using a two-way nested ANOVA showed that the difference in the viability data between concentrations of carbohydrates tested was greater than the difference between each test well, and also greater than the difference between replicate trials; therefore, all data points for a given carbohydrate

and concentration could be pooled, and each bar therefore represents n = 48 replicates since a total of 48 wells of cells (divided between three different plates) were subjected to each treatment. The error bars represent the standard error of the mean (SEM).

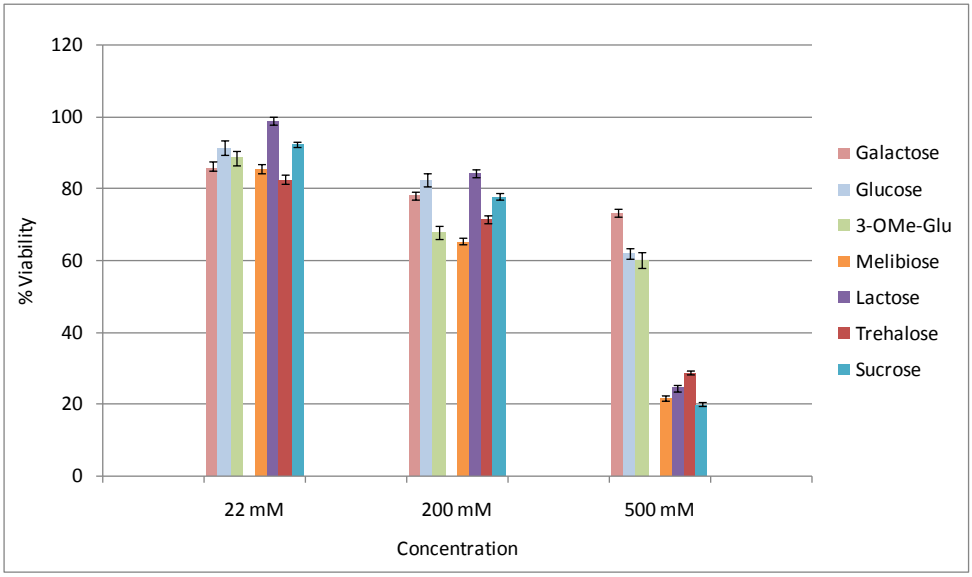

Figure 4.3 MTT cell viability assay of WRL 68 cells in carbohydrate solutions; WRL 68 cells were incubated at 37 °C for 24 h with different concentrations of monosaccharides and disaccharides in EMEM. Optical density (OD) was measured at 570 nm. Cells treated only with EMEM were used as the positive control and were considered to be 100% viable. The error bars indicate SEM.

Figure 4.3 shows that both monosaccharides (galactose, glucose, and 3-*O*-methylglucose), and disaccharides (melibiose, lactose, trehalose, and sucrose) are somewhat cytotoxic to cells at 22 mM and 200 mM in EMEM. Approximately 10-20% of the cells were non-viable after 24 hours exposure to the various carbohydrates at 22 mM, with the exception that 22 mM lactose produced no measurable cytotoxicity. Approximately 15-35% of the cells died after 24 hours exposure to the various carbohydrates at 200 mM. The differences in viability between the 22 mM and 200 mM trials were statistically significant for all carbohydrates. In practice, however, this difference is likely not very important, since the conditions of the cytotoxicity assay are more extreme with respect to time and [above-

zero] temperature, than the conditions encountered with cryopreservation. At 22 mM and 200 mM, the difference in cell viabilities between monosaccharides and disaccharides is not statistically significant. At 500 mM however, the difference between cell viabilities seen with monosaccharides and disaccharides is dramatic. For the monosaccharides, the difference in cell viability between the 200 mM and 500 mM concentrations was minimal. However, 500 mM solutions of disaccharide resulted in significant loss of cell viability: on average only 20% of cells were viable after incubation. These results can be explained by understanding some of the relationships between carbohydrates and cells.

4.5.1.1 Interactions of Carbohydrates and Cells

The cell membrane is only very slightly permeable to polar molecules such as carbohydrates. Carbohydrates penetrate viable cells by slow, bidirectional, transbilayer diffusion, or by rapid, protein-mediated, bidirectional, facilitated diffusion or transport. Facilitated diffusion of carbohydrates across cell membranes is common to almost all cells, and consequently almost all cells transport carbohydrates rapidly down the prevailing carbohydrate concentration gradient into or out of the cell. This transmembrane flux of carbohydrates is mediated by a family of integral membrane proteins (the GLUT protein family), which displays a strong specificity for stereoisomers of pentose and hexose monosaccharides adopting the chair conformation of the pyranose ring. Typical natural substrates for these transport proteins include glucose, galactose, mannose, and xylose, although there is competition between transported carbohydrates for transport.[78] Other monosaccharides, including both galactose and 3-*O*-methylglucose, can permeate through GLUT transporters, although they have a lower affinity than glucose for the GLUT transporters. Further, it has been shown that, in some cell types, the affinity to GLUT transporters is lower for galactose than it is for 3-*O*-methylglucose.[79] Unlike the monosaccharides, disaccharides can only enter the cell via endocytosis, and therefore only enter the cell very slowly at room temperature, if at all.[80]

Further complications arise with cells in culture since most cells in culture have a very limited ability to utilize carbohydrates and do not display the metabolic versatility of the animals from which they originate.[81] Studies on carbohydrate use by mammalian cells conducted prior to 1960 are often flawed as a result of glucose contamination of reagents or conversion of the carbohydrates by serum enzymes. In a slightly more recent study, Burns *et al.* overcame these difficulties, and found that while galactose, lactose, melibiose, and trehalose were neither toxic nor growth inhibitory, they did not promote cell growth when used as the sole energy source (with the exception of trehalose which resulted in 26% cell growth, as compared to glucose, in one cell line). In those trials, cell growth with glucose was taken to be 100%. The authors note that, in general, the disaccharides that support cell growth contain glucose monomers.[82] In a later study, however, Faik and Morgan found that in glucose-free medium, galactose was able to support growth of the mammalian cell line used, though it was not as effective as glucose. [83] The disaccharides lactose and sucrose, on the other hand, did not support cell growth. However, despite the inability of the given cell lines to metabolize the carbohydrates assayed, none of the carbohydrates assayed were found to be toxic to the cells; that is, the carbohydrates neither supported nor inhibited cell growth.

In our study, sufficient glucose for cell growth was present in the cell medium, and therefore, whether or not the cells could metabolize the added monosaccharide or disaccharide should not have had any effect on cell viability. In fact, it has been shown that in rat hepatocytes, the presence of carbohydrate on one side of the membrane is without effect on glucose transport from the other side of the cell membrane.[78] The toxicity seen in our studies, therefore, likely does not result from a direct toxic effect of the carbohydrates added, nor on the cells' ability to metabolize them. However, the tonicity of the carbohydrate solution added may be a source of stress in itself.

When cells are exposed to a hyperosmotic medium, cell shrinkage occurs. This is counteracted by the stimulation of ion uptake from the extracellular fluid, which leads to a regulatory volume increase. For example, Barros showed that HeLa cells exposed to 100 mM solutions of galactose or 3-*O*-methylglucose quickly shrank, before slowly swelling towards their original size. The author found that uptake of the carbohydrates via GLUT transporters preceded the slow volume recovery.[79] On the other hand, Corasanti and co-workers found

that isolated rat hepatocytes exposed to a 200 mM sucrose solution shrank, but did not exhibit regulatory volume increase.[84] The difference between the two findings may be a result of the difference in the permeability of the cells to the carbohydrates employed. It may be that, in general, cells that *cannot* undergo regulatory volume increase are more vulnerable than those that *can* undergo regulatory volume increase. Indirect evidence for this is outlined by Schliess and Haussinger, who noted that hyperosmotic shrinkage increases hepatic susceptibility to stress-induced damage.[85] The authors contend that there appears to be a link between liver cell shrinkage induced by hyperosmolarity, and oxidative stress, and this has also been shown in cell culture studies. The authors speculate that cell shrinkage may trigger apoptotic signal transduction. In our study, the decrease in cell viability of cells exposed to the 200 mM and 500 mM hypertonic carbohydrate solutions, compared to cell viability of cells exposed to the mildly hypertonic 22 mM carbohydrate solution may therefore be due to cell shrinkage and subsequent oxidative stress. The decrease in cell viability at 200 mM is slight, and there is little difference between the monosaccharide and disaccharide trials. It may be that the 200 mM solution is not sufficiently hypertonic to cause significant cell damage. However, the dramatic drop in cell viability when the cells were exposed to the 500 mM hypertonic solution of disaccharides compared to exposure to the same concentration of monosaccharides, may be due to the inability of the cells in the disaccharide solution to undergo regulatory volume increase (since the disaccharides cannot permeate the cell membrane), causing them to be highly susceptible to oxidative stress. Over the course of the 24 hour incubation period, oxidative stress could cause the cells to undergo apoptosis. In view of the evidence presented, we consider this to be a plausible explanation for the experimental outcome. Based on this data, therefore, it seems that the lowest possible concentration of carbohydrate that can afford cryoprotection should be the one employed, particularly when the carbohydrate in question is a disaccharide. This situation will be addressed in relation to the cryopreservation data discussed.

4.5.2 Cytotoxicity of Dimethyl Sulfoxide (DMSO) to WRL 68 Cells

Next, the cytotoxicity of DMSO at four different concentrations was investigated using the MTT assay (Figure 4.4). At a concentration of 2.5%, DMSO had limited toxicity, similar to that of the mono- and disaccharides at 22 mM. Although all the differences in cell viability were statistically significant, the difference in toxicity between 5% and 10% was small. In the presence of 20% DMSO, cell viability dropped below 50%. Since DMSO is known to be toxic, and given the long incubation time, these results were not surprising.

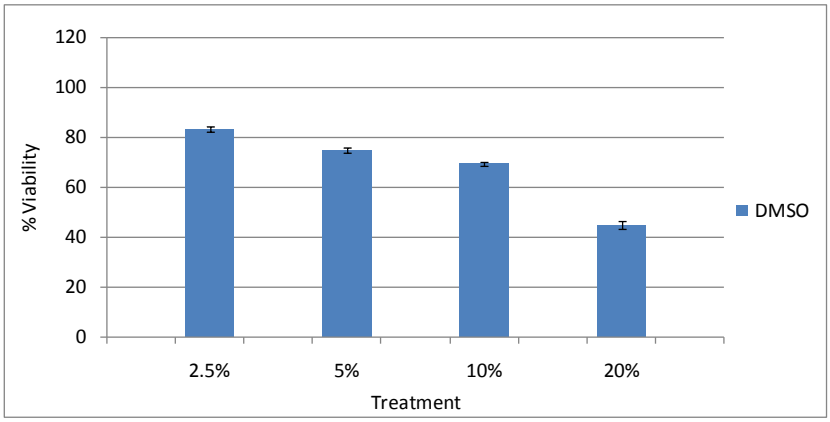

Figure 4.4 MTT cell viability assay of WRL 68 cells in DMSO solutions; WRL 68 cells were incubated at 37 °C for 24 h with different concentrations of DMSO in EMEM. Optical density (OD) was measured at 570 nm. Cells treated only with EMEM were used as the positive control and were considered to be 100% viable. The error bars indicate SEM.

4.6 Permeable versus Impermeable Cryoprotectants

In freeze-tolerant organisms, cryoprotectants are transported across cell membranes using carrier-mediated transporter proteins. The use of carbohydrates and other compounds as cryoprotectants in nature must have evolved in tandem with membrane transporters.[86] As a result, carbohydrates that are effective cryoprotectants in nature may not be effective in cells that are not naturally freeze-tolerant, and consequently, the use of natural cryoprotectants

must be carefully considered and adapted. A number of methods have been developed to load impermeable natural cryoprotectants, including the disaccharide trehalose, into cells. These include the incorporation of a genetically engineered pore-forming protein,[38] use of an extracellular-ATP dependant non-selective pore-forming receptor,[39] or lengthy incubation (up to 2 days) with the trehalose loading medium.[87] However, while some studies have found that the cryoprotectant must be present on both sides of the membrane, numerous studies have shown that this is not necessarily imperative for successful cryopreservation (as discussed previously in this chapter). Specifically for hematopoietic stem cells, both trehalose and sucrose have been shown to be effective extracellular cryoprotectants.[32-34, 36, 37, 40, 41] Similar examples can be found in the hepatocyte cryopreservation literature.[44] Consequently, in our study, no method to ensure cellular uptake of the cryoprotectant was used, regardless of whether permeable or impermeable cryoprotectants were employed. The different cryopreservation agents employed in our studies (monosaccharides, disaccharides, and antifreeze glycoproteins) are likely internalized at different rates, and therefore, it is likely that the intra- and extracellular distribution of each cryoprotectant will be unique.

Our lab previously obtained data regarding the internalization of AFGP 8 and the *C*-serine analogue by WRL 68 cells.[88] As presented in Chapter 2, using confocal microscopy, we found that human liver cells readily internalized AFGP 8 and the *C*-linked AFGP analogue into the cytoplasmic space after only 10 min of incubation at physiological temperature. Neither glycopeptide was internalized at 0 °C. Given the size of these glycoproteins and their hydrophilic nature, it seemed unlikely that internalization was occurring via passive diffusion across the cell membrane. The fact that discrete vesicles were observed suggests that internalization occurred via endocytosis. Further, it has been documented that ATP-dependent endocytosis can be inhibited at 0 °C.[89, 90] The fact that our experiments showed that the glycoproteins were rapidly internalized by human liver cells at 37 °C but not at 0 °C confirmed that internalization is an ATP-dependent process.[91] It has also been shown that receptors highly specific for galactose residues exist on the liver cell membrane and mediate the binding and cellular internalization of glycoproteins presenting galactose residues.[92, 93] When cells were treated with Proteinase K to remove the cell-surface receptors responsible for intracellular signaling events and internalization,[89, 94] no noticeable

difference in internalization of fluorescently labeled AFGP 8 was seen, suggesting that the internalization process is not receptor mediated.

4.7 Cryopreservation Studies with WRL 68 Cells

The first cryopreservation experiments were carried out using WRL 68 cells. This was done since WRL 68 cells are an established cell line, and are therefore more robust than the primary UCB MNCs. Experimental results obtained using cell lines tend to be more easily reproducible than results obtained with a primary cell line. Further, while the WRL 68 cells were readily available, the access to umbilical cord blood was very limited. We subsequently used the results from this work to inform the cryopreservation experiments using umbilical cord blood, although it was kept in mind that different cell types may respond very differently to a given cryopreservation protocol. As outlined earlier, all post-thaw analyses were carried out using flow cytometry with annexin V/7AAD to differentiate between viable cells, early apoptotic cells (which may or may not be committed to the apoptotic pathway), and very late apoptotic/necrotic cells. For all experiments, each condition was carried out at least in duplicate. Statistical analysis was carried out using one-way and two-way ANOVA.

4.7.1 Cryopreservation of WRL 68 Cells with Dimethyl Sulfoxide (DMSO)

The WRL 68 cells were cryopreserved in HTK containing different concentration of cryoprotectants. The only variables we employed in our trials were the type of cryoprotectant (DMSO or carbohydrate) and concentration of cryoprotectant. All other variables were kept constant. As discussed previously, DMSO is the most common cryoprotectant for both hepatocytes and hematopoietic stem cells. Therefore, we first investigated the effect of HTK,

as well as different concentrations of DMSO in HTK. The results of these control experiments are given in Figure 4.5.

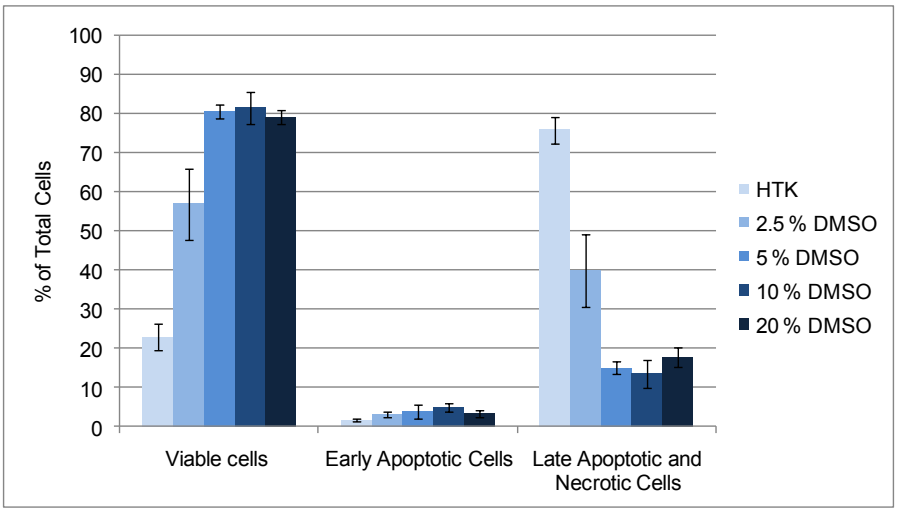

Figure 4.5 Annexin V/7AAD flow cytometry assay of WRL 68 cells after cryopreservation; WRL 68 cells were treated with different concentrations of DMSO in HTK, and then treated according to the standard protocol given in the Chapter 6. The total cell count was taken as 100% of cells. The error bars indicate SEM.

In the absence of DMSO (using only HTK), cell survival was very low. However, we found that 5%, 10% and 20% DMSO were all able to protect around 80% of cells. Given our use of uncontrolled rate freezing conditions, we considered the 80% cell survival rate with DMSO as the sole cryoprotectant to be a satisfactory result, and concluded that the cryopreservation protocol was adequate. As discussed, hepatocytes are normally cryopreserved with 10% DMSO, and as a result, we were somewhat surprised to find that there was no statistical difference between the cell survival obtained with 10% and 5% DMSO. Not surprisingly, cell survival was markedly reduced when the DMSO concentration was further decreased to 2.5%. Interestingly, although the MTT cytotoxicity data had indicated that increasing DMSO concentration was associated with increasing cytotoxicity (Figure 4.5), this same trend was not found in the cryopreservation studies; that is, for cryopreservation, increasing DMSO concentrations did not correlate to decreasing viability. However, this was not necessarily unexpected. In the cytotoxicity (MTT) assay, cells were exposed to DMSO for 24 hours at 37 °C in order to assess the long-term effects of DMSO on

cells at physiological temperatures, while in the cryopreservation assay, cells had limited exposure to DMSO at room temperature. On the other hand, it should be noted that when cells were cryopreserved with 5%, 10% or 20% DMSO, only 80% of the cells were found to be viable after cryopreservation, and some of the cell death may be attributable to the cytotoxicity of DMSO. In any case, based on these trials we concluded that 5% was an appropriate concentration of DMSO to combine with the various concentrations of carbohydrates employed.

4.7.2 Cryopreservation of WRL 68 Cells with Carbohydrates

The results of the first trials where carbohydrates were employed as cryoprotectants are given in Figures 4.6 and 4.7. Carbohydrates were tested as the sole cryoprotectant (Figure 4.6) and as co-cryoprotectants in the presence of 5% DMSO (Figure 4.7). In both cases, carbohydrates were tested at concentrations of 22 mM, 200 mM, and 500 mM. The lower bars (dark blue) show the percentage of viable cells, and the upper, smaller bars (pale blue) show the percentage of early apoptotic cells. As was previously discussed, if 7AAD is used alone, the viable and early apoptotic cells cannot be distinguished, and the percentage of completely viable cells is overestimated. This is a problem because only completely viable cells can be used for transplantation or research. In our work, the viable and apoptotic cell fractions were differentiated using Annexin V. We found that in both cases (carbohydrates alone or carbohydrates with DMSO), the percentage of early apoptotic cells was low.

Based on the literature precedent given at the beginning of this chapter, we did not expect any of the carbohydrates to be effective cryoprotectants at 22 mM when used as the sole cryoprotectant. Further, since the disaccharides showed much greater cytotoxicity at 500 mM compared to the monosaccharides, we expected that disaccharides would be slightly poorer cryoprotectants than the monosaccharides.

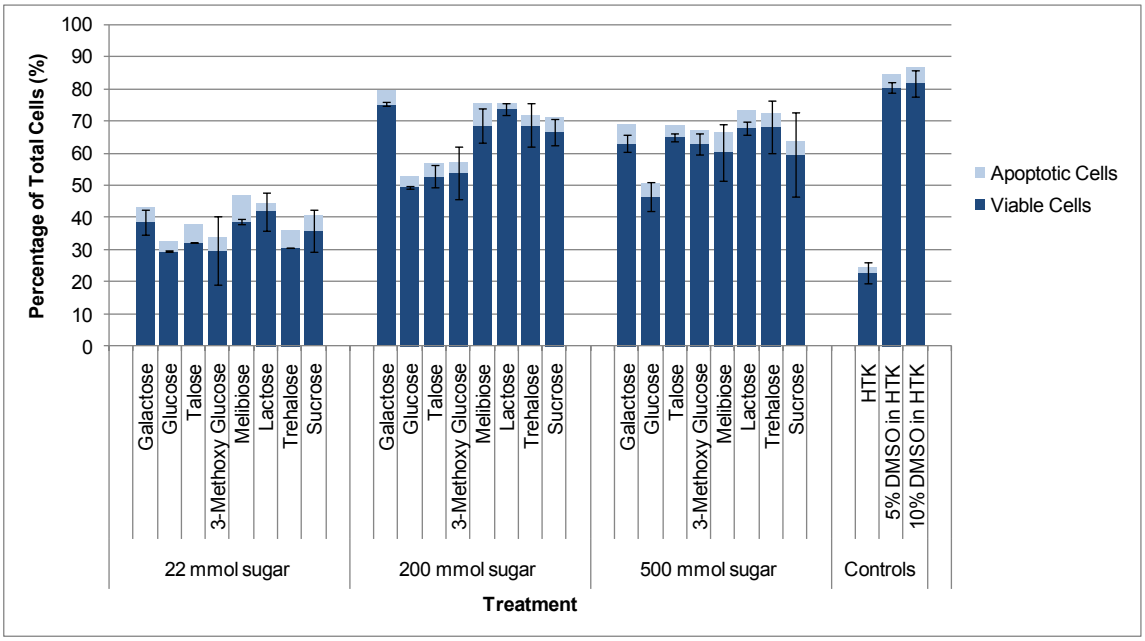

Figure 4.6 Annexin V/7AAD flow cytometry assay of WRL 68 cells after cryopreservation; WRL 68 cells were treated with different concentrations of different carbohydrates in HTK, and then treated according to the standard protocol given in Chapter 6. The total cell count was taken as 100% of cells. The error bars indicate SEM.

As predicted, at a concentration of 22 mM, carbohydrates were not able to provide significant cryoprotection: fewer than 50% of cells were found to be viable after cryopreservation (Figure 4.6). However, 22 mM carbohydrate did increase the percentage of viable cells by 10-20% compared to HTK alone. The data for the trials where carbohydrate concentrations of 200 mM, and 500 mM were used was somewhat surprising. The biggest difference between the mono- and disaccharides was seen at 200 mM, rather than at 500 mM, as had been predicted based on the cytotoxicity data. At 200 mM, while galactose protected 75% of cells, the percentage of viable cells recovered with any of the other monosaccharides was at least 20% lower. A 200 mM solution of any of the disaccharides returned roughly 65-75% viable cells - values comparable to galactose. Increasing the carbohydrate concentration from 200 mM to 500 mM was accompanied by a slight general decrease in cell viability for all carbohydrates except for galactose and glucose. Monosaccharides at 500 mM protected 60-65% of cells, with the exception of glucose, which provided less than 50% viability after cryopreservation. Somewhat unexpectedly, at 500

mM, all disaccharides similarly protected 60-70% of cells. In general, therefore, the cell viability was lower at 500 mM than at 200 mM, but little difference was seen between the set of mono- and disaccharides. This data did not seem to be consistent with the cytotoxicity data obtained for 200 mM and 500 mM carbohydrate solutions (Figure 4.3): while there was a big difference in the *cytotoxicity* of mono- and disaccharides at 500 mM, this did not translate into a difference in *cryopreservation* activity between the mono- and disaccharides at the same concentration. The difference between the results of the two experiments (cytotoxicity and cryopreservation) was likely partly due to the very different conditions for the two experiments: the cells to be cryopreserved remained unfrozen for only a very short period of time - the samples are at room temperature for only 15 minutes before they are placed in the freezer - while the cytotoxicity studies have a 24 h incubation period at 37 °C. While it was important to ascertain what the relatively long-term effects of the cryoprotectants (carbohydrates and DMSO) were, future work should include MTT assays carried out with incubation times that are more representative of the cryopreservation conditions.

In any case, some parallels can be drawn between the carbohydrate data and the DMSO data. In the DMSO trials, the increasing cytotoxicity (as measured by the MTT assay) that accompanied increasing DMSO concentration was not mirrored by a decrease in cryopreservation ability (as measure with the annexin V/7AAD assay) with increasing DMSO concentration. That is, the toxicity of DMSO does not seem to affect the survival of cells through cryopreservation. The carbohydrate cryopreservation data, on the other hand, indicates that increasing the concentration of carbohydrates generally results in a slight decrease in viability. If the nature of the carbohydrate toxicity was chemical, we could expect that this toxicity would be negated by the short amount of time the cells are exposed to them during cryopreservation, as it is for DMSO. Since this was not entirely the case, it is possible that the rapid addition of high concentrations of carbohydrates does indeed cause physical stress to the cells (osmotic shock), and that it is this physical stress, rather than a chemical toxicity of the carbohydrates towards WRL 68 cells, that results in the lower cell viability seen at high carbohydrate concentration in the cytotoxicity study. Further, the conditions imposed by disaccharides that are detrimental to cells at physiological temperature (dehydration) may be *beneficial* to cells during cryopreservation. That is, the

conditions imposed by high concentrations of extracellular cryoprotectants may be beneficial for WRL 68 cell survival during cryopreservation.

Lastly, it was initially surprising that glucose was not an effective cryoprotectant at any concentration, since many organisms (including the wood frog)[95] use glucose as their sole cryoprotectant. However, as Toner *et al.* speculated, "since glucose is rapidly metabolized, the concentration in the cytosol may have been insufficient to protect the cells." [45] From our study it seems that glucose is a poor extracellular cryoprotectant.

4.7.3 Cryopreservation of WRL 68 Cells with Carbohydrates and 5% Dimethyl Sulfoxide (DMSO)

Since the data in Figure 4.6 confirmed that carbohydrates on their own can affect cryopreservation outcomes, we were then interested in whether or not using both a carbohydrate and DMSO in the cryopreservation medium (HTK) would have a synergistic effect, and thereby increase the percentage of viable cells after cryopreservation. We expected an enhancement in cell viability, especially when the non-permeating disaccharides were combined with the permeating cryoprotectant DMSO, since, despite the fact that non-permeating cryoprotectants are reportedly ineffective during slow-freezing, and their primary use is with fast-freezing protocols, non-permeating cryoprotectants have been used to enhance the effect of permeating cryoprotectants.[9, 96] To this end, we repeated each of the trials given in Figure 4.6, and included 5% DMSO in the reaction medium. The results are presented in Figure 4.7. Comparing Figures 4.6 and 4.7, it was immediately obvious that the addition of 5% DMSO to carbohydrate solutions increased the percentage of viable cells found post-cryopreservation, with the exception that the difference between the outcomes with 200 mM galactose alone and 200 mM galactose with 5% DMSO was minimal. Interestingly, there were no significant differences in cell viability between the three concentrations of carbohydrates used with 5% DMSO. Further, there were no trials of carbohydrates with 5% DMSO that were significantly better than 5% DMSO used alone. Therefore, it does not seem that the mixing of these two cryoprotectants had a positive synergistic effect.

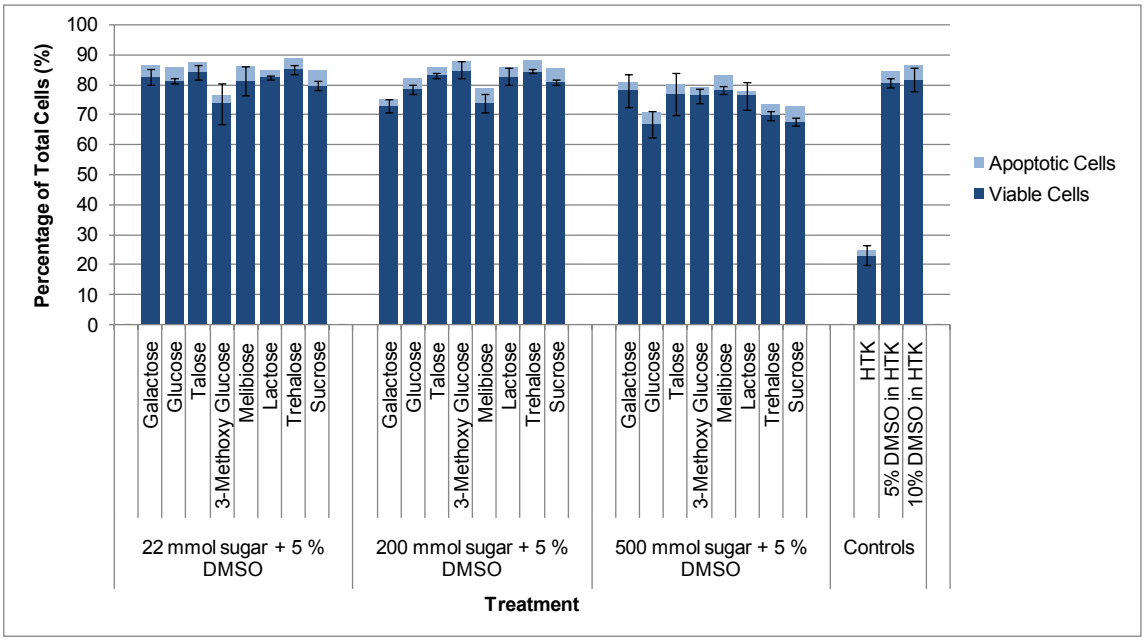

Figure 4.7 Annexin V/7AAD flow cytometry assay of WRL 68 cells after cryopreservation; WRL 68 cells were treated with different concentrations of different carbohydrates with 5% DMSO in HTK, and then treated according to the standard protocol given in Chapter 6. The total cell count was taken as 100% of cells. The error bars indicate SEM.

There were also no significant differences between the monosaccharides and disaccharides at any concentration. There were however, a few slight differences within each concentration. At 22 mM, there were no statistically significant differences, although 3-*O*-methylglucose produced slightly poorer results compared to the other carbohydrates. Similarly, at 200 mM most carbohydrates provided similar cell survival outcomes, although at this concentration, galactose and melibiose had slightly poorer outcomes. This is of some interest, since galactose and melibiose exhibited the best RI activity (chapter 2, Figure 2.11). A discussion of RI activity and cryopreservation will be re-visited later in this chapter. Finally, at carbohydrate concentrations of 500 mM, and particularly with glucose, trehalose, and sucrose, cell survival was slightly lower than it was with 5% DMSO alone.

4.7.4 Cryopreservation of WRL 68 Cells with Combinations of Carbohydrates and Dimethyl Sulfoxide (DMSO)

All of the different combinations of carbohydrates and DMSO will be discussed. However, it was informative to consider all of the raw data gathered as a whole. Therefore, the data for all of the carbohydrates is given in Appendix 2. As an example, Figure 4.8 shows all of the trials that were carried out using galactose.

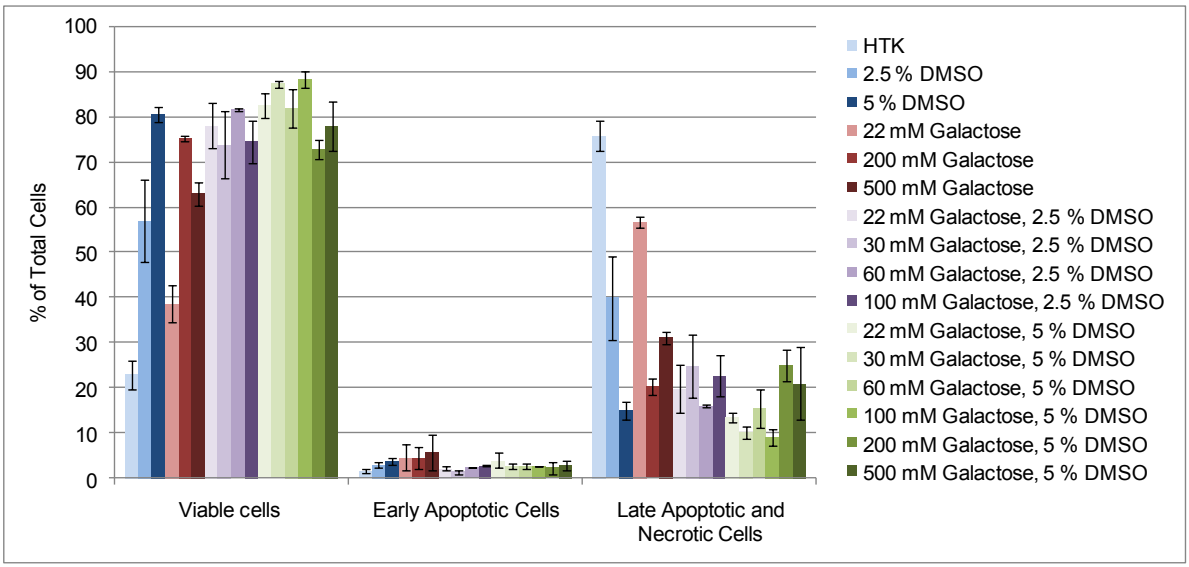

Figure 4.8 Annexin V/7AAD flow cytometry assay of WRL 68 cells after cryopreservation; WRL 68 cells were treated with different concentrations of galactose and DMSO in HTK, and then treated according to the standard protocol given in Chapter 6. The total cell count was taken as 100% of cells. The error bars indicate SEM.

As discussed previously, the annexin V/7AAD flow cytometry assay provides raw data that seems to be able to distinguish between late apoptotic and necrotic cells. In practice, however, the two types of cells *cannot* be distinguished and have therefore been combined to give one category: late apoptotic/necrotic cells.

Looking at the entire collection of data, it appeared that the percentage of viable cells found was inversely related to the percentage of late apoptotic/necrotic cells. The percentage

of early apoptotic cells, on the other hand, seemed to remain relatively constant, showing no correlation to the number of viable cells. In order to determine whether this observation was valid, we constructed plots of viable cells versus late apoptotic/necrotic cells (Figure 4.9), and viable cells versus early apoptotic cells (Figure 4.10).

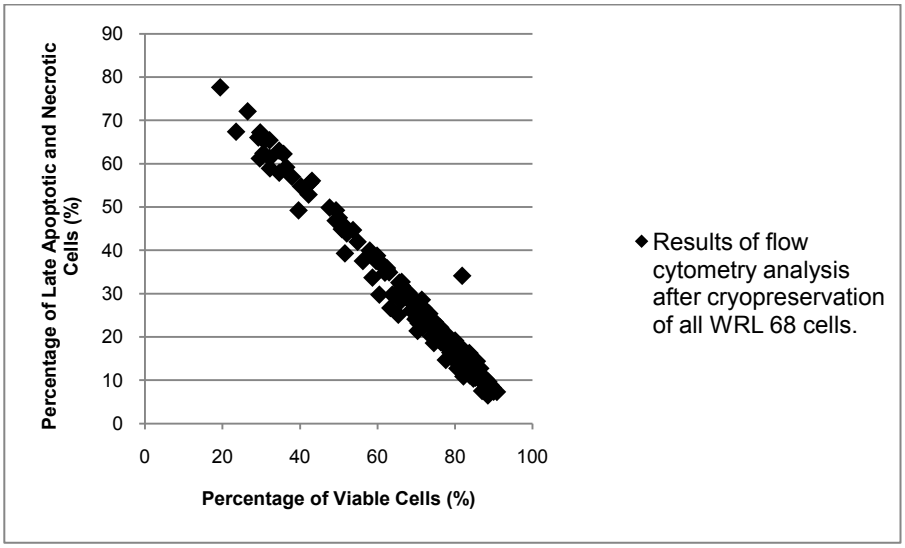

Figure 4.9 Percentage of viable cells versus percentage of late apoptotic/necrotic cells as determined by Annexin V/7AAD flow cytometry assay of WRL 68 cells after cryopreservation; WRL 68 cells were treated with different concentrations of carbohydrates and DMSO in HTK, and then treated according to the standard protocol given in Chapter 6. The total cell count was taken as 100% of cells.

From Figure 4.9, we determined that there was a negative correlation between viable cells and late apoptotic/necrotic cells. Although there may be two relationships present between the two groups of cells, it can be said that generally, an increase in the percentage of viable cells led to a decrease in the percentage of late apoptotic/necrotic cells and vice versa. We felt that this conclusion was appropriate for the purposes of the presentation of the data of this study. Figure 4.10 showed that the relationship between the percentage of viable cells and the percentage of early apoptotic cells was more complex. There seemed to be several relationships between the two groups of cells; that is, the percentage of early apoptotic cells appeared to be influenced by multiple factors within the experiment.

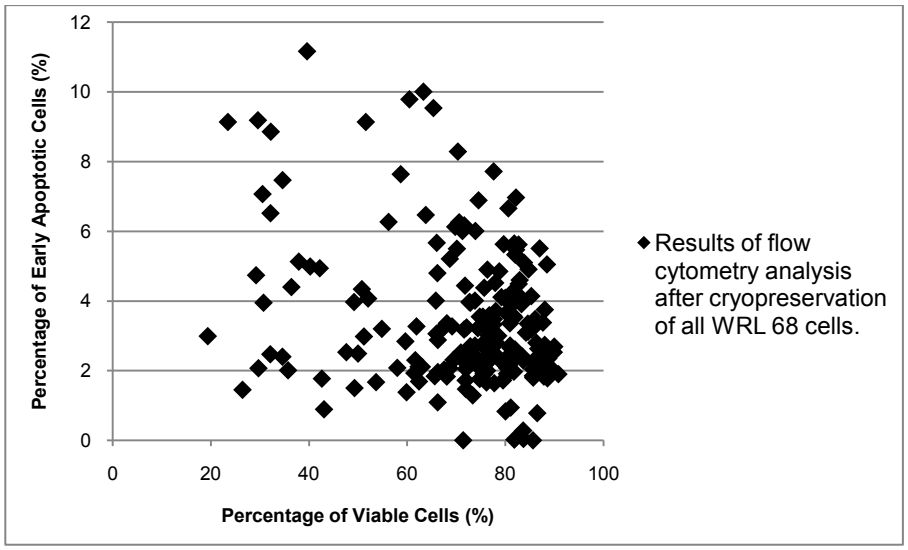

Figure 4.10 Percentage of viable cells versus percentage of early apoptotic cells as determined by Annexin V/7AAD flow cytometry assay of WRL 68 cells after cryopreservation; WRL 68 cells were treated with different concentrations of carbohydrates and DMSO in HTK, and then treated according to the standard protocol given in Chapter 6. The total cell count was taken as 100% of cells.

No conclusions were drawn regarding the relationship between the percentage of viable cells and the percentage of early apoptotic cells. However, the percentage of early apoptotic cells was quite low, and therefore this group, while not negligible, was left from the graphs in order to simplify the discussion of the results. Consequently, the presentation of the data was simplified, with each Figure showing only the number of viable cells obtained with each treatment. The remainder of the data is presented in this fashion, and the complete data set is included in Appendix 2.

4.7.4.1 Cryopreservation of WRL 68 Cells with Carbohydrates and Dimethyl Sulfoxide (DMSO)

One of the goals for our work in cryopreservation was the development of a cryopreservation agent and protocol that would allow us to either reduce the amount of DMSO required for successful cryopreservation, or to replace DMSO entirely with a more innocuous cryoprotective agent (a carbohydrate or an AFGP 8 analogue). Despite the lack of evidence for a synergistic effect when carbohydrates were combined with 5% DMSO, we did not want to preclude the possibility of achieving a synergistic effect with different concentrations of carbohydrates and DMSO. Consequently, we next assayed the cryopreservation potential of carbohydrates at 22 mM with 2.5% DMSO (Figure 4.11). The results from the previous trials for both 22 mM carbohydrate alone, and 22 mM carbohydrate with 5% DMSO were included for comparison.

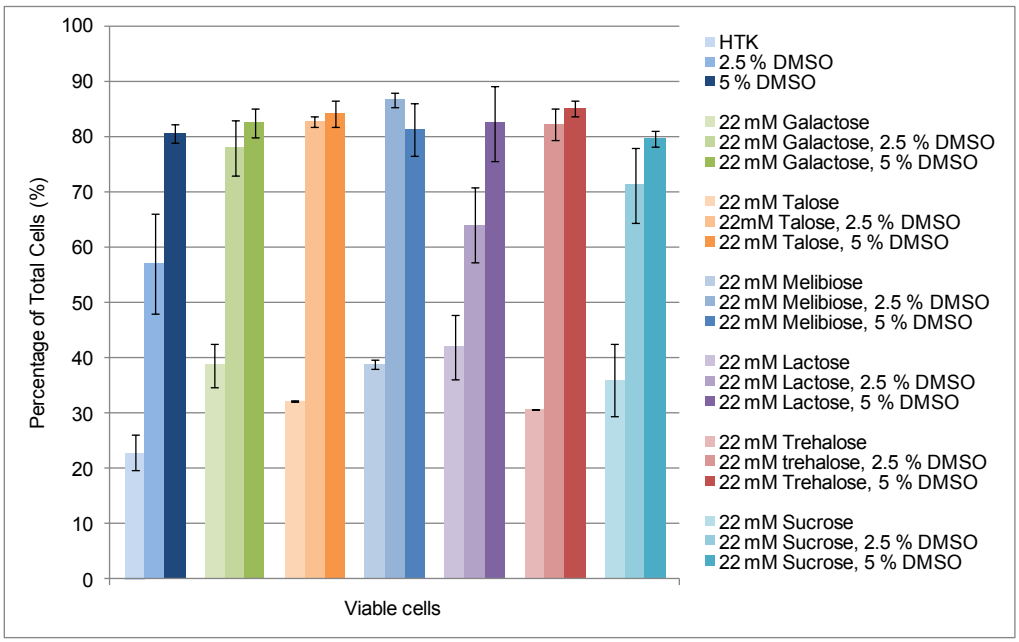

Figure 4.11 Annexin V/7AAD flow cytometry assay of WRL 68 cells after cryopreservation; WRL 68 cells were treated with different concentrations of carbohydrates and DMSO in HTK, and then treated according to the standard protocol given in Chapter 6. The total cell count was taken as 100% of cells. The error bars indicate SEM.

On its own, 2.5% DMSO performed relatively poorly, leaving fewer than 60% of the cells viable after cryopreservation. However, we found that with every carbohydrate assayed, the addition of 2.5% DMSO improved the cryopreservation outcome over that of either compound used alone (although the difference between 2.5% DMSO alone and either lactose or sucrose with 2.5% DMSO was not statistically significant). We were surprised to find that for galactose, talose, melibiose, and trehalose, the cryopreservation outcome with 22 mM carbohydrate with 2.5% DMSO was as good as that with 5% DMSO used alone. Further, the trial with melibiose provided a significantly *better* viability outcome than that with 5% DMSO alone. This data therefore suggests that the addition of galactose, talose, melibiose, or trehalose to the cryopreservation medium allows the amount of DMSO to be reduced from 5% to 2.5% without compromising cell viability. Motivated by these results, we investigated the effects of combinations of higher concentrations of carbohydrates with 2.5% and 5% DMSO on cell viability post-thaw.

Given the precedent outlined earlier in this chapter - that 30 mM trehalose, or 60 mM sucrose could successfully cryopreserve UCB MNCs - and since the trials using WRL 68 cells were carried out in part to inform our UCB trials, we tested both 30 mM and 60 mM carbohydrate solutions for the cryopreservation of WRL 68 cells. Further, in order to assay a concentration intermediate to 22 mM and 200 mM, trials with 100 mM carbohydrate were also carried out. The results are summarized in Figures 4.12 and 4.13.

Only galactose, melibiose, and trehalose were used at 30 mM in combination with 2.5% DMSO, since these carbohydrates had provided the highest cell viability when combined with 5% DMSO (Figure 4.7). Using 30 mM carbohydrate solutions gave similar outcomes to those seen with 22 mM (Figure 4.11). At 30 mM all of the carbohydrate trials seemed to increase cell viability over results when 2.5% DMSO was used alone, although only the difference between trehalose with 2.5% DMSO and 2.5% DMSO alone was statistically significant. When 30 mM of carbohydrate was used in combination with 5% DMSO, within statistical error, all carbohydrates were at least as effective as 5% DMSO alone. Specifically, when trehalose, melibiose, or sucrose was combined with 5% DMSO, the percentage of viable cells after cryopreservation increased by 5-8% over the percentage of viable cells recovered with 5% DMSO alone. Further, within statistical error, there was no

difference in the viability outcome between 30 mM carbohydrate combined with 2.5% or 5% DMSO.

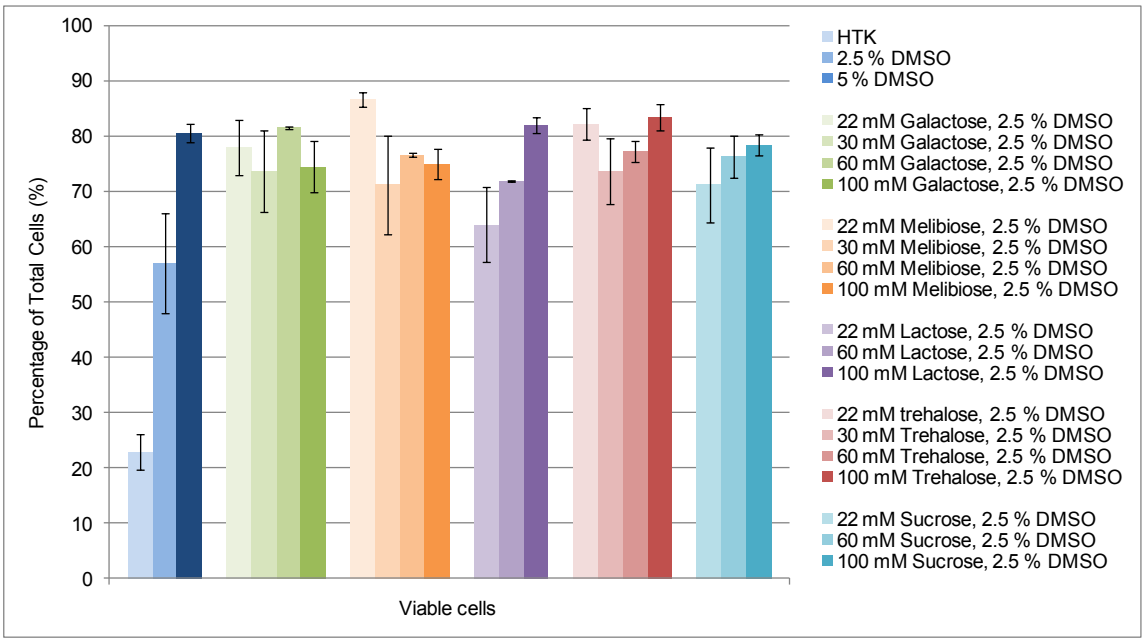

Figure 4.12 Annexin V/7AAD flow cytometry assay of WRL 68 cells after cryopreservation; WRL 68 cells were treated with different concentrations of carbohydrates and 2.5% DMSO in HTK, and then treated according to the standard protocol given in Chapter 6. The total cell count was taken as 100% of cells. The error bars indicate SEM.

In addition to galactose, melibiose, and trehalose, the disaccharides lactose and sucrose were tested at 60 mM. Unlike the combination of 30 mM carbohydrate and 2.5% DMSO, combining 60 mM carbohydrate with 2.5% DMSO resulted in a significantly higher percentage of viable cells after cryopreservation than 2.5% DMSO alone for every carbohydrate tested. In fact, 60 mM galactose, trehalose, and sucrose with 2.5% DMSO were as good as 5% DMSO used alone. Therefore, it seems that the carbohydrates and DMSO had a synergistic effect that improved the cryopreservation outcome over that when either was used alone. Further, with the exception of lactose, when 60 mM carbohydrate was used in combination with 5% DMSO, the results were very similar to those with 30 mM carbohydrate with 5% DMSO: all carbohydrates were at least as effective as 5% DMSO alone. Further, when 60 mM melibiose, trehalose, or sucrose were combined with 5%

DMSO, cell viability was increased by 6-9% over that when 5% DMSO was used alone (differences were statistically significant). Interestingly, for experiments with both 30 mM and 60 mM carbohydrate, it was the same three carbohydrates (the disaccharides melibiose, trehalose, and sucrose) that produced the highest percentage of viable cells.

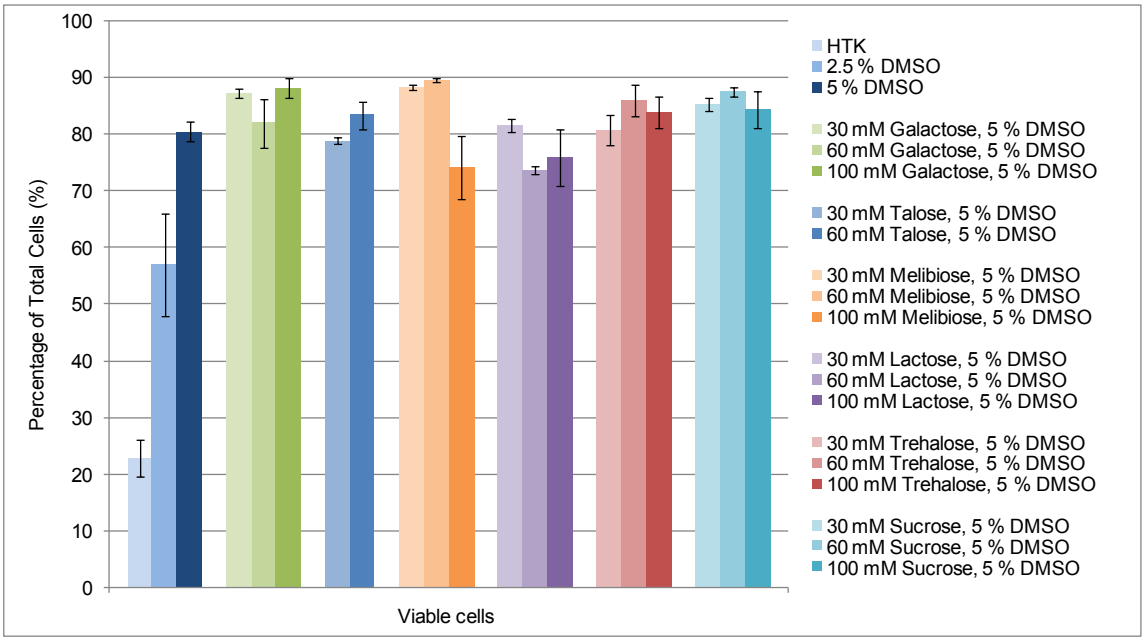

Figure 4.13 Annexin V/7AAD flow cytometry assay of WRL 68 cells after cryopreservation; WRL 68 cells were treated with different concentrations of carbohydrates with 5% DMSO in HTK, and then treated according to the standard protocol given in Chapter 6. The total cell count was taken as 100% of cells. The error bars indicate SEM.

For all carbohydrates assayed, 100 mM carbohydrate with 2.5% or 5% DMSO resulted in better cryoprotection than was obtained with 2.5% DMSO alone (differences were statistically significant), and with the exception of melibiose, carbohydrates with 2.5% DMSO were as good as 5% DMSO used alone. Only 100 mM galactose with 5% DMSO afforded statistically better viability than 5% DMSO used alone.

The cytotoxicity of carbohydrates at concentrations between 22 mM and 200 mM was not tested, and therefore it is unknown whether or not cytotoxicity of the carbohydrates is playing a role in their cryopreservation ability. However, since even carbohydrates at a

concentration of 500 mM have a cryoprotective effect despite the cytotoxicity seen with the MTT viability assay - the disaccharides in particular were very cytotoxic at this concentration - the potential cytotoxicity at the intermediate concentrations (30 mM, 60 mM, and 100 mM) was not a major concern.

The reproducibility of cryopreservation trials using WRL 68 cells was generally good; however, the results of trials carried out using 2.5% DMSO alone or in combination with carbohydrates had poorer reproducibility (as evidenced by the larger SEM associated with them) than when 5% DMSO was used alone or in combination with carbohydrates. It may be that the cells used in some of the trials with 2.5% DMSO were of poor quality. It is possible that some of the trials yielding poorer results were carried out with cells that were no longer in an active growth phase, or with cells whose passage number was too advanced. Cell cultures that have been split and re-grown too many times may begin to show unusual activity, and ideally, the WRL 68 cells are in an active growth phase prior to cryopreservation, since this is known to improve cryopreservation outcomes.

In summary, we found that, in general, there was not a significant difference in cryopreservation outcome regardless of whether carbohydrates were used at 22, 30, 60, or 100 mM, although in general, carbohydrates at 60 mM when combined with 5% DMSO provided slightly better results than the other concentrations. In any case, since there was little difference among these results, we focused on the original concentrations assayed, that is, on 22 mM, 200 mM, and 500 mM. Importantly, this data (the intermediate concentrations) shows that the addition of low concentrations of galactose, talose, melibiose, or trehalose to the cryopreservation medium allows the amount of DMSO to be reduced from 5% to 2.5% without compromising cell viability.

4.7.5 Cryopreservation of WRL 68 Cells with Carbohydrates: Significant Successes using Carbohydrates

Figure 4.14 shows all of the carbohydrate and DMSO combinations that resulted in significantly greater viability after cryopreservation than that obtained with 5% DMSO alone.

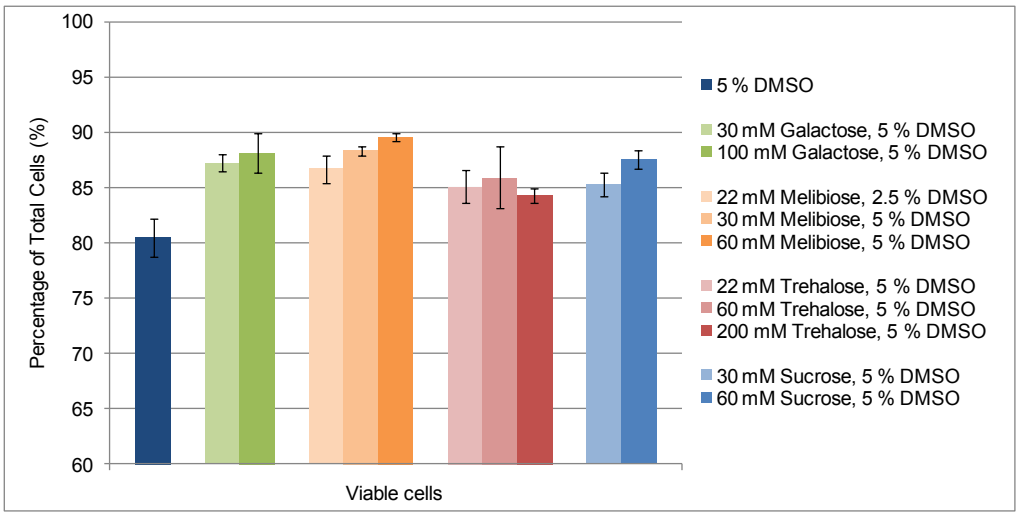

Figure 4.14 Annexin V/7AAD flow cytometry assay of WRL 68 cells after cryopreservation; WRL 68 cells were treated with different concentrations of carbohydrates and DMSO in HTK, and then treated according to the standard protocol given in Chapter 6. The total cell count was taken as 100% of cells. The error bars indicate SEM.

Only four carbohydrates - one monosaccharide (galactose), and three discaccharides (melibiose, trehalose, and sucrose) - appear in this data set. As was shown previously, no carbohydrate used alone, and no carbohydrate at a concentration of 500 mM, regardless of DMSO concentration, resulted in viability greater than that seen with 5% DMSO. Further, combining carbohydrates with 5% DMSO was generally superior than combining them with 2.5% DMSO. Interestingly, melibiose, at only 22 mM and combined with only 2.5% DMSO, resulted in significantly greater viability than that obtained using 5% DMSO alone. While several carbohydrates when combined with 2.5% DMSO resulted in cell viability that was as good as 5% DMSO used alone, melibiose was the only carbohydrate that provided significantly *greater* viability than 5% DMSO used alone. The greatest viability was

obtained using 60 mM melibiose with 5% DMSO, although this result was not significantly different from 100 mM galactose with 5% DMSO. Interestingly, while only four carbohydrates provided superior cryoprotection, each was effective over a broad range of concentrations. Therefore, this data indicates that, in the presence of DMSO, the *type* of carbohydrate is more important than its *concentration.*

4.7.6 Cryopreservation of WRL 68 Cells: Mechanism of Action of Carbohydrates

As was seen in Figure 4.6, with the exception of galactose, disaccharides were better cryoprotectants than monosaccharides. This may be partly due to the difference in their cell permeability: monosaccharides are permeating cryoprotectants, while disaccharides are non-permeating cryoprotectants. As discussed in Chapter 1, permeating cryoprotectants (monosaccharides and DMSO) protect cells by reducing excessive cellular shrinking, a phenomenon linked to cell death during slow freezing. Non-permeating cryoprotectants dehydrate the cell before freezing, however, they have been found to be largely ineffective during slow freezing, and cannot protect against solution effects since they cannot penetrate to the cell interior. Disaccharides may also function by stabilizing the cell membranes; the cryoprotection afforded by the disaccharides trehalose, and sucrose, has been attributed to their ability to stabilize the cell membrane by a similar mechanism to that attributed to DMSO.[97] It is thought that DMSO is able to stabilize the cell membrane through an electrostatic interaction of the sulfoxide group with the polar head groups of the phospholipids.[98] However, it has also been shown that glucose can stabilize small unilamellar vesicles (SUVs) during cryopreservation, maintaining their structural integrity and permeability.[99] Interestingly, however, glucose was a poor cryoprotectant in our study, while galactose was as effective a cryoprotectant as the disaccharides. The similarity in outcomes among galactose and the disaccharides can potentially be explained by exploring the rate of internalization of each. As previously discussed, while cells are largely impermeable to disaccharides, monosaccharides including galactose, glucose, talose, and 3-*O*-methylglucose are transported into cells through the GLUT transporters. Of these monosaccharides, the GLUT transporters have the lowest affinity for galactose. It may be

that due to the short time that the cells are exposed to the carbohydrates prior to cryopreservation, the slow uptake of galactose results in a high extracellular galactose concentration. galactose may therefore have more in common with the disaccharides than with the other monosaccharides, and this may partially explain the similarity in cryopreservation outcomes.

While the different colligative mechanisms of action and membrane stabilization ability of monosaccharides and disaccharides can be used to rationalize some of the differences in cryopreservation activity seen in this study, we still sought a comprehensive explanation. Since our interest was in the relationship between RI activity and cryopreservation, we next turned to an investigation of this relationship.

4.7.6.1 Cryopreservation of WRL 68 Cells Versus Recrystallization Inhibition (RI) Activity

As outlined in Chapter 2, the RI activity of carbohydrates at 22 mM had previously been determined (Figure 2.11; Tam and co-workers[100]), and that study had informed our cryopreservation studies. As discussed in section 4.3, the remaining concentrations at which carbohydrate cryopreservation activity was assessed (30, 60, 100, 200, and 500 mM) were chosen based on precedent in the cryopreservation literature. While the cryopreservation studies were carried out, our lab assessed the RI activity of the monosaccharides at 220 mM – that is, at 10 times the concentration initially assayed, and the highest concentration at which sugars could be tested. Our lab found that all sugars showed increased RI activity at increased concentration.[101] Therefore, the RI activity of the disaccharides was now also assessed at 220 mM, and all of the RI data was plotted against the corresponding cryopreservation data such that while RI data at 22 mM was plotted against cryopreservation data at 22 mM, RI data at 220 mM was plotted against cryopreservation data at 200 mM (Figure 4.19). This unusual approach was therefore taken since the RI and cryopreservation studies had been developed separately; however, since we were interested in the general relationship between RI and cryopreservation activity, the correlation graphs obtained were sufficient for our study.

Specifically, RI activity was measured as a ratio of the average mean grain size (MGS) of the sample in phosphate-buffered saline (PBS) to the average MGS of PBS measured on the same day. The percentage of viable cells was the percentage of viable cells after cryopreservation with a solution of carbohydrate (*without* the addition of DMSO) in HTK, as determined by flow cytometry assay, and the average of these trials was reported. Figure 4.15, therefore, shows the average percentage of viable cells after cryopreservation plotted against the RI ratio of the same treatment.

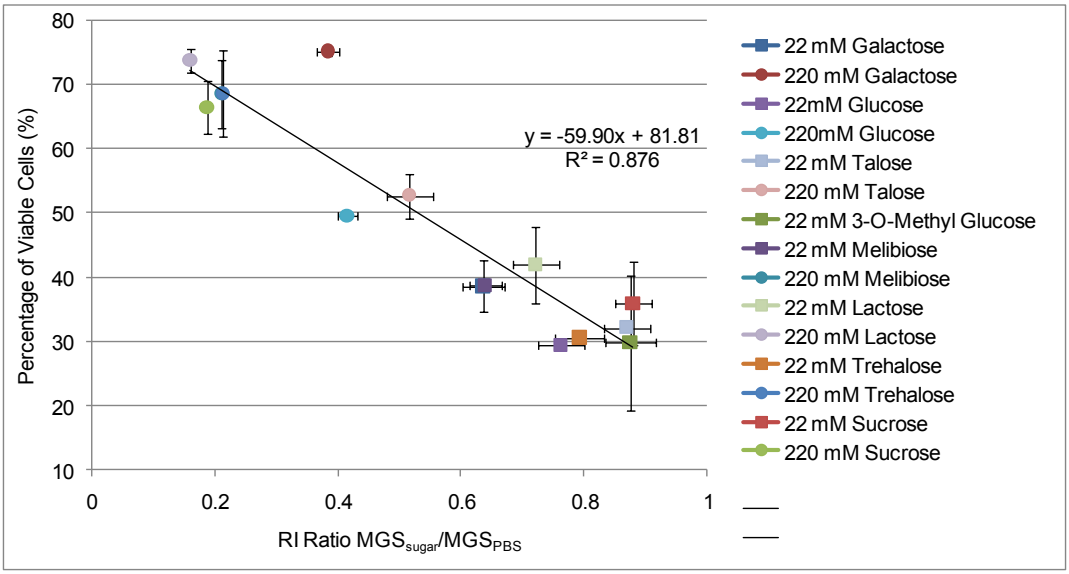

Figure 4.15 Percentage of viable cells versus the RI ratio (sample/PBS) for the same treatment; percentage of viable cells was obtained by Annexin V/7AAD flow cytometry assay of WRL 68 cells after cryopreservation, where the total cell count was taken as 100% of cells. RI ratio of carbohydrates at 220 mM was compared to cryopreservation data of 200 mM carbohydrates. Cryopreservation and RI data were obtained according to the protocols given in Chapter 6. The error bars indicate SEM.

From Figure 4.15, we were pleasantly surprised to discover that there was a good correlation (R^2 = 0.87) between the RI and cryopreservation activities of carbohydrates: the greater the RI activity of a carbohydrate at a given concentration, the greater its cryopreservation activity at that concentration. Carbohydrates had better RI activity at 220

mM than at 20 mM, and carbohydrates were better cryoprotectants at 200 mM than at 22 mM. The best cryopreservation outcomes were obtained with trehalose, lactose, sucrose, and melibiose, each at 200 mM, and these carbohydrates also had the best RI activity at 220 mM. As was previously seen, even at 200 mM, glucose and 3-*O*-methylglucose were poor cryoprotective agents, and both carbohydrates had RI activity that was poorer than that of the disaccharides at the same concentration. Interestingly, galactose presented unusual data: although its RI activity at 200 mM was poorer than that of the four disaccharides (trehalose, lactose, sucrose, and melibiose), it provided similarly successful cryopreservation outcomes. As previously discussed, this unusual data may be related to the rate at which the various carbohydrates are internalized by the cells. Finally, carbohydrates tested at 22 mM had neither good RI activity nor were they good cryopreservation agents.

The nature and formation of both intra- and extracellular ice during the cooling and warming phases of cryopreservation are a concern with all cryopreservation protocols. Although there are other concerns associated with cryopreservation, there are several ways by which ice recrystallization inhibitors can help mitigate the damage caused by ice. Our cryopreservation protocol employed slow-cooling, and therefore, as outlined in Chapter 1, the cells may be subject to osmotic stress upon thawing as a result of solute-uptake during freezing,[102] destabilization of the plasma membrane due to cell dehydration,[103] and/or increasing solute concentration causing a concomitant increase in intracellular sodium levels that could cause the cell to burst with the influx of water during thawing.[104] While fast-freezing injury was not expected to be a problem under our cryopreservation conditions, since we did not use controlled freezing conditions, the cells may still have encountered some of the problems associated with fast-freezing. These include: ice growth through membrane pores, which may allow both mechanical damage to the cell membrane and intracellular ice formation;[105] formation of intracellular ice caused by nucleation by the cell membrane; or cell membrane rupture resulting from thermal fluctuations during cooling.[106] In any case, if a glassy state formed, intracellular ice formation may also occur using a slow cooling protocol as a result of devitrification during warming.[107] Further, once the cryopreservation temperature has been reached, the size of the fraction of unfrozen water seems to play an important role in determining cell survival and the mechanism of cell injury. Particularly, when the unfrozen fraction drops below 10%, the cells may become

trapped in small channels between ice-crystals, which may cause adverse cell-cell and cell-ice interactions.[108] The effects of slow- or fast-warming are more complicated. Although ice-recrystallization may play a role in slow warming, this effect is more pronounced when cells are frozen using a fast-freezing protocol.[105]

Recrystallization inhibitors may therefore mitigate the damage incurred during cryopreservation in several ways. The cellular damage caused by a small unfrozen fraction of water may be mitigated if the ice crystals remain small. Small ice crystals may allow cells to avoid deformation of the cell membrane, and may limit the formation of small channels in extracellular ice, thereby limiting detrimental cell-cell - and perhaps cell-ice - contact. Further, any growth of ice through membrane pores would be less harmful to the cell if the ice crystals in the membrane remained small, and similarly, intracellular ice formation may be rendered innocuous if crystal growth is avoided. This last point is supported by Toner and Fowler,[109] who further predict that "A possible future for cryopreservation research may lie in the development of cryopreservation protocols that manage intracellular ice so that it is non-lethal, rather than attempt its prevention.[110] The correlation we found between RI and cryopreservation would also seem to support this. Lastly, although there does appear to be a correlation between RI and cryopreservation activities of carbohydrates, without further study other mechanisms should not be discounted.

4.7.7 Assessing the Cryopreservation Activity of the Ornithine Analogue

The next objective was to determine the cryopreservation potential of ornithine analogue **14**, as well as that of native AFGP 8. As discussed in Chapter 2, the cytotoxicity of AFGP 8 to WRL 68 cells was previously determined by our lab.[88] It was found that AFGP 8 was cytotoxic to WRL 68 cells when added at concentrations of 2 and 4 mg/mL. While cytotoxicity data was not obtained for the ornithine analogue (**14**), it was found that the related serine analogue **16** was not cytotoxic to WRL 68 cells at similar concentrations. The cytotoxicity of AFGP 8 was not expected to be due to osmotic effects, since the concentration used was very low, especially compared to the concentration of carbohydrates

assayed. While the carbohydrate studies were carried out using concentrations of 22 mM to 500 mM, both AFGP 8 and analogue **14** were used at low micromolar concentrations. Further, it was determined that AFGP 8 induced apoptosis at physiological temperature, while serine analogue **16** appeared to suppress caspase-3/7 activity *in vitro*, thereby inhibiting apoptosis. With these findings in mind, we assayed the cryopreservation activity of AFGP 8 and analogue **14** using WRL 68 cells, and the results are shown in Figures 4.16 and 4.17, respectively.

Since we had a limited supply of AFGP 8, we tested its cryopreservation activity only at 0.5 mg/mL and 1.0 mg/mL. Unfortunately, we did not have sufficient material to carry out a second trial, and were therefore unable to test the reproducibility of our results. Since the ornithine analogue **14** was synthesized in the lab, we were able to test its cryopreservation activity at higher concentrations. Analogue **14** was therefore tested at 1 mg/mL, 5 mg/mL, and 10 mg/mL, and each trial was carried out in duplicate.

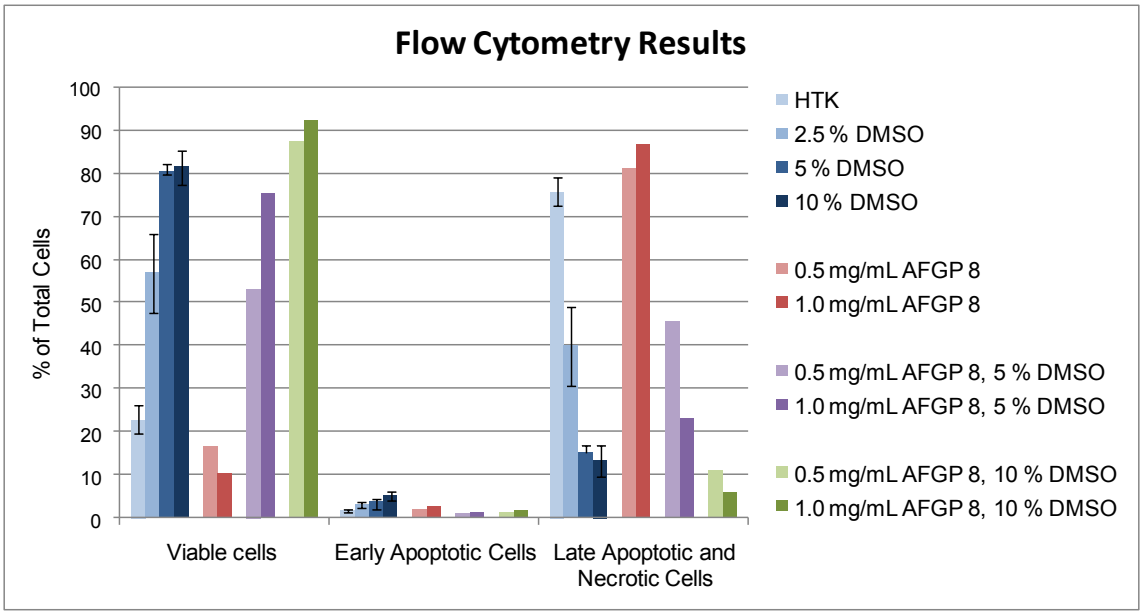

Figure 4.16 Annexin V/7AAD flow cytometry assay of WRL 68 cells after cryopreservation; WRL 68 cells were treated with different concentrations of AFGP 8 and DMSO in HTK, and then treated according to the standard protocol given in Chapter 6. The total cell count was taken as 100% of cells. The error bars indicate SEM.

Given the correlation between RI and cryopreservation activities that we found in our study of carbohydrates, the cryopreservation results obtained with AFGP 8 were surprising. AFGP 8 has much better RI activity than any of the carbohydrates, as well as better RI activity than the ornithine analogue **14** (refer to Chapter 3, Figures 2.8 and 2.11), yet it proved to be a poor cryoprotectant at the concentrations assayed. When AFGP 8 was used at 0.5 mg/mL or 1.0 mg/mL in the absence of DMSO, the percentage of viable cells after cryopreservation was poorer than when HTK was used alone. Further, in this trial, AFGP 8 was more effective at the lower of the two concentrations. Similarly, the addition of AFGP 8 at either concentration to 5% DMSO provided poorer results than when 5% DMSO was used alone, although, 1 mg/mL AFGP 8 with 5% DMSO was more effective than 0.5 mg/mL AFGP 8 with 5% DMSO. When either concentration of AFGP 8 was combined with 10% DMSO, a greater percentage of viable cells was recovered than when DMSO was used alone. This result was encouraging: it suggests that given the appropriate concentrations of AFGP 8 and DMSO, it may be possible to find cryopreservation conditions that increase the percentage of viable cells after cryopreservation compared to 5% DMSO alone, or that allow the percentage of DMSO used to be reduced, without reducing the percentage of viable cells. Interestingly, in all trials that included AFGP 8, the percentage of early apoptotic cells was lower than when DMSO was used alone. This seems to corroborate the data obtained previously by our lab that showed that AFGP 8 induces apoptosis. That is, it may be those cells that do not remain viable are committed to the apoptotic pathway by AFGP 8, and these cells would be then found in the late apoptotic/necrotic cell fraction. However, the data does not preclude a necrotic mechanism of cell death. Since only one trial was carried out for each condition, these results should be treated with some caution.

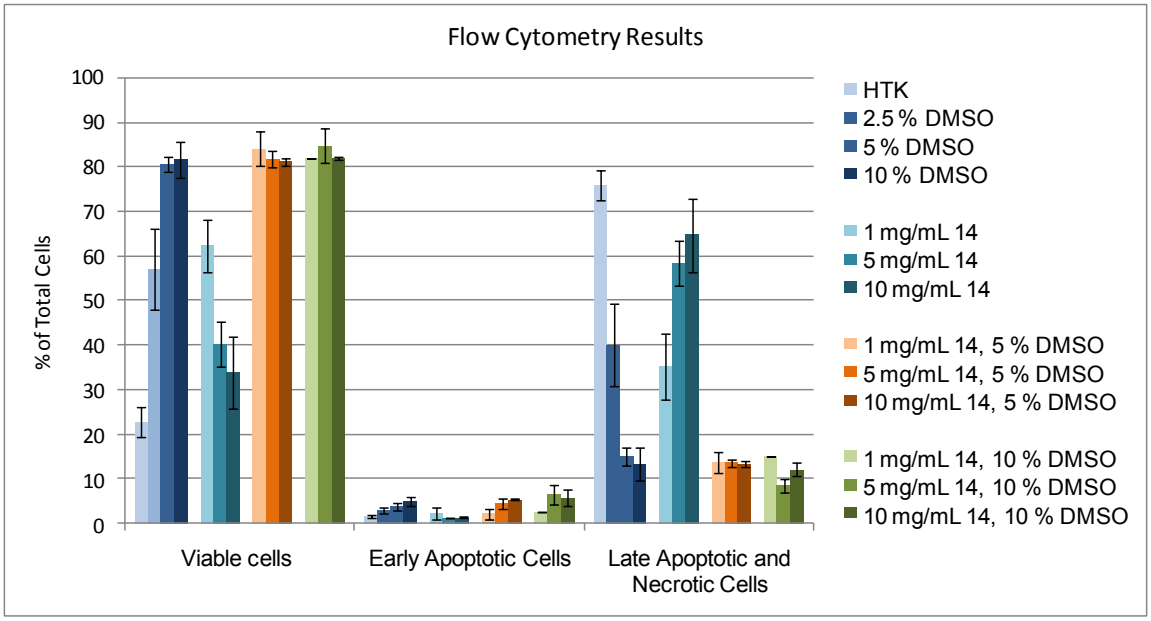

Figure 4.17 Annexin V/7AAD flow cytometry assay of WRL 68 cells after cryopreservation; WRL 68 cells were treated with different concentrations of ornithine analogue **14** and DMSO in HTK, and then treated according to the standard protocol given in Chapter 6. The total cell count was taken as 100% of cells. The error bars indicate SEM.

The cryopreservation outcomes when ornithine analogue **14** was employed (Figure 4.17) were significantly different from those seen with AFGP 8. Interestingly, analogue **14** at 1 mg/mL was as effective as 2.5% DMSO used alone. At 5 mg/mL and 10 mg/mL, on the other hand, analogue **14** resulted in a lower percentage of viable cells than either 1 mg/mL analogue **14**, or 2.5% DMSO used alone, although the result was not as poor as that obtained with HTK alone. When analogue **14** at any concentration was combined with 5% or 10% DMSO, the percentage of viable cells recovered was the same as when either 5% or 10% DMSO was used alone. Therefore, although the combination of analogue **14** with DMSO did not improve the cryopreservation outcome over that when DMSO was used alone, unlike the combination of AFGP 8 and 5% DMSO, analogue **14** combined with 5% DMSO did not negatively affect the outcome compared to that when 5% DMSO was used alone. It would be interesting to test analogue **14** at 0.5 mg/mL as well as with 2.5% DMSO.

4.7.8 Cryopreservation Studies with WRL 68 Cells: Summary

We have shown that it is possible to improve the cryopreservation potential of a 5% DMSO solution by the addition of low concentrations of carbohydrates, and further, that the addition of low concentrations of carbohydrates can allow the concentration of DMSO in the cryopreservation medium to be reduced from 5% to 2.5% without compromising cell viability. Galactose, melibiose, lactose, trehalose, and sucrose at various concentrations ranging from 22 mM to 100 mM and combined with 2.5% DMSO were as successful at protecting cells during cryopreservation as was 5% DMSO used alone. When galactose, melibiose, and trehalose at various concentrations ranging from 22 mM to 200 mM were combined with 5% DMSO, cell viability was greater than that seen when 5% DMSO was used alone. Most interestingly, at only 22 mM, melibiose combined with only 2.5 % DMSO also proved to be superior to 5% DMSO alone. This indicates that low concentrations of carbohydrates can be used for successful cryopreservation. Taken together, the data collected indicates that, in the presence of DMSO, the *type* of carbohydrate is more important than its *concentration.*

Particularly when carbohydrates were used alone, with the exception of galactose, the disaccharides were generally superior cryoprotectants over the monosaccharides; therefore, it appears that carbohydrates were most successful when used as extracellular cryoprotectants. When carbohydrates were used alone, the best results were seen at 200 mM, and some carbohydrates were as successful as 5% DMSO alone. Carbohydrate concentrations of around 200 mM seem to have the appropriate tonicity in order to dehydrate WRL 68 cells appropriately for successful cryopreservation.

Analysis of cryopreservation activity versus RI activity revealed a relationship between the two properties. At a given concentration, carbohydrates that had good RI activity were found to be good cryoprotectants, while poor RI activity was linked with poor cryopreservation activity. Carbohydrates with good RI activity may therefore be able to effectively manage the ice formed during cryopreservation.

Following, AFGP 8 and the ornithine analogue **14** were assayed for cryopreservation activity. The preliminary cryopreservation data obtained for AFGP 8 and the ornithine analogue **14** was encouraging. While AFGP 8 performed poorly when used on its own or in combination with 5% DMSO, it provided superior results when combined with 10% DMSO compared to the outcome when 10% DMSO was used alone. However, since we were interested in reducing the amount of DMSO used in cryopreservation, this outcome was not of practical interest. Analogue **14** provided very different results; at only 1 mg/mL, analogue **14** was as effective as 2.5% DMSO used alone. Increasing the concentration of analogue **14**, however, resulted in decreasing cell viability. Analogue **14** should be tested at a variety of concentrations centered on 1 mg/mL in order to identify an optimal concentration for cryopreservation. Although AFGP 8 had better RI activity than analogue **14**, it generally had poorer cryopreservation activity. Our lab had previously determined that AFGP 8 caused WRL 68 cells to undergo apoptosis at physiological temperatures. The related AFGP 8 serine analogue **16** showed no pro-apoptotic effect, but rather seemed to inhibit caspace-3/7 activation. The cryopreservation results suggest that analogue **14** may be similarly cytoprotective. Pursuing this dual approach of RI activity to manage ice, and apoptosis inhibition to mitigate the effects of stress, both accomplished by *one* cryoprotectant, may provide a superior cryoprotective agent and warrants further study.

4.8 Cryopreservation of Umbilical Cord Blood (UCB):

The cryopreservation activity of carbohydrates was further tested using UCB cells. The UCB studies were performed as described earlier in this chapter and in almost the same manner as the experiments with the WRL 68 cell line. The only difference between the two protocols was in the freezing medium employed: where HTK was used for the WRL 68 cells, cell growth medium (RPMI) supplemented with bovine serum albumin (BSA) and pentaspan was used for the UCB cells (the cell growth medium with the given supplements will be referred to as RPMI hereafter). As for the WRL 68 cells, UCB cells were cryopreserved using different concentration of cryoprotectants in cell freezing medium, and all post-thaw analyses were carried out using flow cytometry with annexin V/7AAD. All trials were

carried out at least in duplicate. The only variables we employed in our trials were the type of cryoprotectant (DMSO or carbohydrate) and concentration of cryoprotectant. All other variables were kept constant. The data for the MNCs and the $CD34^+$ fraction of the MNCs are presented in separate graphs for each treatment type (DMSO or carbohydrate).

4.8.1 Cryopreservation of Umbilical Cord Blood (UCB) with Dimethyl Sulfoxide (DMSO)

As discussed previously, DMSO is the most common cryoprotectant for both hepatocytes and HSCs. Therefore, we first attempted the cryopreservation of UCB with different concentrations of DMSO in RPMI. The MNC fraction was evaluated with RPMI alone, as well as with 5% and 10% DMSO in RPMI. The $CD34^+$ fraction was only evaluated with 5% DMSO. The results of these control experiments are given in Figure 4.18 and 4.19.

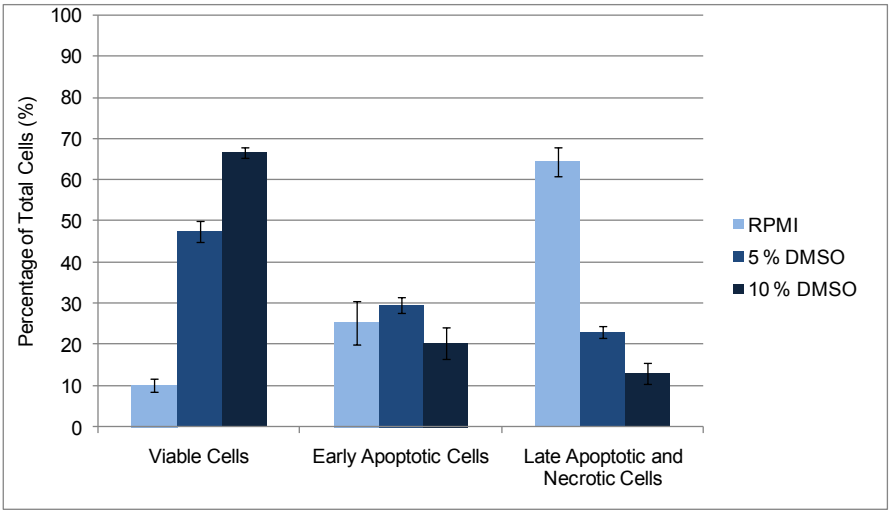

Figure 4.18 Annexin V/7AAD flow cytometry assay of UCB MNCs after cryopreservation; UCB cells were treated with different concentrations of DMSO in RPMI, and then treated according to the standard protocol given in Chapter 6. The total MNC count was taken as 100% of cells. The error bars indicate SEM.

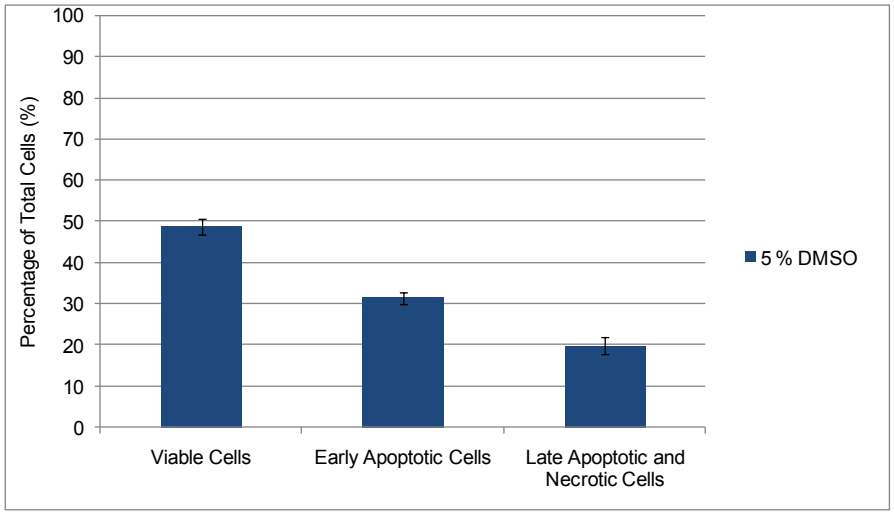

Figure 4.19 Annexin V/7AAD flow cytometry assay of UCB $CD34^+$ cells after cryopreservation; UCB cells were treated with different concentrations of DMSO in RPMI, and then treated according to the standard protocol given in Chapter 6. The total $CD34^+$ cell count was taken as 100% of cells. The error bars indicate SEM.

In the absence of DMSO (using only RPMI), cell survival was very low (about 10%). This result was not unexpected, since RPMI is a cell growth medium, and not a cryopreservation solution. Since it has been reported that 5% DMSO is as effective as 10% DMSO for maintaining cell viability through cryopreservation, we were surprised that in our trials, UCB cells treated with 5% DMSO in RPMI yielded only 47% viable MNCs, and 49% viable $CD34^+$ cells after cryopreservation, while treatment with 10% DMSO yielded 76% viable MNCs. Further, these percentages were significantly lower than the percentage of viable cells found when WRL 68 cells were cryopreserved with either 5% or 10% DMSO. Interestingly, for all DMSO treatments, the percentage of cells in early apoptosis was much higher for UCB cells (comprising 30% and 31% of total cells for MNC and $CD34^+$, respectively, with 5% DMSO treatment) than for WRL 68 cells (where early apoptosis comprised only 5% of total cells with 5% DMSO treatment). For all DMSO treatments, the percentage of UCB MNCs and $CD34^+$ cells in early apoptosis was higher than the percentage of cells in late apoptotis/necrosis. This was different from the result obtained for WRL 68 cells cryopreserved with DMSO, where, for the same treatment, the percentage of cells in early apoptosis was always lower than the percentage of cells in late apoptosis/necrosis. In

fact, as discussed, the percentage of WRL 68 cells found to be in early apoptosis was lower than the percentage of WRL 68 cells in late apoptosis/necrosis for *all* treatments, including all carbohydrate, and carbohydrate with DMSO treatments. The trends found with the UCB cryopreservation data will be explored as more data is presented.

4.8.2 Cryopreservation of Umbilical Cord Blood (UCB): Pre-Cryopreservation Data

The higher percentage of viable WRL 68 cells as compared to the percentage of viable MNC and $CD34^+$ cells after cryopreservation with 5% or 10% DMSO may be due to the greater hardiness of cell lines compared to primary cells. Given that we used un-optimized cryopreservation conditions, it is reasonable to expect that the percentages of viable cells recovered could be improved. It is an important consideration, however, that the difference in hardiness between the WRL 68 cell line, and the UCB primary cells likely means that the number of viable cells before cryopreservation was likely significantly different for the two cell types; the number of viable cells is expected to be greater for the cell line than for the primary cells. Importantly, the cultured WRL 68 cells were collected during a growth phase, and prior to collection, any non-adherent (non-viable) cells were removed by successive washes using EMEM. The remaining cells were detached and counted using a hemacytometer with trypan blue staining (to avoid counting any non-viable cells), and aliquoted into cryopreservation vials. The percentage of viable, non-apoptotic WRL 68 cells prior to cryopreservation was determined to be about 95% (data not shown). The UCB cells, on the other hand, were obtained from another research lab, in vials stored on ice. Although the cells were similarly counted prior to cryopreservation using a hemacytometer with trypan blue staining, the non-viable cells could not be separated from the viable cells, nor could the percentage of apoptotic cells be determined with the trypan blue technique. The pre-cryopreservation percentages of viable, early apoptotic, and late apoptotic or necrotic UCB MNC and $CD34^+$ cells were determined for a number of randomly selected samples of UCB cells using the annexin V/7AAD flow cytometry assay. The data is presented in Figures 4.20 and 4.21.

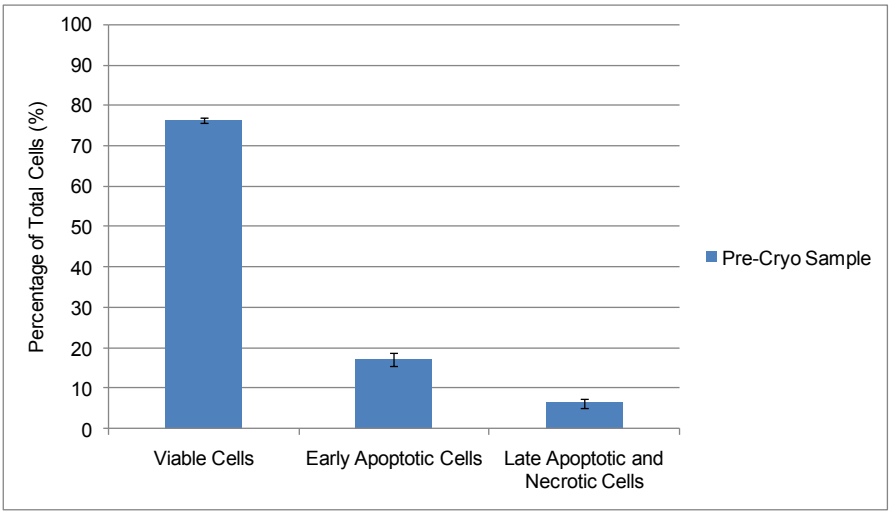

Figure 4.20 Annexin V/7AAD flow cytometry assay of UCB MNCs prior to cryopreservation; the total $CD34^+$ cell count was taken as 100% of cells. The error bars indicate SEM.

Before undergoing cryopreservation, only 76% of the MNCs, and 74% of the $CD34^+$ cells were viable in the UCB samples tested. The early apoptotic fraction made up 17% and 18% of the MNC and $CD34^+$ cells, respectively, and the late apoptotic/necrotic fraction made up 6% and 8% respectively. These percentages were consistent over multiple samples, as alluded to by the low SEM reported. Since the number of viable cells in the post-cryopreservation sample is of vital importance for a successful transplantation outcome, the relative number of viable cells pre- and post-cryopreservation is less important than the absolute number of viable cells in a sample found post-cryopreservation. Consequently, the percentage of viable (and early and late apoptotic/necrotic) cells found post-cryopreservation was reported as determined by the annexin V/7AAD flow cytometry assay, and not as a ratio of the pre- and post-cryopreservation outcomes. Given that a lower percentage of the UCB cells compared to WRL cells were found to be viable pre-cryopreservation, we were reasonably satisfied with the percentage of viable cells recovered after cryopreservation with 5% and 10% DMSO, and we therefore considered these control trials as evidence that our cryopreservation protocol was adequate.

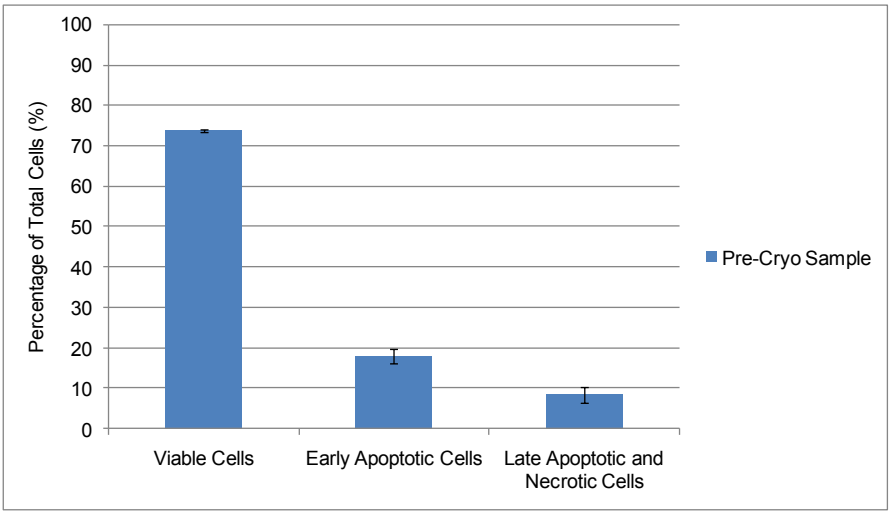

Figure 4.21 Annexin V/7AAD flow cytometry assay of UCB $CD34^+$ cells prior to cryopreservation; the total $CD34^+$ cell count was taken as 100% of cells. The error bars indicate SEM.

Two more points should be considered when analyzing the results of UCB cryopreservation. First, UCB will show some variation between samples due to the heterogeneity of the human population. Secondly, the total number of $CD34^+$ cells is significantly lower than the number of MNCs in each experiment. As a result, the error associated with the $CD34^+$ cell results was greater than for the MNCs, and this translates into larger error bars associated with the $CD34^+$ cell data compared to the MNC data.

4.8.3 Cryopreservation of Umbilical Cord Blood (UCB) with Carbohydrates and Dimethyl Sulfoxide (DMSO)

Six carbohydrates were tested for their cryopreservation activity: three monosaccharides (galactose, glucose, and 3-*O*-methylglucose) and three disaccharides (melibiose, trehalose, and sucrose). As for DMSO, the $CD34^+$ cell fraction was not evaluated for every treatment.

4.8.3.1 Cryopreservation of Umbilical Cord Blood (UCB) with Galactose

The cryopreservation activity of galactose on UCB cells was assessed first (Figures 4.22 and 4.23). The addition of galactose to RPMI with and without 5% DMSO provided very different cryopreservation outcomes with the UCB MNCs than was seen with the WRL 68 cells. Using galactose alone, WRL 68 cell survival (percentage of viable cells) after cryopreservation was greatest at 200 mM, and lowest at 22 mM (Figure 4.6), with cell survival at 500 mM falling in-between. For UCB cells, however, higher concentrations of galactose resulted in higher percentages of viable cells after cryopreservation than lower concentrations of galactose. Interestingly, while cryopreservation of WRL 68 cells with 22 mM galactose resulted in significantly more viable cells than HTK alone (negative control), cryopreservation of UCB MNCs with 22 mM galactose did not increase the viability over that obtained using RPMI alone. The cell survival trend for galactose with 5% DMSO was similar for both UCB MNCs and WRL 68 cells; the lower concentrations of galactose (22 mM and 60 mM) resulted in greater cell viability after cryopreservation than the higher concentrations of galactose (200 mM and 500 mM). However, the difference between the low and high concentrations was more pronounced in the UCB MNCs than had been seen with the WRL 68 cells (Figures 4.22 and 4.8, respectively).

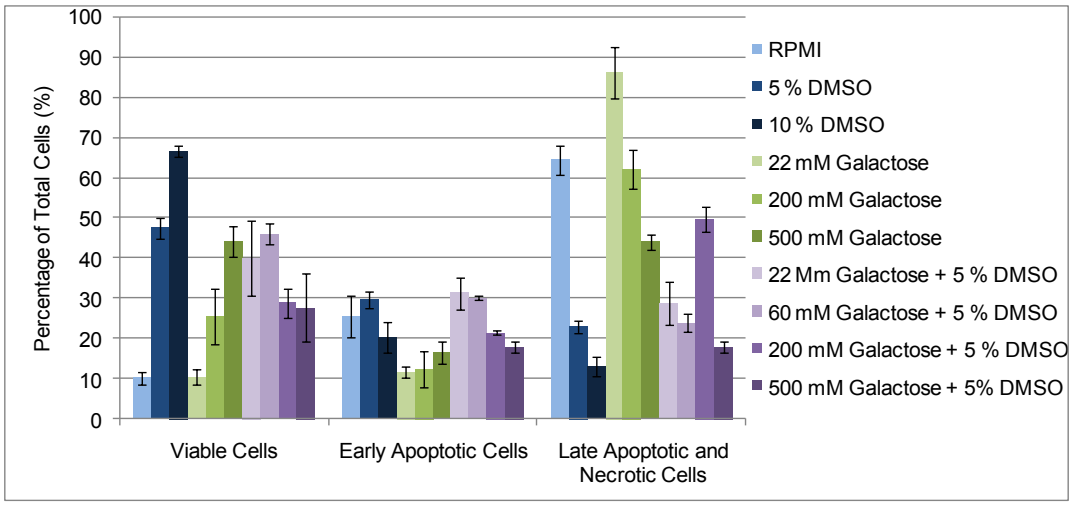

Figure 4.22 Annexin V/7AAD flow cytometry assay of UCB MNCs after cryopreservation; UCB cells were treated with different concentrations of galactose and DMSO in RPMI, and then treated according to the standard protocol given in Chapter 6. The total MNC count was taken as 100% of cells. The error bars indicate SEM.

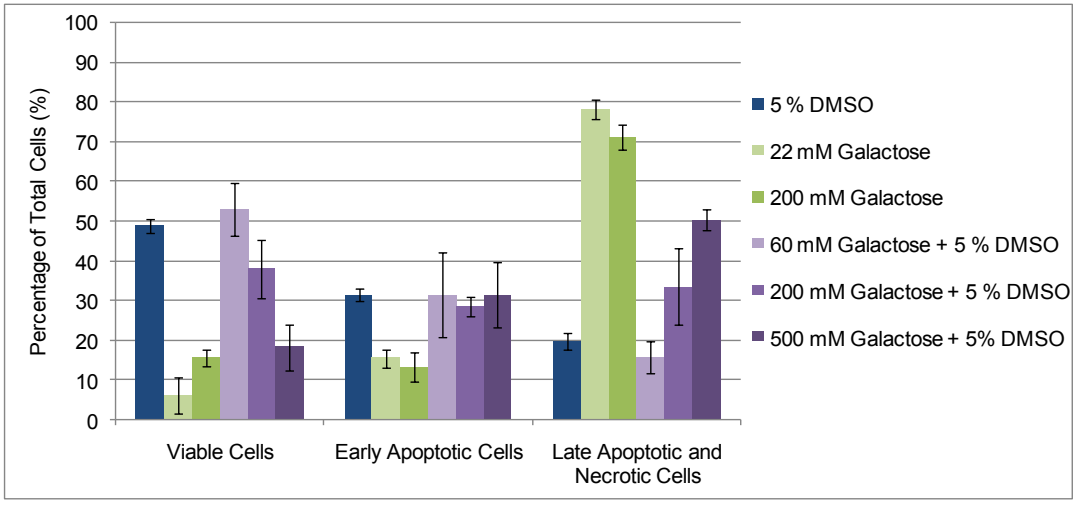

Figure 4.23 Annexin V/7AAD flow cytometry assay of UCB $CD34^+$ cells after cryopreservation; UCB cells were treated with different concentrations of galactose and DMSO in RPMI, and then treated according to the standard protocol given in Chapter 6. The total $CD34^+$ cell count was taken as 100% of cells. The error bars indicate SEM.

Lastly, as was the case when DMSO was used alone for the cryopreservation of WRL 68 cells, the most striking difference between the cryopreservation outcome of the two cell types was in the percentage of early apoptotic cells: not only did the percentage of early apoptosis rise as high as 31% in the UCB cells (and only as high as 6% in the WRL cells), for the UCB MNC fraction, the percentage of early apoptotic cells was not necessarily lower than the percentage of late apoptotic/necrotic cells. For the WRL 68 cells, on the other hand, the percentage of early apoptotic cells was always lower than the percentage of late apoptotic/necrotic cells. Inspection of the rest of the results for both the WRL 68 and UCB MNCs revealed that these trends are roughly true for every treatment employed. However, the WRL 68 and UCB MNCs are dramatically different cell types, and so it is not surprising that the same treatment provided different outcomes. The differences between the outcomes of the same treatments on the two cell types will not be discussed further in terms of specific treatments, however, a general discussion of the effects of carbohydrates on the two cell types will follow.

Returning to the discussion of the data shown in Figures 4.22 and 4.23: it was found that three treatments (500 mM galactose, 22 mM galactose with 5% DMSO, and 60 mM galactose with 5% DMSO) were as good as 5% DMSO alone in terms of the number of viable cells recovered after cryopreservation, (although of these concentration, data for $CD34^+$ cells was only recorded with 60 mM galactose with 5% DMSO). No treatments were as good as 10% DMSO alone. In general, the results of the galactose treatments on the viability of $CD34^+$ cells were very similar to those for the entire MNC fraction.

4.8.3.2 Cryopreservation of UCB with Combinations of Carbohydrates and Dimethyl Sulfoxide (DMSO): Correlations Between Cell Populations

When the trials carried out with WRL 68 cells were first analyzed, it appeared that there was a correlation between the percentage of viable cells and the percentage of late apoptotic/necrotic cells. Visual inspection of the results obtained with UCB cells, however, did not reveal any clear trends. In order to help determine whether or not any correlations

existed in the UCB data, we plotted viable versus early apoptotic cells, as well as viable versus late apoptotic/necrotic cells, for all MNC and $CD34^+$ cell data. Figures 4.24 and 4.25 show the MNC data, and Figures 4.30 and 4.31 show the $CD34^+$ cell data.

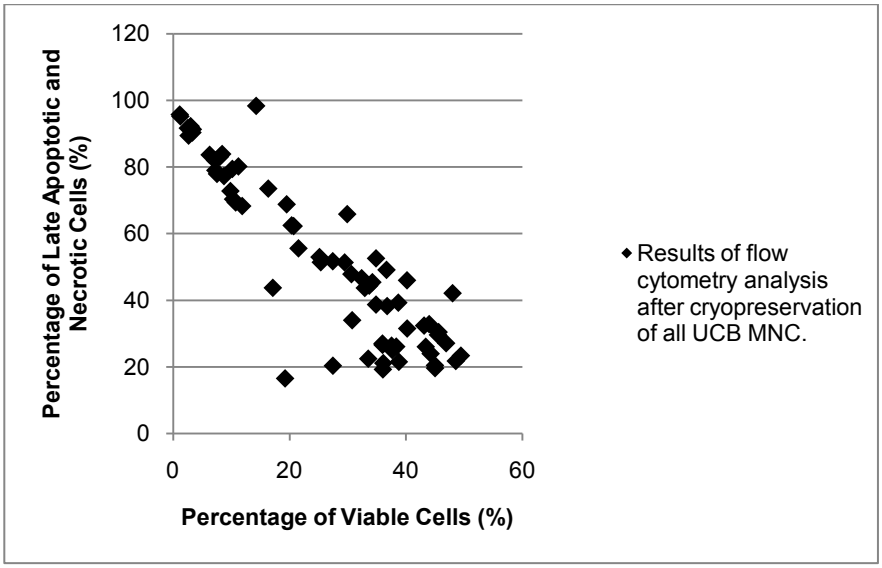

Figure 4.24 Percentage of viable cells versus percentage of late apoptotic/necrotic cells as determined by Annexin V/7AAD flow cytometry assay of MNCs after cryopreservation; UCB cells were treated with different concentrations of carbohydrates and DMSO in RPMI, and then treated according to the standard protocol given in Chapter 6. The total cell count was taken as 100% of cells.

Figure 4.24 seems to show that there exists a negative correlation between viable and late apoptotic/necrotic cells. However, as was seen with the WRL 68 cells, there seemed to be at least two correlations present, and further, there also appeared to be a third, positive, correlation. Interestingly, Figure 4.25 also showed at least two positive correlations between viable and early apoptotic cells, as well as one negative correlation.

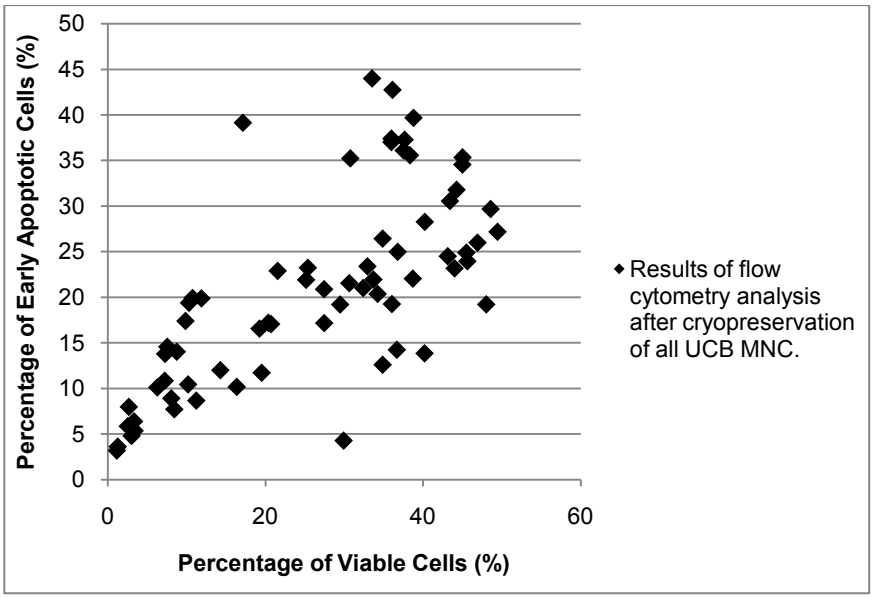

Figure 4.25 Percentage of viable cells versus percentage of early apoptotic cells as determined by Annexin V/7AAD flow cytometry assay of MNCs after cryopreservation; UCB cells were treated with different concentrations of carbohydrates and DMSO in RPMI, and then treated according to the standard protocol given in Chapter 6. The total cell count was taken as 100% of cells.

Figures 4.26 and 4.27 present the data obtained from $CD34^+$ cells. As for the MNC fraction, several positive and negative correlations seemed to be present between both viable cells and late apopotic/necrotic cells, and viable cells and early apoptotic cells. For both MNCs and $CD34^+$ cell types, we attempted to isolate the treatments associated with each correlation (eg. monosaccharides vs. disaccharides, treatments with DMSO vs. treatments without DMSO, etc.) but were unable to determine the contributing factors from the data available. Determining the underlying factors that were responsible for the different correlations seen with both UCB cells and WRL 68 cells presents intriguing prospects for future work. In the present case the implications of Figures 4.28-4.31 were that while the WRL 68 data could be adequately described using only the viable cell fraction, all of the UCB data will be described in order to discuss the cryopreservation outcomes of each treatment.

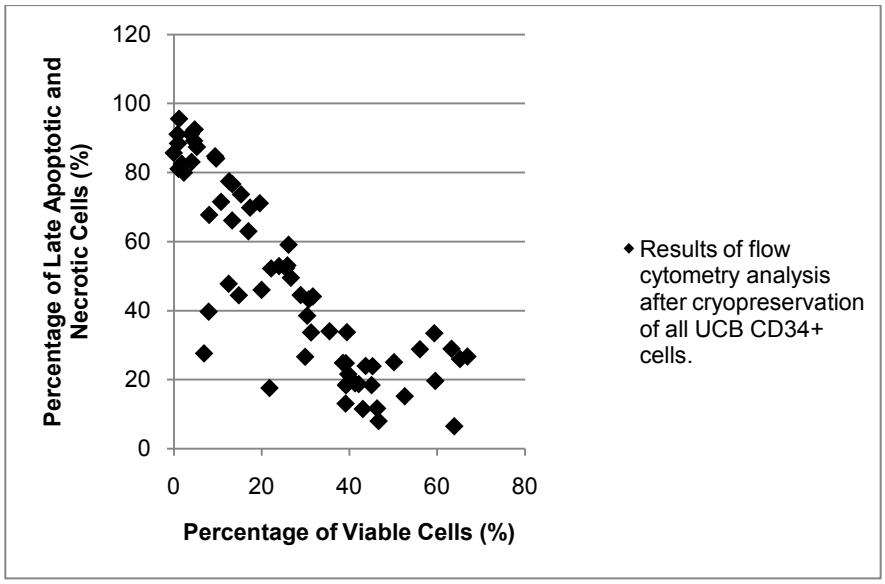

Figure 4.26 Percentage of viable cells versus percentage of late apoptotic/necrotic cells as determined by Annexin V/7AAD flow cytometry assay of $CD34^+$ cells after cryopreservation; UCB cells were treated with different concentrations of carbohydrates and DMSO in RPMI, and then treated according to the standard protocol given in Chapter 6. The total cell count was taken as 100% of cells.

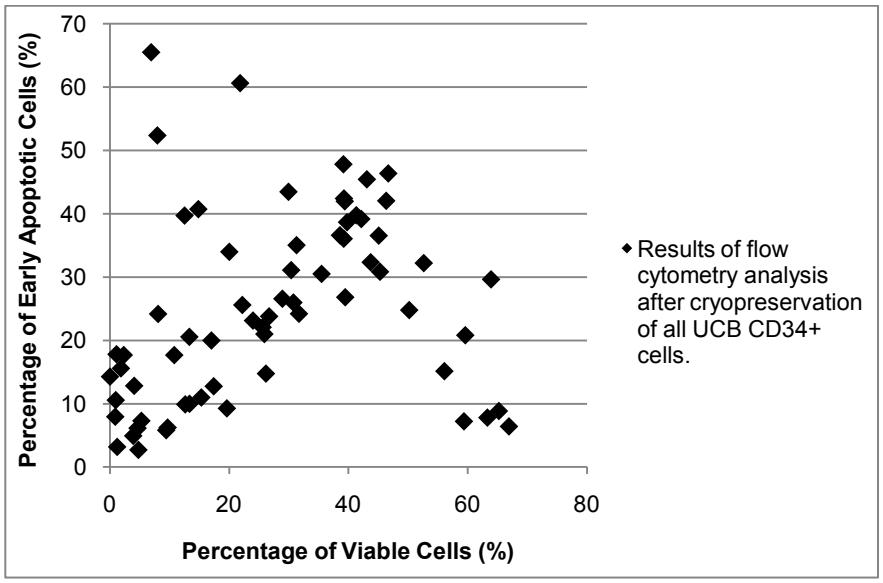

Figure 4.27 Percentage of viable cells versus percentage of early apoptotic cells as determined by Annexin V/7AAD flow cytometry assay of $CD34^+$ cells after cryopreservation; UCB cells were treated with different concentrations of carbohydrates and DMSO in RPMI, and then treated according to the standard protocol given in Chapter 6. The total cell count was taken as 100% of cells.

4.8.3.3 Cryopreservation of Umbilical Cord Blood (UCB) with Glucose and 3-O-Methylglucose

Glucose and 3-*O*-methylglucose did not seem to have any cryopreservation activity with UCB cells (Figures 4.28 and 4.29). Both 22 mM and 200 mM glucose were only as good at protecting cells during cryopreservation as RPMI alone, and 22 mM and 200 mM 3-*O*-methylglucose were significantly poorer than RPMI alone. The same treatments were equally poor at protecting the respective $CD34^+$ cell populations. When either carbohydrate was added to RPMI, the percentage of early apoptotic MNCs decreased compared to those samples cryopreserved using only RPMI; however, the percentage of late apoptotic/necrotic cells increased. That both of these carbohydrates – glucose and 3-*O*-methylglucose – gave similar results is not wholly unexpected since the latter is a derivative of the former.

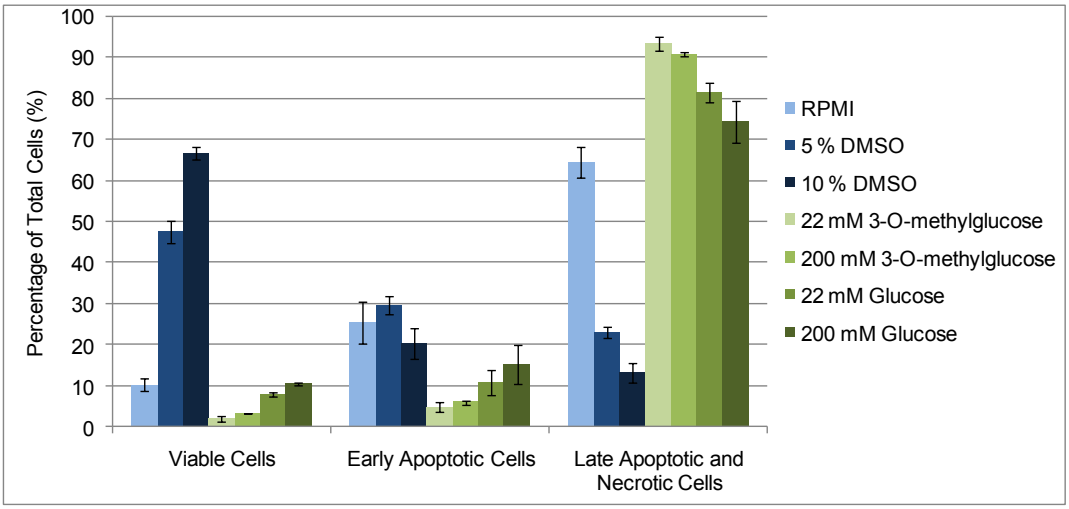

Figure 4.28 Annexin V/7AAD flow cytometry assay of UCB MNCs after cryopreservation; UCB cells were treated with different concentrations of glucose, 3-*O*-methylglucose and DMSO in RPMI, and then treated according to the standard protocol given in Chapter 6. The total MNC count was taken as 100% of cells. The error bars indicate SEM.

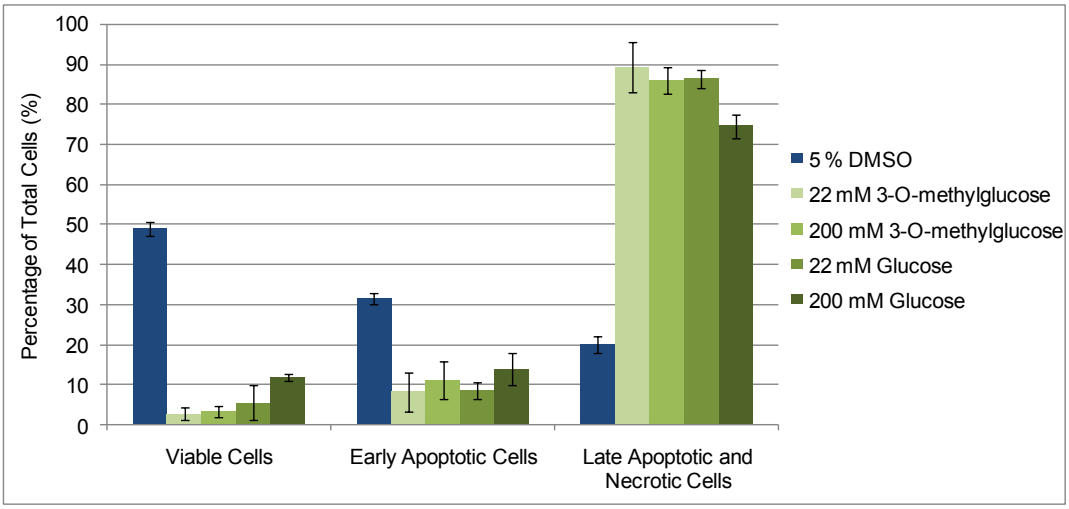

Figure 4.29 Annexin V/7AAD flow cytometry assay of UCB $CD34^+$ cells after cryopreservation; UCB cells were treated with different concentrations of glucose, 3-*O*-methylglucose and DMSO in RPMI, and then treated according to the standard protocol given in Chapter 6. The total $CD34^+$ cell count was taken as 100% of cells. The error bars indicate SEM.

4.8.3.4 Cryopreservation of Umbilical Cord Blood (UCB): Melibiose

The results obtained with the disaccharide melibiose were similar to those obtained using the monosaccharide galactose. The results for melibiose are presented in Figures 4.30 and 4.31. Notably, when either carbohydrate was used without DMSO, cell viability after cryopreservation increased with increasing carbohydrate concentration. However, unlike 500 mM galactose, 500 mM melibiose was not as effective as 5% DMSO alone. No treatments with either carbohydrate were as effective as 10% DMSO alone. When carbohydrates were combined with 5% DMSO, however, 22 mM melibiose provided as many viable cells after cryopreservation as 5% DMSO alone. Results using 22 mM melibiose with 5% DMSO and 60 mM melibiose with 5% DMSO were not significantly different. As was the case for galactose, when low concentrations (22 mM and 60 mM) of melibiose were combined with 5% DMSO, the percentage of early apoptotic cells was equal to or greater than the percentage of late apoptotic/necrotic cells after cryopreservation. For all other treatments, the percentage of early apoptotic cells was significantly smaller than the percentage of late

apoptotic/necrotic cells. This was true for both the MNCs and $CD34^+$ cell fractions. In fact, as will be seen for the trehalose and sucrose data presented following, this proved to be true for all of the carbohydrates tested with UCB cells.

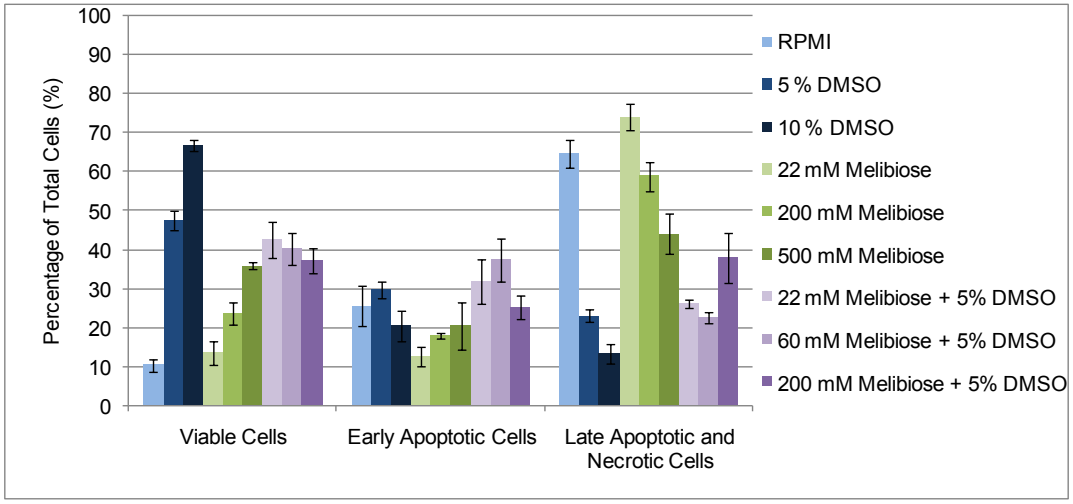

Figure 4.30 Annexin V/7AAD flow cytometry assay of UCB MNCs after cryopreservation; UCB cells were treated with different concentrations of melibiose and DMSO in RPMI, and then treated according to the standard protocol given in Chapter 6. The total MNC count was taken as 100% of cells. The error bars indicate SEM.

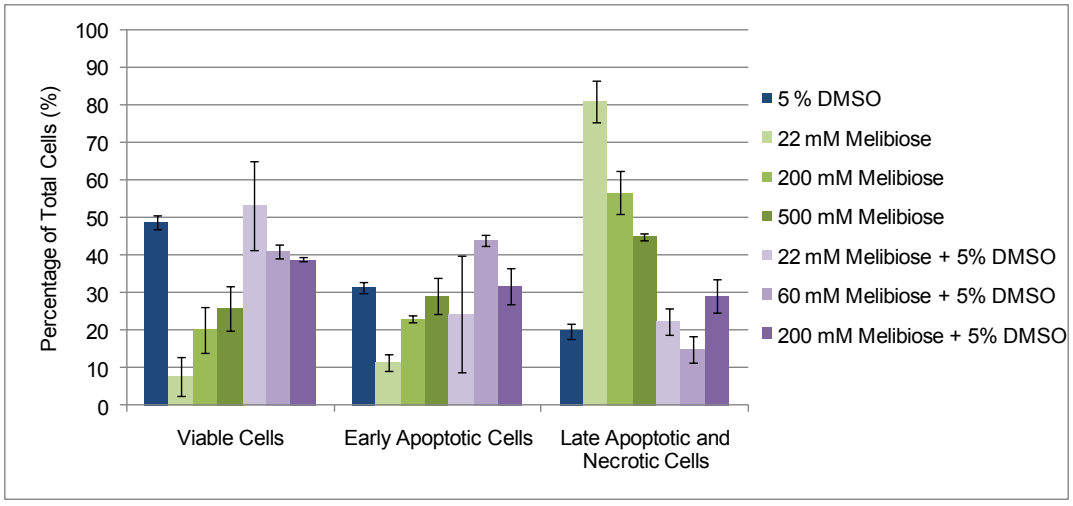

Figure 4.31 Annexin V/7AAD flow cytometry assay of UCB $CD34^+$ cells after cryopreservation; UCB cells were treated with different concentrations of melibiose and DMSO in RPMI, and then treated according to the standard protocol given in the Chapter 6. The total $CD34^+$ cell count was taken as 100% of cells. The error bars indicate SEM.

4.8.3.5 Cryopreservation of Umbilical Cord Blood (UCB) with Trehalose

When used on its own, trehalose proved to be as poor a cryoprotective agent for UCB cells as glucose (Figures 4.32 and 4.33). Cryopreservation with 22 mM trehalose resulted in a lower percentage of viable MNCs (1%) after cryopreservation than cryopreservation with RPMI alone. While cryopreservation with 200 mM trehalose provided a higher percentage of viable MNCs (8%), this result was not better than that obtained when RPMI was used alone. As was seen with galactose and melibiose, the addition of 5% DMSO to the carbohydrate solutions dramatically increased cell viability after cryopreservation. While only 22 mM trehalose with 5% DMSO was as effective as 5% DMSO alone, there was no statistically significant difference between 22 mM, 60 mM, and 200 mM trehalose when each was combined with 5% DMSO. All treatments used had the same effect on MNC and $CD34^+$ cell survival.

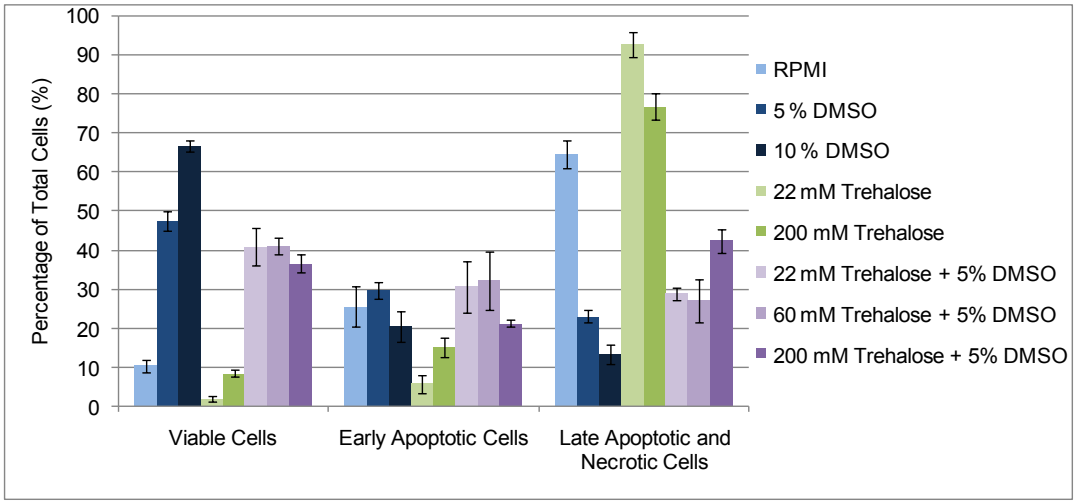

Figure 4.32 Annexin V/7AAD flow cytometry assay of UCB MNCs after cryopreservation; UCB cells were treated with different concentrations of trehalose and DMSO in RPMI, and then treated according to the standard protocol given in Chapter 6. The total MNC count was taken as 100% of cells. The error bars indicate SEM.

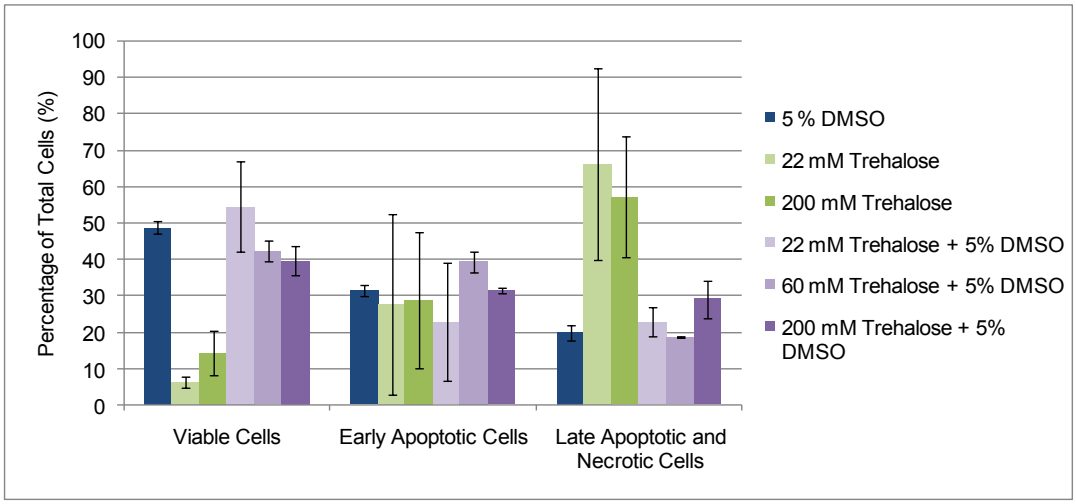

Figure 4.33 Annexin V/7AAD flow cytometry assay of UCB $CD34^+$ cells after cryopreservation; UCB cells were treated with different concentrations of trehalose and DMSO in RPMI, and then treated according to the standard protocol given in Chapter 6. The total $CD34^+$ cell count was taken as 100% of cells. The error bars indicate SEM.

4.8.3.6 Cryopreservation of Umbilical Cord Blood (UCB) with Sucrose

Compared to the other disaccharides tested, sucrose had poor RI activity, as well as relatively poor cryopreservation activity when tested with WRL 68 cells. However, when applied to the cryopreservation of UCB cells, sucrose was as effective a cryoprotectant as were galactose and melibiose for most treatments, and more effective than trehalose across all treatments (Figures 4.34 and 4.35). As for galactose, melibiose, and trehalose used alone, increasing the concentration of sucrose resulted in an increased percentage of viable cells. The addition of 5% DMSO further improved the cryopreservation activity of sucrose, and the greatest cell viability was seen with 22 mM sucrose with 5% DMSO and 60 mM sucrose with 5% DMSO; both treatments were as good as 5% DMSO used alone. Unfortunately, the errors associated with the $CD34^+$ cell data were large, and that data was therefore not informative.

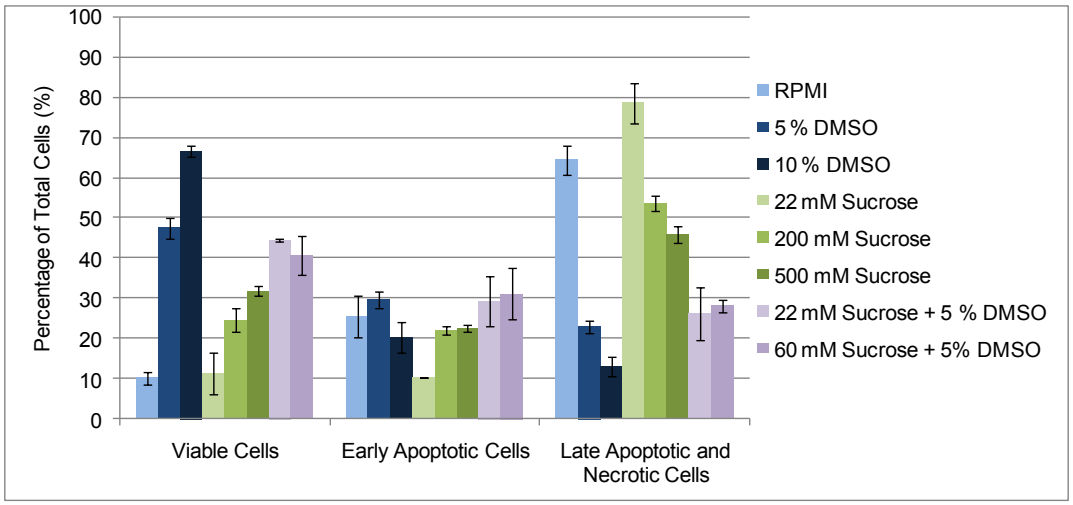

Figure 4.34 Annexin V/7AAD flow cytometry assay of UCB MNCs after cryopreservation; UCB cells were treated with different concentrations of sucrose and DMSO in RPMI, and then treated according to the standard protocol given in Chapter 6. The total MNC count was taken as 100% of cells. The error bars indicate SEM.

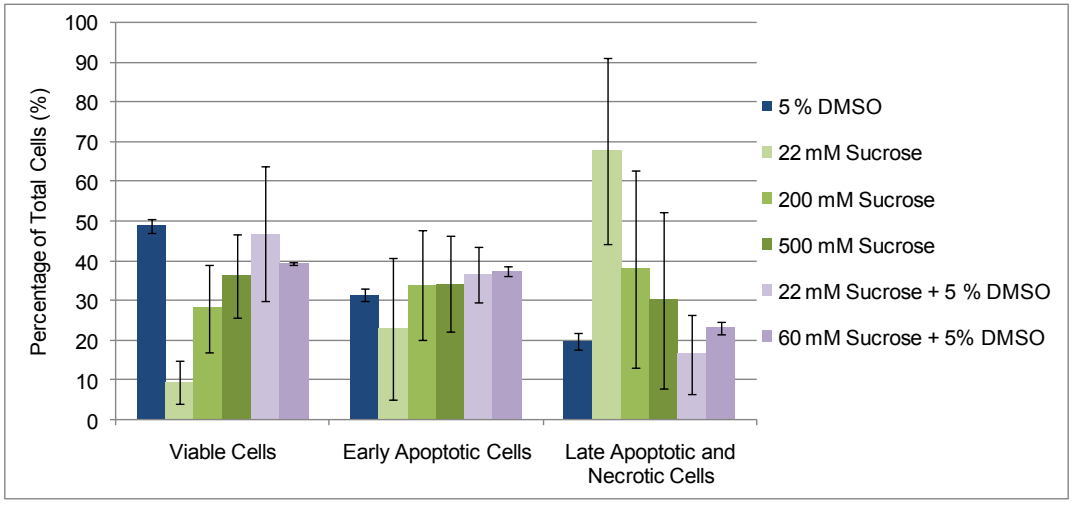

Figure 4.35 Annexin V/7AAD flow cytometry assay of UCB $CD34^+$ cells after cryopreservation; UCB cells were treated with different concentrations of DMSO in RPMI, and then treated according to the standard protocol given in Chapter 6. The total $CD34^+$ cell count was taken as 100% of cells. The error bars indicate SEM.

4.8.4 Cryopreservation of Umbilical Cord Blood (UCB): Significant Successes Using Carbohydrates

Figures 4.36 and 4.37 show all of the cryopreservation treatments that provided a percentage of viable cells equal to the percentage of viable cells obtained after cryopreservation with 5% DMSO alone. Unfortunately, no treatments were found to be better than 5% DMSO used alone, and therefore, no treatments were as good as 10% DMSO used alone (refer to Figure 4.18).

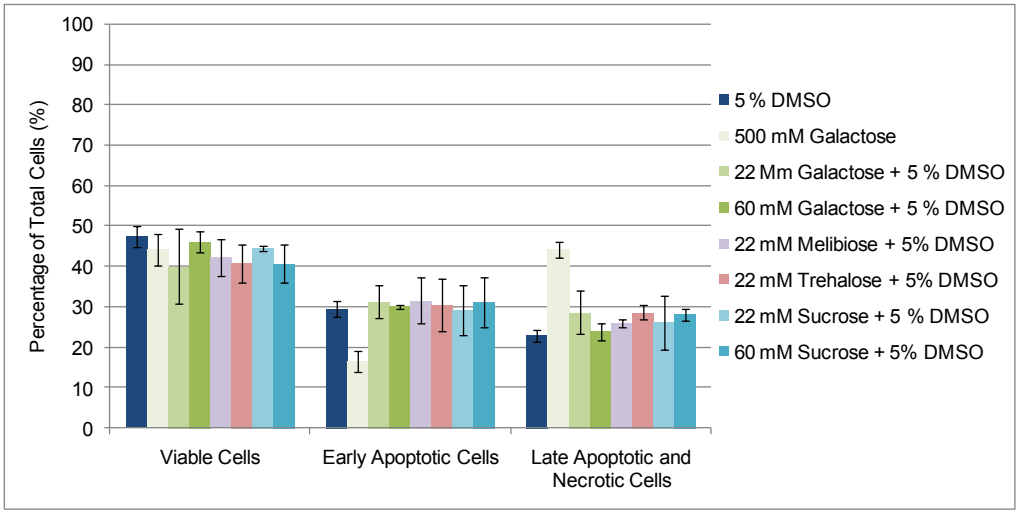

Figure 4.36 Annexin V/7AAD flow cytometry assay of UCB MNCs after cryopreservation; UCB cells were treated with different concentrations of carbohydrates and DMSO in RPMI, and then treated according to the standard protocol given in Chapter 6. The total MNC count was taken as 100% of cells. The error bars indicate SEM.

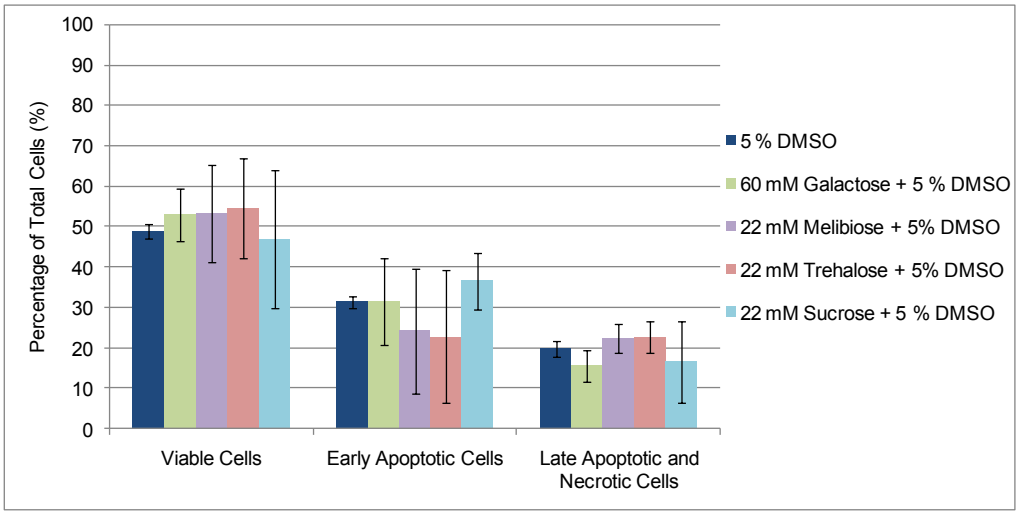

Figure 4.37 Annexin V/7AAD flow cytometry assay of UCB MNCs after cryopreservation; UCB cells were treated with different concentrations of carbohydrates and DMSO in RPMI, and then treated according to the standard protocol given in Chapter 6. The total $CD34^+$ cell count was taken as 100% of cells. The error bars indicate SEM.

As was found for WRL 68 cells, galactose, melibiose, trehalose, and sucrose afforded the greatest protection to cells during cryopreservation. However, galactose could provide cryoprotection in the absence of DMSO. Interestingly, galactose was most effective at 500 mM, the highest concentration tested, when used as the sole cryoprotectant. Further, while the percentages of viable, early apoptotic, and late apoptotic/necrotic cells for all trials where carbohydrates were combined with 5% DMSO were equivalent to the percentages obtained with 5% DMSO used alone, the distribution of cells was different when galactose was used as the sole cryoprotectant; that is, the percentage of early apoptotic cells was lower, and the percentage of late apoptotic/necrotic cells was higher than in all other trials. Although cytotoxicity testing was not carried out with UCB cells, it is likely that carbohydrates will subject the cells to osmotic stress at 500 mM, and may therefore be harmful to the cells. In fact, it was found that for the WRL 68 cells, carbohydrate concentrations of 500 mM greatly reduced cell viability in the cytotoxicity assay, and further, carbohydrates were generally poorer cryoprotectants at 500 mM than at 200 mM. In the UCB cells, it may be that the distribution of cells in the three categories is a reflection of the osmotic effect of a 500 mM carbohydrate solution: it is possible that galactose at 500 mM was able to protect some cells

from cryopreservation-induced damage, and possibly inhibited some cryopreservation-induced apoptosis, while other cells became necrotic as a result of osmotic shock. It could also be argued that this distribution of cells indicates that galactose rapidly causes cells to undergo apoptosis. However, while this study alone cannot be used to rule out an apoptotic mechanism of cell death, galactose is not a known inducer of apoptosis and therefore the latter explanation does not seem likely. This result also serves to highlight the different outcomes that may be seen among different cell types exposed to the same cryopreservation conditions. Unfortunately, the $CD34^+$ data was not recorded for the trials that employed galactose at 500 mM, nor those where 22 mM galactose with 5% DMSO was used. Of the trials for which data was available for both the MNC and $CD34^+$ fractions, only 60 mM sucrose with 5% DMSO was not as effective at protecting $CD34^+$ cells as it was at protecting MNCs. In general, however, MNCs and $CD34^+$ cells were similarly affected for all treatments; however, as was mentioned previously, the $CD34^+$ data suffers from poor reproducibility, and therefore the data should be treated with some caution. In order to improve the reliability of the data, more trials should be carried out per treatment. Next, based on our work with WRL 68 cells, we investigated RI as a possible cryoprotective mechanism.

4.8.5 Cryopreservation of Umbilical Cord Blood (UCB) Versus Recrystallization Inhibition (RI) Activity

The cryopreservation of UCB cells by carbohydrates may occur via the same mechanisms discussed for the cryopreservation of WRL 68. The same arguments for the action of permeable and impermeable cryoprotectants, and colligative properties versus membrane protection can be made. As was done for the WRL 68 cells, we explored the possibility of a relationship between the RI and cryopreservation activities of carbohydrates. Although the cell type is different, and may be somewhat more or less susceptible to cryo-damage, the formation of ice is a problem for all cell types.

The RI versus cryopreservation data for UCB cells was prepared in the same manner as that for the WRL 68 cell studies. RI activity measured as a ratio of the average mean grain size (MGS) of the sample in PBS to the average MGS of PBS measured on the same day, was plotted against the percentage of viable cells as measured by flow cytometry after cryopreservation with a solution of carbohydrate (without the addition of DMSO) in RPMI. As before, the average of the data from the cryopreservation trials is reported, and RI data at 22 mM and 220 mM was plotted against cryopreservation data at 22 mM and 200 mM, respectively. Figures 4.36 and 4.37, therefore, show the average percentage of viable cells after cryopreservation plotted against the RI ratio of the sample, for MNCs and $CD34^+$ cells, respectively.

It can be seen in Figures 4.38 and 4.39 that the relationship between RI and cryopreservation potential is not clear for UCB cells. While there may be some correlation between cryopreservation activity and RI, the correlation is certainly not as strong as it was in the WRL 68 study. The linear regression performed on the MNC data (Figure 4.38) had a poor R^2 value ($R^2 = 0.49$), while the linear regression performed on the $CD34^+$ data (Figure 4.39) had a better R^2 vlaue of 0.73. However, both should be viewed with caution since the error association with each cryopreservation data point is quite large, and the linear regression was carried out using only the average data values.

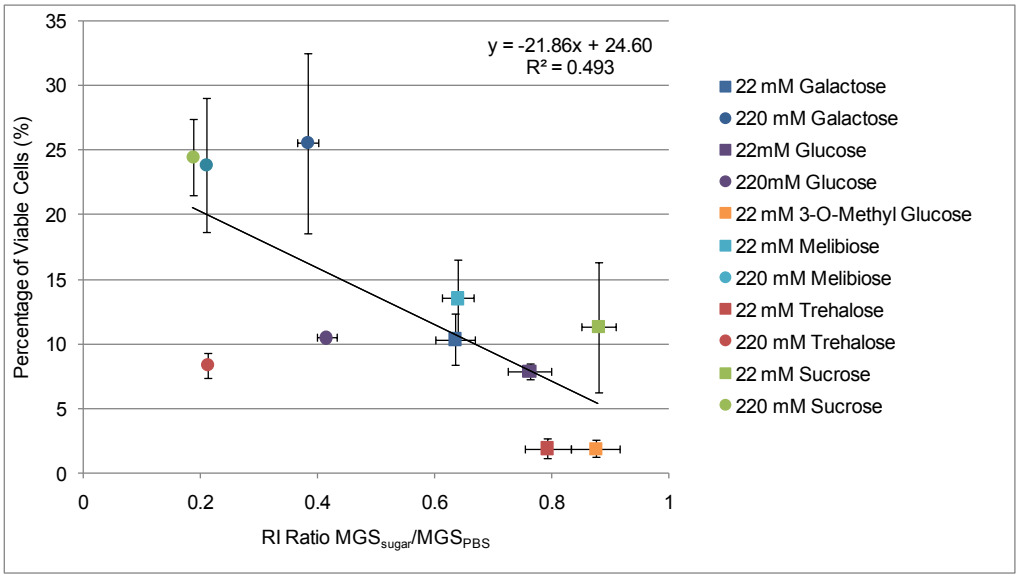

Figure 4.38 Percentage of viable MNCs versus the RI ratio (sample/PBS) for the same treatment; percentage of viable cells was obtained by Annexin V/7AAD flow cytometry assay of UCB cells after cryopreservation, where the total cell count was taken as 100% of cells. RI ratio of carbohydrates at 220 mM was compared to cryopreservation data of 200 mM carbohydrates. Cryopreservation and RI data were obtained according to the protocols given in Chapter 6. The error bars indicate SEM.

Part of the difficulty in ascertaining whether or not a correlation exists lies with the difficulty of reproducibility in the UCB study. As discussed previously, the fact that the UCB cells are primary cells from a heterogeneous population has a negative impact on the reproducibility of our results. In order to improve reproducibility, more trials for each treatment should be carried out. Unfortunately, in this study, our access to UCB cells was limited. It is hoped, however, that these trials will inform future studies, and increase the efficiency with which the available resources can be used.

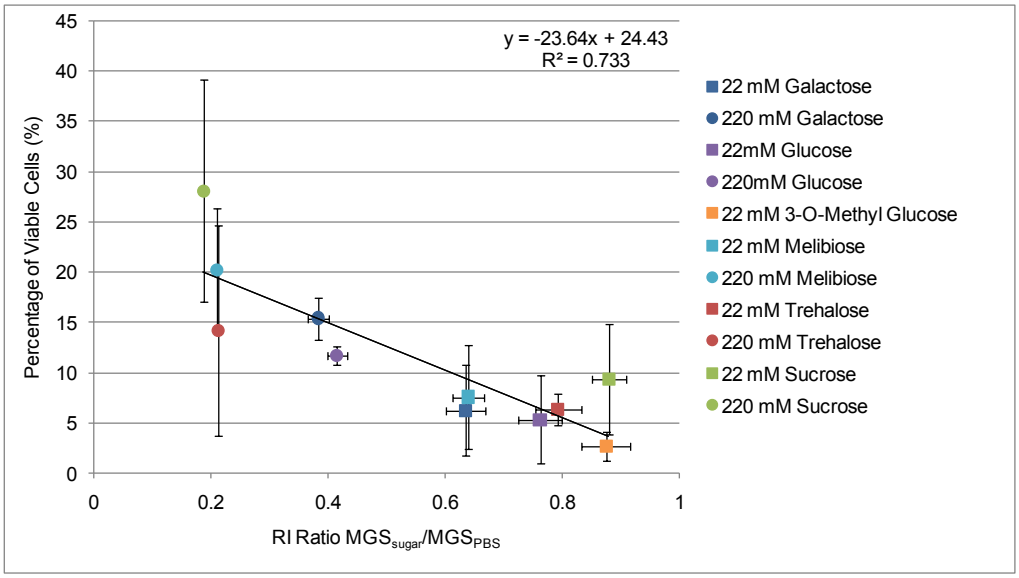

Figure 4.39 Percentage of viable $CD34^+$ cells versus the RI ratio (sample/PBS) for the same treatment; percentage of viable cells was obtained by Annexin V/7AAD flow cytometry assay of UCB cells after cryopreservation, where the total cell count was taken as 100% of cells. RI ratio of carbohydrates at 220 mM was compared to cryopreservation data of 200 mM carbohydrates. Cryopreservation and RI data were obtained according to the protocols given in Chapter 6. The error bars indicate SEM.

Despite the problems inherent to this study, the data in Figures 4.38 and 4.39 indicates that there may be a correlation between the RI and cryopreservation activity of the carbohydrates tested, and further trials to pursue this relationship are warranted. A correlation between RI and cryopreservation activities does not preclude the ability of carbohydrates to protect cells via their colligative properties or through membrane stabilization, however, studying the RI and cryopreservation relationship will likely prove to be invaluable to our understanding of cryopreservation.

4.8.6 Cryopreservation of Umbilical Cord Blood (UCB): Summary

In this study, we found that galactose, melibiose, trehalose, and sucrose at various concentrations, ranging from 22 mM to 60 mM and combined with 5% DMSO were all as effective at protecting MNCs and $CD34^+$ cells during cryopreservation as 5% DMSO alone. Interestingly, galactose at 500 mM, and *without* DMSO, was also as effective as 5% DMSO used alone. While no treatments with carbohydrates were as effective as 10% DMSO used alone (which also provided greater cell viability than 5% DMSO alone), our results suggest that carbohydrates are able to protect UCB cells during cryopreservation, and therefore merit further study. The general trends seen with both MNCs and $CD34^+$ cells were somewhat different from the general trends in the WRL 68 cell data. For both MNCs and $CD34^+$ cells, increasing carbohydrate concentration generally resulted in increased cell viability, when carbohydrates were used alone. Conversely, it appeared that when carbohydrates were used with 5% DMSO, increasing carbohydrate concentration resulted in decreasing cell viability. This trend is particularly interesting given that disaccharides at 500 mM were found to be very cytotoxic to WRL 68 cells. Although the cytotoxicity study were not carried out using UCB cells, since it was speculated that the mode of cytotoxicity of the hypertonic carbohydrate solutions was likely mechanical damage – specifically, osmotic shock resulting from extreme volume excursions – it is likely that some cytotoxicity would have been seen with the UCB cells as well. As was discussed for the WRL 68 cells, since cells are impermeable to disaccharides, and given the trend in increasing cell survival with increasing carbohydrate concentration, it may be that the dehydrating conditions imposed on cells by the high concentrations of extracellular cryoprotectant are beneficial for the cryopreservation of UCB cells. In general, 500 mM carbohydrate solutions without DMSO were most effective for UCB cell cryopreservation and this should therefore be used as a starting point to optimize both the carbohydrate concentration, as well as other components of the cryopreservation protocol.

Lastly, as previously discussed regarding WRL 68 cells, we had found that there was likely a relationship between the RI and cryopreservation activity of carbohydrates. In the UCB study, we found further evidence of this relationship, although the correlation with

MNC's and $CD34^+$ cells were not as good as they were for the WRL 68 cells. Since there is evidence that the correlation holds for UCB cells, additional treatments, as well as additional replicates for treatments already assayed should be carried out in order to further explore the nature of the RI/cryopreservation relationship.

With these studies, we have established a good foundation from which to increase our knowledge and expand the potential of cryopreservation.

1. Skoric, D.; Balint, B.; Petakov, M.; Sindjic, M.; Rodic, P., Collection strategies and cryopreservatino of umbilical cord blood. *Transfusion Medicine* **2007,** 17, 107-113.
2. Clarke, D. M.; Yadock, D. J.; Nicoud, I. B.; Matthew, A. J.; Heimfeld, S., Improved post-thaw recovery of peripheral blood stem/progenitor cells using a novel intracellular-like cryopreservation solution. *Cytotherapy* **2009,** 11, 472-479.
3. Liseth, K.; Abrahamsen, J. F.; Bjorsvik, S.; Grottebo, K.; Bruserud, O., The viability of cryopreserved PBPC depends on the DMSO concentration and the concentration of nucleated cells in the graft. *Cytotherapy* **2005,** 7, 328-333.
4. Akkok, C. A.; Liseth, K.; Nesthus, I.; Lokeland, T.; Tefre, K.; Bruserud, O.; Abrahamsen, J. F., Autologous peripheral blood progenitor cells cryopreserved with 5 and 10 percent dimethyl sulfoxide alone give comparable hematopoietic reconstitution after transplantation. *Transfusion* **2008,** 48, 877-883.
5. Abrahamsen, J. F.; Rusten, L.; Bakken, A. M.; Bruserud, O., Better preservation of early hematopoietic progenitor cells when human peripheral blood progenitor cells are cryopreserved with 5 percent dimethylsulfoxide instead of 10 percent dimethylsulfoxide. *Transfusion* **2004,** 44, 785-789.
6. Rowley, S. D.; Feng, Z.; Chen, L.; Holmberg, L.; Heimfeld, S.; MacLeod, B.; Bensinger, W. I., A randomized phase III clinical trial of autologous blood stem cell transplantation comparing cryopreservation using dimethylsulfoxide *vs* dimethylsulfoxide with hydroxyethylstarch. *Bone Marrow Transplantation* 31, 1043-1051.
7. Abrahamsen, J. F.; Bakken, A. M.; Bruserud, O., Cryopreserving human peripheral blood progenitor cells with 5-percent rather than 10-percent DMSO results in less apoptosis and necrosis in $CD34^+$ cells. *Transfusion* **2002,** 42, 1573-1580.
8. Hunt, C. J.; Armitage, S. E.; Pegg, D. E., Cryopreservation of umbilical cord blood: 2. Tolerance of $CD34^+$ cells to multimolar dimethyl sulphoxide and the effect of cooling rate on recovery after freezing and thawing. *Cryobiology* **2003,** 46, 76-87.
9. Berz, D.; McCormack, E. M.; Winer, E. S.; Colvin, G. A.; Quesenberry, P. J., Cryopreservation of hematopoietic stem cells. *American Journal of Hematology* **2007,** 82, (6), 463-472.
10. Ludlow, J. W.; Bruce, A. T.; Kulik, M. J.; Meheux, S. O.; McCoy, D. W.; Asfeldt, T. M., Allogeneic cell therapy for the treatment of liver disease. *Progress in Transplantation* **2005,** 15, 178-184.
11. Terry, C.; Dhawan, A.; Mitry, R. R.; Hughes, R. D., Cryopreservation of isolated human hepatocytes for transplantation: State of the art. *Cryobiology* **2006,** 53, 149-159.
12. Arikura, J.; Kobayashi, N.; Okitsu, T.; Noguchi, H.; Totsugawa, T.; Watanabe, T.; Matsumura, T.; Maruyama, M.; Kosaka, Y.; Tanaka, N.; Onodera, K.; Kasai, S., UW solution: a promising tool for cryopreservation of primarily isolated rat hepatocytes. *Journal of Hepato-Biliary-Pancreatic Surgery* **2002,** 9, 742-749.
13. Mitry, R. R.; Hughes, R. D.; Dhawan, A., Progress in human hepatocytes: isolation, culture & cryopreservation. *Seminars in Cell and Developmental Biology* **2002,** 13, 463-467.
14. Terry, C.; Mitry, R.; Lehec, S. C.; Muiesan, P.; Rela, M.; Heaton, N. D.; Hughes, R. D.; Dhawan, A., The effects of cryopreservation on human hepatocytes obtained from different sources of liver tissue. *Cell Transplantation* **2005,** 14, 585-594.
15. Feng, X.-N.; Xu, X.; Zheng, S.-S., Current status and perspective of liver preservation solutions. *Hepatobiliary & Pancreatic Diseases International* **2006,** 5, (4), 490-494.

16. Meyer, T. P. H.; Hofmann, B.; Zaisserer, J.; Jacobs, V. R.; Fuchs, B.; Rapp, S.; Weinauer, F.; Burkhart, J., Analysis and cryopreservation of hematopoietic stem and progenitor cells from umbilical cord blood. *Cytotherapy* **2006,** 8, 265-276.
17. Li, A. P., Human hepatocytes: isolation, cryopreservation and applications in drug development. *Chemico-Biological Interactions* **2007,** 168, 16-29.
18. Son, J. H.; Kim, K.-H.; Nam, Y.-K.; Park, J.-K.; Kim, S.-K., Optimization of cryoprotectants for cryopreservation of rat hepatocyte. *Biotechnology Letters* **2004,** 26, 829-833.
19. Lloyd, T. D. R.; Orr, S.; Skett, P.; Berry, D. P.; Dennison, A. R., Cryopreservation of hepatocytes: a review of current methods for banking. *Cell and Tissue Banking* **2003,** 4, 3-15.
20. Stephenne, X.; Najimi, M.; Sokal, E. M., Hepatocyte cryopreservation: is it time to change the strategy? *World Journal of Gastroenterology* **2010,** 16, 1-14.
21. Hunt, C. J.; Armitage, S. E.; Pegg, D. E., Cryopreservation of umbilical cord blood: 1. Osmotically inactive volume, hydraulic conductivity and permeability of $CD34^+$ cells to dimethyl sulphoxide. *Cryobiology* **2003,** 46, 61-75.
22. Tarasov, A. I.; Petrenko, A. Y.; Jones, D. R. E., The osmotic characteristic of human fetal liver-derived hematopoietic stem cell candidates. *Cryobiology* **2004,** 48, 333-340.
23. Woods, E. J.; Pollok, K. E.; Byers, M. A.; Perry, B. C.; Purtteman, J.; Heimfeld, S.; Gao, D., Cord blood stem cell cryopreservation. *Transfusion Medicine and Hemotherapy* **2007,** 34, 276-285.
24. Branch, D. R.; Calderwood, S.; Cecuiti, M. A.; Herst, R.; Solh, H., Hematopoietic progenitor cells are resistant to dimethyl sulfoxide toxicity. *Transfusion* **1994,** 34, (10), 887-890.
25. Yang, H.; Zhao, H.; Acker, J. P.; Liu, J. Z.; Akabutu, J.; McGann, L. E., Effect of dimethyl sulfoxide on post-thaw viability assessment of $CD45^+$ and $CD34^+$ cells of umbilical cord blood and mobilized peripheral blood. *Cryobiology* **2005,** 51, 165-175.
26. Laroche, V.; McKenna, D. H.; Moroff, G.; Schierman, T.; Kadidlo, D.; McCullough, J., Cell loss and recovery in umbilical cord blood processing: a comparison of postthaw and postwash samples. *Transfusion* **2005,** 45, 1909-1916.
27. Loretz, L. J.; Li, A. P.; Flye, M. W.; Wilson, A. G. E., Optimization of cryopreservation procedures for rat and human hepatocytes. *Xenobiotica* **1989,** 19, (5), 489-498.
28. Diener, B.; Utesch, D.; Beer, N.; Durk, H.; Oesch, F., A method for the cryopreservation of liver parenchymal cells for studies of xenobiotics. *Cryobiology* **1993,** 30, 116-127.
29. Solves, P.; Mirabet, V.; Planelles, D.; Carbonell-Uberos, F.; Roig, R., Influence of volume reduction and cryopreservation methodologies on quality of thawed umbilical cord blood units for transplantation. *Cryobiology* **2008,** 56, 152-158.
30. Rubinstein, P.; Dobrila, L.; Rosenfield, R. E.; Adamson, J. W.; Migliaccio, G.; Migliaccio, A. R.; Taylor, P. E.; Stevens, C. E., Processing and cryopreservation of placental/umbilical cord blood for unrelated bone marrow reconstitution. *Proceedings of the National Academy of Science* **1995,** 92, 10119-10122.
31. Jubert, C.; Wagner, E.; Bizier, S.; Vachon, M.-F.; Duval, M.; Champagne, M. A., Length of cord blood unit cryopreservation does not impact hematopoietic engraftment. *Transfusion* **2008,** 48, 2028-2029.

32. Zhang, X. B.; Li, K.; Yau, K. H.; Tsang, K. S.; Fok, T. F.; Li, C. K.; Lee, S. M.; Yuen, P. M. P., Trehalose ameliorates the cryopreservation of cord blood in a preclinical system and increases the recovery of CFUs, long-term culture-initiating cells, and nonobese diabetic-SCID repopulationg cells. *Transfusion* **2003,** 43, 265-272.
33. Sasnoor, L. M.; Kale, V. P.; Limaye, L. S., Supplementation of conventional freezing medium with a combination of catalase and trehalose results in better protection of surface molecules and functionality of hematopoietic cells. *Journal of Hematotherapy and Stem Cell Research* **2003,** 12, 553-564.
34. Sasnoor, L. M.; Kale, V. P.; Limaye, L. S., A combination of catalase and trehalose as additives to conventional freezing medium results in improved cryoprotection of human hematopoietic cells with reference to in vitro migration and adhesion properties. *Transfusion* **2005,** 45, 622-633.
35. Limaye, L. S.; Kale, V. P., Cryopreservation of human hematopoietic cells with membrane stabilizers and bioantioxidants as additives in the conventional freezing medium. *Journal of Hematotherapy and Stem Cell Research* **2001,** 10, 709-718.
36. Sasnoor, L. M.; Kale, V. P.; Limaye, L. S., Prevention of apoptosis as a possible mechanism behind improved cryoprotection of hematopoietic cells by catalase and trehalose. *Transplantation* **2005,** 80, 1251-1260.
37. Scheinkonig, C.; Kappicht, S.; Kolb, H.-J.; Schleuning, M., Adoption of long-term cultures to evaluate the cryoprotective potential of trehalose for freezing hematopoietic stem cells. *Bone Marrow Transplantation* **2004,** 34, 531-536.
38. Buchanan, S. S.; Gross, S. A.; Acker, J. P.; Toner, M.; Carpenter, J. F.; Pyatt, D. W., Cryopreservation of stem cells using trehalose: evaluation of the method using a human hematopoietic cell line. *Stem Cells and Development* **2004,** 13, 295-305.
39. Buchanan, S. S.; Menze, M. A.; Hand, S. C.; Pyatt, D. W.; Carpenter, J. F., Cryopreservation of human hematopoietic stem and progenitor cells loaded with trehalose: transient premeabilization via the adenosine triphospoate-dependent P2Z receptor channel. *Cell Preservation Technology* **2005,** 3, 212-222.
40. Petrenko, Y. A.; Jones, D. R. E.; Petrenko, A. Y., Cryopreservation of human fetal liver hematopoietic stem/progenitor cells using sucrose as an additive to the cryoprotective medium. *Cryobiology* **2008,** 57, 195-200.
41. Rodrigues, J. P.; Paraguassu-Braga, F. H.; Carvalho, L.; Abdelhay, E.; Bouzas, L. F.; Porto, L. C., Evaluation of trehalose and sucrose as cryoprotectants for hematopoietic stem cells of umbilical cord blood. *Cryobiology* **2008,** 56, 144-151.
42. Terry, C.; Dhawan, A.; Mitry, R. R.; Lehec, S. C.; Hughes, R. D., Preincubation of rat and human hepatocytes with cytoprotectants prior to cryopreservation can improve viability and function upon thawing. *Liver Transplantation* **2005,** 11, 1533-1540.
43. Silva, J. M.; Day, S. H.; Nicoll-Griffith, D. A., Induction of cytochrom-P450 in cryopreserved rat and human hepatocytes. *Chemico-Biological Interactions* **1999,** 121, 49-63.
44. Katenz, E.; Vondran, F. W. R.; Schwartlander, R.; Pless, G.; Gong, X.; Cheng, X.; Neuhaus, P.; Sauer, I. M., Cryopreservation of primary hepatocytes: The benefit of trehalose as an additional cryoprotective agent. *Liver Transplantation* **2007,** 13, 38-45.
45. Sugimachi, K.; Roach, K. L.; Rhoads, D. B.; Tompkins, R. G.; Toner, M., Nonmetabolizable glucose compounds impart cryotolerance to primary rat hepatocytes. *Tissue Engineering* **2006,** 12, (3), 579-588.

46. Miyamoto, Y.; Suzuki, S.; Nomura, K.; Enosawa, S., Improvement of hepatocyte viability after cryopreservation by supplementatino of long-chain oligosaccharide in the freezing medium in rats and humans. *Cell Transplantation* **2006,** 15, (10), 911-919.
47. Fotakis, G.; Timbrell, J. A., In vitro cytotoxicity assays: comparison of LDH, netural red, MTT and protein assay in hepatoma cell lines following exposure to cadmium chloride. *Toxicology Letters* **2006,** 160, 171-177.
48. Edmondson, J. M.; Armstrong, L. S.; Martinez, A. O., A rapid and simple MTT-based spectrophotometric assay for determining drug sensitivity in monolayer cultures. *Methods in Cell Science* **1988,** 11, (1), 15-17.
49. Goodwin, C. J.; Holt, S. J.; Downes, S.; Marshall, N. J., Microculture tetrazolium assays: a comparison between two new tetrazolium salts, XTT and MTS. *Journal of Immunological Methods* **1995,** 179, (1), 95-103.
50. El-Gewely, M. R., Tetrazolium dyes as tools in cell biology. *Biotechnology Annual Review* **2005,** 11, 127-152.
51. Schmidt-Mende, J.; Hellstrom-Lindberg, E.; Joseph, B.; Zhivotovsky, B., Freezing induces artificial cleavage of apoptosis-related proteins in human bone marrow cells. *Journal of Immunological Methods* **2000,** 245, 91-94.
52. Abrahamsen, J. F.; Bakken, A. M.; Bruserud, O.; Gjertsen, B. T., Technical Report. Flow cytometric measurement of apoptosis and necrosis in cryopreserved PBPC concentrates from patients with malignant diseases. *Bone Marrow Transplantation* **2002,** 29, 165-171.
53. Baust, J. M.; Vogel, M. J.; Snyder, K. K.; Buskirk, R. G. v.; Baust, J. G., Activation of mitochondrial-associated apoptosis contributes to cryopreservation failure. *Cell Preservation Technology* **2007,** 5, 155-163.
54. Lu, X.; Proctor, S. J.; Dickinson, A. M., The effect of cryopreservation on umbilical cord blood endothelial progenitor cell differentiation. *Cell Transplantation* **2008,** 17, 1423-1428.
55. Baust, J. M., Molecular mechanisms of cellular demise associated with cryopreservation failure. *Cell Preservation Technology* **2002,** 1, 17-31.
56. Brand, A.; Eichler, H.; Szczepiorkowski, Z. M.; Hess, J. R.; Kekomaki, R.; McKenna, D. H.; Pamphilon, D.; Reems, J.; Sacher, R. A.; Takahashi, T. A.; Watering, L. M. G. v. d., Viability does not necessarily reflect the hematopoietic progenitor cell potency of a cord blood unit: results of an interlaboratory exercise. *Transfusion* **2008,** 48, 546-549.
57. Morera, C.; Villanueva, M. A., Heat treatment and viability assessment by Evans blue in cultured *Symbiodinium kawagutii* cells. *World Journal of Microbiology and Biotechnology* **2009,** 25, 1125-1128.
58. Yoo, K. H.; Lee, S. H.; Kim, H.-J.; Sung, K. W.; Jung, H. L.; Cho, E. J.; Park, H. K.; Kim, H. A.; Koo, H. H., The impact of post-thaw colony-forming units-granulocyte/macrophage on engraftment following unrelated cord blood transplantation in pediatric recipients. *Bone Marrow Transplantation* **2007,** 39, 515-521.
59. Yang, H.; Acker, J. P.; Cabuhat, M.; McGann, L. E., Effects of incubation temperature and time after thawing on viability assessment of peripheral hematopoietic progenitor cells cryopreserved for transplantation. *Bone Marrow Transplantation* **2003,** 32, 1021-1026.
60. Koopman, G.; Reutelingsperger, C. P.; Kuijten, G. A.; Keehnen, R. M.; Pals, S. T.; Oers, M. H. v., Annexin V for blood cytometric detection of phosphatidylserine expression on B cells undergoing apoptosis. *Blood* **1994,** 84, 1415-1420.

61. Vermes, I.; Haanen, C.; Steffens-Nakken, H.; Reutelingsperger, C., A novel assay for apoptosis. Flow cytometric detection of phosphatidylserine expression on early apoptotic cells using fluorescein labelled Annexin V. *Journal of Immunological Methods* **1995,** 184, 39-51.
62. Engeland, M. v.; Nieland, L. J. W.; Ramaekers, F. C. S.; Schutte, B.; Reutelingsperger, C. P. M., Annexin V-affinity assay: a review on an apoptosis detection system based on phosphatidylserine exposure. *Cytometry* **1998,** 31, 1-9.
63. Vermes, I.; Haanen, C.; Reutelingsperger, C., Flow cytometry of apoptotic cell death. *Journal of Immunological Methods* **2000,** 243, 167-190.
64. Xiao, M.; Dooley, D. C., Assessment of cell viability and apoptosis in human umbilical cord blood following storage. *Journal of Hematotherapy and Stem Cell Research* **2003,** 12, 115-122.
65. George, T. C.; Basiji, D. A.; Hall, B. E.; Lynch, D. H.; Ortyn, W. E.; Perry, D. J.; Seo, M. J.; Zimmerman, C. A.; Morriessey, P. J., Distinguishing modes of cell death using the ImageStream (R) Multispectral Imaging Flow Cytometer. *Cytometry Part A* **2004,** 59A, 237-245.
66. Tait, J. F., Imaging of Apoptosis. *The Journal of Nuclear Medicine* **2008,** 49, 1573-1576.
67. Belloc, F.; Belaud-Rotureau, M. A.; Lavignolle, V.; Bascans, E.; Braz-Pereira, E.; Durrieu, F.; Lacombe, F., Flow cytometry detection of caspase 3 activation in preapoptotic leukemic cells. *Cytometry* **2000,** 40, 151-160.
68. Span, L. F. R.; Pennings, A. H. M.; Vierwinden, G.; al., e., The dynamic process of apoptosis analyzed by flow cytometry using Annexin-V/propidium iodide and a modified in situ end labeling technique. *Cytometry* **2002,** 47, 24-31.
69. Hammill, A. K.; Uhr, J. W.; Scheuermann, R. H., Annexin V staining due to loss of membrane asymmetry can be reversible and precede commitment to apoptotic death. *Experimental Cell Research* **1999,** 251, 16-21.
70. Laumonier, C.; Segers, J.; Laurent, S.; Michel, A.; Coppee, F.; Belayew, A.; Elst, L. V.; Muller, R. N., A new peptidic vector for molecular imaging of apoptosis, identified by phage display technology. *Journal of Biomolecular Screening* **2006,** 11, 537-545.
71. Shynkar, V. V.; S., A.; Klymchenko; Kunzelmann, C.; Duportail, G.; Muller, C. D.; Demchenko, A. P.; Freyssinet, J.-M.; Mely, Y., Fluorescent biomembranes probe for ratiometric detection of apoptosis. *Journal of the American Chemical Society* **2007,** 129, 2187-2193.
72. Sartor, M.; Antonenas, V.; Garvin, F.; Webb, M.; Bradstock, K. F., Recovery of viable $CD34^+$ cells from cryopreserved hemopoietic progenitor cell products. *Bone Marrow Transplantation* **2005,** 36, 199-204.
73. Heimfeld, S., HLA-identical stem cell transplantation: is there an optimal CD34 cell dose? *Bone Marrow Transplantation* **2003,** 31, 839-845.
74. Zubair, A. C.; Kao, G.; Daley, H.; Schott, D.; Freedman, A.; Ritz, J., $CD34^+$ CD38- and $CD34^+$ HLA-DR- cells in BM stem cell grafts correlate with short-term engraftment but have no influence on long-term hematopoietic reconstitution after autologous transplantation. *Cytotherapy* **2006,** 8, 399-407.
75. Rowley, S. D.; Feng, Z.; Yadock, D.; Holmberg, L.; MacLeod, B.; Heimfeld, S., Post-thaw removal of DMSO does not completely abrogate infusional toxicity of the need for pre-infusion histamine blockade. *Cytotherapy* **1999,** 1, 439-446.

76. Nasr, M. B.; Jenhani, F., A contribution to a study of apoptosis of hematopoietic stem cells $CD34^+$ by flow cytometry before and after cryopreservation. *Transfusion Clinique et Biologique* **2008,** 15, 91-97.
77. Shim, J.-S.; Cho, B.; Kim, M.; Park, G.-S.; Shin, J.-C.; Hwang, H.-K.; Kim, T.-G.; Oh, I.-H., Early apoptosis in $CD34^+$ cells as potential heterogeneity in quality of cryopreserved umbilical cord blood. *British Journal of Haematology* **2006,** 135, 210-213.
78. Carruthers, A., Facilitated diffusion of glucose. *Physiological Reviews* **1990,** 70, (4), 1135-1176.
79. Barros, L. F., Measurement of sugar transport in single living cells. *European Journal of Physiology.* **1999,** 437, 763-770.
80. Oliver, A. E.; Jamil, K.; Crowe, J. H.; Tablin, F., Loading human mesenchymal stem cells with trehalose by fluid-phase endocytosis. *Cell Preservation Technology* **2004,** 2, 35-49.
81. Morgan, M. J.; Faik, P., Carbohydrate metabolism in cultured animal cells. *Bioscience reports* **1981,** 1, 669-686.
82. Burns, R. L.; Rosenberger, P. G.; Klebe, R. J., Carbohydrate preferences of mammalian cells. *Journal of Cellular Physiology* **1976,** 88, 307-316.
83. Faik, P.; Morgan, M. J., A method for the isolation of chinese hamster cell variants with an altered ability to utilise carbohydrates. *Cell Biology International Reports* **1977,** 1, (6), 555-562.
84. Corasanti, J. G.; Gleeson, D.; Boyer, J. L., Effects of osmotic stresses on isolated rat hepatocytes I. Ionic mechanisms of cell volume regulation. *American Journal of Physiology: Gastrointestinal and Liver Physiology* **1990,** 258, G290-G298.
85. Schliess, F.; Haussinger, D., The cellular hydration state: a critical determinant for cell death and survival. *Biological Chemistry* **2002,** 383, 577-583.
86. Storey, K. B.; Storey, J. M., Natural freezing survival in animals. *Annual Review of Ecology and Systematics* **1996,** 27, 365-386.
87. Ji, L.; Pablo, J. J. d.; Palecek, S. P., Cryopreservation of adherent human embryonic stem cells. *Biotechnology and Bioengineering* **2004,** 88, 299-312.
88. Liu, S.; Wang, W.; von Moos, E.; Jackman, J.; Mealing, G.; Monette, R.; Ben, R. N., *In vitro* studies of antifreeze glycoprotein (AFGP) and a *C*-linked AFGP analogue. *Biomacromolecules* **2007,** 8, 1456-1462.
89. Stoorvogel, W.; Oorschot, V.; Neve, B., A novel method for measuring protein expression at the cell surface. *Journal of Cell Science* **1993,** 106, 1201-1209.
90. Avery, S. V.; Lloyd, D.; Harwood, J. L., Temperature-dependent changes in plasma-membrane lipid order and the phagocytotic activity of the amoeba *Acanthamoeba castellanii* are closely correlated. *Biochemistry Journal* **1995,** 312, 811-816.
91. Mamdouh, Z.; Giocondi, M.-C.; Laprade, R.; Grimellec, C. L., Temperature dependence of endocytosis in renal epithelial cells in culture. *Biochimica et Biophysica Acta* **1996,** 1282, 171-173.
92. Kelm, S.; Schauer, R., The galactose-recognizing system of rat peritoneal macrophages; identification and characterization of the receptor molecule. *Hoppe-Seyler's Physiological Chemistry* **1988,** 369, 693-704.
93. Kouyoumdjian, M.; Borges, D. R.; Prado, E. S.; Prado, J. L., Identification of receptors in the liver that mediate endocytosis of circulating tissue kallikreins. *Biochimica et Biophysica Acta* **1989,** 980, 299-304.

94. Stoorvogel, W.; Geuze, H. J.; Griffith, J. M.; Schwartz, A. L.; Strous, G. J., Relations between the intracellular pathways of the receptors for transferrin, asialoglycoprotein, and mannose 6-phosphate in human hepatoma cells. *Journal of Cell Biology* **1989,** 108, 2137-2148.
95. Storey, K. B., Organ-specific metabolism during freezing and thawing in a freeze-tolerant frog. *American Journal of Physiology: Regulatory, Integrative and Comparative Physiology* **1987,** 253, 292-297.
96. Kuleshova, L. L.; Gouk, S. S.; Hutmacher, D. W., Vitrification as a prospect for cryopreservation of tissue-engineered constructs. *Biomaterials* **2007,** 28, 1585-1596.
97. Anchordoguy, T. J.; Rudolph, A. S.; Carpenter, J. F.; Crowe, J. H., Modes of interaction of cryoprotectants with membrane phospholipids during freezing. *Cryobiology* **1987,** 24, 324-331.
98. Anchordoguy, T. J.; Cecchini, C. A.; Crowe, J. H.; Crowe, L. M., Insight into the cryoprotective mechanism of dimethyl sulfoxide for phospolipid bilayers. *Cryobiology* **1991,** 28, 467-473.
99. Strauss, G.; Schurtenberger, P.; Hauser, H., The interaction of saccharides with lipid bilayer vesicles: stabilization during freeze-thawing and freeze-drying. *Biochimica et Biophysica Acta* **1986,** 858, 169-180.
100. Tam, R. Y.; Ferreira, S. S.; Czechura, P.; Chaytor, J. L.; Ben, R. N., Hydration index: a better parameter for explaining small molecule hydration in inhibition of ice recrystallization. *Journal of the American Chemical Society* **2008,** 130, 17494-17501.
101. Chaytor, J. L.; Tokarew, J., In.
102. Fahy, G. M.; A. M. Karow, J., Ultrastructure-function correlative studies for cardiac cryopreservation. V. Absence of a correlation between electrolyte toxicity and cryoinjury in the slowly frozen, cryoprotected rat heart. *Cryobiology* **1977,** 14, 418-427.
103. Steponkus, P. L.; Lynch, D. V., Freeze/thaw-induced destabilization of the plasma membrane and the effects of cold acclimation. *Journal of Bioenergetics and Biomembranes* **1989,** 21, (1), 21-41.
104. Muldrew, K., The salting-in hypothesis of post-hypertonic lysis. *Cryobiology* **2008,** 57, 251-256.
105. Mazur, P., Freezing of living cells: mechanisms and implications. *American Journal of Physiology: Cell Physiology* **1984,** 247, C125-C142.
106. Steponkus, P. L.; Dowgert, M. F.; Gordon-Kamm, W. J., Destabilization of the plasma membrane of isolated plant protoplasts during a freeze-thaw cycle: the influence of cold acclimation. *Cryobiology* **1983,** 20, 448-465.
107. Karlsson, J. O. M.; Toner, M., Long-term storage of tissues by cryopreservation: critical issues. *Biomaterials* **1996,** 17, 243-256.
108. Pegg, D. E.; Diaper, M. P.; Skaer, H. L.; Hunt, C. J., The effect of cooling rate and warming rate on the packing effect in human erythrocytes frozen and thawed in the presence of 2 M glycerol. *Cryobiology* **1984,** 21, 491-502.
109. Fowler, A. J.; Toner, M., Prevention of Hemolysis in Rapidly Frozen Erythrocytes by Using a Laser Pulse. *Annals of the New York Academy of Science* **1998,** 858, 245-252.
110. Fowler, A. J.; Toner, M., Cryo-injury and biopreservation. *Annals of the New York Academy of Science* **2005,** 1066, 119-135.

Chapter 5: Conclusions

The goals of this work were first, to manipulate the hydrophobicity and hydration of antifreeze glycoprotein (AFGP) 8 analogues in order to elucidate the effect of each on antifreeze activity - both thermal hysteresis (TH) and recrystallization inhibition (RI) activity - and secondly, to explore the cryopreservation ability of both an AFGP 8 analogue and simple carbohydrates, and relate the outcomes to RI activity.

5.1 Goal 1: Design of New C-Linked AFGP 8 Analogues

The first goal of this work was to modify the physical properties of selected AFGP 8 analogues in an attempt to tailor antifreeze activity. Specifically, modifications that affected the hydrophobicity and hydration characteristics of these AFGP analogues and the subsequent effect on TH and RI activity were examined. Two series of analogues were to be synthesized.

Objective 1.1: Investigating the Importance of Hydrophobicity of C-Linked AFGP 8 Analogues to Recrystallization Inhibition (RI) Activity (Series I Analogues)

In order to try to gain a better understanding of the involvement of hydrophobic effects in RI, we designed a new series of AFGP analogues that possessed a variety of hydrophobic groups in the pseudo-anomeric position. We hypothesized that the introduction of the hydrophobic elements (R groups) to the ornithine analogue would lead to an increase in RI activity over that of the original ornithine analogue. We expected that the RI activity would increase with increased hydrophobicity of the R group.

We attempted to use a variation on methodology using a thiazolidine thione chiral auxiliary developed by Urpi and co-workers. The methodology should have allowed us to

simultaneously install the desired R group at the pseudo-anomeric position and determine the orientation about the anomeric centre. Unfortunately, we were unable to synthesize the series I analogues.

Objective 1.2: Investigating the Importance of Hydrophobicity of C-Linked AFGP 8 Analogues to Recrystallization Inhibition (RI) Activity (Series II Analogues)

With this second series of analogues, we were primarily interested in manipulating the *hydration* of the polymers: the carbohydrates of the Series II analogues are dehydroxylated at C2 and C3. The absence of the hydroxyl group at C2 could mean that this series of analogues will have greater hydration - that is, a worse "fit" into the three-dimensional hydrogen-bonded network of water - than the original ornithine analogue, and we hypothesized that this modification would increase RI activity.

We initially intended to synthesize only those Series II analogues where R = H or R = Me; however, since Series I analogues were not available, we expanded our synthesis to include a number of different hydrophobic groups. The key intermediates in the Series II analogues were available using the methodology developed by Urpi and co-workers, and the desired R group was easily installed at the pseudo-anomeric position using a thiazolidine thione chiral auxiliary. Unfortunately, the polymer building blocks bearing R groups other than H could not be adequately purified for peptide synthesis; however, the unsubstituted building blocks were readily available and provided their respective polymers via solid-phase peptide synthesis.

In the meantime, our lab showed that deprotected building blocks, as well as *C*-linked carboxylic acid carbohydrate derivatives could be tested for RI activity. This conclusion provided us with a means to test compounds bearing the R groups we had hoped to install on the polymers. Four deprotected building blocks, as well as a series of *C*-linked carboxylic acid galactal derivatives bearing a variety of hydrophobic groups were successfully synthesized and tested for antifreeze activity.

5.1.1 Antifreeze Activity Testing: Thermal Hysteresis (TH) and Recrystallization Inhibition (RI)

All of the newly synthesized compounds (shown in Chapter 3, Figure 3.1) were tested for both TH and RI activity. None of the compounds tested showed any TH activity, although both polymers showed evidence of dynamic ice shaping (DIS). Since TH activity is not desirable for cryopreservation, the absence of TH activity in any of the compounds was encouraging. RI activity, on the other hand, was observed for all compounds; however, all compounds showed poorer RI activity that either galactose or the ornithine analogue.

Of the *C*-linked carboxylic acid galactal derivatives, those derivatives bearing aromatic R groups all presented RI activity equivalent to that of the α-*C*-linked carboxylic acid galactose derivative. Based on the RI activity of analogues previously studied in our lab, the RI activity of the α-anomers was expected to be greater than that of their respective β-anomers. This was found to be true for both R = H, and R = Me, and in fact, the β-anomers did not show any RI activity. We speculated that the newly synthesized *C*-linked carboxylic acid galactal derivatives may be positioned differently at the ice-water interface than either α-*C*-linked carboxylic acid galactose or 2-deoxygalactose, and importantly, we concluded that that increasing the hydrophobicity of *C*-linked carbohydrate derivatives does not *necessarily* improve RI activity.

The RI activity of the building blocks varied significantly among the four compounds tested, and was much poorer than that of any of AFGP 8, the ornithine analogue, or galactose. With one exception, the building blocks were more active than PBS, and the RI activity of the α-anomers was significantly greater than that of the β-anomers. The absence or presence of a double bond in the carbohydrate moiety is the only difference among the building blocks and the results showed that the presence of the double bond did in fact reduce RI activity compared to the saturated building block. The double bond likely changed the orientation of the hydroxyl groups, and this conformational change was therefore the likely cause of the difference in RI activity, although the orientation of the anomeric side-chain may have played a role as well.

The best RI activity was seen with the α-*C*-linked polymer, and as expected the α-anomer had better activity than its β-*C*-linked counterpart. As discussed, this was true for all sets of α- and β-linked compounds tested. In fact, the difference in RI between α- and β-anomers was similar for each of the three types of compounds (polymer, building block, or carbohydrate derivative).

When the data for the newly synthesized polymers and the corresponding building blocks and *C*-linked carboxylic acid galactal derivatives were compared to the ornithine analogue and its corresponding components, it was clear that the trend in RI activity among the three components was not always the same; therefore the RI of one component cannot be used to predict the RI activity of another. With this data set, no general conclusions could be derived regarding the trend among the three components.

Lastly, it was found that the RI activity of the α-linked polymer was equivalent to that of the ornithine analogue in which galactose has been substituted with glucose. Since the nature of the carbohydrate moiety was the only difference between the two polymers, it appeared that the carbohydrate moiety of the newly synthesized analogue is equivalent to that of glucose in terms of its contribution to the RI activity of the polymer. This result reinforced previous conclusions that a non-axial hydroxyl group at C2 (even *no* hydroxyl group as was the case with the analogue) improves RI activity. Therefore, an analogue based on the new α-linked polymer that also incorporates a hydrophobic group, perhaps on the carbohydrate, may indeed prove to be a potent RI inhibitor.

5.2 Goal 2: Investigating the Cryopreservation Potential of the Ornithine Analogue and Several Carbohydrates in Vitro

Objective 2.1 Assessing the Cryopreservation Activity of Carbohydrates

Based on the extensive work done by our lab on the effect of hydration of carbohydrates on RI, we investigated the cryopreservation potential of several carbohydrates,

representing a spectrum of RI activity. We tested the monosaccharides (galactose, glucose, 3-*O*-methylglucose, and talose) and four disaccharides (melibiose, lactose, trehalose, and sucrose) for cryopreservation activity with the human embryonic liver cell line WRL 68 and umbilical cord blood (UCB) cells. Post-cryopreservation analysis using the annexin V/7AAD flow cytometry assay with allowed the delineation of the viable, early apoptotic, and late apoptotic/necrotic cell populations.

First, the cytotoxicity to WRL 68 cells of the carbohydrates at 22, 200, and 500 mM, and DMSO at 2.5%, 5%, 10%, and 20%, was determined using the MTT assay. Both monosaccharides, and disaccharides were found to be slightly cytotoxic to cells at 22 mM and 200 mM. For the monosaccharides, the difference in cell viability between the 200 mM and 500 mM concentrations was minimal. However, 500 mM solutions of disaccharide resulted in significant loss of cell viability: on average only 20% of cells were viable after incubation with 500 mM carbohydrate. Since none of the carbohydrates are known to be cytotoxic, we attributed this difference in viability to the difference in permeability of cells to monosaccharides versus disaccharides. High concentrations of impermeable cryoprotectants such as disaccharides cause cells to undergo extreme osmotic excursions that can lead to cell death. The cytotoxicity of DMSO also increased with increasing concentration; while 2.5% DMSO reduced cell viability by about 20% compared to the control, at 20% DMSO, fewer than 50% of cells were viable. Since DMSO is known to be toxic, and given the long incubation time, the increasing cytotoxicity seen with increasing concentration was not surprising.

The cryopreservation trials with WRL 68 cells were carried out with carbohydrates at concentrations of 22, 200, and 500 mM, without DMSO or combined with 2.5% or 5% DMSO. Three intermediate concentrations of carbohydrates combined with DMSO were also assayed. Correlation graphs revealed a negative relationship between viable and late apoptotic cells. While there are likely two different relationships, their slopes are similar, and we concluded that, for the purposes of the presentation of the data for this study, an increase in the percentage of viable cells leads to a decrease in the percentage of late apoptotic/necrotic cells. No conclusions could be drawn regarding the relationship between the viable and early apoptotic cell populations.

From the trials with DMSO alone, we concluded that 5% was an appropriate concentration of DMSO to combine with the different concentrations of carbohydrates employed. When carbohydrates were used as the sole cryoprotectant, a concentration of 22 mM was insufficient to protect cells. With the exception of galactose, the monosaccharides were poor cryoprotective agents at 200 mM, while the disaccharides protected almost 30% more cells at 200 mM than at 22 mM. With the exception of galactose and glucose, cell viability after cryopreservation was poorer at 500 mM than at 200 mM. Notably, no concentrations of carbohydrate alone were as protective as 5% DMSO.

This study showed that low concentrations of carbohydrates can be used for successful cryopreservation, particularly when combined with DMSO. It was found that the addition of galactose, talose, melibiose, or trehalose to the cryopreservation medium allowed the amount of DMSO to be reduced from 5% to 2.5% without compromising cell viability. Further, ten combinations were found to be superior cryoprotectants than 5% DMSO used alone. The ten combinations included only four carbohydrates – galactose, melibiose, trehalose, and sucrose – were represented and only one carbohydrate, melibiose at 22 mM, was used with 2.5% DMSO, rather than 5% DMSO. In general, it was found that there was little difference in cryopreservation outcome among the intermediate concentrations of carbohydrates employed. We concluded that, in the presence of DMSO, the *type* of carbohydrate was more important that its *concentration* for a successful cryopreservation outcome, and further, carbohydrates are most effective when employed as extracellular cryoprotectants. While the cryopreservation ability of carbohydrates can be attributed to their colligative properties and the ability of some carbohydrates to stabilize the cell membrane, we found that the cryopreservation activity of carbohydrates correlated well with their RI activity. Carbohydrates with good RI activity may therefore be able to effectively manage the ice formed during cryopreservation. This was a significant finding and merits further exploration.

The umbilical cord blood (UCB) mononuclear cells (MNCs) and hematopoietic stem cells (CD34+ cells) were more sensitive to cryopreservation than the WRL 68 cells. The relationship between the cell populations (viable, early apoptotic, late apoptotic/necrotic

cells) of MNCs and CD34+ cells after cryopreservation was complex, and no clear correlations were found. Since it has been reported that 5% DMSO and 10% DMSO solutions are equally effective as cryopreservation agents we were surprised that in our trials, 10% DMSO protected more cells through cryopreservation than 5% DMSO.

Carbohydrates used alone were generally significantly poorer cryoprotectants than 5% DMSO alone, with the exception of galactose, which, at 500 mM was as good as 5% DMSO alone. However, when glucose, 3-*O*-methylglucose, or trehalose, were used as the sole cryoprotectant, cell viability was *poorer* than in the absence of any cryoprotectant. Interestingly, the general trends seen with the UCB trials were quite different from those seen with the WRL 68 cells. Most strikingly, when carbohydrates were used alone, cell viability was highest at 500 mM. When 5% DMSO was added to the carbohydrates this trend was reversed and lower concentrations of carbohydrates were more successful than higher concentrations. No combination of carbohydrate and DMSO proved to be a better cryoprotectant than 5% used alone. Interestingly, as was found for the WRL 68 cells, galactose, melibiose, trehalose, and sucrose were superior cryoprotectants compared to the other carbohydrates tested. Since cells are impermeable to disaccharides, and given the trend in increasing cell survival with increasing carbohydrate concentration, it may be that high concentrations of extracellular cryoprotectant are beneficial for the cryopreservation of UCB cells.

The relationship between RI and cryopreservation potential was less clear for UCB cells. While there may be some correlation between cryopreservation activity and RI, the correlation was not as strong as that found in the WRL 68 study. Part of the difficulty in ascertaining whether or not a correlation exists lies with the difficulty of reproducibility in the UCB study. As discussed previously, the fact that the UCB cells are primary cells has the biggest negative impact on the reproducibility of our results; the samples will vary due to the heterogeneity in the human population, and further, primary cells are less hardy than a cell line. In order to improve reproducibility, more trials for each treatment should be carried out. Unfortunately, in this study, our access to UCB cells was limited.

In conclusion, with WRL 68 cells, we have shown that it is possible to improve the cryopreservation potential of a 5% DMSO solution by the addition of low concentrations of carbohydrates, and further, that the addition of low concentration of carbohydrates can allow the concentration of DMSO in the cryopreservation medium to be reduced without adversely affecting the cryopreservation outcome. With UCB cells, we have shown that galactose can be substituted for 5% DMSO without decreasing cell viability after cryopreservation. This study confirms previous reports that carbohydrates can be successfully used as cryoprotectants. Since carbohydrates allow the amount of DMSO to be reduced, their used in cryopreservation protocols should reduce the risks associated with transplanting samples cryopreserved with high concentrations of DMSO. Further, to the best of our knowledge, a relationship between cryopreservation and recrystallization activity has not been previously explored and this relationship merits further investigation, and may prove to be both a valuable tool for the design of novel cryopreservation agents or novel combinations of cryopreservation agents.

Objective 2.2: Assessing the Cryopreservation Activity of the Ornithine Analogue

The preliminary cryopreservation data obtained with AFGP 8 and particularly, with the ornithine analogue, were encouraging. At the concentration tested, AFGP 8 was a poor cryoprotectant unless it was combined with 10% DMSO. The ornithine analogue, at only 1 mg/mL, was as effective as 2.5% DMSO alone. Interestingly, higher concentrations of the ornithine analogue were less effective. Based on cytotoxicity data obtained prior to this study, we proposed that the ornithine analogue may have apoptosis inhibition activity. We concluded that the ornithine analogue shows significant potential as a cryoprotectant, and optimization studies of the ornithine analogue at a variety of concentrations centered on 1 mg/mL should be carried out in an attempt to determine the optimal concentration for cryopreservation.

5.3 Future Directions

5.3.1 Analogue Synthesis and Recrystallization Inhibition (RI)

It is of interest to append aromatic groups to the pseudo-anomeric position *C*-linked carboxylic acid galactose derivatives, rather than to the galactal analogues as was done in this study, in order to study the influence of the additional groups in isolation. Using a different synthetic route should allow for the incorporation of hydrophobic groups at another location on the polymer or building block as well. The preliminary results presented here suggest that this would be an important series of analogues to consider.

We found that the RI activity of the AFGP 8 analogues (peptides) could not be correlated to that of their component building block or *C*-linked carboxylic acid carbohydrate derivatives. It may be possible, however, to discern a trend if a larger sample set is employed, and this would be an important avenue to explore.

5.3.2 Cryopreservation Studies with WRL 68 cells and Umbilical Cord Blood (UCB)

Cytotoxicity studies were carried out with long incubation times in order to assess the cytotoxicity potential of each cryoprotectant. As a compliment to the cytotoxicity assays carried out in this study, future work should include MTT assays with shorter incubation times, in order for the assays to be more representative of cryopreservation conditions.

From the cryopreservation studies employing combinations of carbohydrates and DMSO, the discovery of multiple relationships between the cell populations was interesting, and it would be valuable to probe a larger data set in order to elucidate the nature of the different relationships, and determine the common attributes of the cryoprotectants responsible for each. Such a study would almost certainly be enlightening.

While AFGP 8 showed poor cryopreservation potential, preliminary cryopreservation data obtained for the ornithine analogue at 1 mg/mL was encouraging, and optimization

studies should be carried out to improve the cryopreservation outcomes. The serine analogue previously synthesized in our lab seemed to inhibit caspase 3/7 activation, and it should be determined whether or not the ornithine analogue possesses this activity. Conversely, the cryopreservation activity of the serine analogue should be investigated. Pursuing this dual approach of RI activity to manage ic, and apoptosis inhibition to mitigate the effects of stress, both accomplished by *one* cryoprotectant, may provide a superior cryoprotective agent and warrants further study.

The correlation between cryopreservation and RI was a significant finding. Further work to explore this correlation and determine whether or not it can be used predictively should be carried out. Work should include cryopreservation and RI testing of additional carbohydrates, and particularly for the UCB data, the reproducibility of the results must be addressed.

This study only addressed the use of single carbohydrates with and without DMSO in the cryopreservation medium. Since the carbohydrates possess different physical properties, perhaps the combination of different carbohydrates would improve cryopreservation outcomes. For example, disaccharides have been used to enhance the effect of permeating cryoprotectants, and therefore it would be interesting to investigate the effect of combinations of disaccharides and monosaccharides in cryopreservation solutions.

It is hoped that the conclusions derived from this study will continue to be considered and will inform future studies.

Chapter 6: Experimental

Table of Contents

6.1 General Experimental.....215

6.2 Compound Preparation Procedures and Experimental Data.....216
(S)-4-(((9H-fluoren-9-yl)methoxy)carbonylamino)-5-(benzyloxy)-5-oxopentan-1-aminium 2,2,2-trifluoroacetate (37): 219
General procedure A. Preparation of (S)- and (R)-thiazolidinone chiral auxiliaries (38 and 43):[3] 219
(S)-1-(4-benzyl-2-thioxothiazolidin-3-yl)ethanone (38a) and (R)-1-(4-benzyl-2-thioxothiazolidin-3-yl)ethanone (43a): 220
(S)-1-(4-benzyl-2-thioxothiazolidin-3-yl)propan-1-one (38b) and (S)-1-(4-benzyl-2-thioxothiazolidin-3-yl)propan-1-one (43b): 221
(S)-1-(4-benzyl-2-thioxothiazolidin-3-yl)butan-1-one (38c): 221
(S)-1-(4-benzyl-2-thioxothiazolidin-3-yl)-2-methylpropan-1-one (38d): 222
(S)-1-(4-benzyl-2-thioxothiazolidin-3-yl)-2-phenylethanone (38e): 223
(S)-1-(4-benzyl-2-thioxothiazolidin-3-yl)-3-phenylpropan-1-one (38f): 223
(S)-1-(4-benzyl-2-thioxothiazolidin-3-yl)-2-(4-methoxyphenyl)ethanone (38g): 224
(S)-1-(4-benzyl-2-thioxothiazolidin-3-yl)-2-(4-bromophenyl)ethanone (38h): 225
(S)-1-(4-benzyl-2-thioxothiazolidin-3-yl)-2-(4-nitrophenyl)ethanone (38i): 225
(S)-1-(4-benzyl-2-thioxothiazolidin-3-yl)octan-1-one (38j): 226
(2R,3R)-2-(acetoxymethyl)-3,4-dihydro-2H-pyran-3,4-diyl diacetate (44):[4] 227
(S)-2-Aamino-3-phenylpropan-1-ol (57) and (R)-2-Amino-3-phenylpropan-1-ol (62):[5] 227
(S)-4-benzylthiazolidine-2-thione (58) and (S)-4-benzylthiazolidine-2-thione (63):[6] 228
2-(4-methoxyphenyl)acetyl chloride (65): 229
2-(4-nitrophenyl)acetyl chloride (67): 229
2-(4-bromophenyl)acetyl chloride (69): 230
(2R,3S,4S,5S,6S)-2-(acetoxymethyl)-6-(phenylthio)tetrahydro-2H-pyran-3,4,5-triyl triacetate (72):[7] 230
(2R,3R,4S,5R,6S)-2-(hydroxymethyl)-6-(phenylthio)tetrahydro-2H-pyran-3,4,5-triol (73):[7] 231
(2R,3S,4S,5R,6S)-3,4,5-tris(benzyloxy)-2-(benzyloxymethyl)-6-(phenylthio)tetrahydro-2H-pyran (74):[8] 231
(3S,4S,5S)-3,4,5-tris(benzyloxy)-6-(benzyloxymethyl)tetrahydro-2H-pyran-2-ol (75):[9] 232
(2S,3S,4S,5S,6R)-3,4,5-tris(benzyloxy)-6-(benzyloxymethyl)tetrahydro-2H-pyran-2-yl 2,2,2-trichloroacetimidate (76):[10] 232
(2R,3S,4S,5R,6R)-2-(acetoxymethyl)-6-bromotetrahydro-2H-pyran-3,4,5-triyl triacetate (81):[11] 233
(3R,4S,5S)-3,4,5-tris(benzyloxy)-6-(benzyloxymethyl)tetrahydro-2H-pyran-2-yl acetate (82):[13] 234

(2R,3S,4S,5R,6R)-3,4,5-tris(benzyloxy)-2-(benzyloxymethyl)-6-methoxytetrahydro-2H-pyran (84) and (2R,3S,4S,5R,6S)-3,4,5-tris(benzyloxy)-2-(benzyloxymethyl)-6-methoxytetrahydro-2H-pyran (85): 234
(2R)-1-((S)-4-benzyl-2-thioxothiazolidin-3-yl)-3-hydroxy-2-methyl-5-phenylpentan-1-one (87):[14] 235
(S)-3-allyl-4-benzylthiazolidine-2-thione (89): 236
General procedure B. Preparation of substituted coupling products (90 and 91):[3] 237
((2R,3R,6R)-3-acetoxy-6-(2-((S)-4-benzyl-2-thioxothiazolidin-3-yl)-2-oxoethyl)-3,6-dihydro-2H-pyran-2-yl)methyl acetate (90a): 238
((2R,3R,6S)-3-acetoxy-6-((R)-1-((S)-4-benzyl-2-thioxothiazolidin-3-yl)-1-oxopropan-2-yl)-3,6-dihydro-2H-pyran-2-yl)methyl acetate (90b): 239
((2R,3R,6S)-3-acetoxy-6-((R)-1-((S)-4-benzyl-2-thioxothiazolidin-3-yl)-3-methyl-1-oxobutan-2-yl)-3,6-dihydro-2H-pyran-2-yl)methyl acetate (90d): 239
((2R,3R,6S)-3-acetoxy-6-((R)-2-((S)-4-benzyl-2-thioxothiazolidin-3-yl)-2-oxo-1-phenylethyl)-3,6-dihydro-2H-pyran-2-yl)methyl acetate (90e): 240
((2R,3R,6S)-3-acetoxy-6-((R)-1-((S)-4-benzyl-2-thioxothiazolidin-3-yl)-1-oxo-3-phenylpropan-2-yl)-3,6-dihydro-2H-pyran-2-yl)methyl acetate (90f): 241
((2R,3R,6S)-3-acetoxy-6-((R)-2-((S)-4-benzyl-2-thioxothiazolidin-3-yl)-1-(4-methoxyphenyl)-2-oxoethyl)-3,6-dihydro-2H-pyran-2-yl)methyl acetate (90g): 242
((2R,3R,6S)-3-acetoxy-6-((R)-1-((S)-4-benzyl-2-thioxothiazolidin-3-yl)-1-oxooctan-2-yl)-3,6-dihydro-2H-pyran-2-yl)methyl acetate (90j): 243
((2R,3R,6S)-3-acetoxy-6-(2-((R)-4-benzyl-2-thioxothiazolidin-3-yl)-2-oxoethyl)-3,6-dihydro-2H-pyran-2-yl)methyl acetate (91a): 244
((2R,3R,6R)-3-acetoxy-6-((S)-1-((R)-4-benzyl-2-thioxothiazolidin-3-yl)-1-oxopropan-2-yl)-3,6-dihydro-2H-pyran-2-yl)methyl acetate (91b): 244
((2R,3R,6S)-3-acetoxy-6-((R)-1-(benzylamino)-1-oxopropan-2-yl)-3,6-dihydro-2H-pyran-2-yl)methyl acetate (102):adapted from Larossa *et al.*[3] 245
(S)-benzyl 1-(9H-fluoren-9-yl)-12,12-dimethyl-3,10-dioxo-2,11-dioxa-4,9-diazatridecane-5-carboxylate (104):[15] 246
(2S)-benzyl 2-(((9H-fluoren-9-yl)methoxy)carbonylamino)-5-(2-((2R,6R)-5-acetoxy-6-(acetoxymethyl)-5,6-dihydro-2H-pyran-2-yl)acetamido)pentanoate (105a): 247
(S)-benzyl 2-(((9H-fluoren-9-yl)methoxy)carbonylamino)-5-((R)-2-((2S,5R,6R)-5-acetoxy-6-(acetoxymethyl)-5,6-dihydro-2H-pyran-2-yl)propanamido)pentanoate (105b): 248
(S)-2-(((9H-fluoren-9-yl)methoxy)carbonylamino)-5-(2-((2S,5R,6R)-5-acetoxy-6-(acetoxymethyl)tetrahydro-2H-pyran-2-yl)acetamido)pentanoic acid (106a): 249
(S)-benzyl 2-(((9H-fluoren-9-yl)methoxy)carbonylamino)-5-(2-((2S,5R,6R)-5-acetoxy-6-(acetoxymethyl)-5,6-dihydro-2H-pyran-2-yl)acetamido)pentanoate (107a): 250
(S)-benzyl 2-(((9H-fluoren-9-yl)methoxy)carbonylamino)-5-((S)-2-((2R,5R,6R)-5-acetoxy-6-(acetoxymethyl)-5,6-dihydro-2H-pyran-2-yl)propanamido)pentanoate (107b): 251
(S)-2-(((9H-fluoren-9-yl)methoxy)carbonylamino)-5-(2-((2R,5R,6R)-5-acetoxy-6-(acetoxymethyl)tetrahydro-2H-pyran-2-yl)acetamido)pentanoic acid (108a): 252
General procedure C. Preparation of alcohol galactal derivatives (109):[3, 16] 253
((2R,3R,6S)-3-acetoxy-6-((S)-1-hydroxypropan-2-yl)-3,6-dihydro-2H-pyran-2-yl)methyl acetate (109b-α): 254

((2R,3R,6R)-3-acetoxy-6-((R)-1-hydroxypropan-2-yl)-3,6-dihydro-2H-pyran-2-yl)methyl acetate (109b-β):.....254
((2R,3R,6S)-3-acetoxy-6-((S)-2-hydroxy-1-phenylethyl)-3,6-dihydro-2H-pyran-2-yl)methyl acetate (109e):.....255
((2R,3R,6S)-3-acetoxy-6-(1-hydroxy-3-phenylpropan-2-yl)-3,6-dihydro-2H-pyran-2-yl)methyl acetate (109f): 256
((2R,3R,6S)-3-acetoxy-6-((S)-2-hydroxy-1-(4-methoxyphenyl)ethyl)-3,6-dihydro-2H-pyran-2-yl)methyl acetate (109g):.....256
((2R,3R)-3-acetoxy-6-(1-oxo-3-phenylpropan-2-yl)-3,6-dihydro-2H-pyran-2-yl)methyl acetate (110f):[17, 18] 257
((2R,3R)-3-acetoxy-6-(1-(4-methoxyphenyl)-2-oxoethyl)-3,6-dihydro-2H-pyran-2-yl)methyl acetate (110g):[19].....258
General procedure D. Preparation of substituted carboxylic acid derivatives – removal of the chiral auxiliary (111 and 120):[20] 259
2-((2R,5R,6R)-5-acetoxy-6-(acetoxymethyl)-5,6-dihydro-2H-pyran-2-yl)acetic acid (111a): 259
(R)-2-((2S,5R,6R)-5-acetoxy-6-(acetoxymethyl)-5,6-dihydro-2H-pyran-2-yl)propanoic acid (111b): 260
(R)-2-((2S,5R,6R)-5-acetoxy-6-(acetoxymethyl)-5,6-dihydro-2H-pyran-2-yl)-2-phenylacetic acid (111e): 260
(R)-2-((2S,5R,6R)-5-acetoxy-6-(acetoxymethyl)-5,6-dihydro-2H-pyran-2-yl)-3-phenylpropanoic acid (111f): 261
(R)-2-((2S,5R,6R)-5-acetoxy-6-(acetoxymethyl)-5,6-dihydro-2H-pyran-2-yl)-2-(4-methoxyphenyl)acetic acid (111g):.....262
((2R,3R,6S)-3-acetoxy-6-(2-(methoxy(methyl)amino)-2-oxoethyl)-3,6-dihydro-2H-pyran-2-yl)methyl acetate (112):[21] 262
(S)-2-(((9H-fluoren-9-yl)methoxy)carbonylamino)-5-(2-((2S,5R,6R)-5-acetoxy-6-(acetoxymethyl)-5,6-dihydro-2H-pyran-2-yl)acetamido)pentanoic acid (115a): 263
((2R,3R,6S)-3-acetoxy-6-((R)-1-(methoxy(methyl)amino)-1-oxopropan-2-yl)-3,6-dihydro-2H-pyran-2-yl)methyl acetate (116):[21] 264
(S)-2-(((9H-fluoren-9-yl)methoxy)carbonylamino)-5-(2-((2R,5R,6R)-5-acetoxy-6-(acetoxymethyl)-5,6-dihydro-2H-pyran-2-yl)acetamido)pentanoic acid (117a): 265
2-((2S,5R,6R)-5-acetoxy-6-(acetoxymethyl)-5,6-dihydro-2H-pyran-2-yl)acetic acid (120a): 266
(S)-2-((2R,5R,6R)-5-acetoxy-6-(acetoxymethyl)-5,6-dihydro-2H-pyran-2-yl)propanoic acid (120b): 266
(S)-2-amino-5-(2-((2R,5R,6R)-5-hydroxy-6-(hydroxymethyl)-5,6-dihydro-2H-pyran-2-yl)acetamido)pentanoic acid (121):.....267
(S)-2-amino-5-(2-((2S,5R,6R)-5-hydroxy-6-(hydroxymethyl)-5,6-dihydro-2H-pyran-2-yl)acetamido)pentanoic acid (122):.....268
(S)-2-amino-5-(2-((2S,5R,6R)-5-hydroxy-6-(hydroxymethyl)tetrahydro-2H-pyran-2-yl)acetamido)pentanoic acid (123):.....269
(S)-2-amino-5-(2-((2R,5R,6R)-5-hydroxy-6-(hydroxymethyl)tetrahydro-2H-pyran-2-yl)acetamido)pentanoic acid (124):.....270
General Procedure D: Preparation of substituted carboxylic acid derivatives – deprotection (125 and 126): 270

2-((2R,5R,6R)-5-hydroxy-6-(hydroxymethyl)-5,6-dihydro-2H-pyran-2-yl)acetic acid (125a): 271
(R)-2-((2S,5R,6R)-5-hydroxy-6-(hydroxymethyl)-5,6-dihydro-2H-pyran-2-yl)propanoic acid (125b): 272
(R)-2-((2S,5R,6R)-5-hydroxy-6-(hydroxymethyl)-5,6-dihydro-2H-pyran-2-yl)-2-phenylacetic acid (125e): 272
(R)-2-((2S,5R,6R)-5-hydroxy-6-(hydroxymethyl)-5,6-dihydro-2H-pyran-2-yl)-3-phenylpropanoic acid (125f): 273
(R)-2-((2S,5R,6R)-5-hydroxy-6-(hydroxymethyl)-5,6-dihydro-2H-pyran-2-yl)-2-(4-methoxyphenyl)acetic acid (125g): 274
2-((2S,5R,6R)-5-hydroxy-6-(hydroxymethyl)-5,6-dihydro-2H-pyran-2-yl)acetic acid (126a): 274
(S)-2-((2R,5R,6R)-5-hydroxy-6-(hydroxymethyl)-5,6-dihydro-2H-pyran-2-yl)propanoic acid (126b): 275
(2R,3S,4R,5S)-2-(acetoxymethyl)-6-allyltetrahydro-2H-pyran-3,4,5-triyl triacetate (127):[22] 275
(2R,3R,4R,5R,6R)-2-allyl-6-(hydroxymethyl)tetrahydro-2H-pyran-3,4,5-triol (129):[22] 276
(2R,3S,4R,5S,6R)-2-(acetoxymethyl)-6-allyltetrahydro-2H-pyran-3,4,5-triyl triacetate (130): 277
(2R,4S,5S,6R)-2-(acetoxymethyl)-6-(2-oxoethyl)tetrahydro-2H-pyran-3,4,5-triyl triacetate (131):[11] 277
2-((2R,3S,4R,5S,6R)-3,4,5-triacetoxy-6-(acetoxymethyl)tetrahydro-2H-pyran-2-yl)acetic acid (132):[11] 278
(2R,3S,4R,5S,6R)-2-(2-((S)-4-(((9H-fluoren-9-yl)methoxy)carbonylamino)-5-(benzyloxy)-5-oxopentylamino)-2-oxoethyl)-6-(acetoxymethyl)tetrahydro-2H-pyran-3,4,5-triyl triacetate (133):[11] 279
(S)-2-(((9H-fluoren-9-yl)methoxy)carbonylamino)-5-(2-((2R,3S,4R,5S,6R)-3,4,5-triacetoxy-6-(acetoxymethyl)tetrahydro-2H-pyran-2-yl)acetamido)pentanoic acid (134):[11] 280

6.3 Procedures for Assessing Antifreeze Activity 281
6.3.1: Assessing Thermal Hysteresis (TH) and Dynamic Ice-Shaping (DIS) Activities 281
6.3.2: Assessing Recrystallization Inhibition (RI) Activity 281

6.4 Methods for Assessing Cytotoxicity and Cryopreservation Activity 282
6.4.1 Cell Culture 282
6.4.1 MTT Cytotoxicity Assay 282
6.4.3 Cryopreservation 283
6.4.4 Flow Cytometry 284

6.5 Statistical Analysis 284

6.1 General Experimental

All anhydrous reactions were performed in flame-dried glassware under a positive pressure of dry argon or nitrogen. Air or moisture-sensitive reagents and anhydrous solvents were transferred with oven-dried syringes or cannulae. All flash chromatography was performed with E. Merck silica gel 60 (230-400 mesh) or Silicycle Ultrapure SiliaFlash-F60 (230-400 mesh). Analytical thin layer chromatography (TLC) was performed with 0.2 mm pre-coated silica gel plates 60 F254 (E. Merck). Preparatory thin layer chromatography was performed using Silicycle Glass Backed TLC Extra Hard Layer, 60 Å. Components were visualized by illumination with a short-wavelength ultraviolet light and/or staining (ceric ammonium molybdate stain solution, potassium permanganate solution, or iodine).

All solvents used for reactions were distilled unless aqueous systems. Tetrahydrofuran (THF) and diethyl ether were distilled from sodium-potassium amalgam/benzophenone under nitrogen. Dichloromethane, triethylamine, benzene and diisopropylethylamine (DIPEA) were distilled from calcium hydride. *N*,*N*-dimethylformamide (DMF) was stored over activated molecular sieves. *n*-Butyl-lithium was titrated according to the method of Burchat et al immediately prior to using to determine the concentration in solution.[1]

Solid-phase peptide synthesis (SPPS) was performed using Fmoc-Gly-Wang resin (Novabiochem). SPPS reactions were monitored using the ninhydrin (Kaiser) test to detect the existence of free amino groups. The ninhydrin test was performed by adding two drops of a mixture solution (5 g of ninhydrin in 100 mL ethanol, 80 g liquefied phenol in 20 mL ethanol, and 2 mL of 0.001 M aqueous potassium cyanide to 98 mL of pyridine) to a sampling of resin and heating to 120 ºC. A dark blue solution indicated the existence of free amino groups. ^{1}H (300, 400 or 500 MHz), and ^{13}C (75, 100 or 125 MHz), spectra were obtained at ambient temperature on a Bruker Avance 300, Bruker Avance 400, Bruker Avance 500, or Varian Inova 500 spectrometer. Deuterated chloroform ($CDCl_3$), deuterated methanol (CD_3OD), deuterated water (D_2O) were used for NMR experiments. Chemical shifts are reported in ppm downfield from TMS and corrected using the solvent residual signal as a reference.[2] Splitting patterns are designated as follows: s, singlet; d, doublet; t,

triplet; q, quartet; m, multiplet and br, broad. Low resolution mass spectroscopy (MS) was performed on a Micromass Quatro- LC Electrospray spectrometer with a pump rate of 20 μL/min using electrospray ionization (ESI). Polymers were analyzed using a Voyager DE-Pro matrix-assisted desorption ionization-time of flight (MALDI-TOF) (Applied Biosystem, Foster City, CA) mass spectrometer operated in the reflectron/positive-ion mode with DHB in 20% EtOH/H2O as the MALDI matrix. Infrared absorption spectra (IR) were recorded on a Shimadzu FTIR- 8400S spectrometer as a neat film from 4000 cm-1 to 650 cm-1.

6.2 Compound Preparation Procedures and Experimental Data

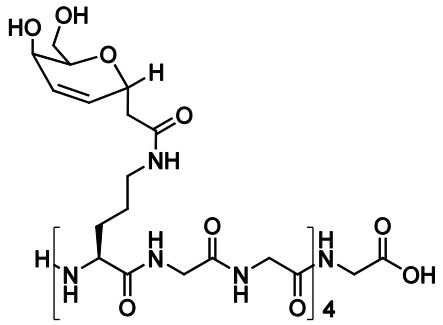

This polypeptide (**33a**) was synthesizes using linear solid-phase synthesis starting from Fmoc-Gly-Wang resin (0.070 g) with loading capacity of 0.6-0.65 mmol/g was employed for the synthesis of the polymer. The resin was allowed to swell for 1 h in DMF. The resin was washed three times with DMF. A solution of 2% piperidine and 2% DBU in DMF was added and the reaction was stirred for 20 minutes. The solution was drained and the beads were again treated with a solution of 2% piperidine and 2% DBU in DMF for 20 minutes before draining and washing with DMF. The solution was then removed and the resin was washed with DMF. A Kaiser test was positive. The beads were washed three times with DMF. For the coupling reaction performed with Fmoc-Gly-OH, a pre-mixed solution of Fmoc-Gly-Gly-OH (0.136 g, 6 equ.), HOBT (0.016 g, 6 equ.), HCTU (0.159 g, 6 equ.), and DIPEA (0.134 mL, 12 equ.) in DMF was added to the reaction vessel. Nitrogen was bubbled through the reaction mixture and the coupling reaction was allowed to run for 4 h, and the solution was

subsequently drained. At this time, a negative result was obtained for the Kaiser test. The beads were washed with DMF, re-suspended in DMF, and left stirring overnight. The beads were treated with a solution of 2% piperidine and 2% DBU in DMF for 20 minutes. The solution was drained and the beads were again treated with a solution of 2% piperidine and 2% DBU in DMF for 20 minutes before draining and washing with DMF. A Kaiser test gave a positive result. For the coupling reactions performed with building block (**117a**), a premixed solution of **117a** (0.039 g, 1.5 eq.), HOBT (0.003 g, 0.45 eq.), HCTU (0.026 g, 1.5 eq.) and DIPEA (0.022 mL, 3 eq.) in DMF was added to the reaction vessel. The reaction mixture was allowed to stir for 24 hours, at which time a negative Kaiser test result was obtained. Following the last coupling reaction, the Fmoc protecting group was removed with a solution of 20% piperidine in DMF. The resin was washed successively with DMF and CH_2Cl_2, and dried for 2 hours. The resin was treated with a 50% solution of TFA in CH_2Cl_2 for 45 minutes. The solution was filtered and the resin was washed with CH_2Cl_2. All filtrate was collected and concentrated under reduced pressure to give the crude product. The crude polymer was purified by reverse-phase HPLC. Lyophilization of the purified product yielded the pure polymer **33a** as a white lyophilized solid.

^{1}H NMR (400 MHz, $CDCl_3$) δ 5.92-5.89 (4H, m), 5.85-5.78 (4H, m), 4.73 (4H, m), 3.87-3.83 (16 H, m), 3.73 (4H, m), 3.62-3.52 (12H, m), 3.08 (8H, m), 2.53-2.49 (4H, m), 2.31-2.28 (4H, m), 1.74 (4H, m), 1.60 (4H, m), 1.44 (8H, m)

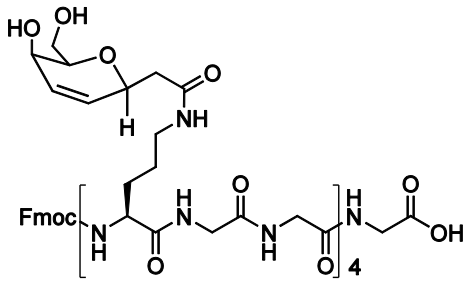

This polypeptide (**34a**) was synthesizes using linear solid-phase synthesis starting from Fmoc-Gly-Wang resin (0.070 g) with loading capacity of 0.6-0.65 mmol/g was employed for the synthesis of the polymer. The resin was allowed to swell for 1 h in DMF. The resin was washed three times with DMF. A solution of 2% piperidine and 2% DBU in DMF was added

and the reaction was stirred for 20 minutes. The solution was drained and the beads were again treated with a solution of 2% piperidine and 2% DBU in DMF for 20 minutes before draining and washing with DMF. The solution was then removed and the resin was washed with DMF. A Kaiser test was positive. The beads were washed three times with DMF. For the coupling reaction performed with Fmoc-Gly-OH, a pre-mixed solution of Fmoc-Gly-Gly-OH (0.098 g, 6 equ.), HOBT (0.011 g, 6 equ.), HCTU (0.115 g, 6 equ.), and DIPEA (0.097 mL, 12 equ.) in DMF was added to the reaction vessel. Nitrogen was bubbled through the reaction mixture and the coupling reaction was allowed to run for 4 h, and the solution was subsequently drained. At this time, a negative result was obtained for the Kaiser test. The beads were washed with DMF, re-suspended in DMF, and left stirring overnight. The beads were treated with a solution of 2% piperidine and 2% DBU in DMF for 20 minutes. The solution was drained and the beads were again treated with a solution of 2% piperidine and 2% DBU in DMF for 20 minutes before draining and washing with DMF. A Kaiser test gave a positive result. For the coupling reactions performed with building block (**115a**), a premixed solution of **115a** (0.028 g, 1.5 eq.), HOBT (0.002 g, 0.45 eq.), HCTU (0.019 g, 1.5 eq.) and DIPEA (0.016 mL, 3 eq.) in DMF was added to the reaction vessel. The reaction mixture was allowed to stir for 24 hours, at which time a negative Kaiser test result was obtained. Following the last coupling reaction, the Fmoc protecting group was removed with a solution of 2% piperidine and 2% DBU in DMF. The resin was washed successively with DMF and CH_2Cl_2, and dried for 2 hours. The resin was treated with 50% solution of TFA in CH_2Cl_2 for 45 minutes. The solution was filtered and the resin was washed with CH_2Cl_2. All filtrate was collected and concentrated under reduced pressure to give the crude product. The crude polymer was purified by reverse-phase HPLC. Lyophilization of the purified product yielded the pure polymer **34a** as a white lyophilized solid.

^{1}H NMR (400 MHz, $CDCl_3$) δ 5.87-5.84 (4H, m), 5.77-5.75 (4H, m), 4.72 (4H, m), 3.83-3.79 (18H, m), 3.60-3.52 (14H, m), 3.08-3.05 (8H, m), 2.40-2.31 (8H, m), 1.70 (4H, m), 1.60-1.56 (4H, m), 1.45-1.37 (8H, m)

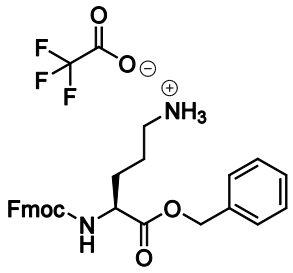

(S)-4-(((9H-fluoren-9-yl)methoxy)carbonylamino)-5-(benzyloxy)-5-oxopentan-1-aminium 2,2,2-trifluoroacetate (37):

To a solution of **104** (4.0 g, 8.80 mmol) in DCM (20 mL), was added TFA (20 mL). The reaction mixture was stirred for 1 hour. The reaction mixture was concentrated, and subsequently re-dissolved in toluene, and again concentrated. This was repeated 3 more times to give **37** (4.1 g, 100 %) as a white foam.

^{1}H NMR (400 MHz, MeOD) 7.79 (2H, d, *J* = 7.6 Hz), 7.64 (2H, dd, *J* = 7.3, 3.2 Hz), 7.40-7.29 (9H, m), 5.17 (2H, s), 4.42 (1H, dd, *J* = 10.4, 6.8 Hz), 4.31-4.23 (2H, m), 4.18 (1H, t, *J* = 6.8 Hz), 2.92 (2H, d, *J* = 7.2 Hz), 1.96 (1H, m), 1.78-1.70 (3H, m)

^{13}C NMR (100 MHz, $CDCl_3$) δ 173.3, 158.8, 145.3, 142.7, 137.2, 129.6, 129.4, 129.3, 128.9, 128.2, 128.2, 126.3, 126.2, 121.0, 68.1, 55.1, 40.2, 29.4, 25.3

MS (ESI) Calcd. for $C_{27}H_{29}N_2O_4$+ (M^+) 445.5296, found 445.5

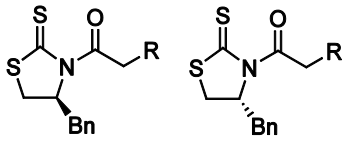

General procedure A. Preparation of (S)- and (R)-thiazolidinone chiral auxiliaries (38 and 43):[3]

A solution of **58** or **63** in dry THF in a round-bottom flask was cooled to -78 °C using a dry-ice/actone bath. Subsequently, *n*Buli was added dropwise and the solution was stirred at -78 °C for 0.5 h. The appropriate acyl chloride was then added, and the reaction mixture was then stirred at -78 °C for 0.5 h. The reaction was slowly warmed to room temperature over 0.5 h. The reaction mixture was quenched with a solution of 10% K_2CO_3 in H_2O. The

aqueous layer was extracted with DCM and the organic layer was washed with H_2O. The combined organic layers were washed with brine, dried over $MgSO_4$ and concentrated. The auxiliary was purified from the residue by recrystallization or by silica flash chromatography.

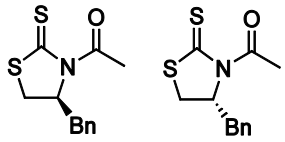

(S)-1-(4-benzyl-2-thioxothiazolidin-3-yl)ethanone (38a) and (R)-1-(4-benzyl-2-thioxothiazolidin-3-yl)ethanone (43a):

The title compound was prepared from **58** or **63** (8.69 g, 41.5 mmol), acetyl chloride (3.54 mL, 49.8 m mol), and 2.4 M *n*BuLi (17.3 mL, 41.5 mmol) in THF (150 mL) using general procedure A. Recrystallization of the residue from ethanol and minimal DCM gave **38a** or **43a**, respectively as yellow needles (9.54 g, 91 %).

R*f* 0.3 (Hexanes/EtOAc, 3:1)

^{1}H NMR (400 MHz, $CDCl_3$) δ 7.37-7.26 (5H, m), 5.38 (1H, m), 3.38 (1H, ddd, *J* = 11.5, 7.2, 1.0 Hz), 3.22 (1H, dd, *J* = 13.2, 3.8 Hz), 3.04 (1H, dd, *J* = 13.2, 10.6 Hz), 2.89 (1H, d, *J* = 11.6 Hz), 2.80 (3H, s)

^{13}C NMR (100 MHz, $CDCl_3$) δ 201.5, 170.7, 136.5, 129.4, 128.9, 127.2, 68.2, 36.7, 31.8, 27.0

Accurate Mass Calcd. for $C_{12}H_{13}NOS_2$ $(M)^+$ 251.0439, found 251.0445

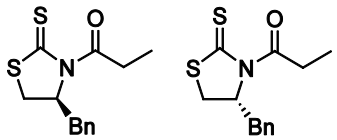

(S)-1-(4-benzyl-2-thioxothiazolidin-3-yl)propan-1-one (38b) and (S)-1-(4-benzyl-2-thioxothiazolidin-3-yl)propan-1-one (43b):

The title compound was prepared from **58** or **63** (0.92 g, 4.41 mmol), propionyl chloride (0.46 mL, 5.3 m mol), and 2.5 M *n*BuLi (1.7 mL, 4.4 mmol) in THF (20 mL) using general procedure A. Recrystallization of the residue from ethanol and minimal DCM and ethanol gave **38b** or **43b**, respectively as yellow needles (1.04 g, 89 %).

R*f* 0.3 (Hexanes/EtOAc, 3:1)

^{1}H NMR (400 MHz, $CDCl_3$) δ 7.36-7.27 (5H, m), 5.38 (1H, ddd, *J* = 10.7, 7.2, 3.8 Hz), 3.47-3.36 (2H, m), 3.22 (1H, dd, *J* = 13.1, 3.7 Hz), 3.18-3.02 (3H, m), 2.88 (1H, d, *J* = 11.5 Hz), 1.19 (3H, t, *J* = 7.2 Hz)

^{13}C NMR (100 MHz, $CDCl_3$) δ 201.1, 174.9, 136.6, 129.4, 128.9, 127.2, 68.6, 36.7, 32.3, 31.9, 8.8

IR νmax (neat): 708, 750, 1261, 1456, 1705, 2931, 3028 cm^{-1}

Accurate Mass Calcd. for $C_{13}H_{15}NOS_2$ $(M)^+$ 265.0595, found 265.0654.

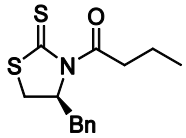

(S)-1-(4-benzyl-2-thioxothiazolidin-3-yl)butan-1-one (38c):

This compound was synthesized by John F. Trant (NSERC summer student).

The title compound was prepared from **58** (3.0 g, 14.3 mmol), butyryl chloride (1.5 mL, 14.3 m mol), and 2.5 M *n*BuLi (6.9 mL, 17.2 mmol) in THF (80 mL) using general procedure A. Purification by silica flash chromatography 25 % ethyl acetate in hexanes gave **38c** as a yellow solid (3.8 g, 96 %).

R*f* 0.9 (hexanes/EtOAc, 2:1)

^{1}H NMR (400 MHz, $CDCl_3$) δ 7.35-7.27 (5H, m), 5.37 (1H, ddd, *J* = 10.8, 7.1, 3.9 Hz), 3.35 (2H, m), 3.21 (1H, dd, *J* = 13.2, 3.8 Hz), 3.11 (1H, m), 3.04 (1H, dd, *J* = 13.1, 10.5 Hz), 2.86 (1H, d, *J* = 11.5 Hz), 1.73 (2H, m), 0.98 (3H, t, *J* = 7.4 Hz)

^{13}C NMR (100 MHz, $CDCl_3$) δ 201.0, 173.8, 136.5, 129.3, 128.8, 127.1, 68.5, 40.2, 36.7, 31.8, 18.1, 13.5; **IR** νmax (neat): 700, 743, 1029, 1255, 1454, 1693, 2960, 3024 cm^{-1}

Accurate Mass Calcd. for $C_{14}H_{17}NOS_2$ $(M)^+$ 279.0752, found 279.0697

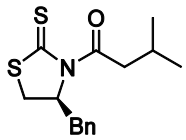

(S)-1-(4-benzyl-2-thioxothiazolidin-3-yl)-2-methylpropan-1-one (38d):

This compound was synthesized by John F. Trant (NSERC summer student).

The title compound was prepared from **58** (2.0 g, 9.6 mmol), 3-methylbutanoyl chloride (1.4 mL, 11.5 m mol), and 2.5 M *n*BuLi (3.8 mL, 9.6 mmol) in THF (54 mL) using general procedure A. Recrystallization of the residue from ethanol and minimal DCM gave **38d** as a yellow solid (2.14 g, 82 %).

R*f* 0.7 (hexanes/EtOAc, 3:1)

^{1}H NMR (400 MHz, $CDCl_3$) δ 7.36-7.25 (5H, m), 5.37 (1H, ddd, *J* = 10.6, 6.8, 3.9 Hz), 3.37 (1H, ddd, *J* = 11.5, 7.2, 0.9 Hz), 3.14 (4H, m), 2.87 (1H, d, *J* = 11.5 Hz), 2.23 (1H, m), 1.00 (3H, d, *J* = 6.7 Hz), 0.97 (3H, d, *J* = 6.6 Hz)

^{13}C NMR (100 MHz, $CDCl_3$) δ ^{13}C NMR (100 MHz, $CDCl_3$) δ 201.0 173.3, 136.5, 129.4, 128.8, 127.1, 68.6, 46.8, 36.8, 31.8, 25.3, 22.5, 22.3

IR νmax (neat): 700, 744, 1689, 2954, 3026 cm^{-1}

Accurate Mass Calcd. for $C_{15}H_{19}NOS_2$ $(M)^+$ 293.0908, found 293.0889

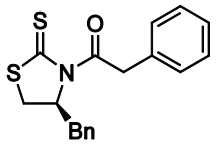

(S)-1-(4-benzyl-2-thioxothiazolidin-3-yl)-2-phenylethanone (38e):

The title compound was prepared from **58** (2.0 g, 9.6 mmol), 2-phenylacetyl chloride (1.52 mL, 11.4 mmol), and 2.4 M *n*BuLi (3.98 mL, 9.6 mmol) in THF (30 mL) using general procedure A. Recrystallization of the residue from ethyl acetate gave **38e** as yellow needles (1.10 g, 35 %).

R*f* 0.6 (hexanes/EtOAc, 3:1)

^{1}H NMR (400 MHz, $CDCl_3$) δ 7.36-7.22 (10H, m), 5.34 (1H, ddd, *J* = 10.6, 6.9, 3.8 Hz), 4.64 (2H, q, *J* = 17.2 Hz), 3.37 (1H, ddd, *J* = 11.5, 7.1, 0.7 Hz), 3.24 (1H, dd, *J* = 13.1, 3.6 Hz), 3.04 (1H, dd, *J* = 13.1, 10.7 Hz), 2.88 (1H, d, *J* = 11.6 Hz)

^{13}C NMR (100 MHz, $CDCl_3$) δ 201.2, 172.2, 136.3, 133.7, 129.7, 129.4, 128.8, 128.4, 127.1, 127.1, 68.9, 44.5, 36.6, 31.8

MS (EI) Calcd. for $C_{18}H_{17}NOS_2$ $(M)^+$ 327.4637, found 327

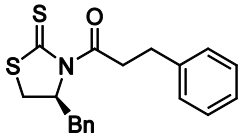

(S)-1-(4-benzyl-2-thioxothiazolidin-3-yl)-3-phenylpropan-1-one (38f):

The title compound was prepared from **58** (0.4 g, 1.9 mmol), hydrocinnamoyl chloride (0.34 mL, 2.3 m mol), and 2.4 M *n*BuLi (0.80 mL, 1.9 mmol) in THF (20 mL) using general procedure A. Recrystallization of the residue from ethanol gave **38f** as yellow crystals (0.42 g, 64 %).

R*f* 0.3 (DCM/MeOH, 9:1)

^{1}H NMR (400 MHz, $CDCl_3$) δ 7.38-7.20 (10H, m), 5.34 (1H, ddd, *J* = 10.6, 6.9, 3.9 Hz), 3.72 (1H, ddd, *J* = 17.2, 9.1, 5.8 Hz), 3.53 (1H, ddd, *J* = 17.2, 9.0, 6.6 Hz), 3.31 (1H, ddd, *J* =

11.5, 7.2, 0.7 Hz), 3.23 (1H, dd, *J* = 13.2, 3.8 Hz), 3.13-2.96 (3H, m), 2.85 (1H, d, *J* = 11.6 Hz)

^{13}C NMR (100 MHz, $CDCl_3$) δ 201.0, 173.0, 140.3, 136.4, 129.3, 128.8, 128.4, 128.4, 126.1, 126.1, 68.5, 39.8, 36.6, 31.9, 30.7

Accurate Mass Calcd. for $C_{19}H_{19}NOS_2$ $(M)^+$ 341.0908, found 341.0910

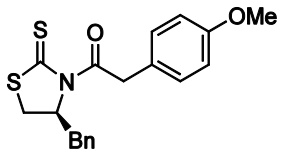

(S)-1-(4-benzyl-2-thioxothiazolidin-3-yl)-2-(4-methoxyphenyl)ethanone (38g):

The title compound was prepared from **58** (2.1 g, 10.0 mmol), **65** (2.2 g, 12.0 mmol), and *n*BuLi (4.0 mL, 10.0 mmol) in THF (8 mL) using general procedure A. Recrystallization of the residue from ethanol and minimal DCM and ethanol gave **38g** as yellow crystals (2.8 g, 82 %).

R*f* 0.9 (hexanes/EtOAc, 3:1)

^{1}H NMR (400 MHz, $CDCl_3$) δ 7.34-7.26 (5H, m), 7.17 (2H, m), 6.89 (2H, m), 5.34 (1H, ddd, *J* = 10.5, 6.7, 3.8 Hz), 4.59 (2H, q, *J* = 17.2 Hz), 3.80 (3H, s), 3.38 (1H, ddd, *J* = 11.5, 7.2, 0.9 Hz), 3.25 (1H, dd, *J* = 13.1, 3.6 Hz), 3.05 (1H, dd, *J* = 13.1, 10.7 Hz), 2.89 (1H, d, *J* = 11.6 Hz)

^{13}C NMR (100 MHz, $CDCl_3$) δ 201.2, 172.6, 158.6, 136.4, 130.7, 129.3, 128.8, 127.1, 125.7, 113.9, 69.0, 55.1, 43.6, 36.6, 31.8

IR νmax (neat): 702, 746, 1558, 1693, 2960, 3026 cm^{-1}

Accurate Mass Calcd. for $C_{19}H_{19}NO_2S_2$ $(M)^+$ 357.0857, found 357.0845.

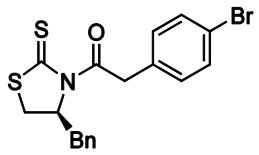

(S)-1-(4-benzyl-2-thioxothiazolidin-3-yl)-2-(4-bromophenyl)ethanone (38h):

This compound was synthesized by John F. Trant (NSERC summer student).

The title compound was prepared from **58** (2.3 g, 11.0 mmol), **69** (3.85g, 16.5 mmol), and 2.5 M *n*BuLi (4.4 mL, 11.0 mmol) in THF (20 mL) using general procedure A. Recrystallization of the residue from ethanol and minimal DCM and ethanol gave **38h** as an orange solid (1.74 g, 40 %). **R*f*** 0.8 hexanes/EtOAc, 3:1)

^{1}H NMR (500 MHz, $CDCl_3$) δ 7.47-7.44 (2H, m), 7.33-7.30 (2H, m), 7.27-7.24 (3H, m), 7.12-7.09 (2H, m), 5.24 (1H, ddd, *J* = 10.6, 6.9, 3.9), 4.65 (1H, d, *J* = 17.3 Hz), 4.51 (1H, d, *J* = 17.3 Hz), 3.38 (1H, ddd, *J* = 8.0, 7.1, 0.8 Hz), 3.22 (1H, dd, *J* = 13.1, 3.7 Hz), 3.04 (1H, dd, *J* = 13.1, 10.6 Hz), 2.89 (1H, d, *J* = 11.6 Hz)

^{13}C NMR (125 MHz, $CDCl_3$) δ 201.3, 171.6, 136.2, 132.7, 131.5, 131.4, 129.3, 128.8, 127.2, 121.2, 68.8, 43.9, 43.9, 36.6, 31.9

IR νmax (neat): 702, 740, 1693, 2854, 2923, 3026 cm^{-1}

Accurate Mass Calcd. for $C_{18}H_{16}NOS_2Br$ $(M)^+$ 406.9836, found 406.9848.

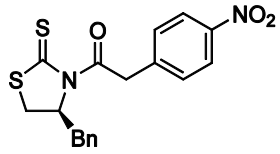

(S)-1-(4-benzyl-2-thioxothiazolidin-3-yl)-2-(4-nitrophenyl)ethanone (38i):

This compound was synthesized by John F. Trant (NSERC summer student).

The title compound was prepared from **58** (2.1 g, 10.0 mmol), **67** (2.40 g, 12.4 mmol), and 2.5 M *n*BuLi (4.0 mL, 10.0 mmol) in THF (60 mL) using general procedure A. Purification by silica flash chromatography 20 % ethyl acetate in hexanes gave **38i** as a yellow solid (0.235 g, 6 %).

R*f* 0.6 (hexanes/EtOAc, 3:1)

^{1}H NMR (400 MHz, $CDCl_3$) δ 8.22-8.10 (2H, m), 7.42-7.40 (2H, m), 7.36-7.28 (5H, m), 5.39 (1H, ddd, *J* = 10.6, 6.8, 4.1 Hz), 4.87 (1H, d, *J* = 17.3 Hz), 4.63 (1H, d, *J* = 17.3 Hz), 3.44 (1H, ddd, *J* = 11.6, 7.2, 0.8 Hz), 3.24 (1H, dd, *J* = 13.2, 3.9 Hz), 3.07 (1H, dd, *J* = 13.2, 10.4 Hz), 2.95 (1H, d, *J* = 11.6 Hz)

^{13}C NMR (100 MHz, $CDCl_3$) δ 201.6, 170.6, 147.2, 141.3, 136.1, 130.8, 129.4, 128.9, 127.3, 123.6, 68.8, 44.3, 36.8, 32.1

Accurate Mass Calcd. for $C_{18}H_{16}N2O_3S_2$ $(M)^+$ 372.0602, found 372.05106

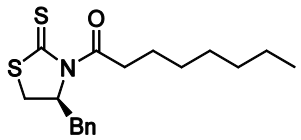

(S)-1-(4-benzyl-2-thioxothiazolidin-3-yl)octan-1-one (38j):

This compound was synthesized by John F. Trant (NSERC summer student).

The title compound was prepared from **58** (2.5 g, 11.9 mmol), octanoyl chloride (2.45 mL, 14.3 m mol), and 2.5 M *n*BuLi (4.76 mL, 11.9 mmol) in THF (70 mL) using general procedure A. Recrystallization of the residue from ethanol gave **38j** as yellow crystals (2.96 g, 77 %). **R*f*** 0.8 (hexanes/EtOAc, 3:1)

^{1}H NMR (400 MHz, $CDCl_3$) δ 7.38-7.25 (5H, m), 5.37 (1H, m), 3.41-3.31 (2H, m), 3.25-3.00 (3H, m), 2.88 (1H, m), 1.68 (2H, m), 1.78-1.60 (2H, m), 1.37-1.27 (8H, m), 0.89 (1H, m)

^{13}C NMR (100 MHz, $CDCl_3$) δ 201.1, 174.2, 136.6, 129.4, 128.9, 127.2, 68.6, 38.5, 36.7, 31.9, 31.7, 29.1, 24.7, 22.6, 14.1

MS (EI) Calcd. for $C_{18}H_{25}NOS_2$ $(M)^+$ 335.5272, found 335

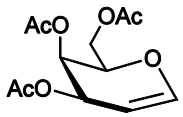

(2R,3R)-2-(acetoxymethyl)-3,4-dihydro-2H-pyran-3,4-diyl diacetate (44):[4]

To a suspension of zinc dust (14.40 g, 220.2 mmol) in EtOAc (148 mL), was added 1-methylimidazole (2.92 mL, 36.7 mmol). The reaction mixture was stirred vigorously and heated to reflux, at which point **81** (15.09 g, 36.7 mmol) in EtOAc (37 mL) was added dropwise. The reaction mixture was maintained at reflux for 0.5 h, and then cooled to room temperature. The reaction mixture was filtered through celite, and the filtrate was washed sequentially with a 10 % aqueous solution of HCl, an aqueous saturated solution of $NaHCO_3$, H_2O, and brine. The aqueous fractions were re-extracted with EtOAc. The combined organic fractions were dried over $MgSO_4$ and concentrated. Purification by silica flash chromatography in 20 % ethyl acetate in hexanes gave **44** (7.548 g, 76 %) as a clear, colourless oil.

R*f* 0.2 (hexanes/EtOAc, 3:1)

^{1}H NMR (400 MHz, $CDCl_3$) δ 6.46 (1H, dd, *J* = 6.3, 1.7 Hz), 5.55 (1H, ddt, *J* = 2.7, 1.8, 1.1 Hz), 5.42 (1H, td, *J* = 4.5, 1.6 Hz), 4.72 (1H, ddd, *J* = 6.3, 2.7, 1.5 Hz), 4.32 (1H, m), 4.29-4.19 (2H, m), 2.12 (3H, s), 2.08 (3H, s), 2.02 (3H, s)

^{13}C NMR (100 MHz, $CDCl_3$) δ 170.5, 170.3, 170.1, 145.4, 98.8 72.8, 63.9, 63.7, 61.9, 20.8, 20.7, 20.6

MS (ESI) Calcd. for $C_{12}H_{16}O_7$ $(M+Na)^+$ 295.2410, found 295.3

All spectral data was in accordance with the literature.[4]

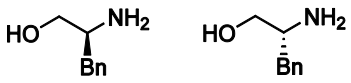

(S)-2-Aamino-3-phenylpropan-1-ol (57) and (R)-2-Amino-3-phenylpropan-1-ol (62):[5]

$LiAlH_4$ (3.4 g, 89.6 mmol) was added to dry THF (300 mL) in a 500 mL round-bottom flask cooled in an ice-bath. L- or D-Phenylalanine (10.0 g, 60.3 mmol) was added portion-wise.

The mixture was stirred at 0 °C for 0.5 h. The reaction flask was then warmed slowly to room temperature. The mixture was heated to reflux and stirred for 18 h. The reaction flask was then cooled in an ice bath, and the mixture was diluted with Et_2O. The reaction was quenched by sequential slow addition of H_2O (3.4 mL), 15% NaOH (aqueous, saturated solution; 3.4 mL), and H_2O (10.2 mL). The mixture was filtered through celite, and the filtrate was concentrated. Recrystallization from toluene gave **57** or **62**, respectively, as white needles (5.5 g, 60 %).

R*f* 0.3 (DCM/MeOH, 9:1)

^{1}H NMR (400 MHz, $CDCl_3$) δ 7.33-7.29 (2H, m), 7.25-7.18 (3H, m), 3.64 (1H, dd, *J* = 10.6, 3.9 Hz), 3.38 (1H, dd, *J* = 10.6, 7.2 Hz), 3.12 (1H, m), 2.80 (1H, dd, *J* = 13.5, 5.2 Hz), 2.53 (1H, dd, *J* = 13.5, 8.6 Hz)

^{13}C NMR (100 MHz, $CDCl_3$) δ 138.6, 129.2, 128.6, 126.4, 66.4, 54.1, 41.0

MS (EI^+): Calcd for $C_9H_{13}NO$ $(M+H)^+$ 152.2136, found 152

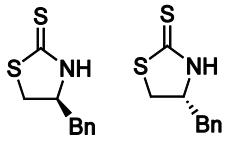

(S)-4-benzylthiazolidine-2-thione (58) and (S)-4-benzylthiazolidine-2-thione (63):[6]

The title compound was prepared by the addition of CS_2 (11.42 g, 180.9 mmol) and KOH (1M solution in H_2O, 180 mL) to **57** or **62** (5.47 g, 36.2 mmol). The solution was heated to reflux and stirred for 48 h. The reaction mixture was cooled and diluted with DCM. The aqueous layer was extracted with DCM and the organic layer was washed with H_2O. The combined organic layers were washed with brine, dried over $MgSO_4$ and concentrated. Silica flash chromatography using 20 % EtOAc in hexanes gave **58** or **63**, respectively, as white solids (6.56 g, 87 %).

R*f* 0.8 (Hexanes/EtOAc, 1:1)

^{1}H NMR (400 MHz, $CDCl_3$) δ 7.38-7.28 (3H, m), 7.22-7.10 (2H, m), 4.46 (1H, qd, *J* = 14.5, 7.6, 7.3, 7.3 Hz), 3.61 (1H, dd, *J* = 11.2, 7.6 Hz), 3.34 (1H, dd, *J* = 11.2, 6.9 Hz), 3.01 (2H, dd, *J* = 8.2, 2.2 Hz)

^{13}C NMR (100 MHz, $CDCl_3$) δ 201.1, 135.9, 129.2, 129.0, 127.6, 65.0, 40.2, 38.4

IR νmax (neat): 698, 739, 1461, 1720, 2941, 3130 cm^{-1}

Accurate Mass Calcd. for $C_{10}H_{11}NS_2$ $(M)^+$ 209.0333, found 209.0331.

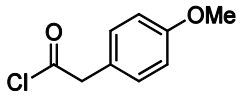

2-(4-methoxyphenyl)acetyl chloride (65):

To a solution of 2-(4-methoxyphenyl)acetic acid (2 g, 12.04 mmol) in DCM (34 mL), oxalyl chloride (3.1 g, 36 mmol) was added slowly. A water-cooled condenser was placed on the round-bottom flask and DMF (cat.) was slowly added through the condenser. The reaction mixture was heated to reflux and stirred for 0.5 h. The reaction mixture was allowed to cool and concentrated to give **65** as a yellow oil, which was used as is (2.2 g, quantitative).

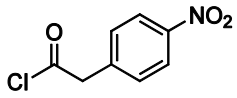

2-(4-nitrophenyl)acetyl chloride (67):

This compound was synthesized by John F. Trant (NSERC summer student).

To a solution of 2-(4-nitrophenyl)acetic acid (2.2 g, 12.0 mmol) in DCM (60 mL), oxalyl chloride (3.1 g, 24.1 mmol) was added slowly. A water-cooled condenser was placed on the round-bottom flask and DMF (cat.) was slowly added through the condenser. The reaction mixture was heated to reflux and stirred for 0.5 h. The reaction mixture was allowed to cool and concentrated to give **67** as an orange oil, which was used as is (2.4 g, quantitative).

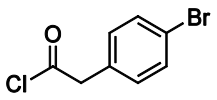

2-(4-bromophenyl)acetyl chloride (69):

This compound was synthesized by John F. Trant (NSERC summer student).

To a solution of 2-(4-bromophenyl)acetic acid (3.6 g, 16.6 mmol) in DCM (90 mL), oxalyl chloride (6.46 g, 49.8 mmol) was added slowly. A water-cooled condenser was placed on the round-bottom flask and DMF (cat.) was slowly added through the condenser. The reaction mixture was heated to reflux and stirred for 0.5 h. The reaction mixture was allowed to cool and concentrated to give **69** as an orange oil, which was used as is (3.9 g, quantitative).

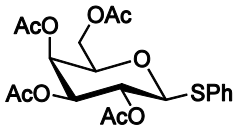

(2R,3S,4S,5S,6S)-2-(acetoxymethyl)-6-(phenylthio)tetrahydro-2H-pyran-3,4,5-triyl triacetate (72):[7]

A solution of β-D-galactose pentaacetate (10 g, 25.6 mmol) in DCM (250 mL) was cooled to 0 ºC. Thiophenol (5.64 g, 51.2 mmol) was then added dropwise. The solution was stirred for 0.5 h, before $BF_3{\cdot}Et_2O$ (12.7 g, 89.6 mmol) was added slowly. TH reaction mixture was stirred overnight at room temperature. The reaction mixture was diluted with DCM, and washed with saturated aqueous $NaHCO_3$, H_2O, and brine. The organic layer was dried over MgSO4, and concentrated. Silica flash chromatography gave **72** as a white solid (10.60 g, 94 %).

^{1}H NMR (300 MHz, $CDCl_3$) δ 7.53-7.50 (2H, m), 7.33-7.30 (3H, m), 5.42 (1H, dd, *J* = 3.3, 0.7 Hz), 5.26 (1H, dd, *J* = 18.1, 8.2 Hz), 5.05 (1H, dd, *J* = 10.0, 3.3 Hz), 4.72 (1H, d, 10.0 Hz), 4.2 (1H, dd, *J* = 11.3, 7.1 Hz), 4.1 (1H, dd, *J* = 11.3, 6.2 Hz), 3.94 (1H, m), 2.10 (3H, s), 2.08 (3H, s), 2.02 (3H, s), 1.95 (3H, s)

All spectral data was in accordance with the literature.[7]

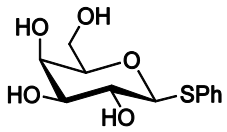

(2R,3R,4S,5R,6S)-2-(hydroxymethyl)-6-(phenylthio)tetrahydro-2H-pyran-3,4,5-triol (73):[7]

A solution of NaOMe in MeOH (pH 12) was added to **72** (9.8 g, 22.3 mmol). The reaction was stirred at room temperature for overnight. The reaction mixture was neutralized with Amberlite® IR-120H ion-exchange resin. The resin was removed by filtration, and the filtrate was concentrated to give **73** as a clear, colourless oil (5.14 g, 96 %), which was used as is.

^{1}H NMR (300 MHz, CD_3OD) δ 7.48-7.46 (2H, m), 7.24-7.12 (3H, m), 4.59 (1H, d, *J* = 9.6 Hz), 3.90 (1H, m), 3.80 (2H, m), 3.64 (2H, m), 3.50 (1H, dd, *J* = 6.2, 3.2 Hz)

All spectral data was in accordance with the literature.[7]

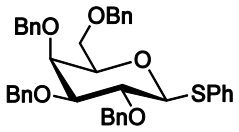

(2R,3S,4S,5R,6S)-3,4,5-tris(benzyloxy)-2-(benzyloxymethyl)-6-(phenylthio)tetrahydro-2H-pyran (74):[8]

To a solution of **73** (4.95 g, 20.6 mmol) in DMF (150 mL), NaH (2.18 g, 90.6 mmol) was carefully added. The reaction mixture was stirred for 2 hours at room temperature, and then cooled to 0 ºC. Subsequently, TBAI (0.739 g, 2.0 mmol) was added, followed by the dropwise addition of BnBr (15.5 g, 90.6 mmol). The reaction mixture was stirred at room temperature for overnight. The reaction was quenched with careful addition of MeOH, and subsequently diluted with EtOAc. The organic layer was washed with H_2O and brine, dried over $MgSO_4$, and concentrated. Silica flash chromatography gave **74** as a white solid (6.78 g, 52 %).

^{1}H NMR (300 MHz, $CDCl_3$) δ 7.60-7.54 (2H, m), 7.41-7.29 (20H, m), 7.21-7.16 (3H, m), 4.98 (1H, d, *J* = 11.5 Hz), 4.76 (2H, q, *J* = 10.1 Hz), 4.73 (2H, d, *J* = 1.76 Hz), 4.63 (2H, d, *J*

= 11.1 Hz), 4.45 (2H, q, *J* = 11.6 Hz), 3.99 (1H, d, *J* = 2.7 Hz), 3.94 (1H, t, *J* = 9.4 Hz), 3.67-3.59 (4H, m)

All spectral data was in accordance with the literature.[8]

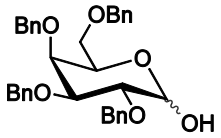

(3S,4S,5S)-3,4,5-tris(benzyloxy)-6-(benzyloxymethyl)tetrahydro-2H-pyran-2-ol (75):[9]

To a solution of **74** (6.5 g, 10.27 mmol) and in a solution of acetone (5 mL) and water (45 mL) was added *N*-bromosuccinimide (3.66 g, 20.54 mmol). The reaction mixture was stirred for 2 h, and then concentrated. The crude product was diluted with EtOAc, and washed with a saturated aqueous solution of $NaHCO_3$, water, and brine. The aqueous layers were in turn washed with EtOAc. The combined organic layers were dried over $MgSO_4$ and concentrated. Silica flash chromatography gave **75** (5.16 g, 93%), as an anomeric mixture, as a clear, colourless oil.

^{1}H NMR (300 MHz, $CDCl_3$) δ 7.38-7.29 (m, 20H, 5.29 (1H, m), 4.96 (m, 1H), 4.85-4.57 (m, 8H), 3.95 (dd, 2H), 3.64-3.57 (m, 3H)

All spectral data was in accordance with the literature.[9]

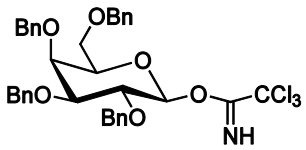

(2S,3S,4S,5S,6R)-3,4,5-tris(benzyloxy)-6-(benzyloxymethyl)tetrahydro-2H-pyran-2-yl 2,2,2-trichloroacetimidate (76):[10]

To a solution of **75** (1.0 g, 1.85 mmol) in DCM (18 mL), under N_2, potassium carbonate (0.639 g, 4.63 mmol) was slowly added. The reaction mixture was stirred for 10 minutes, and trichloroacetonitrile (1.07 g, 7.40 mmol) was subsequently added dropwise. The reaction mixture was stirred at room temperature for overnight. The reaction mixture was diluted with

DCM, and washed with H_2O and brine. The organic extracts were dried over $MgSO_4$, and concentrated to give **76** (1.16 g, 92 %) as a clear, pale yellow oil, and was used as is.

^{1}H NMR (300 MHz, $CDCl_3$) δ 8.55 (1H, s), 7.27-7.17 (20 H, m), 5.67 (1H, d, *J* = 8.0 Hz), 4.89-4.82 (2H, m), 4.76-4.66 (3H, m), 4.56 (1H, m), 4.42-4.32 (2H, m), 4.02 (1H, dd, *J* = 9.6, 8.1 Hz), 3.91 (1H, m), 3.68 (1H, t, *J* = 6.4 Hz), 3.61-3.55 (3H, m)

All spectral data was in accordance with the literature.[10]

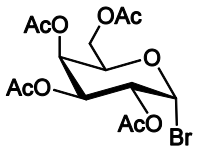

(2R,3S,4S,5R,6R)-2-(acetoxymethyl)-6-bromotetrahydro-2H-pyran-3,4,5-triyl triacetate (81):[11]

β-D-galactose pentaacetate (20.0 g, 51.2 mmol) was added to a round bottom flask and cooled to 0 ºC. HBr (30 % in acetic acid; 120 mL) was subsequently added portionwise. The reaction was stirred at room temperature for 45 minutes. The reaction mixture was subsequently diluted with DCM, and washed with H_2O until the organic layer was neutralized to pH 7, and brine. The organic extracts were dried over $MgSO_4$, and concentrated to give **81** (19.17 g, 91 %) as white crystals.

R*f* 0.3 (hexanes/EtOAc, 6:4)

^{1}H NMR (400 MHz, $CDCl_3$) δ 6.71 (1H, d, *J* = 4.0 Hz), 5.52 (1H, dd, *J* = 3.3, 1.3 Hz), 5.40 (1H, dd, *J* = 10.7, 3.3 Hz), 5.05 (1H, dd, *J* = 10.7, 3.9 Hz), 4.49 (1H, t, *J* = 6.7 Hz), 4.15 (2H, ddd, *J* = 32.2, 11.4, 6.6 Hz), 2.16 (3H, s), 2.12 (3H, s), 2.06 (3H, s), 2.02 (3H, s)

All spectral data was in accordance with the literature.[12]

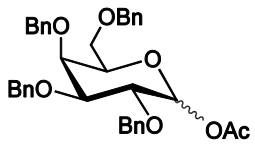

(3R,4S,5S)-3,4,5-tris(benzyloxy)-6-(benzyloxymethyl)tetrahydro-2H-pyran-2-yl acetate (82):[13]

Acetic anhydride (1 mL) and pyridine (1 mL), and DMAP (0.01 g, 0.09 mmol) were added to **75** (0.50 g, 0.925 mmol) at 0 ºC. The reaction was stirred overnight at room temperature. The reaction was diluted with DCM and washed with an aqueous saturated solution of $CuSO_4$ (4x), H_2O, and brine. The organic fractions were combined, dried over $MgSO_4$, and concentrated. Silica flash chromatography gave **82** as a white solid (o.490 g, 91 %).

^{1}H NMR (300 MHz, $CDCl_3$) δ 7.38-7.27 (20H, m), 5.56 (1H, d, *J* = 8.1 Hz), 4.96-4.54 (6H, m), 4.18-4.08 (2H, m), 3.99 (1H, m), 3.96 (1H, dd, J = 7.5, 2.1 Hz), 3.67 (1H, m), 3.59-3.55 (3H, m), 2.02 (3H, s)

All spectral data was in accordance with the literature.[13]

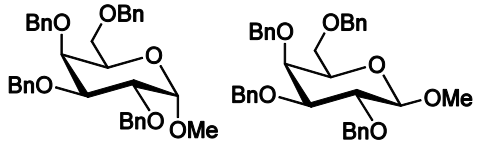

(2R,3S,4S,5R,6R)-3,4,5-tris(benzyloxy)-2-(benzyloxymethyl)-6-methoxytetrahydro-2H-pyran (84) and (2R,3S,4S,5R,6S)-3,4,5-tris(benzyloxy)-2-(benzyloxymethyl)-6-methoxytetrahydro-2H-pyran (85):

MeI (0.263 g, 1.85 mmol) was added to a solution of **75** (0.50 g, 0.925 mmol) in DCM (1 mL). The reaction mixture was stirred at room temperature for overnight. The reaction mixture was diluted with DCM, and washed with H_2O and brine. The organic fractions were dried over $MgSO_4$, and concentrated. Silica flash chromatography gave **84** (0.05 g, 10 %) and **85** (0.09 g, 18 %).

(2R,3S,4S,5R,6R)-3,4,5-tris(benzyloxy)-2-(benzyloxymethyl)-6-methoxytetrahydro-2H-pyran (**84**):

^{1}H NMR (300 MHz, $CDCl_3$) δ 7.35-7.27 (20H, m), 4.92 (2H, dd, *J* = 13.3, 11.4 Hz), 4.77-4.68 (3H, m), 4.62 (1H, d, *J* = 11.7 Hz), 4.43 (2H, d, *J* = 4.3 Hz), 4. 27 (1H, d, *J* = 7.7 Hz), 3.89 (1H, d, *J* = 2.9 Hz), 3.80 (1H, dd, *J* = 9.6, 7.7 Hz), 3.61-3.50 (4H, m), 3.55 (3H, s)

^{13}C NMR (125 MHz, $CDCl_3$) δ 151.6, 138.8, 138.6, 138.5, 137.9, 128.4, 128.3, 128.2, 128.2, 128.1, 128.1, 127.7, 127.7, 127.7, 127.6, 127.5, 98.8, 89.2, 79.1, 76.4, 75.1, 74.7, 73.6, 73.5, 73.3, 69.2, 69.0, 55.3

MS (ESI) Calcd. for $C_{35}H_{38}NO_6$ $(MNH_4)^+$ 572.7111, found 572.2

(2R,3S,4S,5R,6S)-3,4,5-tris(benzyloxy)-2-(benzyloxymethyl)-6-methoxytetrahydro-2H-pyran (**85**):

^{1}H NMR (300 MHz, $CDCl_3$) δ 7.40-7.28 (20H, m), 4.94 (1H, d, *J* = 11.5 Hz), 4.84 (2H, dd, *J* = 12.0, 3.7 Hz), 4.75-4.67 (3H, m), 4.57 (1H, d, *J* = 11.5 Hz), 4.48 (1H, d, *J* = 11.8 Hz), 4.39 (1H, d, *J* = 11.8 Hz), 4.03 (1H, dd, *J* = 11.0, 3.3 Hz), 3.94-3.87 (3H, m), 3.51 (2H, d, *J* = 6.4 Hz), 3.37 (3H, s)

^{13}C NMR (125 MHz, $CDCl_3$) δ 138.8, 138.6, 138.5, 137.9, 128.4, 128.3, 128.3, 128.1, 128.1, 127.9, 127.8, 127.5, 127.5, 127.5, 105.0, 82.1, 79.6, 75.1, 74.4, 73.5, 73.4, 73.3, 73.0, 68.8, 57.0, 30.9

MS (ESI) Calcd. for $C_{35}H_{38}O_6$ $(MNH_4)^+$ 572.7111, found 572.2

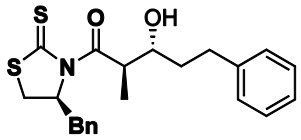

(2R)-1-((S)-4-benzyl-2-thioxothiazolidin-3-yl)-3-hydroxy-2-methyl-5-phenylpentan-1-one (87):[14]

A solution of (S)-chiral auxiliary **38b** (0.10 g, 0.377 mmol) in DCM (1 mL) was cooled to 0 °C using an ice-bath. $TiCl_4$ (1M in DCM, 0.829 mL, 0.829 mmol), was added and the solution was stirred for 5 min. The reaction mixture was cooled to -78 °C using a dry-

ice/acetone bath. Et_3N (0.084 g, 0.829 mmol) was subsequently added, and the reaction mixture was stirred at -78 °C for 0.5 h, and at room temperature for 0.5 h. The reaction mixture was subsequently cooled to -78 °C, and $SnCl_4$ (1M in DCM, 0.829 mL, 0.829 mmol) and hydrocinnamaldehyde (0.101 g, 0.754 mmol) in DCM (1 mL) were then added. The reaction mixture was stirred at room temperature for 0.3 h, and then cooled to -78 °C. The reaction mixture was quenched with a saturated aqueous solution of NH_4Cl, and subsequently warmed to room temperature. The aqueous layer was extracted with DCM and the organic layer was washed with H_2O. The combined organic layers were washed with brine, dried over $MgSO_4$ and concentrated. Purification by silica flash chromatography in 10 % ethyl acetate in hexanes gave **96** as a yellow solid (0.138 g, 92 %). The same procedure was repeated, replacing Et_3N (0.084 g, 0.829 mmol) with (-)-sparteine (0.194 g, 0.829 mmol). Purification by silica flash chromatography in 10 % ethyl acetate in hexanes gave **87** as a yellow solid (0.139 g, 93 %).

R*f* 0.4 (hexanes:EtOAc, 8:2)

^{1}H NMR (300 MHz, $CDCl_3$) δ 7.41-7.18 (10H, m), 5.37 (1H, ddd, *J* = 10.7, 7.0, 4.0 Hz), 4.49 (1H, dq, *J* = 6.9, 2.8 Hz), 3.97 (1H, ddd, *J* = 9.0, 3.8, 3.0 Hz), 3.40 (1H, dd, *J* = 11.7, 7.1 Hz), 3.23 (1H, dd, *J* = 12.9, 4.0 Hz), 3.09 (1H, d, *J* = 3.1 Hz), 2.92 (1H, d, *J* = 11.5 Hz), 2.97-2.81 (1H, m), 2.76-2.65 (1H, m), 1.92 (1H, m), 1.71 (1H, m), 1.31 (3H, d, *J* = 6.9 Hz)

^{13}C NMR (75 MHz, $CDCl_3$) δ 201.3, 178.4, 141.6, 136.2, 129.4, 128.9, 128.4, 128.4, 127.2, 125.8, 71.3, 68.6, 43.1, 36.7, 35.8, 32.1, 32.0, 10.5

MS (ESI) Calcd. for $C_{22}H_{25}NO_2S_2$ $(M+H)^+$ 400.5773, found 400.0, $(M+NH_4)^+$ 417.6079, found 417.0, $(M+Na)^+$ 422.5592, found, 442.8

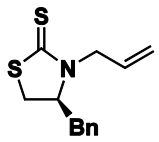

(S)-3-allyl-4-benzylthiazolidine-2-thione (89):

A solution of (S)-chiral auxiliary **38b** (0.10 g, 0.377 mmol) in DCM (1 mL) was cooled to 0 °C using an ice-bath. $TiCl_4$ (1M in DCM, 0.829 mL, 0.829 mmol), was added and the

solution was stirred for 5 min. The reaction mixture was cooled to -78 °C using a dry-ice/acetone bath. Et_3N (0.084 g, 0.829 mmol) was subsequently added, and the reaction mixture was stirred at -78 °C for 0.5 h, and at room temperature for 0.5 h. The reaction mixture was subsequently cooled to -78 °C, and $SnCl_4$ (1M in DCM, 0.829 mL, 0.829 mmol) and allyl bromide (0.091 g, 0.754 mmol) in DCM (1 mL) were then added. The reaction mixture was stirred at room temperature for 0.3 h, and then cooled to -78 °C. The reaction mixture was quenched with a saturated aqueous solution of NH_4Cl, and subsequently warmed to room temperature. The aqueous layer was extracted with DCM and the organic layer was washed with H_2O. The combined organic layers were washed with brine, dried over $MgSO_4$ and concentrated. Purification by silica flash chromatography in 10 % ethyl acetate in hexanes gave **89** as a yellow solid (0.084 g, 89 %).

R*f* 0.2 (hexanes/EtOAc, 9:1)

^{1}H NMR (400 MHz, $CDCl_3$) δ 7.32-7.19 (5H, m), 5.92 (1H, tdd, *J* = 16.9, 10.0, 6.9 Hz), 5.26 (1H, ddd, *J* = 17.0, 2.71, 1.4 Hz), 5.14 (1H, ddd, *J* = 10.1, 2.0, 1.3 Hz), 4.67 (1H, dddd, 8.9, 7.8, 6.5, 5.4 Hz), 3.76 (2H, m), 3.29 (1H, dd, *J* = 10.9, 7.8 Hz), 3.13 (2H, m), 2.72 (1H, dd, *J* = 13.6, 9.0 Hz)

^{13}C NMR (100 MHz, $CDCl_3$) δ 129.3, 128.5, 126.5, 77.7, 40.1, 39.1, 35.5

MS (EI) Calcd. for $C_{13}H_{15}NS_2$ $(M)^+$ 249.3949, found 249

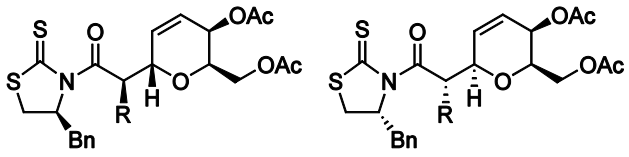

General procedure B. Preparation of substituted coupling products (90 and 91):[3]

A solution of (S)- or (R)-chiral auxiliary (**38** or **43**) in DCM was cooled to 0 °C using an ice-bath. $TiCl_4$ in DCM was added and the solution was stirred for 5 min. The reaction mixture was cooled to -78 °C using a dry-ice/acetone bath. Et_3N was subsequently added, and the reaction mixture was stirred at -78 °C for 0.5 h, and at room temperature for 0.5 h. The reaction mixture was subsequently cooled to -78 °C, and $SnCl_4$ in DCM and **44** in DCM

were then added. The reaction mixture was stirred at room temperature for 0.3 h, and then cooled to -78 °C. The reaction mixture was quenched with a saturated aqueous solution of NH_4Cl, and subsequently warmed to room temperature. The aqueous layer was extracted with DCM and the organic layer was washed with H_2O. The combined organic layers were washed with brine, dried over $MgSO_4$ and concentrated. The wanted compound was purified by silica flash chromatography.

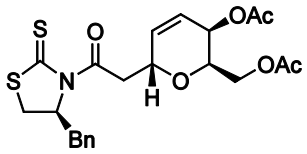

((2R,3R,6R)-3-acetoxy-6-(2-((S)-4-benzyl-2-thioxothiazolidin-3-yl)-2-oxoethyl)-3,6-dihydro-2H-pyran-2-yl)methyl acetate (90a):

The title compound was prepared from **38b** (3.58 g, 14.3 mmol) and **44** (1.94 g, 7.13 mmol) in DCM (71 mL) using general procedure B. $TiCl_4$ (1M in DCM, 15.7 mL, 15.7 mmol), $SnCl_4$ (1M in DCM, 15.7 mL, 15.7 mmol), and Et_3N (2.19 mL, 15.7 mmol) were added. Purification by silica flash chromatography 20 % ethyl acetate in hexanes gave **90a** as a yellow solid (2.24 g, 68 %).

R*f* 0.3 (hexanes/EtOAc, 3:2)

^{1}H NMR (400 MHz, $CDCl_3$) δ 7.36-7.28 (5H, m), 6.12 (1H, dd, *J* = 10.3, 3.0 Hz), 6.05 (1H, ddd, *J* = 10.2, 4.9, 2.1 Hz), 5.43 (1H, ddd, *J* = 10.6, 7.0, 3.9 Hz), 5.11 (1H, dd, *J* = 5.1, 2.6 Hz), 5.01 (1H, tdd, *J* = 7.8, 5.0, 2.4 Hz), 4.20 (2H, ddd, *J* = 18.1, 11.3, 6.3 Hz), 4.11 (1H, dt, *J* = 6.6, 6.3, 2.6 Hz), 3.60 (2H, m), 3.42 (1H, dd, *J* = 11.8, 7.6 Hz), 3.24 (1H, dd, *J* = 13.4, 3.5 Hz), 3.04 (1H, dd, *J* = 13.2, 10.7 Hz), 2.92 (1H, d, *J* = 11.5 Hz), 2.09 (3H, s), 2.08 (3H, s)

^{13}C NMR (100 MHz, $CDCl_3$) δ 201.4, 170.6, 170.4, 170.3, 136.2, 133.9, 129.3, 128.8, 127.2, 122.6, 69.5, 68.6, 68.5, 63.5, 62.6, 40.7, 36.8, 32.1, 20.9, 20.8

MS (ESI) $C_{22}H_{25}NO_6S_2$ $(M+Na)^+$ 486.5568, found 486.4

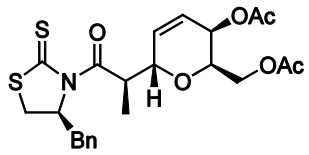

((2R,3R,6S)-3-acetoxy-6-((R)-1-((S)-4-benzyl-2-thioxothiazolidin-3-yl)-1-oxopropan-2-yl)-3,6-dihydro-2H-pyran-2-yl)methyl acetate (90b):

The title compound was prepared from **38b** (2.45 g, 9.6 mmol) and **44** (1.3 g, 4.79 mmol) in DCM (14 mL) using general procedure B. $TiCl_4$ (1M in DCM, 10.5 mL, 10.5 mmol), $SnCl_4$ (1M in DCM, 10.5 mL, 10. 5 mmol), and Et_3N (1.47 mL, 10.5 mmol) were added. Purification by silica flash chromatography 20 % ethyl acetate in hexanes gave **90b** as a yellow solid (1.79 g, 78 %).

R*f* 0.3 (hexanes/EtOAc, 8:2)

^{1}H NMR (400 MHz, $CDCl_3$) δ 7.35-7.27 (5H, m), 6.01 (2H, dd, *J* = 4.4, 1.2 Hz), 5.43 (1H, m), 5.15 (1H, m), 5.10 (1H, m), 4.64 (1H, d, *J* = 8.8 Hz), 4.21 (2H, m), 4.06 (1H, m), 3.38 (1H, dd, *J* = 11.4, 7.3 Hz), 3.22 (1H, dd, *J* = 13.2, 4.1 Hz), 3.05 (1H, dd, *J* = 13.2, 13.4 Hz), 2.88 (1H, d, *J* = 11.7 Hz), 2.09 (3H, s), 2.07 (3H, s), 1.32 (3H, d, *J* = 6.9 Hz)

^{13}C NMR (100 MHz, $CDCl_3$) δ 201.5, 175.2, 170.7, 170.5, 136.3, 132.9, 129.4, 129.4, 127.3, 123.1, 73.5, 69.3, 68.8, 63.8, 62.9, 40.7, 37.1, 31.7, 20.9, 20.8, 15.0

MS (ESI) Calcd. for $C_{23}H_{27}NO_6S_2$ $(M+Na)^+$ 500.5834, found 500.3

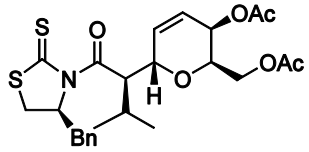

((2R,3R,6S)-3-acetoxy-6-((R)-1-((S)-4-benzyl-2-thioxothiazolidin-3-yl)-3-methyl-1-oxobutan-2-yl)-3,6-dihydro-2H-pyran-2-yl)methyl acetate (90d):

The title compound was prepared from **38d** (0.25 g, 0.86 mmol) and **44** (0.10 g, 0.37 mmol) in DCM (4 mL) using general procedure B. $TiCl_4$ (1M in DCM, 0.81 mL, 0.81 mmol), $SnCl_4$ (1M in DCM, 0.81 mL, 0.81 mmol), and Et_3N (0.11 mL, 0.81 mmol) were added.

Purification by silica flash chromatography 20 % ethyl acetate in hexanes gave **90d** as a yellow solid (0.069 g, 37 %).

R*f* 0.8 (hexanes/EtOAc, 1:1)

^{1}H NMR (400 MHz, $CDCl_3$) δ 7.37-7.34 (2H, m), 7.30-7.29 (3H, m), 5.99 (1H, ddd, *J* = 10.4, 5.2 1.8 Hz), 5.95 (1H, dd, *J* = 10.5, 2.9 Hz), 5.46 (1H, dd, *J* = 10.1, 4.6 Hz), 5.33 (1H, ddd, *J* = 10.9, 6.7, 4.5 Hz), 5.09 (1H, dd, *J* = 5.1, 2.5 Hz), 4.71 (1H, m), 4.25-4.17 (2H, m), 4.10 (1H, ddd, *J* = 7.3 4.9, 2.4 Hz), 3.34 (1H, dd, *J* = 11.4, 6.8 Hz), 3.25 (1H, dd, *J* = 13.2, 4.1 Hz), 3.06 (1H, dd, *J* = 13.2, 10.2 Hz), 2.90 (1H, d, *J* = 11.6 Hz), 2.30 (1H, dtd, *J* = 13.6, 6.8, 4.6 Hz), 2.09 (3H, s), 2.06 (3H, s), 1.05 (3H, d, *J* = 7.1, 1.02 (3H, d, *J* = 6.8 Hz)

^{13}C NMR (100 MHz, $CDCl_3$) δ 202.3, 173.7, 170.6, 170.5, 136.2, 133.3, 129.5, 128.9, 127.3, 122.6, 72.2, 68.9, 68.7, 63.8, 62.0, 48.1, 36.8, 32.3, 30.0, 20.9, 20.8, 20.2, 18.6

MS (ESI) Calcd. for $C_{25}H_{31}NO_6S_2$ $(M+H)^+$ 506.6547, found 506.4, $(M+Na)^+$ 528.6365, found 528.3

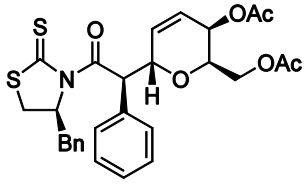

((2R,3R,6S)-3-acetoxy-6-((R)-2-((S)-4-benzyl-2-thioxothiazolidin-3-yl)-2-oxo-1-phenylethyl)-3,6-dihydro-2H-pyran-2-yl)methyl acetate (90e):

The title compound was prepared from **38e** (0.23 g, 0.74 mmol) and **44** (0.10 g, 0.37 mmol) in DCM (4 mL) using general procedure B. $TiCl_4$ (1M in DCM, 0.81 mL, 0.81 mmol), $SnCl_4$ (1M in DCM, 0.81 mL, 0.81 mmol), and Et_3N (0.11 mL, 0.81 mmol) were added. Purification by silica flash chromatography 25 % ethyl acetate in hexanes gave **90e** as a yellow solid (0.18 g, 92 %).

R*f* 0.3 (hexanes/EtOAc, 3:1)

^{1}H NMR (400 MHz, $CDCl_3$) δ 7.39-7.27 (10H, m), 6.64 (1H, d, *J* = 9.9 Hz), 6.19 (1H, dd, *J* = 10.4, 3.0 Hz), 6.08 (1H, ddd, *J* = 10.3, 5.4, 2.0 Hz), 5.20 (1H, m), 5.08 (1H, m), 5.01 (1H,

m), 4.04 (1H, dd, *J* = 6.2, 2.8 Hz), 4.11 (2H, ddd, *J* = 7.3, 5.0, 2.8 Hz), 3.28 (1H, dd, *J* = 13.2, 4.1 Hz), 3.08 (2H, ddd, *J* = 20.2, 12.5, 8.6 Hz), 2.77 (1H, d, *J* = 11.5Hz), 2.05 (3H, s), 1.94 (3H, s)

^{13}C NMR (100 MHz, $CDCl_3$) δ 201.7, 172.6, 170.5, 170.4, 136.2, 135.4, 133.0, 129.4, 129.0, 128.9, 128.6, 128.0, 127.3, 123.3, 74.4, 69.2, 68.8, 63.5, 62.8, 50.3, 36.9, 31.8, 20.8, 20.7

MS (ESI) Calcd. for $C_{28}H_{29}NO_6S_2$ $(M+H)^+$ 540.6709, found 540.3, $(M+Na)^+$ 562.6527 found 562.3

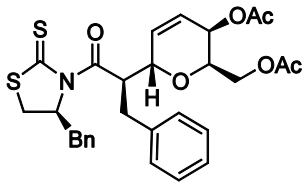

((2R,3R,6S)-3-acetoxy-6-((R)-1-((S)-4-benzyl-2-thioxothiazolidin-3-yl)-1-oxo-3-phenylpropan-2-yl)-3,6-dihydro-2H-pyran-2-yl)methyl acetate (90f):

The title compound was prepared from **38f** (1.28 g, 3.75 mmol) and **44** (0.51 g, 1.87 mmol) in DCM (19 mL) using general procedure B. $TiCl_4$ (1M in DCM, 4.12 mL, 4.12 mmol), $SnCl_4$ (1M in DCM, 4.12 mL, 4.12 mmol), and Et_3N (0.58 mL, 4.12 mmol) were added. Purification by silica flash chromatography 25 % ethyl acetate in hexanes gave **90f** as a yellow solid (0.32 g, 31 %).

R*f* 0.6 (hexanes/EtOAc, 1:1)

^{1}H NMR (400 MHz, $CDCl_3$) δ 7.33-7.14 (10H, m), 6.03 (1H, ddd, *J* = 10.2, 5.2, 1.9 Hz), 5.96 (1H, dd, *J* = 10.3, 2.9 Hz), 5.63 (1H, dt, *J* = 10.8, 4.8 Hz), 5.13 (1H, dd, *J* = 5.1, 2.1 Hz), 4.77 (1H, m), 4.67 (1H, m), 4.31-4.21 (3H, m), 3.41 (1H, dd, *J* = 13.2, 4.7 Hz), 3.11 (1H, dd, *J* = 13.2, 4.4 Hz), 2.86 (2H, ddd, *J* = 18.8, 13.2, 13.6 Hz), 2.55 (1H, d, *J* = 11.2 Hz), 2.47 (1H, dd, *J* = 11.2, 6.7 Hz), 2.11 (3H, s), 2.08 (3H, s)

^{13}C DEPT NMR (100 MHz, $CDCl_3$) δ 132.5, 129.3, 138.6, 128.4, 128.4, 127.0, 126.6, 122.5, 73.6, 69.2, 68.4, 63.7, 63.1, 45.8, 38.6, 36.7, 32.0, 20.7, 20.7

MS (ESI) Calcd. for $C_{29}H_{31}NO_6S_2$ $(M+H)^+$ 554.6975, found 554.186, $(M+NH_4)^+$ 571.7280, found 571.222, $(M+Na)^+$ 576.6793, found 576.174.

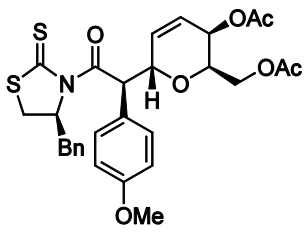

((2R,3R,6S)-3-acetoxy-6-((R)-2-((S)-4-benzyl-2-thioxothiazolidin-3-yl)-1-(4-methoxyphenyl)-2-oxoethyl)-3,6-dihydro-2H-pyran-2-yl)methyl acetate (90g):

The title compound was prepared from **38g** (0.83 g, 2.2 mmol) and **44** (0.30 g, 1.1 mmol) in DCM (10 mL) using general procedure B. $TiCl_4$ (1M in DCM, 2.4 mL, 2.4 mmol), $SnCl_4$ (1M in DCM, 2.4 mL, 2.4 mmol), and Et_3N (0.34 mL, 2.4 mmol) were added. Purification by silica flash chromatography 20 % ethyl acetate in hexanes gave **90g** as a yellow solid (0.485 g, 77 %).

R*f* 0.7 (hexanes/EtOAc, 1:1)

^{1}H NMR (400 MHz, $CDCl_3$) δ 7.36-7.27 (7H, m), 6.85 (2H, m), 6.55 (1H, d, *J* = 9.8 Hz), 6.17 (1H, dd, *J* = 10.4, 3.0 Hz), 6.07 (1H, ddd, *J* = 10.3, 5.4, 2.0 Hz), 5.20 (1H, m), 5.07 (1H, dd, *J* = 5.2, 2.0 Hz), 4.95 (1H, m), 4.05 (3H, m), 3.49 (3H, s), 3.28 (1H, dd, *J* = 13.2, 4.1 Hz), 3.14-3.03 (2H, m), 2.77 (1H, d, *J* = 11.5 Hz), 2.04 (3H, s), 1.97 (3H, s)

^{13}C DEPT NMR (100 MHz, $CDCl_3$) δ 201.6, 173.0, 170.5, 170.5, 159.3, 136.3, 133.1, 130.1, 129.5, 128.9, 127.4, 127.3, 123.2, 114.1, 74.4, 69.3, 68.8, 63.5, 62.9, 55.2, 49.6, 36.9, 31.9, 20.9, 20.8

MS (ESI) Calcd. for $C_{29}H_{31}NO_7S_2$ $(M+H)^+$ 592.6787, found 592.3

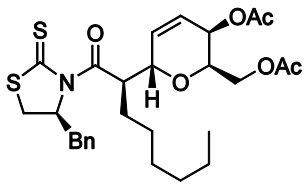

((2R,3R,6S)-3-acetoxy-6-((R)-1-((S)-4-benzyl-2-thioxothiazolidin-3-yl)-1-oxooctan-2-yl)-3,6-dihydro-2H-pyran-2-yl)methyl acetate (90j):

The title compound was prepared from **38j** (0.71 g, 2.20 mmol) and **44** (0.30 g, 1.10 mmol) in DCM (11 mL) using general procedure B. $TiCl_4$ (1M in DCM, 2.4 mL, 2.4 mmol), $SnCl_4$ (1M in DCM, 2.4 mL, 2.4 mmol), and Et_3N (0.34 mL, 2.4 mmol) were added. Purification by silica flash chromatography 20 % ethyl acetate in hexanes gave **90j** as a yellow solid (0.35 g, 58 %).

R*f* 0.7 (hexanes/EtOAc, 1:1)

^{1}H NMR (400 MHz, $CDCl_3$) δ 7.36-7.33 (2H, m), 7.30-7.28 (3H, m), 5.99 (2H, m), 5.39 (1H, ddd, *J* = 10.8, 6.8, 4.2 Hz), 5.26 (1H, m), 5.09 (1H, m), 4.65 (1H, m), 4.23-4.17 (2H, m), 4.09 (1H, ddd, *J* = 7.6, 4.8, 2.6 Hz), 3.35 (1H, dd, *J* = 11.6, 7.1 Hz), 3.23 (1H, dd, *J* = 13.3, 4.0 Hz), 3.05 (1H, dd, *J* = 13.2, 10.5 Hz), 2.90 (1H, d, *J* = 11.4 Hz), 2.08 (3H, s), 2.06 (3H, s), 1.84 (2H, m), 1.30-1.25 (8H, m), 0.86 (3H, t, *J* = 6.9 Hz)

^{13}C NMR (100 MHz, $CDCl_3$) δ 201.6, 175.0, 170.6, 170.5, 136.3, 132.9, 129.5, 128.9, 128.3, 122.9, 73.2, 69.3, 68.8, 63.8, 63.0, 45.0, 36.9, 31.6, 30.4, 29.4, 26.3, 22.6, 20.9, 20.8, 14.0

MS (ESI) Calcd. for $C_{28}H_{38}NO_6S_2$ $(M+H)^+$ 548.7344, found 548.5, $(M+Na)^+$ 570.7163, found 570.4

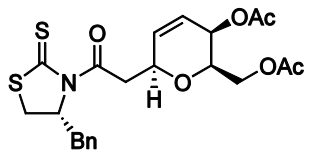

((2R,3R,6S)-3-acetoxy-6-(2-((R)-4-benzyl-2-thioxothiazolidin-3-yl)-2-oxoethyl)-3,6-dihydro-2H-pyran-2-yl)methyl acetate (91a):

The title compound was prepared from **43a** (1.0 g, 3.98 mmol) and **44** (0.54 g, 1.99 mmol) in DCM (20 mL) using general procedure B. $TiCl_4$ (1M in DCM, 4.38 mL, 4.38 mmol), $SnCl_4$ (1M in DCM, 4.38 mL, 4.38 mmol), and Et_3N (0.61 mL, 4.38 mmol) were added. Purification by silica flash chromatography 25 % ethyl acetate in hexanes gave **91a** as a yellow solid (0.40 g, 43 %).

R*f* 0.4 (hexanes/EtOAc, 3:2)

^{1}H NMR (400 MHz, $CDCl_3$) δ 7.37-7.28 (5H, m), 6.04 (2H, m), 5.35 (1H, ddd, *J* = 10.6, 6.9, 4.0 Hz), 5.08 (1H, m), 4.74 (1H, m), 4.19 (2H, dq, *J* = 11.4, 6.4 Hz), 3.94 (1H, m), 3.57 (1H, dd, *J* = 17.5, 8.1 Hz), 3.51-3.41 (2H, m), 3.25 (1H, dd, *J* = 13.2, 3.9 Hz), 3.05 (1H, dd, *J* = 13.2, 10.5 Hz), 2.92 (1H, d, *J* = 11.6 Hz), 2.08 (3H, s), 2.04 (3H, s);

^{13}C NMR (100 MHz, $CDCl_3$) δ 201.3, 170.7, 170.6, 170.6, 136.4, 135.1, 129.4, 128.9, 127.2, 123.3, 73.9, 71.5, 68.6, 63.8, 62.8, 43.7, 36.8, 32.3, 21.0, 20.8

MS (ESI) Calcd. for $C_{22}H_{25}NO_6S_2$ $(M+Na)^+$ 486.5568, found 486.4

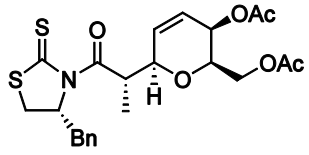

((2R,3R,6R)-3-acetoxy-6-((S)-1-((R)-4-benzyl-2-thioxothiazolidin-3-yl)-1-oxopropan-2-yl)-3,6-dihydro-2H-pyran-2-yl)methyl acetate (91b):

The title compound was prepared from **43b** (3.24 g, 12.6 mmol) and **44** (1.72 g, 6.3 mmol) in DCM (63 mL) using general procedure B. $TiCl_4$ (1M in DCM, 13.9 mL, 13.9 mmol), $SnCl_4$ (1M in DCM, 13.9 mL, 13.9 mmol), and Et_3N (1.94 mL, 13.9 mmol) were added.

Purification by silica flash chromatography 20 % ethyl acetate in hexanes gave **91b** as a yellow solid (2.32 g, 76 %).

R*f* 0.9 (DCM/Et_2O, 1:1)

^{1}H NMR (400 MHz, $CDCl_3$) δ 7.36-7.27 (5H, m), 6.09 (1H, ddd, *J* = 10.1, 5.5, 2.1 Hz), 5.99 (1H, dd, *J* = 10.2, 1.2 Hz), 5.55 (1H, m), 5.03 (1H, td, *J* = 5.3, 2.0 Hz), 4.90 (1H, dq, *J* = 6.8, 4.5 Hz), 4.73 (1H, m), 4.16 (2H, d, *J* = 6.0 Hz), 3.90 (1H, dt, *J* = 6.1, 2.2 Hz), 3.38 (1H, dd, *J* = 11.7, 7.6 Hz), 3.21 (1H, dd, *J* = 13.2, 3.6 Hz), 3.02 (1H, dd, *J* = 13.2, 10.6 Hz), 2.91 (1H, dd, *J* = 11.6, 1.5 Hz), 2.00 (3H, s), 1.82 (3H, s), 1.23 (3H, d, *J* = 6.9 Hz)

^{13}C NMR (100 MHz, $CDCl_3$) δ 201.1, 174.7, 170.7, 170.6, 136.4, 133.9, 129.4, 129.0, 127.3, 123.7, 75.5, 73.7, 68.9, 63.8, 63.4, 43.0, 37.5, 31.7, 20.8, 20.5, 11.3

IR νmax (neat): 702, 735, 1229, 1709, 1732, 2923, 3048 cm^{-1}

MS (ESI) Calcd. for $C_{23}H_{27}NO_6S_2$ $(M+Na)^+$ 500.5834, found 500.3

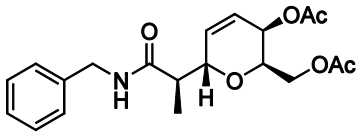

((2R,3R,6S)-3-acetoxy-6-((R)-1-(benzylamino)-1-oxopropan-2-yl)-3,6-dihydro-2H-pyran-2-yl)methyl acetate (102):adapted from Larossa *et al.*[3]

To a solution of **90b** (0.050 g, 0.105 mmol) in DCM (1 mL), was added benzylamine (0.011 g, 0.105 mmol), and Et_3N (0.016 g, 0.115 mmol). The reaction mixture was stirred at room temperature for 16 h. The reaction mixture was diluted with DCM and washed with a saturated aqueous solution of $NaHCO_3$, H_2O, and brine. The aqueous layer was subsequently washed with DCM. The combined organic layers were washed with brine, dried over $MgSO_4$ and concentrated. Purification by silica flash chromatography with 20 % EtOAc in hexanes gave **102** (0.035 g, 89 %) as a white solid.

R*f* 0.2 (hexanes/EtOAc, 3:1)

^{1}H NMR (400 MHz, $CDCl_3$) δ 7.35-7.29 (5H, m), 6.12 (1H, m), 5.99 (1H, m), 5.10 (m, 1H), 4.45 (2H, d, *J* = 5.7 Hz), 4.26-4.04 (3H, m), 2.52 (1H, p, *J* = 6.8 Hz), 2.05 (3H, s), 1.99 (3H, s), 1.30 (3H, d, *J* = 7.0 Hz)

MS (ESI) Calcd. for $C_{20}H_{25}NO_6$ $(M+Na)^+$ 398.4054, found 398.3

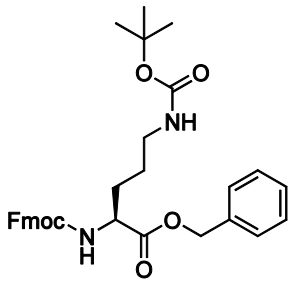

(S)-benzyl 1-(9H-fluoren-9-yl)-12,12-dimethyl-3,10-dioxo-2,11-dioxa-4,9-diazatridecane-5-carboxylate (104):[15]

To a solution of Fmoc-orn(Boc)-OH (**93**) (10.0 g, 22.0 mmol) in DCM (100 mL), was added DCC (5.0 g, 24.2 mmol), BnOH (2.6 g, 24.2 mmol), and DMAP (0.268 g, 2.42 mmol). The reaction mixture was stirred at room temperature for overnight. The reaction mixture was filtered, and the filtrate was diluted with DCM, and washed with a 5 % aqueous solution of acetic acid, H_2O, and brine. The aqueous fractions were then washed with DCM. The combined organic layers were washed with brine, dried over $MgSO_4$ and concentrated. Purification by silica flash chromatography with a gradient of 100 % DCM to 60 % DCM in Et_2O gave **104** (6.46 g, 54 %) as a white solid.

R*f* 0.8 **(**DCM/Et_2O, 4:1)

^{1}H NMR (400 MHz, MeOD) δ 7.77 (2H, d, *J* = 7.5 Hz), 7.60 (2H, d, *J* = 7.4 Hz), 7. 43-7.29 (9H, m), 5.47 (1H, d, *J* = 8.0 Hz), 5.18 (2H, m), 4.50 (1H, bs), 4.46-4.39 (3H, m), 4.21 (1H, t, *J* = 6.9 Hz), 3.11 (2H, dd, *J* = 12.7, 6.9 Hz), 1.89 (1H, m), 1.68 (1H, m), 1.58-1.40 (2H, m), 1.44 (9H, s)

All spectral data was in accordance with the literature.[15]

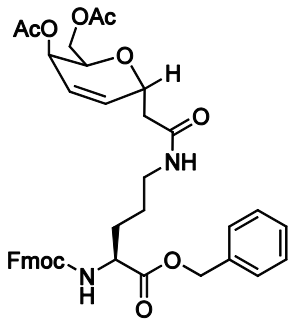

(2S)-benzyl 2-(((9H-fluoren-9-yl)methoxy)carbonylamino)-5-(2-((2R,6R)-5-acetoxy-6-(acetoxymethyl)-5,6-dihydro-2H-pyran-2-yl)acetamido)pentanoate (105a):

To a solution of **111a** (0.489 g, 1.83 mmol) in DCM (20 mL) with molecular sieves was added HBTU (0.763 g, 2.01 mmol). The reaction mixture was stirred at room temperature for 0.3 h, and **37** (1.20 g, 2.38 mmol) and DIPEA (0.709 g, 5.49 mmol) were subsequently added. The reaction mixture was then stirred at room temperature for overnight. The reaction mixture was diluted with DCM, and the organic fraction washed with H_2O, and brine. The aqueous fractions were then washed with DCM. The combined organic layers were dried over $MgSO_4$ and concentrated. Purification by silica flash chromatography with a gradient of 10% EtOAc in hexanes to 25% EtOAc in hexanes to 5% MeOH in DCM, followed by a second purification by silica flash chromatography with 2% MeOH in DCM gave **105a** (0.968 g, 76%) as a clear, colourless, hard gel.

R*f* 0.7 (DCM/MeOH, 95:5)

^{1}H NMR (400 MHz, $CDCl_3$) δ 7.36-7.33 (2H, m), 7.30-7.28 (3H, m), 5.99 (2H, m), 5.39 (1H, ddd, *J* = 10.8, 7.0, 4.1 Hz), 5.26 (1H, ddd, 7.2, 7.7, 6.4 Hz), 5.10 (1H, dd, *J* = 4.1, 2.4 Hz), 4.65 (1H, dd, *J* = 8.9, 1.4 Hz), 4.20 (2H, dd, *J* = 6.2, 4.2 Hz), 4.09 (1H, ddd, *J* = 7.6, 4.8, 2.6 Hz), 3.35 (1H, dd, *J* = 11.3, 6.9 Hz), 3.23 (1H, dd, *J* = 12.9, 4.1 Hz), 3.06 (1H, dd, *J* = 13.2, 10.5 Hz), 2.90 (1H, d, *J* =11.4 Hz), 2.08 (3H, s), 2.07 (3H, s), 1.85 (2H, dd, *J* = 14.4, 7.8 Hz), 1.29-1.25 (8H, m), 0.86 (3H, t, *J* = 6.96 Hz)

^{13}C DEPT135 NMR (100 MHz, $CDCl_3$) δ 201.6, 175.0, 170.6, 170.5, 136.3, 132.9, 129.5, 128.9, 128.3, 127.3, 122.9, 73.2, 69.3, 68.8, 63.8, 63.0, 45.0, 36.9, 32.1, 31.6, 30.4, 29.4, 26.3, 22.6, 20.9, 20.8, 14.0

MS (ESI) Calcd. for $C_{39}H_{42}N_2O_{10}$ $(M+H)^+$ 699.7661, found 699.653, $(M+Na)^+$ 721.7480, found 721.652

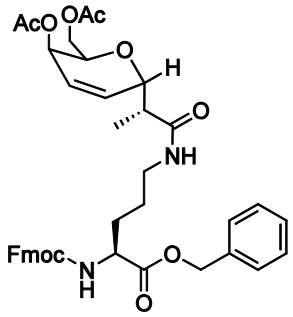

(S)-benzyl 2-(((9H-fluoren-9-yl)methoxy)carbonylamino)-5-((R)-2-((2S,5R,6R)-5-acetoxy-6-(acetoxymethyl)-5,6-dihydro-2H-pyran-2-yl)propanamido)pentanoate (105b):

To a solution of **90b** (0.100 g, 0.216 mmol) in DCM (2 mL), was added **37** (0.101 g, 0.216 mmol), and Et_3N (0.044 g, 0.432 mmol). The reaction mixture was stirred for 1 h. Since the reaction was incomplete, as determined by thin-layer chromatography, additional Et_3N (0.022 g, 0.216 mmol) was added, and the reaction mixture was stirred for an additional 2 h. The reaction mixture was diluted with DCM and washed with a saturated aqueous solution of $NaHCO_3$, H_2O, and brine. The aqueous layer was subsequently washed with DCM. The combined organic layers were washed with brine, dried over $MgSO_4$ and concentrated. Purification by recrystallization from hexanes and MeOH gave **105b** (0.050 g, 38 %) as an off-white solid.

OR:

To a solution of **11b** (0.207 g, 0.723 mmol) in DCM (7.2 mL) was added HBTU (0.302 g, 0.795 mmol), and the reaction mixture was stirred for 1 h. Subsequently, **37** (0.474 g, 0.940 mmol) and DIPEA (0.280 g, 2.17 mmol) were added sequentially, and the reaction mixture was stirred for overnight. The reaction mixture was diluted with DCM and washed with H_2O. The aqueous layer was subsequently washed with DCM. The combined organic layers were washed with brine, dried over $MgSO_4$ and concentrated. Purification by silica flash chromatography with 1 % MeOH in DCM gave **105b** (0.251 g, 49 %) as an off-white solid.

R*f* 0.7 (DCM/MeOH, 9:1)

^{1}H NMR (400 MHz, $CDCl_3$) δ 7.77 (2H, d, *J* = 7.5 Hz), 7.60 (2H, dd, *J* = 7.0, 4.1 Hz), 7.42-7.29 (9H, m), 5.98 (1H, dd, *J* = 10.5, 2.3 Hz), 5.94 (1H, ddd, *J* = 10.5, 4.3, 1.8 Hz), 5.55 (1H, d, *J* = 8.2 Hz), 5.19 (2H, q, *J* = 12.2 Hz), 5.10 (1H, m), 4.45-4.36 (4H, m), 4.25-4.20 (2H, m), 4.16 (1H, dd, *J* = 11.7, 4.2 Hz), 4.06 (1H, td, *J* = 7.8, 3.8 Hz), 3.25 (2H, dd, *J* = 12.5, 6.4 Hz), 2.43 (1H, m), 2.08 (3H, s), 2.06 (3H, s), 1.24 (3H, d, *J* = 6.9 Hz)

^{13}C NMR (100 MHz, $CDCl_3$) δ 173.4, 171.9, 170.7, 170.4, 156.0, 143.8, 143.6, 141.3, 135.1, 132.5, 128.7, 128.6, 128.4, 127.7, 127.1, 125.1, 123.2, 120.0, 120.0, 73.2, 69.2, 67.4, 67.1, 63.8, 62.6, 53.5, 47.1, 44.2, 38.7, 30.1, 25.3, 20.9, 20.8, 14.5

MS (ESI) Calcd. for $C_{40}H_{44}N_2O_{10}$ $(M+Na)^+$ 735.7745, found 735.4

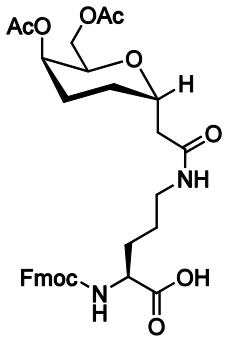

(S)-2-(((9H-fluoren-9-yl)methoxy)carbonylamino)-5-(2-((2S,5R,6R)-5-acetoxy-6-(acetoxymethyl)tetrahydro-2H-pyran-2-yl)acetamido)pentanoic acid (106a):

To a solution of **105a** (0.872 g, 1.25 mmol) in EtOAc (12 mL) and MeOH (12 mL) was added 10% palladium on carbon (0.255 g). The suspension was purged with N_2 (g) and then with H_2 (g). The reaction mixture was stirred at room temperature under H_2 (g) at normal atmosphere for 1 h. The reaction mixture was filtered, and the filtrate was concentrated. Purification by silica flash chromatography with 2% AcOH and 3% MeOH in DCM followed by purification by reverse-phase HPLC gave **106a** (0.194 g, 25%) as a white foam after lyophilization.

R*f* 0.3 (DCM/MeOH, 95:5)

^{1}H NMR (400 MHz, $CDCl_3$) δ 7.79 (2H, d, *J* = 7.5 Hz), 7.67 (2H, t, *J* = 7.3 Hz), 7.39 (2H, t. *J* = 7.4 Hz), 7.31 (2H, dt, *J* = 7.5, 0.9 Hz), 4.89 (1H, m), 4.35 (2H, dd, *J* = 7.0, 1.3 Hz), 4. 27-

4.21 (3H, m), 4.17-4.07 (3 H, m), 3.21 (2H, d, *J* = 2.1 Hz), 2.58 (1H, dd, *J* = 14.0, 8.7 Hz), 2.31 (1H, dd, *J* = 14.1, 5.3 Hz), 2.03 (3H, s), 2.01 (3H, s), 1.98-1.40 (8H, m)

^{13}C NMR (100 MHz, $CDCl_3$) δ 173.2, 172.0, 158.7, 145.4, 145.2, 142.6, 128.8, 128.2, 126.3, 126.3, 121.0, 71.0, 70.2, 69.1, 68.0, 67.6, 62.9, 55.2, 48.5, 43.9, 40.4, 27.0, 26.9, 24.5, 20.9, 20.9

MS (ESI) Calcd. for $C_{32}H_{38}N_2O_{10}$ $(M+H)^+$ 611.6595, found 611.530, $(M+Na)^+$ 633.6413, found 633.504

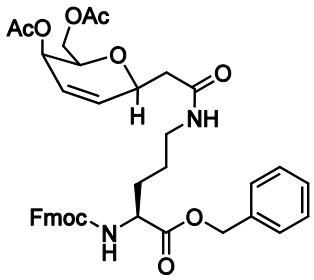

(S)-benzyl 2-(((9H-fluoren-9-yl)methoxy)carbonylamino)-5-(2-((2S,5R,6R)-5-acetoxy-6-(acetoxymethyl)-5,6-dihydro-2H-pyran-2-yl)acetamido)pentanoate (107a):

To a solution of **120a** (0.572 g, 2.10 mmol) in DCM (20 mL) with molecular sieves was added HBTU (0.876 g, 2.31 mmol). The reaction mixture was stirred at room temperature for 0.3 h, and **37** (1.38 g, 2.73 mmol) and DIPEA (0.816 g, 5.49 mmol) were subsequently added. The reaction mixture was then stirred at room temperature for overnight. The reaction mixture was diluted with DCM, and the organic fraction washed with H_2O, and brine. The aqueous fractions were then washed with DCM. The combined organic layers were dried over $MgSO_4$ and concentrated. Purification by silica flash chromatography with a gradient of 1% MeOH in DCM to 2% MeOH in DCM gave **107a** (1.247 g, 85%) as a clear, colourless, hard gel

R*f* 0.8 (DCM/MeOH, 95:5)

^{1}H NMR (400 MHz, $CDCl_3$) δ 7.34-7.28 (5H, m), 5.99 (1H, ddd, *J* = 10.2, 4.9, 1.7 Hz), 5.94 (1H, dd, *J* = 10.4, 2.8 Hz), 5.46 (1H, dd, *J* = 10.1, 4.6 Hz), 5.33 (1H, ddd, *J* = 10.5, 6.7, 4.2 Hz), 5.09 (1H, dd, *J* = 4.9, 2.4 Hz), 4.70 (1H, m), 4.21 (2H, t, *J* = 6.0 Hz), 4.10 (1H, ddd, *J* =

7.6, 5.1, 2.6 Hz), 3.33 (1H, dd, *J* = 11.5, 6.6 Hz), 3.25 (1H, dd, *J* = 13.2, 4.2 Hz), 3.06 (1H, dd, *J* = 13.1, 10.3 Hz), 2.90 (1H, d, *J* = 11.5 Hz), 2.29 (1H, m), 2.09 (3H, m), 2.06 (3H, m), 1.04 (6H, dd, *J* = 11.1, 6.9 Hz)

^{13}C NMR (100 MHz, $CDCl_3$) δ 202.3, 173.7, 170.5, 136.2, 133.3, 129.5, 128.9, 127.3, 122.6, 72.2, 68.9, 68.7, 63.8, 63.0, 48.1, 36.8, 32.3, 30.0, 20.9, 20.8, 20.2, 18.6

MS (ESI) Calcd. for $C_{39}H_{42}N_2O_{10}$ $(M+H)^+$ 699.7661, found 699.630, $(M+Na)^+$ 721.7480, found 721.613

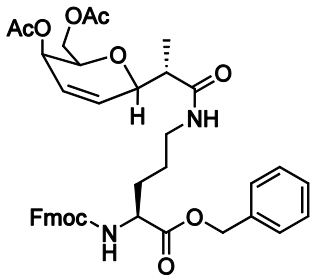

(S)-benzyl 2-(((9H-fluoren-9-yl)methoxy)carbonylamino)-5-((S)-2-((2R,5R,6R)-5-acetoxy-6-(acetoxymethyl)-5,6-dihydro-2H-pyran-2-yl)propanamido)pentanoate (107b):

To a solution of **91b** (2.0 g, 4.19 mmol) in DCM (42 mL), was added **37** (2.34 g, 4.19 mmol), and Et_3N (0.876 g, 6.28 mmol). The reaction mixture was stirred at room temperature for overnight. Since the reaction was incomplete, as determined by thin-layer chromatography, additional Et_3N (0.218 g, 2.15 mmol) was added, and the reaction mixture was stirred at room temperature to overnight. The reaction mixture was diluted with DCM and washed with H_2O, and brine. The aqueous layer was subsequently washed with DCM. The combined organic layers were washed with brine, dried over $MgSO_4$ and concentrated. Purification by silica flash chromatography with a gradient of 100 % hexanes to 50 % EtOAc in hexanes gave **107b** (0.556 g, 61 %) as an off-white foam.

OR

To a solution of **120b** (0.219 g, 0.765 mmol) in DCM (7.7 mL) was added HBTU (0.319 g, 0.841 mmol), and the reaction mixture was stirred for 1 h. Subsequently, **37** (0.502 g, 9.94 mmol) and DIPEA (0.297 g, 2.29 mmol) were added sequentially, and the reaction mixture

was stirred for two days. The reaction mixture was diluted with DCM and washed with H_2O. The aqueous layer was subsequently washed with DCM. The combined organic layers were washed with brine, dried over $MgSO_4$ and concentrated. Purification by silica flash chromatography with 1% MeOH in DCM gave **107b** (0.453 g, 83%) as an off-white solid.

^{1}H NMR (500 MHz, $CDCl_3$) δ 7.76 (2H, d, *J* = 7.6 Hz), 7.60 (2H, m), 7.41-7.29 (9H, m), 6.41 (1H, t, *J* = 5.4 Hz), 6.01 (1H, ddd, *J* = 9.9, 5.4, 1.8 Hz), 5.90 (1H, d, *J* =10.4 Hz), 5.68 (1H, d, *J* = 8,2 Hz), 5.18 (2H, m), 5.08 (1H, m), 4.44-4.38 (2H, m), 4.34 (1H, dd, *J* = 10.5, 7.4 Hz), 4.30 (1H, dd, *J* = 3.6, 1.7 Hz), 4.27 (1H, dd, *J* = 11.8, 7.7 Hz), 4.21 (1H, t, *J* = 6.9 Hz), 4.14 (1H, dd, *J* = 11.6, 4.7 Hz), 3.89 (1H, ddd, *J* = 7.2, 4.7, 2.2 Hz), 3.23 (2H, m), 2.56 (1H, dq, *J* = 7.1, 4.3 Hz), 2.04 (3H, s), 2.03 (3H, s), 1.89 (1H, m), 1.70 (1H, dt, *J* = 14.4, 14.7, 8.6 Hz), 1.55 (2H, m)

^{13}C NMR (125 MHz, $CDCl_3$) δ 173.3, 172.0, 170.7, 170.2, 156.0, 143.9, 143.6, 141.2, 141.2, 135.2, 132.9, 128.6, 128.5, 128.3, 127.7, 127.0, 125.1, 125.0, 123.9, 119.9, 76.1, 74.0, 67.2, 67.0, 63.8, 62.9, 53.8, 47.1, 44.3, 38.7, 38.6, 29.8, 25.7, 20.8, 20.8, 12.3

MS (ESI) Calcd. for $C_{40}H_{44}N_2O_{10}$ $(M+H)^+$ 713.7927, found 713.662, $(M+Na)^+$ 735.7745, found 735.666

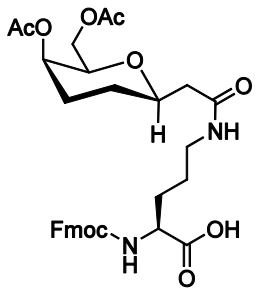

(S)-2-(((9H-fluoren-9-yl)methoxy)carbonylamino)-5-(2-((2R,5R,6R)-5-acetoxy-6-(acetoxymethyl)tetrahydro-2H-pyran-2-yl)acetamido)pentanoic acid (108a):

To a solution of **107a** (0.890 g, 1.27 mmol) in EtOAc (13 mL) and MeOH (13 mL) was added 10% palladium on carbon (0.270 g). The suspension was purged with N_2 (g) and then with H_2 (g). The reaction mixture was stirred at room temperature under H_2 (g) at normal atmosphere for 1 h. The reaction mixture was filtered, and the filtrate was concentrated.

Purification by silica flash chromatography with 2% AcOH and 3% MeOH in DCM followed by purification by reverse-phase HPLC gave **108a** (0.148 g, 19%) as a white foam after lyophilization.

R*f* 0.4 (DCM/MeOH, 95:5)

^{1}H NMR (400 MHz, MeOH) δ 7.76 (2H, d, *J* = 7.5 Hz), 7.65 (2H, t, *J* = 7.6 Hz), 7.36 (2H, t, *J* = 7.4 Hz), 7.28 (2H, dt, *J* = 7.4, 0.8 Hz), 4.84 (1H, m), 4.32 (2H, d, *J* = 7.2 Hz), 4.19 (1H, t, *J* = 7.0 Hz), 4.14 (1H, dd, *J* = 8.9, 6.4 Hz), 4.04 (1H, dd, *J* = 11.2, 5.9 Hz), 3.97 (1H, dd, *J* = 11.3, 6.8 Hz), 3.81 (1H, m), 3.74 (1H, t. *J* = 6.4 Hz), 3.19 (2H, m), 2.01 (3H, s), 1.98-1.93 (4H, m), 1.90-1.47 (8H, m)

MS (ESI) Calcd. for $C_{32}H_{38}N_2O_{10}$ $(M+Na)^+$ 633.6413, found 633.484

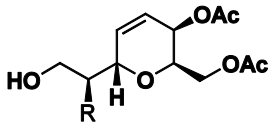

General procedure C. Preparation of alcohol galactal derivatives (109):[3, 16]

A solution of THF and H_2O was added to **90** and $NaBH_4$ was subsequently added. The reaction mixture was stirred at room temperature for 0.3 h. The reaction mixture was diluted with DCM and washed with H_2O, and brine. The aqueous layer was subsequently washed with DCM. The combined organic layers were washed with brine, dried over $MgSO_4$ and concentrated. Purification by silica flash chromatography with 50 % EtOAc in hexanes, gave the final product.

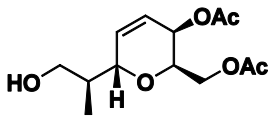

((2R,3R,6S)-3-acetoxy-6-((S)-1-hydroxypropan-2-yl)-3,6-dihydro-2H-pyran-2-yl)methyl acetate (109b-α):

The title compound was prepared from **90b** (1.41 g, 2.96 mmol) and $NaBH_4$ (1.30 g, 2.96 mmol) in THF (20 mL) and H_2O (10 mL) using general procedure C. Purification by silica flash chromatography with 50 % EtOAc in hexanes, gave **109b-α** (0.660 g, 82 %) as a clear, pale yellow oil.

R*f* 0.3 (hexanes/EtOAc, 1:1)

^{1}H NMR (400 MHz, $CDCl_3$) δ 6.03 (1H, d, *J* = 10.6, 2.0 Hz), 5.98 (1H, m), 5.20 (1H, m), 4.40 (1H, ddd, *J* = 5.5, 3.6, 1.9 Hz), 4.27 (1H, dd, *J* = 10.1, 7.7 Hz), 4.19 (2H, m), 3.68 (2H, dq, *J* = 11.0, 5.1 Hz), 2.08 (3H, s), 2.08 (3H, s), 1.93 (1H, m), 1.02 (3H, d, *J* = 7.07 Hz)

^{13}C NMR (100 MHz, $CDCl_3$) δ 170.9, 170.5, 133.3, 123.1, 73.8, 69.9, 65.8, 64.4, 62.5, 39.2, 20.9, 20.8, 12.3

MS (ESI) Calcd. for $C_{13}H_{20}O_6$ $(M+NH_4)^+$, found 290.3, $(M+Na)^+$ 295.2841, found 295.3

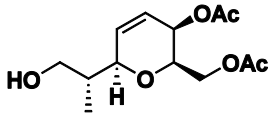

((2R,3R,6R)-3-acetoxy-6-((R)-1-hydroxypropan-2-yl)-3,6-dihydro-2H-pyran-2-yl)methyl acetate (109b-β):

The title compound was prepared from **91b** (2.32 g, 4.86 mmol) and $NaBH_4$ (2.13 g, 4.86 mmol) in THF THF (32 mL) and H_2O (16 mL) using general procedure C. Purification by silica flash chromatography with 50 % EtOAc in hexanes, gave **109b-β** (0.710 g, 54 %) as a clear, pale yellow oil.

R*f* 0.3(hexanes/EtOAc, 1:1)

^{1}H NMR (400 MHz, $CDCl_3$) δ 6.11 (1H, ddd, *J* = 10.2, 5.6, 2.2 Hz), 5.97 (1H, dd, *J* = 10.3, 1.3 Hz), 5.05 (1H, td, *J* = 5.5, 2.0 Hz), 4.37 (1H, dt, *J* = 3.8, 2.0 Hz), 4.18 (1H, d, *J* = 2.4 Hz), 4.17 (1H, d, *J* = 0.9 Hz), 3.88 (1H, m), 3.68-3.58 (2H, m), 2.26 (1H, m), 2.06 (3H, s), 2.06 (3H, s)

MS (ESI) Calcd. for $C_{13}H_{20}O_6$ $(M+H)^+$ 273.3022, found 273.3, $(M+NH_4)^+$ 290.3328, found 290.4, $(M+Na)^+$ 295.2841, found 295.3

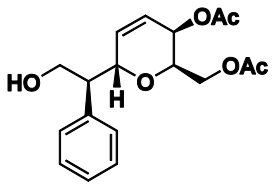

((2R,3R,6S)-3-acetoxy-6-((S)-2-hydroxy-1-phenylethyl)-3,6-dihydro-2H-pyran-2-yl)methyl acetate (109e):

The title compound was prepared from **90e** (1.54 g, 2.85 mmol) and $NaBH_4$ (1.25 g, 1.67 mmol) in THF (18 mL) and H_2O (9 mL) using general procedure C. Purification by silica flash chromatography with 50 % EtOAc in hexanes, gave **109e** (0.592 g, 62 %) as a clear, pale yellow oil.

R*f* 0.3 (hexanes/EtOAc, 1:1)

^{1}H NMR (400 MHz, $CDCl_3$) δ 7.34-7.24 (5H, m), 6.16 (1H, ddd, *J* = 10.4, 2.8, 0.7 Hz), 5.95 (1H, ddd, *J* = 10.4, 4.6, 2.4 Hz), 5.04 (1H, m), 4.74 (1H, m), 4.12 (1H, dd, *J* = 11.6, 8.2 Hz), 4.05-3.91 (4H, m), 3.11 (1H, q, 6.4 Hz), 2.05 (3H, s), 1.95 (3H, s), 1.80 (1H, m)

^{13}C NMR (100 MHz, $CDCl_3$) δ 170.8, 170.4, 138.6, 133.2, 128.8, 128.5, 127.2, 123.2, 72.3, 69.1, 64.1, 64.0, 62.3, 51.2, 20.9, 20.7

MS (ESI) Calcd. for $C_{18}H_{22}O_6$ $(M+Na)^+$ 357.3535, found 357.3

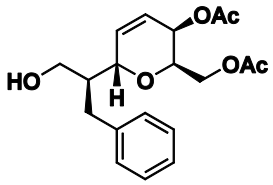

((2R,3R,6S)-3-acetoxy-6-(1-hydroxy-3-phenylpropan-2-yl)-3,6-dihydro-2H-pyran-2-yl)methyl acetate (109f):

The title compound was prepared from **90f** (0.202 g, 0.365 mmol) and $NaBH_4$ (0.160 g, 0.365 mmol) in THF (2.4 mL) and H_2O (1.2 mL) using general procedure C. Purification by silica flash chromatography with 50 % EtOAc in hexanes, gave **109f** (0.083 g, 65 %) as a clear, pale yellow oil.

R*f* 0.3 (hexanes/EtOAc, 1:1)

^{1}H NMR (400 MHz, $CDCl_3$) δ 7.31-7.19 (5H, m), 6.14 (1H, ddd, *J* = 10.4, 2.7, 0.9 Hz), 6.02 (1H, ddd, *J* = 10.4, 4.5, 2.4 Hz), 5.22 (1H, m), 4.51 (1H, ddd, *J* = 6.2, 3.6, 2.5 Hz), 4.33-4.18 (3H, m), 3.67 (1H, dd, *J* = 11.2, 3.4 Hz), 3.60 (1H, dd, *J* = 11.2, 4.9 Hz), 2.93 (1H, dd, *J* = 13.6, 3.8 Hz), 2.74 (1H, dd, *J* =13.5, 10.4 Hz), 2.10 (3H, s), 2.05 (3H, s), 2.01 (1H, m)

MS (ESI) Calcd. for $C_{19}H_{24}O_6$ $(M+Na)^+$ 371.3800, found 371.3

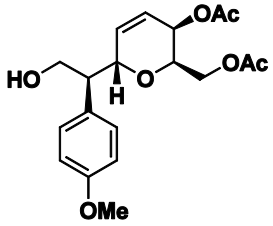

((2R,3R,6S)-3-acetoxy-6-((S)-2-hydroxy-1-(4-methoxyphenyl)ethyl)-3,6-dihydro-2H-pyran-2-yl)methyl acetate (109g):

The title compound was prepared from **90g** (0.95 g, 1.67 mmol) and $NaBH_4$ (0.73 g, 1.67 mmol) in THF (10 mL) and H_2O (5 mL) using general procedure C. Purification by silica flash chromatography with 50 % EtOAc in hexanes, gave **109g** (0.408 g, 67 %) as a clear, yellow oil.

R*f* 0.3 (hexanes/EtOAc, 1:1)

^{1}H NMR (400 MHz, $CDCl_3$) δ 7.21-7.17 (2H, m), 6.87-6.84 (2H, m), 6.12 (1H, ddd, *J* = 10.4, 2.7, 0.8 Hz), 5.93 (1H, ddd, *J* = 10.4, 4.6, 2.4 Hz), 5.04 (1H, m), 4.68 (1H, m), 4.13 (1H, dd, *J* = 116, 8.2 Hz), 4.05-3.88 (4H, m), 3.79 (3H, s), 3.05 (1H, q, *J* = 6.4 Hz), 2.04 (3H, s), 1.98 (3H, s)

^{13}C NMR (100 MHz, $CDCl_3$) δ 170.7, 170.4, 158.7, 133.2, 130.3, 129.7, 123.2, 113.9, 72.3, 69.1, 64.1, 64.1, 62.3, 55.2, 50.2, 50.4, 20.9, 20.8

MS (ESI) Calcd. $C_{19}H_{24}O_7$ $(M+Na)^+$ 387.3794, found 387.3 (MNa^+, 100 %)

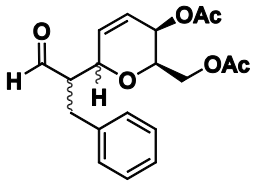

((2R,3R)-3-acetoxy-6-(1-oxo-3-phenylpropan-2-yl)-3,6-dihydro-2H-pyran-2-yl)methyl acetate (110f):[17, 18]

A solution of **90f** (0.042 g, 0.121 mmol) in DCM containing 4Å molecular sieves was stirred for 10 minutes, and NMO (0.008 g, 0.0667 mmol) followed by TPAP (cat.) were added. The reaction mixture was stirred for 2 h. The reaction mixture was diluted with DCM and washed with a saturated aqueous solution of sodium sulfite, a 10% aqueous solution of NaCl, and a sat. aqueous copper (II) sulfate solution. The aqueous layers were washed with DCM. The combined organic layers were dried over $MgSO_4$ and concentrated. Purification by preparative thin layer chromatography gave **110f** as a white solid.

OR

To a solution of SM (0.010 g, 0.029 mmol) in DCM (0.60 mL) containing 4Å molecular sieves was added NMO (0.005 g, 0.043 mmol), followed by TPAP (cat.).The reaction mixture was stirred for 30 minutes. The reaction appeared incomplete by tlc, and therefore $CNCH_3$ was added, and the reaction mixture was stirred for an additional 1.75 h, although no further reaction occurred. The reaction mixture was filtered over a silica plus, and the silica was further rinsed with EtOAc. The wanted compound was recovered by concentration of the filtrate, to give **110f** as a white solid.

R*f* 0.8 (hexanes/EtOAc, 1:1)

^{1}H NMR (400 MHz, $CDCl_3$) δ 9.74 (1H, d, *J* = 1.6 Hz), 7.31-7.19 (5H, m), 6.08 (1H, dd, *J* = 10.6, 2.8 Hz), 6.01 (1H, ddd, *J* = 10.3, 4.5, 2.0 Hz), 5.19 (1H, m), 4.53 (1H, d, *J* = 7.9 Hz), 4.28 (1H, dd, *J* = 11.3, 8.0 Hz), 4.22 (1H, d, *J* = 4.0 Hz), 4.19-4.16 (2H, m), 3.13 (1H, m), 3.05 (1H, m), 2.10 (3H, s), 2.08 (3H, s)

^{13}C NMR (100 MHz, $CDCl_3$) δ 202.1, 170.7, 170.4, 137.9, 132.2, 129.1, 128.7, 126.7, 123.7, 70.4, 69.2, 63.9, 62.6, 56.2, 32.0, 20.9, 20.8

MS (ESI) Calcd. for $C_{19}H_{22}O_6$ $(M+NH_4)^+$ 364.4128, found 364.4, $(M+Na)^+$ 369.3642, found 369.4

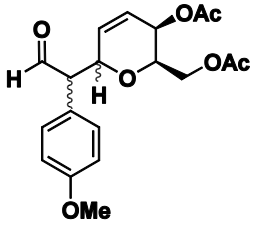

((2R,3R)-3-acetoxy-6-(1-(4-methoxyphenyl)-2-oxoethyl)-3,6-dihydro-2H-pyran-2-yl)methyl acetate (110g):[19]

A solution of $(COCl)_2$ (0.014 mL, 0.165 mmol) in DCM (0.7 mL) was cooled to -60 ºC, and DMSO (0.013 mL, 0.178 mmol) was subsequently added. The reaction mixture was stirred for 10 minutes, and **90g** (0.05 g, 0.137 mmol) was then added, and the reaction mixture was stirred for another 15 minutes. Et_3N (0.077 mL, 0.549 mmol) was added to the reaction mixture, and the reaction vessel was removed from the cold bath. The reaction mixture was quenched with H2O and stirred for overnight. The reaction mixture was diluted with DCM and washed with H_2O. The aqueous layers were washed with DCM, and the combined organic layers were washed with brine, dried over $MgSO_4$, and concentrated to give **110g** as a white solid.

R*f* 0.3 (hexanes/EtOAc, 1:1)

MS (ESI) Calcd. for $C_{19}H_{22}O_7$ $(M+NH_4)^+$ 380.4122, found 380.3, $(M+Na)^+$ 385.3636, found 385.3

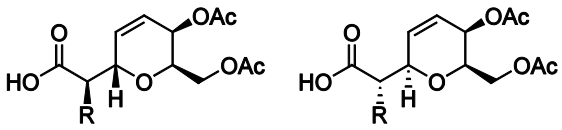

General procedure D. Preparation of substituted carboxylic acid derivatives – removal of the chiral auxiliary (111 and 120):[20]

A solution of LiOH and H_2O_2 in H_2O was stirred for 0.25 h at room temperature. This pre-mixed solution was then added to a solution of coupled product (**90** or **91**) in THF, and the resulting reaction mixture was then stirred for 1 h at room temperature. The reaction mixture was quenched with 10 % aqueous solution of HCl. The aqueous layer was extracted with DCM and the organic layer was washed with H_2O. The combined organic layers were washed with brine, dried over $MgSO_4$ and concentrated. The wanted compound was purified by acid/base extraction: the crude material was dissolved in a saturated aqueous solution of $NaHCO_3$, and the aqueous layer was subsequently acidified to pH 4 with a 10 % aqueous solution of HCl. The aqueous layer was washed with DCM, and subsequently concentrated to provide the wanted compound.

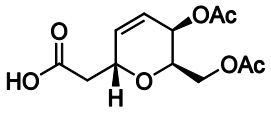

2-((2R,5R,6R)-5-acetoxy-6-(acetoxymethyl)-5,6-dihydro-2H-pyran-2-yl)acetic acid (111a):

The title compound was prepared from **90a** (2.09 g, 4.51 mmol), LiOH (0.22 g, 9.0 mmol) in H_2O (20 mL), and H_2O_2 (0.92 g, 27.1 mmol) in THF (10 mL) using general procedure D. Purification by acid/base extraction gave **111a** as a white solid (0.64 g, 76 %).

R*f* 0.1 (hexanes/EtOAc, 7:3)

^{1}H NMR (400 MHz, $CDCl_3$) δ 6.07-6.06 (2H, m), 5.10 (1H, m), 4.82 (1H, dd, *J* = 9.7, 5.0 Hz), 4.22 (2H, dq, *J* = 11.4, 6.1 Hz), 4.12 (1H, ddd, *J* = 7.5, 5.0, 2.7 Hz), 2.74 (1H, dd, *J* = 15.4, 9.5 Hz), 2.57 (1H, dd, *J* = 15.4, 5.0 Hz), 2.09 (3H, s), 2.07 (3H, s)

^{13}C DEPTQ135 NMR (100 MHz, $CDCl_3$) δ 133.1, 123.2, 69.3, 68.4, 63.3, 36.8

Accurate Mass (ESI) Calcd. for $C_{12}H_{16}O_7$ $(M+Na)^+$ 295.2410 found 295.172

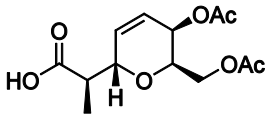

(R)-2-((2S,5R,6R)-5-acetoxy-6-(acetoxymethyl)-5,6-dihydro-2H-pyran-2-yl)propanoic acid (111b):

The title compound was prepared from **90b** (0.16 g, 0.35 mmol), LiOH (0.017 g, 0.71 mmol) in H_2O (2 mL), and H_2O_2 (0.072 g, 2.1 mmol) in THF (1 mL) using general procedure D. Purification by acid/base extraction gave **111b** as a white solid (0.075 g, 74 %).

R*f* 0.1 (hexanes/EtOAc, 7:3)

^{1}H NMR (400 MHz, $CDCl_3$) δ 6.10 (1H, dd, *J* = 10.4, 2.7 Hz), 6.04 (1H, ddd, *J* = 10.3, 4.7, 2.0 Hz), 5.12 (1H, m), 4.45 (1H, td, *J* = 8.0, 1.9 Hz), 4.25 (1H, dd, *J* = 11.6, 8.1 Hz), 4.18 (1H, dd, *J* = 11.6, 4.4 Hz), 4.08 (1H, ddd, *J* = 7.8, 4.3, 3.2 Hz), 2.77 (1H, m), 2.09 (3H, s), 2.08 (3H, s), 1.33 (1H, d, *J* = 7.1 Hz)

^{13}C NMR (100 MHz, $CDCl_3$) δ 178.4, 170.7, 170.4, 132.4, 123.5, 72.8, 69.1, 63.6, 62.7, 42.3, 20.9, 20.8, 13.7

MS (ESI) Calcd. $C_{13}H_{18}O_7$ $(M+Na)^+$ 309.2676, found 309.174

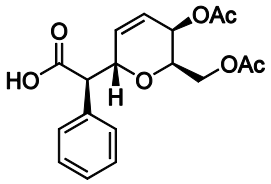

(R)-2-((2S,5R,6R)-5-acetoxy-6-(acetoxymethyl)-5,6-dihydro-2H-pyran-2-yl)-2-phenylacetic acid (111e):

The title compound was prepared from **90e** (0.61 g, 1.2 mmol), LiOH (0.054 g, 2.3 mmol) in H_2O (6 mL), and H_2O_2 (0.69 g, 6.8 mmol) in THF (3 mL) using general procedure C. Purification by acid/base extraction gave **111e** as a white solid (0.17 g, 42 %).

R*f* 0.1 (hexanes/EtOAc, 7:3)

^{1}H NMR (400 MHz, $CDCl_3$) δ 7.38-7.27 (5H, m), 6.27 (1H, dd, *J* = 10.3, 2.7 Hz), 6.08 (1H, ddd, *J* = 10.1, 5.0, 1.5 Hz), 5.05 (2H, d, *J* = 3.4 Hz), 4.92 (1H, d, *J* = 10.3 Hz), 4.01 (1H, m), 3.9 (1H, d, *J* = 10.30), 3.76 (1H, t, *J* = 6.3 Hz), 2.04 (3H, s), 1.9 (3H, s)

^{13}C DEPTQ135 NMR (100 MHz, $CDCl_3$) δ 175.9, 170.8, 170.5, 135.0, 132.8, 128.6, 128.5, 127.8, 123.6, 73.3, 68.5, 63.5, 62.6, 61.7, 20.8, 20.6

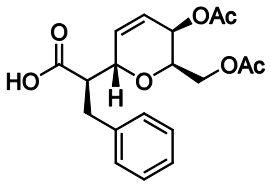

(R)-2-((2S,5R,6R)-5-acetoxy-6-(acetoxymethyl)-5,6-dihydro-2H-pyran-2-yl)-3-phenylpropanoic acid (111f):

The title compound was prepared from **90f** (0.20 g, 0.41 mmol), LiOH (0.020 g, 0.82 mmol) in H_2O (6.4 mL), and H_2O_2 (0.083 g, 2.5 mmol) in THF (9.6 mL) using general procedure C. Purification by acid/base extraction gave **111f** as a white solid (0.12 g, 81 %).

R*f* 0.1 (hexanes/EtOAc, 7:3)

^{1}H NMR (400 MHz, $CDCl_3$) δ 7.30-7.19 (5H, m), 6.10-6.04 (2H, m), 5.12 (1H, m), 4.46 (1H, d, *J* = 8.6 Hz), 4.28-4.19 (2H, m), 4.14 (1H, m), 3.21 (1H, m), 3.06-3.01 (2H, m), 2.97 (1H, dd, *J* = 9.5, 3.1 Hz), 2.10 (3H, s), 2.07 (3H, s)

^{13}C NMR (100 MHz, $CDCl_3$) δ 176.5, 170.8, 170.5, 138.0, 132.3, 128.9, 128.6, 126.7, 123.6, 72.0, 69.0, 63.5, 63.0, 49.7, 35.0, 20.9, 20.8

MS (ESI) Calcd. for $C_{19}H_{22}O_7$ $(M+Na)^+$ 385.3636, found 385.230

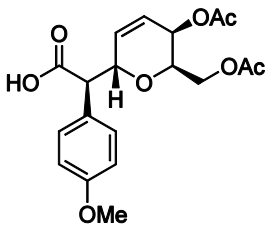

(R)-2-((2S,5R,6R)-5-acetoxy-6-(acetoxymethyl)-5,6-dihydro-2H-pyran-2-yl)-2-(4-methoxyphenyl)acetic acid (111g):

The title compound was prepared from 90g (0.20 g, 0.35 mmol), LiOH (0.017 g, 0.70 mmol) in H_2O (3 mL), and H_2O_2 (0.071 g, 2.1 mmol) in THF (2 mL) using general procedure C. Purification by acid/base extraction gave **111g** as a white solid (0.064 g, 48 %).

R*f* 0.1 (hexanes/EtOAc, 7:3)

^{1}H NMR (400 MHz, MeOD) δ7.31 (2H, m), 6.88 (2H, m), 6.29 (1H, dd, *J* = 10.4, 3.1 Hz), 6.05 (1H, ddd, *J* = 10.3, 5.3, 2.0 Hz), 5.05 (1H, dd, *J* = 5.2, 2.5 Hz), 4.79 (1H, m), 4.13 (1H, m), 4.00 (2H, dd, *J* = 6.2, 2.9 Hz), 3.77 (3H, s), 3.84 (1H, d, *J* = 10.4 Hz), 1.98 (3H, s), 1.83 (3H, s)

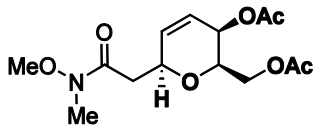

((2R,3R,6S)-3-acetoxy-6-(2-(methoxy(methyl)amino)-2-oxoethyl)-3,6-dihydro-2H-pyran-2-yl)methyl acetate (112):[21]

To a solution of **91a** (0.144 g, 0.311 mmol) in DCM (3 mL) was added N,O-dimethylhydroxylamine hydrochloride (0.061 g, 0.621 mmol) and imidazole (0.085 g, 1.24 mmol). The reaction mixture was stirred at room temperature for 2 h. The reaction mixture was diluted with DCM, and washed with H_2O and brine. The aqueous fractions were then washed with DCM. The combined organic layers were washed with brine, dried over $MgSO_4$ and concentrated. Purification by silica flash chromatography with a gradient of 30 % EtOAc in hexanes to 50 % EtOAc in hexanes gave **112** (0.064 g, 62 %) as a pale yellow oil.

R*f* 0.3 (hexanes/EtOAc, 6:4)

^{1}H NMR (400 MHz, $CDCl_3$) δ 6.12 (1H, dd, *J* = 10.2, 0.9 Hz), 6.00 (1H, ddd, *J* = 10.2, 5.3, 2.1 Hz), 5.09 (1H, m), 4.64 (1H, m), 4.19 (2H, m), 3.94 (1H, dt, *J* = 6.8, 6.6, 2.3 Hz), 3.70 (3H, s), 3.20 (3H, s), 2.96 (1H, dd, *J* = 15.8, 6.2 Hz), 2.58 (1H, dd, *J* = 16.0, 7.4 Hz), 2.07 (3H, s), 2.06 (3H, s)

^{13}C NMR (100 MHz, $CDCl_3$) δ 170.8, 170.6, 135.7, 122.6, 77.2, 73.8, 71.9, 64.0, 62.9, 61.4, 21.0, 20.8

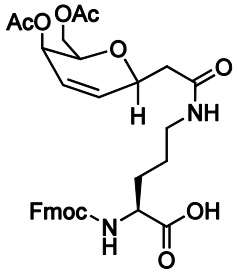

(S)-2-(((9H-fluoren-9-yl)methoxy)carbonylamino)-5-(2-((2S,5R,6R)-5-acetoxy-6-(acetoxymethyl)-5,6-dihydro-2H-pyran-2-yl)acetamido)pentanoic acid (115a):

To a solution of **91a** (0.168 g, 0.360 mmol) in DCM (10 mL) were added **114** (0.17 g, 0.360 mmol) and NEt_3 (0.109 g, 1.09 mmol). The reaction mixture was stirred at room temperature for 3 h. The reaction mixture was diluted with DCM, and the organic fraction washed with a 10% aqueous solution of HCl, H_2O, and brine. The aqueous fractions were then washed with DCM. The combined organic layers were dried over $MgSO_4$ and concentrated. Purification by silica flash chromatography with a solution of EtOAc:H_2O:MeOH:AcOH in a ratio of 10:1:1:1 gave **105a** (0.173 g, 79 %) as a white foam after lyophilization.

R*f* 0.4 (DCM/MeOH/AcOH, 9:0.5:0.5)

^{1}H NMR (400 MHz, $CDCl_3$) δ 7.77 (2H, d, *J* = 7.6 Hz), 7.66 (2H, t, *J* = 7.5 Hz), 7.36 (2H, t, *J* = 7.4 Hz), 7.29 (2H, dt, *J* = 7.3, 0.7 Hz), 6.03 (1H, dd, *J* = 10.2, 0.9 Hz), 5.95 (1H, ddd, *J* = 10.1, 5.2, 2.2 Hz), 5.05 (1H, m), 4.49 (1H, t, *J* = 6.0 Hz), 4.33 (2H, dd, *J* = 7.0, 2.1 Hz), 4.20 (1H, t, *J* = 6.9 Hz), 4.17-4.08 (3H, m), 3.91 (1H, dt, *J* = 6.2, 2.0 Hz), 3.20 (2H, m), 2.42 (2H, d, *J* = 6.6 Hz), 1.99 (3H, s), 1.97 (3H, s), 1.87 (1H, m), 1.73-1.52 (3H, m)

^{13}C NMR (100 MHz, $CDCl_3$) δ 175.9, 172.6, 172.5, 172.1, 158.7, 145.4, 145.2, 142.6, 136.3, 128.8, 128.2, 126.3, 124.1, 121.0, 75.2, 73.6, 68.0, 65.3, 64.1, 55.2, 48.5, 42.5, 40.0, 30.2, 27.0, 20.8, 20.8

Accurate Mass (ESI) Calcd. for $C_{32}H_{36}N_2O_{10}$ $(M+Na)^+$ 631.6254, found 631.359

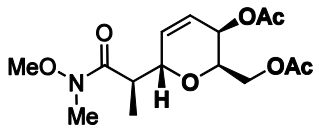

((2R,3R,6S)-3-acetoxy-6-((R)-1-(methoxy(methyl)amino)-1-oxopropan-2-yl)-3,6-dihydro-2H-pyran-2-yl)methyl acetate (116):[21]

To a solution of **90b** (0.390 g, 0.841 mmol) in DCM (8.4 mL) was added N,O-dimethylhydroxylamine hydrochloride (0.328 g, 3.36 mmol) and imidazole (0.344 g, 5.05 mmol). The reaction mixture was stirred at room temperature for 2 h. The reaction mixture was diluted with DCM, and washed with H_2O and brine. The aqueous fractions were then washed with DCM. The combined organic layers were washed with brine, dried over $MgSO_4$ and concentrated. Purification by silica flash chromatography with a gradient of 30 % EtOAc in hexanes to 50 % EtOAc in hexanes gave **116** (0.157 g, 57 %) as a clear, colourless oil.

R*f* 0.3 (hexanes/EtOAc, 6:4)

^{1}H NMR (400 MHz, $CDCl_3$) δ 6.08 (1H, dd, *J* = 10.4, 3.1 Hz), 5.99 (1H, ddd, *J* = 10.3, 5.2, 2.0 Hz), 5.06 (1H, dd, *J* = 5.1, 2.6 Hz), 4.45 (1H, m), 4.23-4.21 (2H, m), 4.03 (1H, m), 3.68 (3H, s), 3.21 (1H, m), 3.19 (3H, s), 2.09 (6H, s), 1.28 (3H, d, *J* = 6.8 Hz)

MS (ESI) Calcd. for $C_{15}H_{23}NO_7$ $(M+H)^+$ 330.3536, found 330.326, $(M+Na)^+$ 352.3354, found 352.290 (MNa^+, 100%).

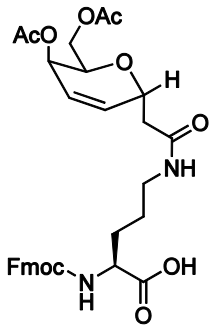

(S)-2-(((9H-fluoren-9-yl)methoxy)carbonylamino)-5-(2-((2R,5R,6R)-5-acetoxy-6-(acetoxymethyl)-5,6-dihydro-2H-pyran-2-yl)acetamido)pentanoic acid (117a):

To a solution of **90a** (1.39 g, 3.0 mmol) in DCM (30 mL) were added **114** (1.40 g, 3.0 mmol) and NEt_3 (1.25 g, 9.0 mmol). The reaction mixture was stirred at room temperature for 3 h. The reaction mixture was diluted with DCM, and the organic fraction washed with a 10% aqueous solution of HCl, H_2O, and brine. The aqueous fractions were then washed with DCM. The combined organic layers were dried over $MgSO_4$ and concentrated. Purification by silica flash chromatography with a solution of EtOAc:H2O:MeOH:AcOH in a ratio of 20:1:1:1 gave **117a** (1.16 g, 63 %) as a white foam after lyophilization.

R*f* 0.4 (DCM/MeOH/AcOH, 9:0.5:0.5)

^{1}H NMR (400 MHz, MeOD) δ 7.77 (2H, d, *J* = 7.5 Hz), 7.66 (2H, t, *J* = 7.5 Hz), 7.37 (2H, t, *J* = 7.4 Hz), 7.29 (2H, dt, *J* = 7.4, 1.0 Hz), 6.05 (1H, dd, *J* = 10.3, 3.0 Hz), 5.96 (1H, ddd, *J* = 10.2, 5.2, 2.1 Hz), 5.04 (1H, dd, *J* = 4.8, 1.1 Hz), 4.68 (1H, tdd, *J* = 9.6, 4.7, 2.4 Hz), 4.32 (2H, m), 4.22-4.08 (4H, m), 3.15 (2H, m), 2.54 (1H, dd, *J* = 14.3, 9.7 Hz), 2.35 (2H, dd, *J* = 14.3, 4.6 Hz), 2.00 (3H, s), 1.99 (3H, s), 1.88 (1H, m), 1.73-1.53 (3H, m)

^{13}C NMR (100 MHz, MeOD) δ; 172.5, 172.1, 158.4, 145.4, 145.3, 142.6, 135.5, 128.8, 128.2, 126.3, 123.5, 121.0, 71.5, 69.4, 67.9, 65.0, 63.9, 49.9, 48.5, 40.2, 39.7, 31.1, 26.9, 20.9, 20.8

Accurate Mass (ESI) Calcd. for $C_{32}H_{36}N_2O_{10}$ $(M+Na)^+$ 631.6254, found 631.312

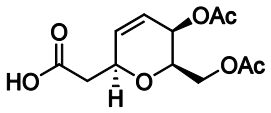

2-((2S,5R,6R)-5-acetoxy-6-(acetoxymethyl)-5,6-dihydro-2H-pyran-2-yl)acetic acid (120a):

The title compound was prepared from **91a** (2.5 g, 5.4 mmol), LiOH (0.26 g, 10.8 mmol) in H_2O (25 mL), and H_2O_2 (1.10 g, 32.4 mmol) in THF (15 mL) using general procedure D. Purification by acid/base extraction gave **190a** as a white solid (0.58 g, 57 %).

R*f* 0.1 (hexanes/EtOAc, 7:3)

^{1}H NMR (400 MHz, $CDCl_3$) δ 6.06-6.05 (2H, m), 5.09 (1H, m), 4.57 (1H, m), 4.20 (2H, m), 3.95 (1H, m), 2.69 (2H, ddd, *J* = 22.4, 16.1, 6.9 Hz), 2.09 (3H, s), 2.07 (3H, s

^{13}C DEPTQ135 NMR (100 MHz, $CDCl_3$) δ 175.3, 170.8, 170.6, 134.1, 123.5, 73.9, 71.2, 63.6, 62.8, 39.4, 20.9, 20.8.

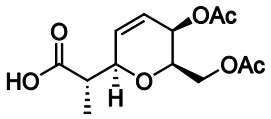

(S)-2-((2R,5R,6R)-5-acetoxy-6-(acetoxymethyl)-5,6-dihydro-2H-pyran-2-yl)propanoic acid (120b):

The title compound was prepared from **120b** (0.56 g, 1.2 mmol), LiOH (0.057 g, 2.4 mmol) in H_2O (4 mL), and H_2O_2 (0.24 g, 7.1 mmol) in THF (12 mL) using general procedure C. Purification by acid/base extraction gave **91b** as a white solid (0.23 g, 67 %).

R*f* 0.1 (hexanes/EtOAc, 7:3)

^{1}H NMR (400 MHz, $CDCl_3$) δ 6.13 (1H, ddd, *J* = 10.1, 5.6, 2.1 Hz), 5.98 (1H, dd, *J* = 10.3, 1.1 Hz), 5.07 (1H, td, *J* = 5.36, 2.0 Hz), 4.49 (1H, dd, *J* = 4.9, 1.8 Hz), 4.22 (2H, dq, *J* = 11.5, 6.4 Hz), 3.96 (1H, m), 2.76 (1H, m), 2.08 (3H, s), 2.07 (3H, s), 1.25 (3H, d, *J* = 7.1)

^{13}C DEPTQ135 NMR (100 MHz, $CDCl_3$) δ 176.3, 170.7, 170.5, 132.5, 124.5, 75.5, 73.8, 63.6, 62.7, 43.3, 20.9, 20.8, 11.4

MS (ESI) Calcd. for $C_{13}H_{18}O_7$ $(M+Na)^+$ 309.2676, found 309.182

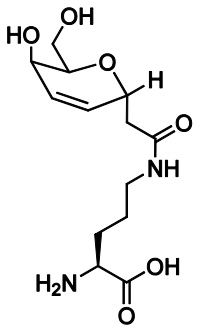

(S)-2-amino-5-(2-((2R,5R,6R)-5-hydroxy-6-(hydroxymethyl)-5,6-dihydro-2H-pyran-2-yl)acetamido)pentanoic acid (121):

To a solution of sodium in methanol was added **117a**. The reaction mixture was stirred at room temperature for 0.5 h. The reaction mixture was neutralized to pH 6 with Amberlite® IR-120H ion-exchange resin, filtered, and concentrated. The crude product was purified by preparative thin layer chromatography with a solution of AcOH:MeOH:H_2O:EtOAc = 0.5:0.5:0.5:8.5. Lyophilization of the purified compound gave **121** as a lyophilized white powder (0.0175 g, 85%).

^{1}H NMR (400 MHz, D_2O) δ 6.07 (1H, ddd, *J* = 10.2, 5.4, 1.9 Hz), 6.01 (1H, dd, *J* = 10.3, 3.0 Hz), 4.6 (1H, m), 3.9 (1H, dd, *J* = 5.3, 2.1 Hz), 3.83 (1H, *J* = ddd, 7.7, 4.1, 2.1 Hz), 3.74-3.61 (5H, m), 3.20 (2H, m), 2.62 (1H, dd, *J* = 14.5, 10.0 Hz), 2.40 (1H, dd, *J* = 14.5, 4.3 Hz), 1.90-1.75 (2H, m), 1.64-1.45 (2H, m)

^{13}C DEPTQ135 NMR (100 MHz, D_2O) δ 174.52, 173.17, 131.67, 125.67, 72.34, 70.31, 61.20, 61.14, 54.46, 38.82, 38.28, 27.87, 24.30

Accurate Mass Calcd. for $C_{13}H_{22}N_2O_6$ $(M+Na)^+$ 325.3133, found 325.238

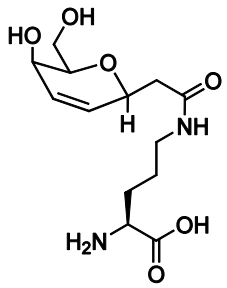

(S)-2-amino-5-(2-((2S,5R,6R)-5-hydroxy-6-(hydroxymethyl)-5,6-dihydro-2H-pyran-2-yl)acetamido)pentanoic acid (122):

To a solution of sodium in methanol was added **115a**. The reaction mixture was stirred at room temperature for 0.5 h. The reaction mixture was neutralized to pH 6 with Amberlite® IR-120H ion-exchange resin, filtered, and concentrated. The crude product was purified by preparative thin layer chromatography with a solution of AcOH:MeOH:H_2O:EtOAc = 0.5:0.5:0.5:8.5. Lyophilization of the purified compound gave **122** as a lyophilized white powder (0.0162 g, 82%).

^{1}H NMR (400 MHz, D_2O) δ 6.05 (1H, ddd, *J* = 10.01, 5.4, 2.1 Hz), 5.96 (1H, dd, *J* = 10.3, 0.9 Hz), 4.54 (1H, m), 4.03 (1H, m), 3.81-3.71 (5H, m), 3.28 (1H, t, *J* = 6.7 Hz), 2.59 (1H, dd, *J* = 14.7, 5.3), 2.53 (1H, dd, *J* = 14.7, 8.3), 1.92-1.86 (2H, m), 1.63 (2H, m)

^{13}C DEPTQ135 NMR (100 MHz, D_2O) δ 174.6, 173.1, 132.5, 126.4, 78.37, 72.2, 61.7, 61.6, 54.5, 41.1, 38.8, 27.9, 24.2

Accurate Mass Calcd. for $C_{13}H_{22}N_2O_6$ $(M+Na)^+$ 325.3133, found 325.201

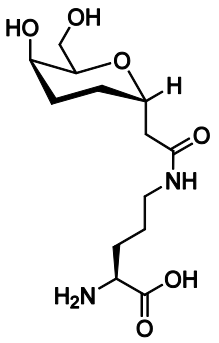

(S)-2-amino-5-(2-((2S,5R,6R)-5-hydroxy-6-(hydroxymethyl)tetrahydro-2H-pyran-2-yl)acetamido)pentanoic acid (123):

To a solution of sodium in methanol was added **106a**. The reaction mixture was stirred at room temperature for 0.5 h. The reaction mixture was neutralized to pH 6 with Amberlite® IR-120H ion-exchange resin, filtered, and concentrated. The crude product was purified by preparative thin layer chromatography with a solution of AcOH:MeOH:H_2O:EtOAc = 0.5:0.5:0.5:8.5. Lyophilization of the purified compound gave **123** as a lyophilized white powder (0.038 g, 76%).

^{1}H NMR (400 MHz, $CDCl_3$) δ 4.15 (1H, qd, *J* = 9.7, 5.0 Hz), 3.80-3.66 (3H, m), 3.62 (1H, dd, *J* = 6.5, 5.7 Hz), 3.54 (1H, dd, *J* = 5.2, 4.2 Hz), 3.12 (2H, t, *J* = 6.8 Hz), 2.61 (1H, dd, *J* = 14.8, 9.3 Hz), 2.31 (1H, dd, *J* = 14.7, 5.1 Hz), 1.89 (1H, m), 1.82-1.69 (2H, m), 1.63-1.40 (3H, m), 1.29 (1H, m)

Accurate Mass Calcd. for $C_{13}H_{24}N_2O_6$ $(M+Na)^+$ 327.3292, found 327.218

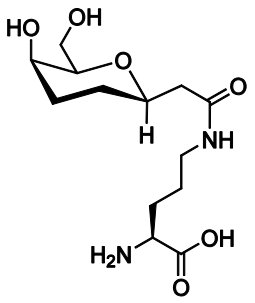

(S)-2-amino-5-(2-((2R,5R,6R)-5-hydroxy-6-(hydroxymethyl)tetrahydro-2H-pyran-2-yl)acetamido)pentanoic acid (124):

To a solution of sodium in methanol was added **108a**. The reaction mixture was stirred at room temperature for 0.5 h. The reaction mixture was neutralized to pH 6 with Amberlite® IR-120H ion-exchange resin, filtered, and concentrated. The crude product was purified by preparative thin layer chromatography with a solution of AcOH:MeOH:H_2O:EtOAc = 0.5:0.5:0.5:8.5. Lyophilization of the purified compound gave **124** as a lyophilized white powder (0.042 g, 84%).

^{1}H NMR (400 MHz, $CDCl_3$) δ 4.23 (1H, t, *J* = 6.3 Hz), 4.00-3.94 (2H, m), 3.79-3.76 (2H, m), 3.72 (1H, dq, *J* = 5.9, 6.3, 1.1 Hz), 3.38 (2H, t, *J* = 6.7 Hz), 2.63 (1H, dd, *J* = 15.5, 8.0 Hz), 2.55 (1H, dd, *J* = 15.5, 2 Hz), 2.17-2.01 (3H, m), 1.94 (1H, m), 1.87-1.62 (4H, m)

Accurate Mass Calcd. for $C_{13}H_{24}N_2O_6$ $(M+Na)^+$ 327.3292, found 327.231

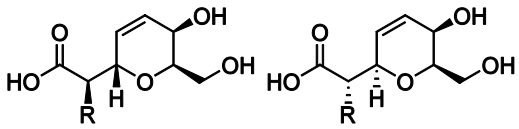

General Procedure D: Preparation of substituted carboxylic acid derivatives – deprotection (125 and 126):

A solution of NaOMe in MeOH at pH 12 was added to the protected carboxylic acid derivative (**111** or **120**). The reaction mixture was stirred for 0.5 h at room temperature. The reaction mixture was neutralized with Amberlite® IR-120H ion-exchange resin. The beads were filtered off and the filtrate was extracted with CH_2Cl_2. The recovered organic solution was concentrated to provide a residue. The wanted compound was purified from the residue

using preparative thin layer chromatography with a solution of AcOH:MeOH:H_2O:EtOAc = 0.5:0.5:0.5:8.5

OR

A solution of 4M aqueous HCl and THF was added to the protected carboxylic acid derivative (**111b**, **111f**). The reaction mixture was stirred for 2 h at 50 °C, and then allowed to cool to room temperature. The reaction mixture was co-evaporated with toluene to dryness, providing a residue. The wanted compound was purified from the residue using preparative thin layer chromatography with a solution of AcOH:MeOH:H_2O:EtOAc = 0.5:0.5:0.5:8.5.

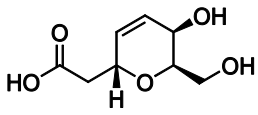

2-((2R,5R,6R)-5-hydroxy-6-(hydroxymethyl)-5,6-dihydro-2H-pyran-2-yl)acetic acid (125a):

The title compound was prepared from **111a** in NaOMe in MeOH (2 mL) using general procedure D. Lyophilization of the purified compound gave **125a** as a white lyophilized solid (0.005 g).

^{1}H NMR (400 MHz, MeOD) δ 6.01-5.91 (2H, m), 4.68 (1H, m), 3.87 (1H, m), 3.77 (1H, m), 3.69 (2H, m), 2.66 (1H, dd, *J* = 15.2, 8.6 Hz), 2.52 (1H, dd, *J* = 15.3, 5.4 Hz)

^{13}C DEPTQ135 NMR (100 MHz, MeOD) δ 131.3, 126.5, 72.8, 69.6, 61.3, 61.2, 37.1

Accurate Mass (ESI) Calcd. for $C_8H_{12}O_5$ $(M+Na)^+$ 211.1676, found 211.105

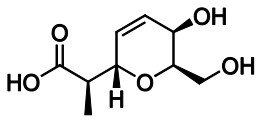

(R)-2-((2S,5R,6R)-5-hydroxy-6-(hydroxymethyl)-5,6-dihydro-2H-pyran-2-yl)propanoic acid (125b):

The title compound was prepared from **111b** (0.050 g, 0.18 mmol) in 4M aqueous HCl (1 mL) and THF (3 mL) according to general procedure E. Lyophilization of the purified compound gave **125b** as a lyophilized white powder (0.0054 g, 15 %).

^{1}H NMR (400 MHz, MeOD) δ 5.99 (1H, dd, *J* = 4.5, 1.4 Hz), 5.97 (1H, d, *J* = 2.4 Hz), 4.26 (1H, td, *J* = 9.3, 2.1 Hz), 3.88 (1H, d, *J* = 4.4 Hz), 3.74-3.70 (3H, m), 2.71 (1H, qd, *J* = 9.22, 7.0 Hz), 1.29 (3H, d, *J* = 7.0 Hz)

^{13}C NMR (100 MHz, MeOD) δ 178.19, 131.51, 128.08, 74.68, 74.60, 62.62, 62.42, 43.47, 14.72

Accurate Mass (ESI) Calcd. for $C_9H_{14}O_5$ $(M+Na)^+$ 225.1942, found 225.125

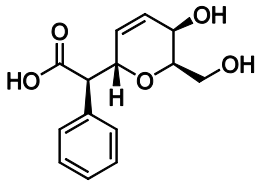

(R)-2-((2S,5R,6R)-5-hydroxy-6-(hydroxymethyl)-5,6-dihydro-2H-pyran-2-yl)-2-phenylacetic acid (125e):

The title compound was prepared from **111e** (0.040 g, 0.12 mmol) in 4M aqueous HCl (1 mL) and THF (3 mL) according to general procedure E. Lyophilization of the purified compound gave **125e** as a lyophilized white powder (0.0059 g, 19 %)

^{1}H NMR (400 MHz, MeOH) δ 7.38 (2H, m), 7.30-7.20 (3H, m), 6.12 (1H, dd, *J* = 10.3, 2.8 Hz), 6.04 (1H, ddd, *J* = 10.3, 5.2, 1.6 Hz), 4.69 (1H, m), 3.87-3.83 (2H, m), 3.76 (1H, dt, *J* = 6.3, 2.38 Hz), 3.55 (1H, dd, *J* = 11.3, 6.0 Hz), 3.39 (1H, dd, *J* = 11.3, 6.6 Hz)

^{13}C NMR (100 MHz, MeOD) δ 138.53, 131.94, 129.75, 129.43, 128.82, 128.36, 75.42, 74.18, 62.52, 62.19, 55.42

MS (ESI) Calcd. for $C_{14}H_{16}O_5$ $(M+NH_4)^+$ 282.3123, found 282.307, $(M+Na)^+$ 287.2636, found 287.131

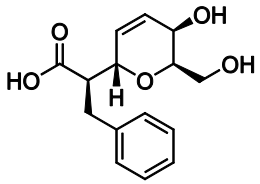

(R)-2-((2S,5R,6R)-5-hydroxy-6-(hydroxymethyl)-5,6-dihydro-2H-pyran-2-yl)-3-phenylpropanoic acid (125f):

The title compound was prepared from **111f** (0.028 g, 0.077 mmol) in NaOMe in MeOH (1 mL) using general procedure D. Lyophilization of the purified compound gave **125f** as a white lyophilized solid (0.0062 g, 29 %).

^{1}H NMR (400 MHz, MeOD) δ 7.26-7.21 (4H, m), 7.16 (1H, m), 6.02 (1H, ddd, *J* = 10.3, 5.2, 1.9 Hz), 5.93 (1H, dd, *J* = 10.3, 3.0 Hz), 4.32 (1H, m), 3.89 (1H, dd, *J* = 5.2, 2.2 Hz), 3.81 (1H, ddd, *J* = 6.9, 4.4, 2.3 Hz), 3.76-3.75 (2H, m), 3.30 (1H, m), 2.91 (2H, m)

Accurate Mass (ESI) Calcd. for $C_{15}H_{18}O_5$ $(M+Na)^+$ 301.2902, found 301.157

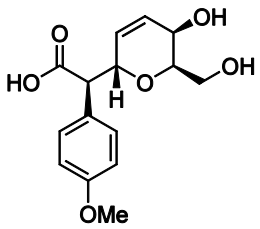

(R)-2-((2S,5R,6R)-5-hydroxy-6-(hydroxymethyl)-5,6-dihydro-2H-pyran-2-yl)-2-(4-methoxyphenyl)acetic acid (125g):

The title compound was prepared from **111g** (0.050 g, 0.13 mmol) in NaOMe in MeOH (5 mL) using general procedure D. Lyophilization of the purified compound gave **125g** as a white lyophilized solid (0.0085 g, 22 %).

^{1}H NMR (400 MHz, MeOD) δ 7.32 (2H, d, *J* = 8.6 Hz), 6.86 (2H, d, *J* = 8.5 Hz), 6.2-6.0 (2H, m), 4.66 (1H, d, *J* = 9.9 Hz), 3.88 (1H, dd, *J* = 5.1, 2.2 Hz), 3.77 (3H, s), 3.59 (2H, dd, *J* = 11.3, 6.0 Hz), 3.44 (2H, dd, *J* = 11.3, 6.6 Hz)

^{13}C NMR (100 MHz, MeOD) δ 160.4, 132.0, 130.4, 128.3, 114.5, 75.6, 75.4, 73.9, 62.3, 62.0, 55.4

Accurate Mass (ESI) Calcd. for $C_{15}H_{18}O_6$ $(M+Na)^+$ 317.2896, found 317.162

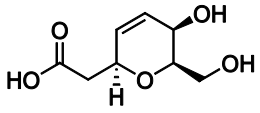

2-((2S,5R,6R)-5-hydroxy-6-(hydroxymethyl)-5,6-dihydro-2H-pyran-2-yl)acetic acid (126a):

The title compound was prepared from **120a** in NaOMe in MeOH (2 mL) using general procedure D. Lyophilization of the purified compound gave **126a** as a white lyophilized solid (0.012 g).

^{1}H NMR (400 MHz, MeOD) δ 5.99 (1H, ddd, *J* = 10.1, 5.3, 2.0 Hz), 5.92 (1H, dd, *J* = 10.2, 0.9 Hz), 4.47 (1H, m), 3.86 (1H, m), 3.71-3.70 (2H, m), 3.57 (1H, m), 2.59 (2H, dq, *J* = 15.9, 6.8)

^{13}C DEPTQ135 NMR (100 MHz, MeOD) δ 174.8, 133.7, 128.4, 80.2, 73.2, 63.2, 63.2, 40.7

Accurate Mass (ESI) Calcd. for $C_8H_{12}O_5$ $(M+Na)^+$ 211.1676, found 211.106

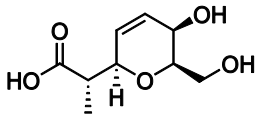

(S)-2-((2R,5R,6R)-5-hydroxy-6-(hydroxymethyl)-5,6-dihydro-2H-pyran-2-yl)propanoic acid (126b):

The title compound was prepared from **120b** (0.070 g, 0.49 mmol) in NaOMe in MeOH (4 mL) using general procedure D. Lyophilization of the purified compound gave **126b** as a white lyophilized solid (0.003 g, 6 %).

^{1}H NMR (400 MHz, $CDCl_3$) δ 6.13 (1H, ddd, *J* = 10.1, 5.6, 2.1 Hz), 5.98 (1H, dd, *J* = 10.3, 1.1 Hz), 5.07 (1H, td, *J* = 5.4, 2.0 Hz), 4.49 (1H, m), 4.22 (2H dq, *J* = 11.5, 6.4 Hz), 3.96 (1H, m), 2.76 (1H, m), 2.08 (3H, s), 2.07 (3H, s), 1.25 (3H, d, *J* = 7.1)

^{13}C NMR (100 MHz, $CDCl_3$) δ 176.3, 170.7, 170.5, 132.5, 124.5, 75.5, 73.8, 63.6, 62.7, 43.3, 20.9, 20.8, 11.4

Accurate Mass (ESI) Calcd. for $C_9H_{14}O_5$ $(M+Na)^+$ 225.1942, found 225.120

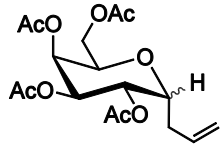

(2R,3S,4R,5S)-2-(acetoxymethyl)-6-allyltetrahydro-2H-pyran-3,4,5-triyl triacetate (127):[22]

To a solution of β-(D)-galactose pentaacetate (8.0 g, 20.5 mmol) in MeCN (40 mL) was added allyltrimethylsilane (4.68 g, 41.0 mmol), and $BF_3{\cdot}Et_2O$ (8.72 g, mmol). The reaction mixture was stirred for overnight at room temperature. The reaction mixture was concentrated and then washed with DCM (3x). The organic fractions were subsequently washed with H_2O (2x), a saturated aqueous solution of $NaHCO_3$ (3x), and brine. The combined organic layers were dried over $MgSO_4$ and concentrated. Purification by silica

flash chromatography with 20 % EtOAc in hexanes gave **127** (4.1 g, 54 %) as anomers, as a yellow oil.

^{1}H NMR (400 MHz, $CDCl_3$) δ 5.75 (1H, dddd, *J* = 17.1, 13.6, 8.4, 5.1 Hz), 5.40 (1H, m), 5.25 (1H, dd, *J* = 9.3, 4.8 Hz), 5.20 (1H, m), 5.14-5.07 (2H, m), 4.28 (1H, td, *J* = 9.9, 4.7 Hz), 4.19 (1H, dd, *J* = 12.5, 8.9 Hz), 4.11-4.04 (2H, m), 2.45 (1H, m), 2.27 (1H, m), 2.10 (3H, s), 2.05 (3H, s), 2.02 (3H, s), 2.01 (3H, s).

Only one isomer represented here. All spectral data was in accordance with the literature.[22]

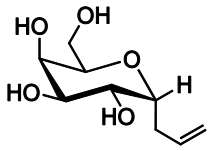

(2R,3R,4R,5R,6R)-2-allyl-6-(hydroxymethyl)tetrahydro-2H-pyran-3,4,5-triol (129):[22]

A solution of NaOMe in MeOH (100 mL, pH 10) was added to **127** (3.8 g, 10.2 mmol). The reaction mixture was stirred at room temperature for overnight. The reaction mixture was brought to pH 6 with Amberlite® IR-120H ion-exchange resin, and then filtered to remove the resin. The filtrate was evaporated to dryness. Toluene was added to the residue, and the mixture was concentrated. The residue was purified by recrystallization from cold MeOH to give **129** (1.96 g, 94 %) as pale pink crystals.

^{1}H NMR (400 MHz, MeOD) δ 5.84 (1H, tdd, *J* = 17.1, 10.2, 7.0 Hz), 5.08 (1H, ddd, *J* = 17.2, 3.2, 1.2 Hz), 5.00 (1H, tdd, *J* = 10.2, 2.2, 1.1 Hz), 3.99-3.84 (3H, m), 3.75-3.62 (4H, m), 2.39 (2H, m), 2.48-2.29 (2H, m).

All spectral data was in accordance with the literature.[22]

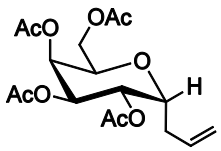

(2R,3S,4R,5S,6R)-2-(acetoxymethyl)-6-allyltetrahydro-2H-pyran-3,4,5-triyl triacetate (130):

A solution of acetic anhydride (8 mL, 76.0 mmol) in pyridine (80 mL) was added to **129** (1.94 g, 9.50 mmol). The reaction mixture was stirred at room temperature for overnight. The reaction was diluted with DCM and washed with a 10 % aqueous solution of HCl, an aqueous saturated solution of $CuSO_4$ (4x), a 10 % aqueous solution of HCl, an aqueous saturated solution of $NaHCO_3$, and brine. The organic fractions were combined, dried over $MgSO_4$, and concentrated. Toluene was added to the residue, and the mixture was evaporated to dryness (3x) to give **130** (1.73 g, 49 %) as a clear, colourless gel.

^{1}H NMR (400 MHz, MeOD) δ 5.76 (1H, tdd, *J* = 17.2, 10.2, 6.9 Hz), 5.42 (1H, m), 5.28 (1H, dd, *J* = 9.3, 5.0 Hz), 5.22 (1H, dd, *J* = 9.3, 3.2 Hz), 5.14 (1H, dddd. *J* = 17.1, 3.0, 1.5 Hz), 5.10 (1H, dd, *J* = 10.1, 2.7, 1.4 Hz), 4.31 (1H, td, *J* = 10.0, 4.8 Hz), 4.21 (1H, dd, *J* = 12.7, 9.0 Hz), 4.12-4.07 (2H, m), 2.13 (3H, s), 2.07 (3H, s), 2.05 (3H, s), 2.03 (3H, s).

All spectral data was in accordance with the literature.[23]

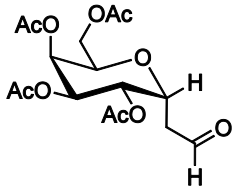

(2R,4S,5S,6R)-2-(acetoxymethyl)-6-(2-oxoethyl)tetrahydro-2H-pyran-3,4,5-triyl triacetate (131):[11]

Through a solution of **130** (1.64 g, 4.41 mmol) in DCM (44 mL) was bubbled O_3 (g) until the solution became blue in colour. Subsequently, N_2 (g) was bubbled through the reaction mixture until the solution became colourless, and PPh_3 (1.39 g, 5.29 mmol) was then added. The reaction mixture was stirred at room temperature for overnight. The reaction mixture

was diluted with DCM, and the organic fraction washed with H_2O and brine. The aqueous fractions were then washed with DCM. The combined organic layers were dried over $MgSO_4$ and concentrated. Purification by silica flash chromatography with a gradient of 20 % toluene in acetone to 25 % toluene in acetone gave **131** (1.49 g, 90 %) as a clear, colourless, very viscous oil.

^{1}H NMR (400 MHz, MeOD) δ 9.73 (1H, d, *J* = 10.6 Hz), 5.43 (1H, m), 5.24 (2H, m), 4.88 (1H, m), 4.33 (1H, m), 4.10 (2H, m), 2.72 (2H, m), 2.36 (1H, m), 2.14-2.04 (12H, m).

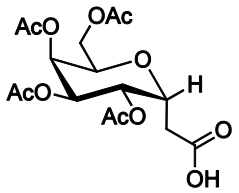

2-((2R,3S,4R,5S,6R)-3,4,5-triacetoxy-6-(acetoxymethyl)tetrahydro-2H-pyran-2-yl)acetic acid (132):[11]

A mixture of KH_2PO_4 (4.45 g, 32.7 mmol) and $NaClO_2$ (2.96 g, 32.7 mmol) in H_2O (15 mL) was sonicated until the solid dissolved. This reaction mixture was added to a solution of **131** (1.46 g, 3.27 mmol) in ^{t}BuOH (18 mL) and *i*PrOH (16.5 mL) cooled to 0 ºC. The reaction mixture was stirred at 0 ºC and 2-methylbut-2-ene (2.89 g, 42.5 mmol) was added. The reaction mixture was stirred at 0 ºC for 0.75 h. The reaction mixture was diluted with EtOAc, and the organic layer was washed with H_2O and brine. The aqueous fractions were then washed with EtOAc. The combined organic layers were dried over $MgSO_4$ and concentrated. Purification by silica flash chromatography with 5 % MeOH in DCM gave **132** (0.472 g, 31 %) as a white foam.

^{1}H NMR (400 MHz, MeOD) δ 5.43 (1H, m), 5.30 (1H, m), 5.17 (1H, m), 4.71 (1H, m), 4.24 (1H, m), 4.14 (2H, m), 2.68 (2H, m), 2.13-2.03 (12 H, m).

All spectral data was in accordance with the literature.[11]

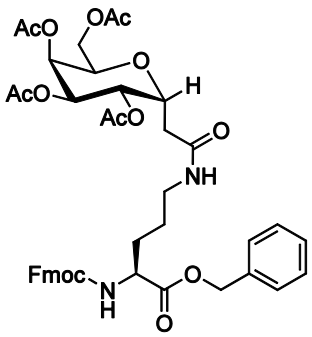

(2R,3S,4R,5S,6R)-2-(2-((S)-4-(((9H-fluoren-9-yl)methoxy)carbonylamino)-5-(benzyloxy)-5-oxopentylamino)-2-oxoethyl)-6-(acetoxymethyl)tetrahydro-2H-pyran-3,4,5-triyl triacetate (133):[11]

To a solution of **132** (0.471 g, 1.21 mmol) in DCM (15 mL) was added HBTU (0.456 g, 1.20 mmol). The reaction was stirred for 0.3 h at room temperature. Subsequently, **37** (0.560 g, 1.00 mmol) and DIPEA (0.155 g, 1.20 mmol) were added to the reaction mixture, and the reaction mixture was stirred at room temperature for overnight. The reaction mixture was diluted with DCM, and the organic layer was washed with H_2O and brine. The aqueous fractions were then washed with DCM. The combined organic layers were dried over $MgSO_4$ and concentrated. Purification by silica flash chromatography with a gradient of 5 % MeOH in DCM to 10 % MeOH in DCM gave **133** (0.639 g, 78 %) as a white powder.

^{1}H NMR (400 MHz, $CDCl_3$) δ 7.77 (2H, d, *J* = 7.4 Hz), 7.60 (2H, d, *J* = 7.2 Hz), 7.42-7.29 (9H, m), 6.15 (1H, m), 5.57 (1H, d, *J* = 8.1 Hz), 5.40 (1H, t, *J* = 3.1 Hz), 5.26 (1H, dd, *J* = 8.4, 4.6 Hz), 5.19-5.14 (3H, m), 4.65 (1H, td, *J* = 9.1, 4.4 Hz), 4.45-4.36 (3H, m), 4.24 (2H, td, *J* = 13.6, 7.9 Hz), 4.15-4.10 (2H, m), 3.26 (2H, dd, *J* = 12.2, 6.2 Hz), 2.52 (1H, dd, *J* = 15.5, 9.6 Hz), 2.39 (1H, dd, *J* = 15.4, 4.3 Hz), 2.11 (3H, s), 2.05 (3H, s), 2.04 (3H, s), 2.00 (3H, s), 1.88 (1H, m), 1.70 (1H, m), 1.60-1.50 (2H, m).

All spectral data was in accordance with the literature.[11]

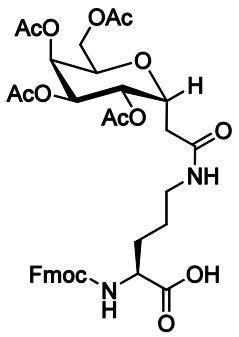

(S)-2-(((9H-fluoren-9-yl)methoxy)carbonylamino)-5-(2-((2R,3S,4R,5S,6R)-3,4,5-triacetoxy-6-(acetoxymethyl)tetrahydro-2H-pyran-2-yl)acetamido)pentanoic acid (134):[11]

To a solution of **133** (1.035 g, 1.27 mmol) in a 1:1 mixture of EtOH and EtOAc (minimum to dissolve all starting material) was added 10% palladium on carbon (0.1 g). The reaction mixture was purged of air and stirred vigorously under H_2 (g) at normal atmosphere for 4 h at room temperature. The reaction mixture was filtered and the filtrate was concentrated. Purification by silica flash chromatography with a gradient of 5 % MeOH in DCM to 10 % MeOH in DCM gave **134** (0.586 g, 63 %) as a white solid. The title compound was added to a larger batch for further purification and solid-phase peptide synthesis, both carried out by Mathieu Leclere.

6.3 Procedures for Assessing Antifreeze Activity

6.3.1: Assessing Thermal Hysteresis (TH) and Dynamic Ice-Shaping (DIS) Activities

TH and DIS activities of carbohydrates were studied using a Clifton nanoliter osmometer (Clifton Technical Physics). The compound being tested was dissolved in distilled water to form a 10 mg/mL solution. Then, a drop (sub-microliter) of solution was introduced into a microscope immersion oil-filled cylindrical well on an aluminum plate. The solution was flash frozen at -40 ºC and then nucleated by slow warming to acquire a stable single ice crystal. The melting and freezing points of the solution were determined by changing the temperature of the system at a constant rate of 10 mOsmol (0.0186 ºC) per 15 seconds.

6.3.2: Assessing Recrystallization Inhibition (RI) Activity

The RI activities were measured using a recrystallization inhibition assay developed by Horwath et al.[24] A 10 μL solution of compound in PBS was dropped from a height of two meters through a shielding tube to a polished aluminum block, which was pre-cooled to -80 °C on dry ice. The "splat cooling" of the solution produced an ice wafer about 1 cm in diameter and 20 μm in thickness. The wafer was then quickly moved onto a microscope cover glass and transferred into a cold chamber, which was dried with continuous air flow to avoid moisture condensing on the ice wafer. The sample was annealed at -6 °C for 30 minutes before the size of the ice grains was photographed using a microscope equipped with an LMPlanF1 20x/0.40 objective. The temperature of the cold chamber was controlled by a Series 800 temperature controller (Alpha Omega Instruments). For each sample drop, three photographs were taken from different areas of the ice wafer. The drop was repeated two additional times to give a total of nine pictures per sample. The size of ice grains was calculated by taking the surface area of twelve random ice grains in each photograph using Domain Recognition Software following the procedure of Jackman *et al*..[25]

6.4 Methods for Assessing Cytotoxicity and Cryopreservation Activity

6.4.1 Cell Culture

Cell culture was undertaken with help from Louise Guolla (Honours B.Sc. student).

WRL 68 human embryonic liver cells (ATCC, CL-48) were cultured in Eagle's minimum essential media (EMEM) (Aldrich, M4655) supplemented with 10% fetal bovine serum (FBS, Hyclone, SH3039703C) and 1% penicillin-streptomycin (Sigma, P4333) T75 flasks (Corning Inc., 430641). Cells were incubated in a 37 °C incubator supplied with 5% CO2. Passage 89 to 104 of WRL 68 cells were used in this study. No evidence of overgrowth or morphological changes consistent with apoptosis was observed. All cells were trypsinized with a trypsin-EDTA solution (Sigma, T4174) for use in experiments.

Umbilical cord blood (UCB) was received in aliquots stored on ice from the Ottawa Hospital Research Institute.

6.4.1 MTT Cytotoxicity Assay

MTT data was collected with the help of Louise Guolla (Honours B.Sc. student).

Cells in culture media were added to half-area 96-well plates in 100µL aliquots and incubated in a 37 °C incubator supplied with 5% CO2 until they reached 100% confluence The cell culture media was then replaced with 40µL fresh cell culture media supplemented with 22, 200, or 500 mM sugar with or without 5% DMSO and incubated at 37 °C for 18h.

Cells incubated with cell culture media without supplement were used as a control. Subsequently, 4µL of MTT solution (3-(4,5-dimethyldiazol-2-yl)-2,5-diphenyl tetrazolium 6 bromide, Sigma, M5655), 5mg/mL in Hank's balanced salt solution (HBSS, Sigma, H8264), was added. Plates were then incubated at 37 °C with 5% CO_2 for 3 h. 100µL of MTT solubilization solution (10% Triton X-100 plus 0.1 N HCl in isopropanol) was added to each well, and each well was aspirated 5 times. Plates were kept in the dark for 18h and the

absorbance of each well was then read at a wavelength of 570 nm with a multiwell plate reader (AD 340C Absorbance Detector, Beckman Coulter, Inc.). Viability was reported as a percentage of the control. All experiments were repeated three times, and 16 wells were used for each condition.

6.4.3 Cryopreservation

This was carried out in collaboration from Luke Wu (Honours B.Sc. and M.Sc student).

WRL 68 cells were cultured and trypsinized as described above. Cells were diluted with culture media and counted using a hemacytometer (BRIGHT-LINE Hemacytometer Set, Hausser Scientific, 1492). Aliquots containing $1x10^7$ cells were added to 15 mL centrifuge tubes and cells were pelleted by centrifugation for 10 min at 2000 g. The supernatant was removed and the cells were resuspended in 1.5 mL HTK (CUSTODIOL ® HTK (Histidine-Tryptophan-Ketoglutarate), Methapharm Inc.) supplemented with sugar to a concentration of 22, 200 or 500 mM with or without DMSO (Sigma, D8418) at a concentration of 5 %. HTK supplemented with DMSO to a concentration of 5 or 10 % served as the positive controls. Cell suspensions were transferred to 1.8 mL cryogenic vials (VWR, CA16001-102) and placed in to a "Mr. Frosty" freezing container (Nalgene ® Mr. Frosty, Sigma, C1562). The container was placed in an ultra-cold freezer (-80°C) for 24 h. According to the manufacturer, "Mr. Frosty" provides a sample cooling rate of approximately 1°C /min. Samples were then stored in [cell cryo tank] in the vapour phase of liquid nitrogen (-150 °C) for 6 days. Following storage, samples were rapidly thawed in a 37 °C water bath with gentle agitation. Thawed samples were transferred to 15 mL centrifuge tubes and slowly diluted to 3 mL by dropwise addition of cell culture medium. After 3 minutes samples were further diluted to 9 mL. Cells were pelleted by centrifugation for 10 minutes at 2000 rpm. The supernatant was decanted and the pellet resuspended in 5 mL EMEM cell culture medium. Centrifuge tubes were stored in a 37 °C water bath for transport.

6.4.4 Flow Cytometry

Flow cytometry data was collected by Luke Wu (Honours B.Sc. and M.Sc student).

After cryopreservation and thawing as described above, the cell count was determined using a hemacytometer and an aliquot containing $1x10^6$ cells was transferred to a 15 mL centrifuge tube and diluted with to 1mL cell culture media. Cells were pelleted by centrifugation for 10 min at 300 g. The supernatant was removed and the pellet was resuspended in 1mL Annexin V-PE binding buffer (PE: phycoerythrin) (BD Pharmingen, Annexin V-PE Apoptosis Detection Kit I, 559763) and 100 µL of the sample was transferred to a flow cytometry tube. Subsequently, 5 µL 7-Actinomycin D (7AAD) and 4 µL Annexin V-PE (BD Pharmingen, Annexin V-PE Apoptosis Detection Kit I, 559763) were added and samples were incubated for 20 min in the dark. Following incubation, samples were diluted to 500 µL with Annexin V-PE binding buffer. Flow cytometry analysis on 10,000 cells was carried out on a BD LSR flow cytometer using CellQuest™ software (Becton Dickinson). Annexin V-PE was measured on FL-2 while 7-AAD was measured on FL-3. Annexin V-PE-/7-AAD- cells were denoted as completely viable, Annexin V-PE+ /7-AAD- cells as early apoptotic, Annexin V-PE+ /7-AAD+ cells as late apoptotic and Annexin V-PE- /7-AAD+ as necrotic. Compensation was set from a single stain experiments with 7-AAD and Annexin V-PE. Aliquots from non-cryopreserved samples labeled with equivalent fluorochromes were used to set the control gate excluding 99% 7-AAD Positive cells. Time between thawing and analysis by flow cytometry was 2 h. All trials were performed at least in duplicate.

6.5 Statistical Analysis

MTT cytotoxicity data analysis was carried out using a two-way nested analysis of variance (ANOVA) model. The nested ANOVA calculations were carried out by Scott Findlay using the statistical package S-Plus v. 8.0 (TIBCO Software Inc.).

Cryopreservation data analysis was carried out using one-way and two-way ANOVA models, using the statistical package S-Plus v. 8.0 (TIBCO Software Inc.).

1. Burchat, A. F.; Chong, J. M.; Nielsen, N., Titration of alkyllithiums with a simple reagent to a blue endpoint. *Journal of Organometallic chemistry* **1997,** 542, 281-283.
2. Gottlieb, H. E.; Kotlyar, V.; Nudelman, A., NMR chemical shifts of common laboratory solvents as trace impurities. *Journal of Organic Chemistry* **1997,** 62, 7512-7515.
3. Larrosa, I.; Romea, P.; Urpi, F.; Balsells, D.; Vilarrasa, J.; Font-Bardia, M.; Solans, X., Unprecedented highly stereoselective α- and β-C-glycosidation with chiral titanium enolates. *Organic Letters* **2002,** 4, 4651-4654.
4. Somsak, L.; Nemeth, I., A simple method for the synthesis of acylated pyranoid glycals under aprotic conditions. *Journal of Carbohydrate Chemistry* **1993,** 12, 679 - 684.
5. McKennon, M. J.; Meyers, A. I., A covalent reduction of amino acids and their derivatives. *Journal of Organic Chemistry* **1993,** 58, 3568-3571.
6. Crimmins, M. T.; King, B. W.; Tabet, E. A.; Chaudhary, K., Asymmetric aldol additions: use of titanium tetrachloride and (-)-sparteine for teh soft enolization of *N*-acyl oxazolidinones, oxazoladinethiones, and thiazolidinethiones. *Journal of Organic Chemistry* **2001,** 66, 894-902.
7. Janczuk, A. J.; Zhang, W.; Andreana, P. R.; Warrick, J.; Wang, P. G., The synthesis of deoxy-α-Gal epitope derivatives for the evaluation of an anti-α-Gal antibody binding. *Carbohydrate Research* **2002,** 337, 1247-1259.
8. Ohlsson, J.; Magnusson, G., Galabiosyl donors; efficient synthesis from 1,2,3,4,6-penta-*O*-acetyl-β-D-galatopyranose. *Carbohydrate Research* **2000,** 329, 49-55.
9. Misra, A. K.; Agnihotri, G., Chloramine-T-mediated chemoselective hydrolysis of thioglycosides into glycosyl hemiacetals under neutral conditions. *Carbohydrate Research* **2004,** 339, 885-890.
10. Bouvet, V. R. Novel AFGP 8 analogues: synthesis and biological evaluation of potent recrystallization inhibitors. University of Ottawa, Ottawa, 2006.
11. Czechura, P.; Tam, R. Y.; Dimitrijevic, E.; Murphy, A. V.; Ben, R. N., The importance of hydration for inhibiting ice recrystallization with C-linked antifreeze glycoproteins. *Journal of the American Chemical Society* **2008,** 130, 2928-2929.
12. Liu, S.; Ben, R. N., *C*-linked galactosyl serine AFGP analogues as potent recrystallization inhibitors. *Organic Letters* **2005,** 7, 2385-2388.
13. Cribiu, R.; Borbas, K. E.; Cumpstey, I., On the synthesis of vinyl and phenyl C-furanosides by stereospecific debenzylative cycloetherification. *Tetrahedron* **2009,** 65, 2022-2031.
14. Cosp, A.; Romea, P.; Talavera, P.; Urpi, F.; Vilarrasa, J.; Font-Bardia, M.; Solans, X., Enantioselective addition of a chiral thiazolidinethione-derived titanium enolate to acetals. *Organic Letters* **2001,** 3, 615-617.
15. Larionov, O. V.; Meijere, A. d., Enantioselective total syntheses of belactosin A, belactosin C, and its homoanalogue. *Organic Letters* **2004,** 6, 2153-2156.
16. Wu, Y.; Shen, X.; Yang, Y.-Q.; Hu, Q.; Huang, J.-H., Enantioselective total synthesis of (+)-brefeldin A and 7-*epi*-brefeldin A. *Journal of Organic Chemistry* **2004,** 69, 2857-3865.
17. Griffith, W. P.; Ley, S. V.; Whitcombe, G. P.; White, A. D., Preparation and use of tetra-n-butylammonium per-ruthenate (TBAP reagent) and tetra-n-propylammonium per-ruthenate (TPAP reagent) as new catalytic oxidants for alcohols. *Journal of the Chemical Society Chemical Communications* **1987**, 1625-1627.

18. Ley, S. V.; Norman, J.; Griffith, W. P.; Marsden, S. P., Tetrapropylammonium perruthenate, $Pr_4N^+RuO_4^-$, TPAP: a catalytic oxidant for organic synthesis. *Synthesis* **1994**, 639-666.
19. Omura, K.; Swern, D., Oxidation of alcohols by "activated dimethyl sulfoxide. A preparative, steric and mechanistic study. *Tetrahedron* **1978,** 34, 1651-1660.
20. Evans, D. A.; Britton, T. C.; Ellman, J. A., Contrasteric carboximide hydrolysis with lithium hydroperoxide. *Tetrahedron Letters* **1987,** 28, 6141-6144.
21. Nahm, S.; Weinreb, S. M., N-Methoxy-N-methylamides as effective acylating agents. *Tetrahedron Letters* **1981,** 22, 3815-3818.
22. BeMiller, J. N.; Yadav, M. P.; Kalabokis, V. N.; Myers, R. W., *N*-Substituted (b-D-galactopyranosylmehtyl)amines, and *C*-b-D-galactopyranosylformamides, and related compounds. *Carbohydrate Research* **1990,** 200, 111-126.
23. mari, S.; Canada, F. J.; Jimenez-Barbero, J.; Bernardi, A.; Marcou, G.; Motto, I.; Velter, I.; Nicotra, F.; Ferla, B. L., Synthesis and conformational analysis of galactose-derived bicyclic scaffolds. *Eruropean Journal of Organic Chemistry* **2006,** 2006, 2925-2933.
24. Horwath, K. L.; Easton, C. M.; Jr., G. J. P.; Myers, K.; Schnorr, I. L., Tracking the profile of a specific antifreeze protein and its contribution to the thermal hysteresis activity in cold hardy insects. *European Journal of Entomology* **1996,** 93, 419-433.
25. Jackman, J.; Noestheden, M.; Moffat, D.; Pezacki, J. P.; Findlay, S.; Ben, R. N., Assessing antifreeze activity of AFGP 8 using domain recognition software. *Biochemical and Biophysical Research Communications* **2007,** 354, 340-344.

Appendix 1 Compound Characterization

^{1}H NMR and ^{13}C NMR

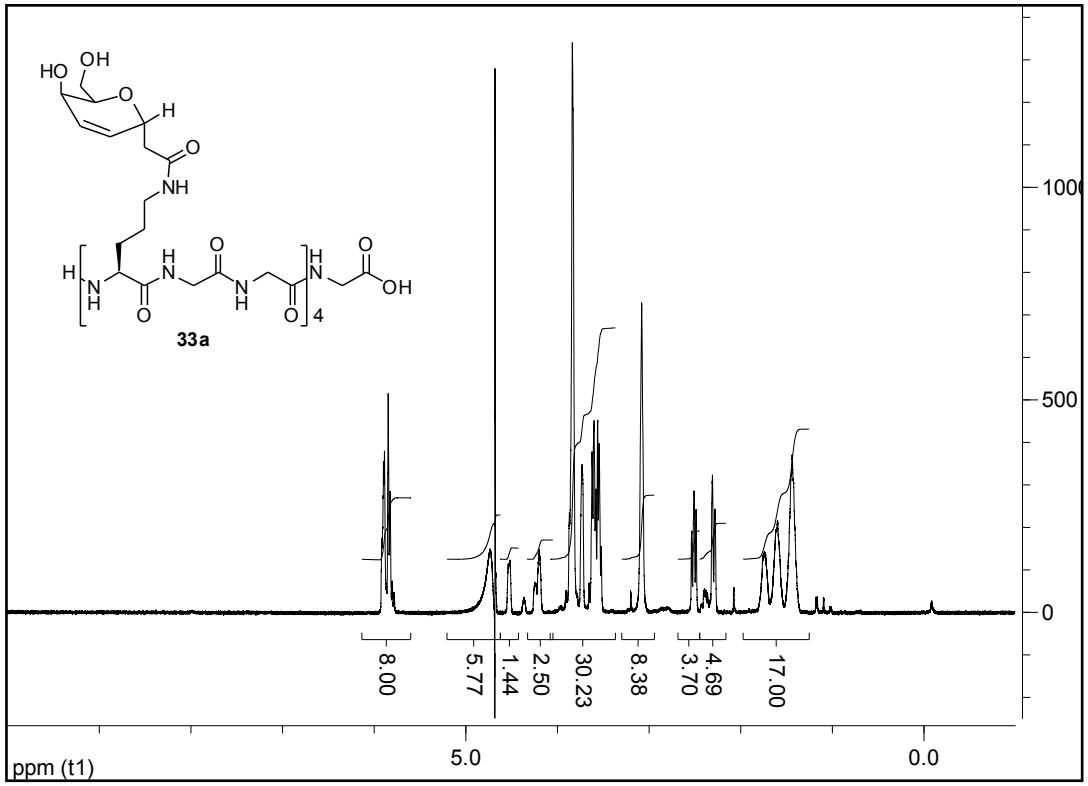

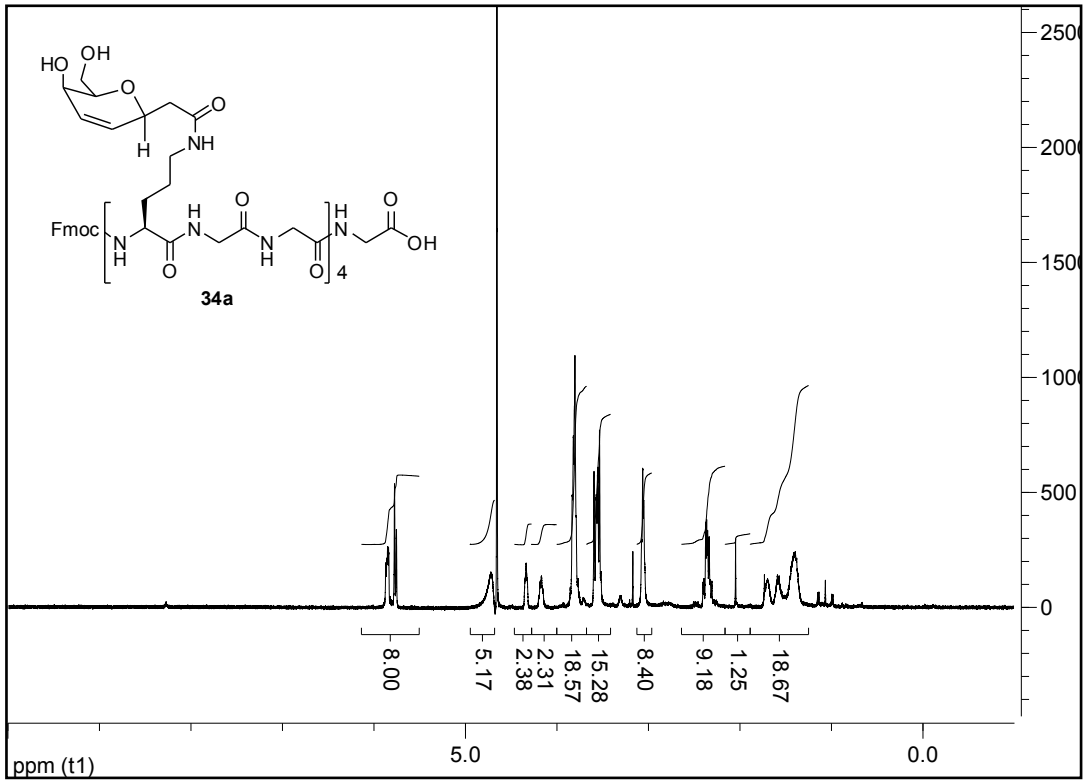
HO
OH
O
O
NH
H
Fmoc
N
H
H
N
O
N
H
O
O
H
N
O
OH
4
34a
8.00
5.17
2.38
2.31
18.57
15.28
8.40
9.18
1.25
18.67
ppm (t1)
5.0
0.0
250
200
150
100
500
0

(S)-4-(((9H-fluoren-9-yl)methoxy)carbonylamino)-5-(benzyloxy)-5-oxopentan-1-aminium 2,2,2-trifluoroacetate (37):

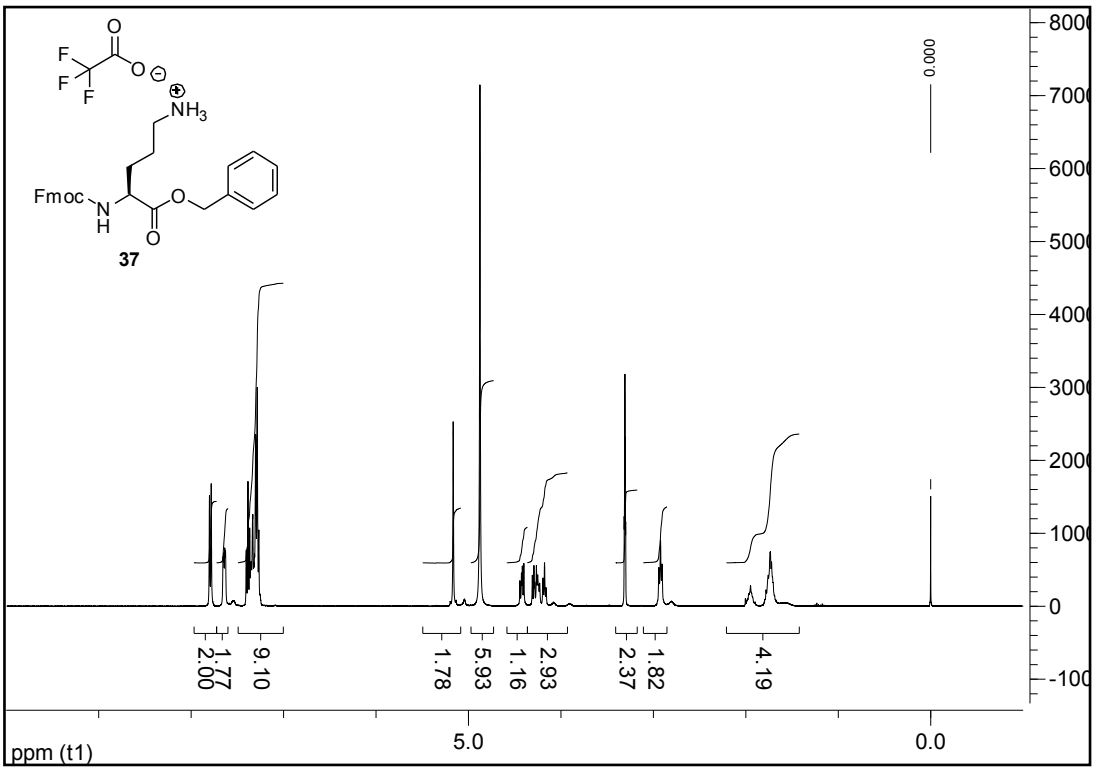

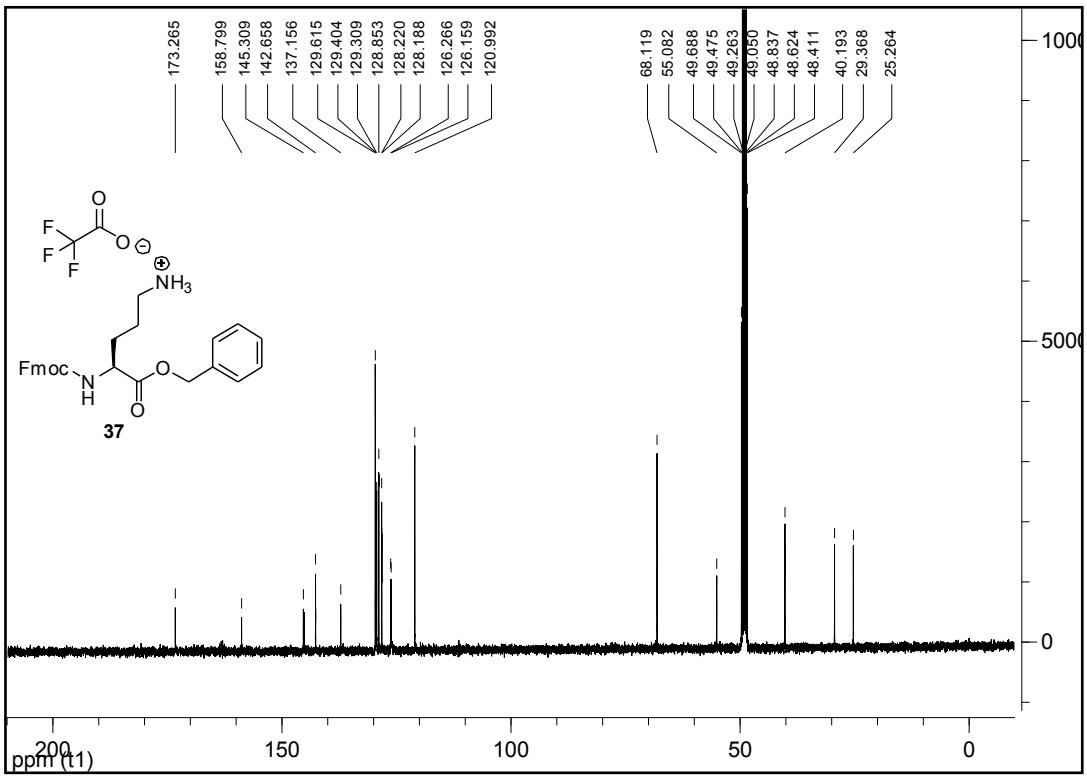

(S)-1-(4-benzyl-2-thioxothiazolidin-3-yl)ethanone (38a) and (R)-1-(4-benzyl-2-thioxothiazolidin-3-yl)ethanone (43a):

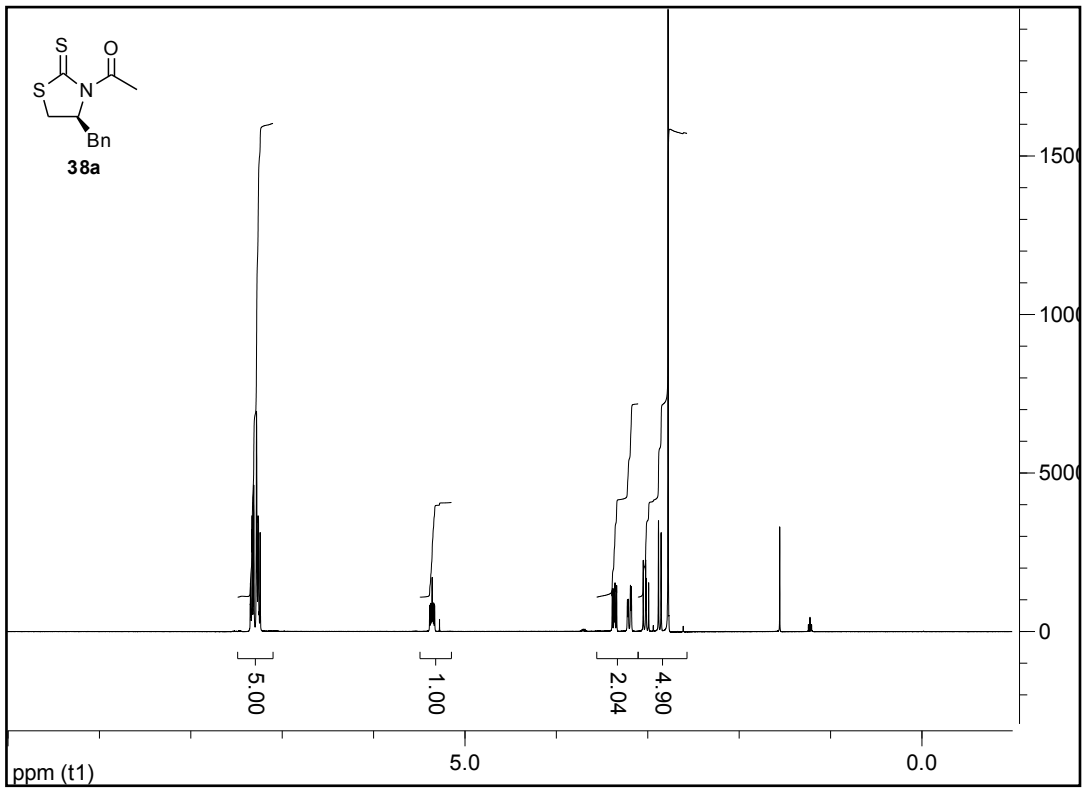

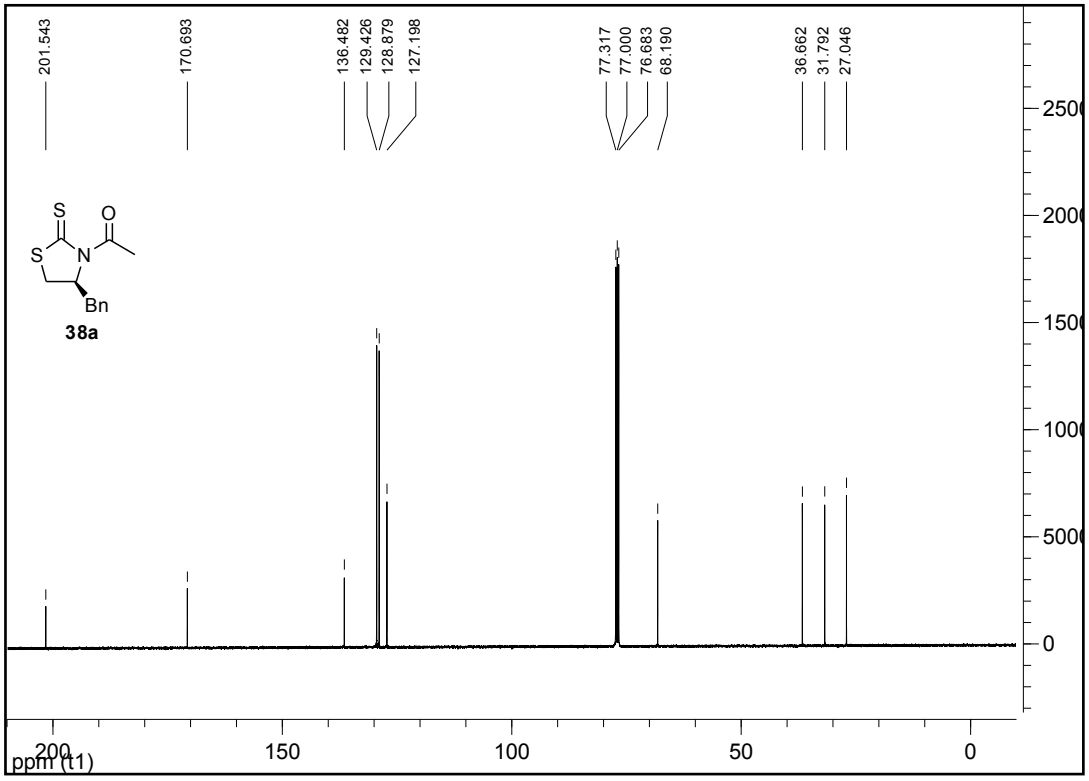

(S)-1-(4-benzyl-2-thioxothiazolidin-3-yl)propan-1-one (38b) and (S)-1-(4-benzyl-2-thioxothiazolidin-3-yl)propan-1-one (43b):

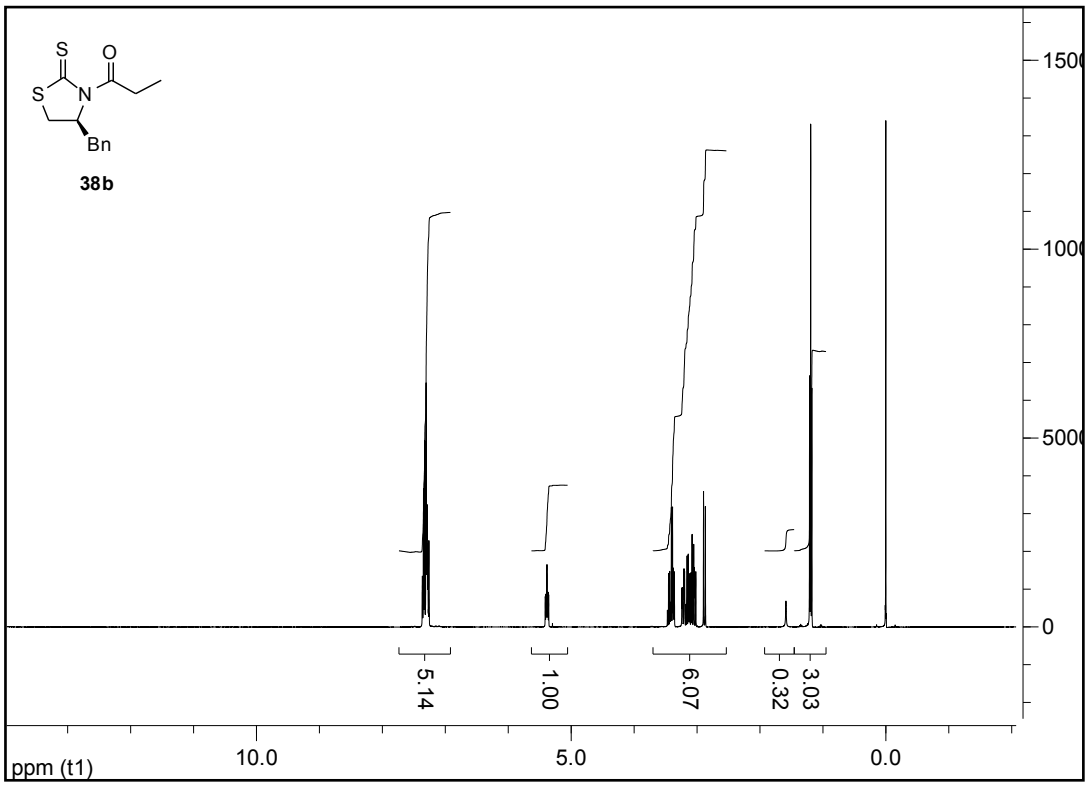

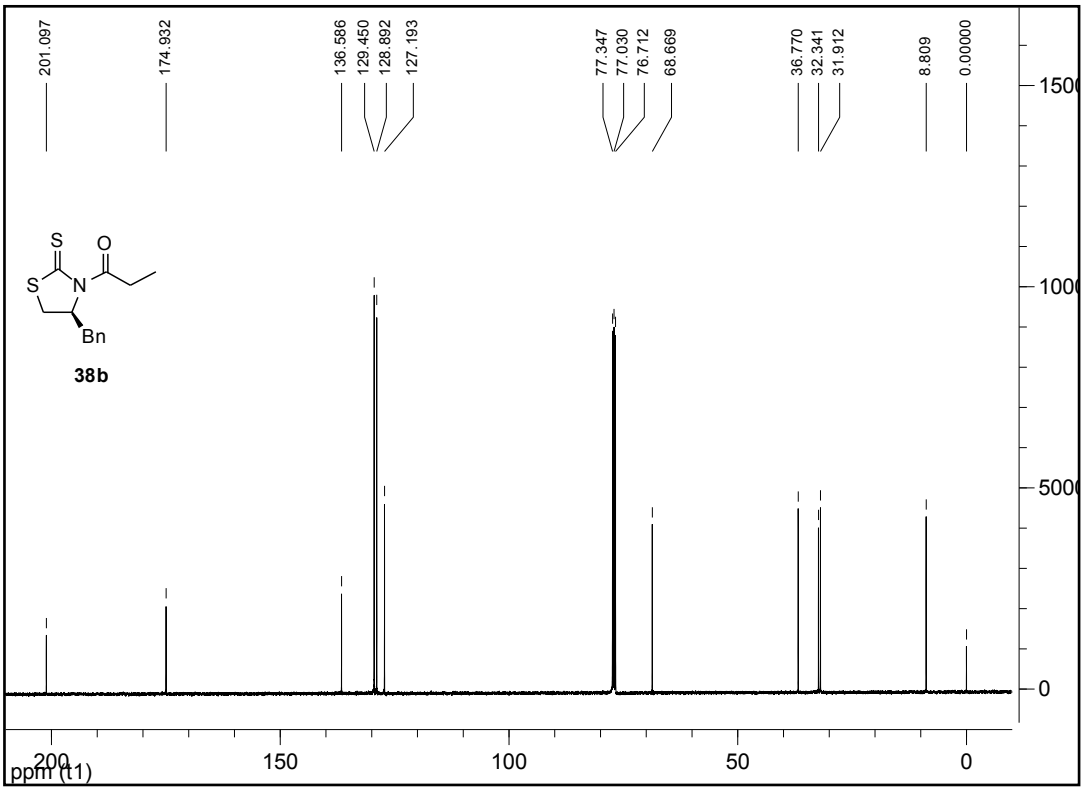

(S)-1-(4-benzyl-2-thioxothiazolidin-3-yl)butan-1-one (38c):

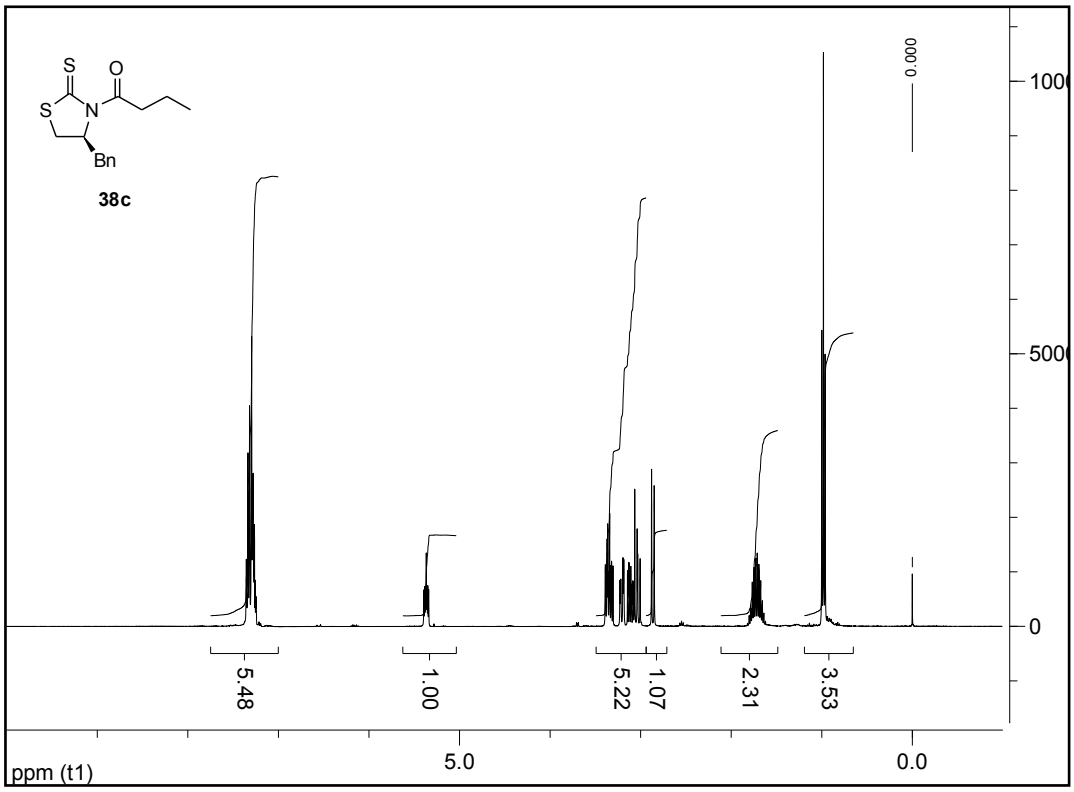

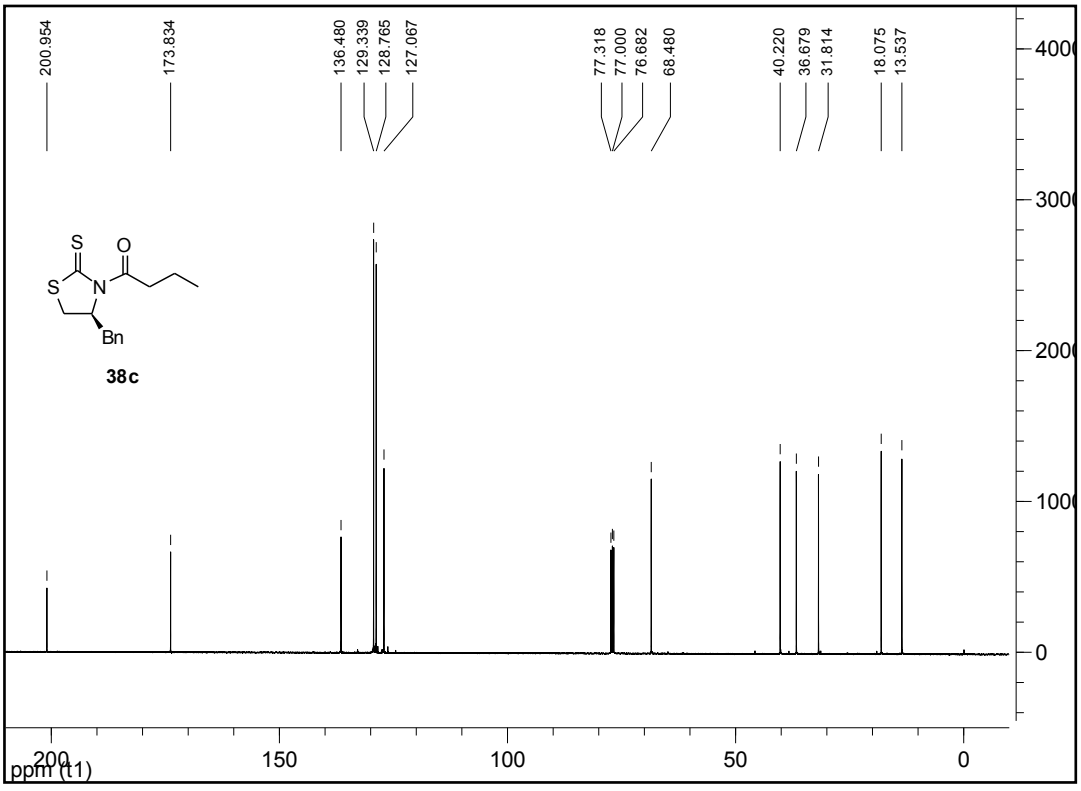

(S)-1-(4-benzyl-2-thioxothiazolidin-3-yl)-2-methylpropan-1-one (38d):

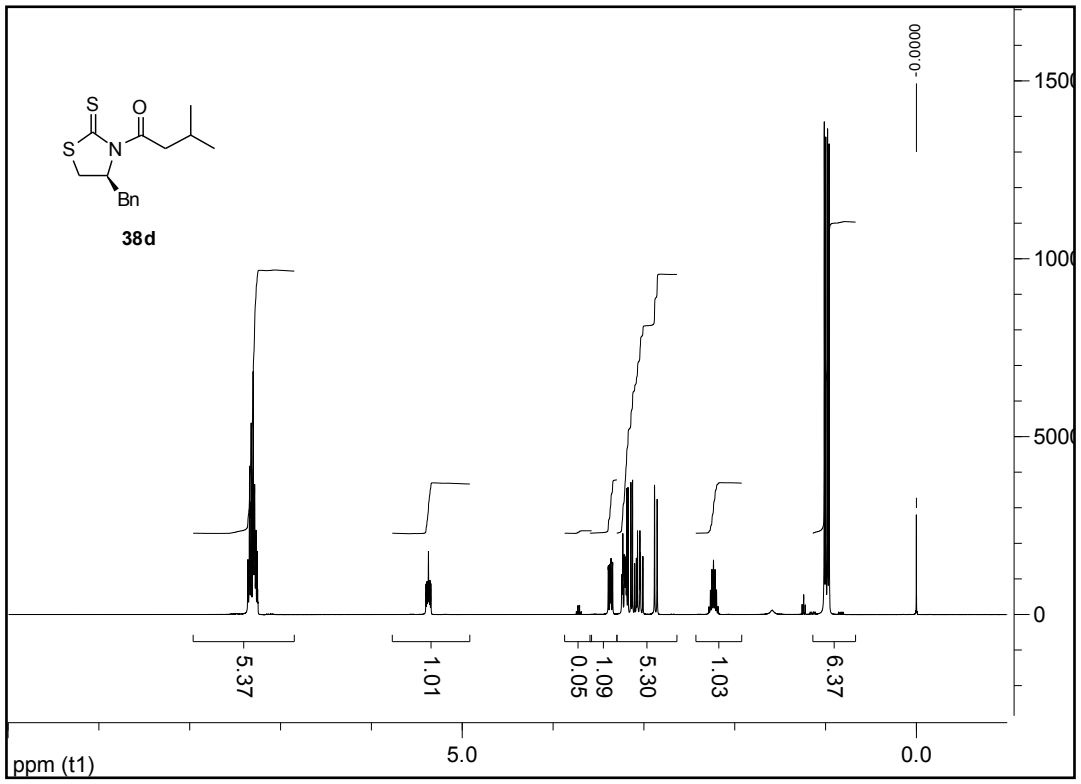

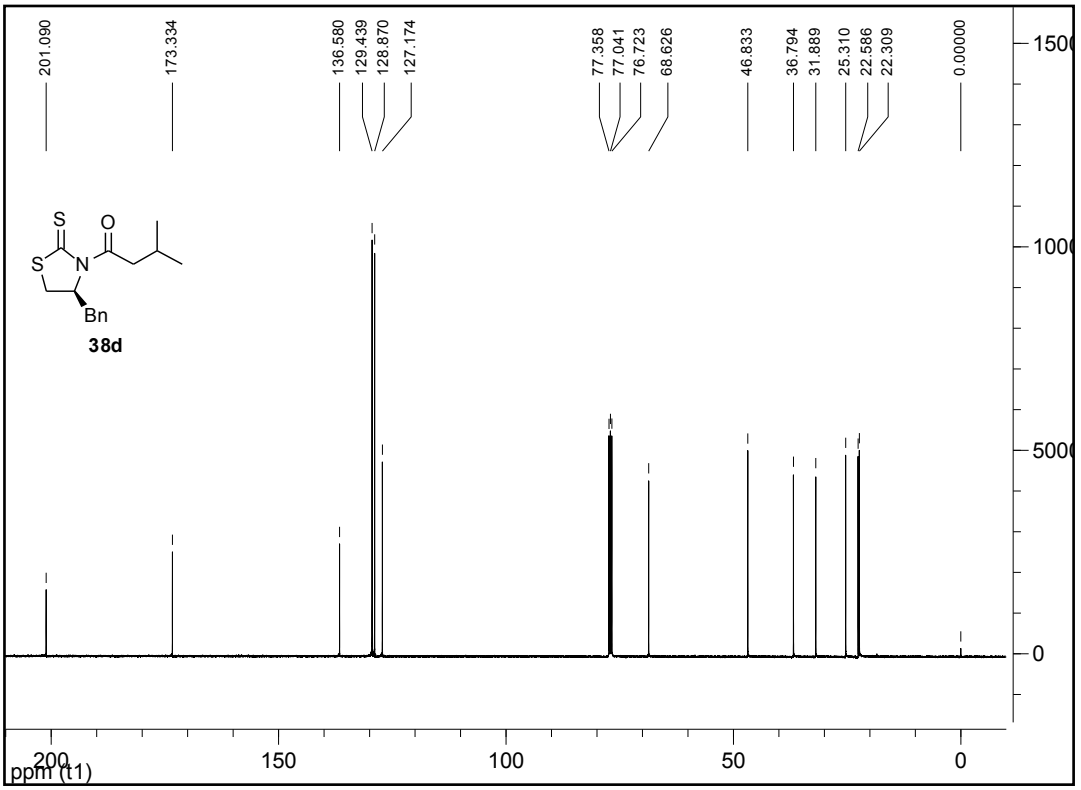

(S)-1-(4-benzyl-2-thioxothiazolidin-3-yl)-2-phenylethanone (38e):

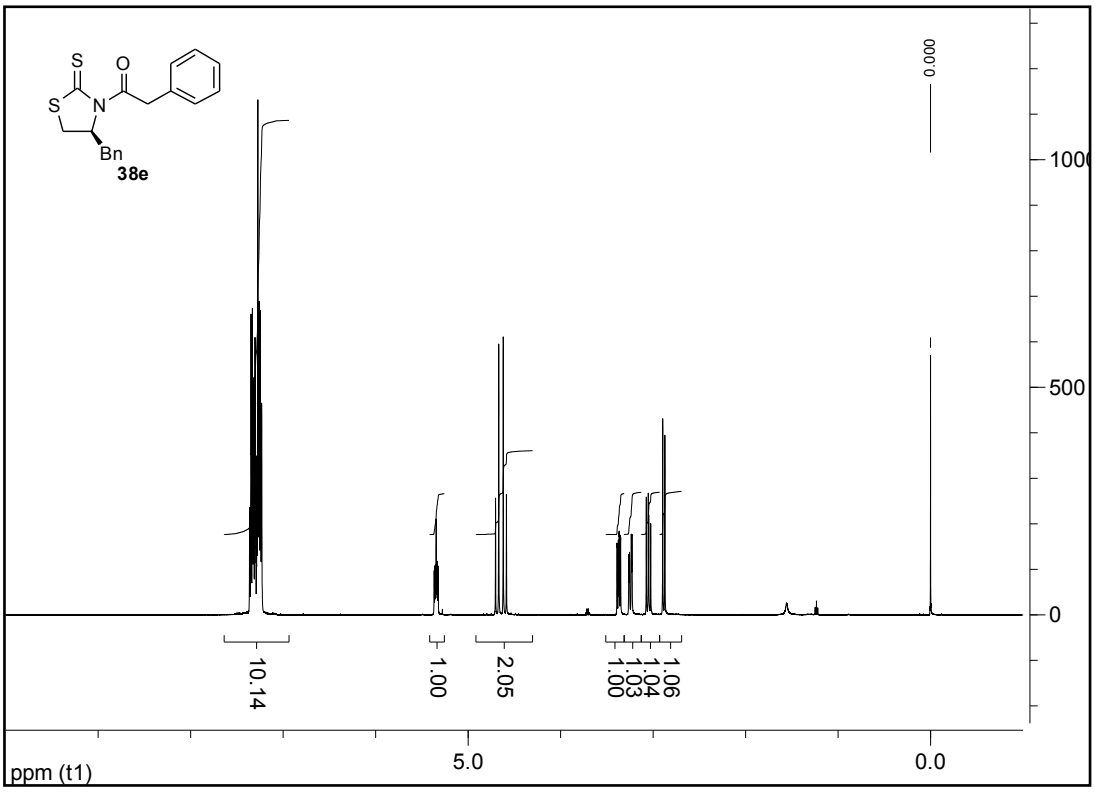

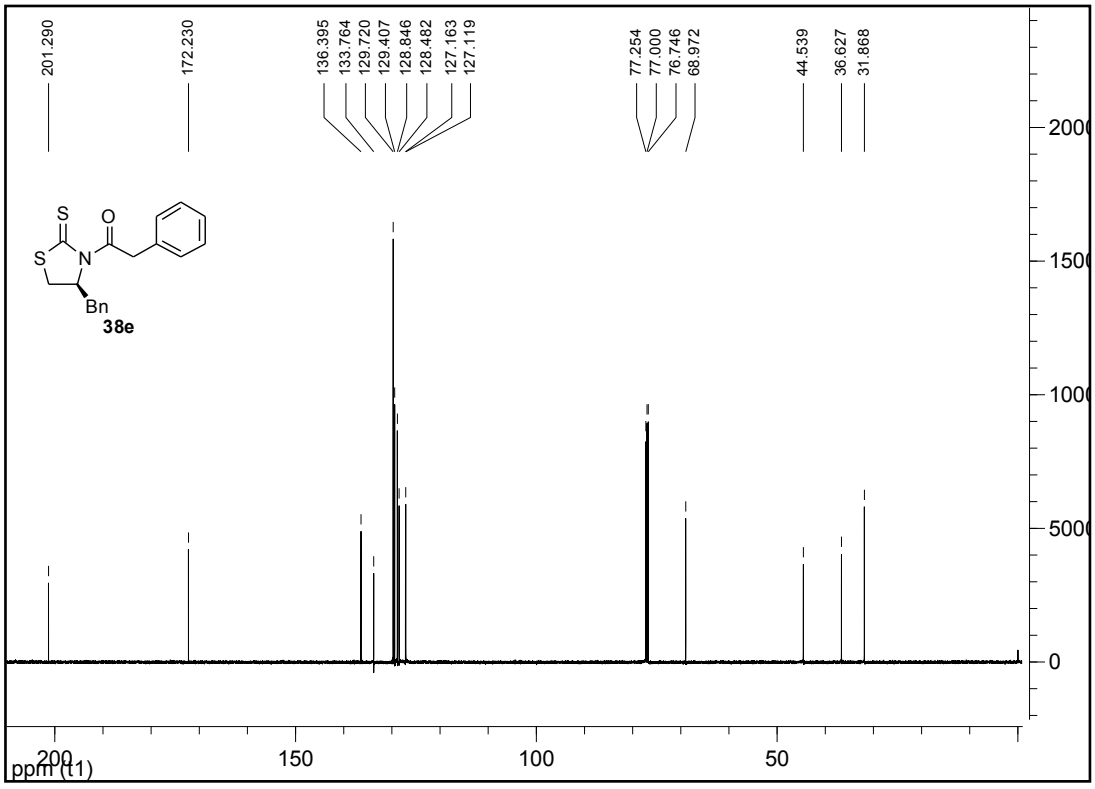

(S)-1-(4-benzyl-2-thioxothiazolidin-3-yl)-3-phenylpropan-1-one (38f):

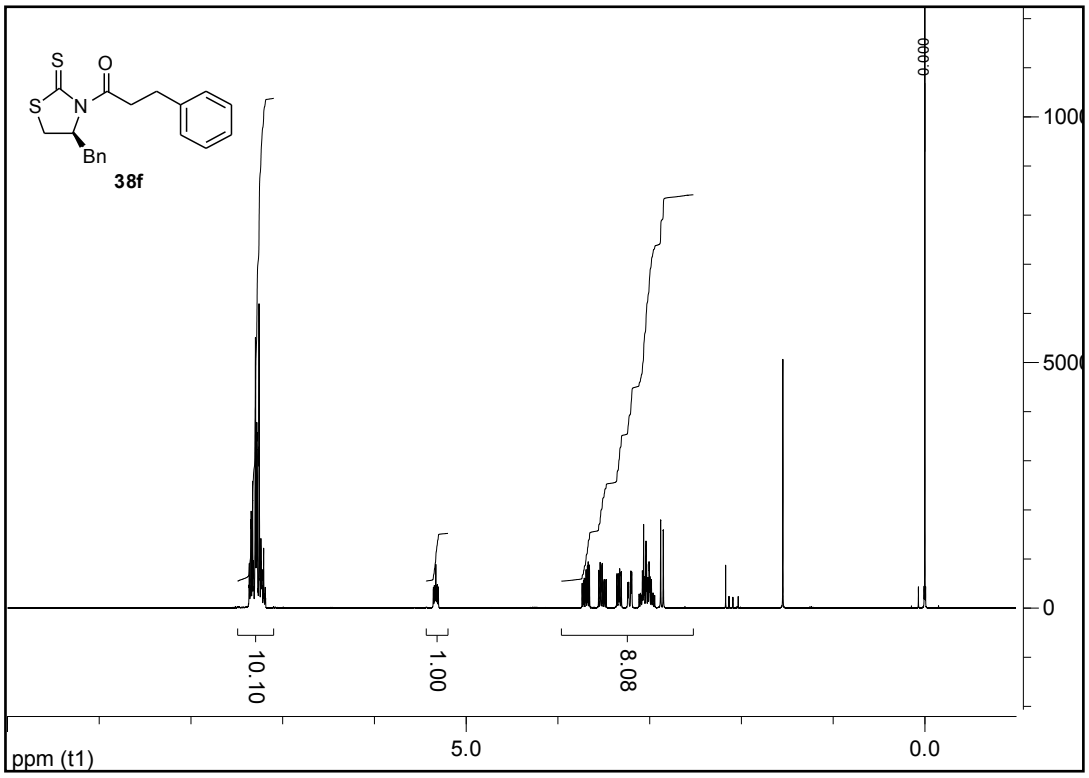

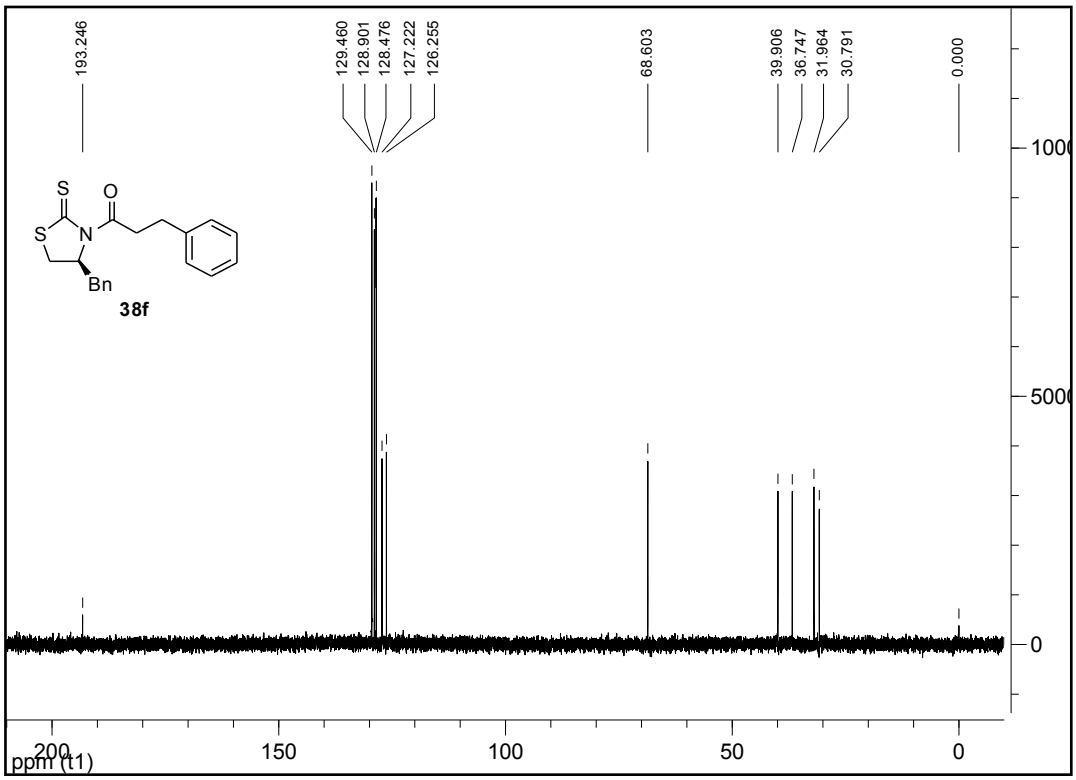

(S)-1-(4-benzyl-2-thioxothiazolidin-3-yl)-2-(4-methoxyphenyl)ethanone (38g):

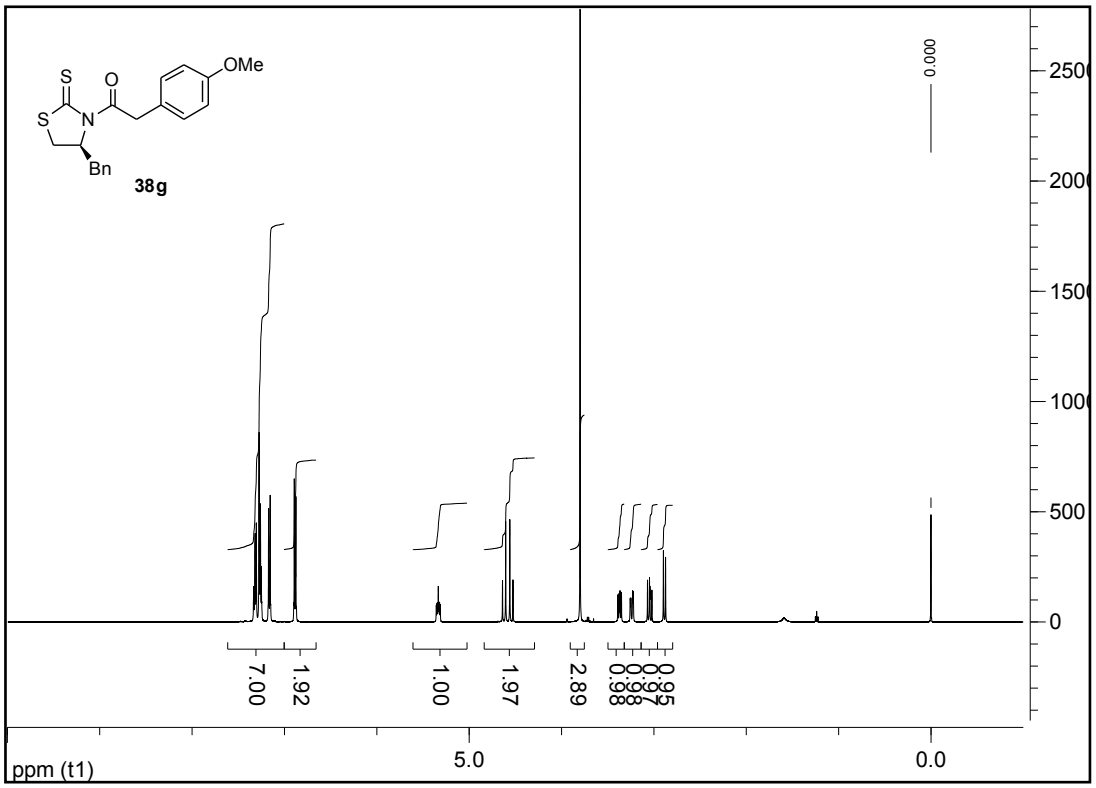

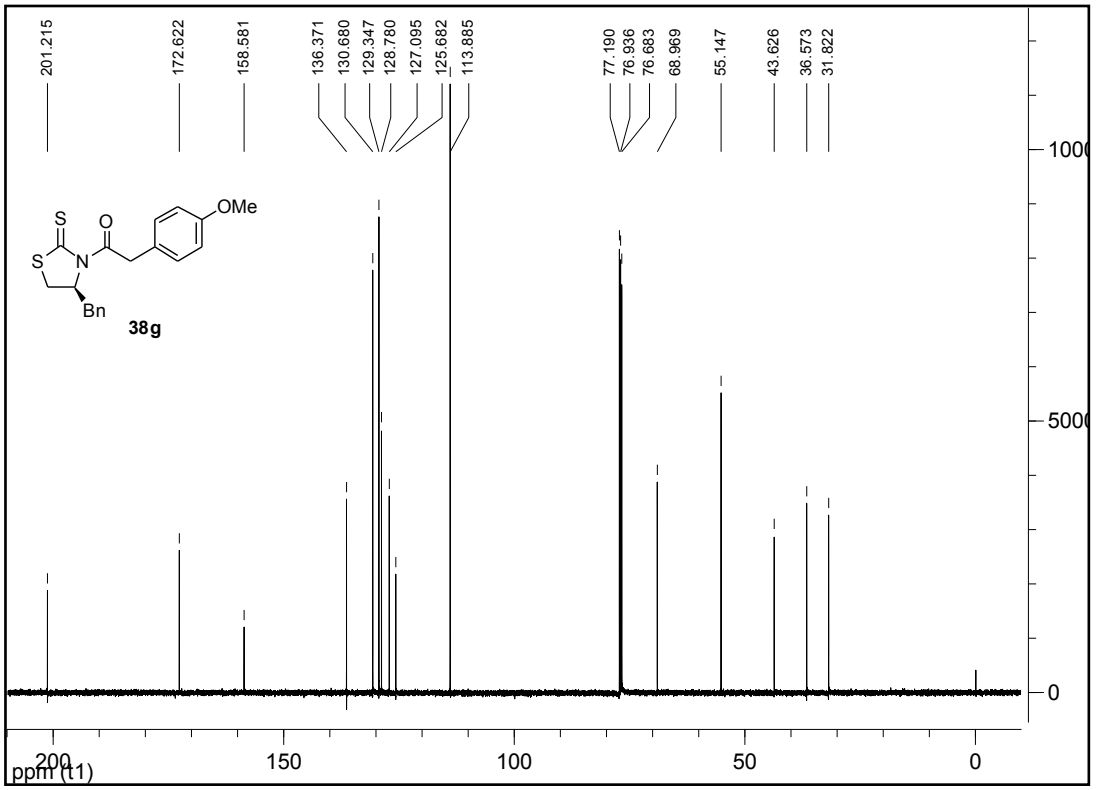

(S)-1-(4-benzyl-2-thioxothiazolidin-3-yl)-2-(4-bromophenyl)ethanone (38h):

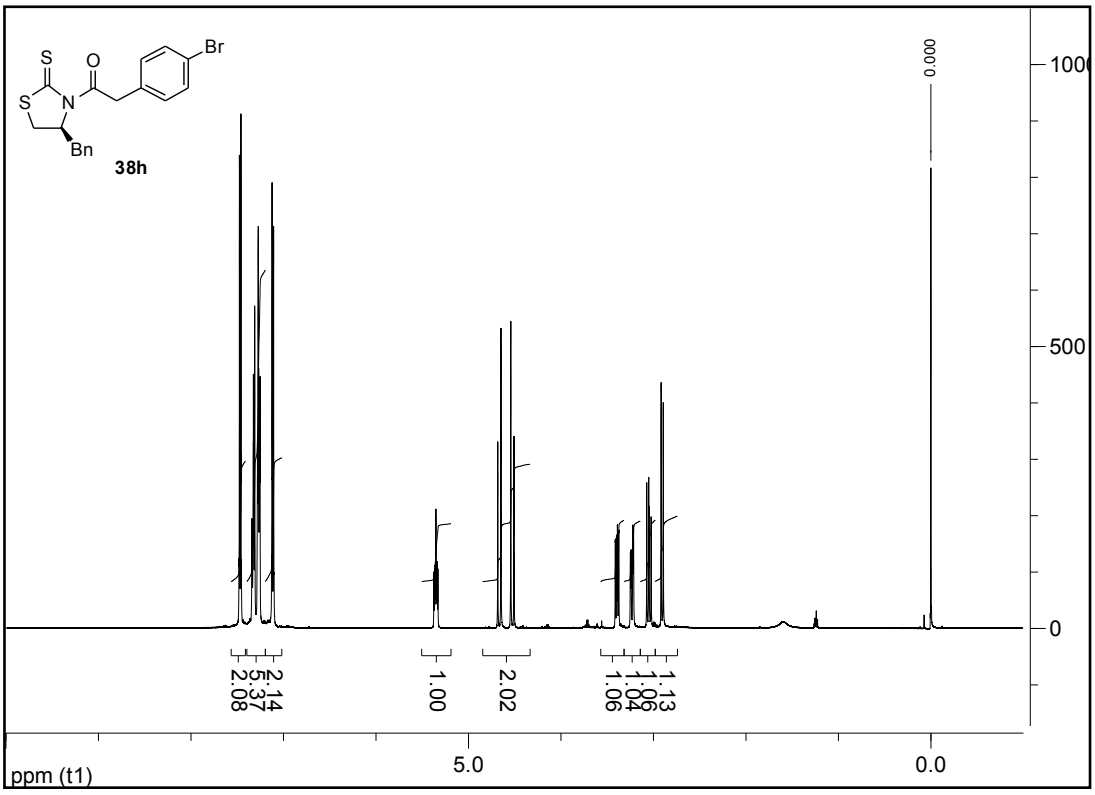

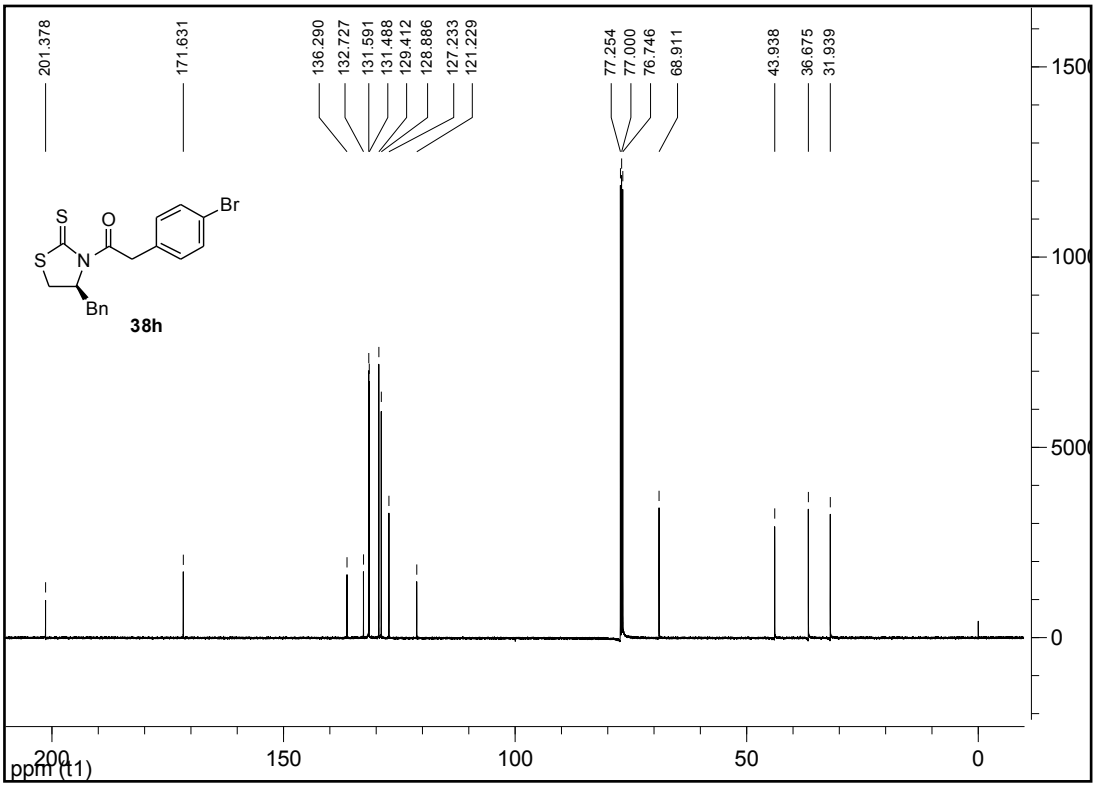

(S)-1-(4-benzyl-2-thioxothiazolidin-3-yl)-2-(4-nitrophenyl)ethanone (38i):

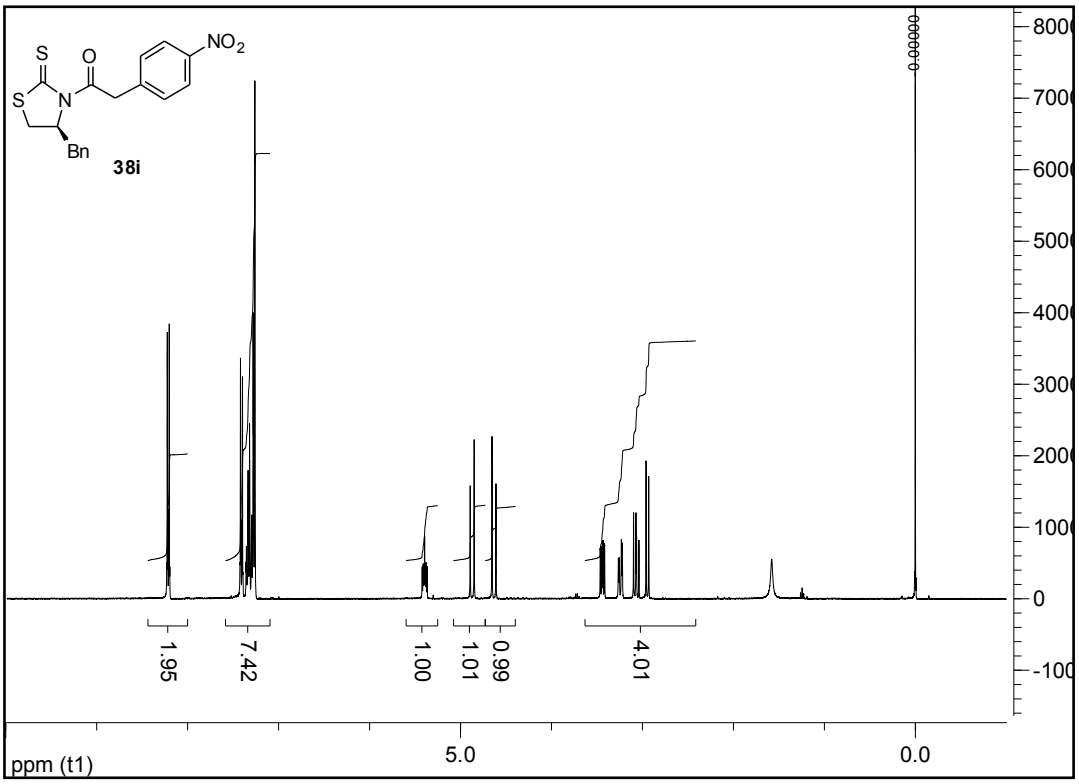

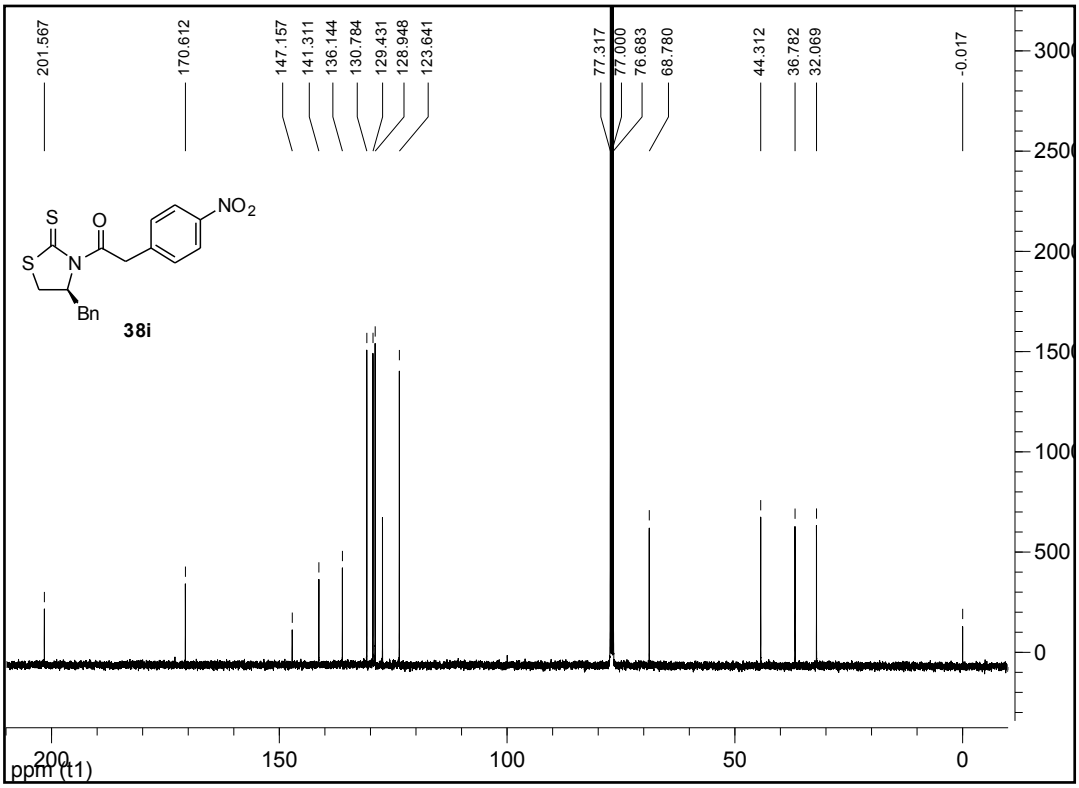

(S)-1-(4-benzyl-2-thioxothiazolidin-3-yl)octan-1-one (38j):

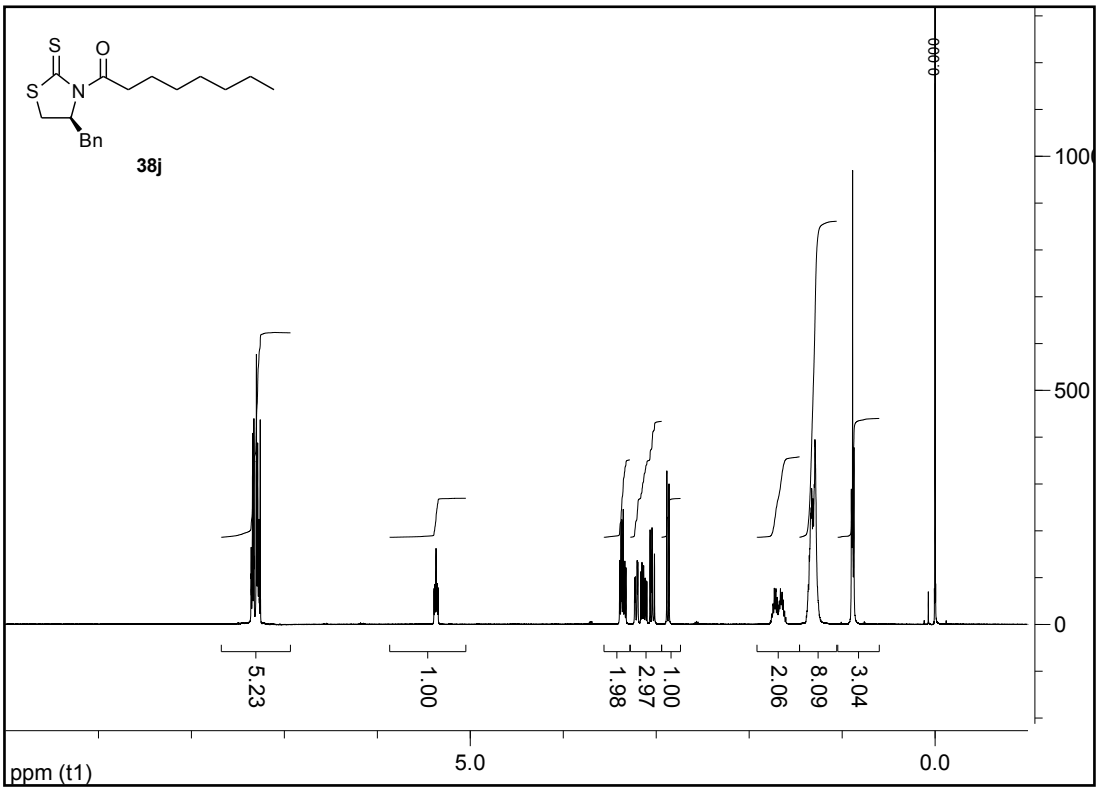

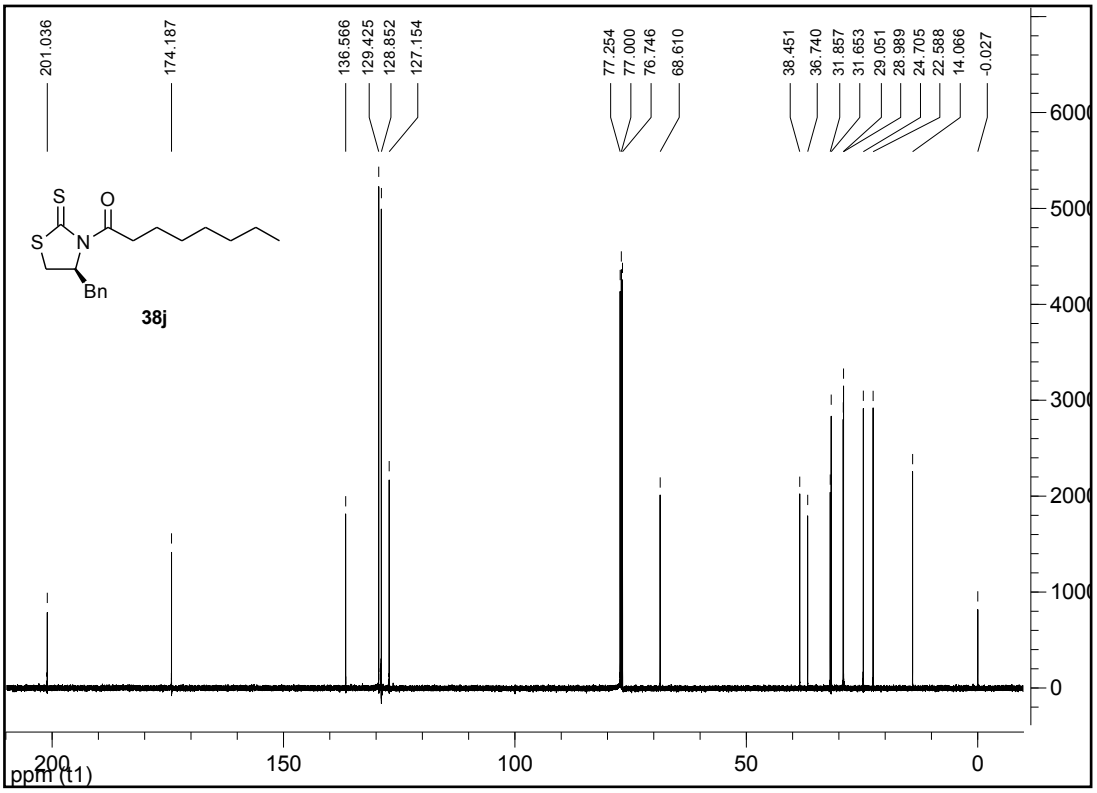

(2R,3R)-2-(acetoxymethyl)-3,4-dihydro-2H-pyran-3,4-diyl diacetate (44):

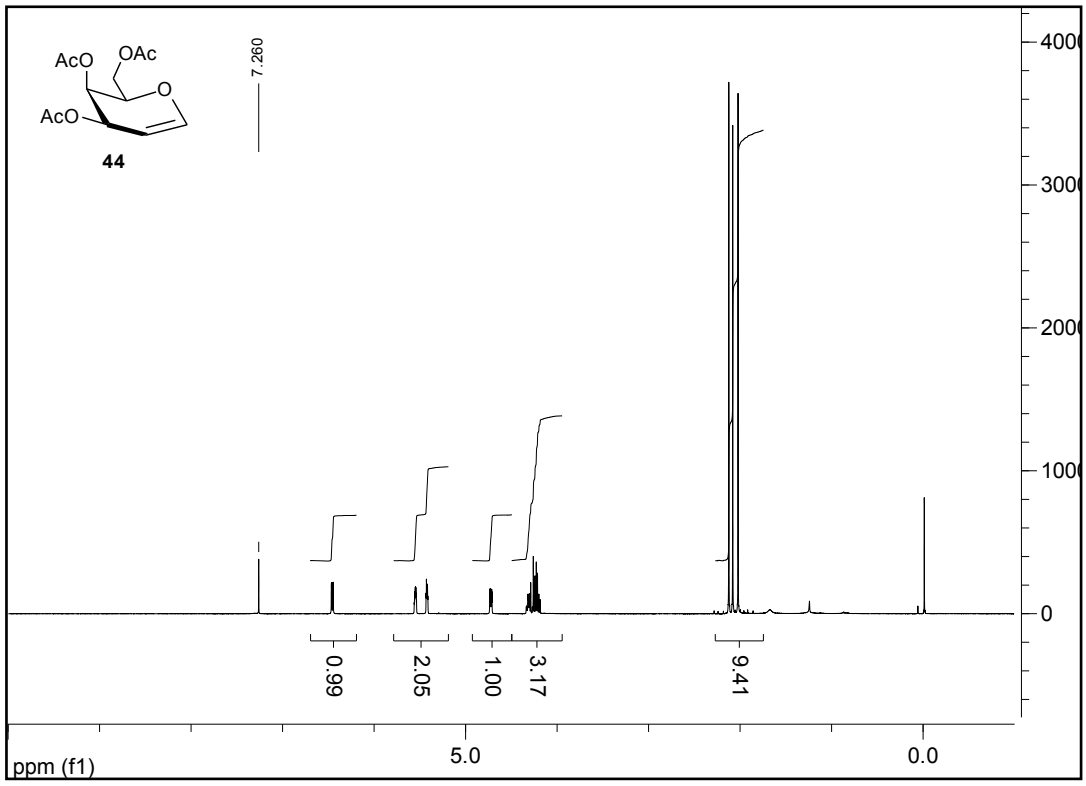

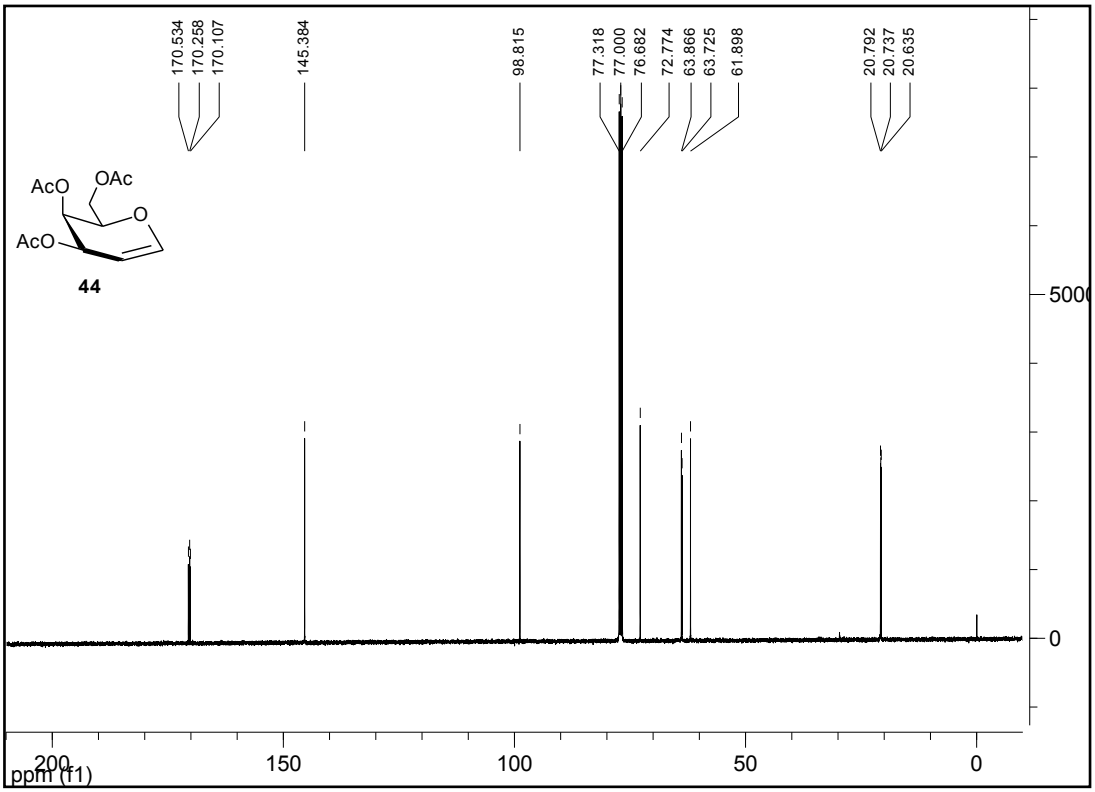

(S)-2-Amino-3-phenylpropan-1-ol (57) and (R)-2-Amino-3-phenylpropan-1-ol (62):

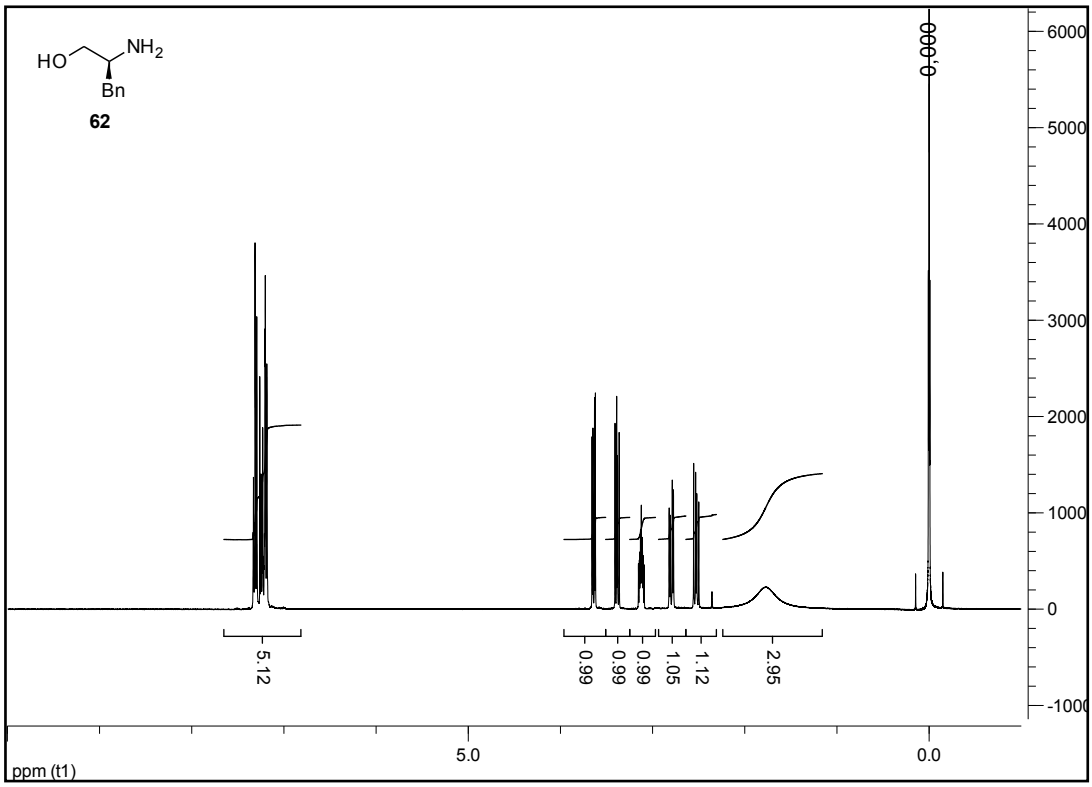

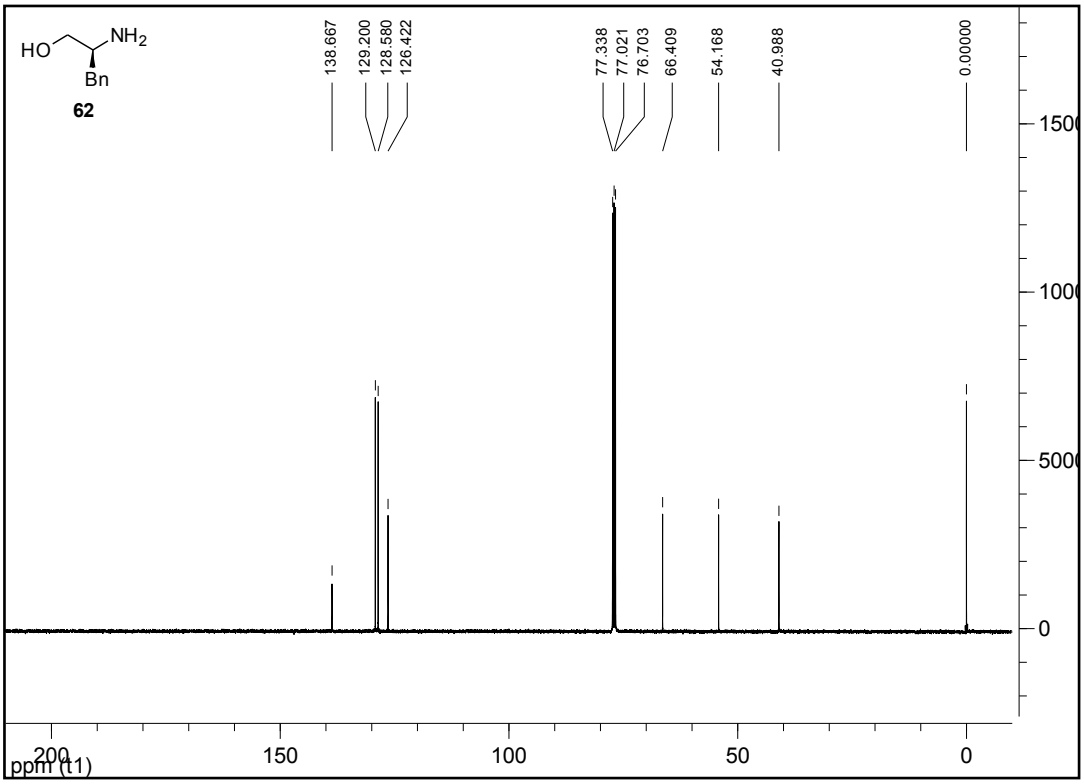

(S)-4-benzylthiazolidine-2-thione (58) and (S)-4-benzylthiazolidine-2-thione (63):

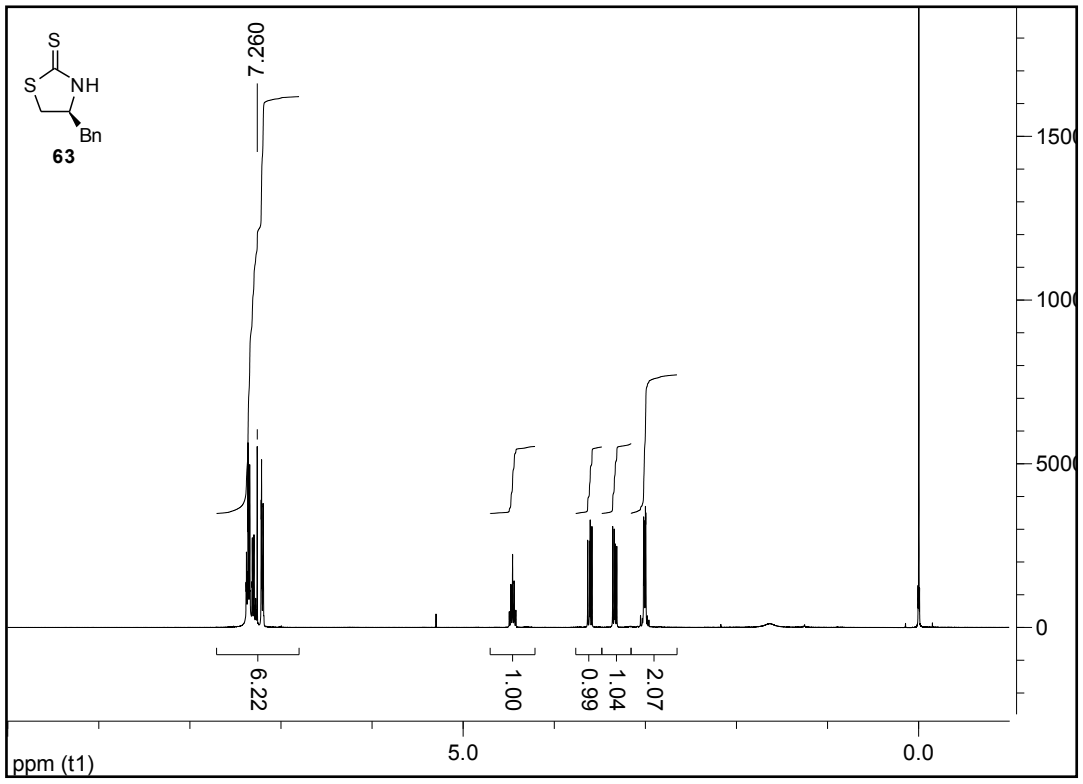

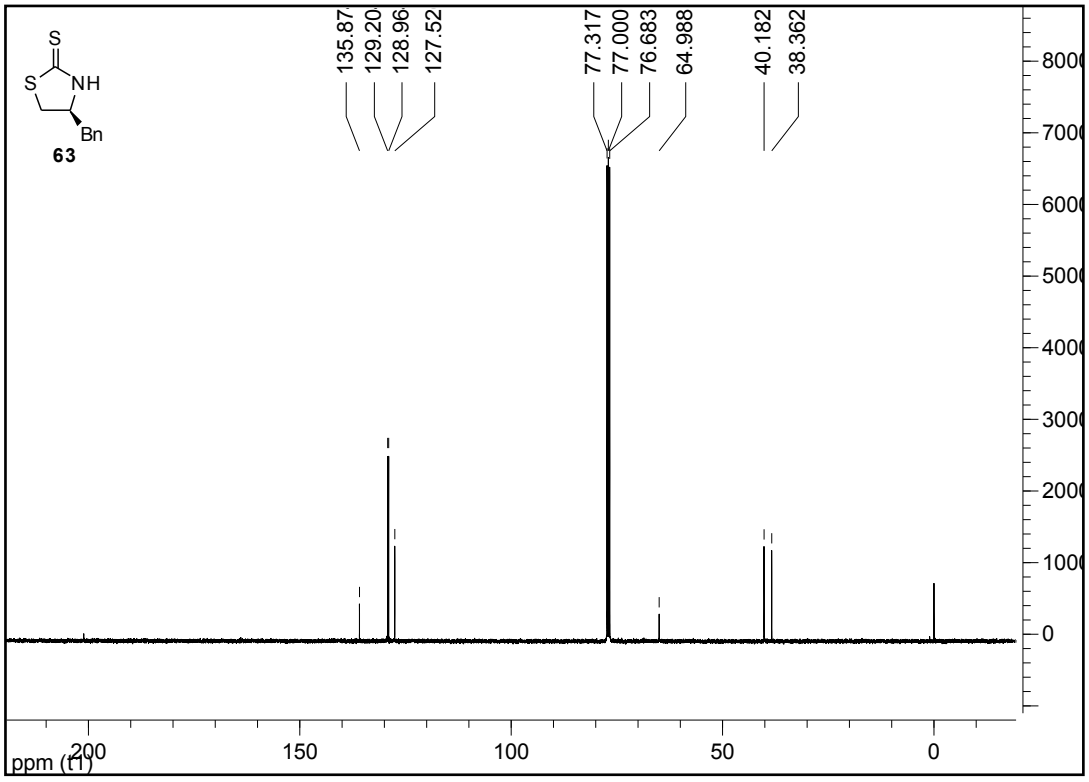

(2R,3S,4S,5S,6S)-2-(acetoxymethyl)-6-(phenylthio)tetrahydro-2H-pyran-3,4,5-triyl triacetate (72):

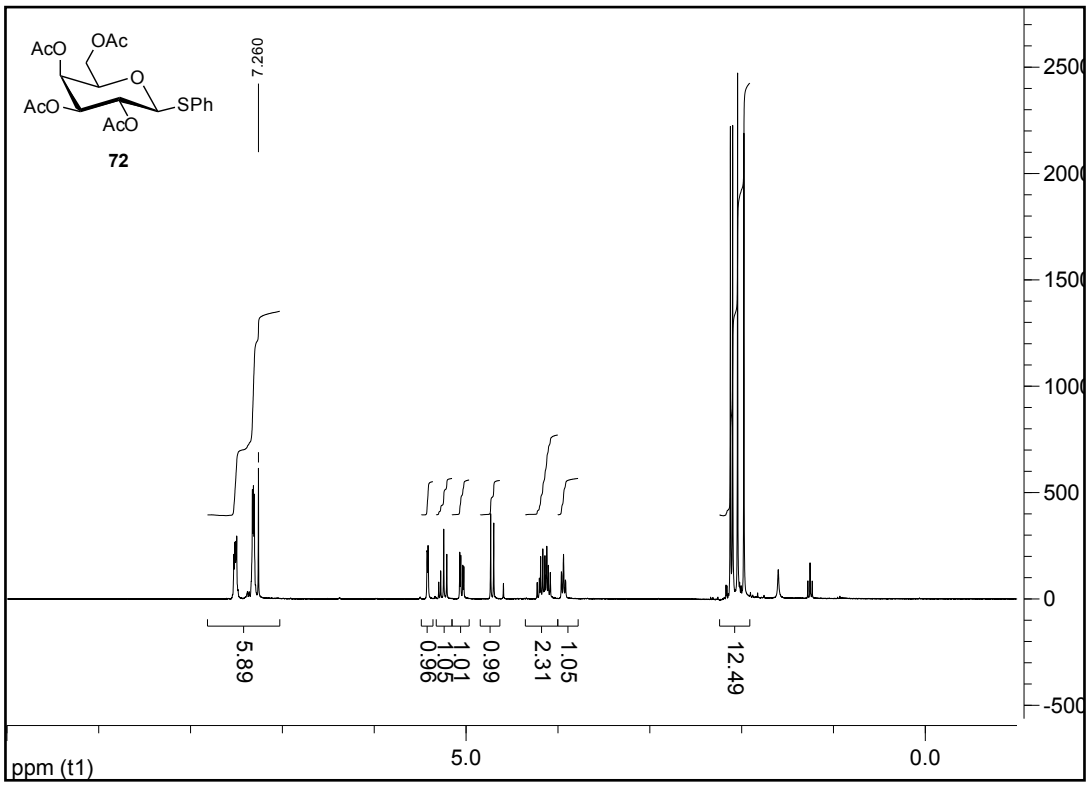

(2R,3R,4S,5R,6S)-2-(hydroxymethyl)-6-(phenylthio)tetrahydro-2H-pyran-3,4,5-triol (73):

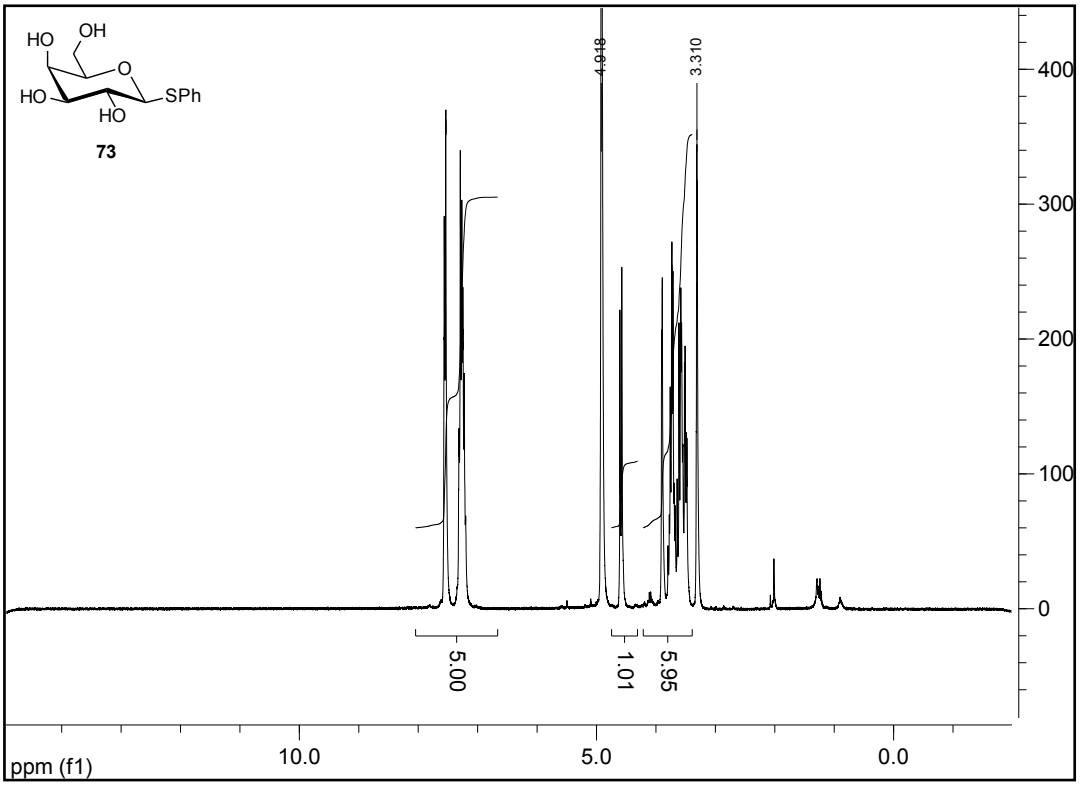

(2R,3S,4S,5R,6S)-3,4,5-tris(benzyloxy)-2-(benzyloxymethyl)-6-(phenylthio)tetrahydro-2H-pyran (74):

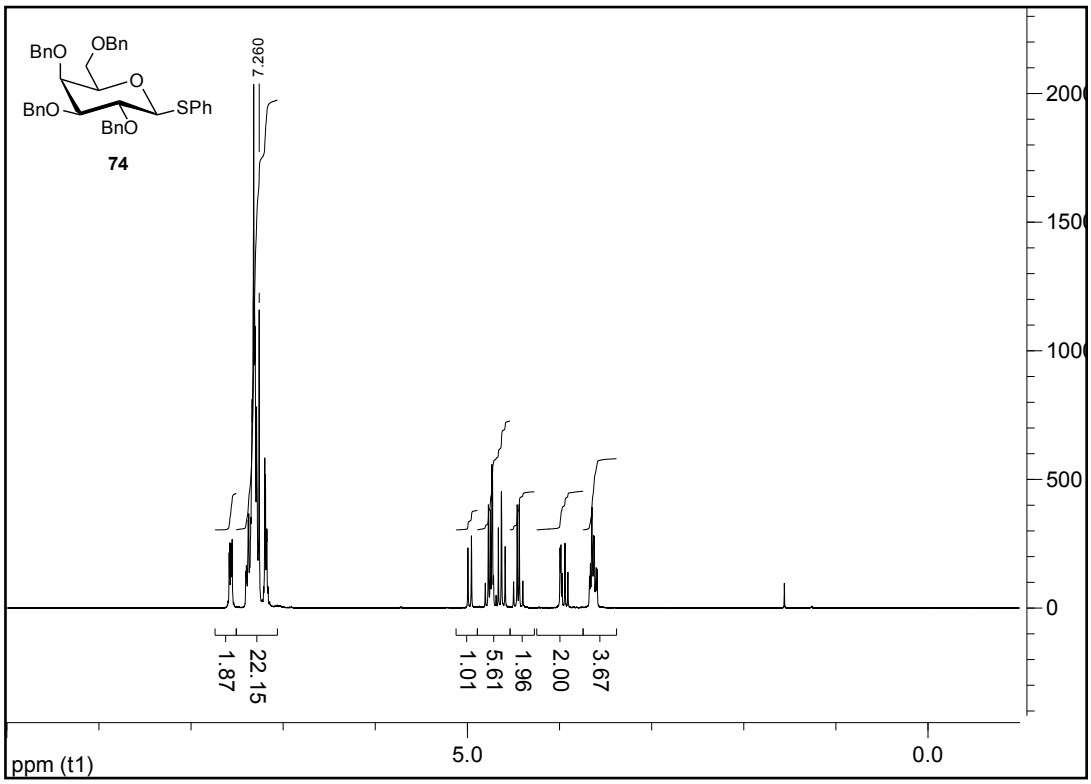

(3S,4S,5S)-3,4,5-tris(benzyloxy)-6-(benzyloxymethyl)tetrahydro-2H-pyran-2-ol (75):

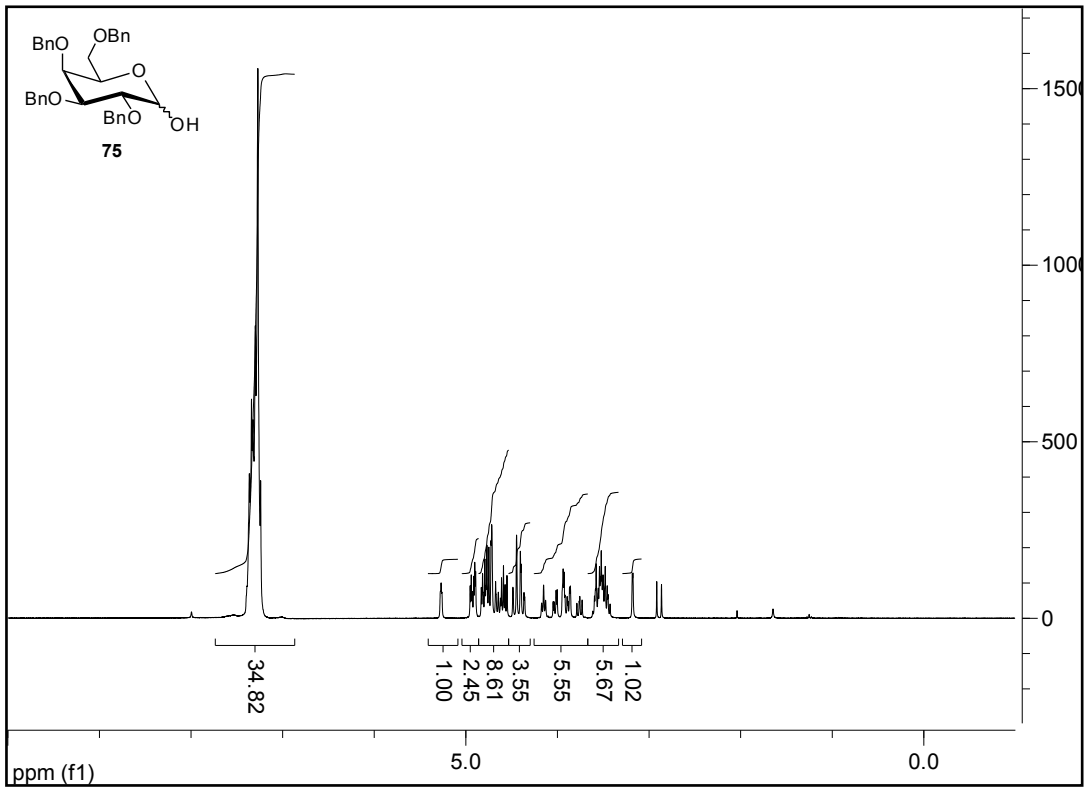

(2S,3S,4S,5S,6R)-3,4,5-tris(benzyloxy)-6-(benzyloxymethyl)tetrahydro-2H-pyran-2-yl 2,2,2-trichloroacetimidate (76):

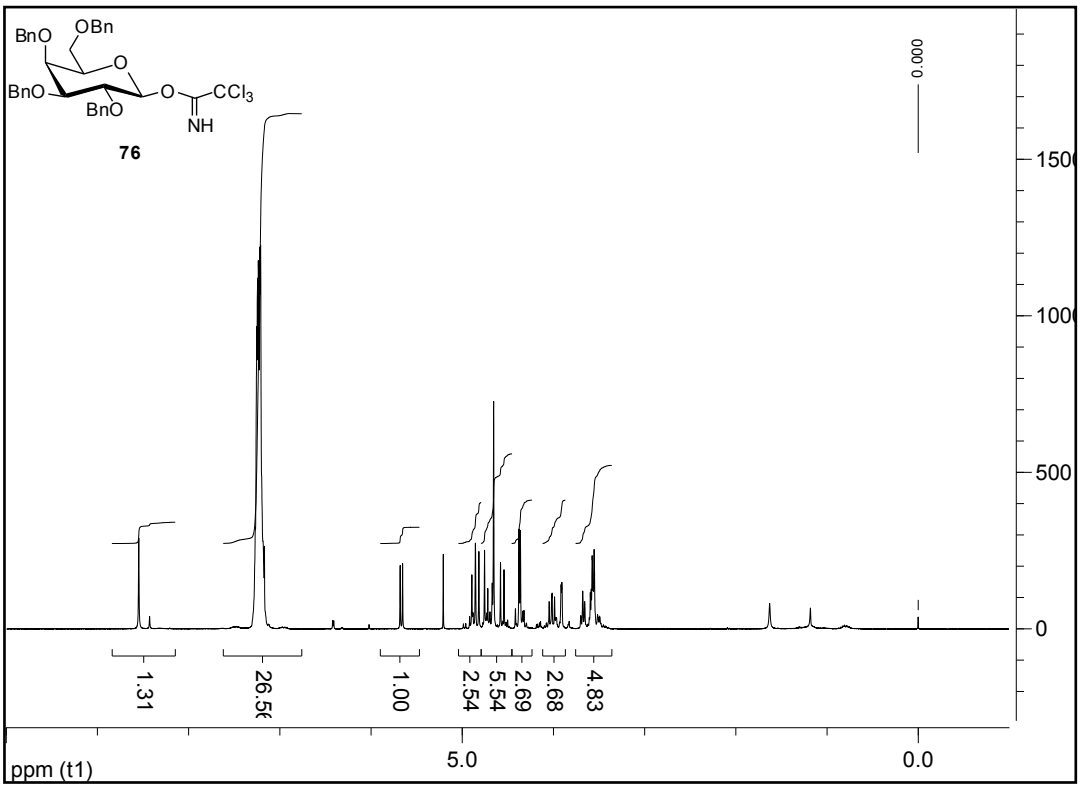

(2R,3S,4S,5R,6R)-2-(acetoxymethyl)-6-bromotetrahydro-2H-pyran-3,4,5-triyl triacetate (81):

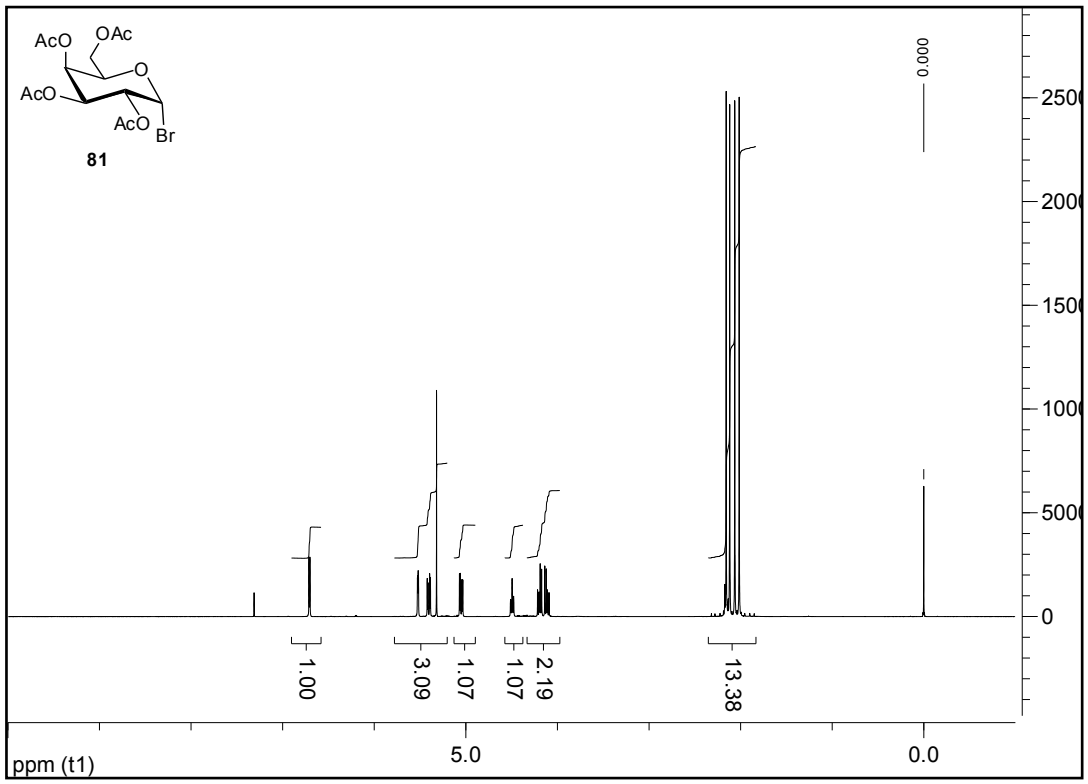

(3R,4S,5S)-3,4,5-tris(benzyloxy)-6-(benzyloxymethyl)tetrahydro-2H-pyran-2-yl acetate (82):

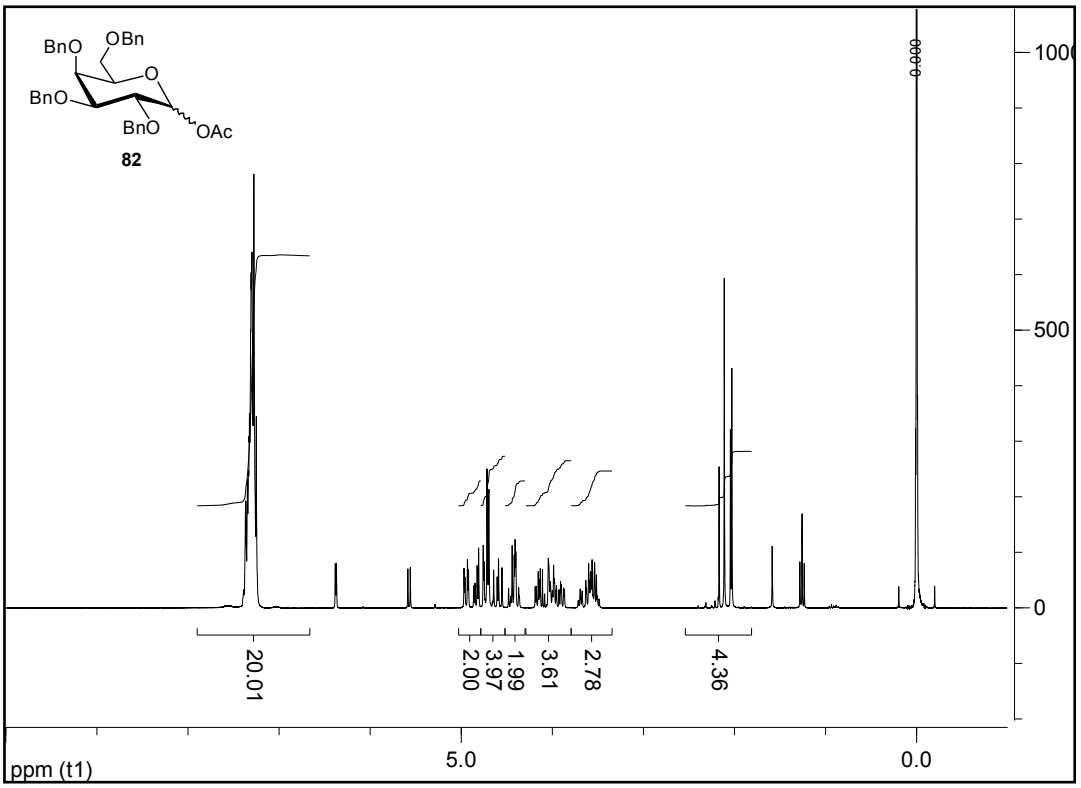

(2R,3S,4S,5R,6R)-3,4,5-tris(benzyloxy)-2-(benzyloxymethyl)-6-methoxytetrahydro-2H-pyran (84):

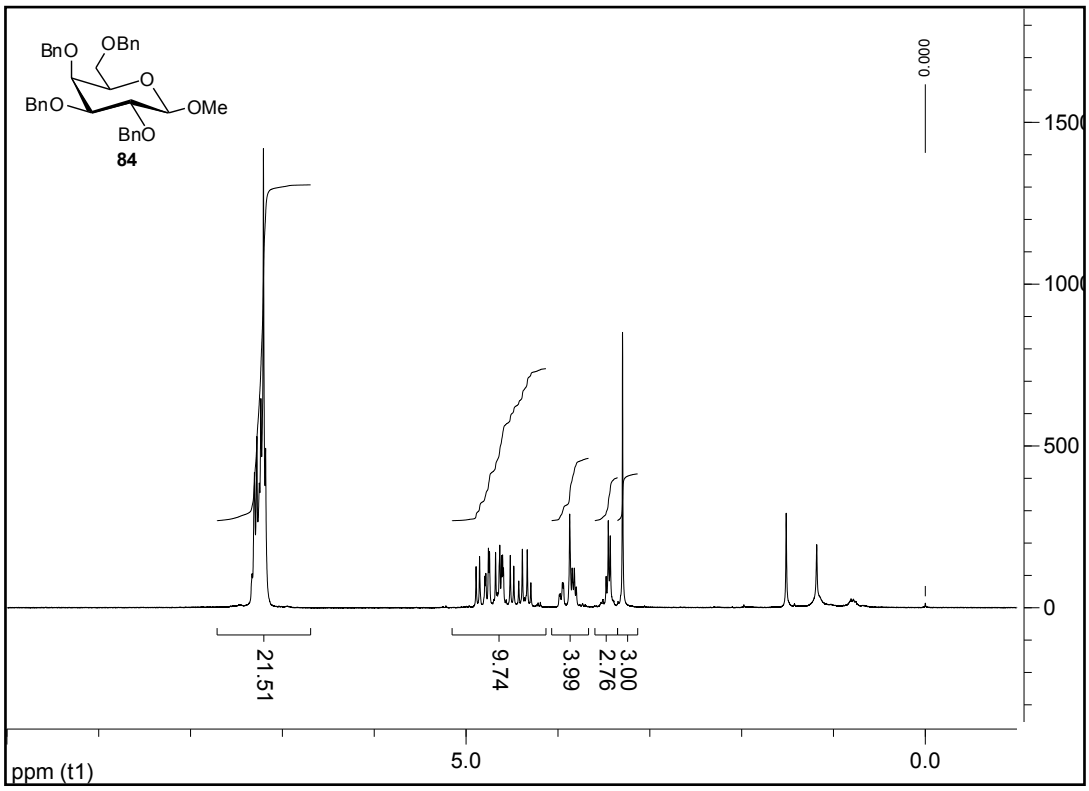

(2R,3S,4S,5R,6S)-3,4,5-tris(benzyloxy)-2-(benzyloxymethyl)-6-methoxytetrahydro-2H-pyran (85):

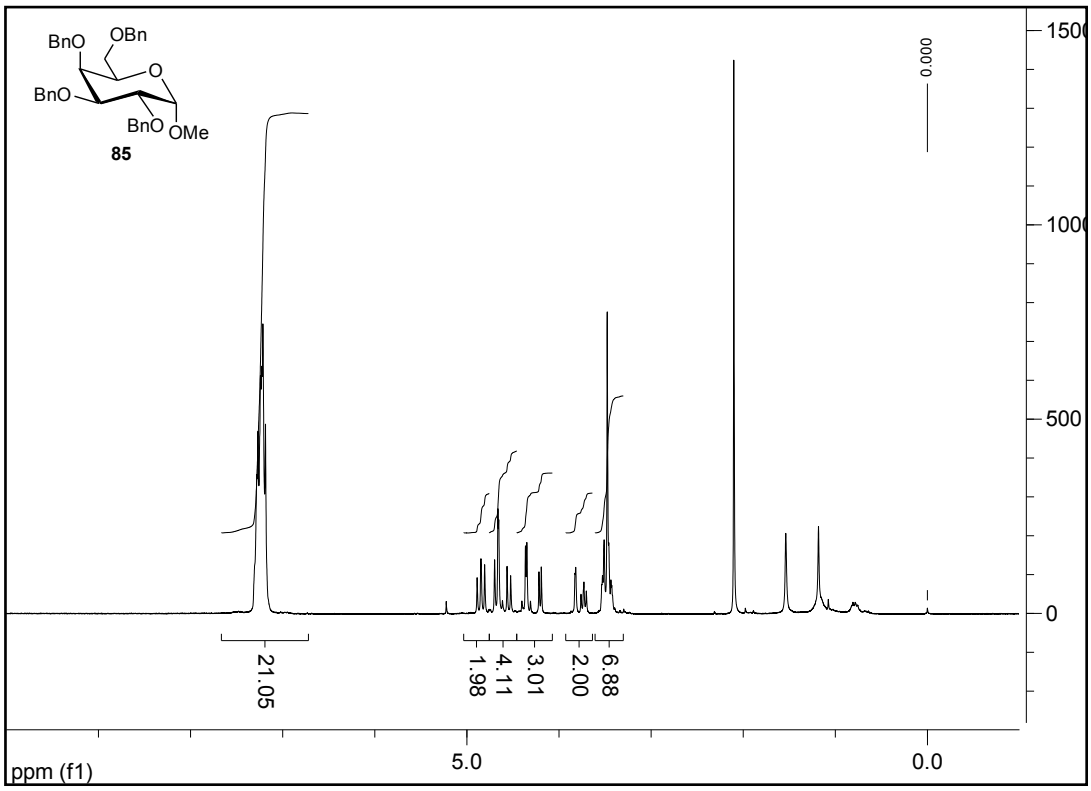

(2R)-1-((S)-4-benzyl-2-thioxothiazolidin-3-yl)-3-hydroxy-2-methyl-5-phenylpentan-1-one (87):

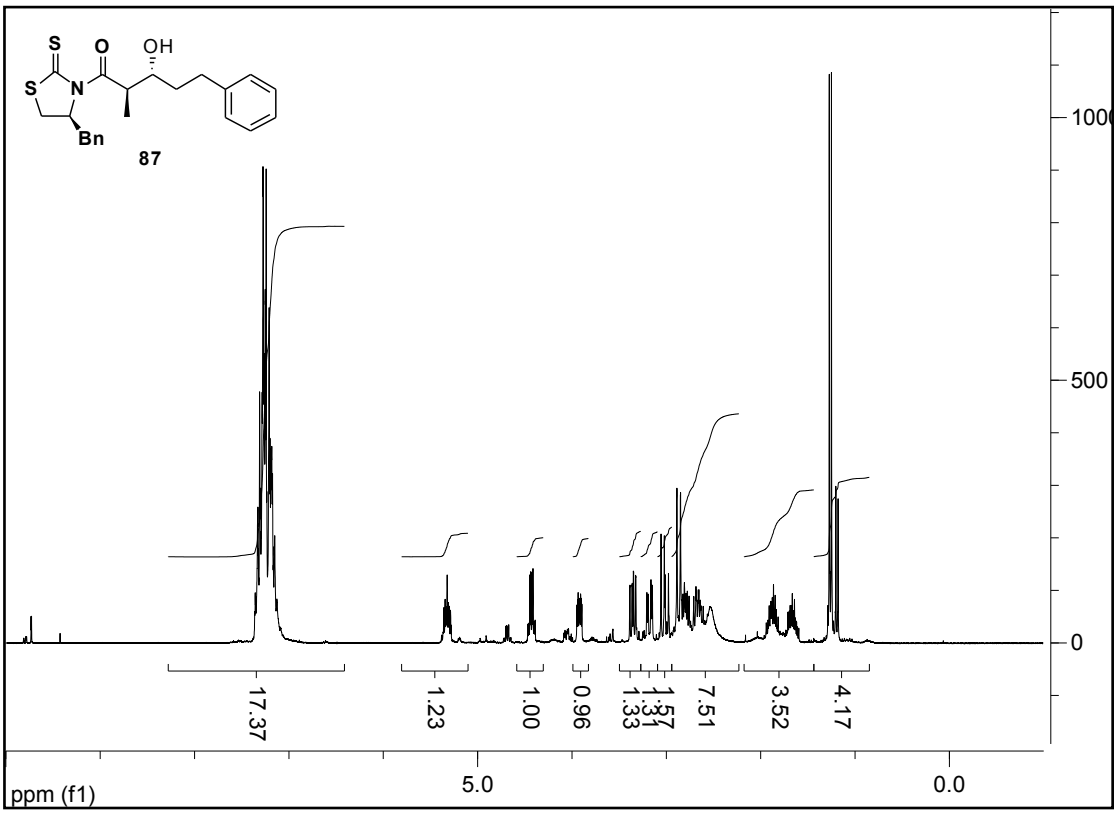

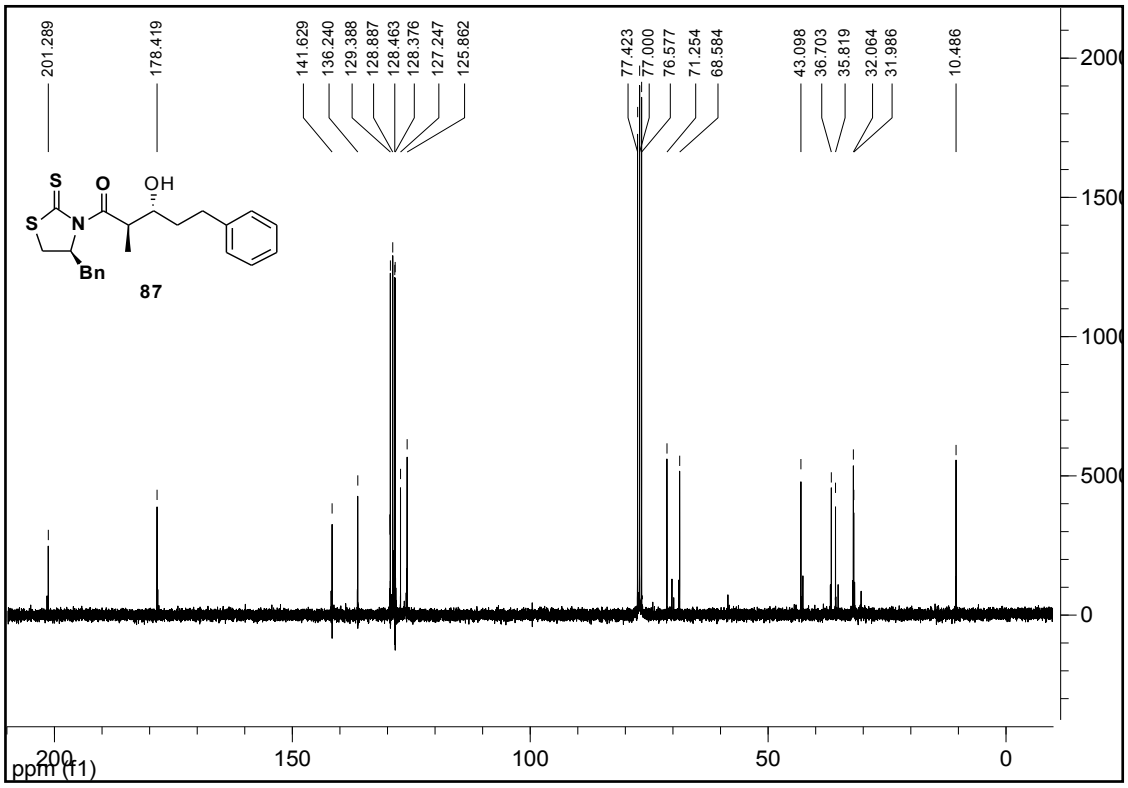

(S)-3-allyl-4-benzylthiazolidine-2-thione (89):

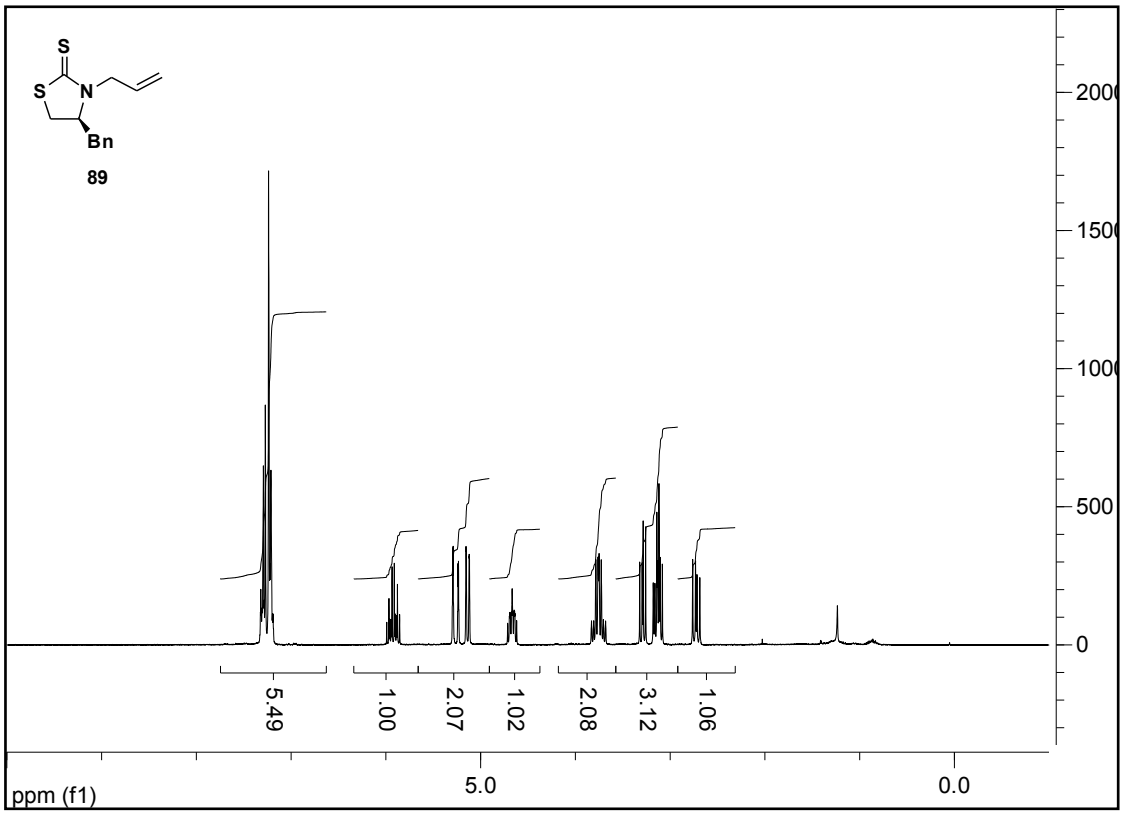

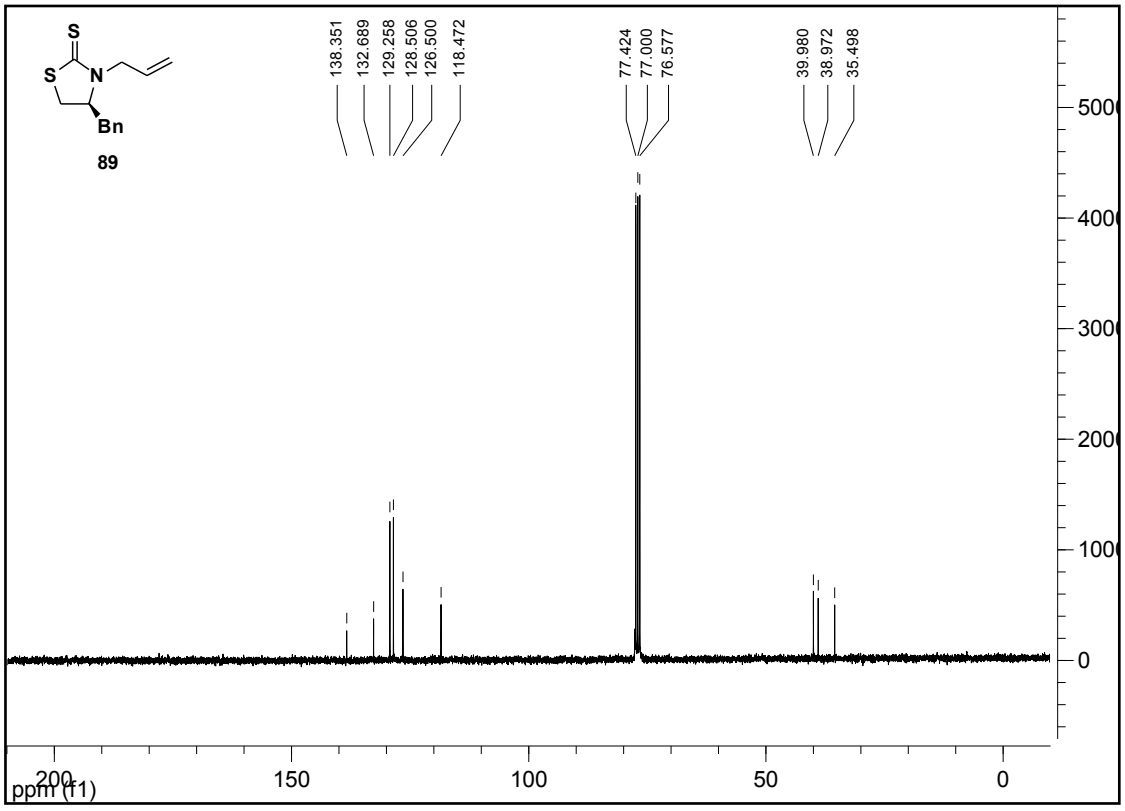

((2R,3R,6R)-3-acetoxy-6-(2-((S)-4-benzyl-2-thioxothiazolidin-3-yl)-2-oxoethyl)-3,6-dihydro-2H-pyran-2-yl)methyl acetate (90a):

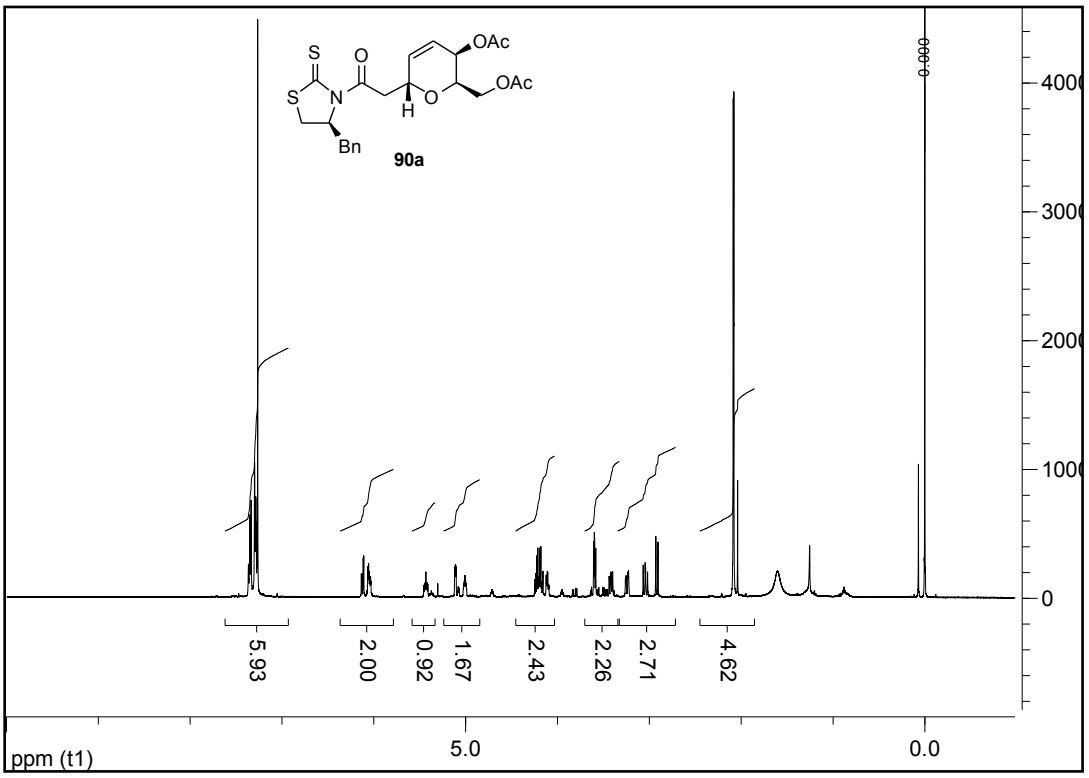

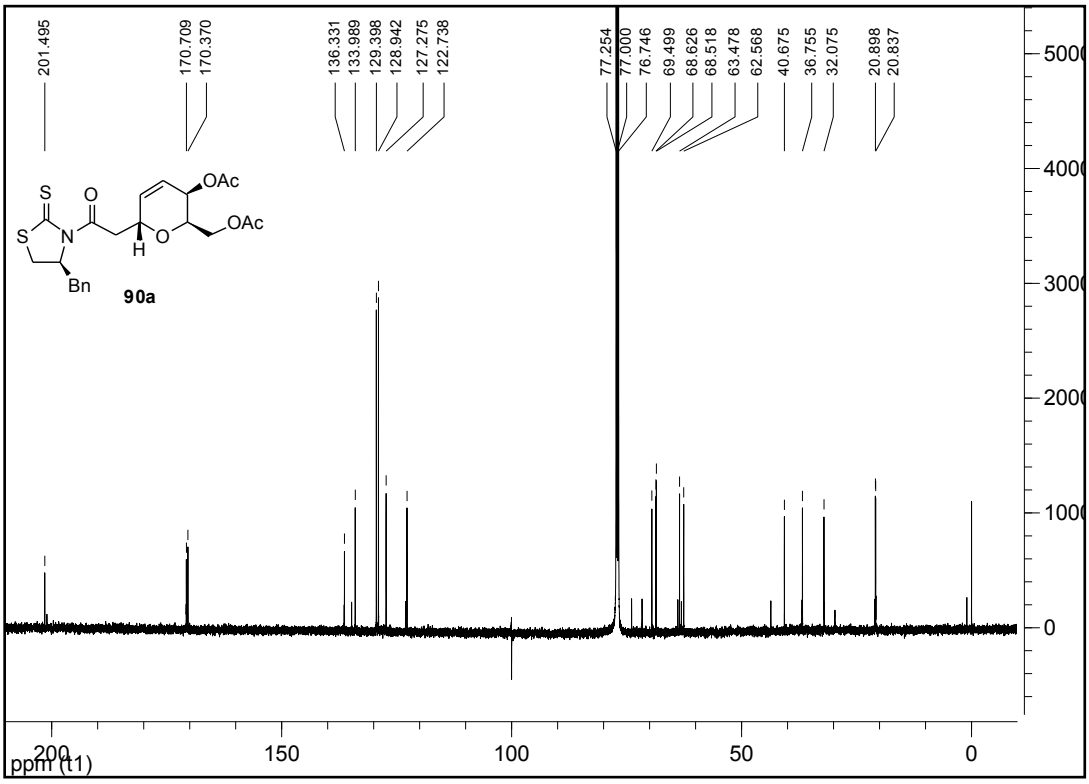

((2R,3R,6S)-3-acetoxy-6-((R)-1-((S)-4-benzyl-2-thioxothiazolidin-3-yl)-1-oxopropan-2-yl)-3,6-dihydro-2H-pyran-2-yl)methyl acetate (90b):

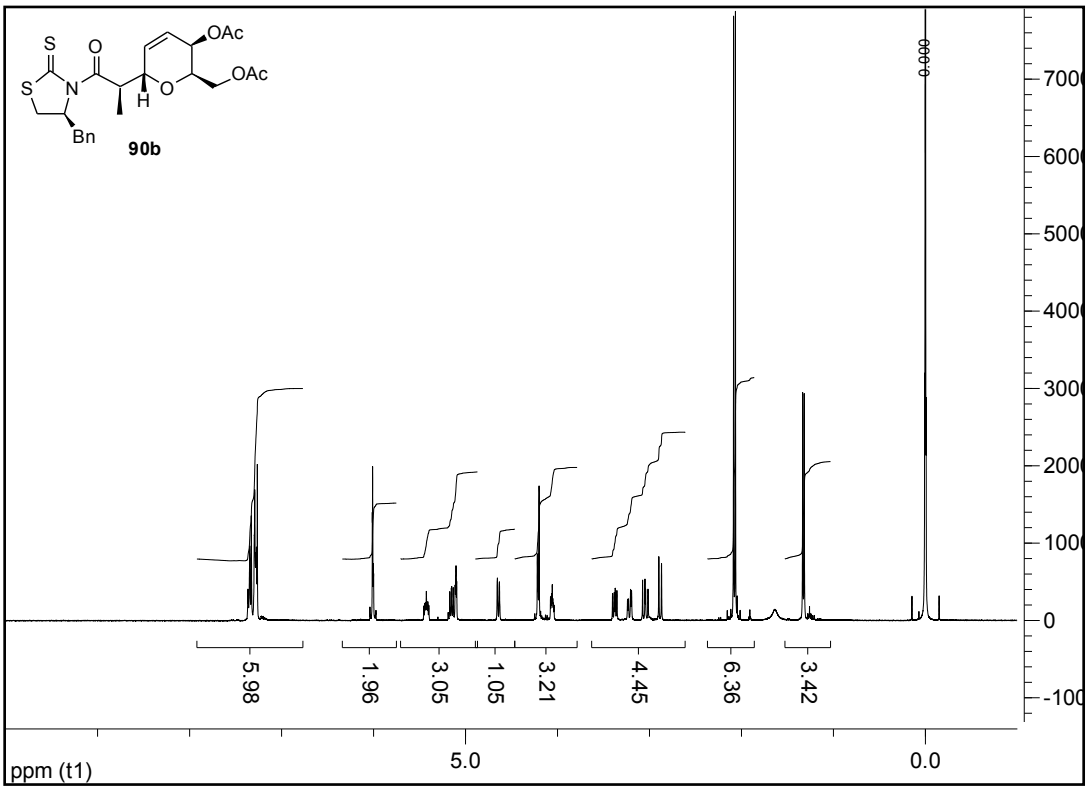

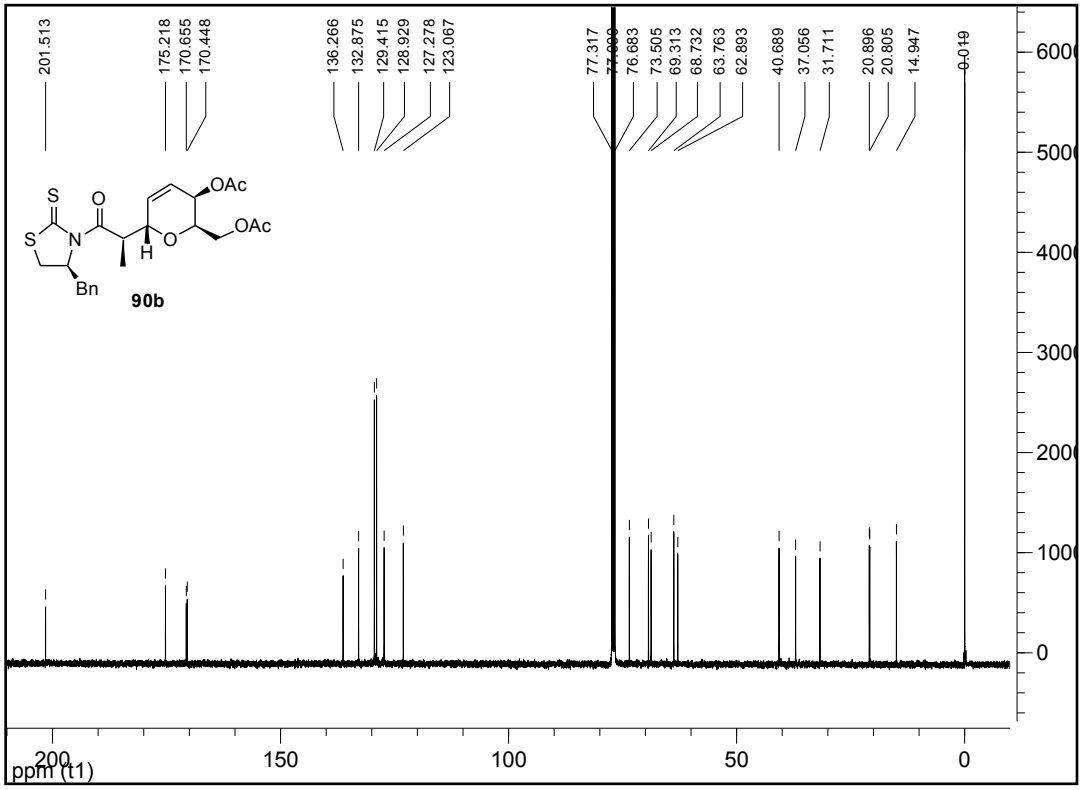

((2R,3R,6S)-3-acetoxy-6-((R)-1-((S)-4-benzyl-2-thioxothiazolidin-3-yl)-3-methyl-1-oxobutan-2-yl)-3,6-dihydro-2H-pyran-2-yl)methyl acetate (90d):

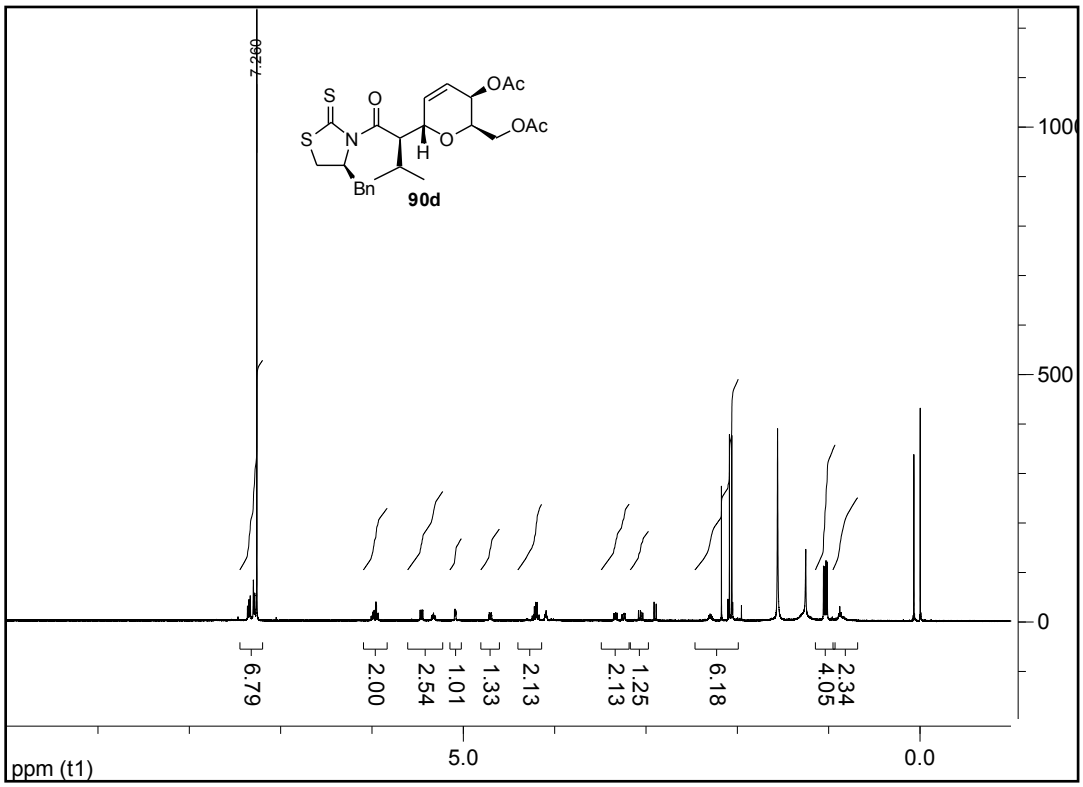

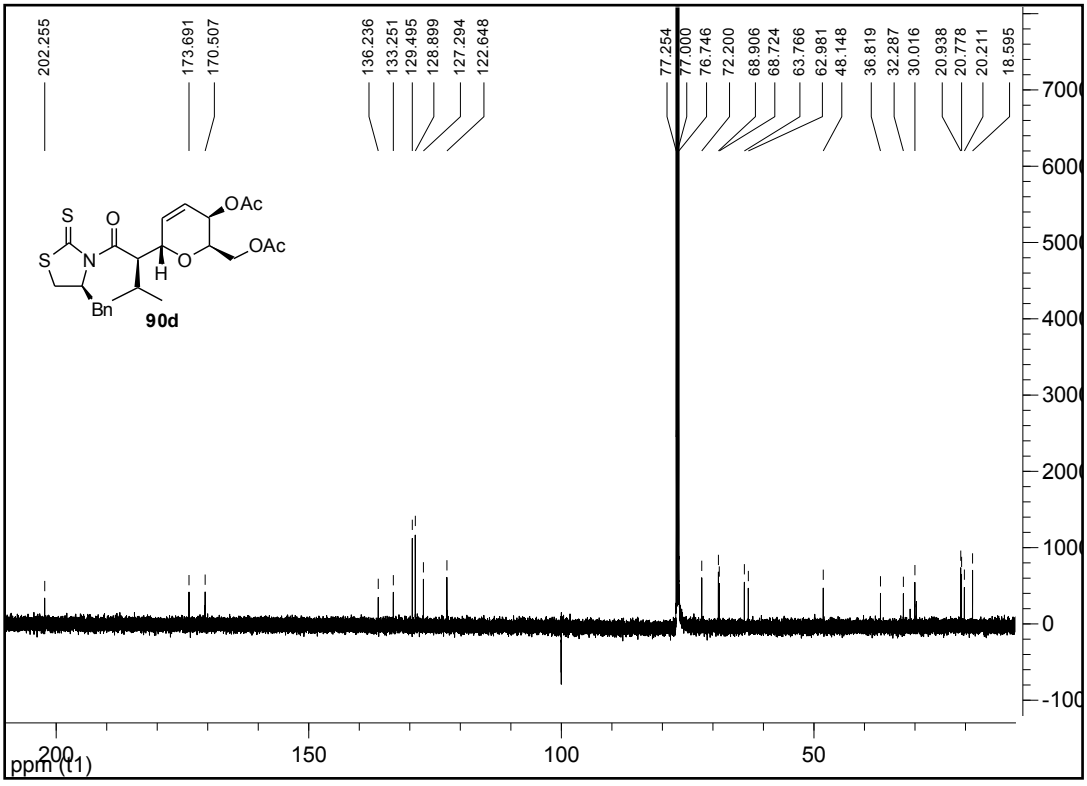

((2R,3R,6S)-3-acetoxy-6-((R)-2-((S)-4-benzyl-2-thioxothiazolidin-3-yl)-2-oxo-1-phenylethyl)-3,6-dihydro-2H-pyran-2-yl)methyl acetate (90e):

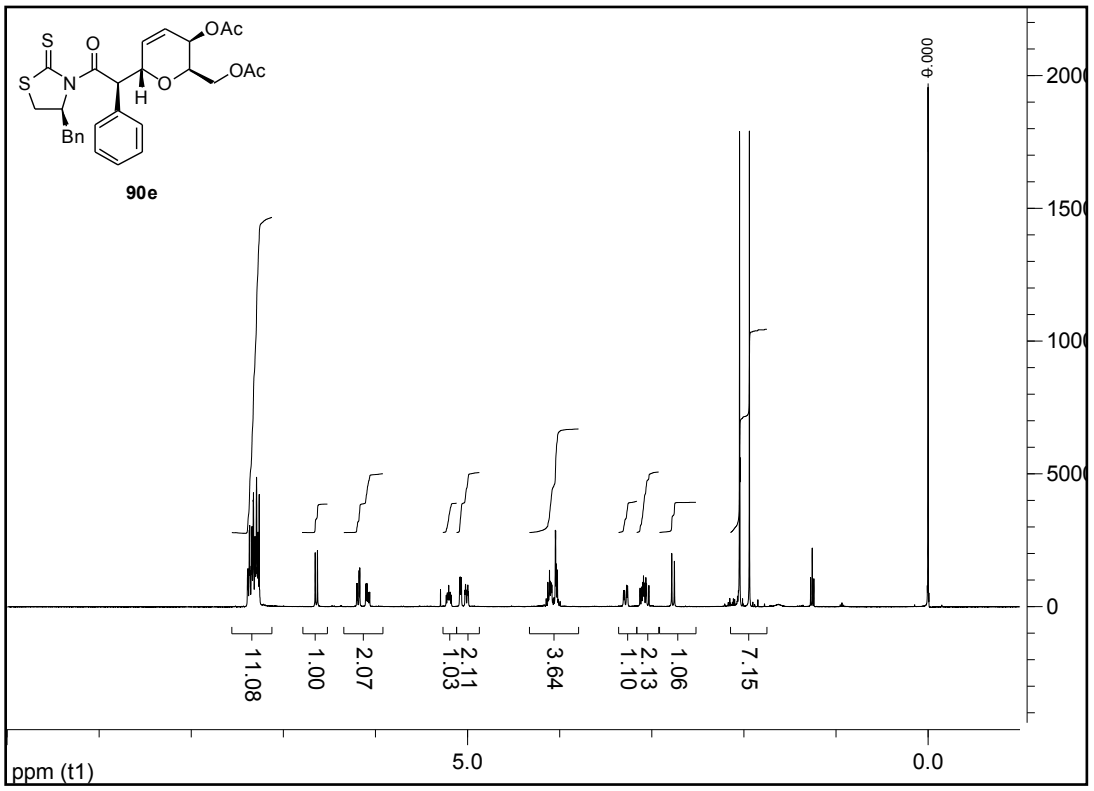

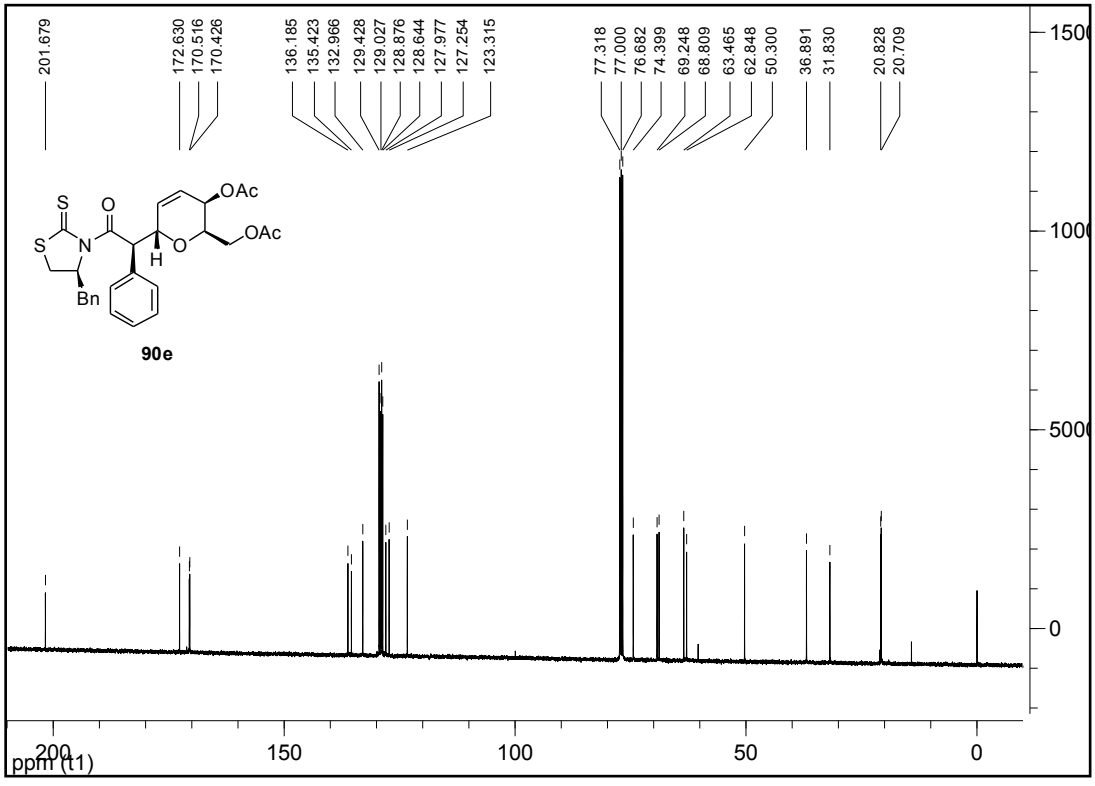

((2R,3R,6S)-3-acetoxy-6-((R)-1-((S)-4-benzyl-2-thioxothiazolidin-3-yl)-1-oxo-3-phenylpropan-2-yl)-3,6-dihydro-2H-pyran-2-yl)methyl acetate (90f):

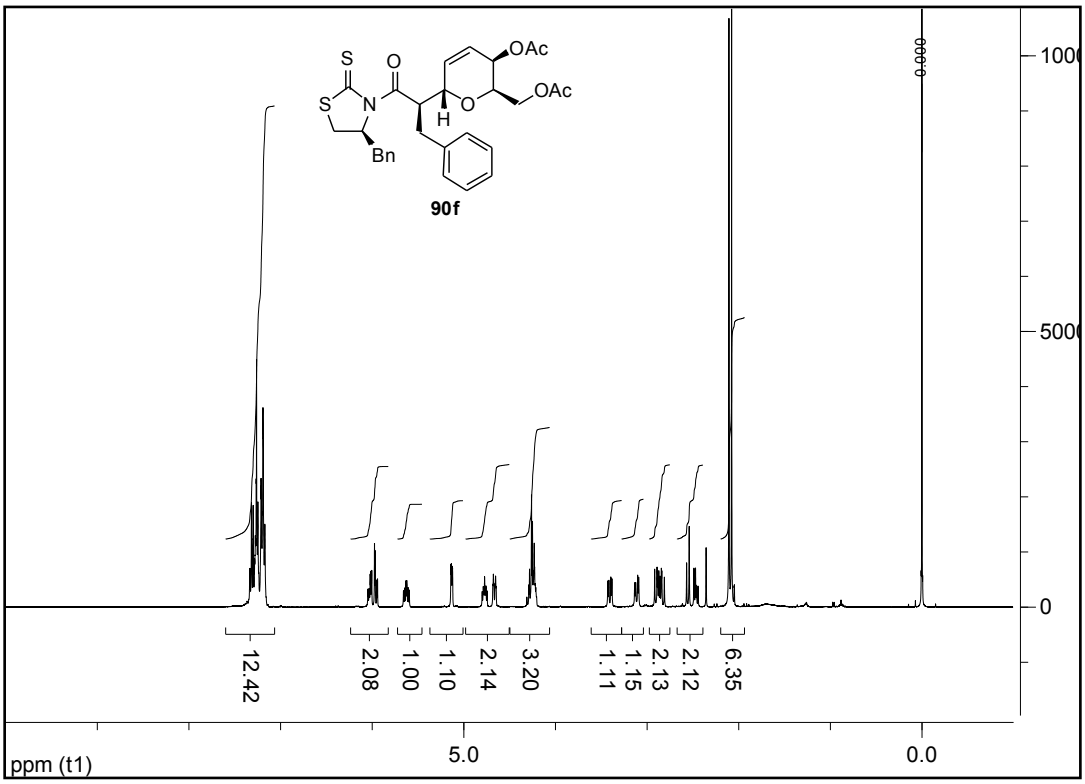

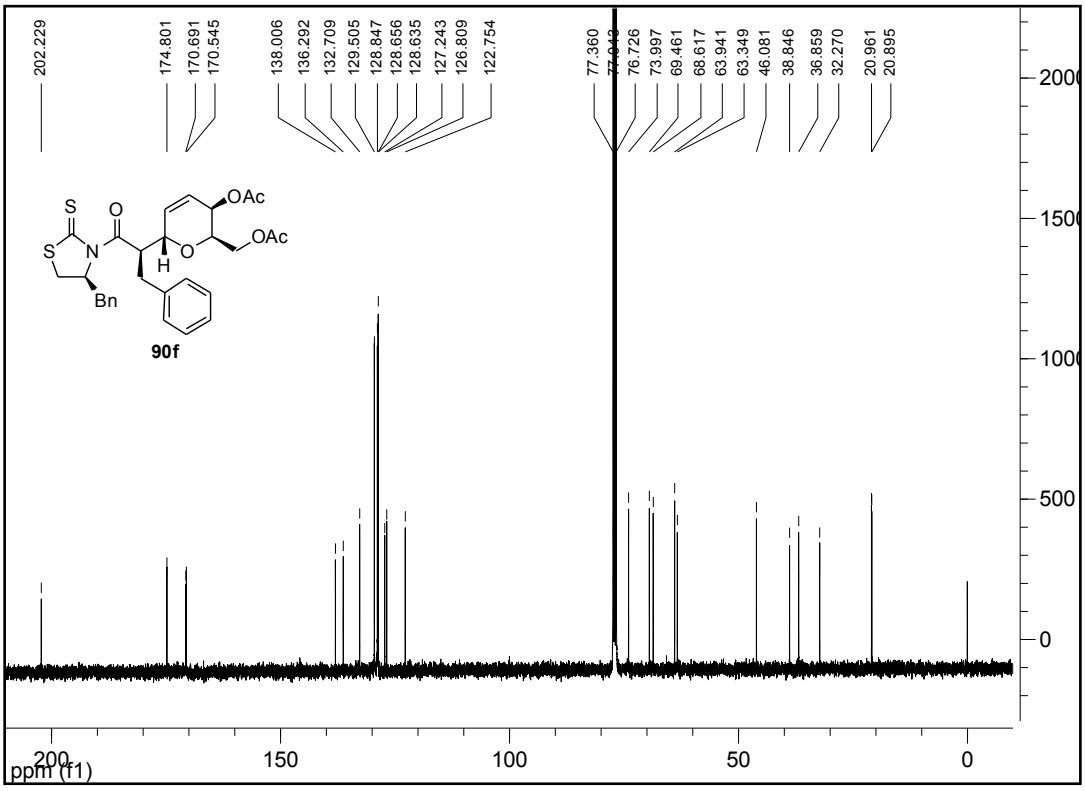

((2R,3R,6S)-3-acetoxy-6-((R)-2-((S)-4-benzyl-2-thioxothiazolidin-3-yl)-1-(4-methoxyphenyl)-2-oxoethyl)-3,6-dihydro-2H-pyran-2-yl)methyl acetate (90g):

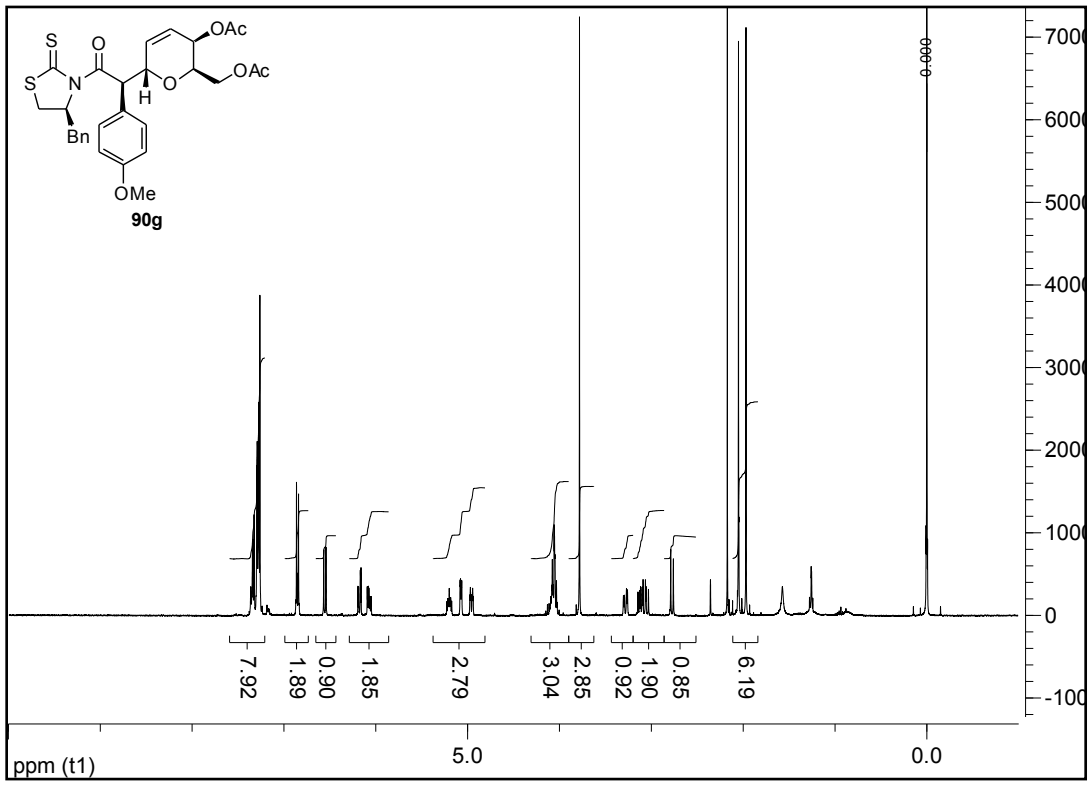

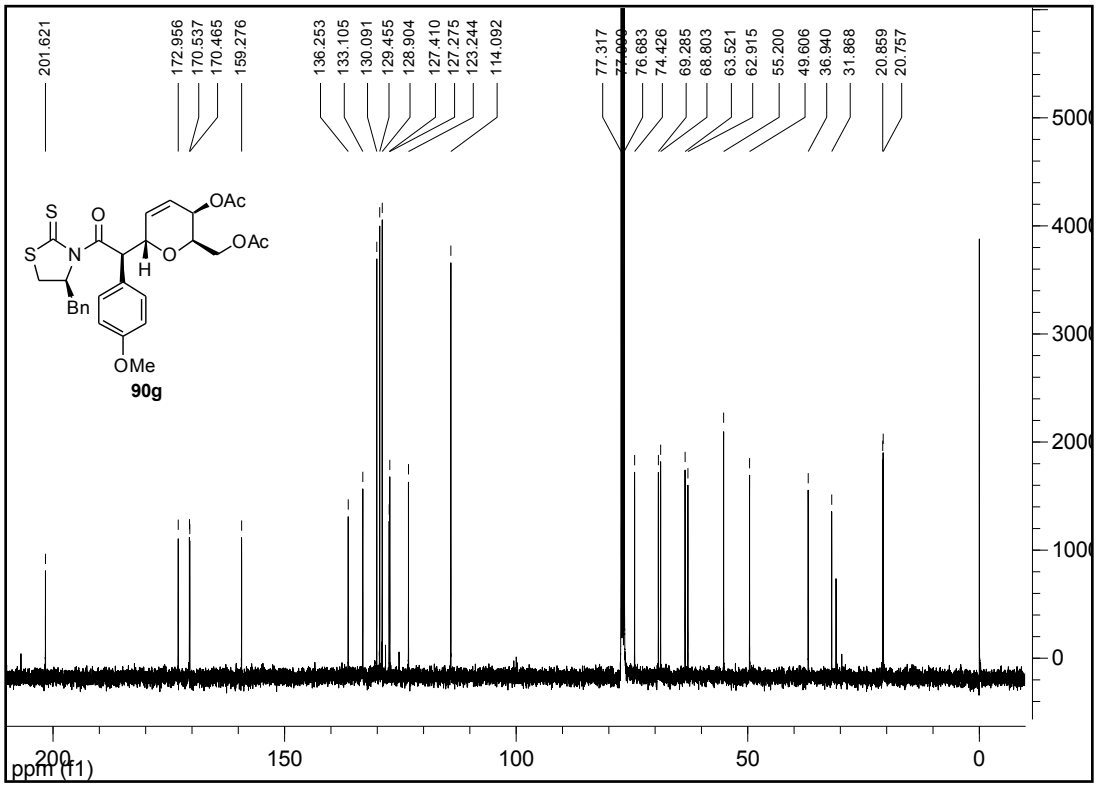

((2R,3R,6S)-3-acetoxy-6-((R)-1-((S)-4-benzyl-2-thioxothiazolidin-3-yl)-1-oxooctan-2-yl)-3,6-dihydro-2H-pyran-2-yl)methyl acetate (90j):

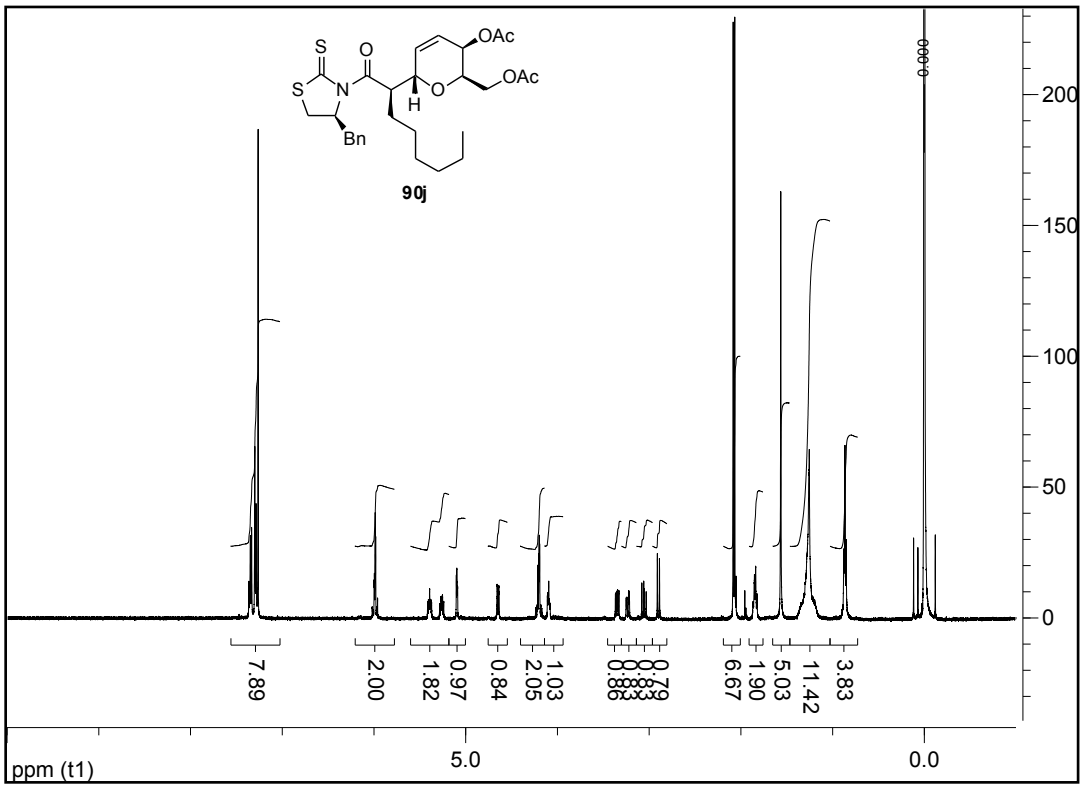

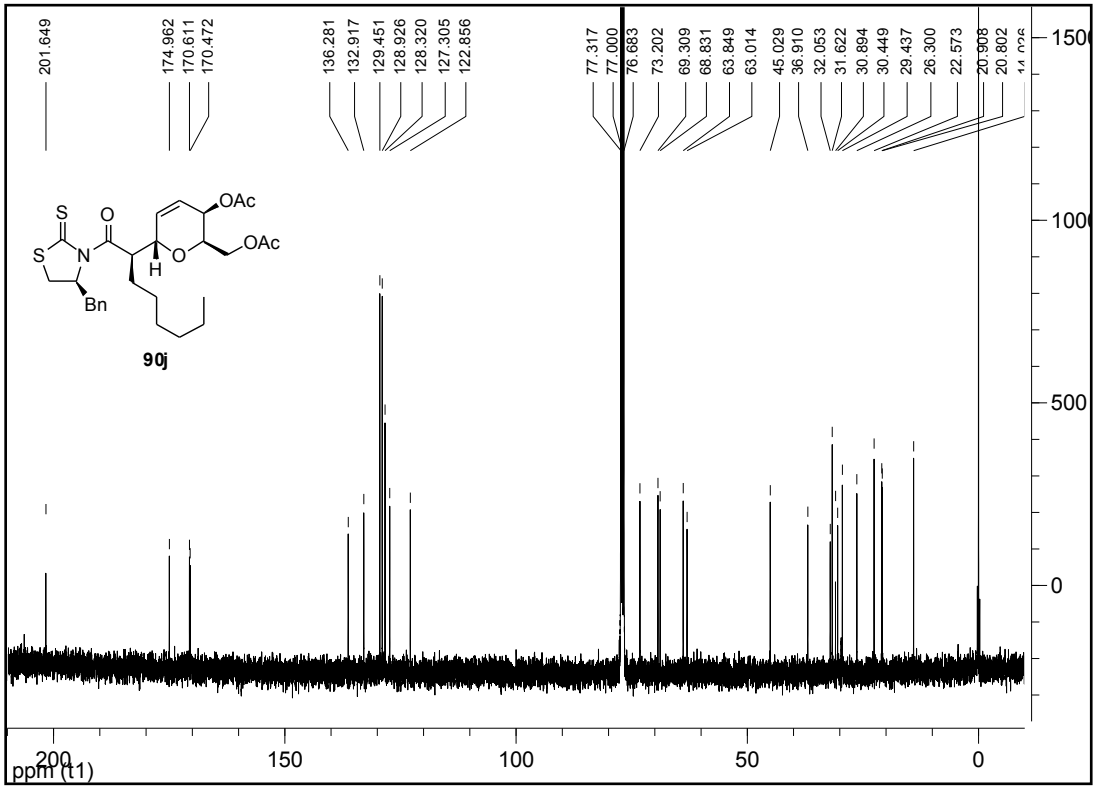

((2R,3R,6S)-3-acetoxy-6-(2-((R)-4-benzyl-2-thioxothiazolidin-3-yl)-2-oxoethyl)-3,6-dihydro-2H-pyran-2-yl)methyl acetate (91a):

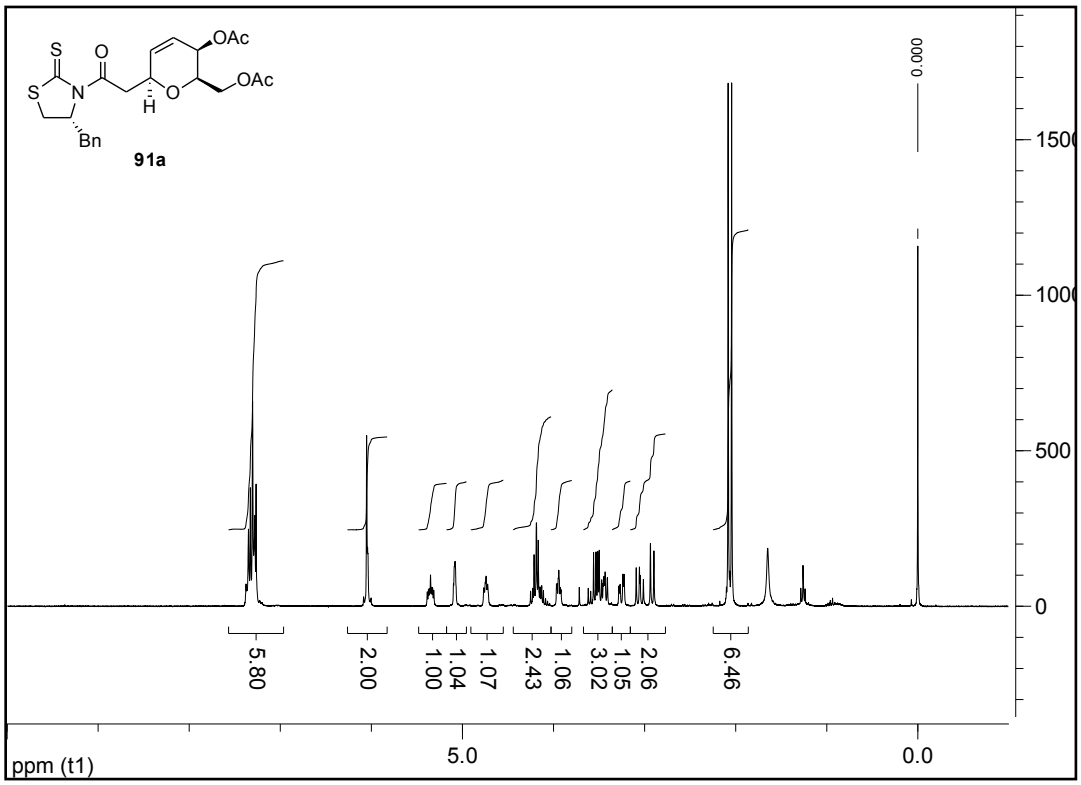

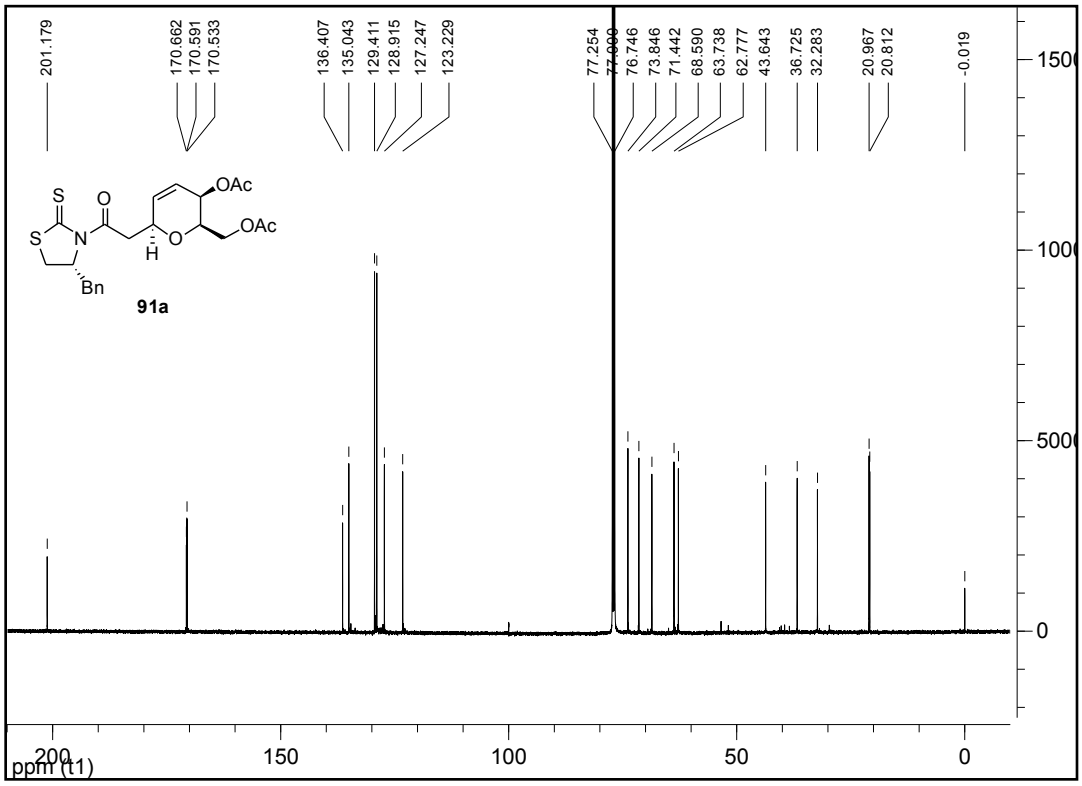

((2R,3R,6R)-3-acetoxy-6-((S)-1-((R)-4-benzyl-2-thioxothiazolidin-3-yl)-1-oxopropan-2-yl)-3,6-dihydro-2H-pyran-2-yl)methyl acetate (91b):

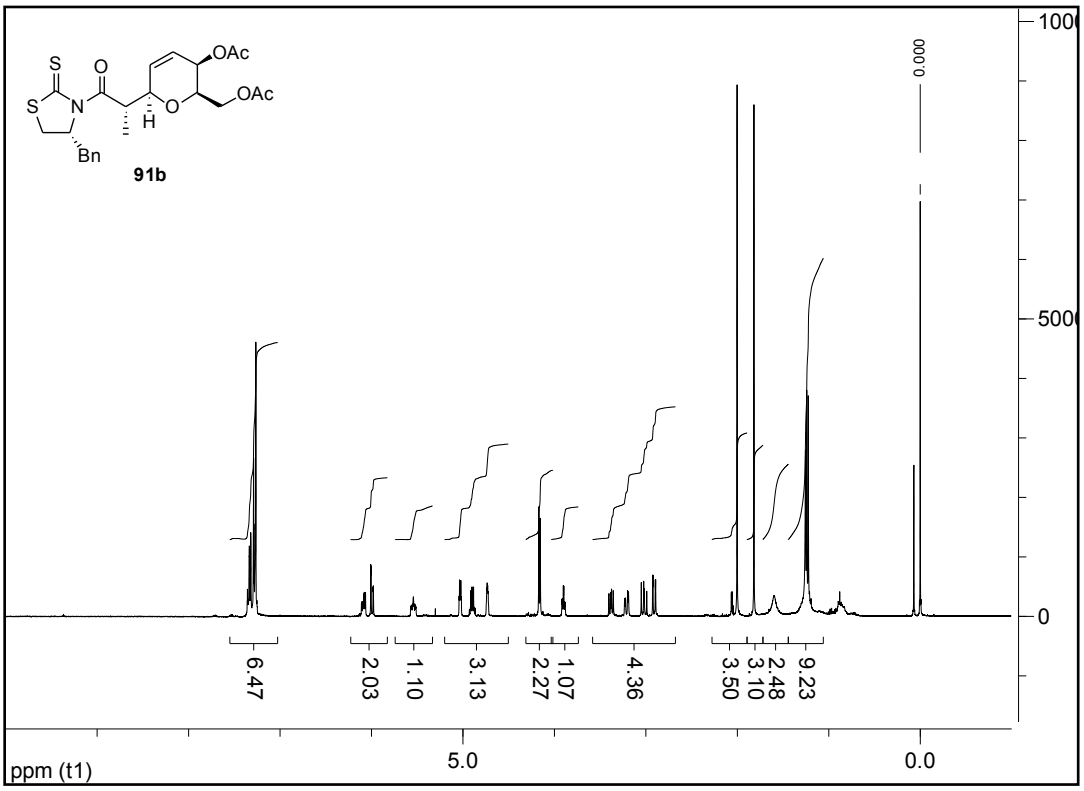

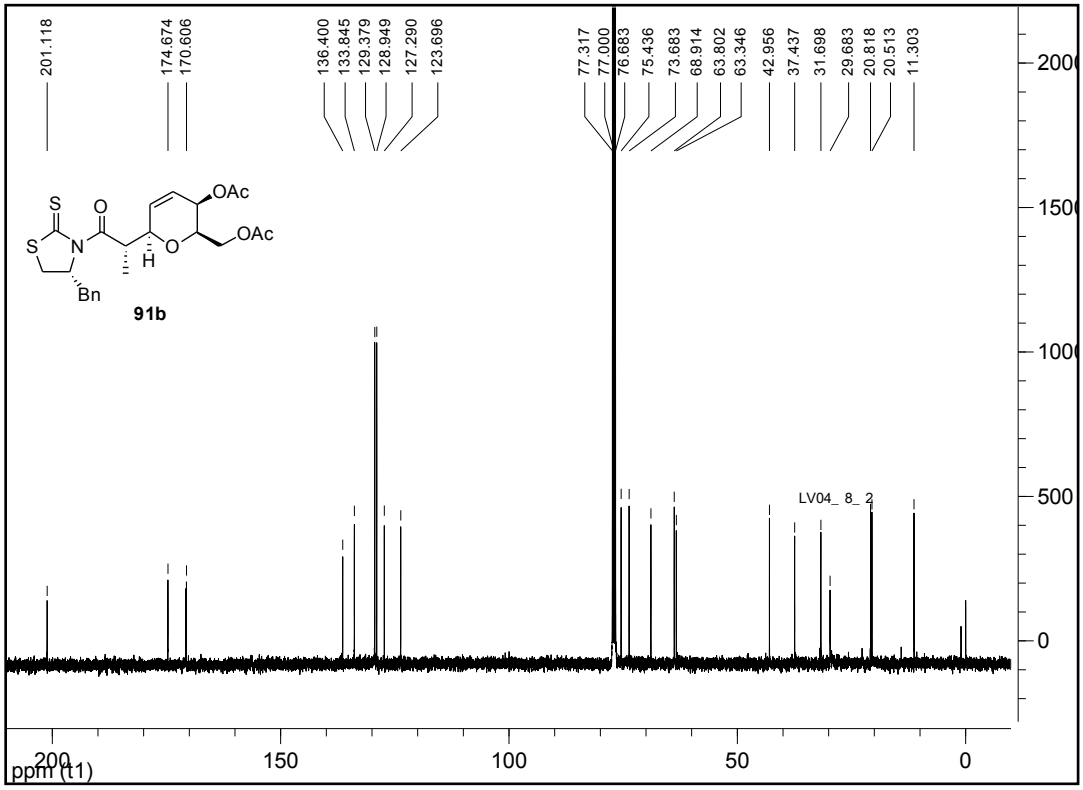

((2R,3R,6S)-3-acetoxy-6-((R)-1-(benzylamino)-1-oxopropan-2-yl)-3,6-dihydro-2H-pyran-2-yl)methyl acetate (102):

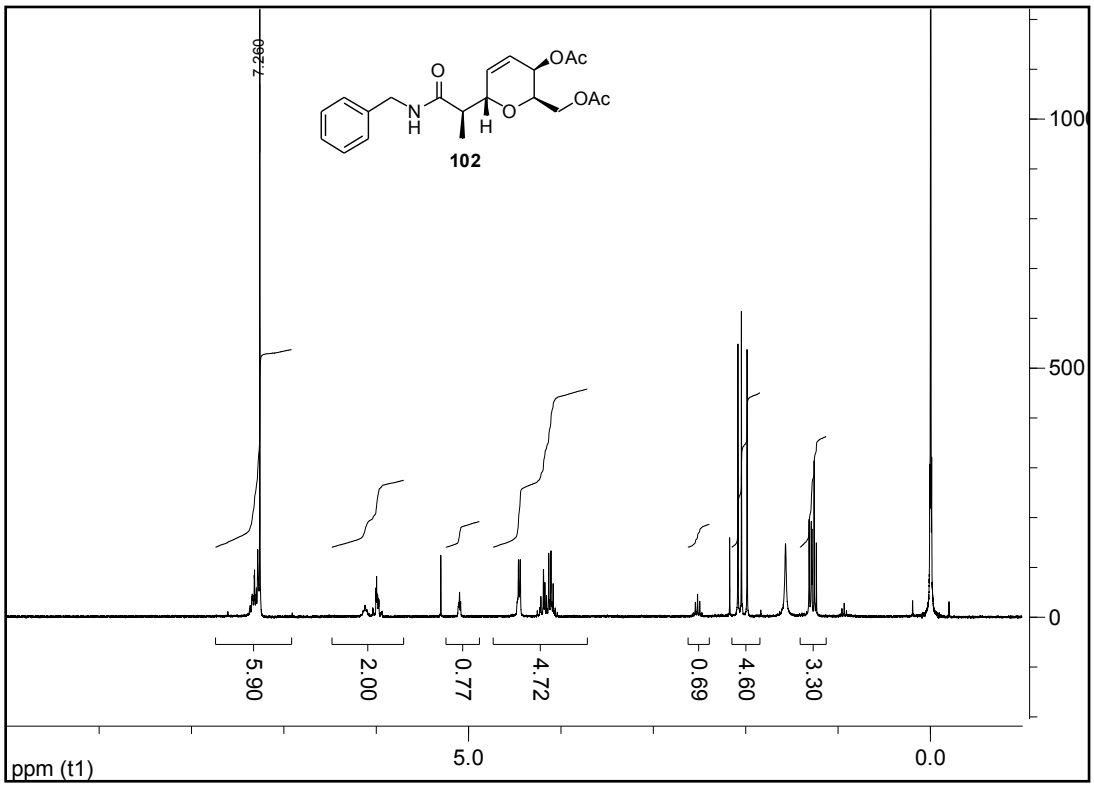

(S)-benzyl 1-(9H-fluoren-9-yl)-12,12-dimethyl-3,10-dioxo-2,11-dioxa-4,9-diazatridecane-5-carboxylate (104):

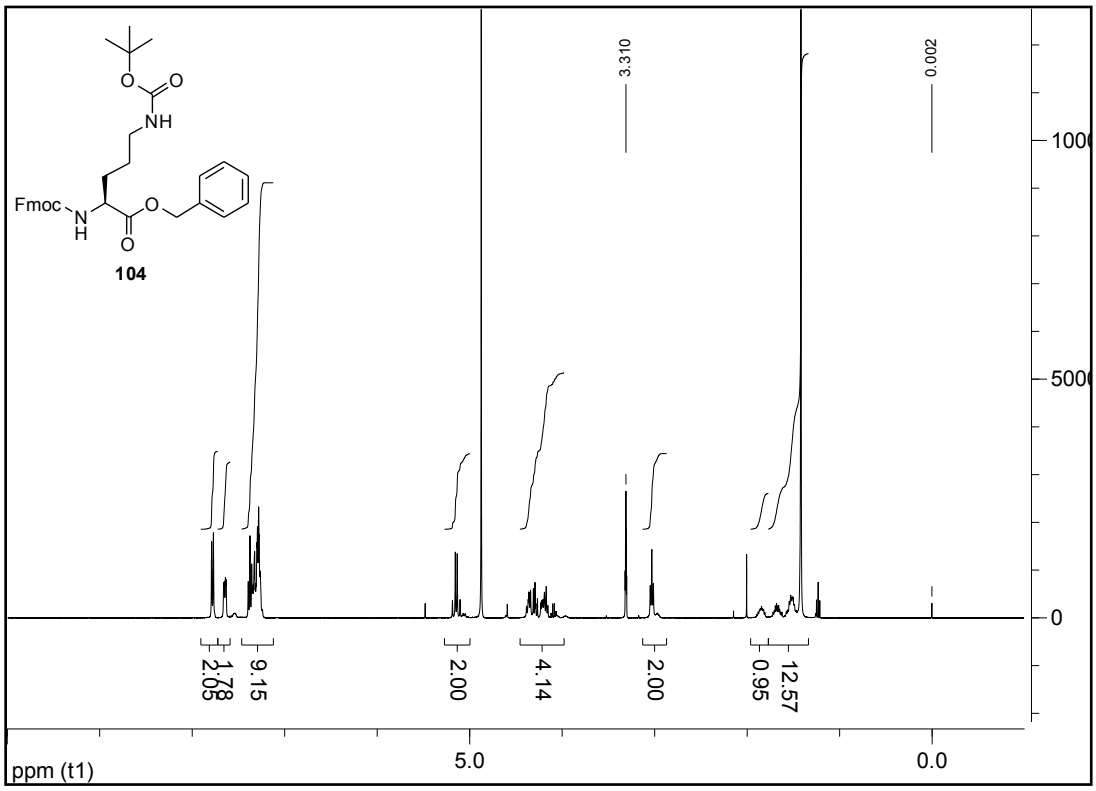

(2S)-benzyl 2-(((9H-fluoren-9-yl)methoxy)carbonylamino)-5-(2-((2R,6R)-5-acetoxy-6-(acetoxymethyl)-5,6-dihydro-2H-pyran-2-yl)acetamido)pentanoate (105a):

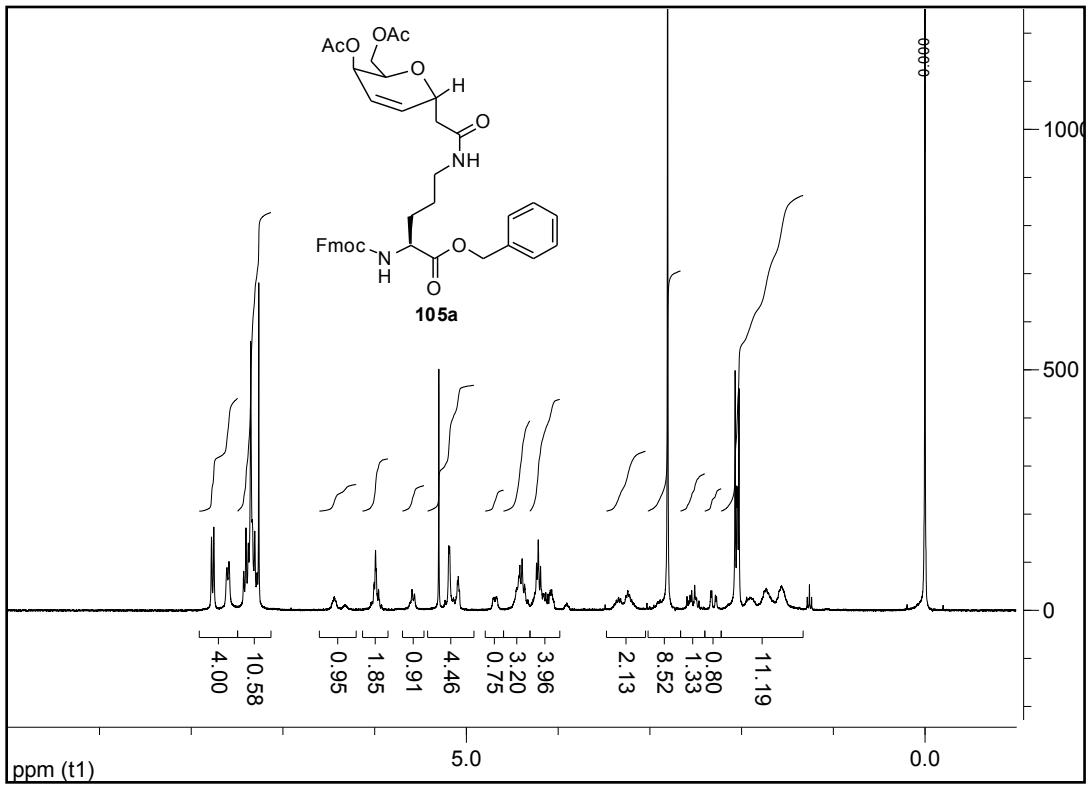

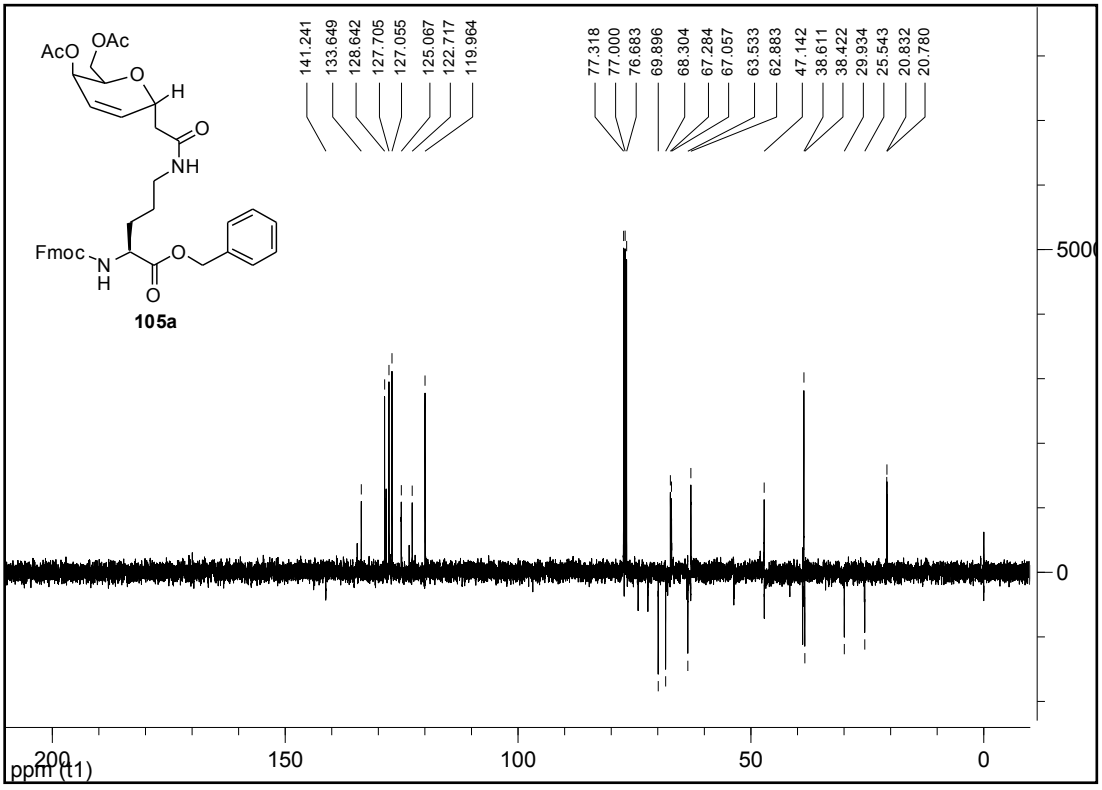

(S)-benzyl 2-(((9H-fluoren-9-yl)methoxy)carbonylamino)-5-((R)-2-((2S,5R,6R)-5-acetoxy-6-(acetoxymethyl)-5,6-dihydro-2H-pyran-2-yl)propanamido)pentanoate (105b):

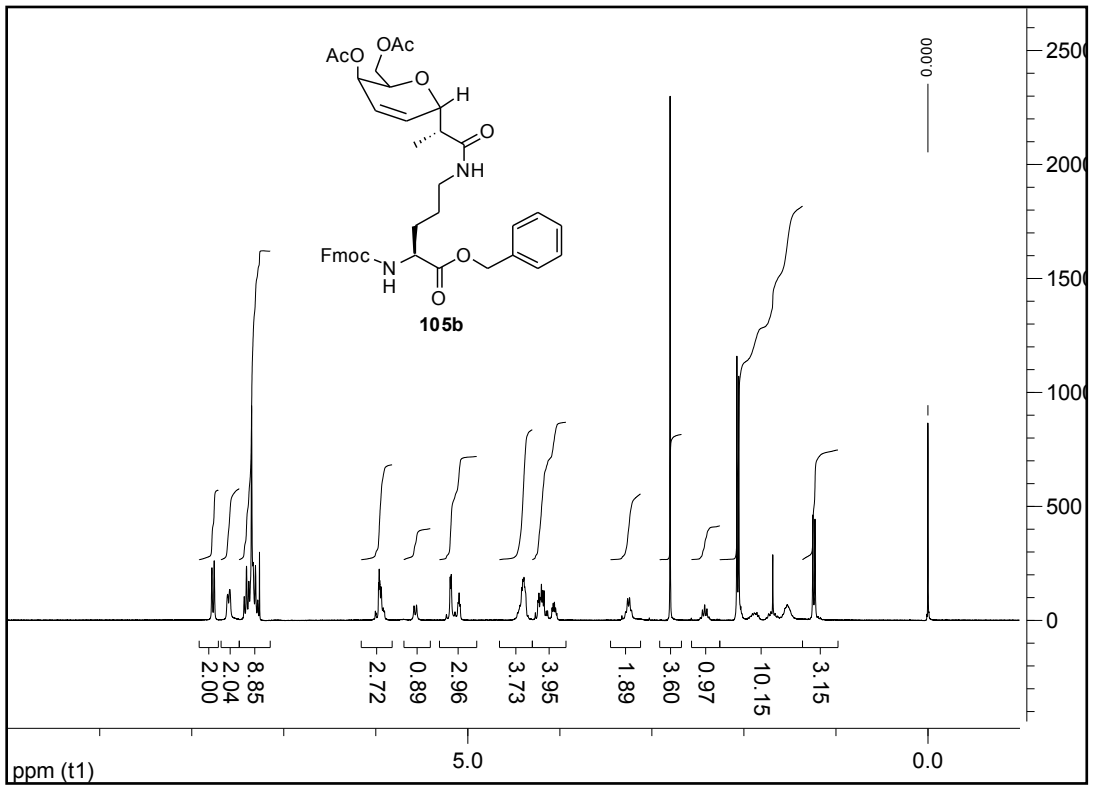

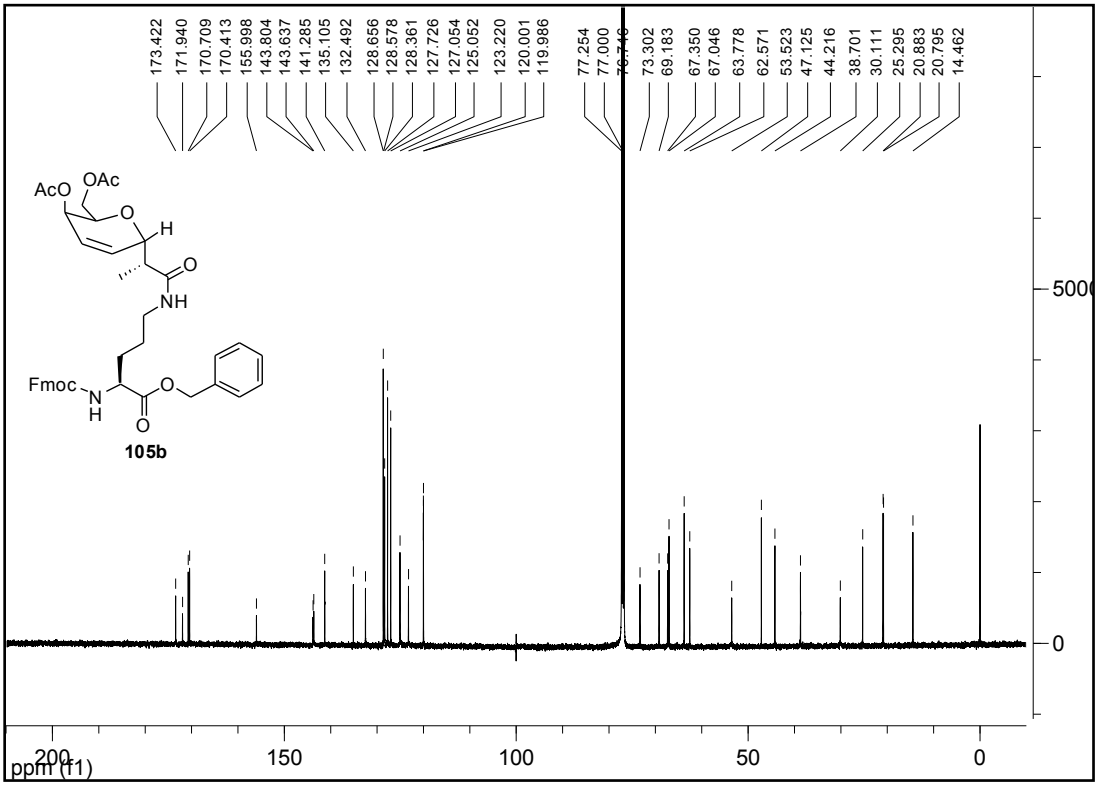

(S)-2-(((9H-fluoren-9-yl)methoxy)carbonylamino)-5-(2-((2S,5R,6R)-5-acetoxy-6-(acetoxymethyl)tetrahydro-2H-pyran-2-yl)acetamido)pentanoic acid (106a):

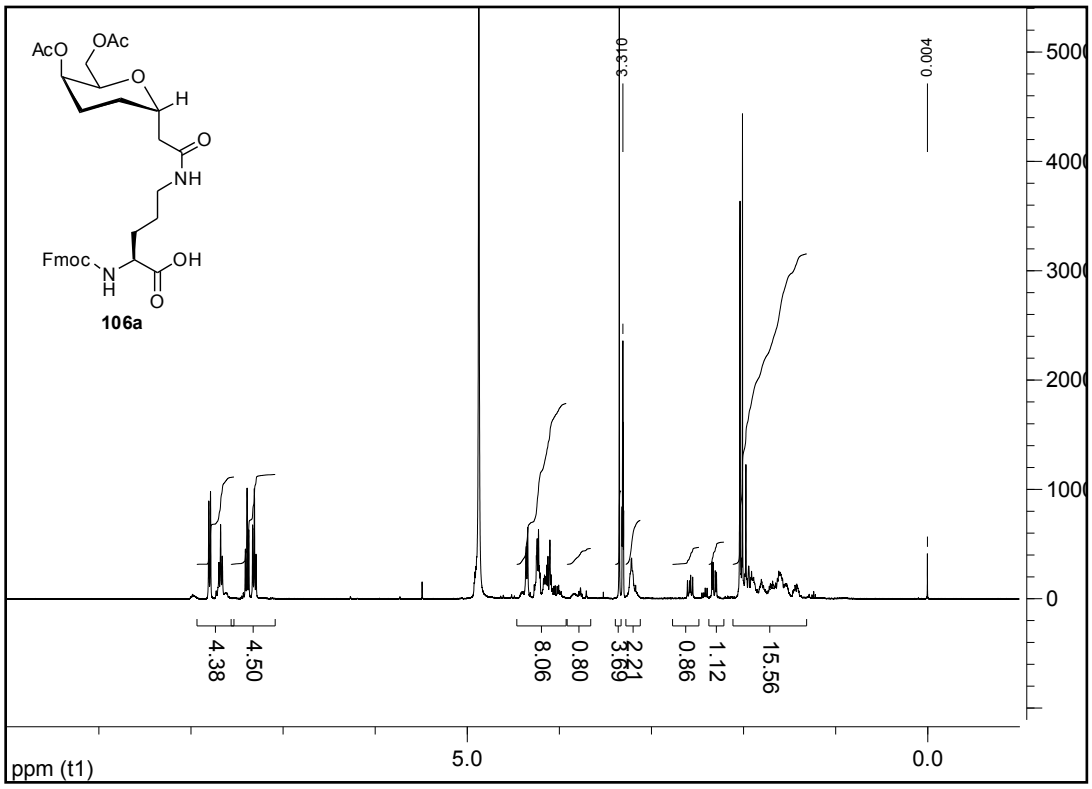

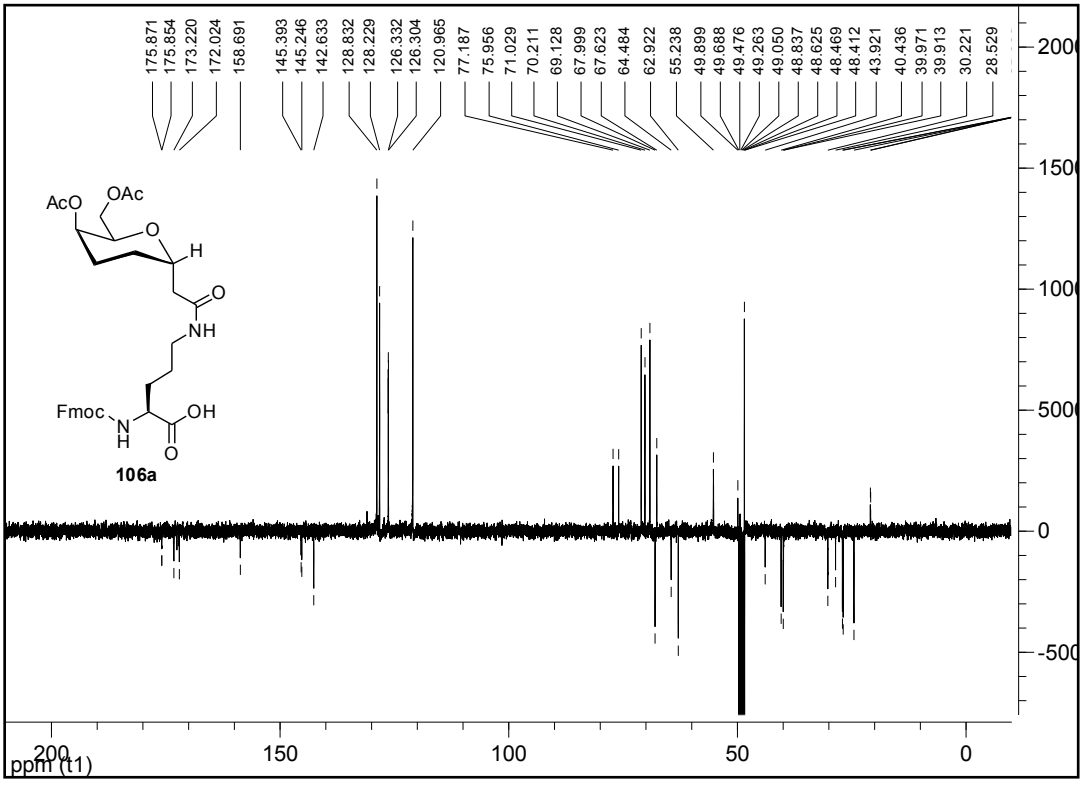

(S)-benzyl 2-(((9H-fluoren-9-yl)methoxy)carbonylamino)-5-(2-((2S,5R,6R)-5-acetoxy-6-(acetoxymethyl)-5,6-dihydro-2H-pyran-2-yl)acetamido)pentanoate (107a):

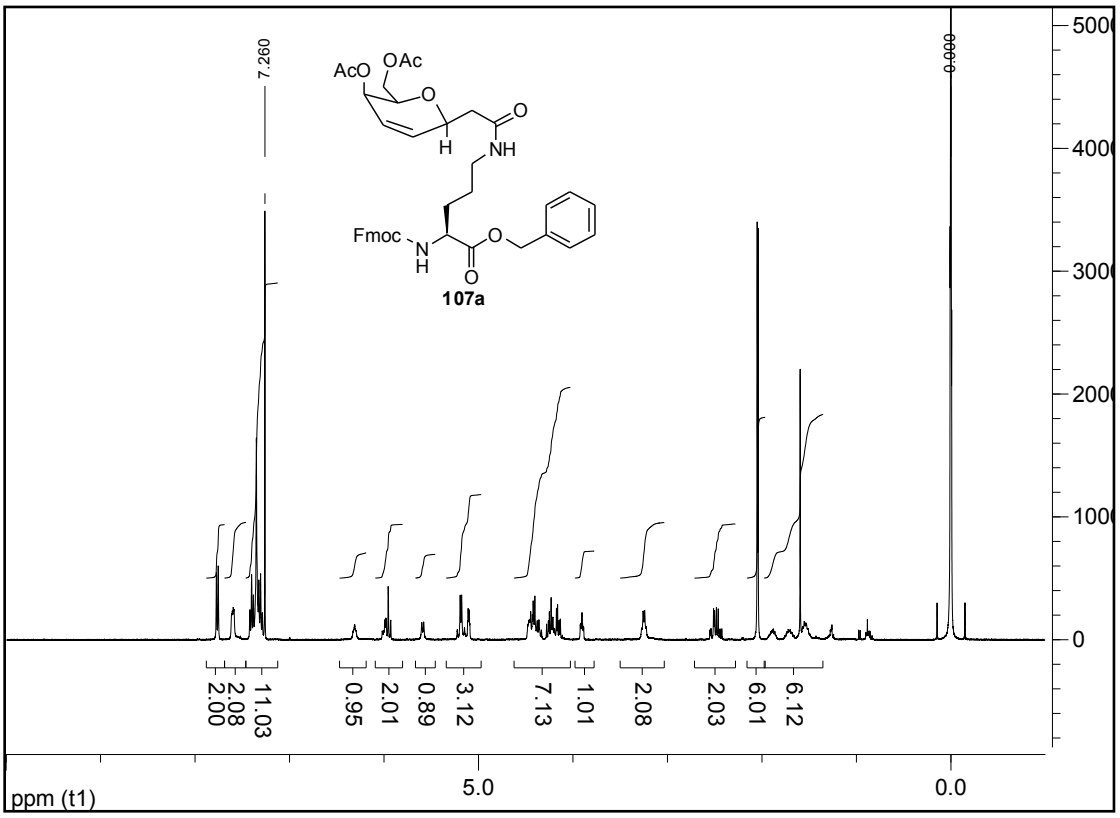

(S)-benzyl 2-(((9H-fluoren-9-yl)methoxy)carbonylamino)-5-((S)-2-((2R,5R,6R)-5-acetoxy-6-(acetoxymethyl)-5,6-dihydro-2H-pyran-2-yl)propanamido)pentanoate (107b):

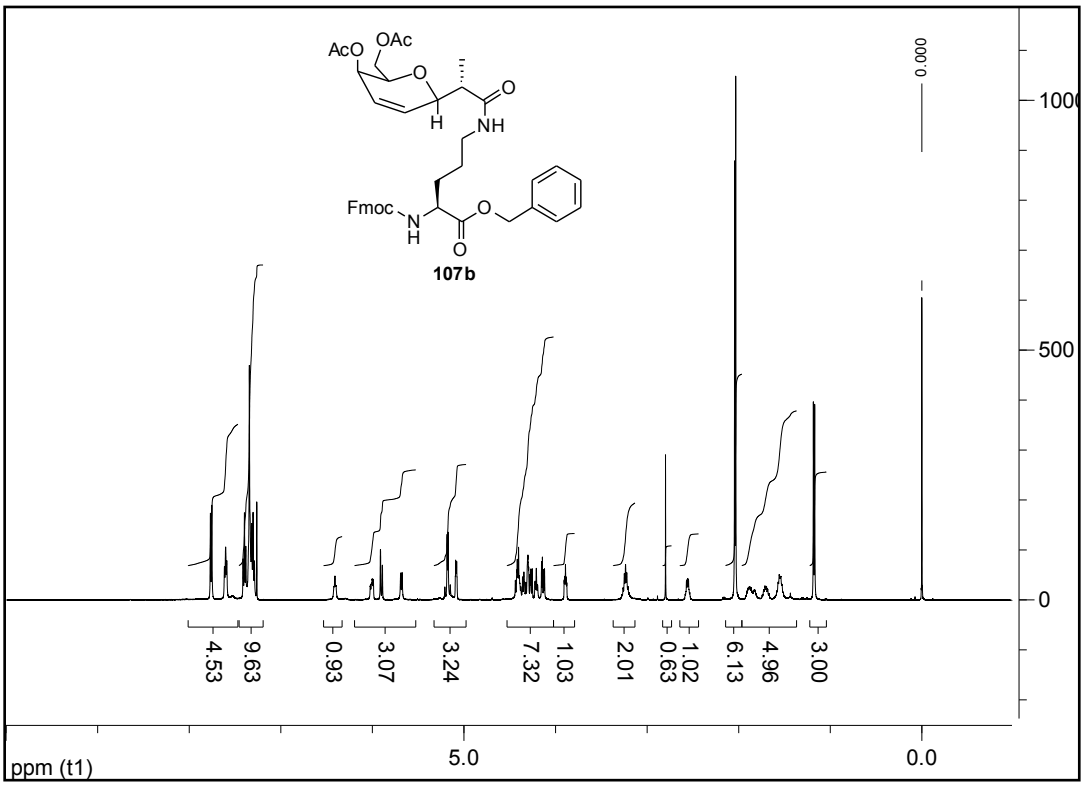

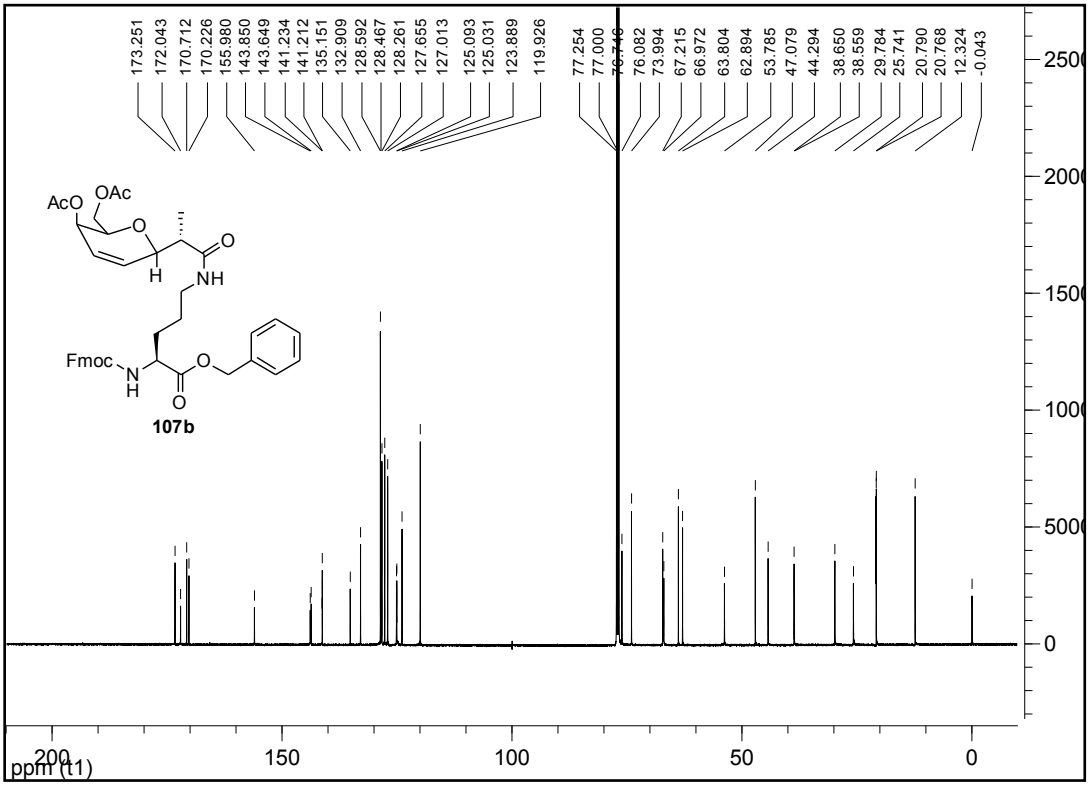

(S)-2-(((9H-fluoren-9-yl)methoxy)carbonylamino)-5-(2-((2R,5R,6R)-5-acetoxy-6-(acetoxymethyl)tetrahydro-2H-pyran-2-yl)acetamido)pentanoic acid (108a):

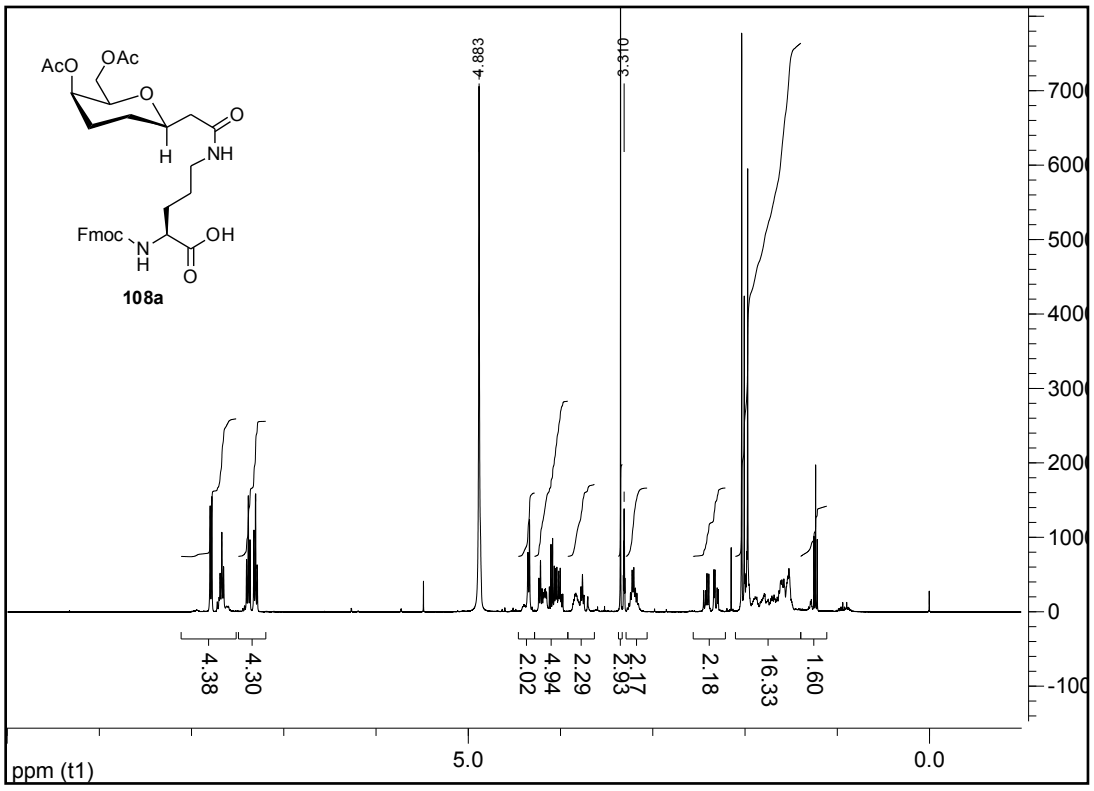

((2R,3R,6S)-3-acetoxy-6-((S)-1-hydroxypropan-2-yl)-3,6-dihydro-2H-pyran-2-yl)methyl acetate (109b-α):

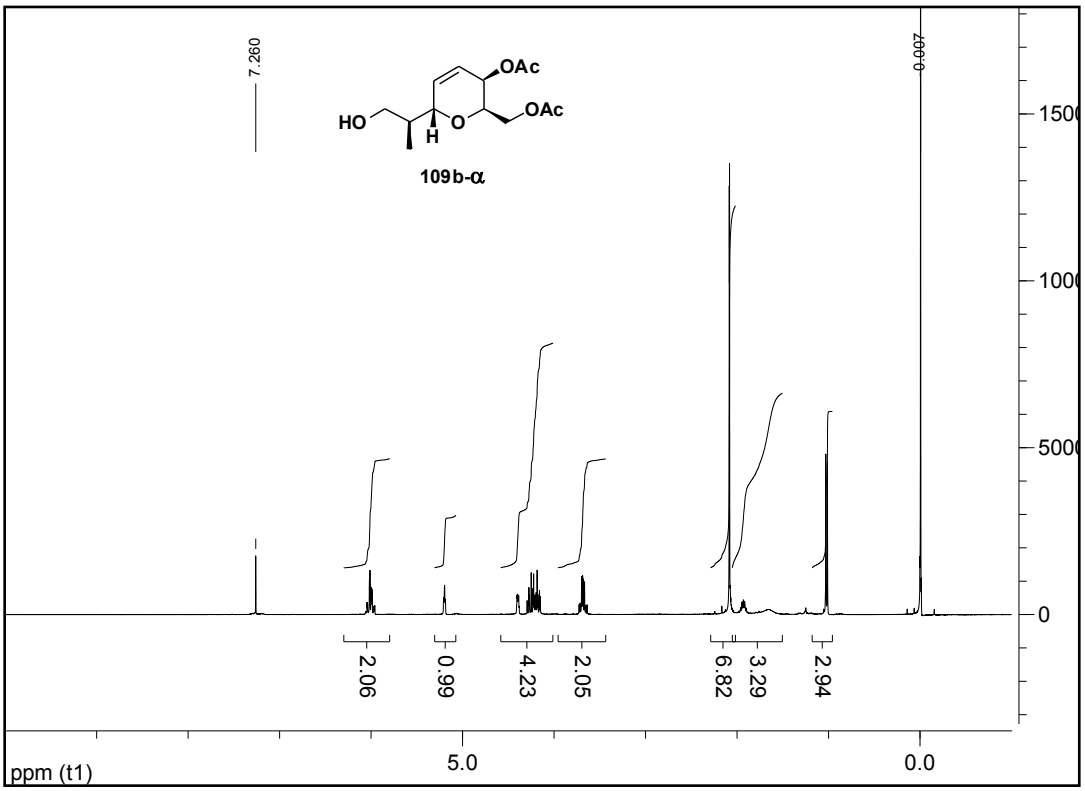

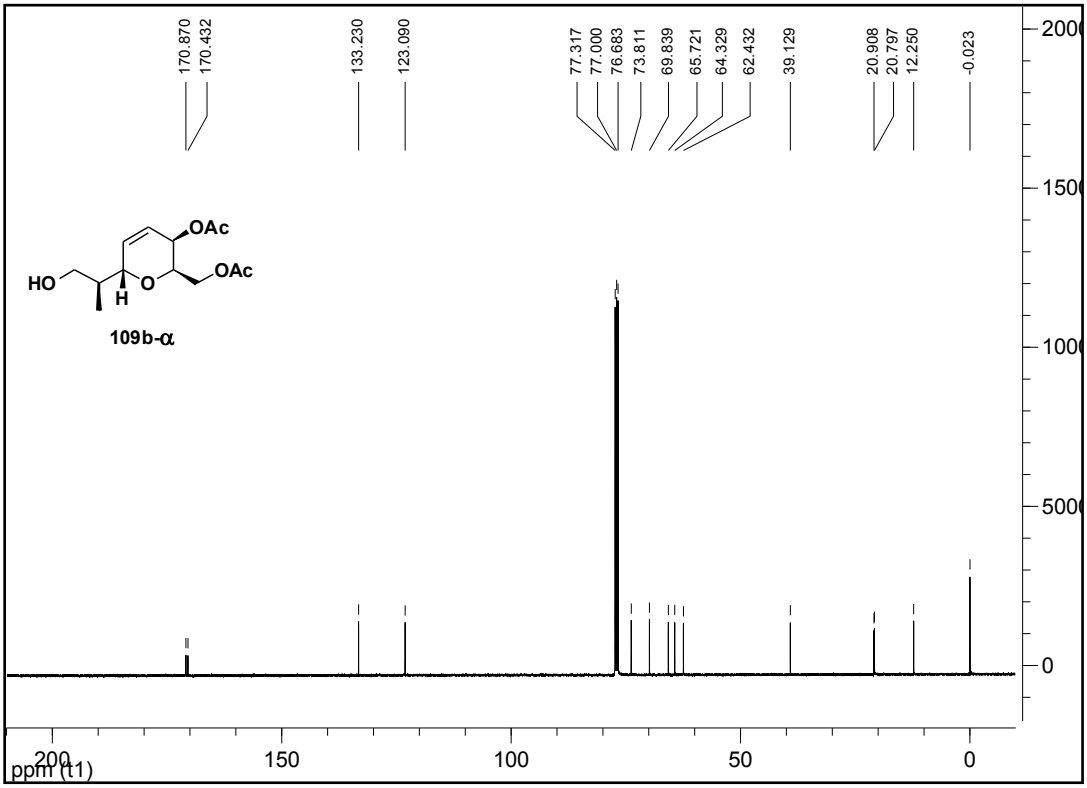

((2R,3R,6R)-3-acetoxy-6-((R)-1-hydroxypropan-2-yl)-3,6-dihydro-2H-pyran-2-yl)methyl acetate (109b-β):

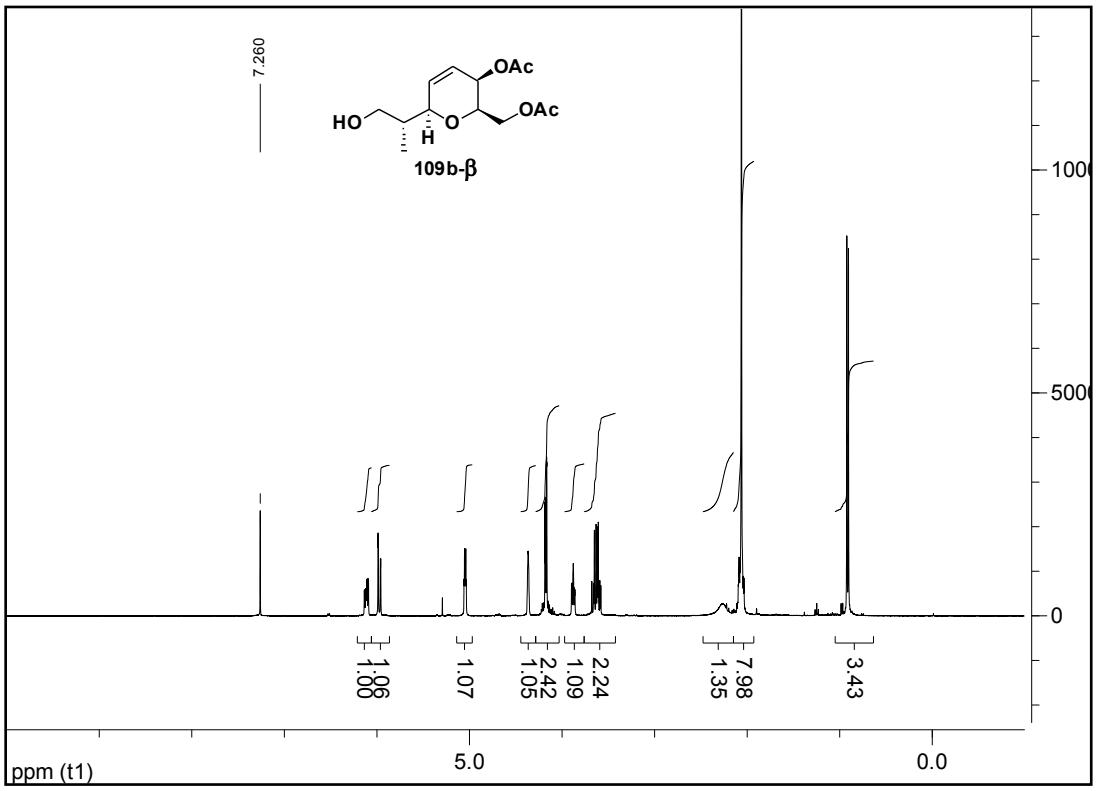

((2R,3R,6S)-3-acetoxy-6-((S)-2-hydroxy-1-phenylethyl)-3,6-dihydro-2H-pyran-2-yl)methyl acetate (109e):

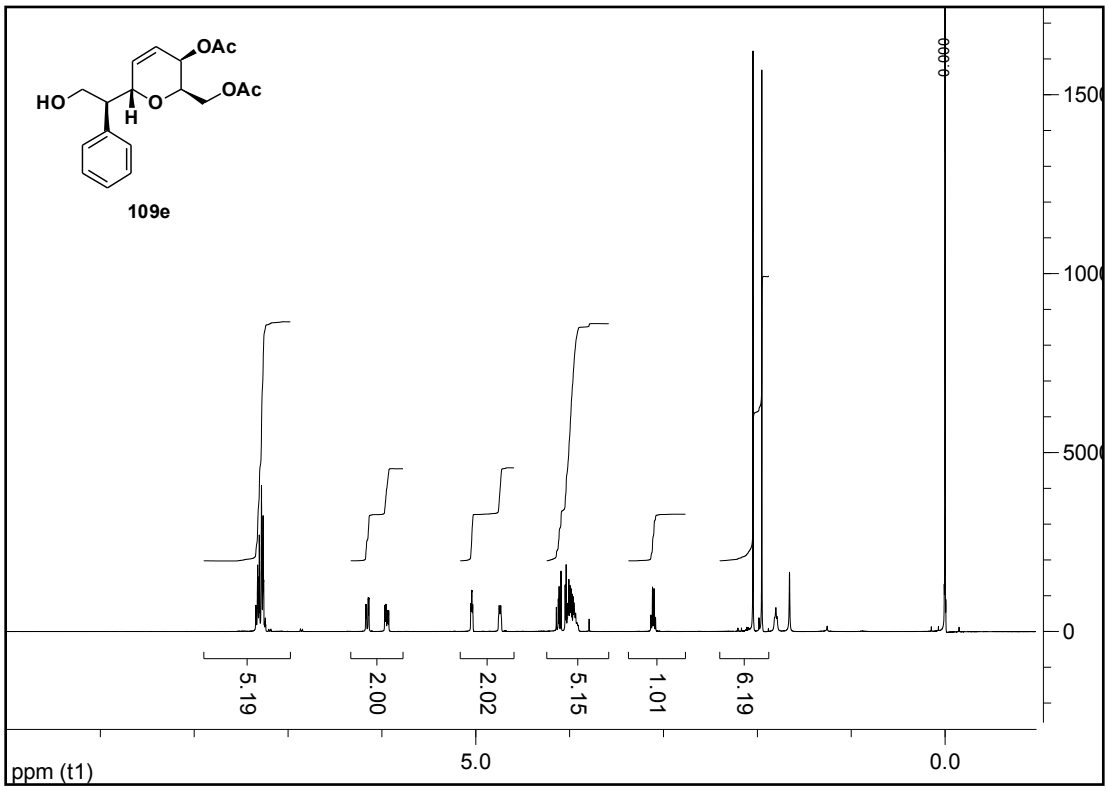

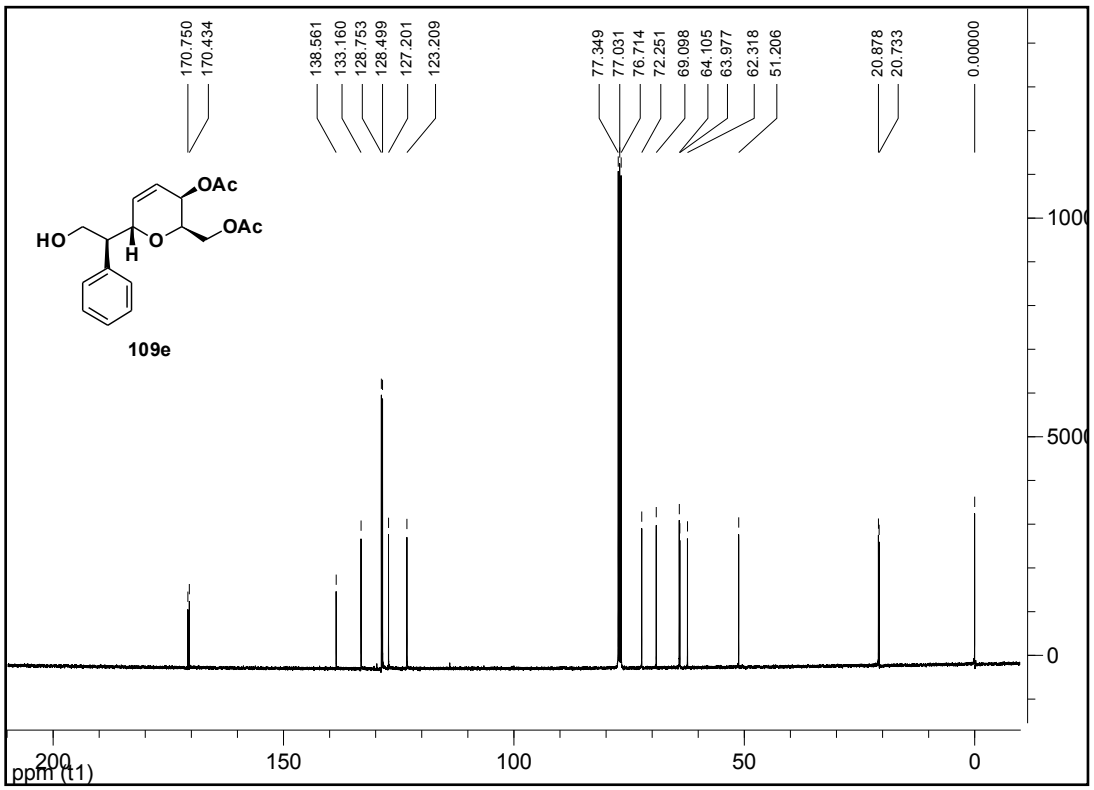

((2R,3R,6S)-3-acetoxy-6-(1-hydroxy-3-phenylpropan-2-yl)-3,6-dihydro-2H-pyran-2-yl)methyl acetate (109f):

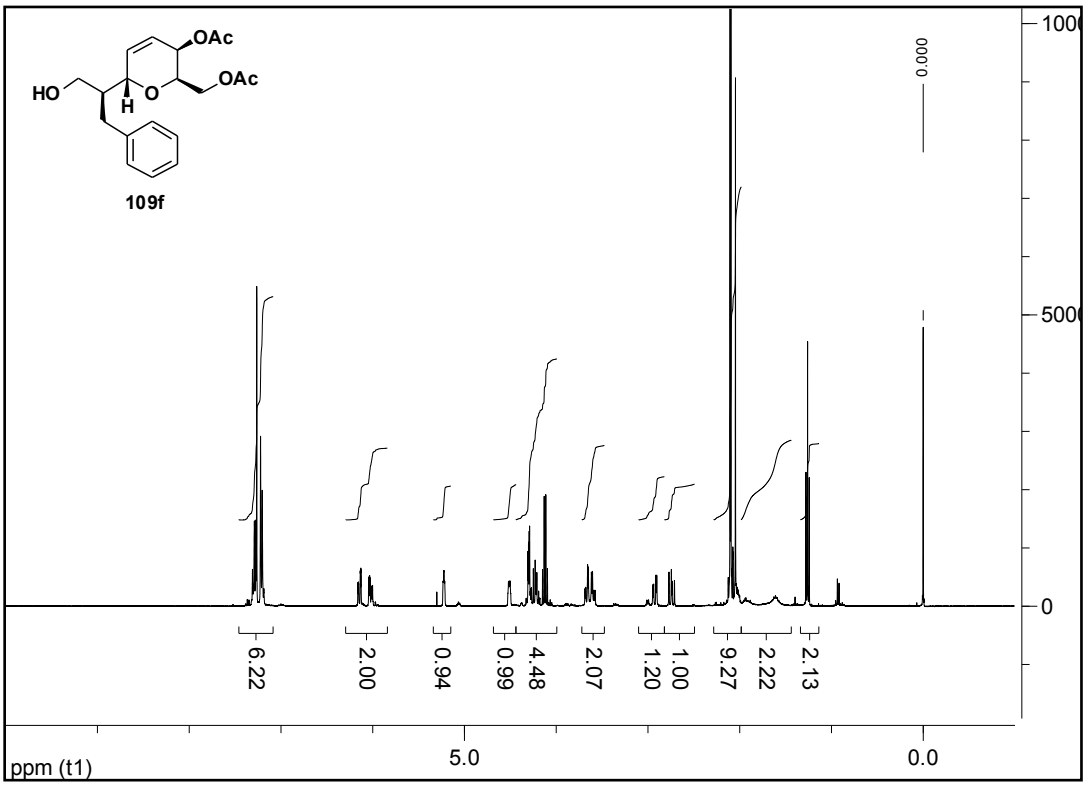

((2R,3R,6S)-3-acetoxy-6-((S)-2-hydroxy-1-(4-methoxyphenyl)ethyl)-3,6-dihydro-2H-pyran-2-yl)methyl acetate (109g):

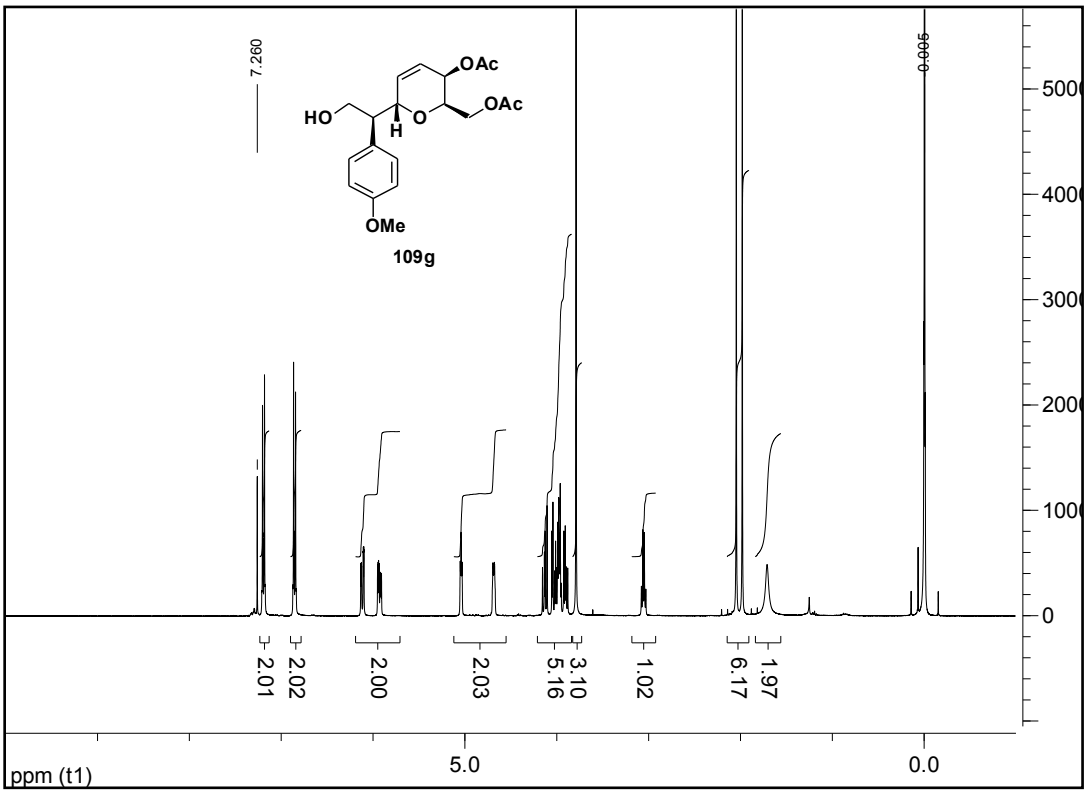

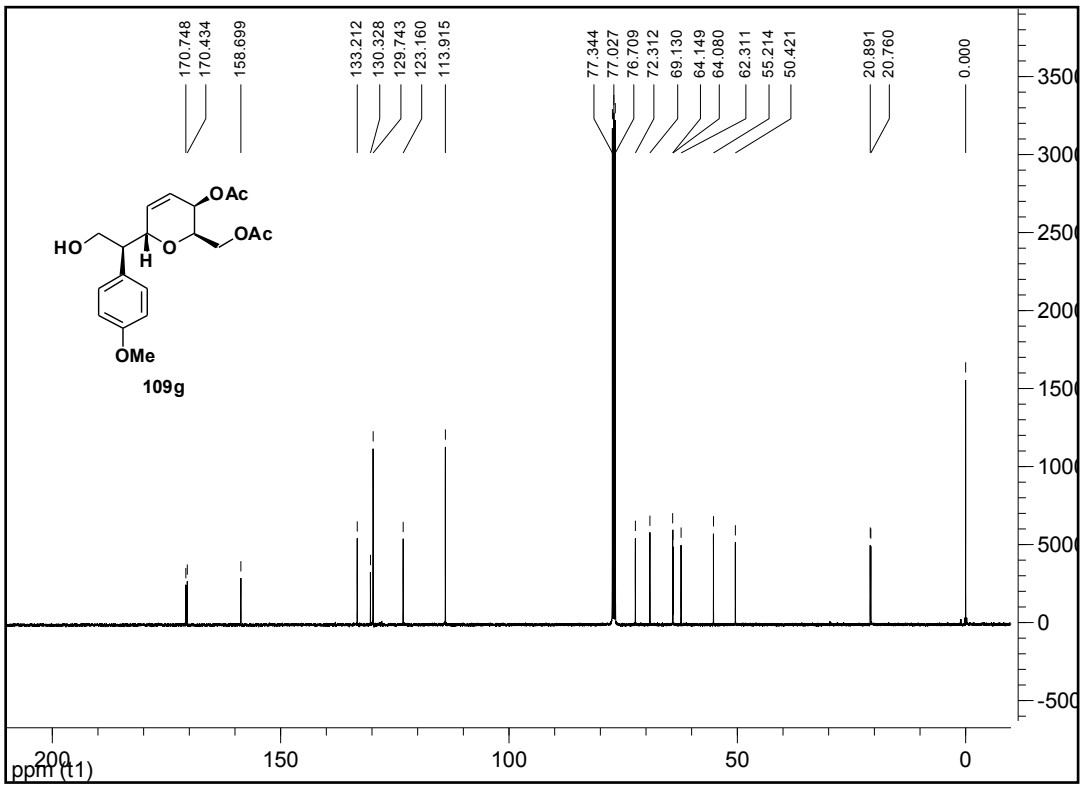

((2R,3R)-3-acetoxy-6-(1-oxo-3-phenylpropan-2-yl)-3,6-dihydro-2H-pyran-2-yl)methyl acetate (110f):

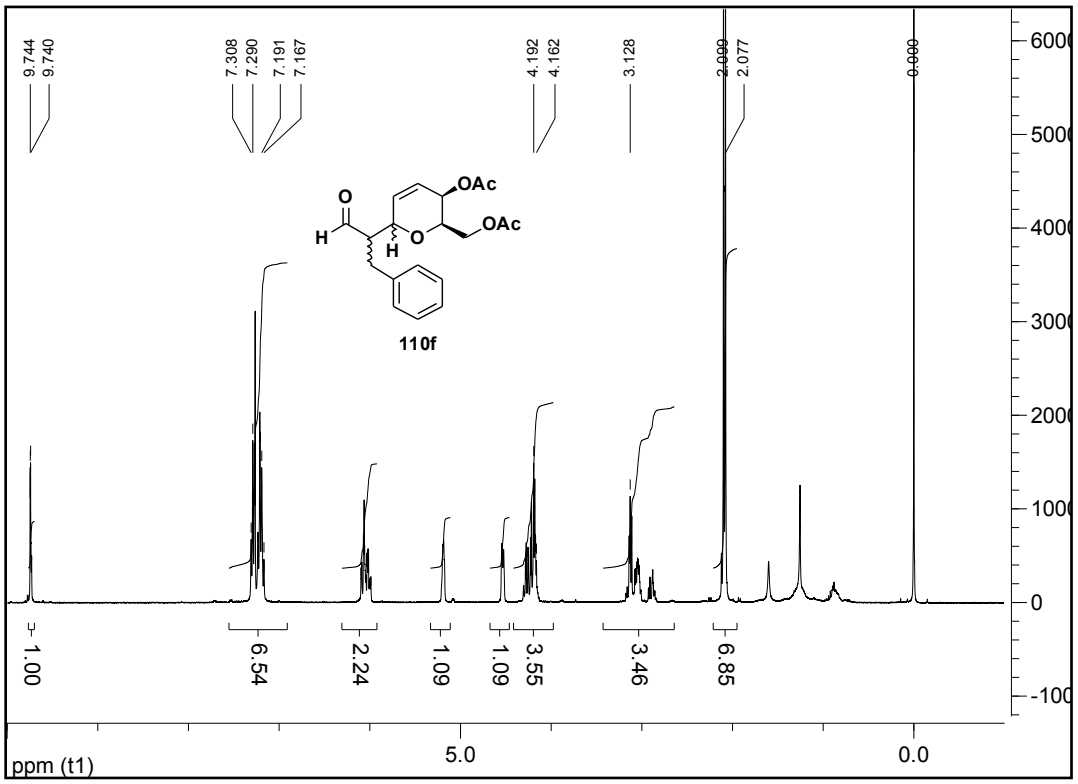

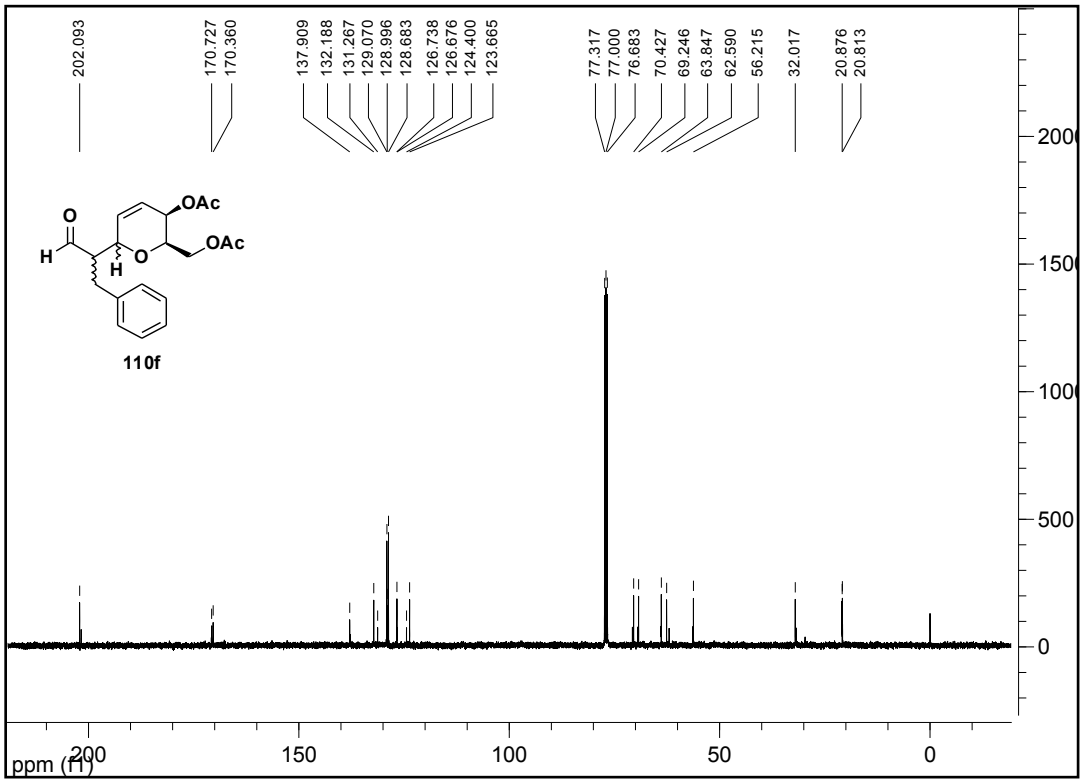

2-((2R,5R,6R)-5-acetoxy-6-(acetoxymethyl)-5,6-dihydro-2H-pyran-2-yl)acetic acid (111a):

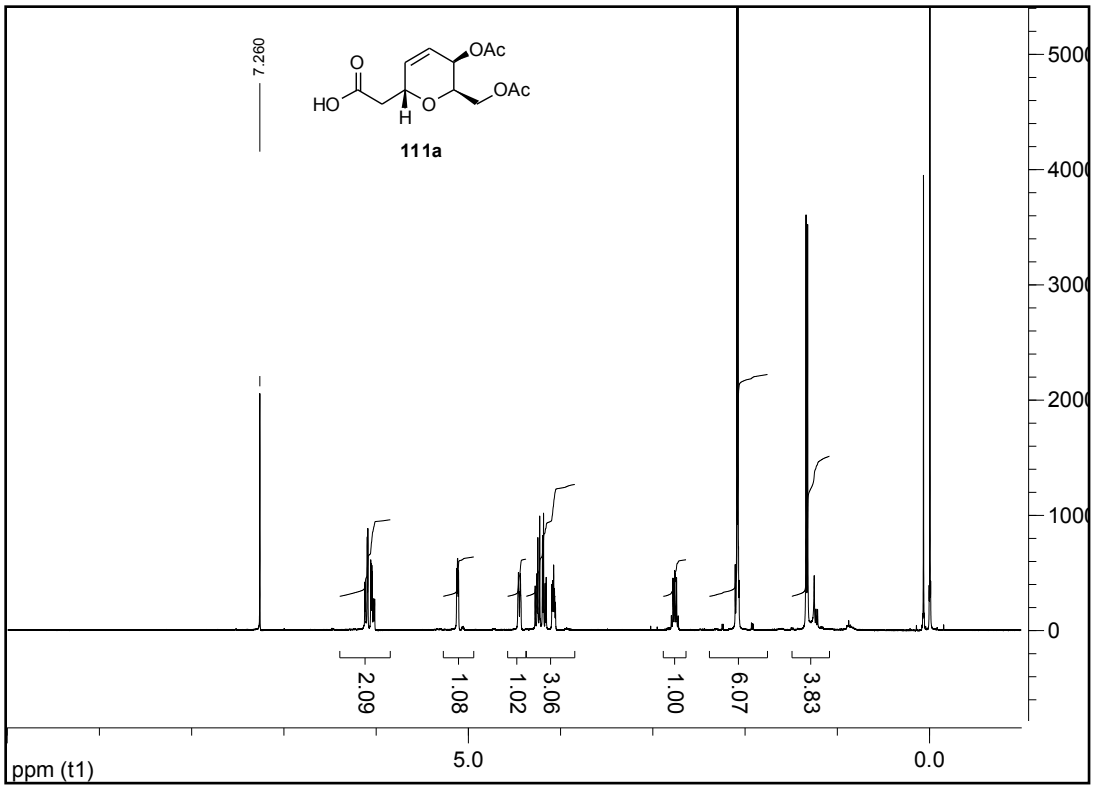

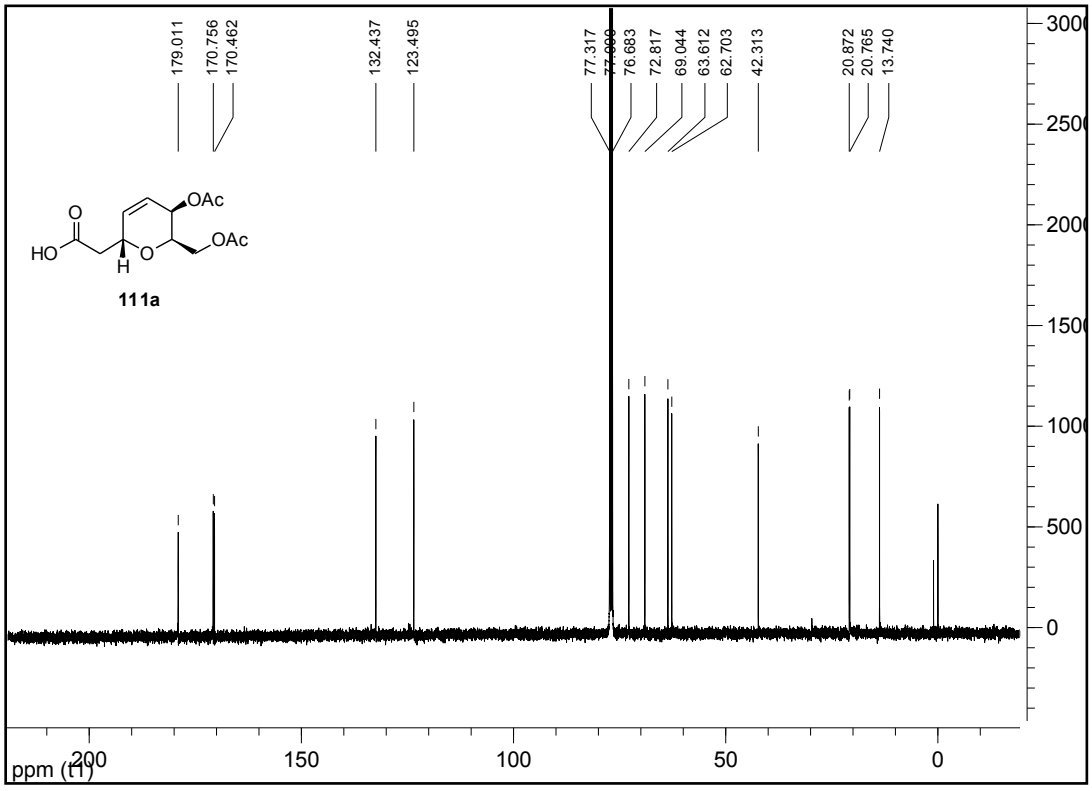

(R)-2-((2S,5R,6R)-5-acetoxy-6-(acetoxymethyl)-5,6-dihydro-2H-pyran-2-yl)propanoic acid (111b):

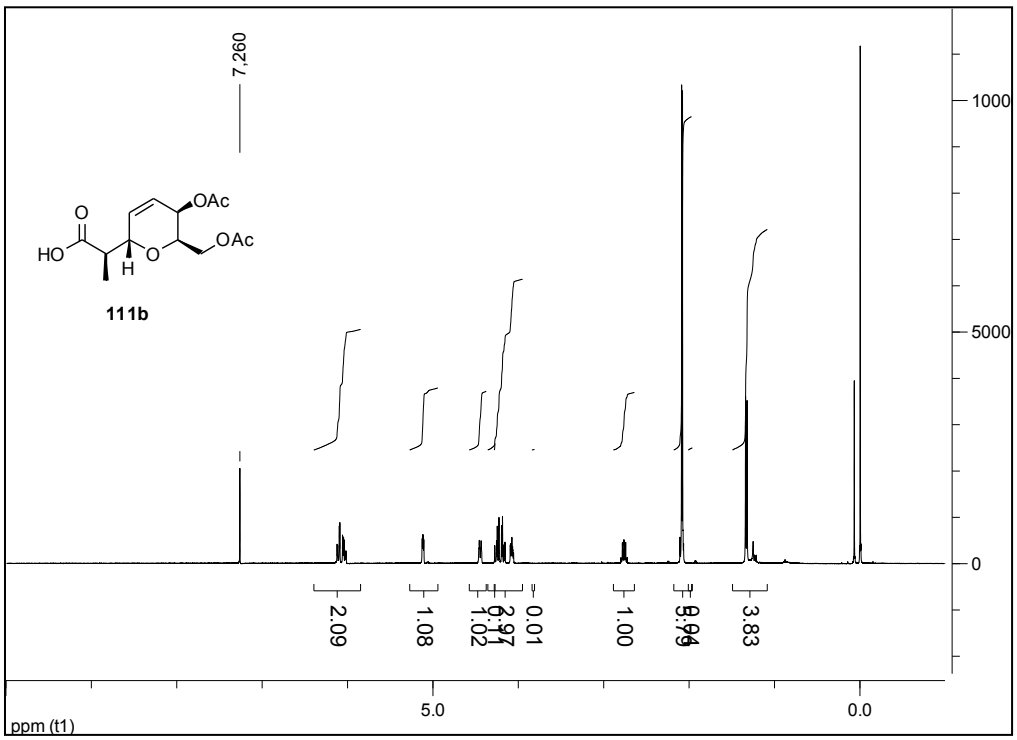

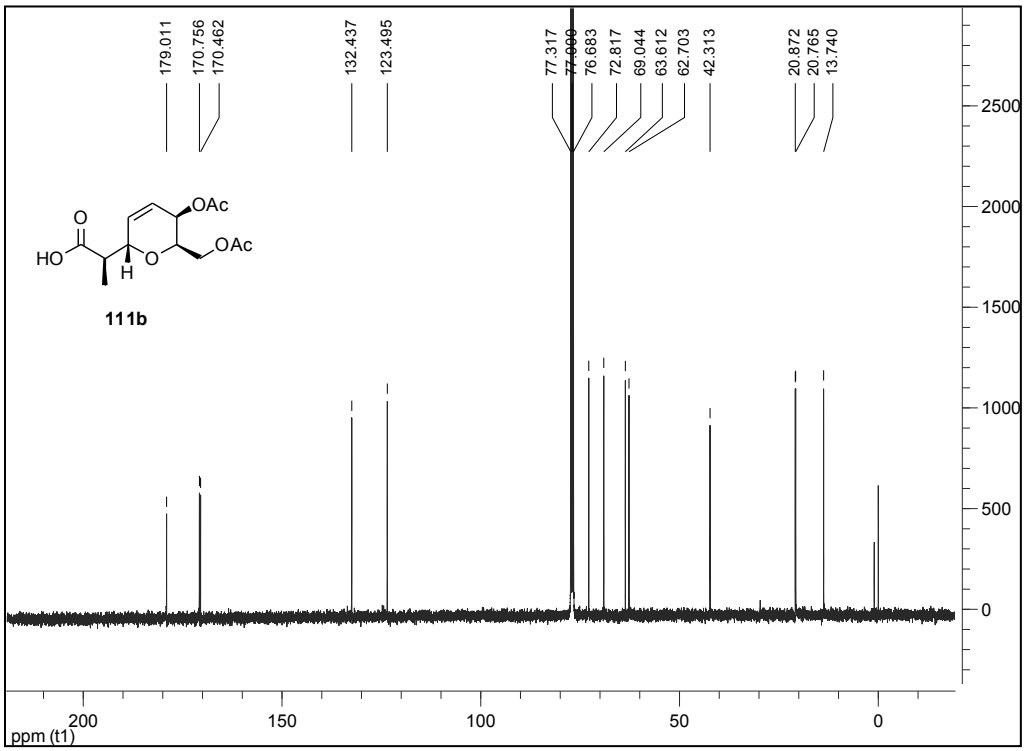

(R)-2-((2S,5R,6R)-5-acetoxy-6-(acetoxymethyl)-5,6-dihydro-2H-pyran-2-yl)-2-phenylacetic acid (111e):

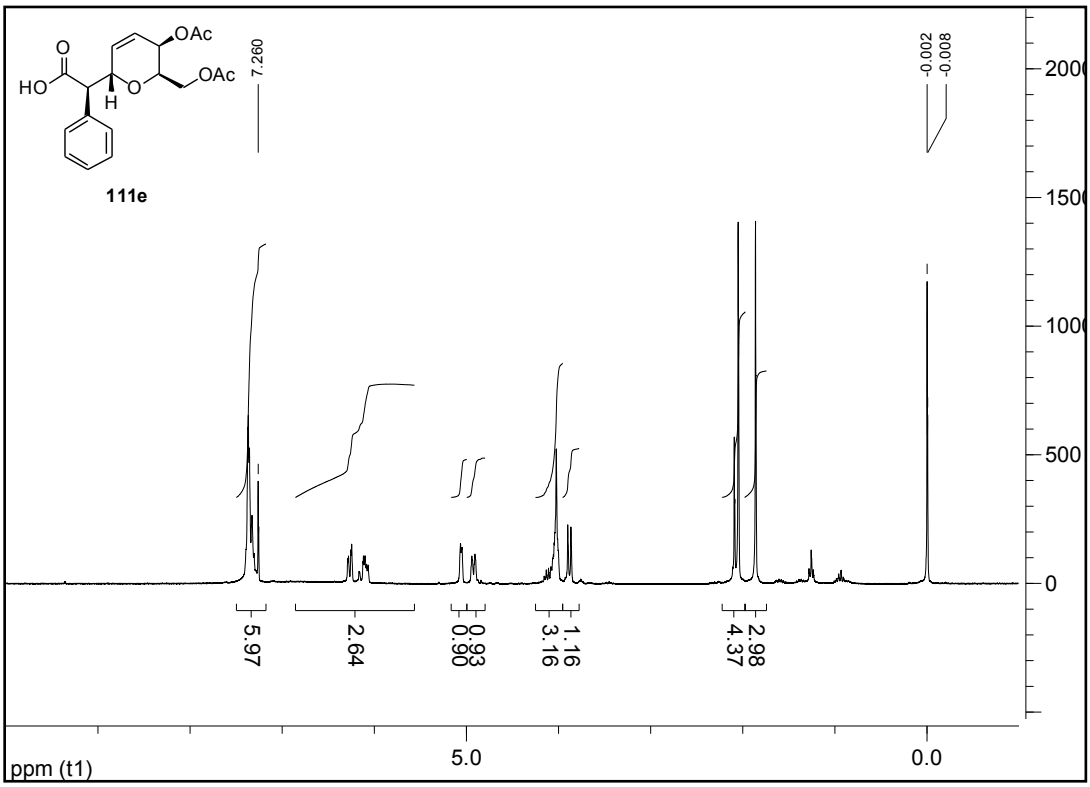

(R)-2-((2S,5R,6R)-5-acetoxy-6-(acetoxymethyl)-5,6-dihydro-2H-pyran-2-yl)-3-phenylpropanoic acid (111f):

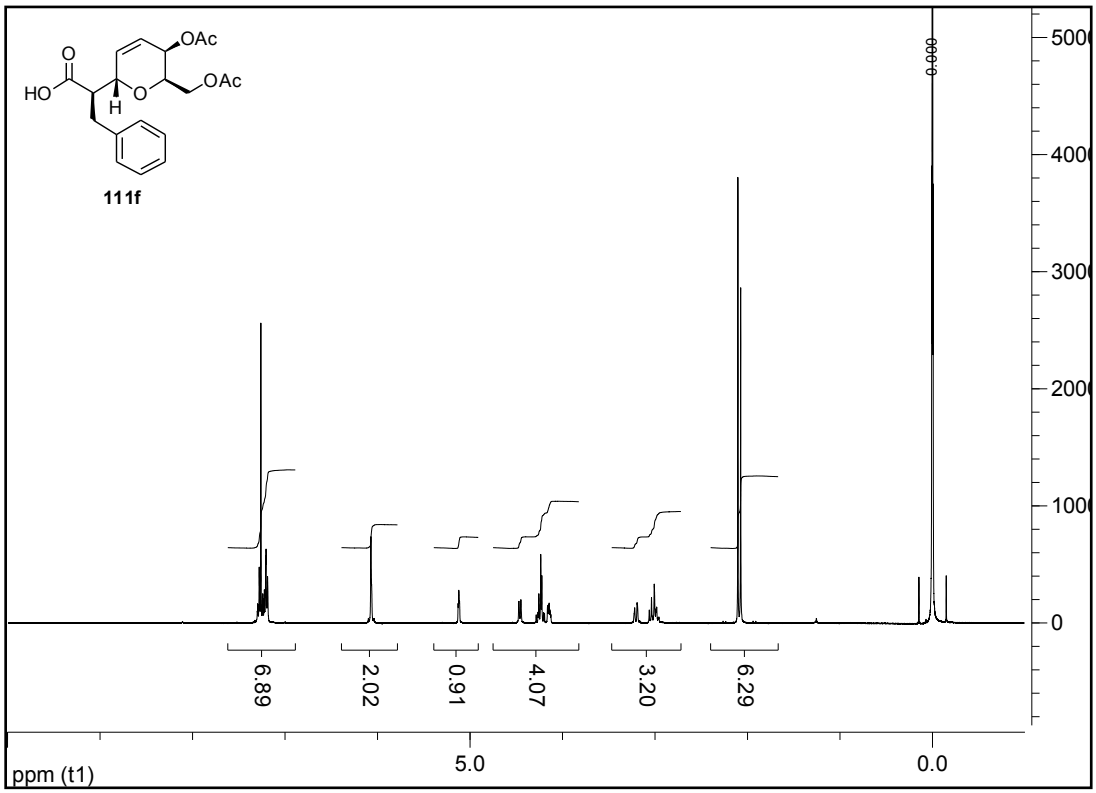

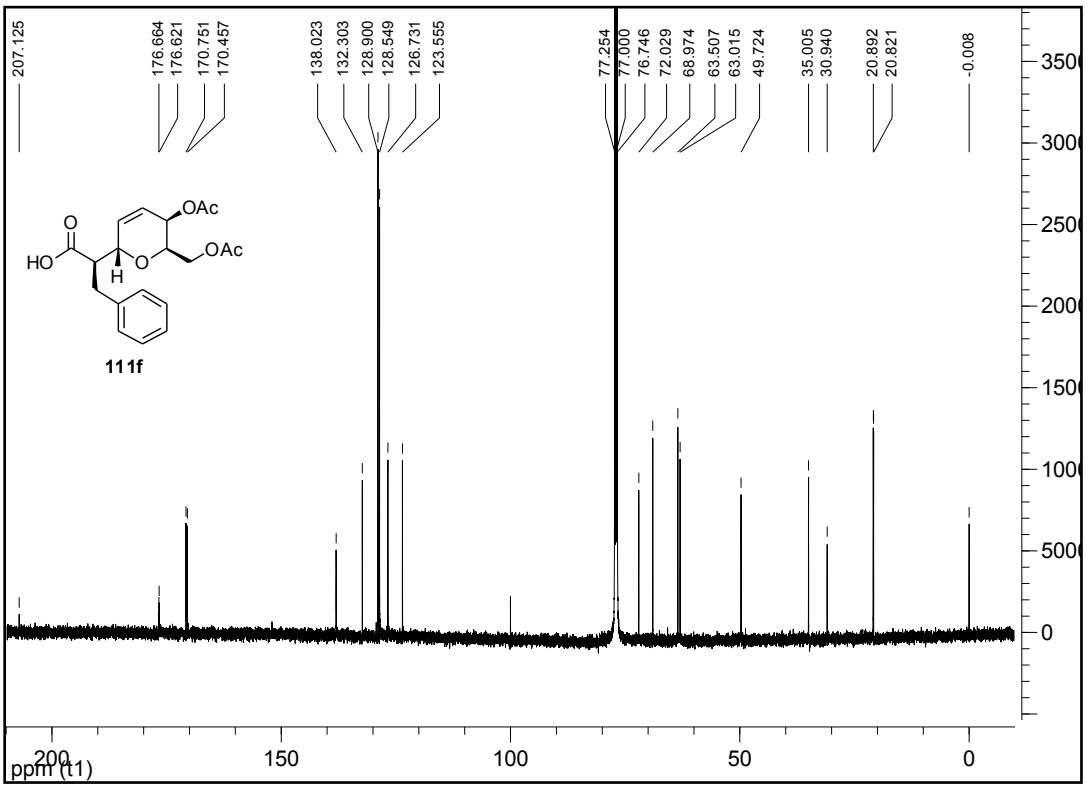

(R)-2-((2S,5R,6R)-5-acetoxy-6-(acetoxymethyl)-5,6-dihydro-2H-pyran-2-yl)-2-(4-methoxyphenyl)acetic acid (111g):

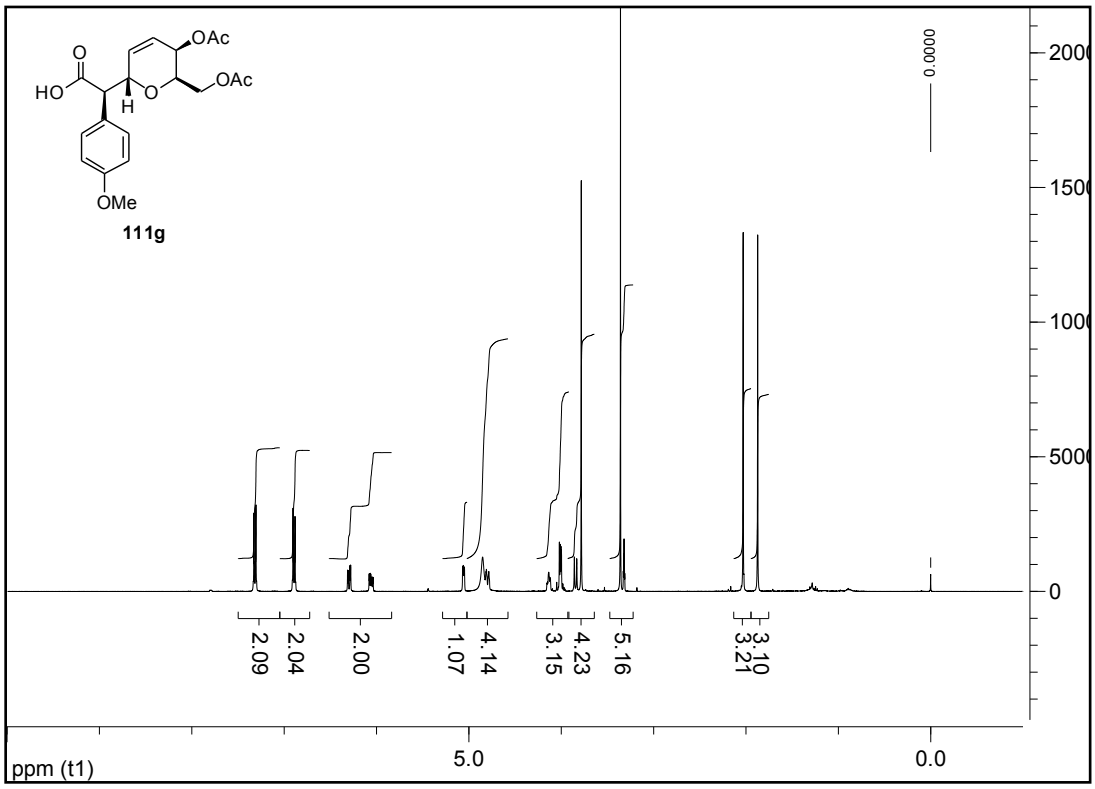

((2R,3R,6S)-3-acetoxy-6-(2-(methoxy(methyl)amino)-2-oxoethyl)-3,6-dihydro-2H-pyran-2-yl)methyl acetate (112):

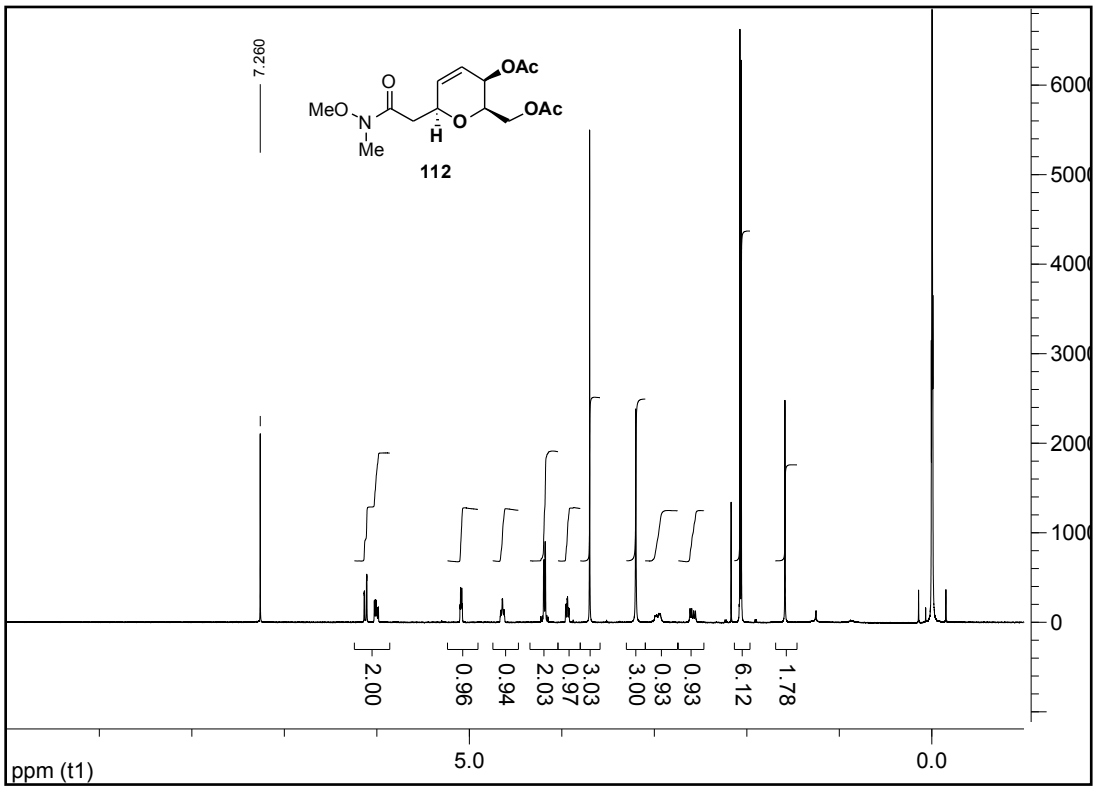

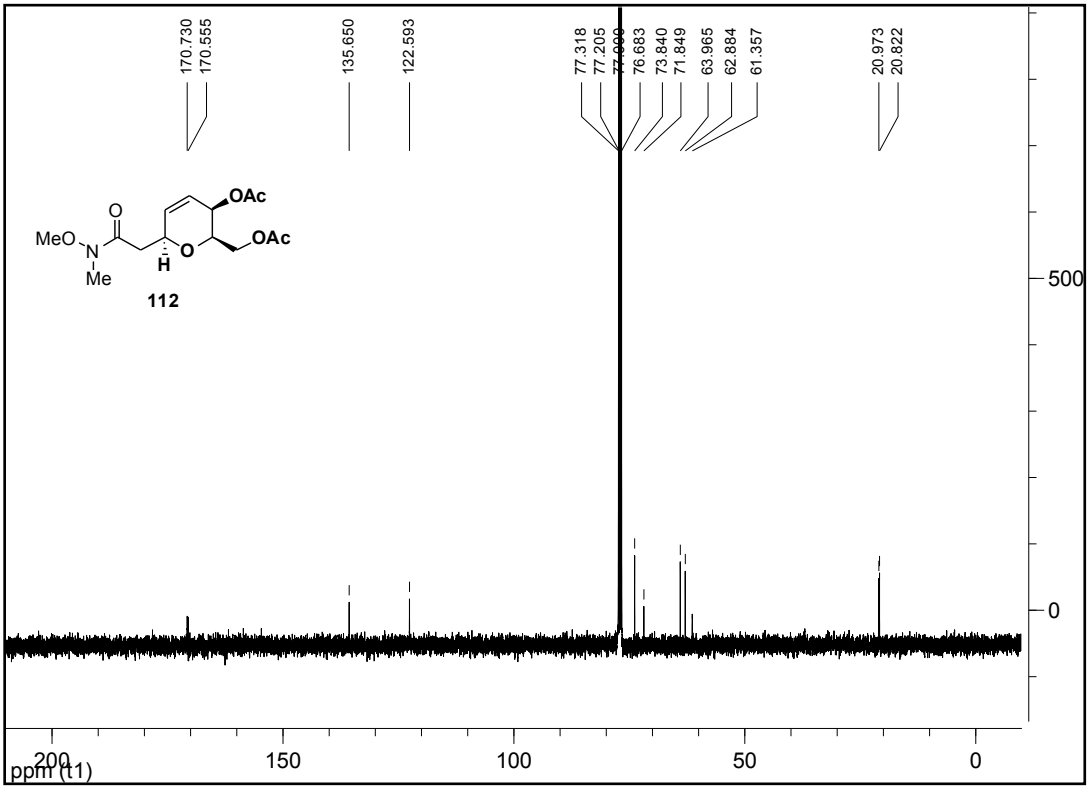

(S)-2-(((9H-fluoren-9-yl)methoxy)carbonylamino)-5-(2-((2S,5R,6R)-5-acetoxy-6-(acetoxymethyl)-5,6-dihydro-2H-pyran-2-yl)acetamido)pentanoic acid (115a):

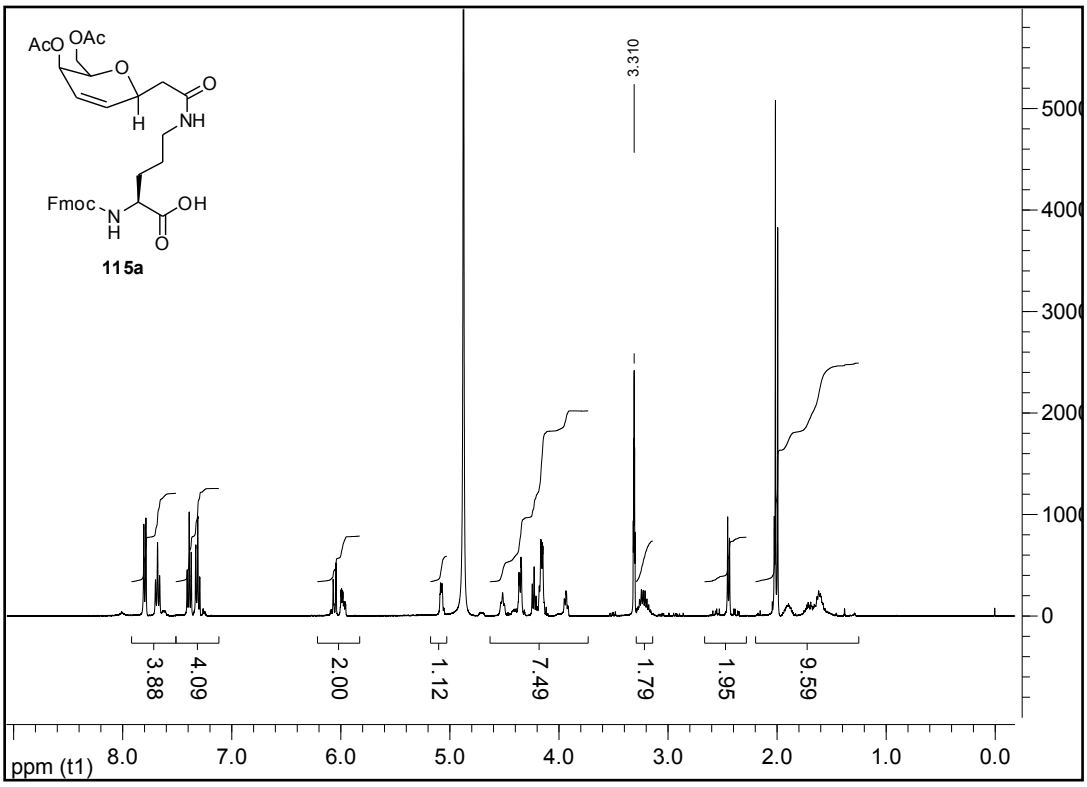

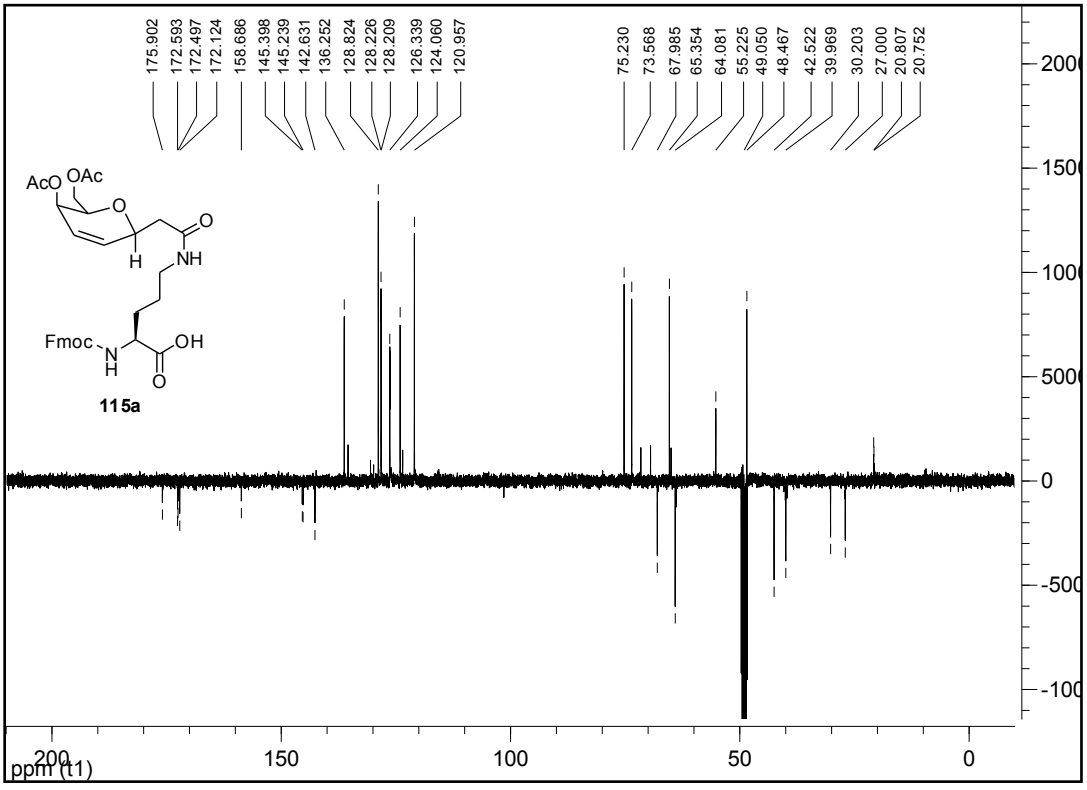

((2R,3R,6S)-3-acetoxy-6-((R)-1-(methoxy(methyl)amino)-1-oxopropan-2-yl)-3,6-dihydro-2H-pyran-2-yl)methyl acetate (116):

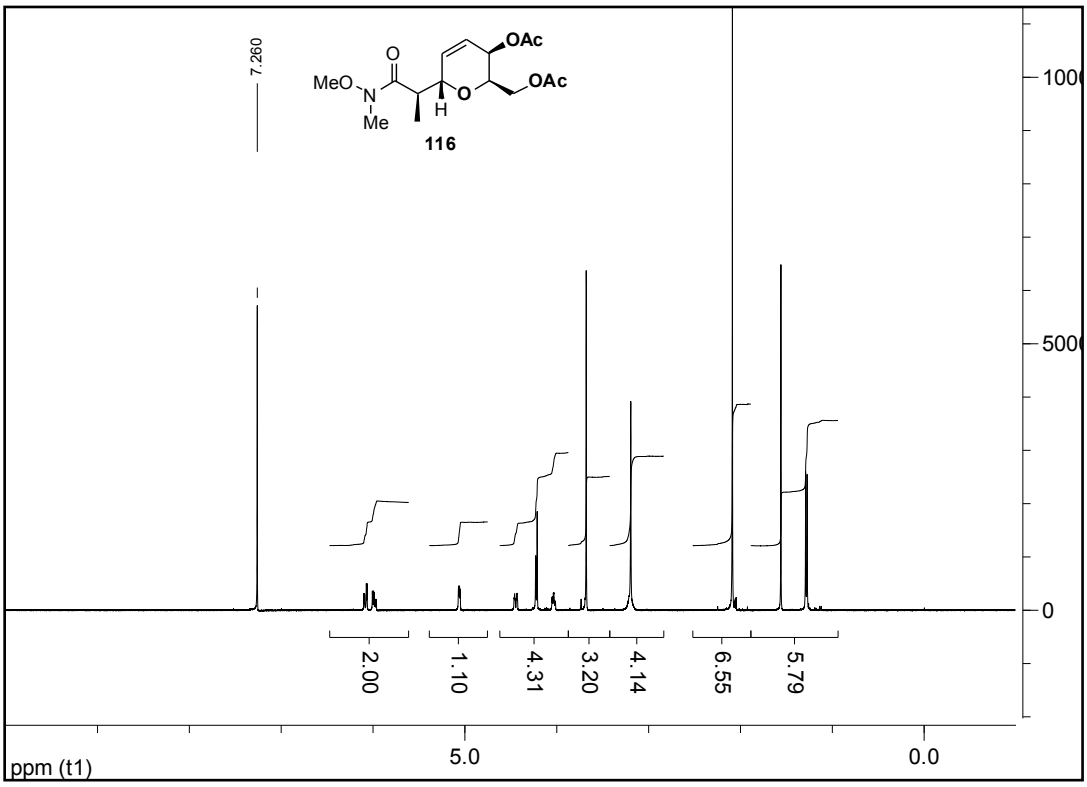

(S)-2-(((9H-fluoren-9-yl)methoxy)carbonylamino)-5-(2-((2R,5R,6R)-5-acetoxy-6-(acetoxymethyl)-5,6-dihydro-2H-pyran-2-yl)acetamido)pentanoic acid (117a):

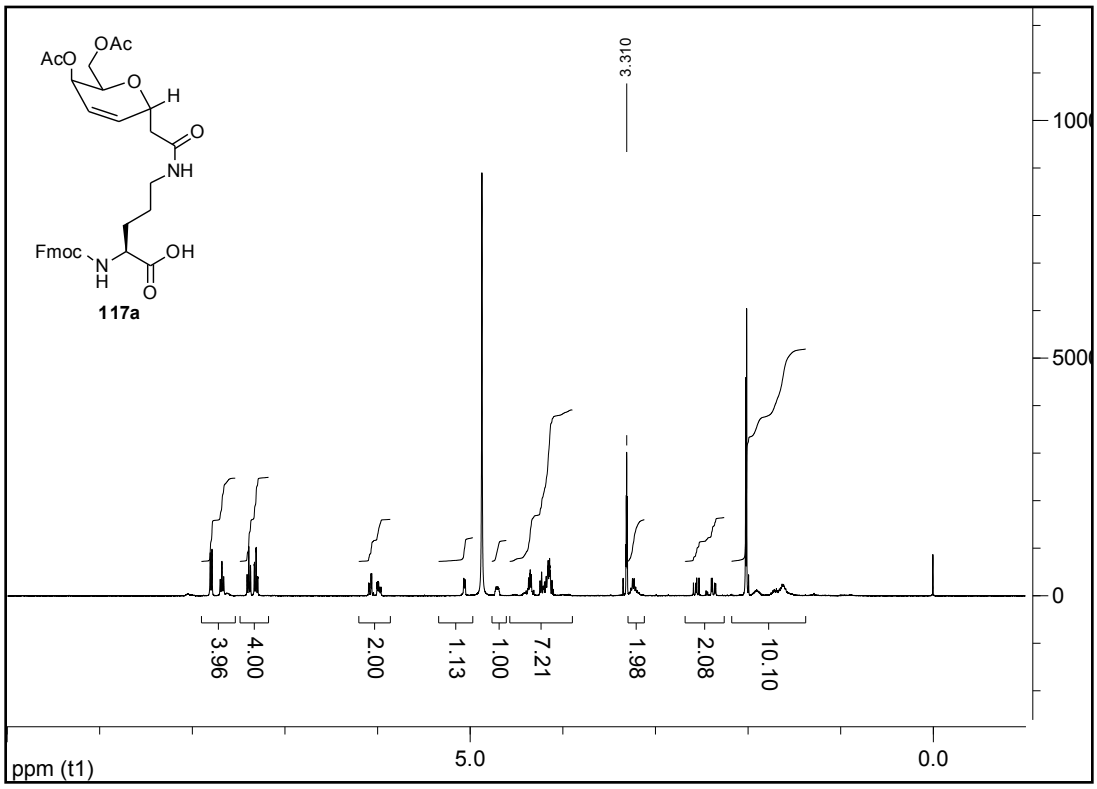

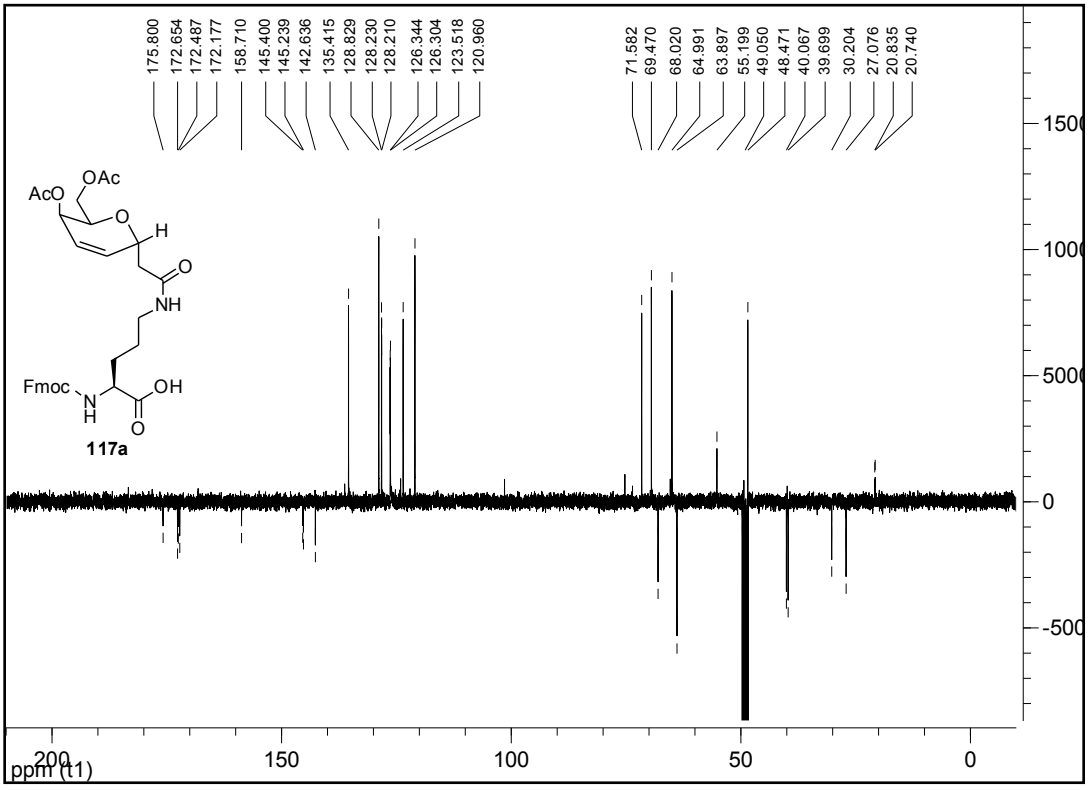

2-((2S,5R,6R)-5-acetoxy-6-(acetoxymethyl)-5,6-dihydro-2H-pyran-2-yl)acetic acid (120a):

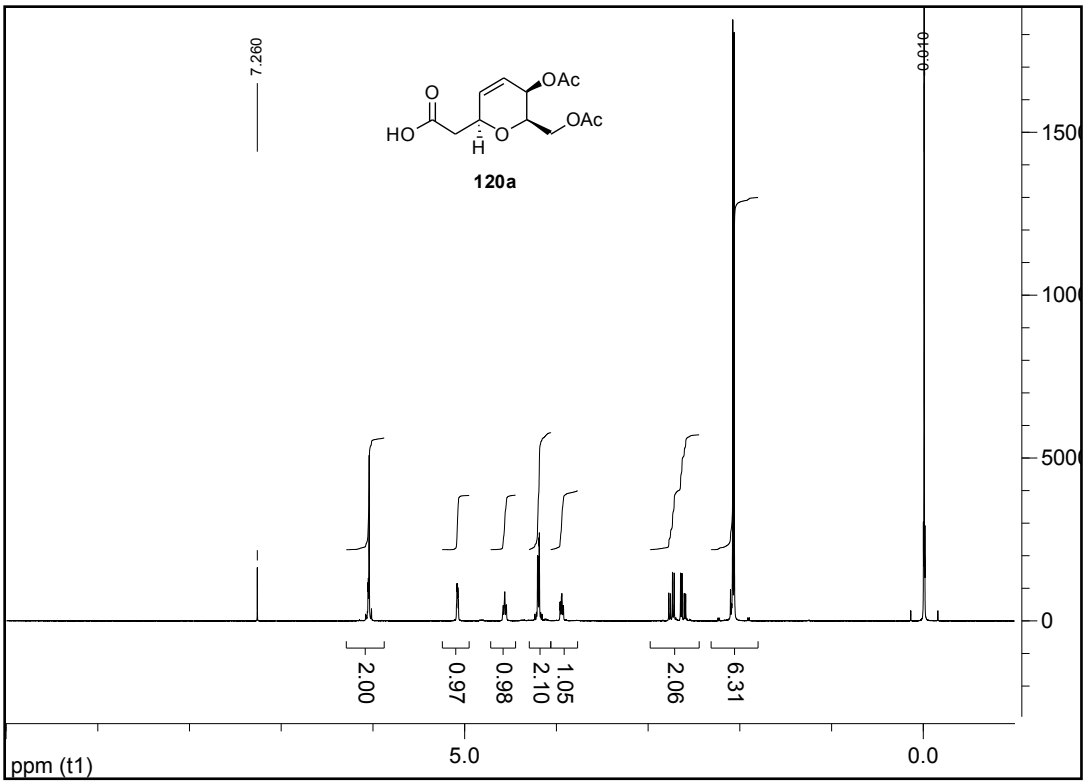

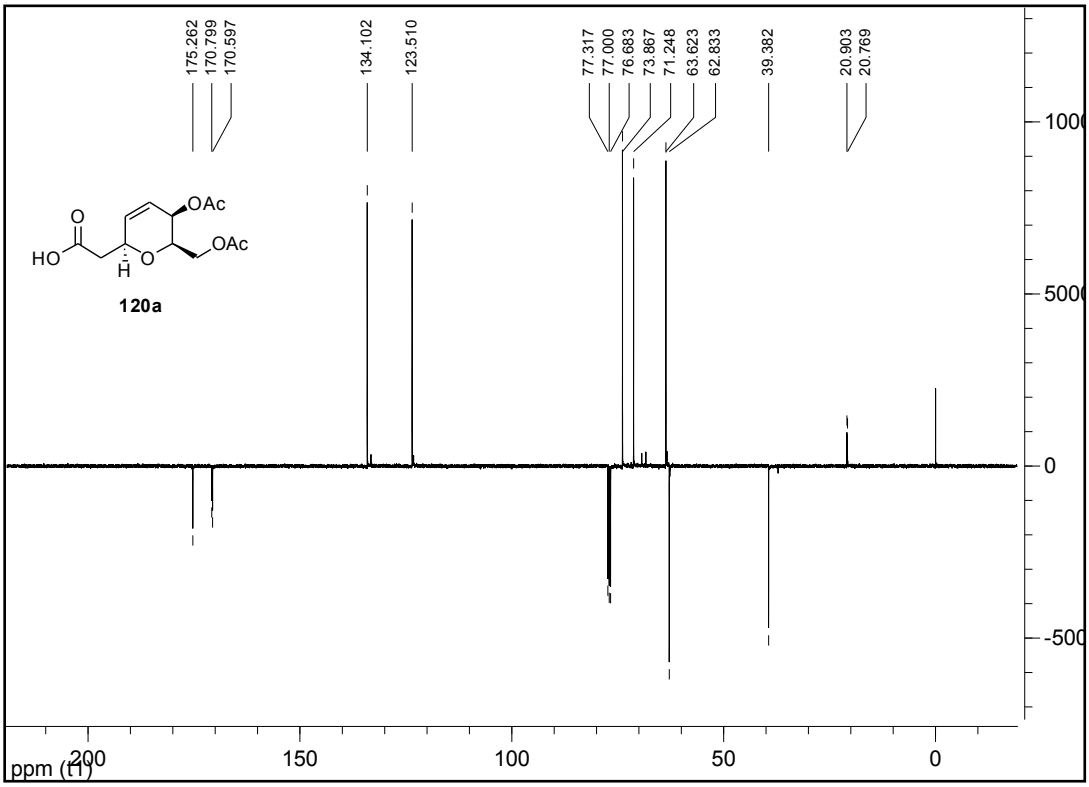

(S)-2-((2R,5R,6R)-5-acetoxy-6-(acetoxymethyl)-5,6-dihydro-2H-pyran-2-yl)propanoic acid (120b):

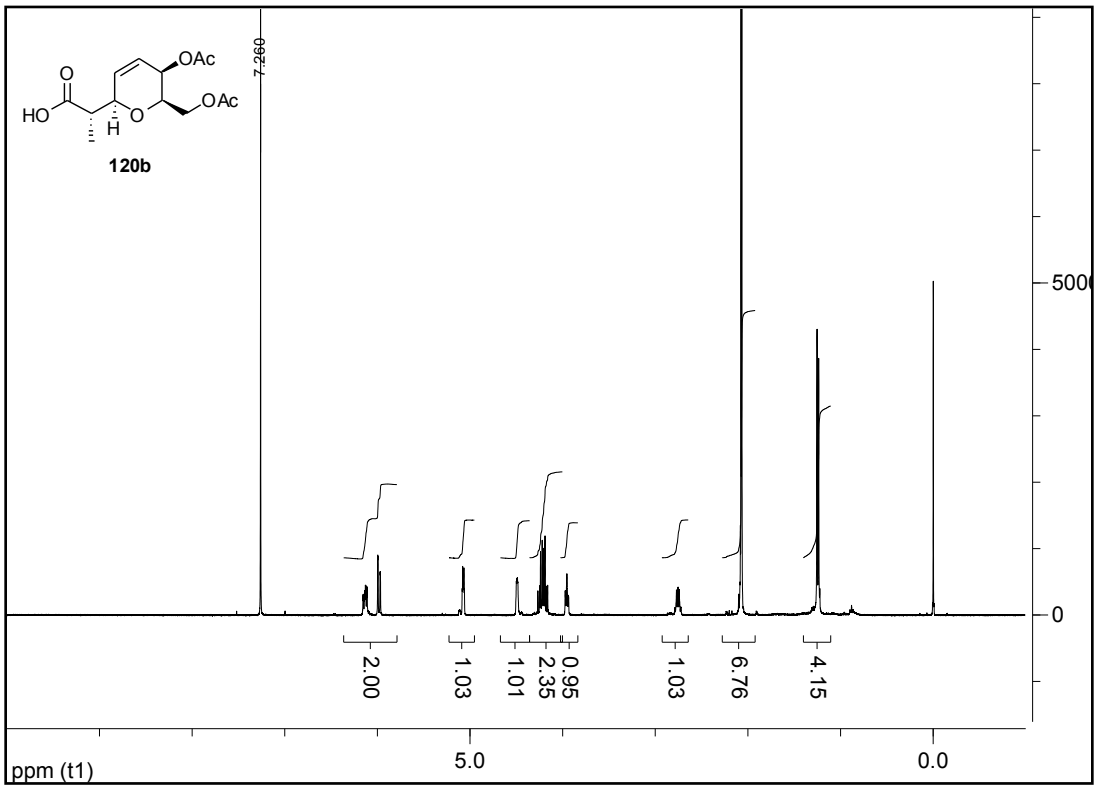

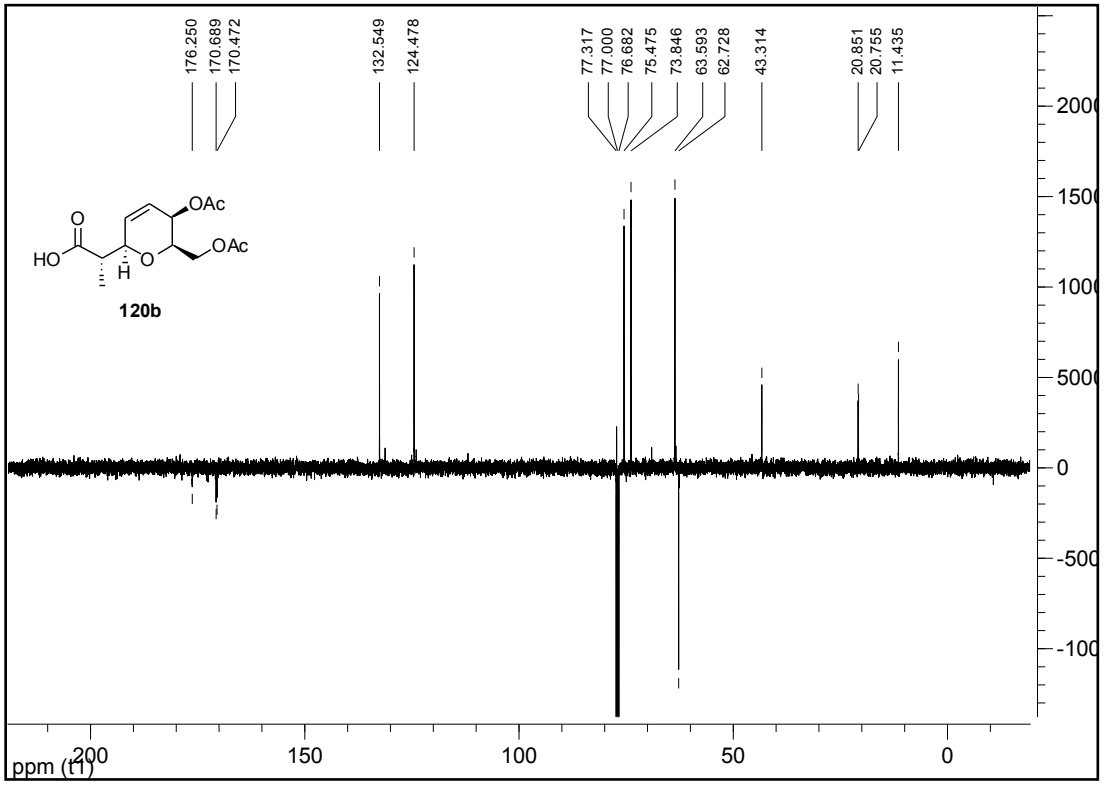

(S)-2-amino-5-(2-((2R,5R,6R)-5-hydroxy-6-(hydroxymethyl)-5,6-dihydro-2H-pyran-2-yl)acetamido)pentanoic acid (121):

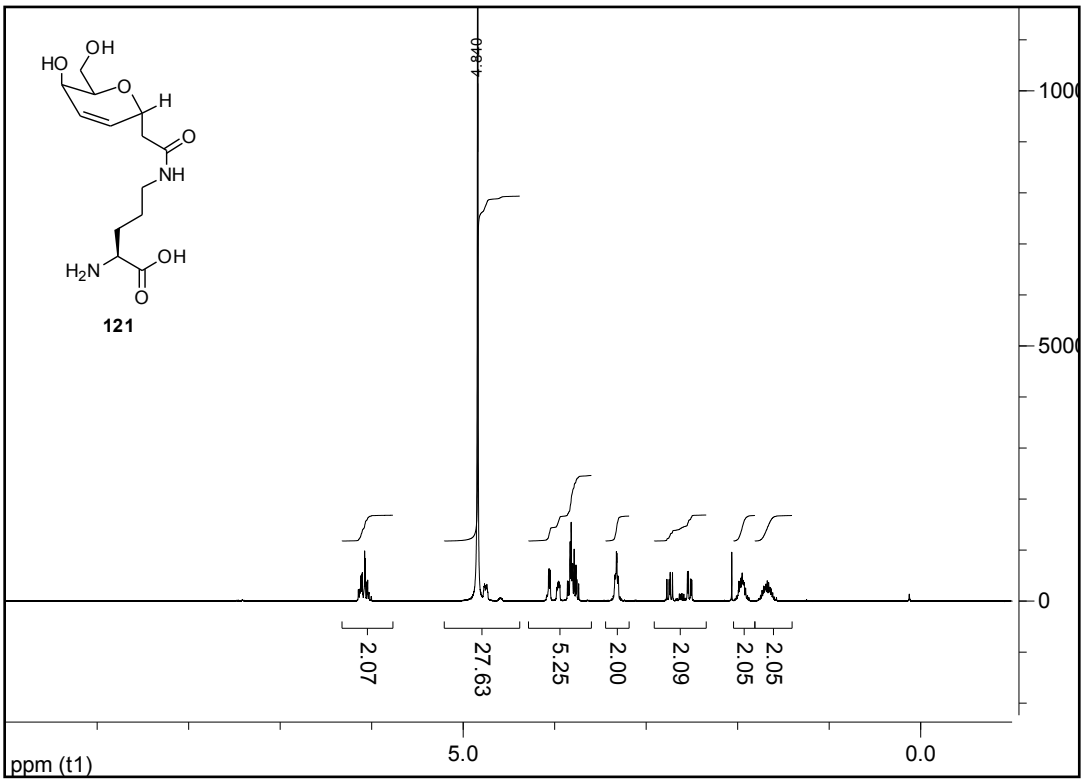

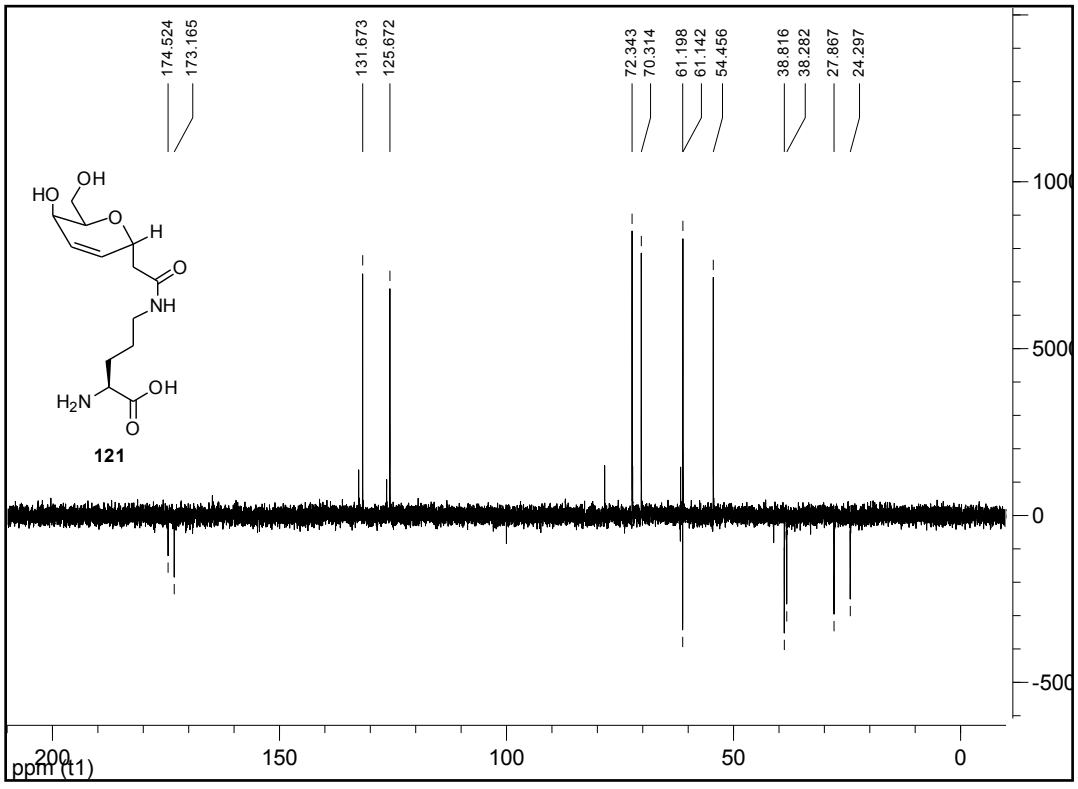

(S)-2-amino-5-(2-((2S,5R,6R)-5-hydroxy-6-(hydroxymethyl)-5,6-dihydro-2H-pyran-2-yl)acetamido)pentanoic acid (122):

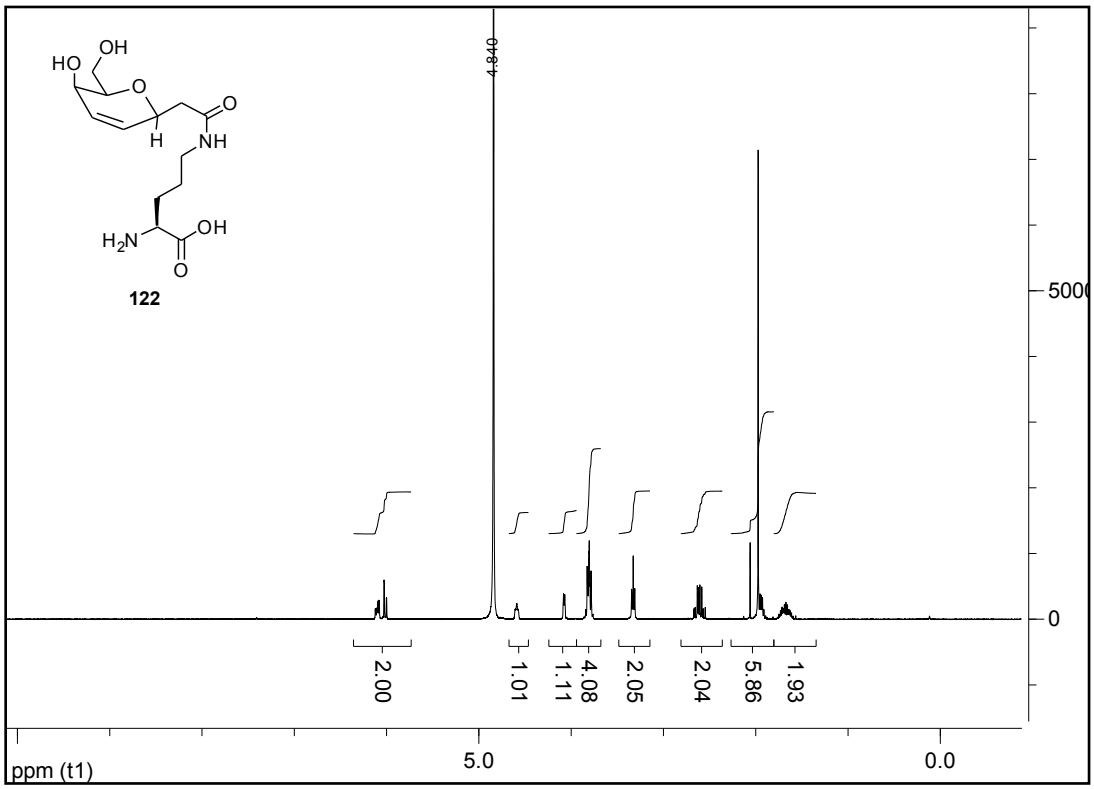

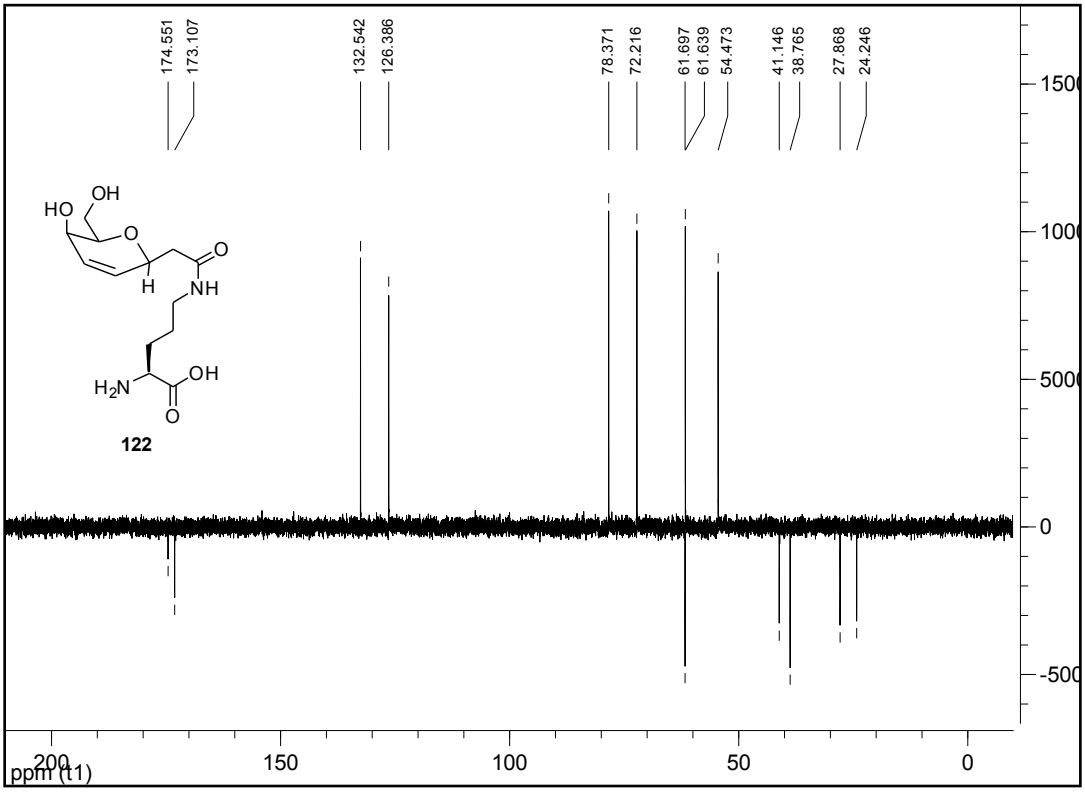

(S)-2-amino-5-(2-((2S,5R,6R)-5-hydroxy-6-(hydroxymethyl)tetrahydro-2H-pyran-2-yl)acetamido)pentanoic acid (123):

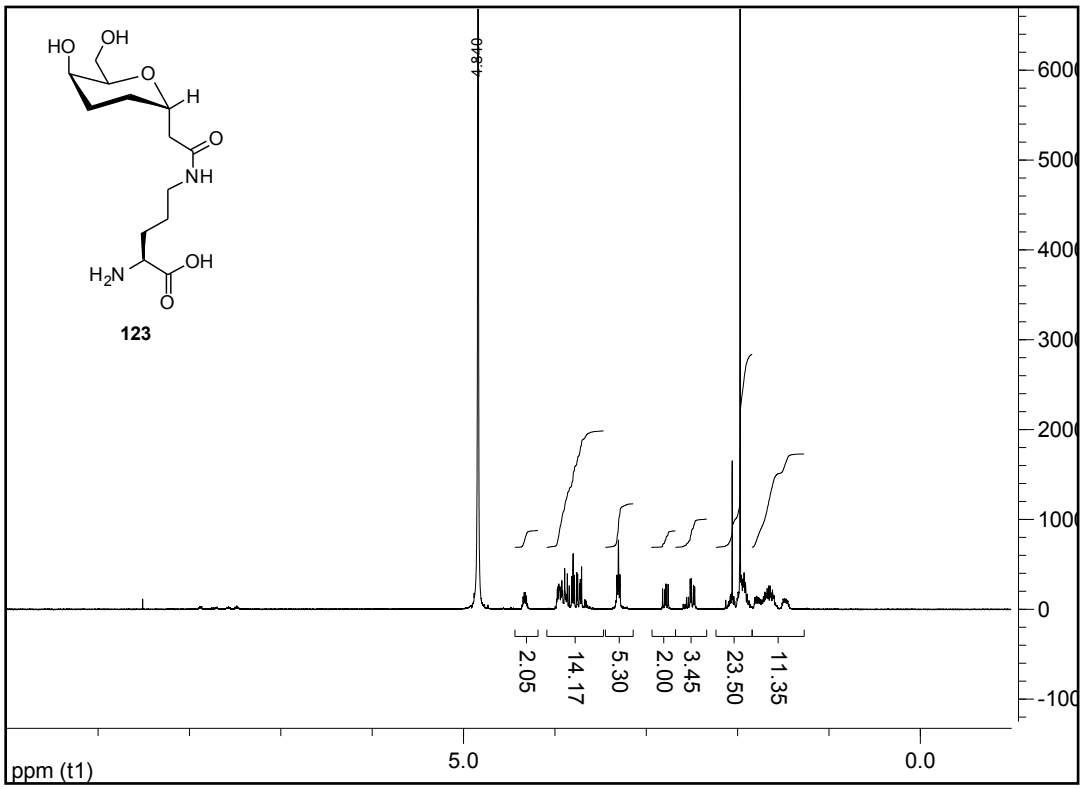

(S)-2-amino-5-(2-((2R,5R,6R)-5-hydroxy-6-(hydroxymethyl)tetrahydro-2H-pyran-2-yl)acetamido)pentanoic acid (124):

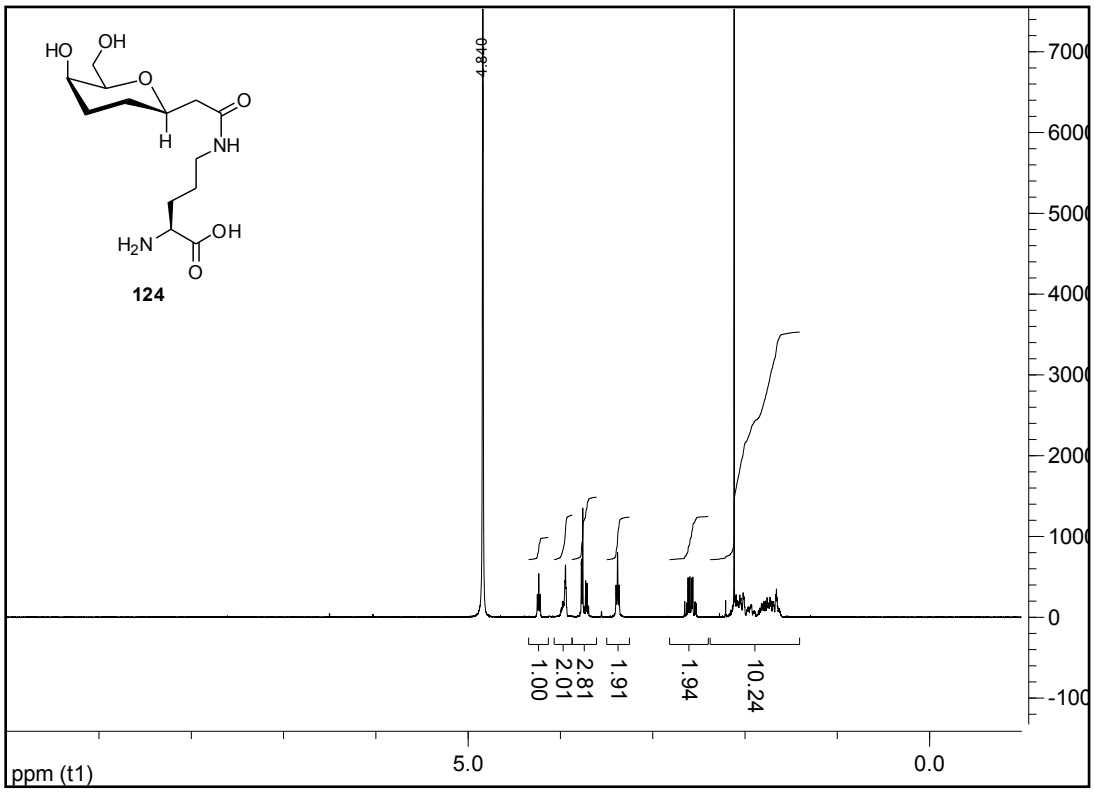

2-((2R,5R,6R)-5-hydroxy-6-(hydroxymethyl)-5,6-dihydro-2H-pyran-2-yl)acetic acid (125a):

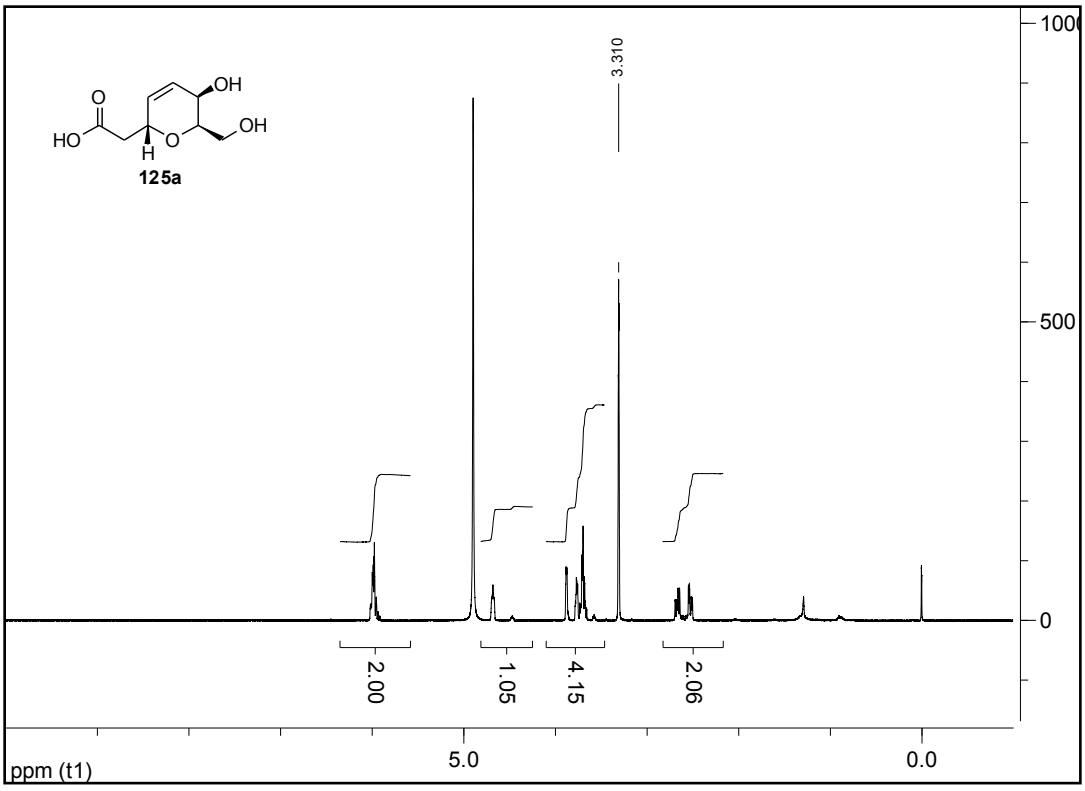

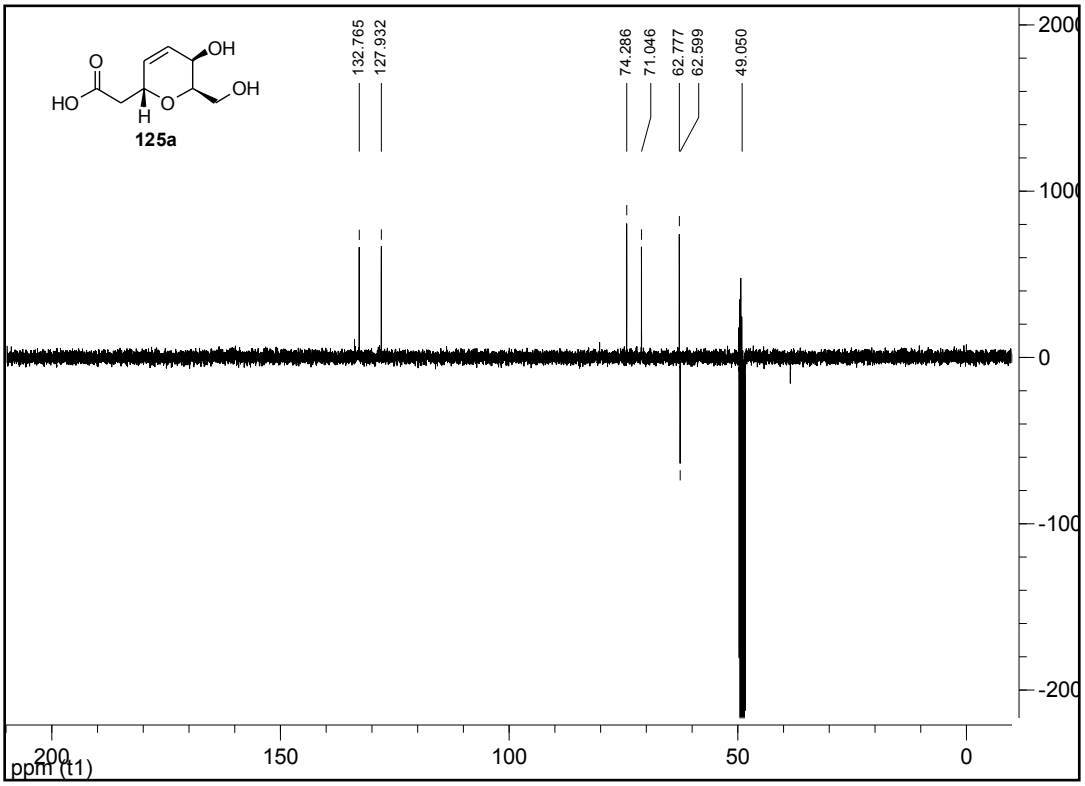

(R)-2-((2S,5R,6R)-5-hydroxy-6-(hydroxymethyl)-5,6-dihydro-2H-pyran-2-yl)propanoic acid (125b):

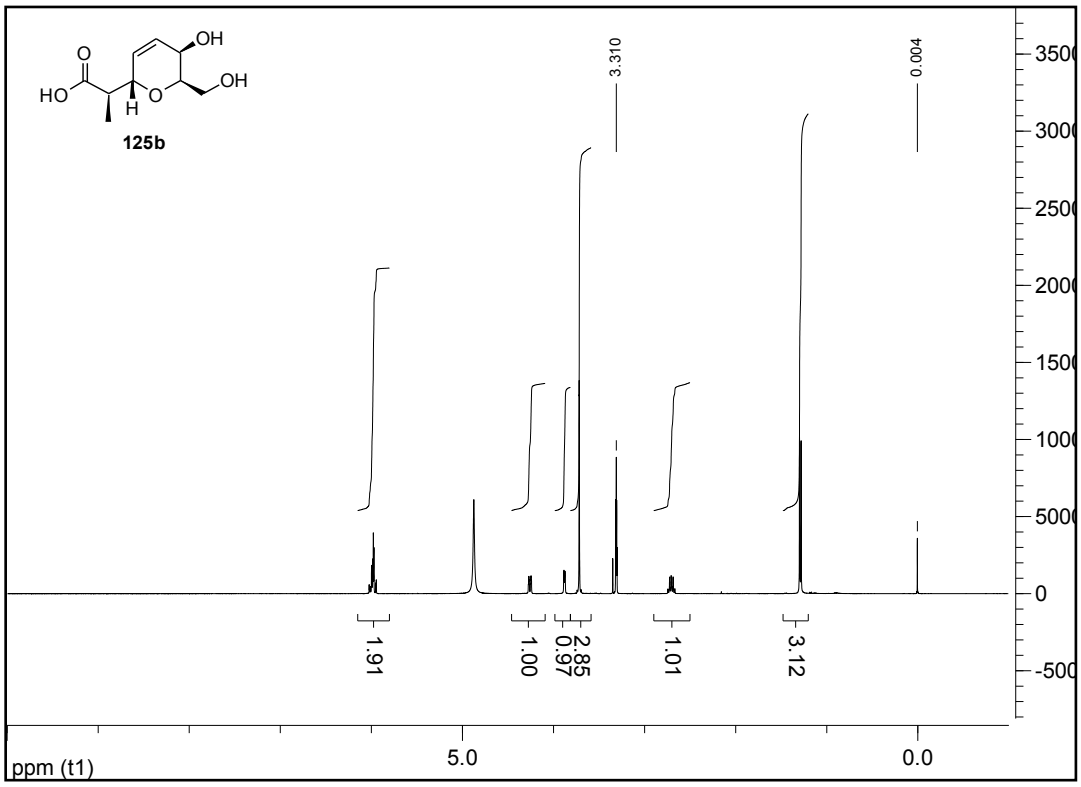

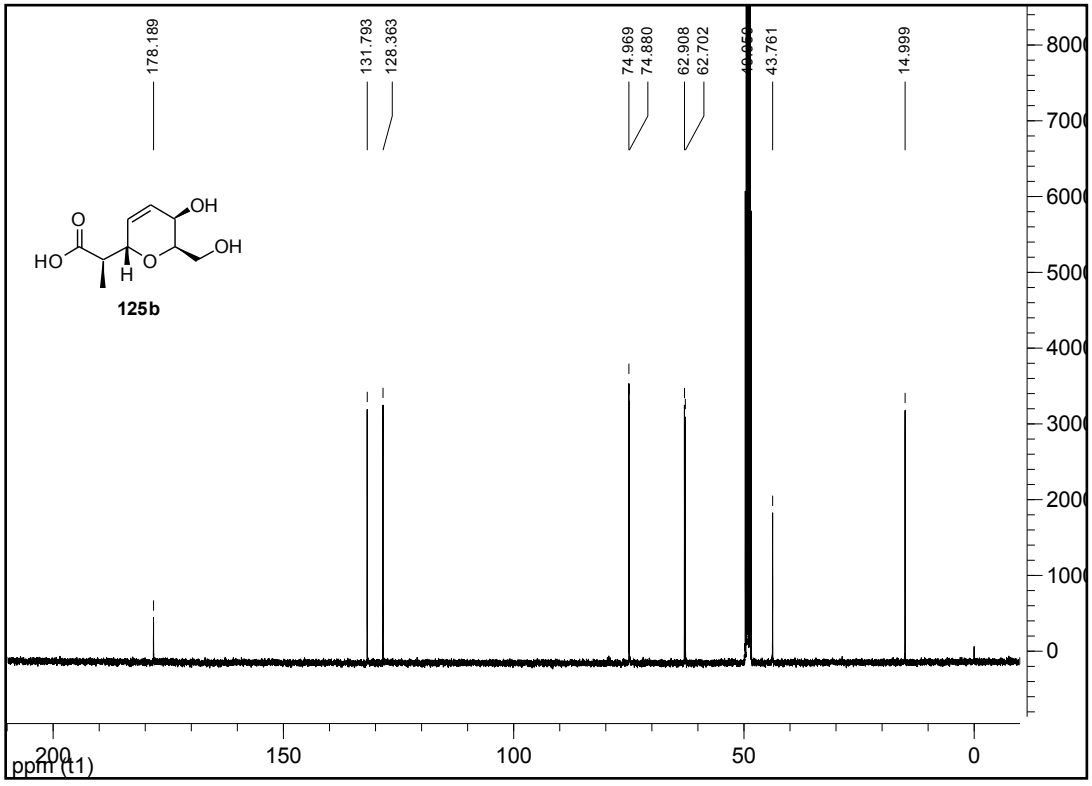

(R)-2-((2S,5R,6R)-5-hydroxy-6-(hydroxymethyl)-5,6-dihydro-2H-pyran-2-yl)-2-phenylacetic acid (125e):

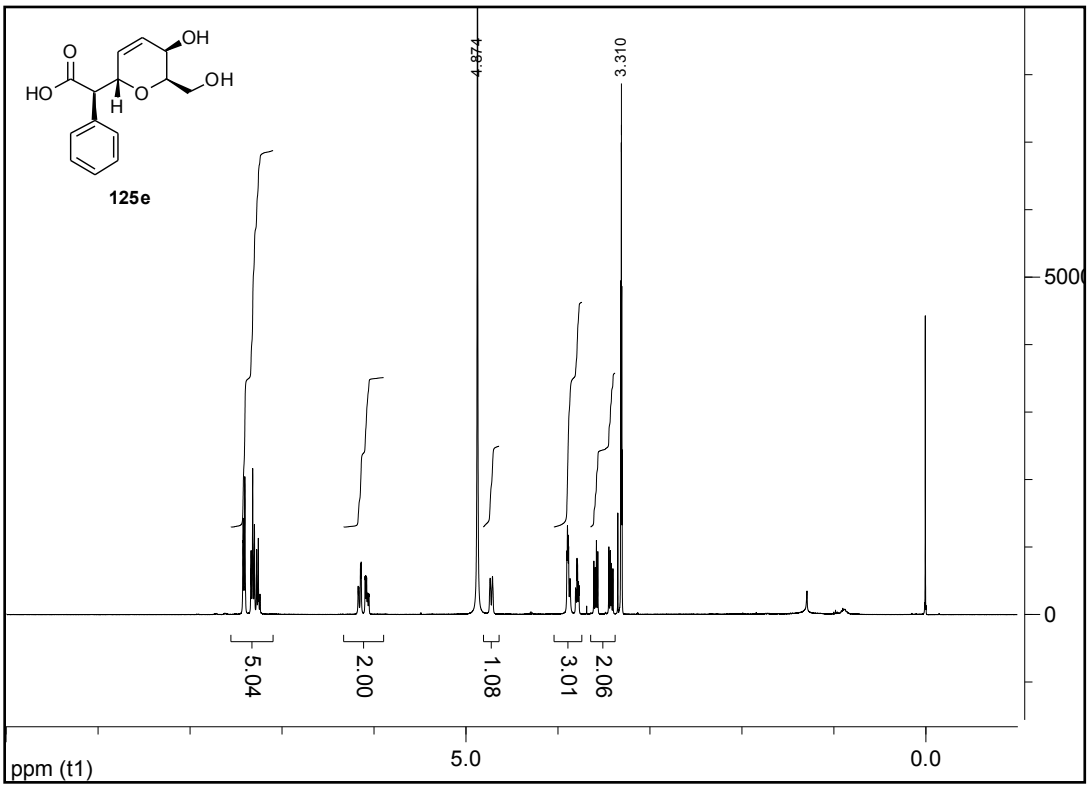

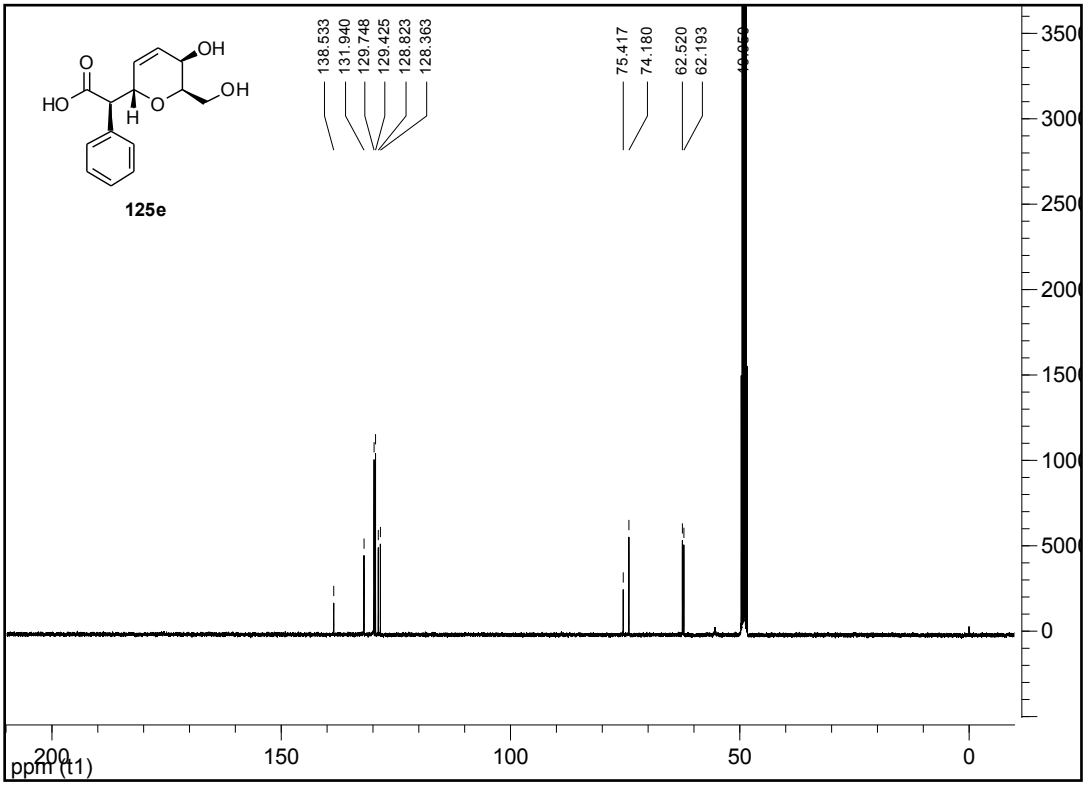

(R)-2-((2S,5R,6R)-5-hydroxy-6-(hydroxymethyl)-5,6-dihydro-2H-pyran-2-yl)-3-phenylpropanoic acid (125f):

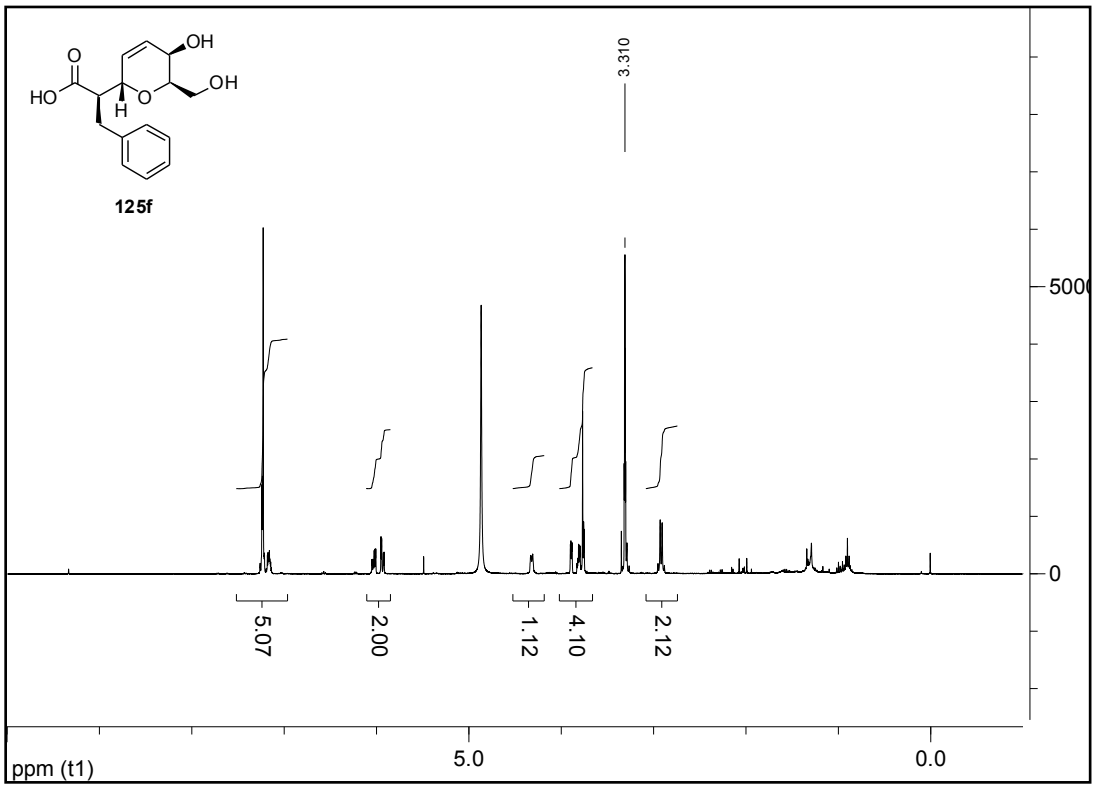

(R)-2-((2S,5R,6R)-5-hydroxy-6-(hydroxymethyl)-5,6-dihydro-2H-pyran-2-yl)-2-(4-methoxyphenyl)acetic acid (125g):

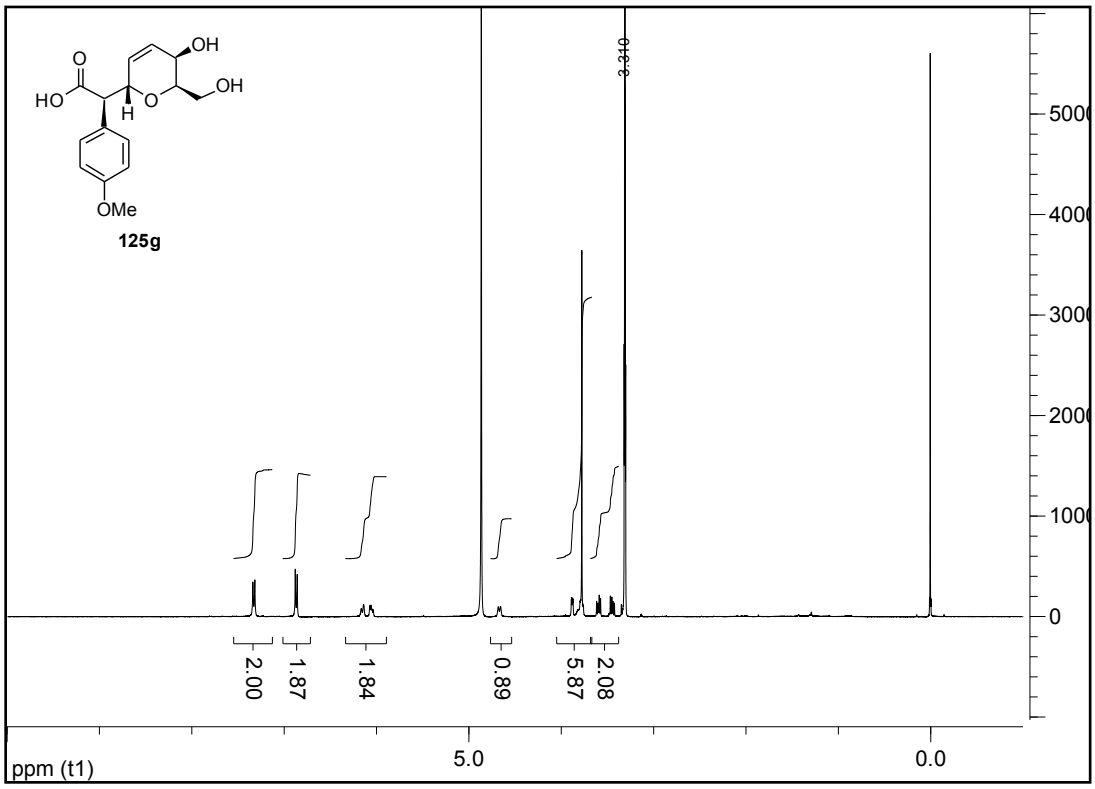

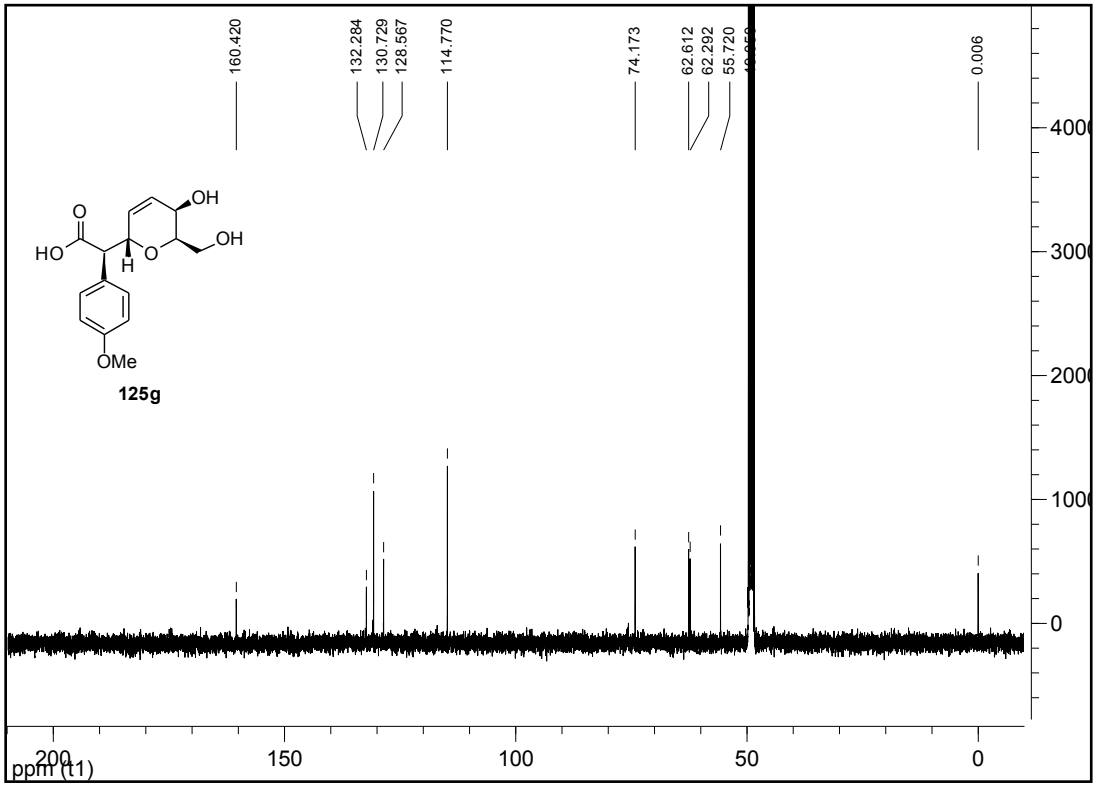

2-((2S,5R,6R)-5-hydroxy-6-(hydroxymethyl)-5,6-dihydro-2H-pyran-2-yl)acetic acid (126a):

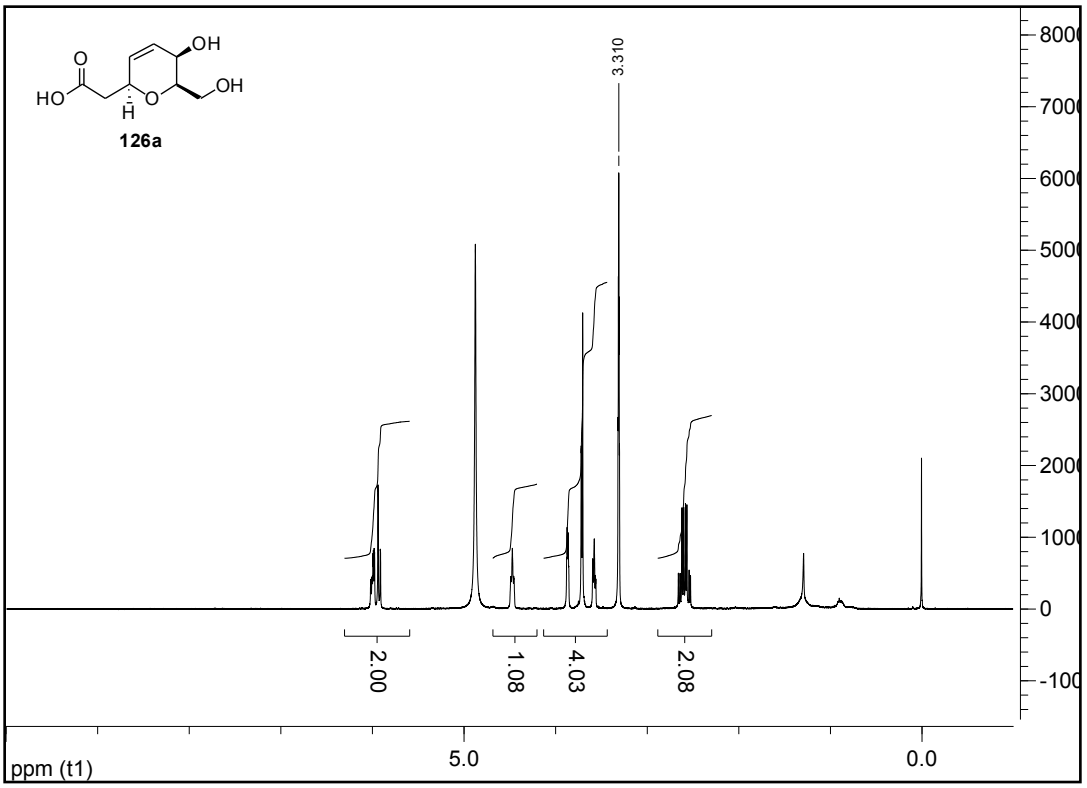

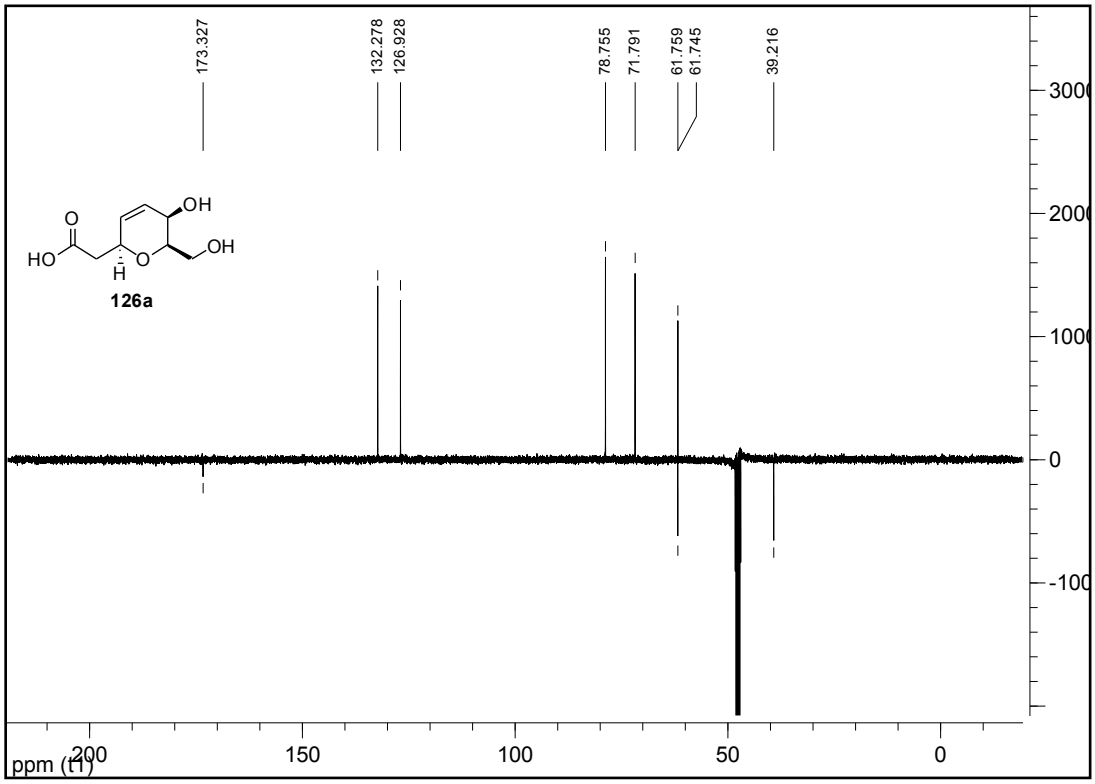

(S)-2-((2R,5R,6R)-5-hydroxy-6-(hydroxymethyl)-5,6-dihydro-2H-pyran-2-yl)propanoic acid (126b):

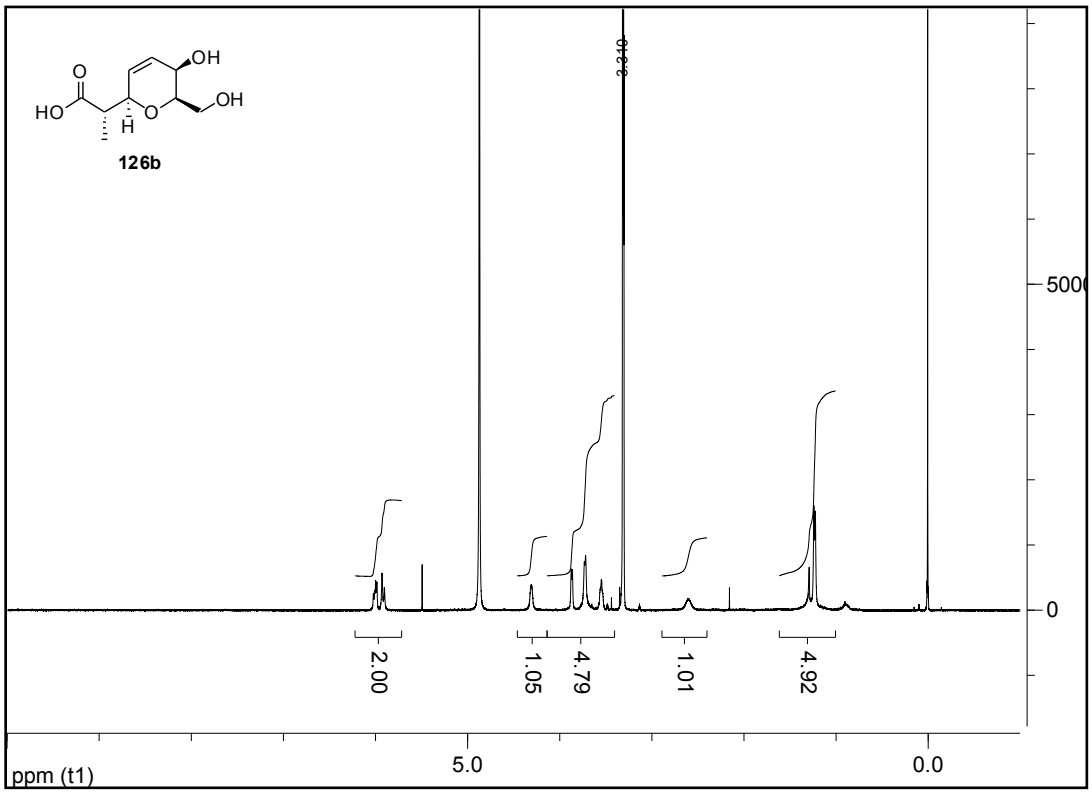

(2R,3S,4R,5S)-2-(acetoxymethyl)-6-allyltetrahydro-2H-pyran-3,4,5-triyl triacetate (127):

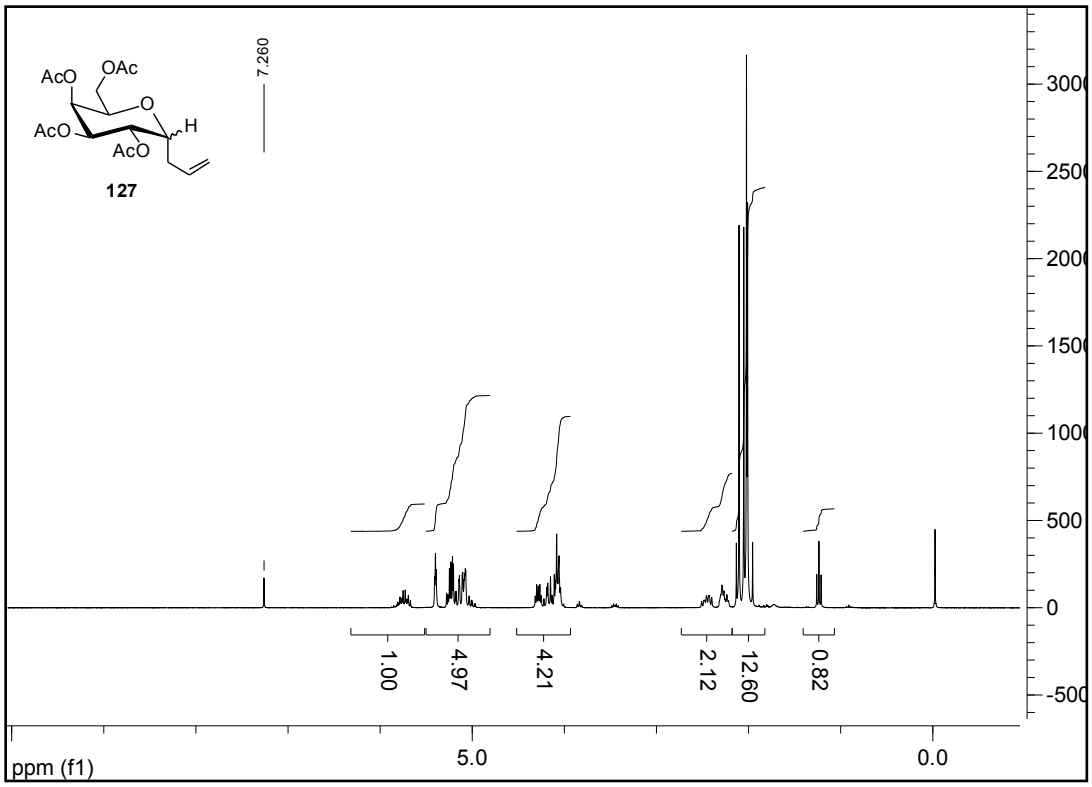

(2R,3R,4R,5R,6R)-2-allyl-6-(hydroxymethyl)tetrahydro-2H-pyran-3,4,5-triol (129):

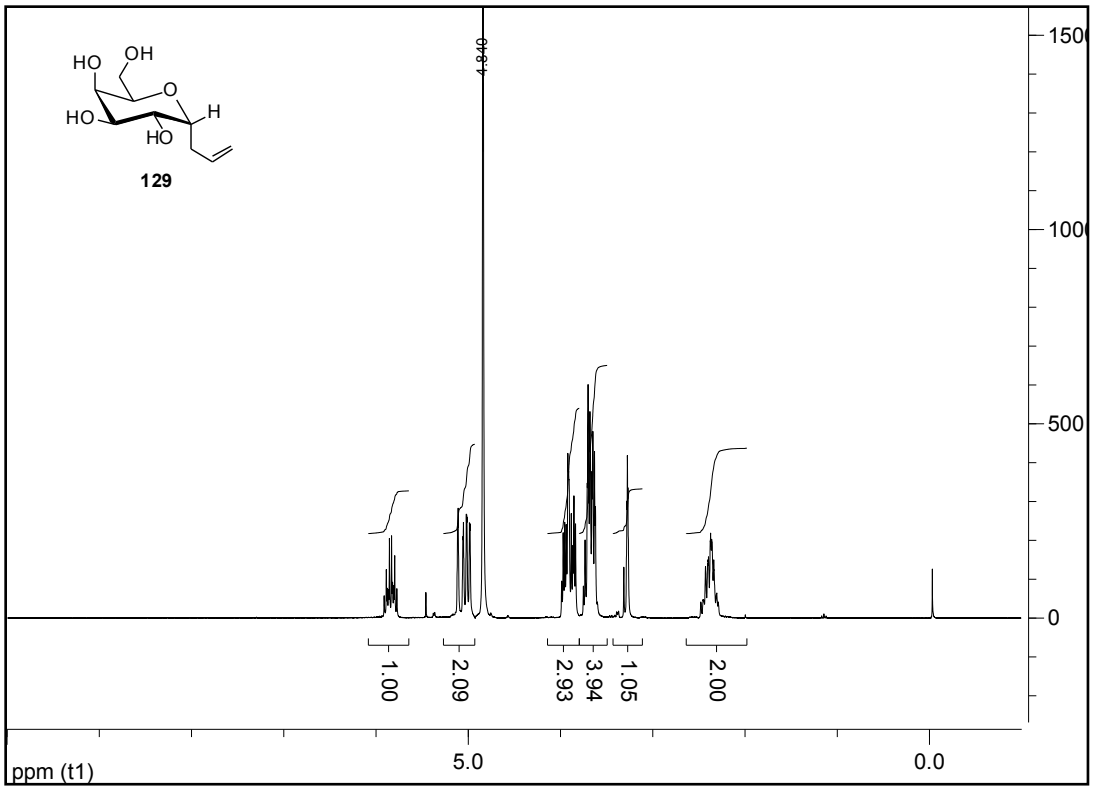

(2R,3S,4R,5S,6R)-2-(acetoxymethyl)-6-allyltetrahydro-2H-pyran-3,4,5-triyl triacetate (130):

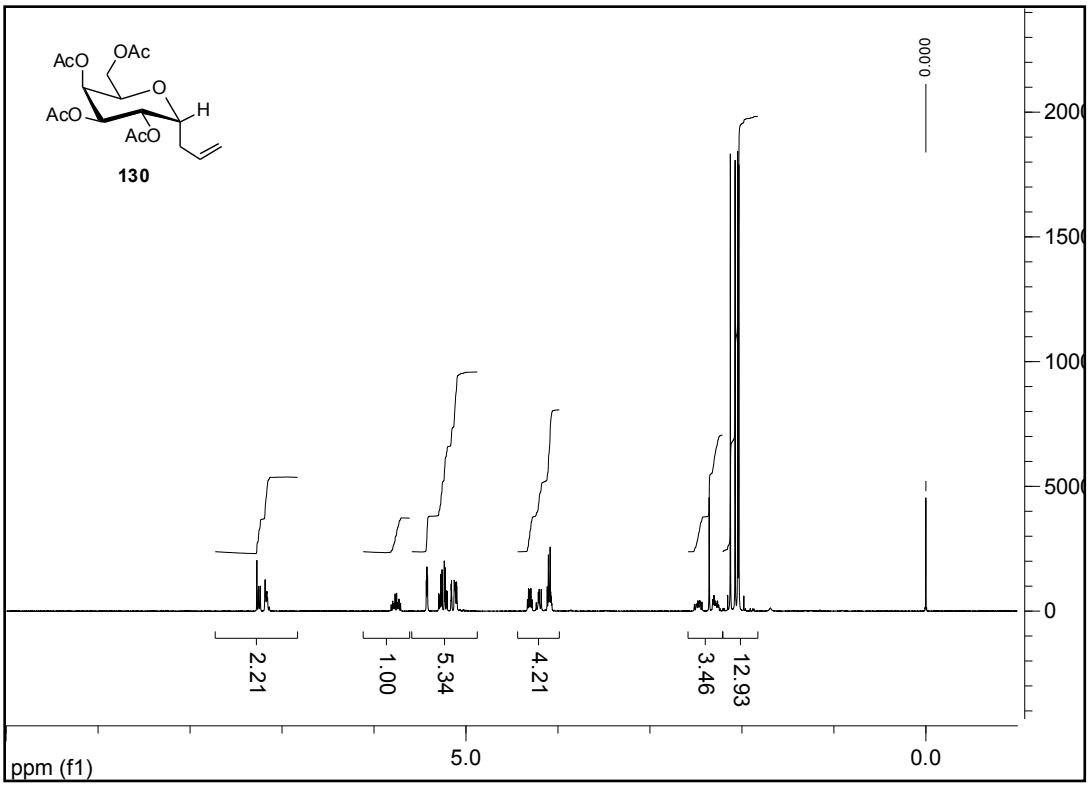

(2R,4S,5S,6R)-2-(acetoxymethyl)-6-(2-oxoethyl)tetrahydro-2H-pyran-3,4,5-triyl triacetate (131):

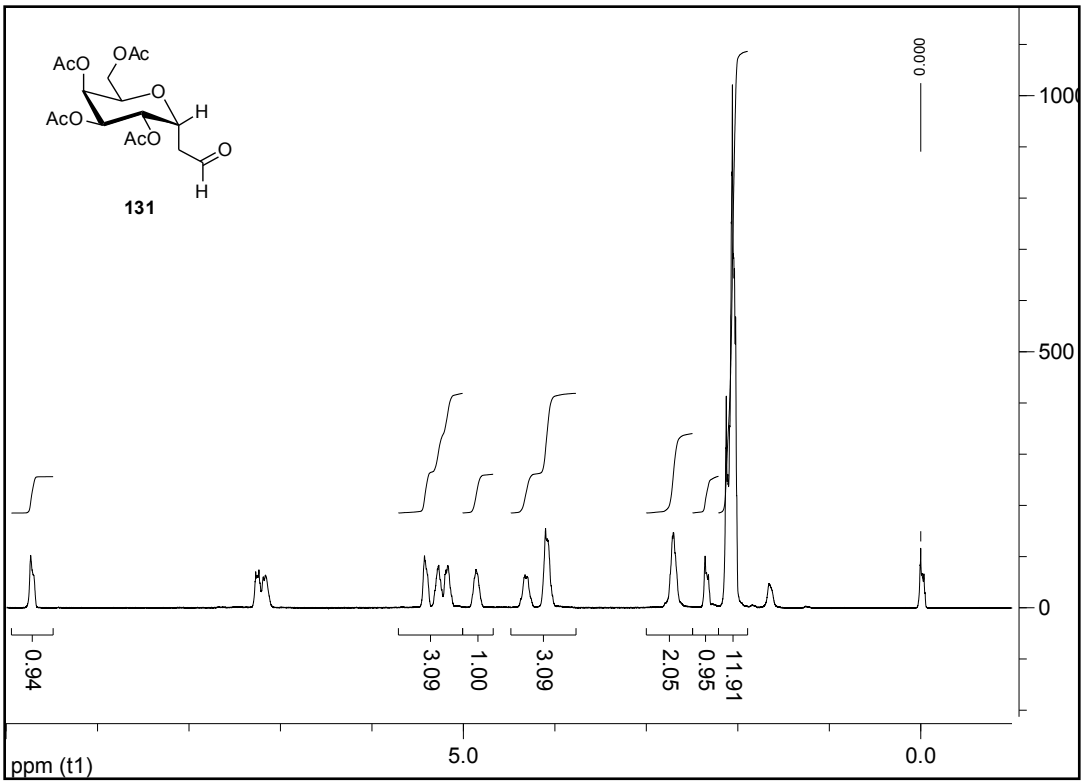

2-((2R,3S,4R,5S,6R)-3,4,5-triacetoxy-6-(acetoxymethyl)tetrahydro-2H-pyran-2-yl)acetic acid (132):

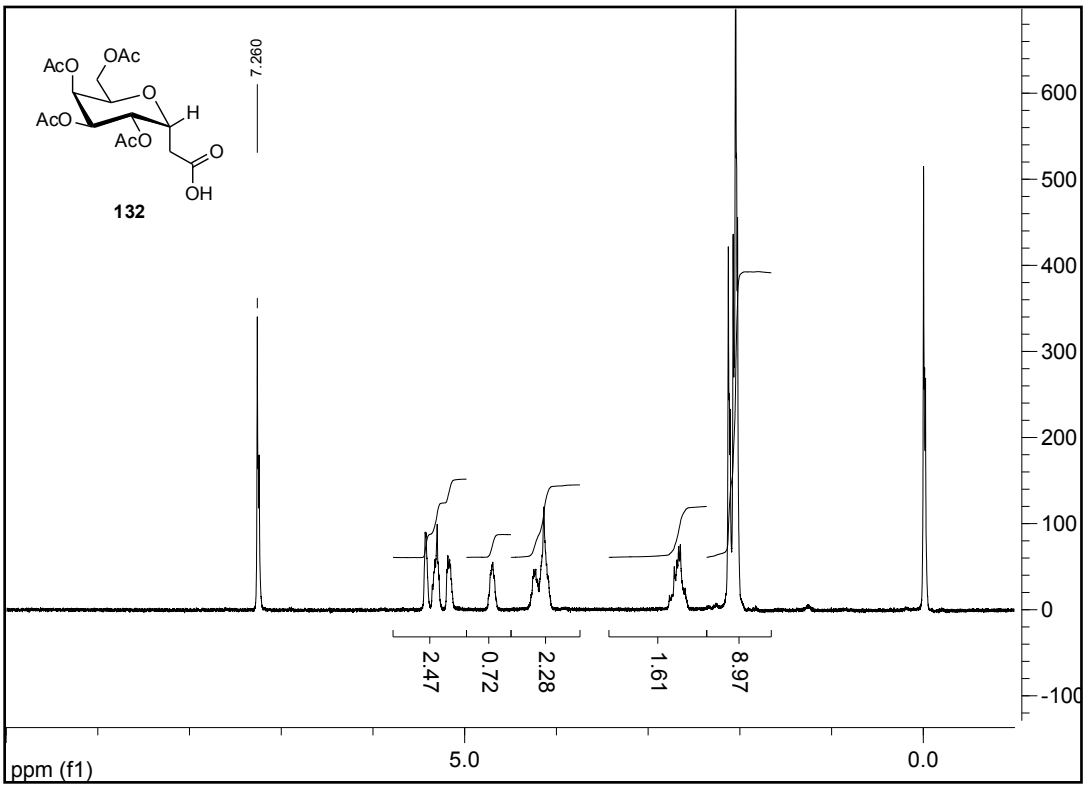

(2R,3S,4R,5S,6R)-2-(2-((S)-4-(((9H-fluoren-9-yl)methoxy)carbonylamino)-5-(benzyloxy)-5-oxopentylamino)-2-oxoethyl)-6-(acetoxymethyl)tetrahydro-2H-pyran-3,4,5-triyl triacetate (133):

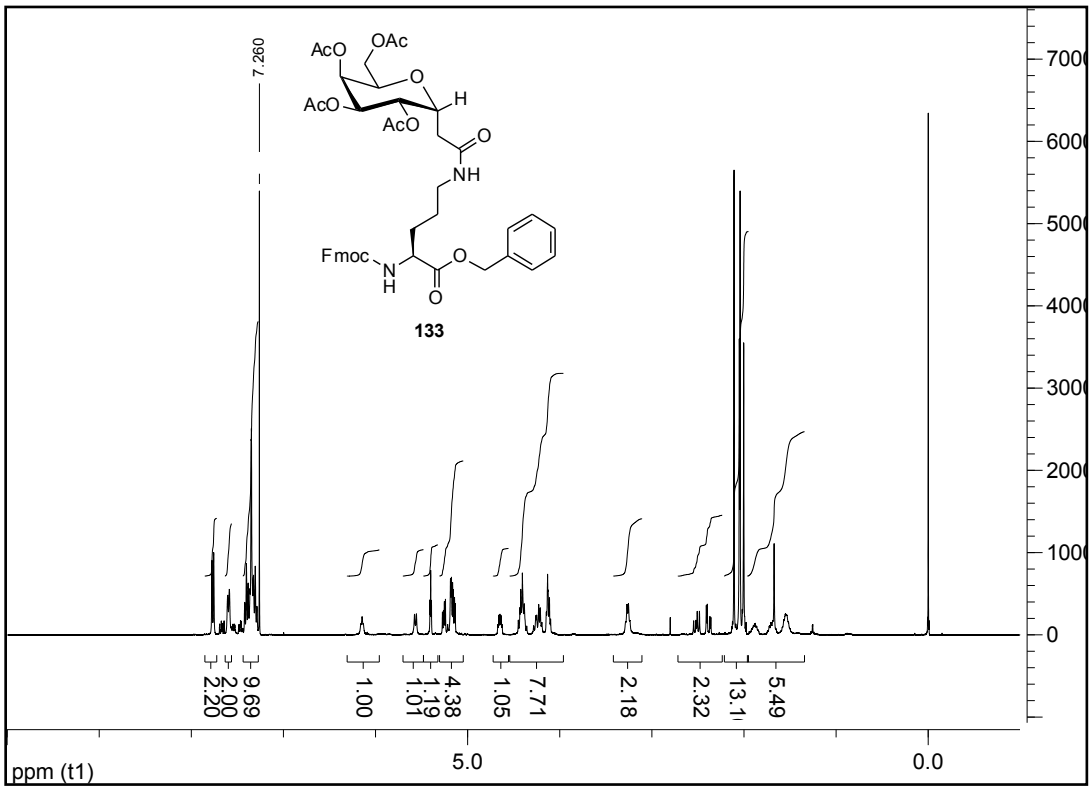

Appendix 2 Cryopreservation Data

Annexin V/7-AAD Flow Cytometry Assay of WRL 68 Cell Trials

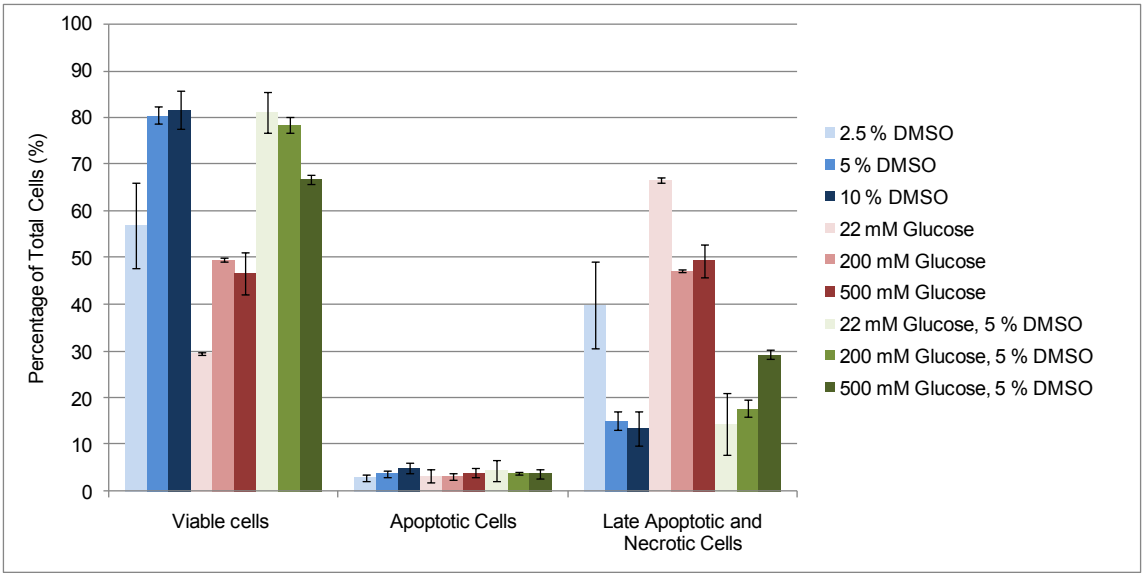

Figure A.1 Annexin V/7AAD flow cytometry assay of WRL 68 cells after cryopreservation; WRL 68 cells were treated with different concentrations of glucose and DMSO in HTK, and then treated according to the standard protocol given in Chapter 6. The total cell count was taken as 100% of cells. The error bars indicate SEM.

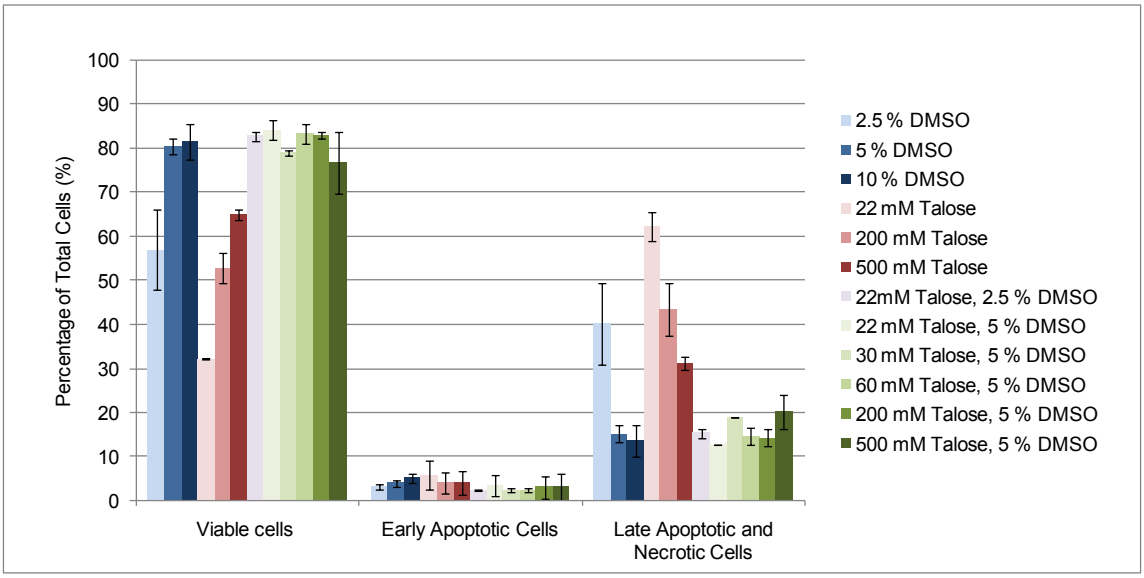

Figure A.2 Annexin V/7AAD flow cytometry assay of WRL 68 cells after cryopreservation; WRL 68 cells were treated with different concentrations of talose and DMSO in HTK, and then treated according to the standard protocol given in Chapter 6. The total cell count was taken as 100% of cells. The error bars indicate SEM.

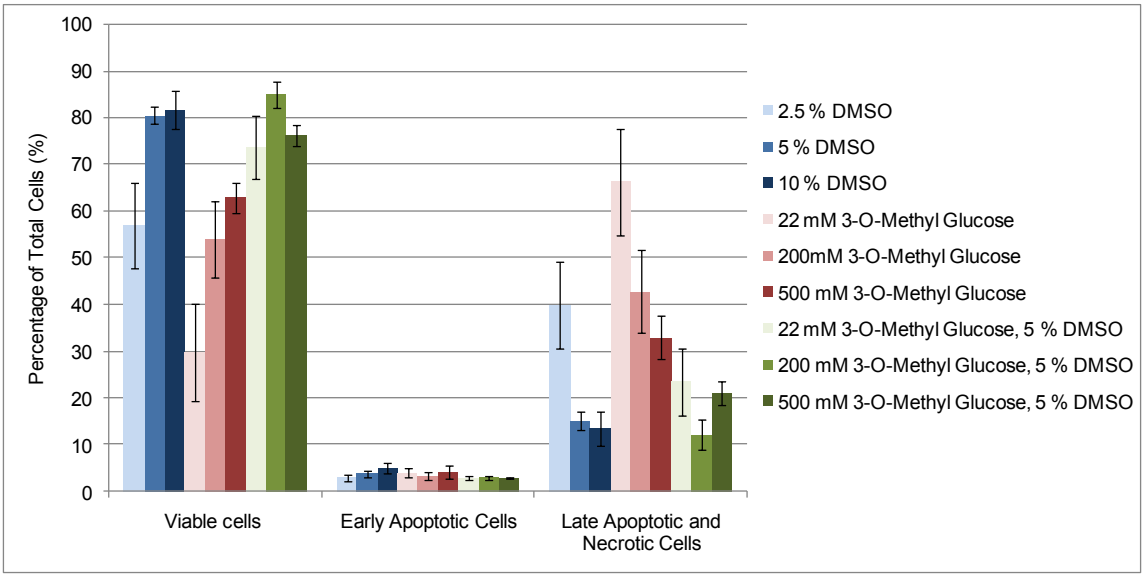

Figure A.3 Annexin V/7AAD flow cytometry assay of WRL 68 cells after cryopreservation; WRL 68 cells were treated with different concentrations of 3-*O*-methylglucose and DMSO in HTK, and then treated according to the standard protocol given in Chapter 6. The total cell count was taken as 100% of cells. The error bars indicate SEM.

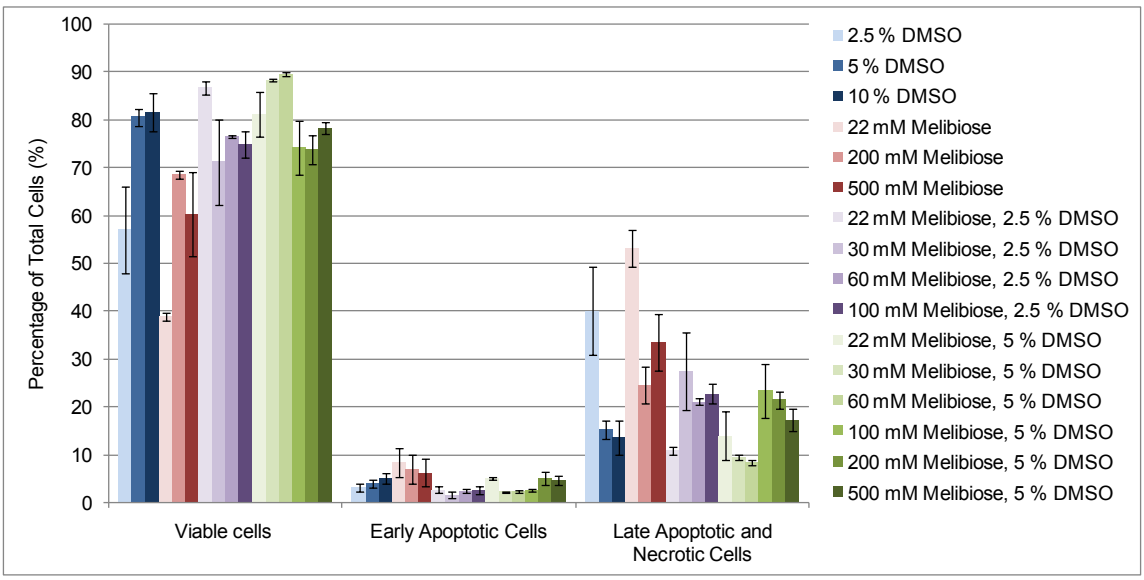

Figure A.4 Annexin V/7AAD flow cytometry assay of WRL 68 cells after cryopreservation; WRL 68 cells were treated with different concentrations of melibiose and DMSO in HTK, and then treated according to the standard protocol given in Chapter 6. The total cell count was taken as 100% of cells. The error bars indicate SEM.

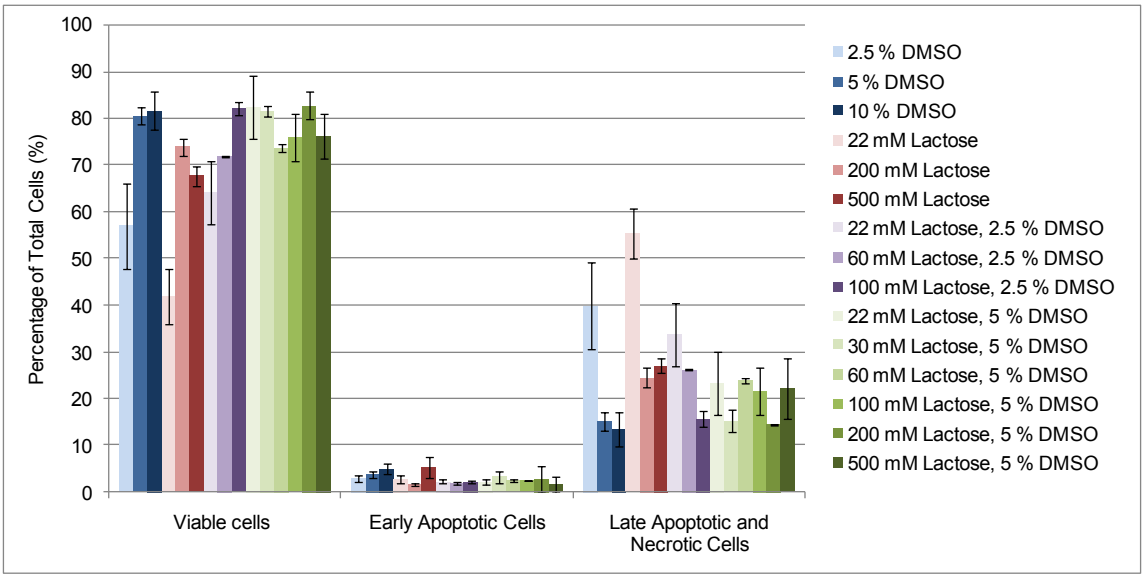

Figure A.5 Annexin V/7AAD flow cytometry assay of WRL 68 cells after cryopreservation; WRL 68 cells were treated with different concentrations of lactose and DMSO in HTK, and then treated according to the standard protocol given in Chapter 6. The total cell count was taken as 100% of cells. The error bars indicate SEM.

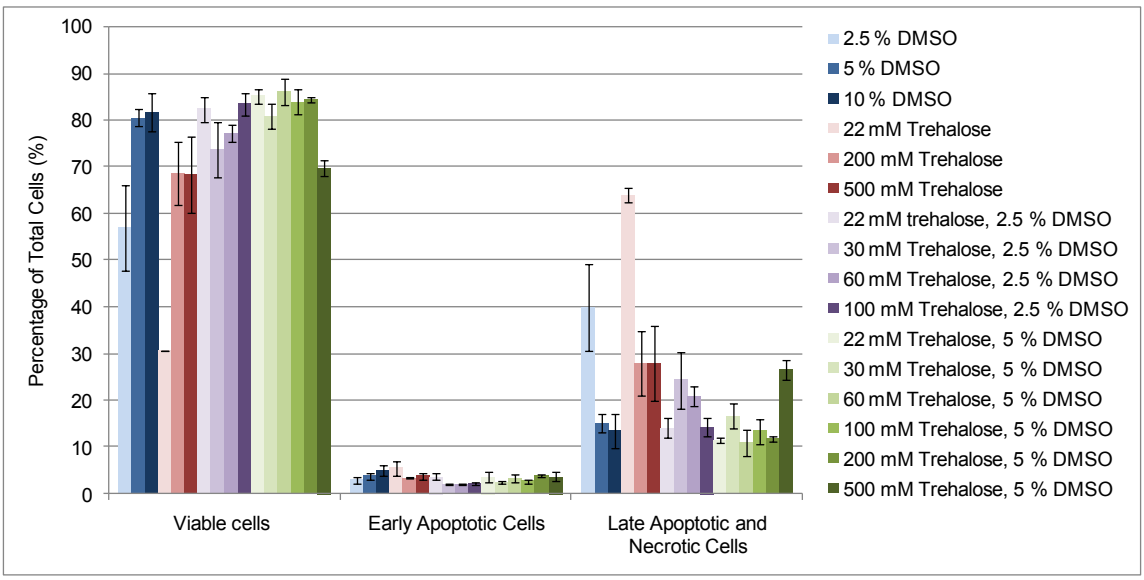

Figure A.6 Annexin V/7AAD flow cytometry assay of WRL 68 cells after cryopreservation; WRL 68 cells were treated with different concentrations of trehalose and DMSO in HTK, and then treated according to the standard protocol given in Chapter 6. The total cell count was taken as 100% of cells. The error bars indicate SEM.

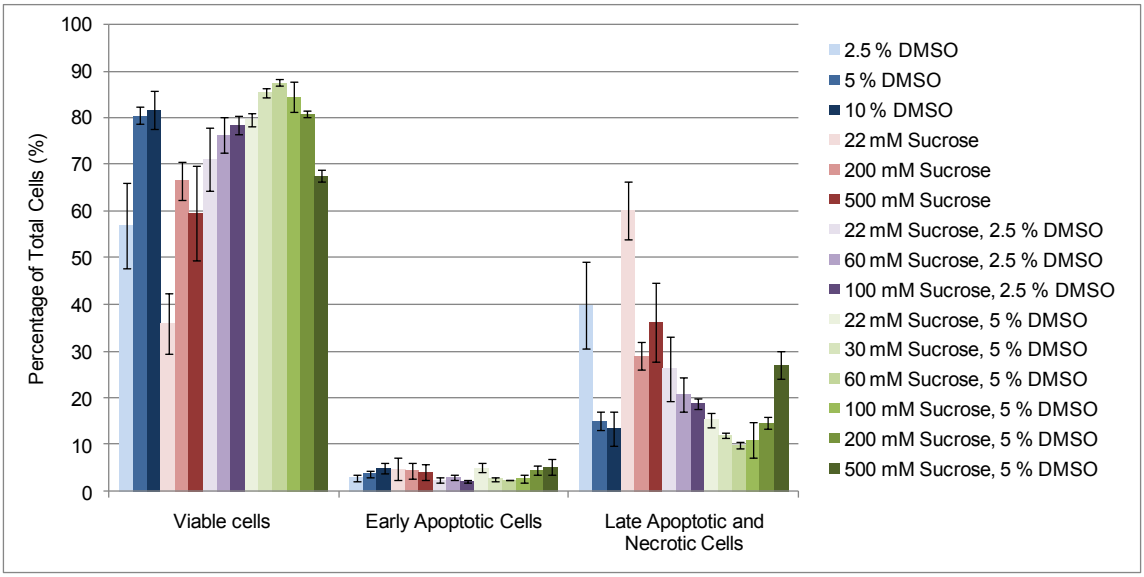

Figure A.7 Annexin V/7AAD flow cytometry assay of WRL 68 cells after cryopreservation; WRL 68 cells were treated with different concentrations of sucrose and DMSO in HTK, and then treated according to the standard protocol given in Chapter 6. The total cell count was taken as 100% of cells. The error bars indicate SEM.